УДК 547.89
КП
№ держреєстрації
Інв. №

МІНІСТЕРСТВО ОСВІТИ ТА НАУКИ УКРАЇНИ
ОДЕСЬКИЙ ДЕРЖАВНИЙ ЕКОЛОГІЧНИЙ УНІВЕРСИТЕТ
(ОДЕКУ)
65016, Одеса-16, вул. Львівська, 15;
тел. (0482) 427767

ЗАТВЕРДЖУЮ
Проректор ОДЕКУ, д.г.н., професор
_____ Ю.С.Тучковенко
2010 _____

З В І Т
ПРО НАУКОВО-ДОСЛІДНУ РОБОТУ

СУПРАМОЛЕКУЛЯРНА ХІМІЯ НА ОСНОВІ КРАУН-ЕТЕРІВ, ОРГАНІЧНИХ КИСЛОТ Й ЛУГІВ

(заключний)

Керівник НДР,
зав. каф. хімії навколишнього середовища,
д.х.н., проф. __ _____ Е.В. Ганін

2010

Рукопис закінчено “___”_____ 2010 р.

СПИСОК АВТОРІВ

Науковий керівник, д.х.н., проф., зав. каф. хімії навколишнього середовища	Е.В. Ганін (участь у всіх розділах)
К.х.н., доцент	Г.І. Герасименко (розділи 3, 4, 9)
К.т.н., доцент	В.Ф.Шевченко (розділ 4, 6, 9)
К.х.н., доцент	Г.В.Федорова (розділи 1, 6)
К.п.н., доцент	М.Г. Горліченко (розділ 4-6, 9)
Ст. викладач	М.Г. Васильева (розділи 1-3, 7,9)
Ст. викладач	С.В.Шевченко (розділи 5, 7, 9)
Асистент	О.М. Ласовська (розділ 6, 8, 9)
Асистент	С.І. Шепеліна (розділ 6, 9)
Нормоконтролер	С.В. Малацковська

РЕФЕРАТ

Звіт з НДР: 281 с., 56 рисунків, 27 додатків.

Об'єкт дослідження – супрамолекулярні сполуки на прикладі комплексів "гість-хазяїн" при використанні у якості молекул "хазяїнів" – O- та N-вмістних краун-етерів різної будови, кислот та лугів, а у якості молекул "гостей" – органічних і неорганічних сполук.

Мета роботи – дослідження синтезу і аналіз нових сполук ("гість-хазяїн") при використанні як "хазяїнів" – краун-етерів різної будівлі, а як "гостей" – органічних і неорганічних сполук, у тому числі біологічно активних сполук, а також лабільних рівноважних розчинів флуорокомплексних кислот.

Метод дослідження – розробка методики й синтез названих супрамолекулярних сполук у виді монокристалів і здійснення рентгеноструктурного дослідження для отриманих продуктів.

Доведена можливість зв'язування азакраун-етерами 4-амінобензойної кислоти, саліцилової кислоти, мефенамової кислоти, ізоніазіду, етіонаміду, протіонаміду, дітіоурацілу, сульфаніламідних препаратів, похідних трифенілметану в стабільні супрамолекулярні комплекси. Розроблено методики і здійснено синтези комплексів силіційфлуороводній кислоти з піридинами. Розроблени методики і здійснені синтези комплексів краун-етерів із флуорокомплексними кислотами силіцію, ніобію, танталу. Зроблено висновки щодо особливостей синтезу нових речовин, які необхідно враховувати при моделюванні біохімічних взаємодій, створенні методик.

Результати НДР використані у матеріалах конференцій, статтях у провідних наукових виданнях.

КРИСТАЛІЧНІ СУПРАМОЛЕКУЛЯРНІ СПОЛУКИ, КРАУН-ЕТЕРІ, СИЛІЦІЙФЛУОРОВОДНЕВА КИСЛОТА, ФЛУОРОКОМПЛЕКСНІ КИСЛОТИ СІЛІЦІЮ, НІОБІЮ, ТАНТАЛУ

Умови одержання звіту: за договором. 65016, Одеса-16, вул. Львівська, 15, ОДЕКУ

ЗМІСТ

	Вступ.....	8
1	Комплекси краун-етерів та 4-амінобензойної кислоти.....	10
2	Комплекси краун-етерів та 2-оксібензойної (саліцилової) кислоти....	13
3	Комплекси азакраун-етерів, піперазину й 2-аміно-2-(гідроксіметіл)пропан-1,3 -диолу з мефенамовою кислотою.....	16
4	Комплексна сполука – пирантел памоат.....	18
5	Комплекси ізоніазиду та органічних дікарбонових кислот	19
6	Супрамолекулярні комплекси 2,4-дітіоурацилу з краун-етерами....	20
7	Комплекси краун-етерів з етіон- й протіонамідом	22
8	Селективна взаємодія молекул "хазяїнів":краун- етерів з похідними трифенілметану	25
9	Комплекси азакраун-етерів та сульфаніламідних препаратів	27
10	Комплекси піперидину і піперазину та сульфаніламідних препаратів.....	29
11	Комплекси кремнефлуороводній кислоти з похідними піридину та краун-етерами	31
12	Синтез і структури комплексів краун- і азакраун-етеров із флуорметаллатами цирконію, гафнію, ніобію й танталу	34
13	Застосування матеріалів досліджень.....	37
	Висновки	45
Додаток А	Копія статті. Molecular complexes of thionicotinamide with 18-membered crown ethers: Synthesis and crystal structures	46
Додаток Б.	Копія статті. Supramolecular associates of p-aminobenzoic acid with N- and N,O-heterocyclic molecules	54
Додаток В.	Копія статті. Кристаллическая структура гексафторосиликата орто-толуидиния	63

Додаток Г. Копія статті. Кристаллические структуры комплексов цис-син-цис изомера дициклогексано-18-краун-6 с гексафортанталатом оксония и с гексафторниобатом оксония 69

Додаток Д. Копія статті. Two new "onium" fluorosilicates, the products of interaction of fluorosilicic acid with 12-membered macrocycles: structures and spectroscopic properties 77

Додаток Е. Копія статті. Hydrogen bonded frameworks of 2-carboxypyridinium hexafluorosilicate and 2-carboxyquinolinium hexafluorosilicate dihydrate 88

Додаток Ж. Копія статті. Structure of oxonium hexafuoroniobate and hexafuorotantalate complexes with crown ethers of diferent dimensionality 96

Додаток З. Копія статті. Crystal Structure of Bis(3-carboxypyridinium) Hexafluorosilicate 107

Додаток І. Копія статті. Structure of Benzo- and Dibenzocrown Ethers and Their H-Bonded Adducts. 4.§ Structural Motifs in the 2,4-Dithiouracil Complexes with 4-Bromo- and 4-Nitrobenzo-18-crown-6, [2.4]Dibenzo- and Thia[1.5]dibenzo-18-crown-6 112

Додаток Й. Копія статті. Crystal Structures of Dioxonium Hexafluorotantalate and Dioxonium Hexafluoroniobate Complexes with Tetrabenzo-30-Crown-10 122

Додаток К. Копія статті. Binding of fluoro-containing anions to hexaazamacrocyclic ligand: competitive interactions of fluoride and tetrafluoroborate anions with hexaprotonated [18]aneN6 130

Додаток Л.	Копія статті. From clusters to coordination polymers in the crown-templated system ZrO_2/HfO_2 (Nb_2O_5/Ta_2O_5) – HF – H_2O – azacrown ether Rarely Observed Metal Oxide Fluoride Anions $[(TaF_5)_2O]^{2-}$ and $[(H_2O)NbF_4O\ NbF_5]^{2-}$ in the Complexes with Azacrown Ethers	137
Додаток М.	Копія статті. Hexafluorosilicates of bis(carboxypyridinium) and bis(2-carboxyquinolinium)	149
Додаток Н.	Копія статті. Inclusion of triphenylmethane derivatives by crown and linear O-containing molecules : selective interactions and crystal structure	156
Додаток О.	Копія статті. Hexafuorosilicates of bis(aminopyridinium). The relationship between H-bonding system and solubility of salts	165
Додаток П.	Копія статті. Синтез и кристаллическая структура гексафторосиликата N,N-диметилбигуанидиния	173
Додаток Р.	Копія статті. Conformational Mobility of 7,16-Bis(4-methoxybenzyl)-1,4,10,13-tetraoxa-7,16-diazacyclooctadecane in Molecular and Proton Transfer Complexes: X-ray and DFT Study	178
Додаток С.	Копія статті. Особенности структуры производных 1,3-дигидропиримидин-2,4-дионов в комплексах с макроциклическими поли– и азаполиэфирами	191
Додаток Т.	Копія статті. Синтез краун-эфиров и их взаимодействие с кремнефтороводородной кислотой	199
Додаток У.	Копія статті. Особенности образования комплексов «хозяин-гость» краун-эфиров с HN-протонодонорными молекулами	206
Додаток Ф.	Копія статті. Селективные взаимодействия краун-эфиров с фторокомплексными кислотами бора, кремния, германия, олова и сурьмы в присутствии воды	214

Додаток Х. Interaction of hexafluorosilicic acid with sulfa drugs. Bis(sulfathiazolium)hexafluorosilicate: Spectral data and crystal structure 221

Додаток Ц. Гексафторосиликаты бис(2-алкилтиокарбамоил-4-пиридиния) 228

Додаток Ш. Persistent CH... π Interactions in Mefenamic Acid Complexes with Cyclic and Acyclic Amines 236

Додаток Щ. Structural study of salicylic acid salts of a series of azacycles and azacrown ethers 247

Додаток Ю. From chains to ladders in the co-crystals with 2,3-thiophene-15-crown-5, 2,3-naphtho-15-crown-5, and bis-(18-crown-6)-stilbene constructed by weak hydrogen bonding 264

Додаток Я. Транспортные взаимодействия краун-эфиров с фторокомплексными кислотами кремния 275

ВСТУП

Молекупярна хімія контролює ковалентні зв'язки. Супрамолекупярна хімія - "хімія за межами молекули". Її ціль - досягнення контролю над міжмолекулярними нековалентними взаємодіями. Супрамолекупярна хімія має справу з більш складними утвореннями, чим окремі молекул, - супрамолекупярними ансамблями утримуваними разом міжмолекулярними єднальними взаємодіями. Це - найвищою мірою міждисциплінарна галузь знання, що поєднує науку і технологію, що перекидає мости від хімії до біології. Результати супрамолекулярних досліджень неодмінно використовується як хімічна база при моделюванні молекулярних і міжмолекулярних взаємодій природних молекул, а взагалі і в навколишньому середовище, а також у спрямованому синтезі супрамолекулярних ансамблів.

[- Comprehensive supramolecular chemistry / Eds. J-M. Lehn, J.L. Atwood, J.E.D. Davies, D.D. MacNicol, F. Wogtle. Oxford - New York - Tokyo: Pergamon, 1996. Vol. 1-11. (мова - англійська);

- Лен Ж-М. Супрамолекулярна хімія: Концепції і перспективи. Новосибірськ: Наука, 1998. 334 с. (мова - російська)

Лен Ж-М. (J-M. Lehn) є лауреатом Нобелівської премії і головним координатором сучасних супрамолекулярних досліджень у Європі й Америці.]

Об'єктами дослідження супрамолекулярної хімії є великі порожнинні молекули і їх комплекси з катіонами, аніонами та нейтральними молекулами, порівняно невеликого розміру. В останні десятиліття синтезовані і достатньо добре вивчені такі надзвичайно цікаві макрогетероциклічні сполуки як краун-етери, криптанди, кавитанди, каліксарени, аннулени, циклофани, катенани, ротаксани. Особливе місце при цьому в хімії макроциклів із ряду причин займають краун-етери, криптанди і їхні гетероаналоги. Такі сполуки здатні утворювати стабільні комплекси з іонами металів, нейтральними органічними сполуками і водою, солюбілюзовати їх в органічні розчинники, або переносити іони через природні і штучні мембрани.

Методами дослідження супрамолекулярної хімії є такі сучасні фізико-хімічні методи досліджень як ПМР, ІЧ, УФ, мас-спектрометрія, рентгеноструктурний аналіз і ін., що забезпечує надійність і однозначну інтерпретацію отриманих результатів.

Однак, далеко не всі закономірності таких взаємодій ретельно вивчені і доведені. Тому дослідження в цьому напрямку є досить актуальними.

Метою даного дослідження є синтез і фізико-хімічне тестування нових оригінальних супрамолекулярних сполук (комплексів "гість-хазяїн") при використанні як порожнинні молекули "хазяїнів" – кисень і азот вмістних краун-етерів різної будівлі, а як молекул "гостей" – органічних і неорганічних сполук, у тому числі порівнянних за розміром і функціональною структурою з краун-етерами, біологічно активних сполук, а також лабільних рівноважних розчинів кислот. Результати цих досліджень можуть бути прийняті до уваги як хімічна основа при моделюванні молекулярних і міжмолекулярних взаємодій природних молекул, а також у спрямованому синтезі інших супрамолекулярних ансамблів. Отримані результати цієї роботи апробовані на міжнародних конференціях, нарадах, симпозіумах і опубліковані в міжнародних журналах.

Задачі дослідження включають аналіз відомих літературних даних і розробку методів синтезу перерахованих вище об'єктів, перетворення їх у монокристали, здійснення рентгеноструктурних досліджень архітектури отриманих супрамолекулярних ансамблів у співавторстві з усілякими інтернаціональними науковими командами, аналіз і узгодження отриманих результатів відносно відомих феноменів включення, накопичення конструктивних висновків.

Термін виконання теми “ Супрамолекулярна хімія на основі краун-етерів, органічних кислот й лугів” з 01.01.2007 р. до 31.12.2010 р.

1 КОМПЛЕКСИ КРАУН-ЕТЕРІВ ТА 4-АМІНОБЕНЗОЙНОЇ КИСЛОТИ

4-Амінобензойна кислота (ПАБК) була віднесена до вітамінів в 1940 р. після того, як Вудс і Фильдс установили, що вона необхідна для розвитку багатьох мікроорганізмів і що дія сульфаніламідних препаратів придушується малими кількостями 4-амінобензойної кислоти, інгібіторами яких вони є.

4-Амінобензойна кислота (вітамін Н) необхідна для біосинтезу деяких вітамінів групи фоліевої кислоти, до складу молекули яких вона входить. До таким вітамінам, наприклад, ставиться птероілглутамінова кислота.

Як речовина, що містить аміногрупу й карбоксил, ПАБК володіє амфотерними властивостями, будучи одночасною й слабкою кислотою й слабкою підставою; водяний розчин при 25° має pH 3,79. Для неї характерні всі хімічні властивості ароматичних з'єднань, пов'язані з її функціональними групами.

4-Амінобензойная кислота утворить численні похідні як по аміногрупі, так і по карбоксильної групі; багато хто із цих похідних мають коштовні лікувальні властивості. Етиловий естер 4-амінобензойної кислоти (анестезин) і метиловий ефір 4-амінобензойної кислоти володіють дуже слабкої (0,01-0,06%) вітамінної активністю вільної кислоти. У той же час діетиламіноетиловий естер 4-амінобензойної кислоти (новокаїн) має активність вільної кислоти. Це порозумівається його легким гідролізом в організмі з утворенням вільного вітаміну.

4-Амінобензойна кислота каталізує біохімічні реакції, пов'язані з синтезом різних з'єднань, шляхом введення в їхню молекулу одновуглецевого з'єднання типу мурашиної кислоти. Прикладом такий реакції служить біосинтез гіпоксантіну.

Метою роботи було визначення можливості синтезу кристалічних молекулярних комплексів краун-етерів з 4-амінобензойною кислотою і виявлення особливостей у взаємодіях цих партнерів комплексоутворення.

Встановлено, що при мимовільному випарі розчинників з розчинів азакраун-етерів – аза-12-краун-4, діаза-12-краун-4, тетрааза-12-краун-4

гексаметілтетрааза-14-краун-4, аза-18-краун-6 та піперидину з 4-амінобензойною кислотою (ПАБК) утворяться кристалічні молекулярні комплекси.

Описані взаємодії можуть бути враховані як складова частина при моделюванні молекулярних взаємодій лікарських молекул.

На рисунках 1.1 – 1.6 приводимо структури комплексів азакраун-етерів з ПАБК.

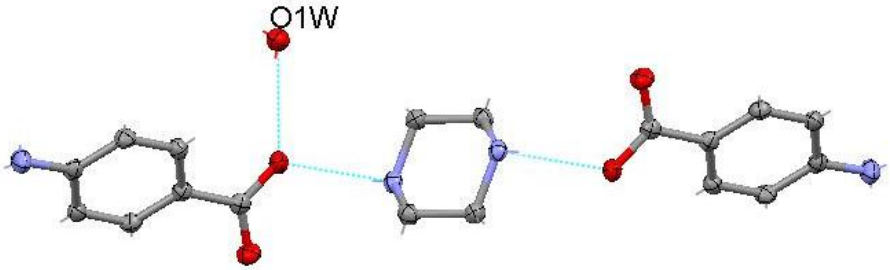

Рисунок 1.1 Структура комплексу піперидину з ПАБК

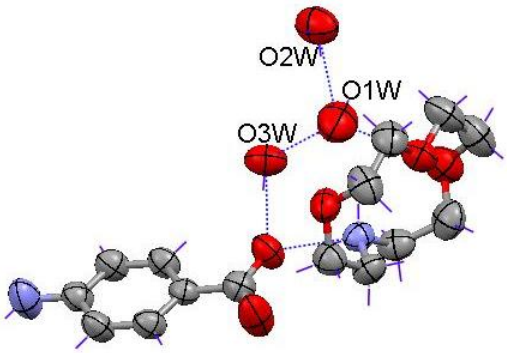

Рисунок 1.2 Структура комплексу аза-12-краун-4 з ПАБК

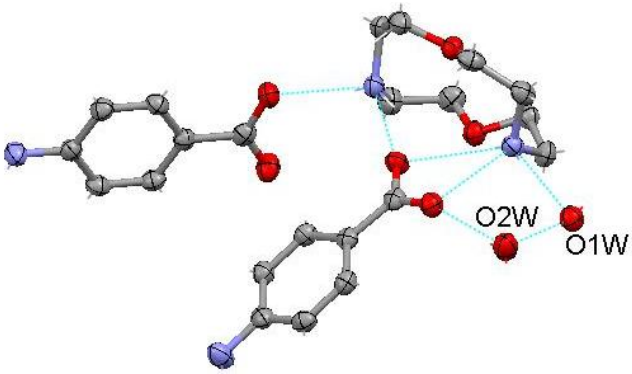

Рисунок 1.3 Структура комплексу діаза-12-краун-4 з ПАБК

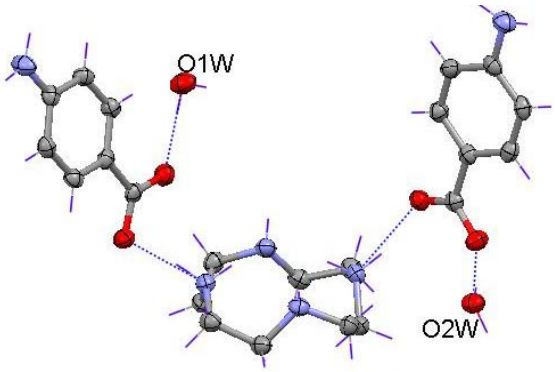

Рисунок 1.4 Структура комплексу тетрааза-12-краун-4 (Cyclen) з ПАБК

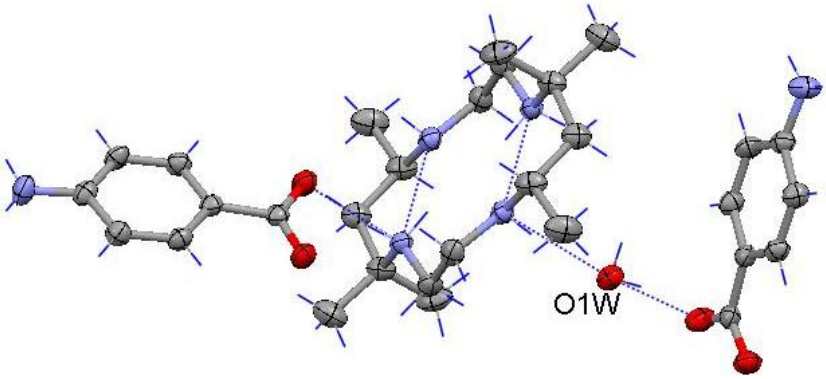

Рисунок 1.5 Структура комплексу гексаметілтетрааза-14-краун-4 (tet B) з ПАБК

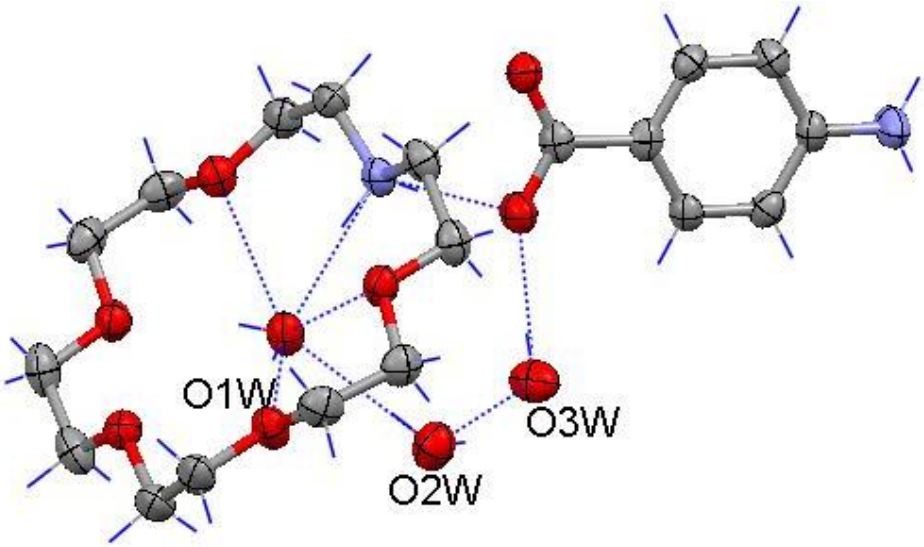

Рисунок 1.6 Структура комплексу аза-18-краун-6 з ПАБК

Компонент комплексу піперидин (Рисунок 1.1) вже використовується у фармакопеї. Тому отримані сполуки можуть представляти інтерес для подальших досліджень з боку біохіміків.

2 КОМПЛЕКСИ КРАУН-ЕТЕРІВ ТА 2-ОКСІБЕНЗОЙНОЇ (САЛІЦИЛОВОЇ) КИСЛОТИ

2-оксібензойна (саліцилова) кислота широко використається у фармацевтичній практиці.

Метою роботи було визначення можливості синтезу кристалічних молекулярних комплексів краун-етерів з саліциловою кислотою і виявлення особливостей у взаємодіях цих партнерів комплексоутворення.

Встановлено, що при мимовільному випарі розчинників з розчинів азакраун-етерів – аза-12-краун-4, аза-18-краун-8, бензо-аза-15-краун-5, гексаметілтетрааза-14-краун-4, з саліциловою кислотою утворюються кристалічні молекулярні комплекси.

Описані взаємодії можуть бути враховані як складова частина при моделюванні молекулярних взаємодій лікарських молекул.

На рисунках 2.1 – 2.4 приводимо структури комплексів азакраун-етерів з саліциловою кислотою

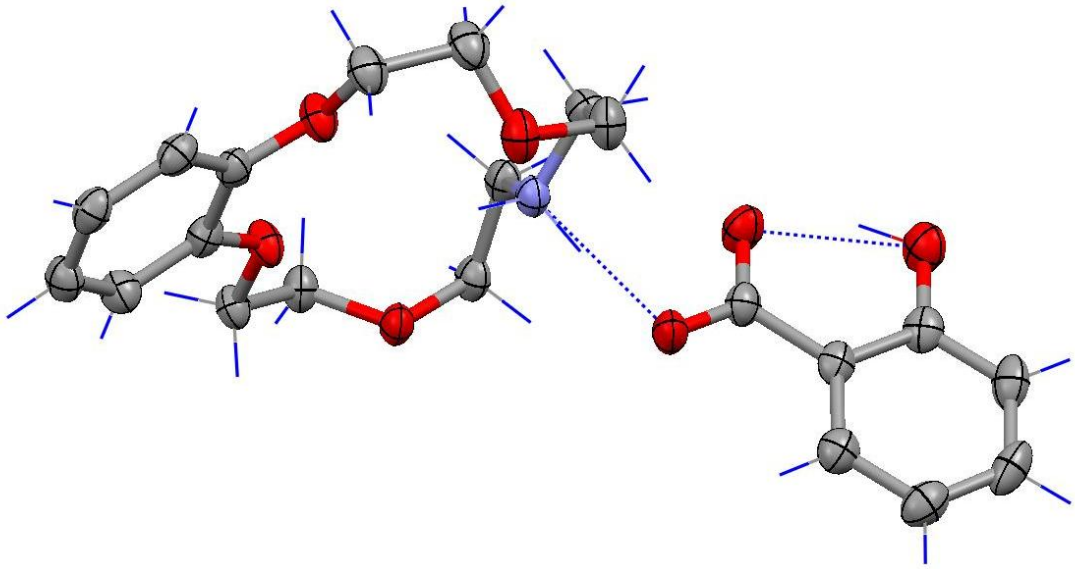

Рисунок 2.1 – Структура комплексу бензо-аза-15-краун-5 з саліциловою кислотою

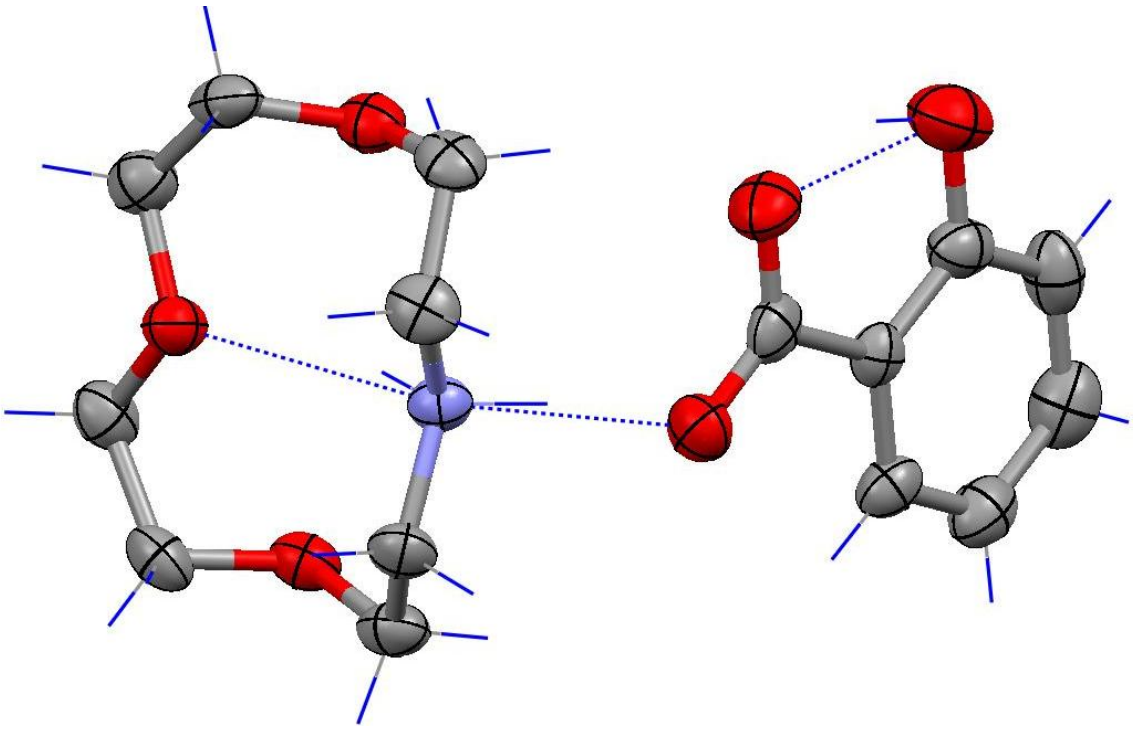

Рисунок 2.2 – Структура комплексу аза-12-краун-4 з саліциловою кислотою

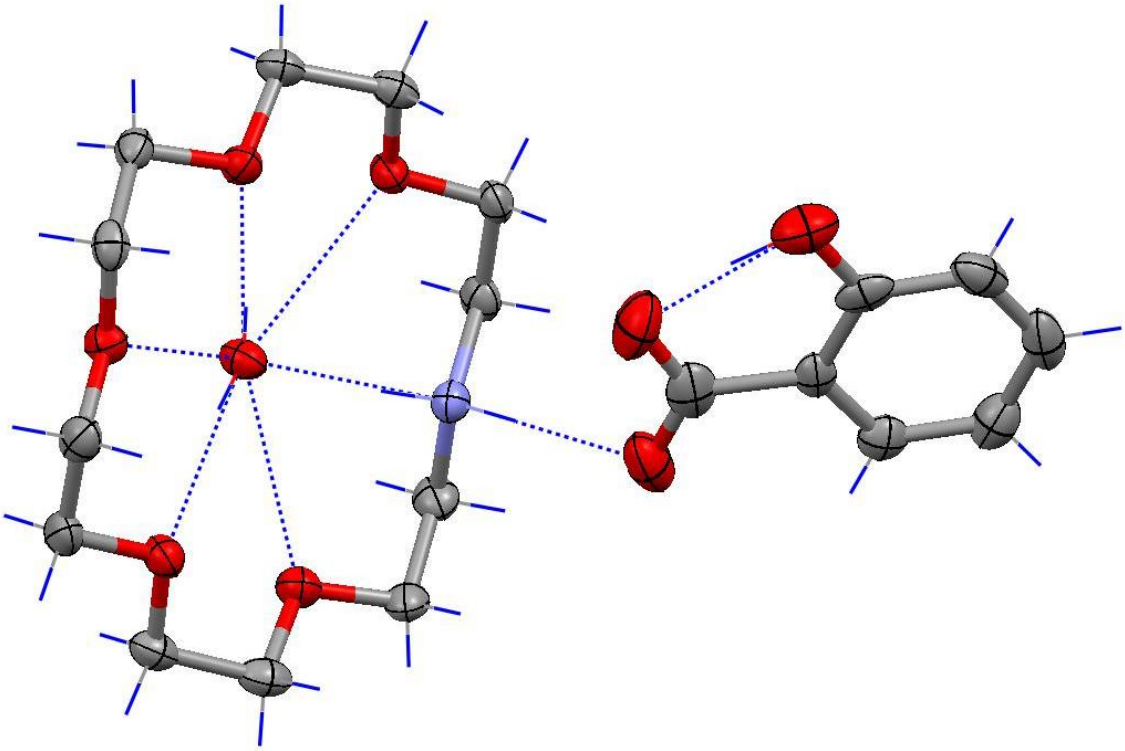

Рисунок 2.3 – Структура комплексу аза-18-краун-6 з саліциловою кислотою

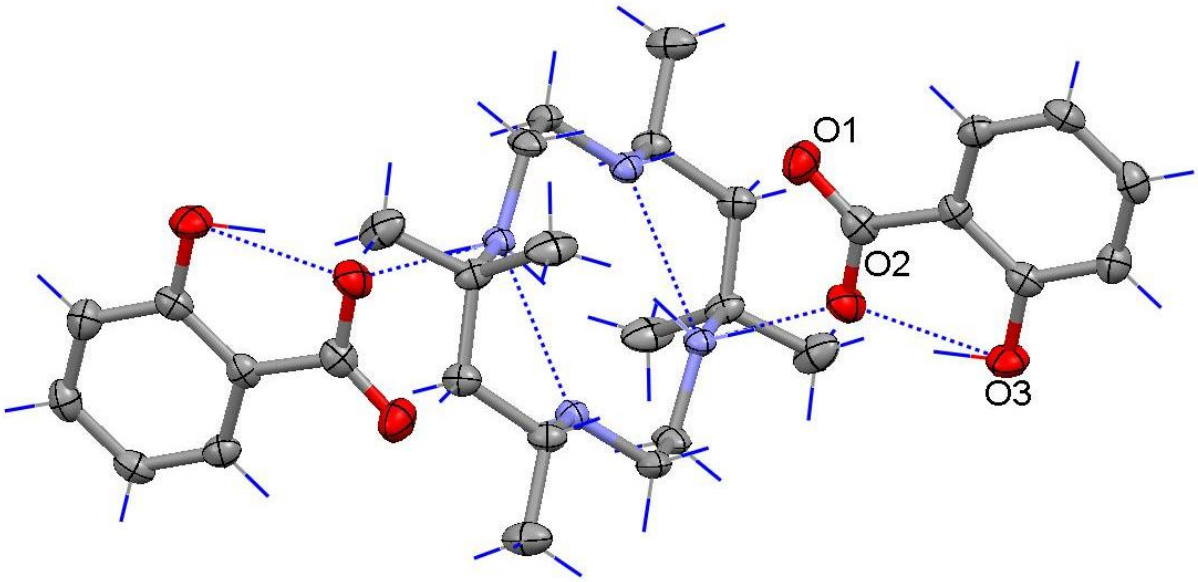

Рисунок 2.4 – Структура комплексу гексаметілтетрааза-14-краун-4 (tet B) з саліциловою кислотою

Пірерідин – 6 членний гетероцикл, широко використовуваний як базовий фрагмент у синтезі лікарських засобів.

Ціль синтезу – визначення можливості отримання кристалічних молекулярних комплексів на основі пірерідину та саліцилової кислоти.

На рисунку 2.5 приводимо структуру комплексу пірерідину з саліциловою кислотою.

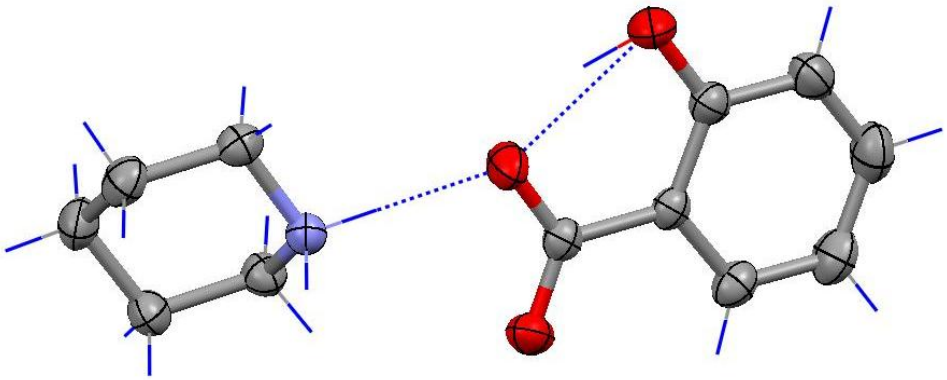

Рисунок 2.5 – Структура комплексу пірерідину та саліцилової кислоти

Виходячи з літературних джерел, цей продукт буде мати більшу хімічну стабільність та кращу засвоюваність.

3 КОМПЛЕКСИ АЗАКРАУН-ЕТЕРІВ, ПІПЕРАЗИНУ Й 2-АМІНО-2-(ГІДРОКСІМЕТІЛ)ПРОПАН-1,3-ДИОЛУ З МЕФЕНАМОВОЮ КИСЛОТОЮ

Мефенамова кислота є похідним антранілової кислоти, що має елементи структурної подібності із саліциловою кислотою і її похідними, застосовуваними як протизапальні засоби. Вона має аналгезивну, жарознижуючу й протизапальну активність, причому як протизапальний засіб перевершує по активності саліцилати. По аналгезивній активності мефенамова кислота рівноцінна бутадіону й перевершує саліцилати, а по жарознижуючій дії дорівнює цим препаратам.

По механізму дії мефенамова кислота близька до іншим нестероїдним протизапальним речовинам. По здатності гнітити біосинтез простагландінов займає проміжне місце між бутадіоном й індометаціном.

Застосовують мефенамову кислоту при ревматизмі, неспецифічному інфекційному поліартриті, артралгіях і м'язових болях, невралгіях, при головному й зубному болі, як жарознижуюче при різних гарячкових станах.

Недоліком кислоти, що обмежує її використання як лікарський засіб, є невисока розчинність у воді. Ефективним способом підвищення розчинності може з'явитися синтез розчинних сольових комплексів мефенамової кислоті з амінами.

Ціль роботи – визначення можливості синтезу кристалічних молекулярних комплексів на базі мефенамової кислоти та азакраун-етерів, а також піперазину і 2-аміно-2-(гідроксіметіл)пропан-1,3-диолу. Не виключено, що цільові продукти будуть мати більшу хімічну стабільність та кращу біологічну засвоюваність.

Взаємодією зазначених компонентів отримано кристалічні молекулярні комплекси.

На рисунках 3.1 – 3.4 приводимо структури комплексів мефенамової кислоти з аміносполуками.

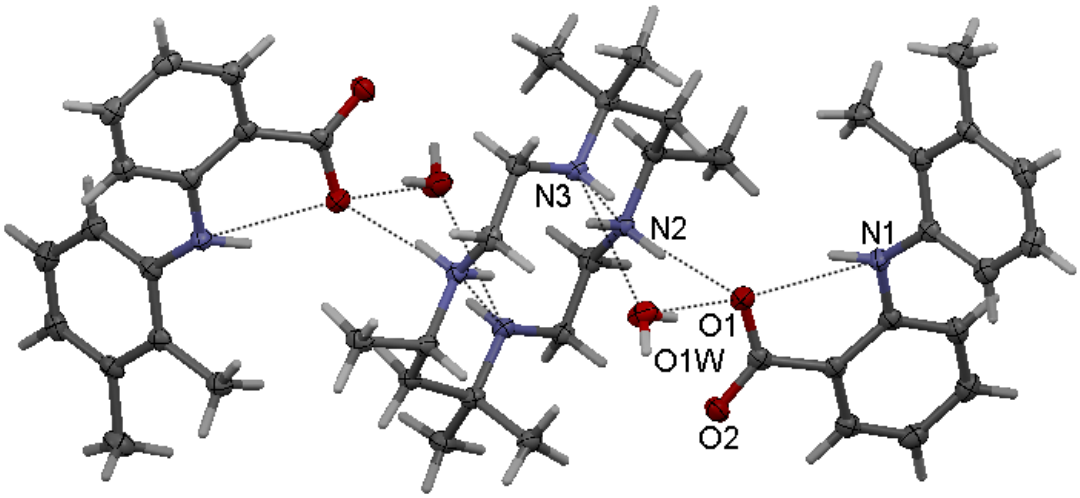

Рисунок 3.1 – Структура комплексу мефенамової кислоти з tet B

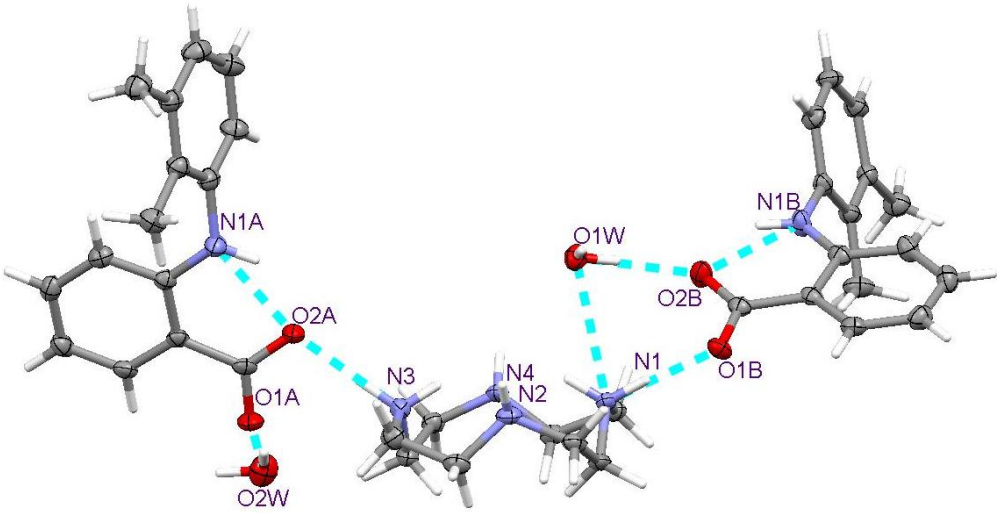

Рисунок 3.2 – Структура комплексу мефенамової кислоти з цікленом

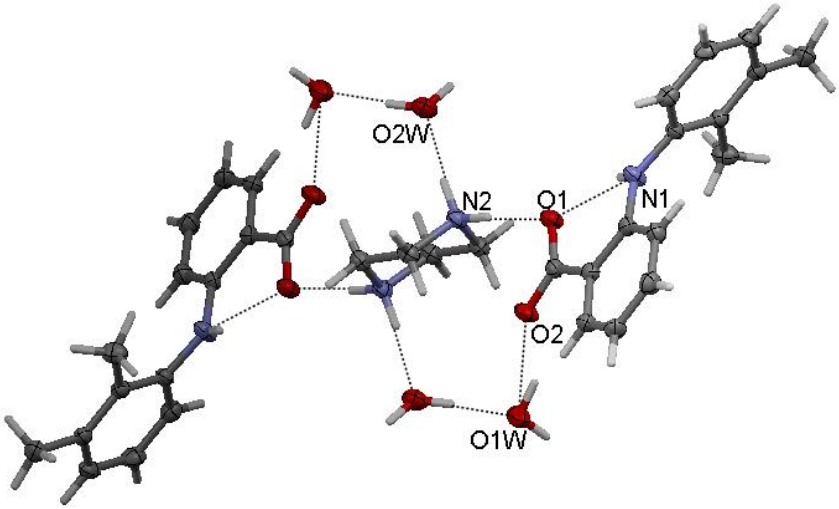

Рисунок 3.3 – Структура комплексу мефенамової кислоти з піперазином

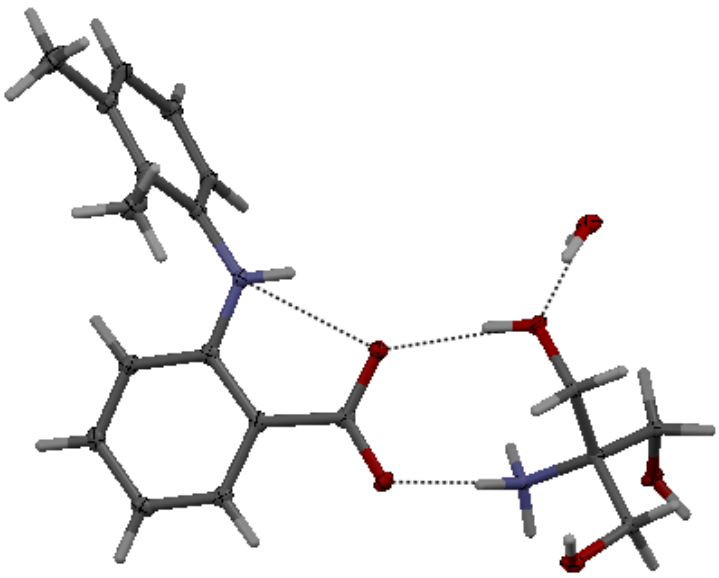

Рисунок 3.4 – Структура комплексу мефенамової кислоти з 2-аміно-2-(гідроксіметіл)пропан-1,3-диолом

Компоненти комплексів, таки як: піперазин і 2-аміно-2-(гідроксиметіл)пропан-1,3-диол вже використовуються у фармакопеї. Тому отримані сполуки можуть представляти інтерес для подальших досліджень з боку біохіміків.

4 КОМПЛЕКСНА СПОЛУКА – ПИРАНТЕЛ ПАМОАТ

Пирантел памоат – комплексна сіль 1, 4, 5, 6-Тетрагідро-1-метил-2-[транс-2-(2-тіеніл)-вініл]-пірімідину з 3-оксі-2-нафтоатойною кислотою.

У зв'язку з високою ефективністю й низькою токсичністю його широко застосовують при лікуванні энтеробіозу в дітей.

Ціль роботи – визначення можливості синтезу моно-кристалічних комплексів пирантел памоату. Рентгеноструктурний опис будови цієї сполуки відсутній.

Встановлено, що при мимовільному випарі розчинників з розчинів 1, 4, 5, 6-Тетрагідро-1-метил-2-[транс-2-(2-тіеніл)-вініл]-пірімідину з 3-оксі-2-нафтоатойною кислотою утворюються моно-кристали комплексу.

На рисунку 4.1 приводимо структуру пирантел памоату.

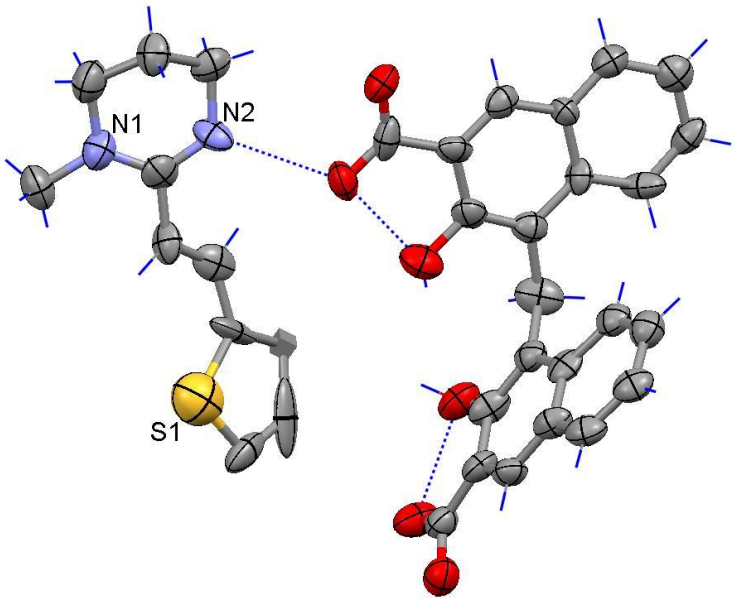

Рисунок 4.1 – Структура комплексу пирантел памоату

5 КОМПЛЕКСИ ІЗОНІАЗИДУ ТА ОРГАНІЧНИХ ДІКАРБОНОВИХ КИСЛОТ

Ізоніазид (isoniazidum) – гідразид ізонікотинової кислоти. Є основним представником похідних ізонікотинової кислоти, що знайшли застосування як протитуберкульозні засоби. Інші препарати цієї групи (фтивазид, етіонамід й ін.) можуть розглядатися як похідні гідразида ізонікотинової кислоти. Ізоніазид має високу бактеріологічну активність відносно мікобактерій туберкульозу. Дія обумовлена здатністю ізоніазиду блокувати активність ферментів, що беруть участь у біосинтезі коллагена.

Ціль роботи – визначення можливості синтезу кристалічних молекулярних комплексів на основі ізоніазиду та органічних дікарбонових кислот. Можливо, що цільові продукти будуть мати більшу хімічну стабільність, кращу засвоюваність, мати менші побічні ефекти.

Встановлено, що при мимовільному випарі розчинників з розчинів ізоніазиду із рядом нетоксичних органічних дікарбонових кислот утворюються кристалічні молекулярні комплекси.

На рисунку 5.1 – 5.3 приводимо структури комплексів ізоніазиду та органічних дікарбонових кислот.

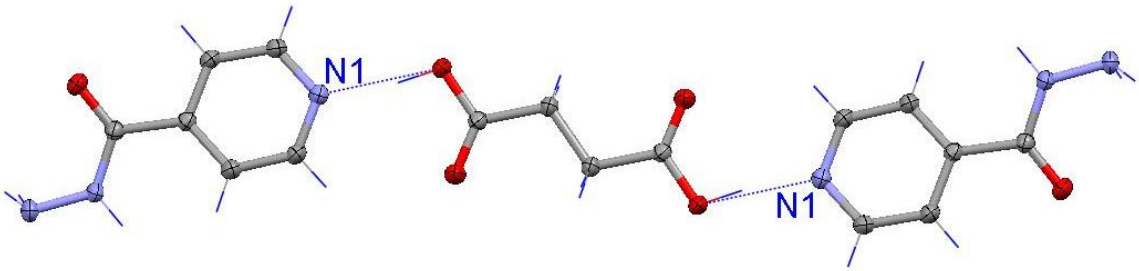

Рисунок 5.1 Структура комплексу ізоніазиду та бурштинової кислоти

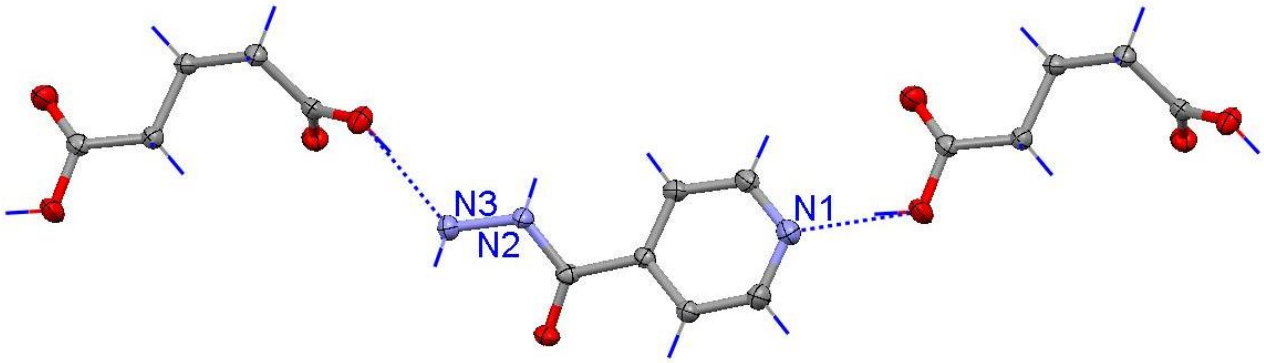

Рисунок 5.2 Структура комплекса ізоніазиду та глутарової кислоти

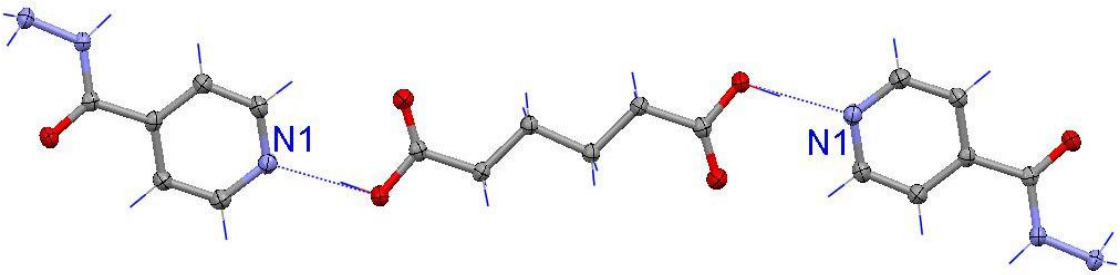

Рисунок 5.3 Структура комплекса ізоніазиду та адипинової кислоти

Такі компоненти комплексів, як перелічені кислоти, вже використовуються у фармакопеї. Тому отримані сполуки можуть представляти інтерес для подальших досліджень з боку біохіміків.

6 СУПРАМОЛЕКУЛЯРНІ КОМПЛЕКСИ 2,4-ДІТІОУРАЦИЛУ З КРАУН-ЕТЕРАМИ

Відомо що 2,4-дітіоурацил існує у 6 таутомерних формах (Рисунок 6.1). Структурні відомості щодо фіксації тій чи іншій форми 2,4-дітіоурацилу у супрамолукуярні або інші комплекси відсутні.

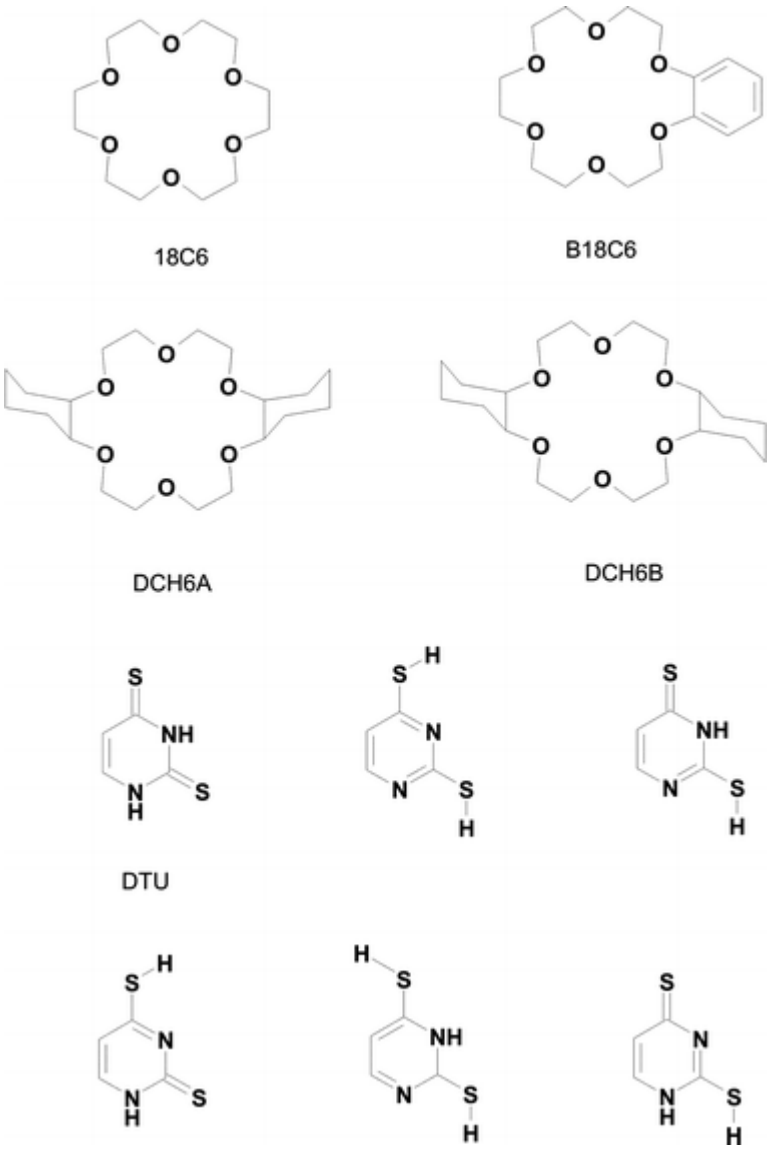

Рисунок 6.1 – Таутомерні форми 2,4-дітіоурацилу та використані краун-етері

Доведено, що краун-етери селективно зв'язують у комплекси лише одну таутомерну форму 2,4-дітіоурацилу – DTU, першу (Рисунок 6.2-6.5).

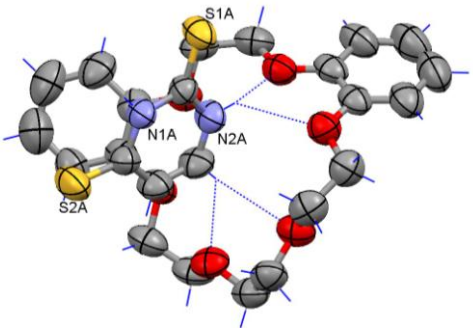

Рисунок 6.2 – Структура комплексу 2,4-дітіоурацилу з бензо-18-краун-6

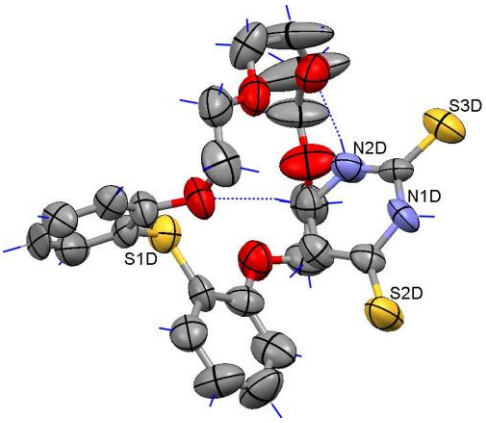

Рисунок 6.3 – Структура комплексу 2,4-дітіоурацилу з дібензо-15-краун-5

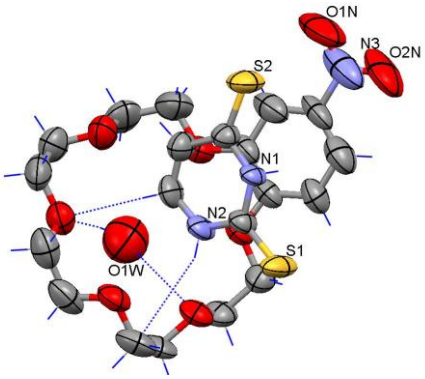

Рисунок 6.4 – Структура комплексу 2,4-дітіоурацилу з 4-нітробензо-18-краун-6

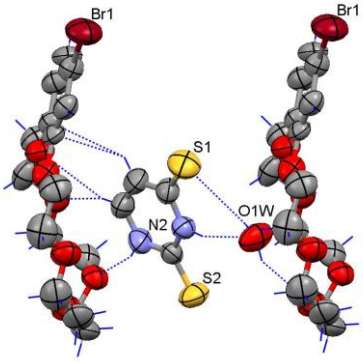

Рисунок 6.5 – Структура комплексу 2,4-дітіоурацилу з 4-бромбензо-18-краун-6

7 КОМПЛЕКСИ КРАУН-ЕТЕРІВ З ЕТІОН- Й ПРОТІОНАМІДОМ

ЕТІОНАМІД (ethionamidum) – тіоамід етилізонікотинової кислоти, або 2-етил-4-тіокарбамоіл-4-піридін. За структурою й антибактеріальними властивостями близький до ізоніазиду, але менш активний, разом з тим діє на стійкі до ізоніазиду штами мікобактерій. Протитуберкульозний препарат. Етіонамід застосовують також для лікування лепри.

ПРОТІОНАМІД (Protionamidum) – тіоамід пропілізонікотинової кислоти, або 2- пропіл-4-тіокарбамоіл-4-піридін.

Хімічно близький до етіонаміду, відрізняється лише заміною етільного радикала у положенні 2 на пропільний. По протитуберкульозній активності істотно не відрізняється від етіонаміду, але краще переноситься. Може застосовуватися в комбінації з ізоніазідом й іншими протитуберкульозними препаратами. Протіонамід рекомендується при поганий переносності етіонаміду.

Ціль роботи – визначення можливості синтезу кристалічних молекулярних комплексів на основі протіонаміду, етіонаміду, краун-етерів та нетоксичних органічних кислот. Цільові продукти будуть мати більшу хімічну стабільність та кращу засвоюваність.

Взаємодією зазначених компонентів отримано кристалічні супрамолекулярні комплекси (Рисунок 7.1 – 7.7).

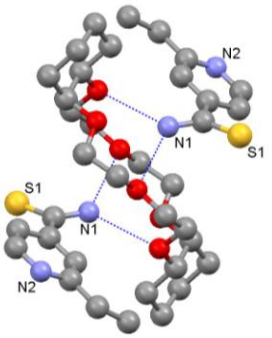

Рисунок 7.1 Структура комплексу етіонаміду та 18-краун-6

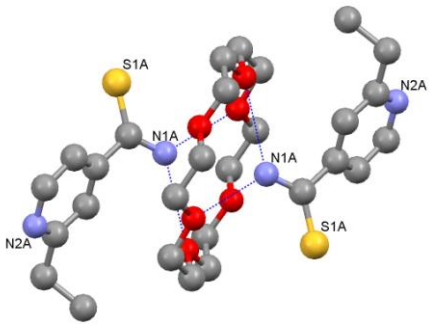

Рисунок 7.2 Структура комплексу етіонаміду та діциклогексано-18-краун-6

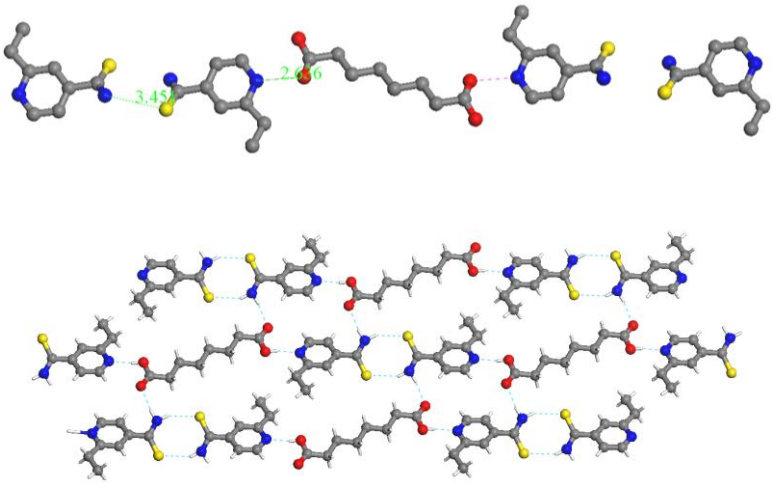

Рисунок 7.3 Структура комплексу етіонаміду та коркової кислоти

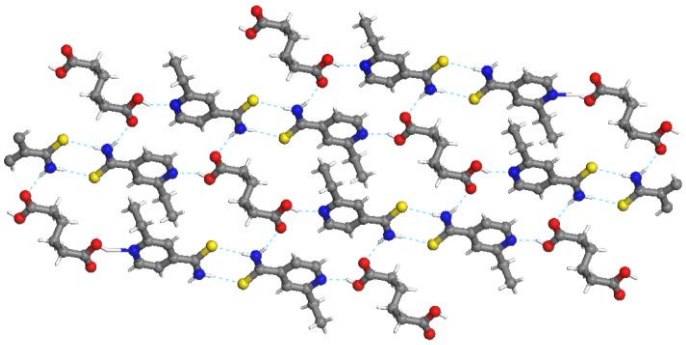

Рисунок 7.4 Структура комплексу етіонаміду та адіпінової кислоти

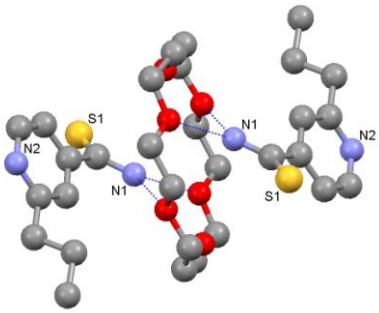

Рисунок 7.5 Структура комплексу протіонаміду та 18-краун-6

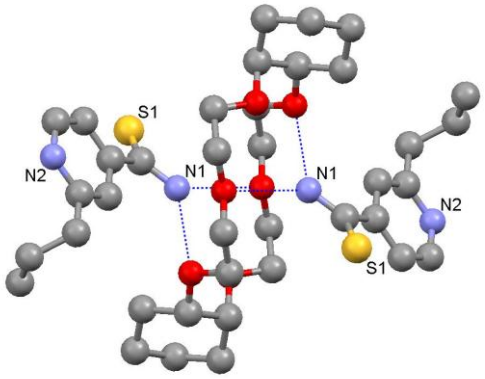

Рисунок 7.6 Структура комплексу протіонаміду та діциклогексано-18-краун-6

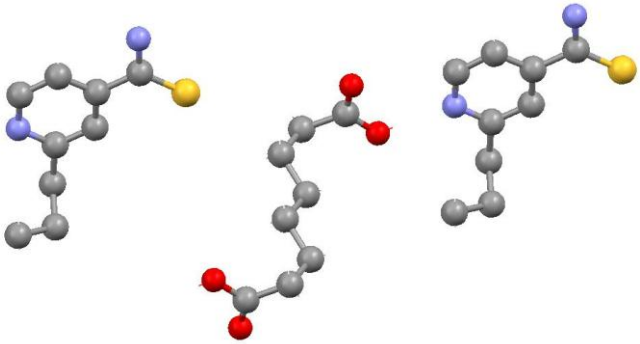

Рисунок 7.7 Структура комплексу протіонаміду та коркової кислоти

Компонент комплексу - адіпінова кислота (Рисунок 3.4) вже використовується у фармакопеї. Тому отримані сполуки можуть становити інтерес для подальших досліджень з боку біохіміків.

8 СЕЛЕКТИВНА ВЗАЄМОДІЯ МОЛЕКУЛ "ХАЗЯЇНІВ": КРАУН- ЕТЕРІВ З ПОХІДНИМИ ТРИФЕНІЛМЕТАНУ

Пошук селективних взаємодій нейтральних молекул, що приводять до утворення молекулярних комплексів моделюючих широко розповсюджені процеси в біологічних системах є одна з пріоритетних задач хімії "гість-хазяїн". Вичерпним керівництвом [Comprehensive supramolecular chemistry / Editors J-M. Lehn, J.L. Atwood, J.E.D. Davies, D.D. MacNicol, F. Wogtle. Oxford – New York –

Tokyo: Pergamon, 1996, Vol. 1-11.] як краун-етери, так і похідні трифенілметану віднесені до молекул "хазяїв", здатним зв'язувати менші по розмірі "гостьові" молекули у комплекси.

Ціль роботи – визначення можливості синтезу кристалічних молекулярних комплексів краун-етерів з похідними трифенілметану і виявлення селективності у взаємодіях цих партнерів комплексоутворення.

Встановлено, що при мимовільному випарі розчинників з розчинів малого "коронанду" – 1,4,7,10-тетраоксациклододекану (12с4) із трифенілметанолом (Іа), 1,1,1-трифенілметіламіном (Іб) і трифенилметантіолом (Ів) утворяться кристалічні молекулярні комплекси – [12с4·2$(C_6H_5)_3COH$] - (III), [12с4·2$(C_6H_5)_3CNH_2$] - (IV), [12с4·2 $(C_6H_5)_3CSH$] - (V) відповідно.

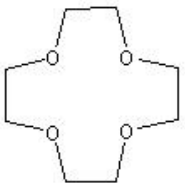

12к4

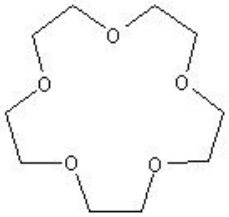

15к5

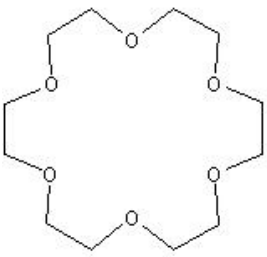

18к6

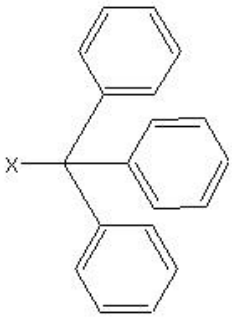

I а-в

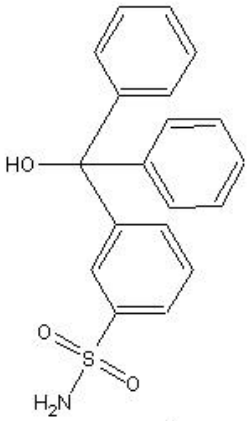

II

Виявлено також, що в цих же умовах при використанні суміші краун-етерів: 12с4, 15с5 та18с6 похідні трифенілметану (Іа,б) селективно утворять кристалічні комплекси лише з 12с4 - (III, IV). Введення в ароматичну частину молекули трифенілметанолу Н-донорної сульфамідної групи істотно змінює результат комплексоутворення. Так при взаємодії 3-(гидроксидифенілметіл)

бензол сульфаміду (II) з названою сумішшю краун-етерів селективне виділяється кристалічний комплекс складу [18к6 · 2 *m*-$H_2NSO_2C_6H_4(C_6H_5)_2COH$] – (VI). Раніше у взаємодії нейтральних молекул з перерахованими краун-етерами селективності відзначено не було. Навпроти, N-(фенілсульфоніл)бензол сульфамід $HN(SO_2C_6H_5)_2$ дає кристалічні молекулярні комплекси як з 12с4, так і з 18с6.

Як приклад, на рисунку 8.1 приводимо структуру комплексу [18к6 · 2 *m*-$H_2NSO_2C_6H_4(C_6H_5)_2COH$] – (VI):

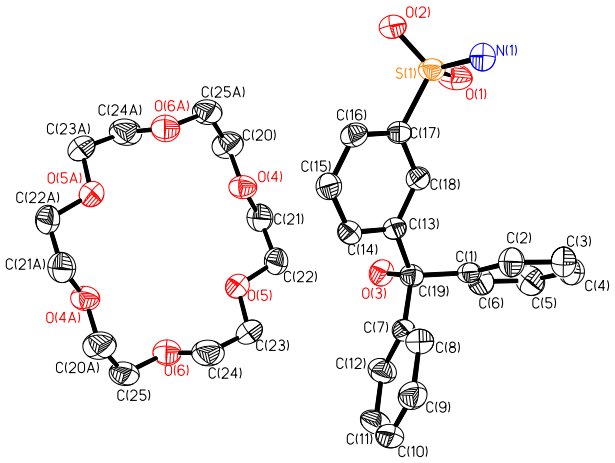

Рисунок 8.1 Структура [18к6 · 2 *m*-$H_2NSO_2C_6H_4(C_6H_5)_2COH$] – (VI)

Таким чином, вперше описані селективні взаємодії краун-етерів з об'ємними похідними трифенілметану кристалічних молекулярних комплексів, що приводять до утворення, (III, IV, VI) і що може бути враховане як складова частина при моделюванні молекулярних взаємодій порівняно великих природних молекул, а також з'явитися хімічною основою поділу сумішей краун-етерів.

9 КОМПЛЕКСИ АЗАКРАУН-ЕТЕРІВ ТА СУЛЬФАНІЛАМІДНИХ ПРЕПАРАТІВ

Сульфаніламідні препарати широко використаються у фармацевтичній практиці як бактерицидні засобі широкої дії.

Метою роботи було визначення можливості синтезу кристалічних молекулярних комплексів азакраун-етерів та сульфаніламідних препаратів і виявлення особливостей у взаємодіях цих партнерів комплексоутворення.

Встановлено, що при мимовільному випарі розчинників з розчинів азакраун-етерів – 5,7,7,12,12,14-гексаметіл-1,4,8,11-тетраазациклотетрадекану (tet B) та 1,4,7,10-тетраазацилододекан (Cyclen) з рядом сульфаніламідних препаратів: етазол, сульфамонометоксин, норсульфазол, сульфален та сульфадимезин, за рахунок міжмолекулярних водневих зв’язків, утворюються кристалічні молекулярні комплекси.

Описані взаємодії можуть бути враховані як складова частина при моделюванні молекулярних взаємодій лікарських молекул.

На рисунках 9.1 – 9.6 приводимо структури комплексів азакраун-етерів з сульфаніламідними препаратами.

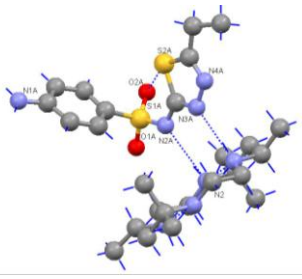

Рисунок 9.1 – Структура комплексу tet B з етазолом

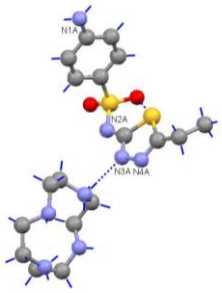

Рисунок 9.2 – Структура комплексу Cyclen з етазолом

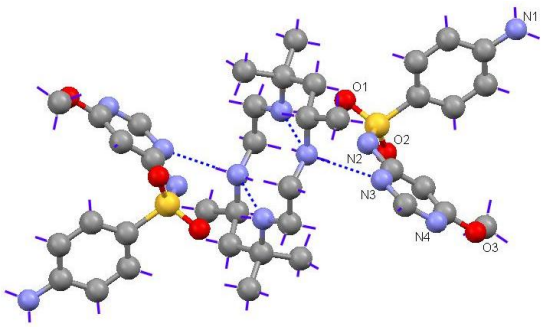

Рисунок 9.3 – Структура комплексу tet B з сульфамонометоксином

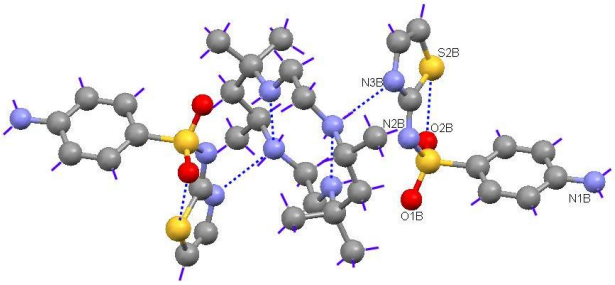

Рисунок 9.4 – Структура комплексу tet B з норсульфазолом

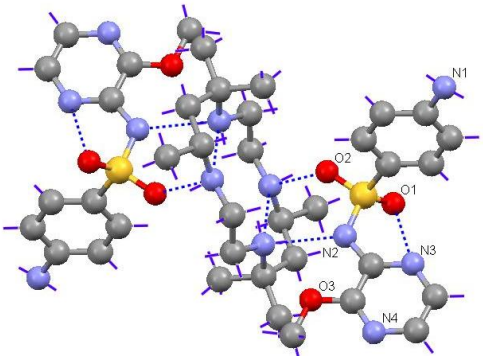

Рисунок 9.5 – Структура комплексу tet B з сульфаленом

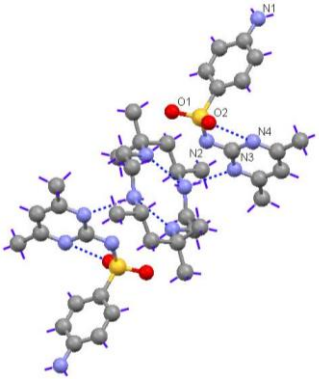

Рисунок 9.6 – Структура комплексу tet B з сульфадимезином

Під час роботи також знайдені умови синтезу нових комплексів саліцилової кислоти з нетоксичними азот-вмістніми гетероциклами, використовуваними у фармакології.

10 КОМПЛЕКСИ ПІПЕРИДИНУ І ПІПЕРАЗИНУ ТА СУЛЬФАНІЛАМІДНИХ ПРЕПАРАТІВ

Піперидин і піперазин широко використовуються у фармакологи як складова частина при приготуванні розчинних лікарських засобів у зв’язку з їх досить низькою токсичністю.

Ціль роботи – визначення умов синтезу монокристалічних комплексів піперидину і піперазину та сульфаніламідних препаратів. Рентгеноструктурний аналіз будови оцих сполук.

Встановлено, що при мимовільному випарі розчинників з розчинів піперидину і піперазину з рядом сульфаніламідних препаратів: норсульфазол, сульфадиметоксин та сульфадимезин, за рахунок міжмолекулярних водневих зв'язків, утворюються кристалічні молекулярні комплекси.

На рисунках 10.1 – 10.5 приводимо структури комплексів піперидину і піперазину з сульфаніламідними препаратами.

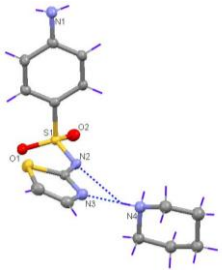

Рисунок 10.1 – Структура комплексу піперидину з норсульфазолом

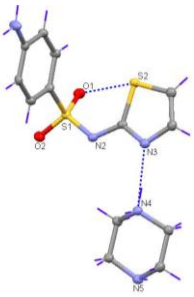

Рисунок 10.2 – Структура комплексу піперазину з норсульфазолом

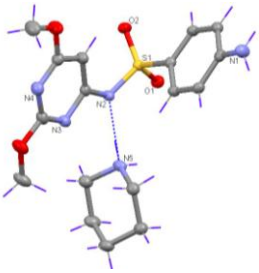

Рисунок 10.3 – Структура комплексу піперидину з сульфадиметоксином

Враховуючи ти обставини, що компоненти комплексів вже використовуються у фармакопеї, отримані сполуки можуть мати інтерес для подальших досліджень з боку біохіміків.

11 КОМПЛЕКСИ КРЕМНЕФЛУОРОВОДНІЙ КИСЛОТИ З ПОХІДНИМИ ПІРИДИНУ ТА КРАУН-ЕТЕРАМИ

Відомо, що архітектура яка реалізується у структурах "онієвих" гексафлуоросілікатів та міжіонні Н-зв'язки в помітному ступені визначають особливості геометрії й фізико-хімічне поводження солей. Робота продовжує початі раніше дослідження про вплив Н-зв'язків на будову й властивості гексафлуоросілікатів ариламонію й присвячена вивченню кристалічної структури гексафлуоросілікатів з похідними піридину та краун-етерами.

Взаємодією зазначених компонентів отримано кристалічні молекулярні комплекси (рисунки 11.1 – 11.10).

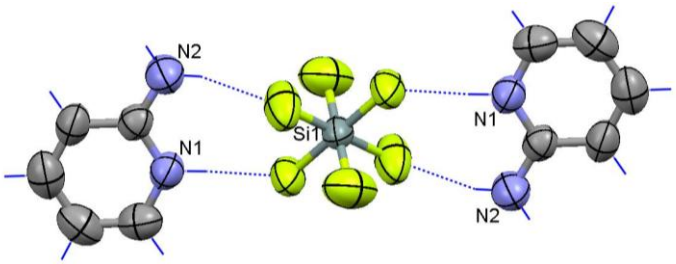

Рисунок 11.1 – Структура гексафлуоросілікату 2-амінопіридинію

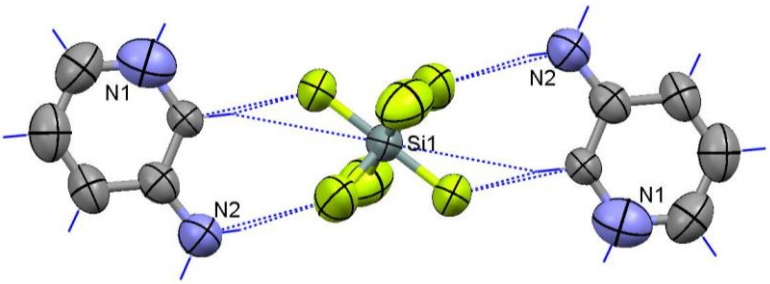

Рисунок 11.2 – Структура гексафлуоросілікату 3-амінопіридинію

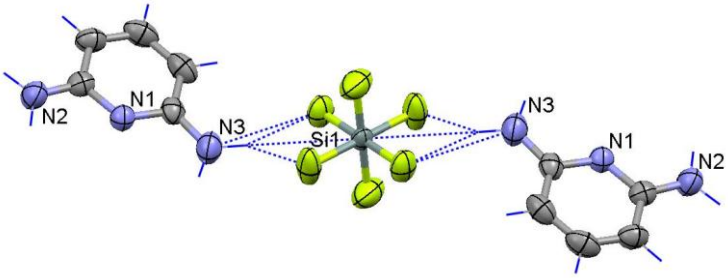

Рисунок 11.3 – Структура гексафлуоросілікату 2,6-діамінопіридинію

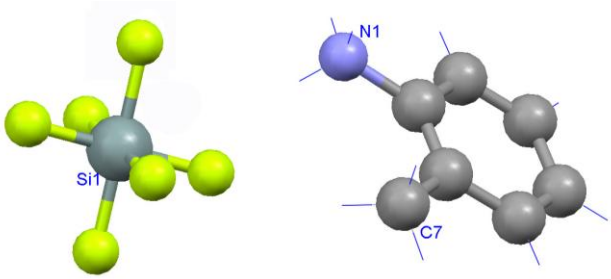

Рисунок 11.4 Структура гексафлуоросілікату 2-толуідинію

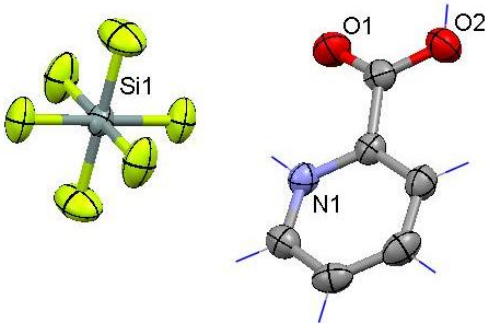

Рисунок 11.5 Структура гексафлуоросілікату 2-піридинкарбонію

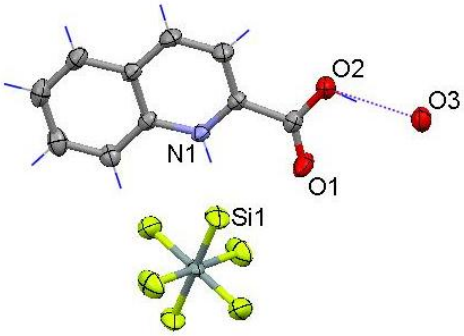

Рисунок 11.6 Структура гексафлуоросілікату 2-толуідінію

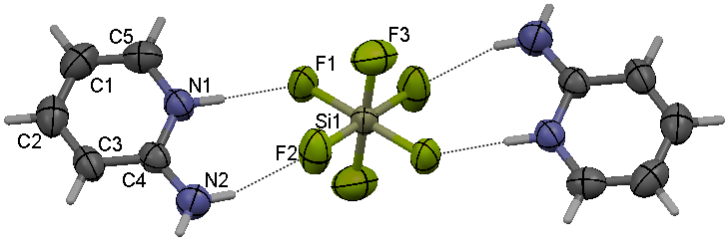

Рисунок 11.7 – Структура гексафлуоросілікату 2-амінопіридинію

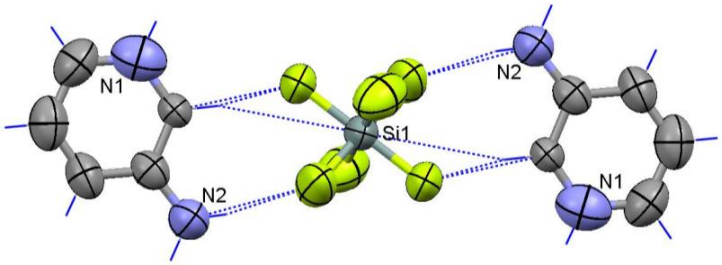

Рисунок 11.8 – Структура гексафлуоросілікату 3-амінопіридинію

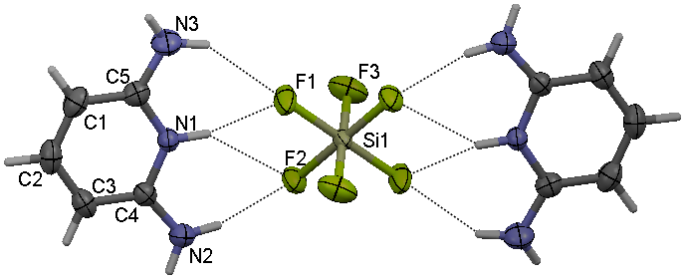

Рисунок 11.9 – Структура гексафлуоросілікату 2,6-діамінопіридинію

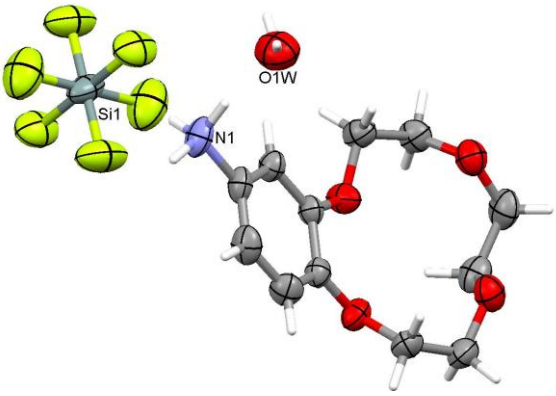

Рисунок 11.9 Структура комплексу кремнефлуороводній кислоти з 4-амінобензо-12-краун-4

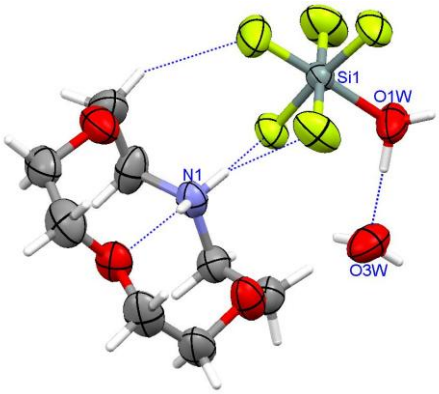

Рисунок 11.10 Структура комплексу кремнефлуороводній кислоти із аза-12-краун-4

Сполуки також охарактеризовані методами ІЧ-, мас-спектрометрії, потенціометрії, розчинності; будова установлена методом РСА.

12 СИНТЕЗ І СТРУКТУРИ КОМПЛЕКСІВ КРАУН- І АЗАКРАУН-ЕТЕРОВ ІЗ ФЛУОРМЕТАЛЛАТАМИ ЦИРКОНІЮ, ГАФНІЮ, НІОБІЮ Й ТАНТАЛУ

Тантал і ніобій мають здатність не викликати в живих тканинах запальних процесів, що дозволяє використати їх у медицині. П'яти окис танталу використається для присипання ран з метою прискорення згортання крові й застосовується при опіках. Чисті металеві ніобій і тантал знаходять застосування при виробництві деталей годин, фотоапаратів, оптичних приладів і хірургічних інструментів. Деякі сплави з нікелем, вольфрамом і ренієм є замінниками платини, іридію й золота.

Флуориди. При розчиненні металевих ніобію й танталу, гідратованих або прожарених п'яти окисей у флуороводній кислоті утворяться комплексні флуороводні кислоти. Склад цих кислот залежить від концентрації HF. При надлишку флуороводній кислоти утворяться флуороніобіева $H_2[NbF_7]$ і флуоротанталова H_2 $[TaF_7]$ кислоти. При недоліку флуороводній кислоти комплексний іон $[MeF_7]^{2-}$ переходить в іон $[MeF_6]^{2-}$, а останній у водяних розчинах гидролизуется до оксифторидов $[MeOF_5]$ $^{2-}$, $[MeOF_4]^-$, $[MeOF_6]^{3-}$ або $[Me_2F_5]^{4-}$. Комплексні флуориди є найбільш стійкими сполуками ніобію й танталу, вони знаходять застосування в аналітичній хімії.

Зростаюче застосування ніобію, танталу, цирконію й гафнію, а також їхніх сполук у різних галузях нової техніки, викликало необхідність у всебічному вивченні цих елементів. Флуоридні комплекси цирконію(IV), гафнію(IV), ніобію(V) і танталу (V) є ключовими сполуками в технології витягу, поділи й очищення зазначених металів від домішок. В основі методу лежить процес екстракції або дробової кристалізації флуорокомплексів з кислих водяних розчинів. Необхідним елементом ефективного керування цим процесом є дані про стан флуорокомплексів у розчинах.

З урахуванням однієї з пріоритетних задач супрамолекулярної хімії по виявленню селективних взаємодій і стабілізації краун-етерами малостійких сполук в стабільні кристалічні сполуки включення, метою роботи було

визначення можливості селективної екстракції і синтезу супрамолекулярних комплексів різноманітних азакраун-етерів з гекса- або гепта-флуорокомплексними кислотами ніобію і танталу а також цирконію та гафнію з їх розчинів у флуороводній кислоті.

Встановлено, що при випаровуванні розчинників з розчинів ніобію і танталу а також цирконію та гафнію і різноманітних азакраун-етерів у флуороводній кислоті, селективне утворюються кристалічні супрамолекулярні комплекси з декафлуоро-оксо-ніобатом, декафлуоро-оксо-танталатом, дека-флуороцирконатом й дека-флуорогафніатом відповідно. Структура деяких синтезованих супрамолекулярних комплексів представлена на рисунках 12.1 – 12.4

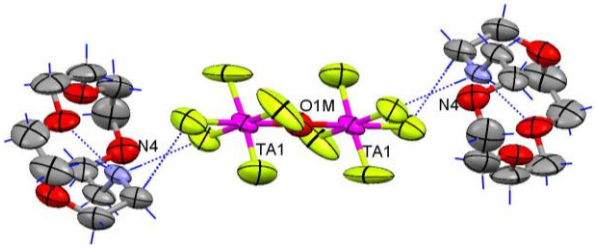

Рисунок 12.1 – Структура комплексу декафлуоро-оксо-танталату з аза-15-краун-5

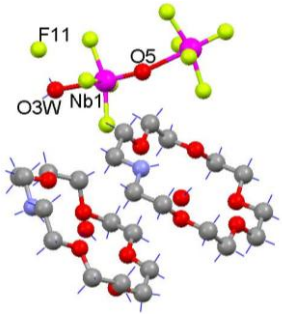

Рисунок 12.2 – Комплекс декафлуоро-оксо-ніобату із аза-18-краун-8

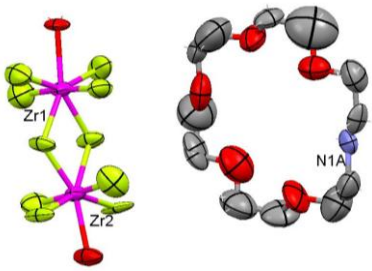

Рисунок 12.3 – Структура комплексу дека-флуороцирконату з аза-18-краун-6

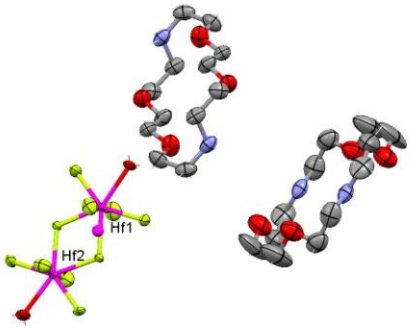

Рисунок 12.4 – Структура комплексу дека-флуорогафніату з діаза-18-краун-6

Одержані кристалічні супрамолекулярні сполуки є прикладом селективної екстракції краун-етером флуорокомплексих кислот ніобію, танталу, цирконію та гафнію з кислотних розчинів; вони стабільні і можуть бути цікавими як контейнери цих кислот. Проведене дослідження показало безумовну перспективність макроциклічних комплексонов для витягу Zr(IV), Hf(IV), Nb(V) і Ta(V) із флуор утримуючих водяних розчинів.

13 ЗАСТОСУВАННЯ МАТЕРІАЛІВ ДОСЛІДЖЕНЬ

Надруковано 27 статей у провідних міжнародних наукових журналах:

1. M.S.Finari, E.V.Ganin, S.-W.Tang, W.-J.Wang,.Yu.A. Simonov // Molecular complexes of thionicotinamide with 18-membered crown ethers: Synthesis and crystal structures //Journal of Molecular Structure (2007) Vol. 826, p. 89–95;

2. B.Moulton, B.S.Luisi, M.S.Fonari, S.S.Basok, E.V.Ganin, V.Ch. Kravtsov // Supramolecular associates of p-aminobenzoic acid with N- and N,O-heterocyclic molecules // New Journal of Chemistry (2007) Vol. 31, No. 4, p. 561-568;

3. В.О.Гельмбольдт, Э.В.Ганин, М.М.Ботошанский, М.С.Фонарь, А.А.Эннан // Кристаллическая структура гексафторосиликата орто-толуидиния // Журнал неорганической химии (2007) Т. 52, № 5, с. 1-5;

4 М.С.Фонарь, О.А.Алексеева, Н.Г.Фурманова, К.А.Лысенко, В.-Д.Ванг, С.-В.Танг, Э.В.Ганин, В.О.Гельмбольдт, Ю.А.Симонов // Кристаллические структуры комплексов цис-син-цис изомера дициклогексано-18-краун-6 с гексафтортанталатом оксония и с гексафторниобатом оксония // Кристаллография (2007) Т.52, № 2, с. 271-276;

5. V.O.Gelmboldt, E.V.Ganin, M.S.Fonari, Yu.A.Simonov, L.V.Koroeva, A.A.Ennan, S.S.Basok, S.Shova, H.Kahlig, V.B.Arion, B.K. Keppler// Two new "onium" fluorosilicates, the products of interaction of fluorosilicic acid with 12-membered macrocycles: structures and spectroscopic properties // Journal Chem. Soc.: Dalton Trans. (2007) p. 2915-2924;

6. V.O.Gelmboldt, E.V.Ganin, K.V. Domasevitch // Hydrogen bonded frameworks of 2-carboxypyridinium hexafluorosilicate and 2-carboxyquinolinium hexafluorosilicate dihydrate // Acta Crystallographica, Section C (2007) C 63, p.o530–o534;

7 M.S.Fonari, Yu.A.Simonov, Wen-Jwu Wang, Shang-Wei Tang, E.V.Ganin, V.O.Gelmboldt, T.S.Chernaya, O.A.Alekseeva, N.G.Furmanova // Structure of oxonium hexafuoroniobate and hexafuorotantalate complexes with crown ethers of diferent dimensionality // Polyhedron (2007) p.2008

8. V. O. Gel'mbol'df, L. Kh. Minacheva, E. V. Ganin, V. S. Sergienko // Crystal Structure of Bis(3-carboxypyridinium) Hexafluorosilicate // Russ. Journal of Inorganic Chem. (2008) Vol.. 53, No. 6, pp. 875-878;

9. M. S. Fonari , Y.A. Simonov, G. Bocelli , E.V. Ganin, Wen-Jwu Wang, S.M. Pluzhnik-Gladyr, V.V. Tkachuk, S.A. Kkotlyar, G.L. Kamalov // Structure of Benzo- and Dibenzocrown Ethers and Their H-Bonded Adducts. 4.§ Structural Motifs in the 2,4-Dithiouracil Complexes with 4-Bromo- and 4-Nitrobenzo-18-crown-6, [2.4]Dibenzo- and Thia[1.5]dibenzo-18-crown-6 // Journal of Inclusion Phenomena (2008) Vol. 61, pp. 367-375;

10. N. G. Furmanova, M. Kh. Rabadanov, T. S. Chernaya, M. S. Fonari;, Yu. A. Simonov, E. V. Ganin, V. O. Gelmboldt', R. Ya. Grigorash', S. A. Kotlyar, G. L. Kamalov // Crystal Structures of Dioxonium Hexafluorotantalate and Dioxonium Hexafluoroniobate Complexes with Tetrabenzo-30-Crown-10 // Crystallography Reports (2008) Vol. 53, No. 2, pp. 246-252;

11 .M.S. Fonari, E.V. Ganin, V.O. Gelmboldt, S.S. Basok, B.S. Luisi, B.Moulton // Binding of fluoro-containing anions to hexaazamacrocyclic ligand: competitive interactions of fluoride and tetrafluoroborate anions with hexaprotonated [18]aneN6 // Inorganic chemistry communications (2008) Vol. 11, No. 5, pp. 497-501;

12. M.S. Fonari, V. Kravtsov, Yu.A. Simonov, E.V. Ganin, V.O. Gelmboldt, K.Suwinska, J. Lipkowski, N.G. Furmanova // From clusters to coordination polymers in the crown-templated system ZrO_2/HfO_2 (Nb_2O_5/Ta_2O_5) – HF – H_2O – azacrown ether Rarely Observed Metal Oxide Fluoride Anions $[(TaF_5)_2O]^{2-}$ and $[(H_2O)NbF_4O\ NbF_5]^{2-}$ in the Complexes with Azacrown Ethers // Polyhedron (2008) Vol. 27, No. 9-10, pp. 2049-2058;

13. V.O. Gelmboldt, L.V. Koroeva, E.V. Ganinb, M.S. Fonari, M.M. Botoshansky. A.A. Ennan // Hexafluorosilicates of bis(carboxypyridinium) and bis(2-carboxyquinolinium) // Journal of Fluorine Chemistry (2008) Vol. 129, No. 7, pp. 632-636.

14. M.S.Fonari, Yu.A.Simonov, W.-J.Wang, S.-W.Tang, E.V.Ganin //Inclusion of triphenylmethane derivatives by crown and linear O-containing molecules: selective interactions and crystal structure // CrystEngComm. (2009) Vol. 2, pp. 94-101.

15. V.O.Gelmboldt, E.V.Ganin, M.S.Fonari, L.V.Koroeva, Y.E.Ivanov, M.M.Botoshansky // Hexafuorosilicates of bis(aminopyridinium). The relationship between H-bonding system and solubility of salts // Journal of Fluorine Chemistry (2009) Vol. 130, № 4, pp. 428-433.

16. Ю.А. Симонов, М.С. Фонарь, Я. Липковский, Э.В. Ганин, А.А. Яволовский,Г.Л. Камалов // Особенности структуры производных 1,3-дигидропиримидин-2,4-дионов в комплексах с макроциклическими поли– и азаполиэфирами // Структурная химия (2009) Т. 50, Приложение, S143 – S149.

17. M.S. Fonari, E.V.Ganin, Y.M.Chumakov, M.M.Botoshansky, K.Suwinska, S.S.Basok, Y.A.Simonov // Conformational Mobility of 7,16-Bis(4-methoxybenzyl)-1,4,10,13-tetraoxa-7,16-diazacyclooctadecane in Molecular and Proton Transfer Complexes: X-ray and DFT Study // New Journal of Chemistry (2009) Vol. 33, No. 8, pp. 1646 - 1656.

18. В.О. Гельмбольдт, Л.Х. Миначева, Э.В. Ганин, В.С. Сергиенко, М.М. Ботошанский // Синтез и кристаллическая структура гексафторосиликата N,N-диметилбигуанидиния // Журнал неорганической химии (2009) Т. 54, № 12, с. 1-4.

19. М.Г. Васильева, М.Г. Горличенко, С.В. Шевченко, О.Н. Ласовская, Э.В. Ганин // Синтез краун-эфиров и их взаимодействие с кремнефтороводородной кислотой // Вістник одеського екологичного університету (2009), Вип. 8, с. 228-232.

20. М.Г. Васильева , М.Г. Горличенко, С.В. Шевченко, С.И.Шепелина, Э.В. Ганин // Особенности образования комплексов «хозяин-гость» краун-эфиров с HN-протонодонорными молекулами // Вістник одеського екологичного університету (2009), Вип. 8, с. 239-244.

21. М.Г. Васильева, Г.И. Герасименко, В.Ф. Шевченко, Э.В. Ганин // Селективные взаимодействия краун-эфиров с фторокомплексными кислотами

бора, кремния, германия, олова и сурьмы в присутствии воды // Вістник одеського екологичного університету (2009), Вип. 8, с. 245-249.

22. Vladimir O. Gelmboldt, Eduard V. Ganin, Larisa V. Koroeva, Mark M. Botoshansky, Marina S. Fonari // Interaction of hexafluorosilicic acid with sulfa drugs. Bis(sulfathiazolium)hexafluorosilicate: Spectral data and crystal structure // Journal of Fluorine Chemistry. (2010), Vol. 131, No. 6. P. 719–723

23. В. О. Гельмбольдт, Э. В. Ганин, Л. Х. Миначева,Л. В. Короева, В. С. Сергиенко // Гексафторосиликаты бис(2-алкилтиокарбамоил-4-пиридиния) // Журнал неорганической химии, (2010), том 55, № 8, С. 1284–1290.

24. Marina S. Fonari, Eduard V. Ganin, Anna V. Vologzhanina, Mikhail Yu. Antipin,and Victor Ch. Kravtsov // Persistent CH... π Interactions in Mefenamic Acid Complexes with Cyclic and Acyclic Amines // Crystal Growth & Design. (2010), (10.1021/cg100518b) Vol. XXX, No. X PP., XXXX PROOF

25. Marina S. Fonari, Eduard V. Ganin, Stepan S. Basok, Konstantin A. Lyssenko, Michael J. Zaworotko ,Victor Ch. Kravtsov // Structural study of salicylic acid salts of a series of azacycles and azacrown ethers // Crystal Growth & Design. (2010), (cg-2010-01002x) PROOF

26. Eduard V. Ganin, Stepan S. Basok, Arkadii A. Yavolovskii, Mark M. Botoshansky and Marina S. Fonari //From chains to ladders in the co-crystals with 2,3-thiophene-15-crown-5, 2,3-naphtho-15-crown-5, and bis-(18-crown-6)-stilbene constructed by weak hydrogen bonding // CrystEngComm. (2010), (CE-ART-04-2010-000155.R1) PROOF

27. М.Г.Васильева, Э.В.Ганин, В.Ф.Шевченко, О.Н.Ласовская // Транспортные взаимодействия краун-эфиров с фторокомплексными кислотами кремния // Вістник одеського екологічного університету. (2010), Вип. 10, С. XXX-XXX.

Представлено 22 тези на міжнародних конференціях:

1. N.Furmanova, E.Ganin, V.Gelmboldt, P.Bourosh, Yu.Simonov, M.Fonari // Isolation of oxonium ions by crown ethers: structural evidence // International Seminar of Inclusion Compounds (ISIC-11). 2007, Kyiv, June 10-15, Abstracts, p. 112.

2. Арион В.Б, Басок С.С., Ганин Э.В., Гельмбольдт В.О., Кепплер Б.К., Кёлиг Х., Короева Л.В., Фонарь М.С., Симонов Ю.А., Шова С., Эннан А.А. // Новый пример стабилизации аниона $[SiF_5(H_2O)]^-$ в составе комплекса “гость-хозяин” с протонированной формой азакраун-эфира // XXIII Международная Чугаевская конференция по координационной химии, 2007, Одесса, 4-7 сентября 2007, Тезисы докладов, с. 272-273.

3. Гельмбольдт В.О., Ганин Э.В., Домасевич К.В., Короева Л.В., Эннан А.А. // Гексафторосиликаты протонированых форм пиридин-2-карбоновой и хинолин-2-карбоновой кислот // XXIII Международная Чугаевская конференция по координационной химии, 2007, Одесса, 4-7 сентября 2007, Тезисы докладов, с. 359.

4. M.S.Fonari, L.Croitor, B.Moulton, B.S. Luisi, S.S. Basok, E.V. Ganin, V.O. Gelmboldt // Binding of tetrafluoroborate and fluoride anions to macrocyclic ligands // The IInd International Conference of the Chemical Society of the Republic of Moldova “Achievements and Perspectives of Modern Chemistry”, 2007, Chisinau, October 1-3, Abstracts of communications, pp. 22.

5. M.Fonari, Yu.Simonov, P.Bourosh, N.Furmanova, T.Chernaya, O.Alexeeva, E.Ganin, V.Gelmboldt // Isolation of oxonium ions by crown ethers of different dimensionality: X-ray study // The IInd International Conference of the Chemical Society of the Republic of Moldova “Achievements and Perspectives of Modern Chemistry”, 2007, Chisinau, October 1-3, Abstracts of communications, pp. 16.

6. V.Ch.Kravtsov, E.V.Ganin, Yu.A.Simonov // Supramolecular structure of multiple component crystals involving anti tubercular drugs and D-tartaric acid // The IInd International Conference of the Chemical Society of the Republic of Moldova “Achievements and Perspectives of Modern Chemistry”, 2007, Chisinau, October 1-3, Abstracts of communications, pp. 78.

7. Yu.Simonov, M.Fonari, G.Duca, E.Ganin, A.Yavolovskii // Specificity of interaction of hydrochlorothiazide and its n-nitroso derivative with 18-membered macrocyclic receptors // XVIII Mendeleev Congress on General and Applied

Chemistry: section 10. "Supramolecular systems in chemistry and biology", 2007, September 23-28, Moscow, Abstract Book, p. 2143.

8. V.Ch. Kravtsov, E. V. Ganin, K. A. Lyssenko // Supramolecular assembly in the system piperidine-organic acid // First international symposium "Supramolecular and nanochemistry: toward applications" (SNCTA-2008). 2008 Kharkov, Ukraine, 25th-29th August, Book of abstracts, p. P2-6.

9. Yu. A. Simonov, M. S. Fonari, V. Ch. Kravtsov, K. Suwinska, J. Lipkowski, O. A. Alekseeva, N. G. Furmanova, S.S. Basok, V.O. Gelmboldt, E.V. Ganin // Crown-templated assembling of the inorganic binuclear fluoro-containing metallates in the system ZrO_2/HfO_2 (Nb_2O_5/Ta_2O_5) – HF – H_2O – azacrown ether // First international symposium "Supramolecular and nanochemistry: toward applications" (SNCTA-2008). 2008 Kharkov, Ukraine, 25th-29th August, Book of abstracts, p. I-14.

10. Гельмбольдт В.О., Ганин Э.В., Домасевич К.В., Иванов Ю.Э., Короева Л.В., Миначева Л.Х., Сергиенко В.С. // Гексафторосиликаты карбоксипиридиния – модели гибридных функциональных материалов// XVII Українська конференція з неорганічної хімії за участю закордонних вчених,присвячена 90-річчю заснування Національної академії наук України. 2008, Львів, Україна, 15-19 вересня 2008, Тези доповідей , с. У31.

11. V.Ch. Kravtsov, E.V. Ganin // X-ray structural study of pyrantel pamoate. Unprecedented conformation of pamoate anion // 4-th International conference on materials science and condensed matter physics. 2008, Chisinau, Moldova, 23-26 September, Absracts, p. 123.

12. V.Ch. Kravtsova, M.S. Fonaria, Yu.A. Simonova, M.Yu.Antipin, E.V. Ganin // Supramolecular crystalline state assembly of salicylic acid with piperidine and azo-containing macrocycles // 4-th International conference on materials science and condensed matter physics. 2008, Chisinau, Moldova, 23-26 September, Absracts, p. 126.

13. В.О. Гельмбольдт, Л.В. Короева, Э.В. Ганин, А.А. Эннан // О взаимосвязи растворимости и строения гексафторосиликатов пиридиния // IV Українська науково-технічна конференція з технології неорганічних речовин "Сучасні

проблеми технології неорганічних речовин " з міжнародною участю. 2008, Дніпродзержинськ, Україна, 14-16 жовтня, Збірник матеріалів конференції - с. 23-24.

14. M.S.Fonari, E.V.Ganin, M.Y.Antipin, V.C.Kravtsov // Crystallographic characterization of mefenamic acid complexes with cyclic and acyclic amines // The International Conference dedicated to the 50th anniversary from the foundation of the Institute of Chemistry of the Moldavian Academy of Sciences. 2009. 26–28 May, Chisinau, Moldova, Book of abstracts, p. PP 026.

15. V.C.Kravtsov, E.V.Ganin, A.V.Vologzhanina, K.A.Lyssenko // Crystalline assembly of anti tubercular drugs with p-toluenesulfonic acid // The International Conference dedicated to the 50th anniversary from the foundation of the Institute of Chemistry of the Moldavian Academy of Sciences. 2009. 26–28 May, Chisinau, Moldova, Book of abstracts, p. PP 085.

16. V.C.Kravtsov, E.V.Ganin // Crystal engineering of pharmaceutical solids involving N-containing cycles/macrocycles and sulfa drugs // The International Conference dedicated to the 50th anniversary from the foundation of the Institute of Chemistry of the Moldavian Academy of Sciences. 2009. 26–28 May, Chisinau, Moldova, Book of abstracts, p. OP 14.

17. E.Goreshnik, V.O.Gelmboldt, L.V.Koroeva, E.V.Ganin // Synthesis, crystal structure, IR-spectral data and some properties of 3,5-diamino-1,2,4-triazolium hexafluorosilicate and tetrafluoroborate // The International Conference dedicated to the 50th anniversary from the foundation of the Institute of Chemistry of the Moldavian Academy of Sciences. 2009. 26–28 May, Chisinau, Moldova, Book of abstracts, p. PP 039.

18. V.O.Gelmboldt, L.V.Koroeva, E.V.Ganin, M.S.Fonari, M.M.Botoshansky, Y.E.Ivanov, A.A.Ennan // Hexafluorosilicates of aminopyridinium: correlation between of H-bonds parameters and solubility of salts// The International Conference dedicated to the 50th anniversary from the foundation of the Institute of Chemistry of the Moldavian Academy of Sciences. 2009. 26–28 May, Chisinau, Moldova, Book of abstracts, p. OP 08.

19. В.Гельмбольдт, Е.Ганін, Л.Короєва, Л.Міначова, В.Сергієнко //Гексафторосилікати біс(2-алкіл-4-тіокарбамоіл-4-піридинію): синтез, будова, властивості //Дванадцята наукова конференція «Львівські хімічні читання - 2009» (Міністерство освіти і науки України). 2009. 1-4 червня. Львів, Україна, Збірник наукових праць, с. У1.

20. В.О. Гельмбольдт. Э.В. Ганин, М.С. фонарь, Ю.А. Симонов, Я. Липковский // Стабилизация фторокомплексов p- и d-элементов в супрамолекулярных соединениях с краун- и азакраун-эфирами // VIII Всероссийская конференция «Химия фтора», 22–25 ноября 2009 года, Черноголовка, Московская обл., НЦЧ РАН, P.87.

21. Evgeny Goreshnik, Vladimir Gelmboldt, Larisa Koroeva, Eduard Ganin // Synthesis, crystal structure and properties of 3,5-diamino-1,2,4-triazolium salts $(LH)_2SiF_6$, $(LH)BF_4$ and $[Cu(LH)_2]2(SiF_6)_3$ // 16th European Symposium on Fluorine Chemistry, Ljubljana, Slovenia, July 18 - 23, 2010. Book of Abstracts. - P. 189.

22. В.О. Гельмбольдт, Э.В. Ганин, Л.В. Короева, М.С. Фонарь, М.М. Ботошанский // Особенности взаимодействия сульфаниламидов с кремнефтороводородной кислотой // Фармація України. Погляд у майбутнє, Харків, 15–17 вересня, 2010. Матеріали VII Національного з’їзду фармацевтів України, Том 1, С. 26.

ВИСНОВКИ

1. Доведена можливість утворення стійких кристалічних супрамолекулярних комплексів 4-амінобензойної, саліцилової, мефенамової кислоти та сульфаніламідних препаратів з азакраун-етерами та різноманітними амінами, які використовуються у фармацевтичній практиці.

2. Встановлена можливість утворення стійких кристалічних супрамолекулярних комплексів ізоніазіду, протіон- й етіонаміду із краун-етерами та дікарбоновими кислотами що використаються у фармакопеї.

3. Синтезом ряду комплексів із краун-етерів та дітіоурацілу експериментально доведена можливість зв'язування О-вмістними гетероциклами урацилів в стабільні супрамолекулярні комплекси. Структурні особливості синтезованих комплексів можуть бути складовій яку необхідно враховувати при моделюванні біохімічних взаємодій.

4. Доведена можливість рідкісної селективної взаємодії класичних молекул "хазяїнів" між собою: краун-етерів з похідними трифенілметану з селективним утворенням стійких кристалічних супрамолекулярних комплексів.

5. Встановлено, що при випаровуванні розчинників з розчинів силіційфлуороводневої кислоті та ряду похідних амінопіридинів селективне утворюються кристалічні супрамолекулярні комплекси з гексафлуоросилікатним аніоном.

6. Доведено, що при випаровуванні розчинників з розчинів флуорокомплексних кислот цирконію, гафнію, ніобію, танталу, які є ключовими сполуками в технології витягу, поділи й очищення зазначених металів від домішок, та ряду О- й N-краун-етерів у флуороводній кислоті, селективне утворюються кристалічні супрамолекулярні комплекси із фіксацією аніонів рідкісної будови.

Додаток А

Копія статті.

“Molecular complexes of thionicotinamide with 18-membered crown ethers: Synthesis and crystal structures”

Available online at www.sciencedirect.com
ScienceDirect
Journal of Molecular Structure 826 (2007) 89 95
Journal of MOLECULAR STRUCTURE
www.elsevier.com/locate/molstruc

Molecular complexes of thionicotinamide with 18-membered crown ethers: Synthesis and crystal structures

Marina S. Fonari [a,*], Eduard V. Ganin [b], Shang-Wei Tang [c], Wen-Jwu Wang [c], Yurii A. Simonov [a]

[a] *Institute of Applied Physics, Academy of Sciences of Moldova, Academy str., 5 MD2028 Chisinau, Republic of Moldova*
[b] *Odessa State Environmental University, Ministry of Education and Science of Ukraine, Odessa, Ukraine*
[c] *Department of Chemistry, Tamkang University, 151 Ying-Chuan Road, Tamsui, Taipei 25137, Taiwan, ROC*

Received 16 March 2006; received in revised form 17 April 2006; accepted 19 April 2006
Available online 24 May 2006

Abstract

The reaction of thionicotinamide (3-thioamidopyridine) with 18-membered crown ethers, 18-crown-6 (18C6), benzo-18-crown-6 (B18C6) and *cis–anti–cis*-dicyclohexyl-18-crown-6 (D18C6) results in the molecular complexes of 1:1 ratio for 18C6 (complex **1**) and B18C6 (complex **2**) and monohydrate of 2:1:1 ratio for D18C6 (complex **3**), respectively. The complexes are sustained by combination of N–H···O, O–H···N and C–H···O hydrogen bonds, and the components are associated into molecular adduct (**1**) or infinite chain (**2** and **3**).
© 2006 Elsevier B.V. All rights reserved.

Keywords: H-bonded adducts; Thionicotinamide; 18-Membered crown ethers; Synthesis and crystal structure

1. Introduction

In the last decade we witnessed an increased interest to the co-crystals including active pharmaceutical ingredient (API) [1–3] with the aim to produce new valuable materials. Crystalline self-assemblies are promising for improving drug solubility, dissolution rate, stability and bioavailability. Supramolecular synthesis is now being widely explored to obtain new pharmaceuticals from known APIs and a benign solid component (cyclodextrins [4–6], carboxylic [7–10] and dicarboxylic acids [11–13], etc.). The recent findings in this topic are summarized in the fresh review paper by Zaworotko and co-workers [14].

Crown ethers (CEs) exhibit themselves as very useful model compounds capable to function as do more complex chemical structures. Moreover, some simple crown ethers exhibit biological activity. These two properties make them very attractive molecules that permit a detailed analysis of interactions that are thought to be important in biology [15]. For several years we are involved in the problem of the molecular recognition of biologically important molecules (nucleic bases, drugs) by macrocyclic molecules, as the model systems mimic substrate–receptor interactions [16,17]. We have analyzed series of complexes, e.g., streptocid (4-aminobenzenesulfonamide) – 18-membered CEs (18-crown-6, dicyclohexyl-18-crown-6, benzo, cyclohexyl-18-crown-6) [18–20], PABA (4-aminobenzoic acid) – CEs (isomers of dicyclohexyl-18-crown-6, aza-12-crown-4) [21,22], hypothiazide (6-chloro-3,4-dihydro-2*H*-1,2,4-benzothiadiazine-7-sulfonamide-1,1-dioxide) – CEs (18-crown-6, dicyclohexyl-18-crown-6) [23,24]. It has been shown that the interaction with the neutral macrocycle results in the genius co-crystals with the primary amino-group involved in the coordination to macrocyclic molecule, while aza-macrocycle is easily protonated and interaction results in an organic salt. The self-assembly of the drug molecules via hydrogen bonds typical for their pure forms is destroyed and is substituted by the interaction with the

* Corresponding author. Tel.: +373 22 73 81 54; fax: +373 22 72 58 87.
E-mail address: fonari.xray@phys.asm.md (M.S. Fonari).

0022-2860/$ - see front matter © 2006 Elsevier B.V. All rights reserved.
doi:10.1016/j.molstruc.2006.04.034

Author's personal copy

macrocyclic molecule [25]. As the rule, the complete rearrangement of the hydrogen bonds occurs, and only the strongest homosynthons typical for the pure form (as that $R_2^2(8)$ combining two carboxylic groups [26]) remain in the complex [20] (Scheme 1).

In continuation of this research, we studied the system thionicotinamide (3-thioamidopyridine) – CE [18-crown-6 (18C6), benzo-18-crown-6 (B18C6) and *cis–anti–cis*-dicyclohexyl-18-crown-6 (D18C6)] and report here on the X-ray crystal structures of three novel complexes.

The thioamide functional group is present in many drugs and agricultural chemicals, and exposure to man can result in inadvertent toxicity. Thus, a large number of potentially useful drugs containing the thioamide group are limited in their use due to the toxic side effects associated with these compounds. The diverse thioamide derivatives have been used as herbicides, antitubercular and antibacterial agents. The associated toxicity of the thioamides is explained to be linked to their oxidative metabolism, especially *S*-oxygenation [27]. Some recent studies were devoted to the synthesis of modified thionicotinamide to decrease its toxicity and maintain the useful medicinal properties [28]. Thionicotinamide is a known xenobiotic. It is a drug used for the treatment of *Chagas disease*, a common health problem in South America [29].

The crystallographic data [30] for this class of compounds are rather scanty. They are restricted by three isomeric thioamidopyridines of general formula $C_6H_6N_2S$, 2-thioamidopyridine [31], 3-thioamidopyridine [32] and 4-thioamidopyridine [33]. The structure of the 2-propyl derivative of 4-thioamidopyridine has also been reported [34]. The structural interest to these compounds has centered on the parameters of the thioamide group and the consequent electron arrangement within the group. Additional features of interest are the non-coplanarity of the pyridine ring with the thioamide group and the hydrogen-bonding schemes. The isomers have three possible coordination sites, and the packing of all of them reveals some common features. The molecules lie in the layers via $R_2^2(8)$ centrosymmetric rings built on NH···S contacts (N···S ~ 3.4 Å, a bit longer than the sum of van der Waals radii) and C(7) chains (contacts NH···N, N···N about 2.96 Å), and then these layers stack along the shortest axis (Scheme 2).

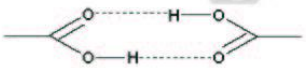

Scheme 1. Homosynthon $R_2^2(8)$ typical for carboxylic acids.

As for the multicomponent adducts involving isomers of thionicotinamide, only its S-oxide monohydrate [35] and thionicotinamidium 3,5-dinitro-4-methylbenzoate 3,5-dinitro-4-methylbenzoic acid adduct [36] are reported. From the viewpoint of crystal packing, it is interesting that only NH···N contact (N···N distance of 2.954 Å) remains in the crystal packing of the first adduct, while weaker NH···S contacts are substituted by the interaction with water molecule as a more powerful H-acceptor, while in the second compound the full rearrangement of the intermolecular interactions occurs, and two homosynthons typical for 3-thionicotinamide itself are substituted by the heterosynthons between thionicotinamidium cations and 3,5-dinitro-4-methylbenzoate anions (or 3,5-dinitro -4-methylbenzoic acid molecules).

The aim of our study is to elucidate the mode of interaction of the drug molecule with the macrocycles and to compare the crystal packing motifs in the complexes.

2. Experimental

Commercially available reagents were used as received. Compounds **1–3** were analyzed for C, H, N and S in a Perkin-Elmer 240 C. The thin-layer chromatographic control of the substance purity was performed on Silufol UV-254 plates. ^{1}H NMR spectra were recorded at 300 MHz on a Varian Oxford 300 NMR spectrometer.

2.1. Synthesis

Compound 1. A solution of 18C6 (0.264 g, 1 mmol) and thionicotinamide (0.138 mg, 1 mmol) in 2 ml of methanol and 3 ml of ethyl acetate was stored for 3–5 days at 20 °C in an open flask. The crystals, separated in a yield of 91% (0.365 g), were suitable for X-ray analysis. Yellow crystals, soluble in methanol, ethanol, acetone, m.p. 120–122 °C. Analysis: found C, 53.71; H, 7.51; N, 6.96; S, 7.97%. $C_{18}H_{30}N_2O_6S$ requires C, 53.68; H, 7.54; N, 6.93; S, 7.94%. ^{1}H NMR (CD_3OD_{d4}, 300 MHz): 3.60 s (24H, 18C6), 7.45 m, 8.26 m, 8.60 m, 9.00 m (4H, CH).

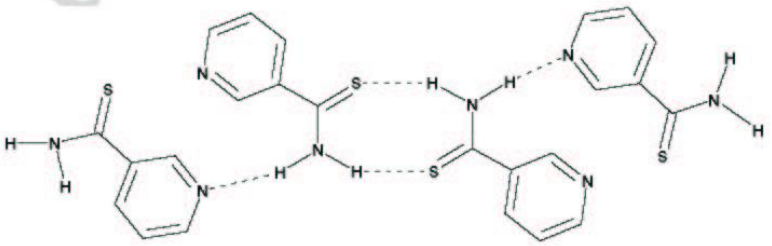

Scheme 2. The mode of association of 3-thionicotinamide molecules in the crystal.

Compound 2. A solution of B18C6 (0.312 g, 1 mmol) and thionicotinamide (0.138 mg, 1 mmol) in 7 ml of methanol and 15 ml ethyl acetate was stored ~3 days at 20 °C in an open flask. The crystals, separated in a yield of 96% (0.430 g), were suitable for X-ray analysis. Yellow crystals, soluble in methanol, ethanol, acetone, m.p. 140–142 ° C. Anal. found C, 58.59; H, 6.83; N, 6.31; S, 7.12%. $C_{22}H_{30}N_2O_6S$ requires C, 58.65; H, 6.71; N, 6.22; S, 7.19%. ^{1}H NMR ($DMSO_{d6}$, 300 MHz): 3.55 m, 3.73 m, 4.05 m (20H, CH_2) and 6.90 m (4H, CH – B18C6), 7.43 m, 8.18 m, 8.64 m, 8.99 m (4H, CH).

Compound 3. A solution of D18C6 (0.372 g, 1 mmol) and thionicotinamide (0.138 g, 1 mmol) in 5 ml of acetone and 5 ml hexane was stored for 3–5 days at 20 °C in an

Table 1
Crystal data summary for complexes 1–3

Complex	1	2	3
CCDC number	601910	601911	601909
Empirical formula	$C_{18}H_{30}N_2O_6S$	$C_{22}H_{30}N_2O_6S$	$C_{32}H_{50}N_4O_7S_2$
Formula weight	402.50	450.54	666.88
Temperature (K)	293(2)	293(2)	293(2)
Crystal system	Monoclinic	Triclinic	Orthorhombic
Space group	*Cc*	*P-1*	*Pccn*
Unit cell dimensions			
a (Å)	17.228(2)	8.471(2)	16.880(1)
b (Å)	8.525(1)	9.866(2)	18.685(1)
c (Å)	14.866(1)	15.111(2)	11.331(1)
α (deg.)	90.0	84.37(1)	90.0
β (deg.)	102.75(2)	84.69(2)	90.0
γ (deg.)	90.0	65.78(2)	90.0
Cell volume (Å^3)	2129.4(3)	1144.2(4)	3573.7(5)
Formula units/unit cell	4	2	4
D_{calc} (g/cm^{-3})	1.256	1.308	1.239
μ (mm^{-1})	0.186	0.181	0.198
$F(000)$	864	480	1432
Crystal dimensions (mm)	$0.55 \times 0.53 \times 0.40$	$0.58 \times 0.46 \times 0.38$	$0.42 \times 0.34 \times 0.25$
θ Range for data collection (deg.)	2.42–27.51	2.27–25.00	2.18–27.00
Limiting indices	$22 \leqslant h \leqslant 17$, $10 \leqslant k \leqslant 11$, $18 \leqslant l \leqslant 19$	$0 \leqslant h \leqslant 9$, $10 \leqslant k \leqslant 11$, $17 \leqslant l \leqslant 17$	$15 \leqslant h \leqslant 21$, $23 \leqslant k \leqslant 23$, $14 \leqslant l \leqslant 14$
Reflections collected/unique	6608/3703 [R(int) – 0.0274]	4304/4008 [R(int) – 0.0103]	20874/3909 [R(int) – 0.0287]
Reflections with $I > 2\sigma(I)$	1667	3505	1865
Refinement method	Full-matrix least-squares on F^2	Full-matrix least-squares on F^2	Full-matrix least-squares on F^2
Data/restraints/parameters	3703/2/253	4008/0/289	3909/0/216
Goodness-of-fit on F^2	0.881	1.020	0.849
Final R indices [$I > 2\sigma(I)$] %	R_1 – 0.0401, wR_2 – 0.0721	R_1 – 0.0332, wR_2 – 0.0930	R_1 – 0.0350, wR_2 – 0.0782
R indices (all data) %	R_1 – 0.0886, wR_2 – 0.0763	R_1 – 0.0390, wR_2 – 0.0960	R_1 – 0.0829, wR_2 – 0.0854
Largest diff. peak and hole (eÅ^{-3})	0.179/ 0.209	0.208/ 0.214	0.187/ 0.232

Table 2
Hydrogen bonding in complexes 1–3

D–H···A	r(D–H) (Å)	r(H···A) (Å)	r(D···A) (Å)	∠(DH···A) (deg)	Symmetry transformation for acceptor
1					
N2–H1N2···O2	0.90(3)	2.10(3)	2.998(4)	176(3)	x, y, z
N2–H2N2···O6	0.93(3)	2.59(3)	3.294(4)	132(2)	x, y, z
2					
N2–H1N2···O4	0.88(2)	2.11(2)	2.989(2)	173(2)	x, y, z
N2–H2N2···O1	0.87(2)	2.43(2)	3.231(2)	153(2)	x, y, z
N2–H2N2···O6	0.87(2)	2.48(2)	3.218(2)	144(2)	x, y, z
3					
N2–H1N2···O2	0.90(2)	2.07(2)	2.934(2)	161(2)	x, y, z
N2–H2N2···O1	0.88(2)	2.10(2)	2.975(2)	170(2)	$x+1, y+1, z+2$
O4–H1O4···N1	0.81(2)	2.16(2)	2.957(2)	165(3)	$x+1/2, y+3/2, z$

Author's personal copy

open flask. The crystals, separated in a yield of 71% (0.235 g), were suitable for X-ray analysis. Yellow crystals, soluble in methanol, ethanol, acetone, m.p. 115–116 °C. Anal. found C, 57.61; H, 7.59; N, 8.38; S, 9.67%. $C_{32}H_{50}N_4O_7S_2$ requires C, 57.63; H, 7.56; N, 8.40; S, 9.62%. ^{1}H NMR (DMSO$_{d6}$, 300 MHz): 1.19–1.71 m and 3.55 m (36H, D18C6), 7.44 m, 8.19 m, 8.65 m, 8.99 m (8H, CH), 9.68 s, 10.04 s (2H, NH; 2H, SH).

2.2. X-ray crystallography

The X-ray intensity data were collected at room temperature on a Bruker CCD diffractometer for **1** and **3** and on a Siemens P4 diffractometer for **2**. The recorded data were corrected for polarization and Lorentz effects. The structure solution and refinement proceeded similarly for all structures using SHELX-97 program package [37]. Direct methods yielded all non-hydrogen atoms of the asymmetric unit. These atoms were treated anisotropically (full-matrix least-squares method on F^2). C-bound hydrogen atoms were placed in calculated positions with their isotropic displacement parameters riding on those of the parent atoms, while the N- and O-bound H-atoms were found from difference syntheses at an intermediate stage of the refinement and were treated isotropically. The X-ray data and the details of the refinement for **1–3** are given in Table 1, H-bonding data are given in Table 2, geometry of thionicotinamide molecule in **1–3** is summarized in Table 3.

Table 3
Selected bond lengths (Å) and angles (deg) for thionicotinamide molecule in complexes **1–3**

	1	2	3
S1–C6	1.653(3)	1.667(2)	1.652(2)
N1–C1	1.297(5)	1.337(2)	1.333(3)
N1–C5	1.361(4)	1.330(2)	1.340(2)
N2–C6	1.318(4)	1.324(2)	1.314(2)
C1–C2	1.367(6)	1.367(3)	1.361(3)
C2–C3	1.381(5)	1.368(2)	1.368(3)
C3–C4	1.369(4)	1.391(2)	1.375(2)
C4–C5	1.378(4)	1.384(2)	1.372(2)
C4–C6	1.465(4)	1.492(2)	1.483(2)
C1–N1–C5	116.1(4)	116.5(2)	116.0(2)
N1–C1–C2	125.2(4)	123.8(2)	123.4(2)
C1–C2–C3	117.4(4)	118.8(2)	119.2(2)
C4–C3–C2	120.5(3)	119.4(2)	119.5(2)
C3–C4–C5	116.5(3)	117.0(1)	117.0(2)
C3–C4–C6	122.3(3)	121.1(1)	121.3(2)
C5–C4–C6	121.1(3)	121.9(1)	121.7(2)
N1–C5–C4	124.2(3)	124.5(2)	124.8(2)
N2–C6–C4	116.1(3)	116.7(1)	115.5(2)
N2–C6–S1	122.8(3)	122.2(1)	122.7(1)
C4–C6–S1	121.0(2)	121.1(1)	121.8(1)

Crystallographic data (cif files) for complexes **1–3** have been deposited with the Cambridge Crystallographic Data Center, CCDC Nos. 601909 (complex **3**), 601910 (complex **1**), and 601911 (complex **2**). Copies of this information may be obtained free of charge from The Director, CCDC, 12 Union Road, Cambridge CB2 1EZ, UK (fax: +44 1233 336 033; E-mail: deposit@ccdc.cam.ac.uk or http://www.ccdc.cam.ac.uk).

3. Results and discussion

Complexes **1** and **2** represent anhydrous co-crystals of 1:1 ratio of thionicotinamide and corresponding crown ether, while **3** is a monohydrate of 2:1:1 stoichiometry. As all three complexes reveal a lot of common features in the complex organization, we present the comparative analysis for **1–3**. Fig. 1 reveals the ORTEP view for complexes **1** and **2**.

These two complexes are very close in structure organization: in **1** the formula unit is sustained by two NH···O hydrogen bonds, with the involvement in these interactions

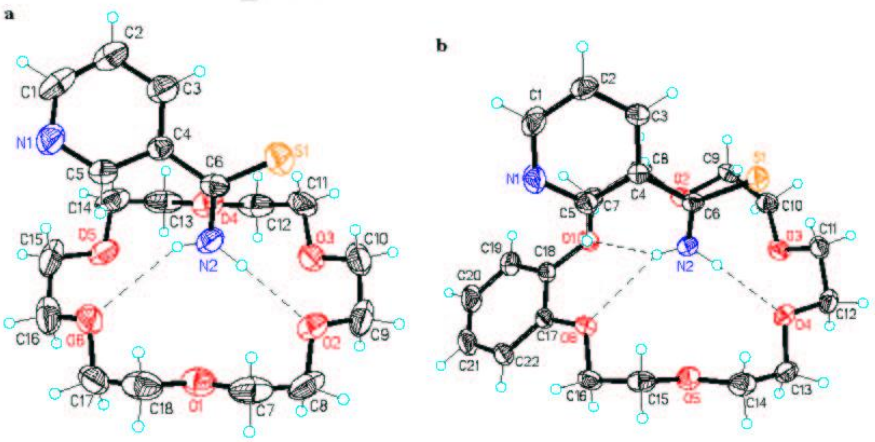

Fig. 1. (a and b). ORTEP view of complexes **1** and **2** with the numbering scheme. Displacement ellipsoids are drawn at the 30% probability level. Hydrogen bonds are shown by dashed lines.

of two crown oxygen atoms, O2 and O6 separated by the oxyethylene fragment. The N···O distances adopt the values 2.998(4) and 3.294(4) Å. It is evident that the second value is rather long as well as the corresponding H(N)···O6 distance, however, this contact contributes to the complex stability. In complex **2** thionicotinamide and B18C6 molecules are held together again through two NH···O hydrogen bonds, single one with the N···O separation of 2.989(2) Å, and the second one which is bifurcated, with two aromatic oxygen atoms O1 and O6 of B18C6, the corresponding N···O distances being 3.218(2) and 3.231(2) Å. The nitrogen atom of thioamide group is situated at 1.720(3) and 1.748(2) Å from the mean plane of six oxygen atoms of the macrocycles in the complexes **1** and **2**, correspondingly. 18C6 in **1** has a crown-like shape typical for D_{3d} conformation with the mean deviation of six oxygen atoms from their least-square plane being within ±0.23 Å. B18C6 in **2** has a more distorted shape with the maximal deviations for O3 and O4 atoms equal to 0.40 and 0.42 Å, correspondingly from the mean plane through all six oxygen atoms where they are fitted within ±0.26 Å. The molecules in the complexes are arranged in such a way that the dihedral angle between the mean planes of crown oxygen atoms and the pyridine ring of thionicotinamide molecule is equal to 36.4(1)° in **1** and 58.8(1)° in **2**, correspondingly. The subtle differences in **1** and **2** are connected with the nature of the CE used, namely with the availability of the phenyl ring in the molecule of B18C6. These differences exhibit themselves in the crystal packing. The packing of **1** does not reveal any specific features besides van der Waals interactions between the neighboring complexes. In contrary, in **2** one may note two short C–H···O contacts, one, C5···O6 functions within the complex (C···O 3.445(2) Å, CHO angle is 164°), while the second one, C3···O3(x 1, y, z) functions between the neighboring complexes translated along a direction (C···O 3.281(2) Å, CHO angle is 133°). These weak interactions combine the complexes in the chains (Fig. 2).

Fig. 3 depicts the ORTEP view of complex **3**. The asymmetric part of the unit cell comprises of one molecule of CE that resides on the inversion center, one thionicotinamide molecule in general position and one water molecule that resides on twofold screw axis. It results in the common complex stoichiometry of 1:2:1. Due to CE position on an inversion center, two thionicotinamide molecules approach its two faces in a similar manner. The molecules in a 1:2 molecular unit are held together by four single inversion-related NH···O hydrogen bonds, N···O distances being 2.957(2) and 2.975(2) Å. These H-bonds are the shortest amongst three studied complexes. In the complex the nitrogen atom of thioamide group deviates at 1.883(2) Å from the mean plane of six oxygen atoms of the D18C6, which are coplanar within ±0.14 Å. The molecules in the complex are arranged in such a way that the dihedral angle between the mean planes of crown oxygen atoms and the pyridine ring of the thionicotinamide molecule is equal to 60.8(1)°.

Water molecule occupies position on twofold screw axis. Via OH···N hydrogen bond with the pyridine nitrogen it binds two neighboring complexes in the corrugated chain. The fragment of the chain is shown in Fig. 4.

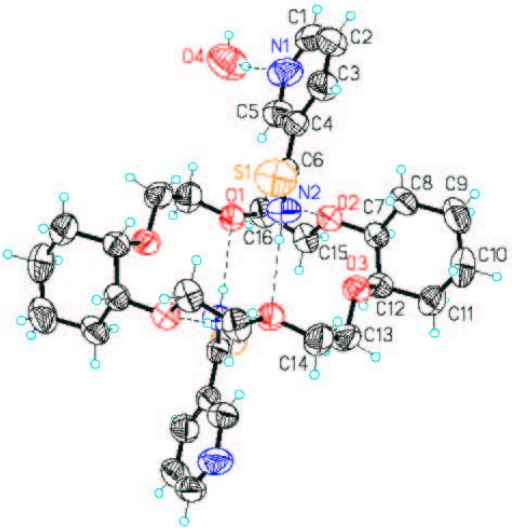

Fig. 3. ORTEP view of complex **3** with the numbering scheme. Displacement ellipsoids are drawn at the 30% probability level. Hydrogen bonds are shown by dashed lines.

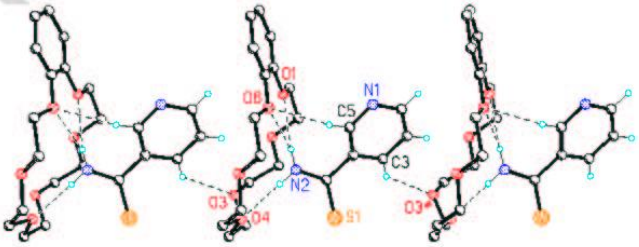

Fig. 2. Chain organization in **2**. C-bound H-atoms of B18C6 molecule are omitted for clarity. Atom marked with a hash (#) is at the symmetry position x 1, y, z.

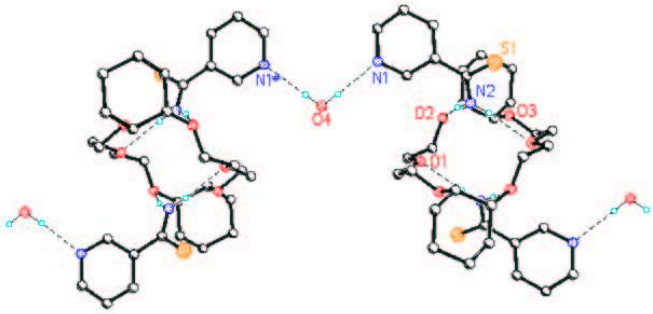

Fig. 4. Chain organization in **3**. C-bound H-atoms are omitted for clarity. Atom marked with a hash (#) is at symmetry position $x + 1/2$, $y + 3/2$, z.

The geometry of thionicotinamide molecule is consistent in **1**–**3** and in pure 3-thionicotinamide [32] (Table 3). The molecule is characterized by the planar pyridine ring with S1 and N2 atoms of the side chain considerably displaced from the plane of the pyridine ring, but C6 atom of the thioamido-group is not significantly displaced from this mean plane. The mean plane through the pyridine ring and the mean plane through the thioamide group [S1/N2/C6] are inclined at an angle of 40.8(1)° in **1**, 24.0(1)° in **2**, and 34.7(1)° in **3** to one another, the same angle in thionicotinamide itself is equal to 33.8°. This non-coplanarity is not uncommon and due to [38] it arises from the steric hindrance between the atoms in the side chain and the ring atoms *ortho* to the side chain.

4. Conclusion

Three molecular complexes of thionicotinamide with 18-membered crown ethers were synthesized in approximately the same conditions and their crystal structures were described. As we noted in Section 1, the molecules of isomers of thionicotinamide are held in the crystal via $R_2^2(8)$ supramolecular synthon (Scheme 2). In the supramolecular adducts with the macrocycles this synthon is destroyed. In all studied complexes the H-donor amino-group forms NH···O hydrogen bonds with the crown ethers' oxygen atoms. The availability of sterically bulky sulfur atom in the thioamide fragment does not permit to create a system of equal NH···O hydrogen bonds that is especially pronounced in complexes **1** and **2**.

Acknowledgements

The research described in this publication was made possible in part by Award No. MRDA-008: BGP-III award MOC2-3063-CS-03 of the Moldovan Research and Development Association (MRDA) and the U.S. Civilian Research & Development Foundation (CRDF). E.V.G. and W.J.W. are indebted to the National Science Council of Taiwan 95-2811-M-032 project for financial support.

Appendix A. Supplementary data

Supplementary data associated with this article can be found, in the online version, at doi:10.1016/j.molstruc.2006.04.034.

References

[1] R.D.B. Walsh, M.W. Bradner, S.G. Fleischman, L.A. Morales, B. Moulton, N. Rodriguez-Hornendo, M.J. Zaworotko, Chem. Commun. (2003) 186.
[2] S.G. Fleischman, S.S. Kuduva, J.A. McMahon, B. Moulton, R.D.B. Walsh, N. Rodriguez-Hornedo, M.J. Zaworotko, Crystal Growth Des. 3 (2003) 909.
[3] Ö. Almarsson, M.J. Zaworotko, Chem. Commun. (2004) 1889.
[4] M.R. Caira, V.J. Griffith, L.R. Nassimbeni, B. van Oudtshoorn, Chem. Commun. (1994) 1061.
[5] M.R. Caira, V.J. Griffith, L.R. Nassimbeni, J. Inclusion Phenom. 32 (1998) 461.
[6] M.R. Caira, D.R. Dodds, J. Inclusion Phenom. 34 (1999) 19.
[7] G. Smith, U.D. Wermuth, J.M. White, Cryst. Eng. Commun. 5 (2003) 58.
[8] J.L. Flippen-Anderson, J.R. Deschamps, A. Brossi, N.H. Greig, Acta Crystallogr. E 58 (2002) o853.
[9] C.B. Aakeröy, J. Desper, B.M.T. Scott, Chem. Commun. (2006) 1445.
[10] R. Banerjee, P.M. Bhatt, N.V. Ravindra, G.R. Desiraju, Crystal Growth Des. 5 (2005) 2299.
[11] V. Sethuraman, N. Stanley, P.T. Muthiah, W.S. Sheldrick, M. Winter, P. Luger, M. Weber, Crystal Growth Des. 3 (2003) 823.
[12] P. Vishweshwar, A. Nangia, V.M. Lynch, Crystal Growth Des. 3 (2003) 783.
[13] M. Hemamalini, P.T. Muthiah, G. Bocelli, A. Cantoni, Acta Crystallogr., Sect. E 59 (2003) o14.
[14] P. Vishweshwar, J.A. Mcmahon, J.A. Bis, M.J. Zaworotko, J. Pharm. Sci. 95 (2006) 499.
[15] G.W. Gokel, W.M. Leevy, M.E. Weber, Chem. Rev. 104 (2004) 2723.
[16] Yu. A. Simonov, M.S. Fonari, G.G. Duca, M.V. Gonta, Ed.V. Ganin, A.A. Yavolovskii, M. Gdaniec, J. Lipkowski, Tetrahedron 61 (2005) 6596.
[17] W.-J. Wang, Ed.V. Ganin, M.S. Fonari, Yu.A. Simonov, G. Bocelli, Org. Biomol. Chem. 3 (2005) 3054.
[18] S.T. Malinovskii, E.V. Ganin, Yu. A. Simonov, V.F. Makarov, Bull. Acad. Sci. Moldova, Phys. Eng. Math. Sci. (1989) 22.
[19] A.A. Dvorkin, M.S. Fonari, S.T. Malinovskii, E.V. Ganin, Yu.A. Simonov, V.F. Makarov, S.A. Kotlyar, N.G. Lukyanenko, Russ. J. Struct. Chem. 30 (1989) 96.
[20] Y.A. Simonov, J. Lipkowski, M.S. Fonari, E.V. Ganin, T.J. Malinowski, Supramol. Chem. 3 (1994) 227.

Author's personal copy

[21] M.S. Fonari, Y.A. Simonov, J. Lipkowski, A.A. Dvorkin, E.V. Ganin, Supramol. Chem. 4 (1994) 43.
[22] S.S. Basok, G. Bocelli, M.S. Fonari, E.V. Ganin, Yu.A. Simonov, Acta Crystallogr., Sect. C 62 (2006) o50.
[23] A.A. Dvorkin, Yu.A. Simonov, J. Lipkowski, M.S. Fonari, T.I. Malinowski, E.V. Ganin, S.A. Kotlyar, Russ. Crystallogr. Rep. 35 (1990) 682.
[24] Y.A. Simonov, M.S. Fonari, G. Bocelli, G. Calestani, J. Lipkowski, K. Suwinska, E.V. Ganin, Supramol. Chem. 4 (1995) 251.
[25] M.S. Fonari, Y.A. Simonov, E.V. Ganin, W.-J. Wang, Acta Crystallogr., Sect. E 62 (2006) o911.
[26] M.C. Etter, J. Am. Chem. Soc. 104 (1982) 1095.
[27] R. Olojo, R.H. Simoyi, J. Phys. Chem. A 108 (2004) 1018.
[28] M. Miletin, J. Hartl, M. Dolezal, Z. Odlerova, K. Kralova, M. Machacek, Molecules 5 (2000) 208.
[29] S. Wendel, Curr. Opin. Hematol. 5 (1998) 406.
[30] F.N. Allen, Acta Crystallogr. B 58 (2002) 380.
[31] T.C. Downie, W. Harrison, E.S. Raper, M.A. Hepworth, Acta Crystallogr., Sect. B 28 (1972) 283.
[32] G.R. Form, E.S. Raper, T.C. Downie, Acta Crystallogr., Sect. B 29 (1973) 776.
[33] J.C. Colleter, M. Gadret, Bull. Soc. Chim. France (1967) 3463.
[34] J.C. Colleter, M. Gadret, M. Gourselle, Acta Crystallogr., Sect. B 26 (1970) 1510.
[35] A.B. Corradi, C. Boga, L. Forlani, P. Sgarabotto, J. Chem. Crystallogr. 29 (1999) 115.
[36] V.R. Pedireddi, A. Ranganathan, S. Chatterjee, Tetrahedron Lett. 39 (1998) 9831.
[37] G.M. Sheldrick, SHELXS97 and SHELXL97, University of Göttingen, Germany, 1997.
[38] T. Takano, Y. Sasado, M. Kakudo, Acta Crystallogr. 21 (1966) 514.

Author's personal copy

Додаток Б

Копія статті.

“Supramolecular associates of p-aminobenzoic acid with N- and N,O-heterocyclic molecules”

PAPER www.rsc.org/njc | New Journal of Chemistry

Supramolecular associates of *p*-aminobenzoic acid with N- and N,O-heterocyclic molecules†

Brian Moulton,[a] Brian S. Luisi,[a] Marina S. Fonari,*[b] Stepan S. Basok,[c] Eduard V. Ganin[d] and Victor Ch. Kravtsov[b]

Received (in Montpellier, France) 13th December 2006, Accepted 29th January 2007
First published as an Advance Article on the web
DOI: 10.1039/b618207k

A series of novel supramolecular multicomponent complexes of *p*-aminobenzoic acid (PABA) with N-containing cyclic molecules and aza-crown ethers, $(H_2PPz)\cdot(PABA)_2\cdot 2H_2O$ (**1**), $(H_2teta)\cdot(PABA)_2\cdot H_2O]$ (**2**), $(H_2cyclen)\cdot(PABA)_2\cdot 2H_2O$ (**3**), (H_2-diazonia-12C4)$\cdot(PABA)_2\cdot 2H_2O$ (**4**), (H-azonia-18C6)$\cdot$(PABA)$\cdot 3H_2O$ (**5**) (PPz = piperazine, teta = *meso*-5,7,7,12,12,14-hexamethyl-1,4,8,11-tetraazacyclotetradecane, cyclen = 1,4,7,10-tetraazacyclododecane, diaza-12-crown-4 = 1,7-dioxa-4,10-diazacyclododecane and aza-18-crown-6 = 1,4,7,10,13-pentaoxa-16-azacyclooctadecane) has been synthesized. Crystallographic studies reveal that all complexes are organic salts formed due to the proton transfer from the carboxylic group of PABA to the amino group of the macrocycle, and thus are comprised of PABA anion, macrocyclic mono- or dication and a variable number of water molecules. In all complexes the cations and anions are associated *via* $(H_2N^+)NH\cdots O(COO^-)$ charge-assisted hydrogen bonds. The number of PABA involved in the complex equals to the number of N-protonated binding sites in the cyclic molecule. Water molecules play a significant role in the formation of the supramolecular architecture.

Introduction

The *p*-aminobenzoic acid (PABA) molecule as well as *p*-aminobenzoate salts are known for their role in biological processes[1] and are well suited for use in supramolecular syntheses based on hydrogen bonding interactions with a variety of organic acids and bases. The presence of favorably arranged carboxylic and amino groups in PABA affords the generation of advantageous hydrogen-bonded arrays because these functional groups can form predictable patterns useful for constructing a wide range of supramolecular assemblies. This property was recognized by Etter and Frankenbach[2] as a possible tool for promoting co-crystallization with the aim of designing acentric organic materials. Since the first PABA structural determination by Alleaume *et al.* in 1966,[3] a number of works devoted to PABA complexes have appeared; however, only three complexes between a neutral PABA molecule and 18-membered O-containing macrocycles, 18-crown-6[4] and *cis*-isomers of dicyclohexano-18-crown-6,[5] have been previously reported. Moreover, only two other studies describe ionic complexes of the *p*-aminobenzoate anion with protonated aza-containing macrocycles (cyclam, 1,4,8,11-tetraazacyclotetradecane,[6] and aza-12-crown-4[7]).

A survey of the Cambridge Structural Database[8] (version 5.27, update August 2006) revealed two known PABA polymorphs. In the α-form, molecules form chains *via* alternating carboxyl–carboxyl and amine–carboxyl homo- and heterosynthons,[9] while only amine–carboxyl heterosynthons are responsible for the 3D association of PABA molecules in the β-polymorph.[10] PABA is known to be neutral, cationic or anionic in its complexes. Complexes of PABA with such molecules as 4-nitropyridine *N*-oxide (1 : 1), 1,3,5-trinitrobenzene, urea, 2-carboxyphenoxyacetic acid, 4,4′-bipyridyl *N,N*-dioxide, carbamazepine, 4,4′-bipyridine, 2,2′-bipyridine[11–18] represent neutral adducts. Lynch and McClenaghan[19] investigated the influence of the pK_a values on the formation of either neutral-component co-crystals or proton-transfer complexes. In a small number of multicomponent compounds, the carboxylic group of PABA (pK_a = 2.38) protonates the amino group of a Lewis base, *e.g.*, diethylamine (1 : 1)[20] or 2-aminopyrimidine (2 : 1).[21] On the other hand, the amino group of PABA is reported to be protonated by such acids as 3,5-dinitrosacicylic, 5-sulfosalicylic or fluorosilicic acid.[22–24]

As a part of our ongoing efforts toward the supramolecular synthesis of new multicomponent solids involving active pharmaceutical ingredients (APIs), we carried out the systematic investigation of the interaction of PABA with azaheterocycles having different ring sizes (6, 12, 14, 18 atoms in the ring) and a variable number of basic nitrogen atoms (n = 1, 2, 4) capable of varying degrees of protonation by acidic moieties (in our case PABA). The ionized acid–base pairs,[25] or salts by

[a] *Department of Chemistry, Brown University, Providence, Rhode Island, 02912, USA*
[b] *Institute of Applied Physics, Academy of Sciences of Moldova, Academiei str., 5 MD-2028 Chişinău, R. Moldova. E-mail: kravtsov.xray@phys.asm.md, fonari.xray@phys.asm.md; Fax: (+373 22) 725887; Tel: (+373 22) 738154*
[c] *A.V. Bogatsky Physico-Chemical Institute, Lustdorfskaya doroga, 86, 65080 Odessa, Ukraine*
[d] *Odessa State Environmental University, Lvovskaya str., 15, 65016 Odessa, Ukraine*
† The HTML version of this article has been enhanced with colour images.

definition, are the most common multiple-component systems involving APIs.[26,27] To the best of our knowledge, this contribution is the first systematic study of PABA interaction with cyclic molecules of different size and chemical nature.

Experimental

Synthesis and crystallization

Complexes **1–4** were obtained in a similar way by mixing of the corresponding macrocycle (1 mmol) with PABA (2 mmol) in a water–methanol solution and heating until completely dissolved. Complex **5** was obtained by dissolving of an equimolar (1 mmol) amount of the corresponding macrocycle and PABA in a hot water–methanol solution. Crystals suitable for X-ray structural determination were obtained by recrystallization from a mixture of methanol and ethyl acetate. Initial crystallization products were characterized by elemental analysis. Melting points for co-crystals were determined and are presented in Table 1 along with the melting points for the parent compounds.

1. $C_{18}H_{28}N_4O_6$: Calc.: C, 54.53; H, 7.12; N, 14.13. Found: C, 54.57; H, 7.16; N, 14.10%.

2. $C_{30}H_{52}N_6O_5$: Calc.: C, 62.47; H, 9.09; N, 14.57. Found: C, 62.45; H, 9.13; N, 14.61%.

3. $C_{22}H_{38}N_6O_6$: Calc.: C, 54.76; H, 7.94; N, 17.42. Found: C, 54.78; H, 7.91; N, 17.46%.

4. $C_{22}H_{36}N_4O_8$: Calc.: C, 54.53; H, 7.49; N, 11.56. Found: C, 54.56; H, 7.45; N, 11.53%.

5. $C_{19}H_{38}N_2O_{10}$: Calc.: C, 50.21; H, 8.43; N, 6.16. Found: C, 50.24; H, 8.47; N, 6.19%.

Structure determinations

X-Ray data for all complexes were collected on a Bruker SMART-APEX CCD diffractometer by ω and φ-scan mode at 90 K using graphite-monochromated Mo-Kα radiation. There was no intensity decay. Structure solutions were performed by direct methods (SHELXS-97) and refined by full-matrix least-squares methods on F^2 (SHELXL-97).[28] Lorentz and polarization corrections were applied for diffracted reflections. In addition, the data were corrected for absorption using SADABS.[29] In all complexes non-hydrogen atoms were refined anisotropically. H atoms attached to carbons were included in idealized positions in a riding model with isotropic temperature factors (1.2 times the parent carbon atom temperature factor), whereas those on N and O(water) atoms were found from difference Fourier maps and refined isotropically. The hydrogen bonding geometry for **1–5** is summarised in Table 2. All the figures were prepared using MERCURY facilities. Displacement ellipsoids are shown with 50% probability level.

Table 1 Melting points for the starting materials and complexes **1–5**

Complex	Starting materials Mp (L)/ °C	Starting materials Mp (PABA)/ °C	Complex Mp/ °C
1 (piperazinium)(PABA)$_2 \cdot 2H_2O$	44 45	188 189	189 190
2 (H_2teta)(PABA)$_2 \cdot H_2O$	97 105	188 189	270 271
3 (H_2cyclen)(PABA)$_2 \cdot 2H_2O$	108 113	188 189	206 207
4 (diazonia12C4)(PABA)$_2 \cdot 2H_2O$	56 57	188 189	126 127
5 (azonia18C6)(PABA) $\cdot 3H_2O$	46 50	188 189	111 112

Crystal/refinement data

1. $C_{18}H_{28}N_4O_6$: M = 396.44, monoclinic, space group $P2_1/c$, a = 6.5739(13), b = 11.597(2), c = 12.604(3) Å, β = 90.13(3)°, V = 960.9(3) Å^3, Z = 2, D_c = 1.370 g cm^{-3}, μ = 0.104 mm^{-1}, specimen: 0.22 × 0.25 × 0.30 mm, 'T' min/max = 0.74, N_t = 7319, N = 1891, N_o = 1685 (R_{int} = 0.0287), GOF on F^2 = 1.005. Final R indices $>I > 2\sigma(I)$]: $R1$ = 0.0373, $wR2$ = 0.1039; R indices (all data): $R1$ = 0.0420, $wR2$ = 0.1073.

2. $C_{30}H_{52}N_6O_5$: M = 576.78, monoclinic, $C2/c$, a = 19.0506(13), b = 12.1200(9), c = 14.4397(10) Å, β = 107.72(1)°, V = 175.8(4) Å^3, Z = 4, D_c = 1.206 g cm^{-3}, μ = 0.083 mm^{-1}, specimen: 0.25 × 0.25 × 0.20 mm, 'T' min/max = 0.87, N_t = 13 533, N = 3646, N_o = 2940 (R_{int} = 0.0321), GOF on F^2 = 1.006. Final R indices [$I > 2\sigma(I)$]: $R1$ = 0.0484, $wR2$ = 0.1211; R indices (all data): $R1$ = 0.0619, $wR2$ = 0.1283.

3. $C_{22}H_{38}N_6O_6$: M = 482.58, monoclinic, $P2_1$, a = 9.6004(19), b = 11.350(2), c = 12.088(2) Å, β = 111.91(3)°. V = 1222.0(4) Å^3, Z = 2, D_c = 1.311 g cm^{-3}, μ = 0.096 mm^{-1}, specimen: 0.20 × 0.20 × 0.40 mm, 'T' min/max = 0.80. N_t = 9148, N = 4232, N_o = 3939 (R_{int} = 0.0272), GOF on F^2 = 1.009. Final R indices [$I > 2\sigma(I)$]: $R1$ = 0.0366, $wR2$ = 0.0881; R indices (all data): $R1$ = 0.0400, $wR2$ = 0.0906.

4. $C_{22}H_{36}N_4O_8$: M = 484.55 monoclinic, Pc, a = 10.9044(14), b = 9.9475(13), c = 12.1429(15) Å, β = 114.267(2)°, V = 1200.8(3) Å^3, Z = 2, D_c = 1.340 g cm^{-3}, μ = 0.102 mm^{-1}, specimen: 0.10 × 0.40 × 0.40 mm, 'T' min/max = 0.58. N_t = 8749, N = 4343, N_o = 4062 (R_{int} = 0.0267), GOF on F^2 = 1.004. Final R indices [$I > 2\sigma(I)$]: $R1$ = 0.0349, $wR2$ = 0.0800; R indices (all data): $R1$ = 0.0381, $wR2$ = 0.0825.

5. $C_{19}H_{38}N_2O_{10}$: M = 454.51, orthorhombic, $Pca2_1$, a = 24.784(4), b = 9.6757(17), c = 10.0867(18) Å, V = 2418.8(7) Å^3, Z = 4, D_c = 1.248 g cm^{-3}, μ = 0.100 mm^{-1}, specimen: 0.10 × 0.30 × 0.30 mm, 'T' min/max = 0.57, N_t = 12 926, N = 3892, N_o = 3038 (R_{int} = 0.0601), GOF on F^2 = 0.996. Final R indices [$I > 2\sigma(I)$]: $R1$ = 0.0424, $wR2$ = 0.0849, R indices (all data): $R1$ = 0.0575, $wR2$ = 0.0913.

CCDC reference numbers 626905–626909.

For crystallographic data in CIF or other electronic format see DOI: 10.1039/b618207k

Results and discussion

Commercially available PABA, N- and N,O-containing cycles, piperazine, *meso*-5,7,7,12,12,14-hexamethyl-1,4,8,11-tetraazacyclotetradecane (teta), 1,4,7,10-tetraazacyclododecane (cyclen), and azacrown ethers, 1,7-dioxa-4,10-diazacyclododecane (diaza-12-crown-4) and 1,4,7,10,13-pentaoxa-16-azacyclooctadecane

This journal is © the Royal Society of Chemistry and the Centre National de la Recherche Scientifique 2007

Table 2 Hydrogen bonding geometry in **1–5** (Å, °)

D H···A	d(D H)	D(H···A)	d(D···A)	∠(DHA)	Symmetry operation for acceptor
1					
N(1) H(1N1)···O(1)	0.90(2)	2.56(2)	3.311(2)	142(2)	x, y + 1/2, z + 1/2
N(1) H(2N1)···O(1W)	0.89(2)	2.04(2)	2.930(2)	178(2)	x + 1, y + 1/2, z + 1/2
N(2) H(1N2)···O(2)	0.92(2)	1.80(2)	2.697(2)	165(2)	x + 2, y + 1, z
N(2) H(2N2)···O(1)	0.95(2)	1.72(2)	2.632(2)	160(2)	x, y, z
O(1W) H(1W1)···O(1)	0.87(2)	1.95(2)	2.804(2)	168(2)	x, y, z
O(1W) H(2W1)···O(2)	0.88(2)	1.92(2)	2.789(2)	168(2)	x + 2, y 1/2, z + 1/2
2					
N(1) H(1N1)···O(2)	0.86(2)	2.07(2)	2.923(2)	170(2)	x, y, z 1/2
N(1) H(2N1)···O(2)	0.89(2)	2.10(2)	2.988(2)	176(2)	x + 1/2, y 1/2, z 1/2
N(2) H(1N2)···O(1W)	0.89(2)	2.16(2)	3.040(1)	172(1)	x + 1, y + 1, z
N(3) H(1N3)···N(2)	0.94(2)	2.01(2)	2.790(2)	139(1)	x, y, z
N(3) H(2N3)···O(1)	0.93(2)	1.78(2)	2.704(2)	171(2)	x, y, z
O(1W) H(1W)···O(1)	0.93(2)	1.82(2)	2.737(1)	168(2)	x + 1, y + 1, z
3					
N(1A) H(1NA)···O(2W)	0.94(2)	1.99(2)	2.928(3)	176(2)	x, y 1, z + 1
N(1A) H(2NA)···O(1A)	0.89(3)	2.03(3)	2.911(3)	170(3)	x 1, y 1/2, z
N(1B) H(1NB)···O(2B)	0.94(3)	2.27(3)	3.098(3)	146(2)	x 2, y 1/2, z 1
N(1B) H(2NB)···O(1W)	0.92(3)	2.14(3)	2.981(3)	152(2)	x 2, y + 1/2, z 1
N(3) H(1N3)···N(4)	0.94(2)	2.29(2)	2.796(3)	113(2)	x, y, z
N(3) H(1N3)···N(2)	0.94(2)	2.34(2)	2.857(2)	114(2)	x, y, z
N(3) H(2N3)···O(1B)	0.92(2)	1.82(2)	2.710(2)	164(2)	x, y, z
N(4) H(1N4)···O(2B)	0.86(2)	2.28(2)	3.116(2)	163(2)	x 1, y 1/2, z 1
N(5) H(1N5)···O(2A)	0.97(3)	1.71(3)	2.656(2)	165(2)	x, y, z
N(5) H(1N5)···O(1A)	0.97(3)	2.45(3)	3.146(2)	129(2)	x, y, z
N(5) H(2N5)···N(2)	0.87(2)	2.37(2)	2.840(3)	114(2)	x, y, z
O(1W) H(1W1)···O(1B)	0.89(3)	1.98(3)	2.850(2)	166(3)	x 1, y 1/2, z 1
O(1W) H(2W1)···O(1A)	0.85(3)	1.92(4)	2.753(2)	167(3)	x, y, z
O(2W) H(1W2)···O(1B)	0.89(3)	1.98(3)	2.869(2)	172(2)	x 1, y + 1/2, z 1
O(2W) H(2W2)···O(2B)	0.91(4)	1.87(4)	2.765(2)	165(3)	x, y, z
4					
N(1A) H(2NA)···O(1B)	0.84(3)	2.36(3)	3.069(3)	143(2)	x, y 1, z 1/2
N(1B) H(1NB)···O(1W)	0.86(3)	2.27(3)	3.105(3)	165(2)	x 1, y 1, z
N(1B) H(2NB)···O(2A)	0.88(3)	2.08(3)	2.942(3)	163(2)	x 1, y 1, z 1/2
N(3) H(3A)···O(1W)	0.88(3)	1.93(3)	2.777(2)	162(2)	x, y, z
N(3) H(3B)···O(1A)	0.90(3)	1.97(3)	2.850(2)	164(2)	x, y, z
N(4) H(4A)···O(1A)	0.91(2)	2.18(2)	2.993(2)	148(2)	x, y, z
N(4) H(4B)···O(1B)	0.98(2)	1.66(2)	2.635(2)	169(2)	x, y, z
O(1W) H(1W1)···O(2B)	0.86(2)	1.87(2)	2.725(2)	172(3)	x + 1, y, z + 1/2
O(1W) H(2W1)···O(2W)	0.87(2)	1.83(2)	2.698(2)	172(3)	x, y, z
O(2W) H(1W2)···O(2A)	0.86(2)	1.98(2)	2.762(2)	150(2)	x, y, z
O(2W) H(2W2)···O(1B)	0.87(3)	1.92(3)	2.758(2)	162(4)	x + 1, y, z
5					
N(1) H(1N1)···O(5)	0.88(3)	2.22(3)	3.061(3)	161(3)	x, y 1, z + 1
N(1) H(2N1)···O(2)	0.90(3)	2.08(3)	2.962(3)	167(3)	x + 1, y, z + 1/2
N(2) H(2N2)···O(1)	0.86(3)	1.91(3)	2.759(3)	170(3)	x, y, z
N(2) H(1N2)···O(1W)	0.98(3)	1.90(3)	2.881(3)	171(3)	x, y, z
O(1W) H(1W1)···O(6)	0.88(6)	1.97(6)	2.838(3)	167(5)	x, y, z
O(1W) H(2W1)···O(4)	0.83(4)	2.26(4)	3.077(3)	170(4)	x, y, z
O(1W) H(2W1)···O(3)	0.83(4)	2.54(4)	2.999(3)	116(3)	x, y, z
O(2W) H(1W2)···O(3W)	0.81(5)	2.04(5)	2.799(3)	156(5)	x, y, z
O(2W) H(2W2)···O(1W)	0.85(4)	2.09(4)	2.938(3)	172(4)	x, y, z
O(3W) H(1W3)···O(2W)	0.82(5)	2.11(5)	2.908(3)	164(4)	x + 3/2, y, z + 1/2
O(3W) H(2W3)···O(1)	0.80(4)	1.99(4)	2.784(3)	175(4)	x, y, z

(aza-18C6) were chosen for complex formation. The macrocycles gradually increase from 6 to 18 ring atoms, and contain one to four 'anchor positions', namely secondary NH-amino groups capable of being protonated to give a mono-, di-, tri- or tetra-cation.[8] In the complexes described herein, only aza-18C6 is protonated by PABA to a single cation, while all the other macrocycles are doubly protonated to form the dications.

In all five complexes the acidic proton transfer occurs from the carboxylic group of PABA molecule to the amino-group of macrocycle. The crystallographic evidence for this proton transfer is the approximately equal C–O distances in the carboxylate group consistent with the carboxylate anion (the most different values in the same COO group are 1.250 and 1.278 Å that correspond to the delocalised C–O bond) and unbiased localisation of two

Fig. 1 ORTEP plot of the compact formula unit in **1**.

hydrogen atoms in the close proximity of macrocyclic nitrogen atoms.

The formula units for five studied complexes **1–5** shown in Fig. 1–5 represent the common view of the hydrated acid–base complexes of the compositions $(H_2L)(PABA)_2 \cdot 2H_2O$ for L = piperazine, cyclen, diaza-12C4 (complexes **1**, **3** and **4**, respectively), $(H_2L)(PABA)_2 \cdot H_2O$ for L = teta (complex **2**), and $(HL)(PABA) \cdot 3H_2O$ for L = aza-18C6 (complex **5**). The hydrogen bonds for **1–5** are listed in Table 2. The ionic components of **1–5** invariably form charge-assisted hydrogen bonds, and the $N(NH_2^+)\cdots O(COO^-)$ distances are the shortest amongst those that sustain the structures. In all materials, the H-bonded complexes form additional hydrogen bonds to water molecules resulting in 3D supramolecular architectures where PABA moieties are involved in both PABA–macrocycle and PABA–PABA interactions. The N–H···O and O–H···O hydrogen bonds provide for intermolecular binding, while N–H···N intramolecular hydrogen bonds were found within $(H_2teta)^{2+}$ and $(H_2cyclen)^{2+}$ dications.

In **1** (Fig. 6(a)) each aminia group is H-bonded to two PABA anions, which act as a bridge between two centrosymmetric piperazinium cations, resulting in a supramolecular chain along [010]. The length of the two hydrogen bonds varies slightly (N···O separations being 2.697 and 2.632 Å), both being the shortest in the structure. The resulting supramolecular synthons are hetero-tetramers corresponding to the $R_4^4(12)$ rings in graph set notation.[30] Furthermore, two inversion center related PABA anions and two water molecules form $R_4^4(20)$ hetero-tetrameric rings, which assemble into corrugated chains *via* shared water molecules (Fig. 6(b)). The combination of these two motifs results in the 3D grid.

In **2** (Fig. 2) the $(H_2teta)^{2+}$ dication resides around an inversion center, and the anion occupies a general position. The acid–base interaction (N···O separations being 2.704(2) Å) is the shortest in the structure; but unlike **1**, only one carboxylate oxygen, O1, participates in the PABA–cycle interaction. Additionally aminia moieties are involved in typical

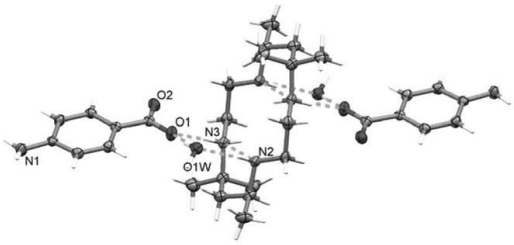

Fig. 2 ORTEP plot of the compact formula unit in **2**.

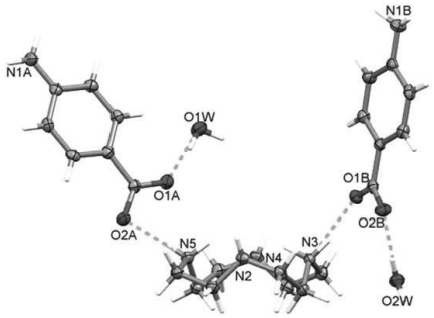

Fig. 3 ORTEP plot of the compact formula unit in **3**.

NH···H intramolecular hydrogen bonds that span the cyclic cavity. The other carboxylate oxygen atom, O2, and the amino-group of PABA are involved in NH···O anion–anion self-associated interactions *via* alternating of $R_2^4(8)$ and $R_4^4(32)$ rings, thus generating a negatively charged sheet as shown in Fig. 7(a). The same anionic sheet was reported in the structure $(cyclamH_2)^{2+} \cdot 2(PABA)^- \cdot H_2O$[6]and resembles the association of neutral PABA molecules in its β-polymorph.[10] The $(H_2teta)^{2+}$ cations are linked to the anionic framework *via* direct NH···O hydrogen bonds and additionally *via* intermediate water molecules. The mode of water incorporation in the crystal structure is depicted in Fig. 7(b).

Complexes **3** and **4** both contain the 12-membered macrocyclic dication, two crystallographically non-equivalent PABA anions (A and B) and two water molecules (Fig. 3 and 4). Although in the both cycles NH_2^+-aminia centers are separated by the chain $[CH_2CH_2O(NH)CH_2CH_2]$ of the same length, the conformations of the molecules are different, due to the different set of donor, acceptor atoms in the rings and the availability of the short intramolecular $NH^+\cdots N$ interactions in $(H_2cyclen)^{2+}$ (Table 2). This results in different modes of interaction with PABA anions, as it is clearly evident from Fig. 3 and 4. In **3**, three charged components are held together *via* two single $NH^+\cdots O$ hydrogen bonds, 2.656(2) and 2.710(2) Å, and the anions are in a 'side arrangement', while in **4** one of the PABA anions acts as a bridge between two

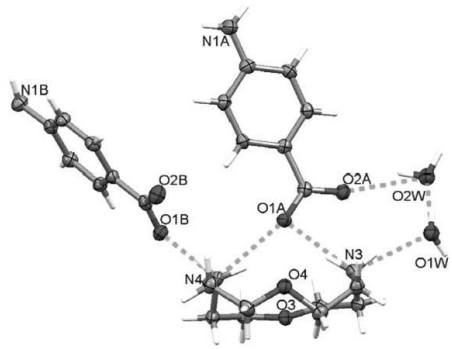

Fig. 4 ORTEP plot of the compact formula unit in **4**.

This journal is © the Royal Society of Chemistry and the Centre National de la Recherche Scientifique 2007

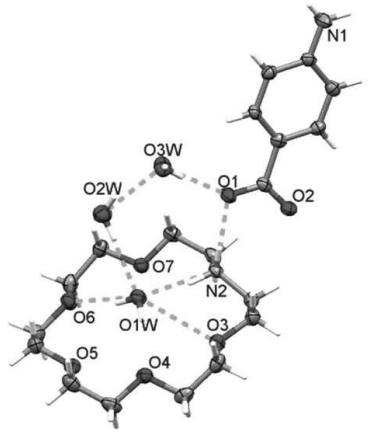

Fig. 5 ORTEP plot of the compact formula unit in **5**.

cyclic nitrogens, N3 and N4, and thus is arranged just above the cyclic cavity. Further differences are evident from the PABA anions arrangements in the crystals. In complex **3** the PABA-A anions form head-to-tail chains due to the $NH_2\cdots O(COO^-)$ interactions (Fig. 8), which alternate with the PABA-B anions without any direct PABA–PABA H-bonded interactions, and are surrounded by water molecules. The connection of two types of anions occurs *via* 12-membered H-bonded ring and combines two PABA-A anions that belong

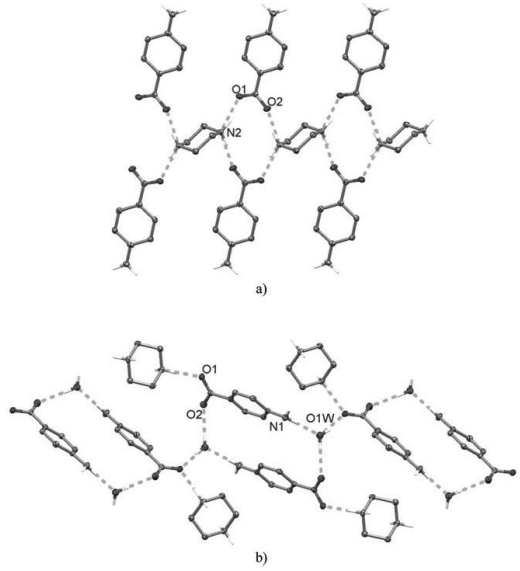

Fig. 6 (a) Fragment of chain combining the opposite-charged components in **1**. (b) Mode of association of PABA anions and water molecules, only few of the piperazinium cations attached to this chain are shown. C-bound H-atoms are omitted for clarity.

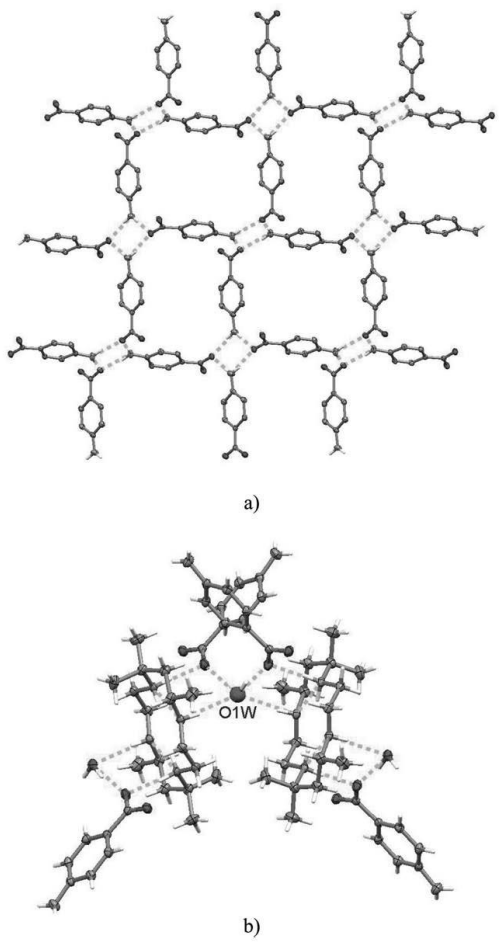

Fig. 7 (a) The negative sheet of PABA anions in **2** sustained by the alternation of $R_2^4(8)$ and $R_4^4(32)$ hydrogen-bonded rings. C-bound H-atoms are omitted for clarity. (b) The mode of water incorporation in the structure.

to the same chain, one PABA-B anion and two different water molecules. It is interesting to note that PABA-B anion appears to be completely hydrated, its carboxylic group and one hydrogen of amino group participate in three $COO^-\cdots O$(-water) and one $NH\cdots O$(water) hydrogen bonds.

In **4** six hydrogen bonds of the $NH^+\cdots O^-$ and $OH\cdots O$ types act within the formula unit shown in Fig. 4, while four other bind the formula units into a supramolecular 3D network: translated along [100] direction complexes are combined into chain *via* bridging O2W water molecule (Fig. 9(a)). The amino-group of each of two symmetrically independent PABA anions (A or B), being hydrogen bonded with its counterpart, forms the ABAB head-to-tail chain (Fig. 9(b)), similar to that found in **3**. Water molecule O1W unites these two structural motifs into 3D grid.

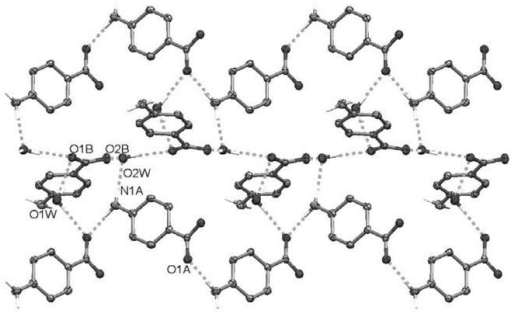

Fig. 8 Fragment of the continuous negative motif in (**3**) built of the alternative rows of PABA-A and -B anions and water molecules; view down the [100] direction. The $R_5^4(12)$ ring in a conditional 'boat' conformation binds three PABA anions (AAB) and two water molecules. C-bound H-atoms and $[H_2cyclen]^{2+}$ cations are omitted for clarity.

Contrary to **1–3**, with the point inclusion of water molecules in those structures, in **4** we observe the association of two water molecules into a two-membered O1W···O2W water cluster, the O···O separation being 2.698(2) Å. These water molecules act as double donors and single acceptors, thus only the O1W water molecule interacts with the macrocycle, while the second O2W water molecule bridges carboxylic groups of A and B anions.

Complex **5** stands aside due to only one cyclic aminia binding site, the largest cavity amongst the discussed heterocycles and the richness in a number of included water molecules. Three incorporated water molecules fulfill different

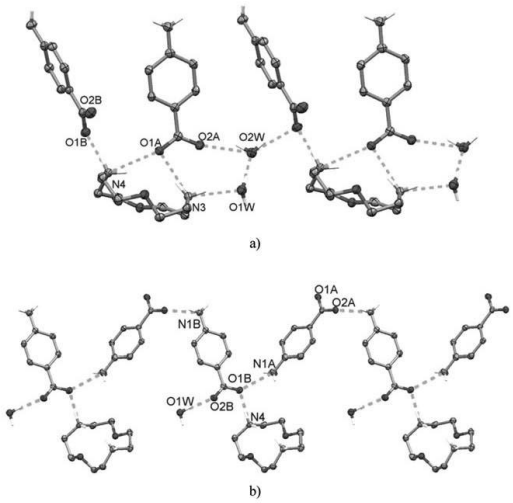

Fig. 9 (a) The hydrogen-bonded chain of complexes (**4**) developed along [100] direction. (b) The chain of alternating A and B PABA anions running along [001] direction. Only a few of the macrocyclic cations are shown. C-bound H-atoms are omitted for clarity.

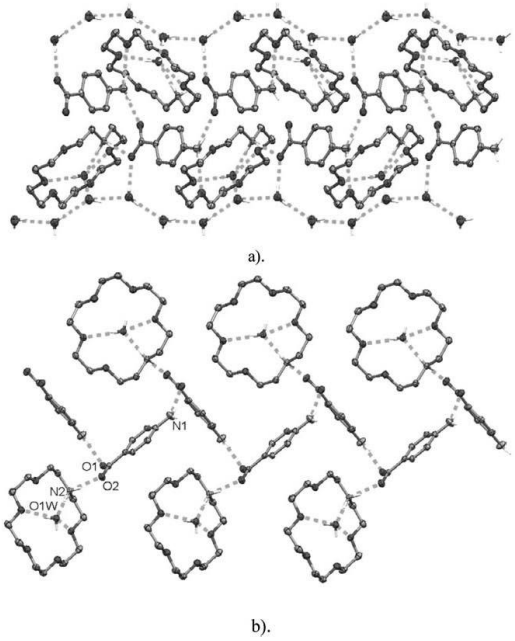

Fig. 10 (a) Fragment of crystal packing in **5** showing the bridging PABA and macrocyclic cation inclusion and water chains, view along [010] direction. (b) Fragment of face-to-tail PABA chain with the macrocyclic cations attached to the PABA carboxylic moiety. C-bound H-atoms are omitted for clarity.

structural functions. Water molecule O1W in a perching mode centers the macrocyclic cavity acting as an H-double donor towards macrocyclic oxygens and as an H-acceptor from one of the aminia hydrogens. The displacement of O1W atom from the mean plane of the macrocyclic heteroatoms equals to 0.918 Å. The same O1W water molecule is H-bonded to the next O2W water molecule, which, alternating with O3W, form the continuous water chain in the structure (Fig. 10(a)). The NH_2^+-group of the macrocycle is characterized by the *exo,endo*-orientation of its hydrogen atoms, that explains the 1 : 1 ratio of the acid–base associate, where the charged units are bound *via* one single $NH^+\cdots O(COO^-)$ hydrogen bond, N2···O1 2.759(3) Å. This structure is also exceptional by the involvement of PABA amino-group in the interactions with the crown oxygen atom of the macrocylic cavity *via* a conventional NH···O hydrogen bond, N1···O5, 3.061(3) Å and, henceforth, the bridging function of both PABA anion and the macrocyclic cation. The robust motif of PABA···PABA head-to-tail association still exists in this structure, combining anions related by the two-fold screw axis (Fig. 10(b)).

The predominant structural features in complexes **1–5** are the interaction of the PABA carboxylic group with the amino-group of cyclic molecule accompanied by a proton transfer and resulting in either single NH···O hydrogen bond in **1–3** and **5**, or bifurcated (two-point) hydrogen bond in **4**. Data mining the CSD[8] reveals no examples for cyclen, diaza-12-

 This journal is © the Royal Society of Chemistry and the Centre National de la Recherche Scientifique 2007

crown-4 and aza-18-crown-6 complexes with carbonic acids, and thus this contribution represents the first examination of such interactions, with a specific emphasis on the interaction of PABA with these cyclic molecules. Examples of interactions between carbonic acids and teta (Refcodes CUTVOC, CUVNOW, CUVNUC, JAHCOL, HUSRUI, WUXJAA) and piperazine (more than 50 hits), reveal that all adducts are organic salts with the carboxylate group involved in the different modes of interaction with the protonated binding site of the ring. The tetrameric mode of two carboxylic groups and two NH_2^+-aminia centers association found in **1**, is typical for piperazinium adducts (BAKYES, BEXCEM10, BEXDAJ01, BEXDIR01, BOCLIO, RIKBIW, ZEMXOE, ZUGQEX), including the formation of $R_4^4(12)$ heterosynthon (HIHJOX, QIBRUO, VAJWUZ). Surprisingly, no chelate-type interaction, common for carboxylic groups and observed for the *p*-aminobenzoate anion in its cyclam complex[6] and for the salicylate anion in complexes with similar macrocycles,[31] was exhibited here. Typical for 'all O-containing' crown ethers, an interaction with the neutral PABA molecule *via* two conventional NH···O(crown) hydrogen bonds with the PABA amino-group exhibits itself only in complex **5** in the form of a rather weak single subsidiary NH(PABA)···O(crown) interaction.

Excluding **1**, two main motifs of PABA anion self-association are observed: in **3–5** the PABA anions are linked into a head-to-tail chain *via* a single NH···O hydrogen bond; the sheet motif similar to that in β-polymorph of PABA is observed only in **2** and in $(cyclamH_2)^{2+} \cdot 2(PABA) \cdot H_2O$.[6]

Water molecules feature different structural functions in the complexes.[32,33] Water point inclusion is registered in **1–3**: in **1** it acts as a double H-donor and single H-acceptor towards three PABA anions and is responsible for their association in the ribbons. Water incorporation in **1** results in a complete violation of any self-association of PABA anions. This situation differs from **2**, where water function, although present, might be considered as a negligible one, adding only a minor component to the binding between the $(H_2teta)^{2+}$ cations and PABA anionic sheet, which is the most ordered and vast fragment of PABA association within **1–5**. The transition from aza-macrocycles to N,O-crown ethers reveals the association of water molecules, acting as a two-membered cluster in **4**, three-membered cluster in bis(1,4,7-trioxa-10-azoniacyclododecane) bis(4-aminobenzoate) trihydrate[7] or as an infinite chain in **5**.

Conclusion

The supramolecular synthesis of the PABA–macrocycle complexes in a water–methanol solution unambiguously leads to the organic hydrated salts. The number of PABA involved in the complex equals to the number of N-protonated binding sites in the cyclic molecule. The present study shows the remarkable coordinating properties of the PABA molecule, and illustrates its ability to achieve a suitable balance between the driving force to coordinate to aminia binding sites of the cyclic molecules and its tendency to self-assemble *via* supramolecular heterosynthons in the structure of the complexes described herein.

The proton transfer within the complex seems to be a favorable factor for aquation, while in the case of the less polar classic O-containing crown ethers the anhydrous adducts have been obtained.[5] In the light of the hot paper[34] addressed to the important factors crucial for the organic crystal hydrates formation, the following generalizations for the studied system PABA–macrocycle could be highlighted. Survey of the hydrogen-bonding arrays easily reveals the significant role of water molecules to balance the number of proton-donor and proton-acceptor sites involved in the intermolecular hydrogen bonding interactions. In all supramolecular associates excluding **2** the sum of proton–acceptor sites for PABA and heterocyclic molecule exceeds the sum of proton-donors, and water molecules compensate this misbalance. Our study shows that the degree of such misbalance correlates with a number of water molecules included in the supramolecular associate. The largest disagreement between the number of H-donors and H-acceptors was found in trihydrate **5**, while only one water molecule per formula unit is involved in the supramolecular associate **2**, where the system PABA-heterocycle reveals a balance of H-binding sites. Thus, the reported crystal structures obviously show the important glue water function, which in all cases serves as an intermediate between the supramolecular reagents.

Acknowledgements

This study is supported by MRDA (Moldova)–CRDF (U.S.) award No. MRDA-008:BGP-III, MOC2-3063-CS-03.

References

1 (*a*) P. J. Osgood, S. H. Moss and D. J. Davies, *J. Invest. Dermatol.*, 1982, **79**(6), 354; (*b*) T. Sahr, S. Ravanel, G. Basset, B. P. Nichols, A. D. Hanson and F. Rebeille, *Biochem. J.*, 2006, **396**(1), 157; (*c*) O. Kornfeld and B. P. Nichols, *FEMS Microbiol. Lett.*, 2005, **251**(1), 137; (*d*) L. M. Elandalloussi, P. M. Rodrigues, R. Afonso, R. B. Leite, P. A. Nunes and M. L. Cancela, *Mol. Biochem. Parasitol.*, 2005, **142**(1), 106; (*e*) I. Meneau, D. Sanglard, J. Bille and P. M. Hauser, *Antimicrob. Agents Chemother.*, 2004, **48**(7), 2610; (*f*) J. Berglez, P. Iliades, W. Sirawaraporn, P. Coloe and I. Macreadie, *Int. J. Parasitol.*, 2004, **34**(1), 95; (*g*) L. A. Castelli, N. P. Nguyen and I. G. Macreadie, *FEMS Microbiol. Lett.*, 2001, **199**(2), 181; (*h*) P. Wang, P. F. Sims and J. E. Hyde, *Parasitology*, 1997, **115**(Pt 3), 223; (*i*) K. Yamasaki, T. Maruyama, U. Kragh-Hansen and M. Otagiri, *Biochim. Biophys. Acta*, 1996, **1295**(2), 147; (*j*) C. B. Lalor, G. L. Flynn and N. Weiner, *J. Pharm. Sci.*, 1994, **83**(11), 1525; (*k*) L. Ma, C. Ramachandran and N. D. Weiner, *J. Pharm. Sci.*, 1992, **81**(11), 1104.
2 (*a*) M. C. Etter and G. A. Frankenbach, *Chem. Mater.*, 1989, **1**, 10–12.
3 (*a*) M. Alleaume, G. Salas-Cimingo and J. Decap, *C. R. Acad. Sci., Ser. C (Chim.)*, 1966, **262**, 416.
4 (*a*) A. Elbasyouny, H. J. Brugge, K. Deuten, M. Dickel, A. Knohel, K. U. Koch, J. Kopf, D. Melzer and G. Rudolph, *J. Am. Chem. Soc.*, 1983, **105**, 6568.
5 M. S. Fonari, Yu. A. Simonov, J. Lipkowski, A. A. Dvorkin and E. V. Ganin, *Supramol. Chem.*, 1994, **4**, 43.
6 C. M. Zakaria, A. J. Lough, G. Ferguson and C. Glidewell, *Acta Crystallogr., Sect. B*, 2004, **60**, 65.
7 S. S. Basok, G. Bocelli, M. S. Fonari, E. V. Ganin and Yu. A. Simonov, *Acta Crystallogr., Sect. C*, 2006, **62**, o50.
8 F. H. Allen and O. Kennard, *Acta Crystallogr., Sect. B*, 2002, **58**, 380–388.
9 T. F. Lai and R. E. Marsh, *Acta Crystallogr.*, 1967, **22**, 885.
10 S. Gracin and A. Fischer, *Acta Crystallogr., Sect. E*, 2005, **61**, o1242.

This journal is © the Royal Society of Chemistry and the Centre National de la Recherche Scientifique 2007

11 R. M. Fuquen, R. H. De A. Santos and J. R. Lechat, *Acta Crystallogr., Sect. C*, 1996, **52**, 220.
12 D. E. Lynch, G. Smith, K. A. Byriel and C. H. L. Kennard, *Chem. Commun.*, 1992, 300.
13 G. Smith, K. E. Baldry, K. A. Byriel and C. H. L. Kennard, *Aust. J. Chem.*, 1997, **50**, 727.
14 K. A. Byriel, D. E. Lynch, G. Smith and C. H. L. Kennard, *Aust. J. Chem.*, 1991, **44**, 1459.
15 R. Moreno-Fuquen, M. Font i Carot, M. Garriga, F. Cano, M. Martinez-Ripoll, J. Valderrama-Naranjo and M. L. Serratto, *Acta Crystallogr., Sect. E*, 2003, **59**, o495.
16 J. A. McMahon, J. A. Bis, P. Vishweshwar, T. R. Shattock, O. L. McLaughlin and M. J. Zaworotko, *Z. Kristallogr.*, 2005, **220**, 340.
17 Ruihu Wang, Feilong Jiang, Youfu Zhou, Lei Han and Maochun Hong, *Inorg. Chim. Acta*, 2005, **358**, 545.
18 J. R. Bowers, G. W. Hopkins, G. P. A. Yap and K. A. Wheeler, *Cryst. Growth Des.*, 2005, **5**, 727.
19 See, for example, besides already mentioned: D. E. Lynch and I. McClenaghan, *Acta Crystallogr., Sect. C*, 2001, **57**, 830.
20 G. Smith, K. A. Byriel and C. H. L. Kennard, *Aust. J. Chem.*, 1999, **52**, 625.
21 D. E. Lynch, G. Smith, D. Freney, K. A. Byriel and C. H. L. Kennard, *Aust. J. Chem.*, 1994, **47**, 1095.
22 G. Smith, D. E. Lynch, K. A. Byriel and C. H. L. Kennard, *Aust. J. Chem.*, 1995, **48**, 1133.
23 G. Smith, U. D. Wermuth and J. M. White, *Acta Crystallogr., Sect. E*, 2005, **61**, o313.
24 V. O. Gelmboldt, A. A. Ennan, E. V. Ganin, Yu. A. Simonov, M. S. Fonari and M. M. Botoshansky, *J. Fluorine Chem.*, 2004, **125**, 1951.
25 Z. J. Li, Yu. Abramov, J. Bordner, J. Leonard, A. Medek and A. V. Trask, *J. Am. Chem. Soc.*, 2006, **128**, 8199.
26 S. G. Fleischman, S. S. Kuduva, J. A. McMahon, B. Moulton, R. D. B. Walsh, N. Rodriguez- Hornedo and M. J. Zaworotko, *Cryst. Growth Des.*, 2003, **3**, 909.
27 P. Vishweshwar, J. A. Mcmahon, J. A. Bis and M. J. Zaworotko, *J. Pharm. Sci.*, 2006, **95**, 499.
28 G. M. Sheldrick, *SHELXS and SHELXL97 Programs for structure refinement and solution*, Göttingen, Germany, 1997.
29 SADABS (Area Detector Absorption Correction), Siemens Industrial Automation, Inc, Madison, WI, 1996.
30 (*a*) M. C. Etter, *Acc. Chem. Res.*, 1990, **23**, 120; (*b*) J. Bernstein, R. E. Davis, I. Shimoni and N.-L. Chang, *Angew. Chem., Int. Ed. Engl.*, 1995, **34**, 1555.
31 (*a*) M. S. Fonari, V. Ch. Kravtsov, Yu. A. Simonov, S. S. Basok and E. V. Ganin, Supramolecular architecture in the co-crystals of azacrown ethers with salicylic acid, in *Moldavian Polish Ukrainian Symposium on Supramolecular Chemistry*, Chisinau, Moldova, October 10 12, 2005, Abstracts, p. 65.
32 (*a*) T. M. Krygowski, S. J. Grabowski and J. Konarski, *Tetrahedron*, 1998, **54**, 11311.
33 (*a*) A. L. Gillon, N. Feeder, R. J. Davey and R. Storey, *Cryst. Growth Des.*, 2003, **3**, 663.
34 (*a*) L. Infantes, L. Fábián and W. D. S. Motherwell, *CrystEngComm*, 2007, **9**, 65.

This journal is © the Royal Society of Chemistry and the Centre National de la Recherche Scientifique 2007

Додаток В
Копія статті.

“Кристаллическая структура гексафторосиликата орто-толуидиния”

ЖУРНАЛ НЕОРГАНИЧЕСКОЙ ХИМИИ, 2007, том 52, № 5, с. 1–5

ФИЗИЧЕСКИЕ МЕТОДЫ ИССЛЕДОВАНИЯ

УДК 541.49:546.284.161-32:547.551

КРИСТАЛЛИЧЕСКАЯ СТРУКТУРА ГЕКСАФТОРОСИЛИКАТА *ОРТО*-ТОЛУИДИНИЯ

© 2007 г. **В. О. Гельмбольдт*, Э. В. Ганин**, М. М. Ботошанский***, М. С. Фонарь****, А. А. Эннан****

**Физико-химический институт защиты окружающей среды и человека Министерства образования и науки Украины и НАН Украины, Одесса*

***Одесский государственный экологический университет, Украина*

****Израильский технологический институт, Хайфа, Израиль*

*****Институт прикладной физики АН Республики Молдова, Кишинев*

Поступила в редакцию 17.08.2006 г.

Методом РСА определено строение комплекса $(o\text{-}CH_3C_6H_4NH_3)_2SiF_6$. В ионной структуре гексафторосиликата анионы SiF_6^{2-} (Si–F 1.595(9)–1.683(17) Å) и катионы $o\text{-}CH_3C_6H_4NH_3^+$ объединены Н-связями NH···F (N···F 2.757(10)–3.25(2) Å). Компоненты структуры объединены в слой, центральную часть которого формируют анионы SiF_6^{2-}, а наружные гидрофобные поверхности – ароматические циклы катионов.

Известно, что реализующиеся в структурах "ониевых" гексафторосиликатов межионные Н-связи в заметной степени определяют особенности геометрии анионов SiF_6^{2-} [1, 2] и физико-химическое поведение солей [3]. Настоящая работа продолжает начатые ранее исследования [4–6] влияния Н-связей на строение и свойства гексафторосиликатов ариламмония и посвящена изучению кристаллической структуры гексафторосиликата *орто*-толуидиния.

ЭКСПЕРИМЕНТАЛЬНАЯ ЧАСТЬ

Синтез. Монокристаллы соединения $(o\text{-}CH_3C_6H_4NH_3)_2SiF_6$ (**I**) получили по методике [4].

РСА. Параметры элементарной ячейки и трехмерный набор интенсивностей отражений для монокристалла I размером 0.24 × 0.14 × 0.01 мм получены на дифрактометре Nonius Kappa CCD (MoK_α-излучение, графитовый монохроматор, ω-сканирование, $2\theta_{max} = 51.0°$) при 293 K. Всего зарегистрировано 5483 отражения ($-16 \le h \le 16$, $-6 \le k \le 6$, $-11 \le l \le 12$), из них 1452 независимых.

Кристаллы I ($C_{14}H_{20}F_6N_2Si$, M = 358.41) моноклинные: a = 14.582(3), b = 5.892(1), c = 10.184(2) Å, β = 105.83(3)°, V = 841.8(3) Å^3, $\rho_{выч}$ = 1.414 г/см^3, μ = 0.198 мм$^{-1}$, $F(000)$ = 372, Z = 2, пр. гр. $P2_1/c$.

Структура расшифрована прямым методом (SHELXS-97 [7]) и уточнена полноматричным анизотропным методом наименьших квадратов (SHELXL-97 [7]).

Окончательные результаты уточнения: R_1 = 0.0525, wR_2 = 0.1167 по отражениям с $I > 2\sigma(I)$, R_1 = 0.1380, wR_2 = 0.1376 по всем отражениям. Значения $\Delta\rho_{max}$, $\Delta\rho_{min}$ составляют 0.212 и –0.145 eÅ^{-3} соответственно.

В центросимметричном гексафторсиликат-анионе атомы фтора разупорядочены по двум позициям с заселенностями 0.602 и 0.398; обе позиции уточнены в анизотропном приближении. Положение атомов водорода при атомах углерода уточнено по модели "наездника". Атомы водорода аммонийной группы, локализованные из разностных синтезов Фурье, уточняли изотропно с применением мягких ограничений (инструкция SADI для расстояний N–H и H···H).

Длины некоторых связей и валентные углы приведены в табл. 1. CIF депонирован в Кембриджском банке структурных данных, номер регистрации CCDC 614304.

РЕЗУЛЬТАТЫ И ИХ ОБСУЖДЕНИЕ

Структурные единицы комплекса I – гексафторосиликат-анионы и катионы *о*-толуидиния, объединенные водородными связями NH···F (рис. 1). Обе позиции разупорядоченных атомов фтора принимают участие в разветвленной системе Н-связей. В табл. 2 приведены геометрические параметры Н-связей для обоих положений разупорядоченного аниона SiF_6^{2-}. Обсуждение струк-

Таблица 1. Длины связей (*d*) и валентные углы (ω) в структуре I

Связь	*d*, Å	Угол	ω, град
Si(1)–F(1)	1.611(10)	F(2)Si(1)F(1)	87.9(4)
Si(1)–F(2)	1.611(5)	F(2)Si(1)F(3)	91.2(4)
Si(1)–F(3)	1.630(5)	F(1)Si(1)F(3)	88.5(5)
Si(1)–F(1')	1.683(17)	F(3')Si(1)F(2')	90.0(7)
Si(1)–F(2')	1.603(6)	F(3')Si(1)F(1')	93.3(8)
Si(1)–F(3')	1.595(9)	F(2')Si(1)F(1')	96.0(7)
C(1)–C(6)	1.344(5)	C(6)C(1)C(2)	121.5(4)
C(1)–C(2)	1.402(5)	C(6)C(1)N(1)	122.1(4)
C(1)–N(1)	1.453(5)	C(2)C(1)N(1)	116.4(4)
C(2)–C(3)	1.343(6)	C(3)C(2)C(1)	119.7(4)
C(3)–C(4)	1.381(6)	C(2)C(3)C(4)	119.7(5)
C(4)–C(5)	1.358(6)	C(5)C(4)C(3)	120.7(5)
C(5)–C(6)	1.405(5)	C(4)C(5)C(6)	120.2(4)
C(6)–C(7)	1.480(5)	C(1)C(6)C(5)	118.2(4)
		C(1)C(6)C(7)	122.4(5)
		C(5)C(6)C(7)	119.4(5)

* Штрихами отмечены позиции атомов F(1)–F(3).

туры базируется только на позиции с большей заселенностью, поскольку общий мотив упаковки остается неизменным. Все атомы водорода аммонийной группы и все атомы фтора аниона SiF_6^{2-} вовлечены в систему Н-связей. Ближайшее окружение катиона формируют три аниона SiF_6^{2-}, занимающих частные позиции и находящихся в вершинах практически равностороннего треугольника со сторонами 5.892, 5.883 и 5.883 Å (рис. 2). Атом азота аммонийной группы отстоит от этой плоскости на 1.75 Å. В свою очередь, каждый анион SiF_6^{2-} занимает позицию в центре гексагона, образующегося в результате сочленения шести ближайших треугольников таким образом, что катионы ориентированы по обе стороны от плоскости анионов. Компоненты структуры объединены в слой, перпендикулярный направлению *a* в кристалле (рис. 4). Центральную часть слоя формируют анионы SiF_6^{2-}, наружные гидрофобные поверхности слоя создаются ароматическими циклами катионов.

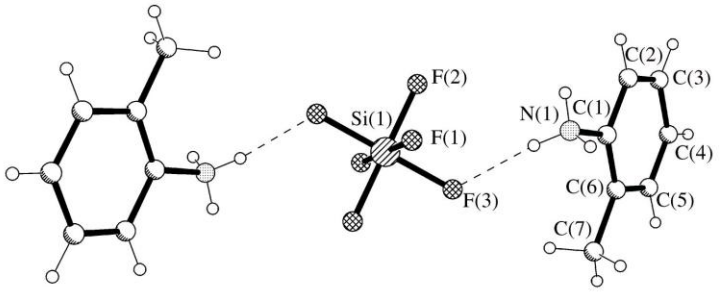

Рис. 1. Строение комплекса I с нумерацией атомов.

Таблица 2. Геометрические параметры Н-связей в структуре I*

D–H···A	Расстояние, Å			Угол DHA, град
	D–H	H···A	D···A	
N(1)–H(1N)···F(1)#2	0.81(2)	2.00(3)	2.797(10)	170(3)
N(1)–H(1N)···F(2)#3	0.81(2)	2.51(3)	3.087(10)	130(3)
N(1)–H(2N)···F(3)	0.79(2)	2.00(3)	2.757(10)	160(4)
N(1)–H(3N)···F(2)#4	0.82(2)	2.13(3)	2.878(10)	153(4)
N(1)–H(1N)···F(1')#2	0.81(2)	2.47(3)	3.25(2)	164(3)
N(1)–H(1N)···F(3')#2	0.81(2)	2.37(3)	2.955(14)	131(3)
N(1)–H(2N)···F(1')	0.79(2)	2.51(4)	3.136(19)	138(3)
N(1)–H(2N)···F(2')	0.79(2)	2.34(3)	2.963(16)	136(3)
N(1)–H(3N)···F(1')#4	0.82(2)	2.26(3)	3.02(2)	155(4)
N(1)–H(3N)···F(3')#5	0.82(2)	2.15(3)	2.820(19)	139(3)

* Преобразования симметрии, используемые для генерации эквивалентных атомов: #1 $-x, -y, -z$; #2 $-x, y + 1/2, -z + 1/2$; #3 $x, -y + 1/2, z + 1/2$; #4 $-x, -y + 1, -z$; #5 $x, y + 1, z$.

В заключение отметим, что фиксируемая неиквивалентность длин связей SI–F аниона SIF_6^{2-} (интервал значениий 1.595(9)–1.683(17) Å) согласуется с мультиплетным (дублетным) характером поглощения колебаний ν(SIF) и $\delta(SIF_2)$ в ИК-спектре I [5], указывающим на понижение симметрии

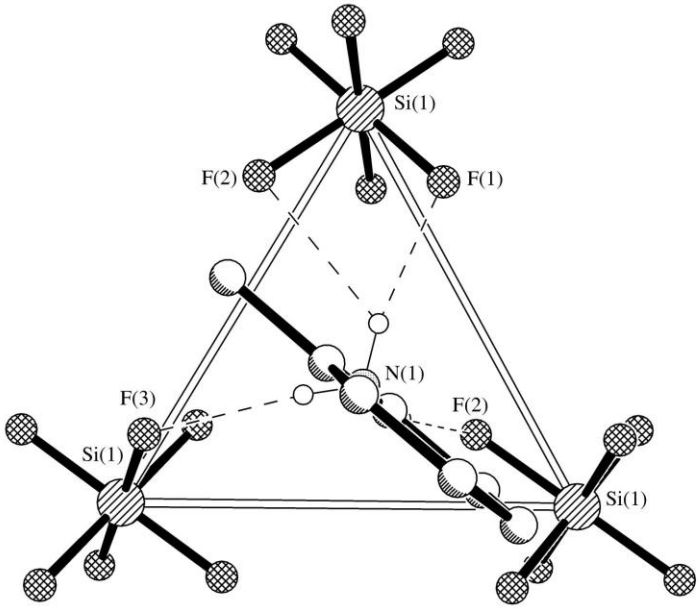

Рис. 2. Ближайшее окружение катиона *о*-толуидиния в кристалле I.

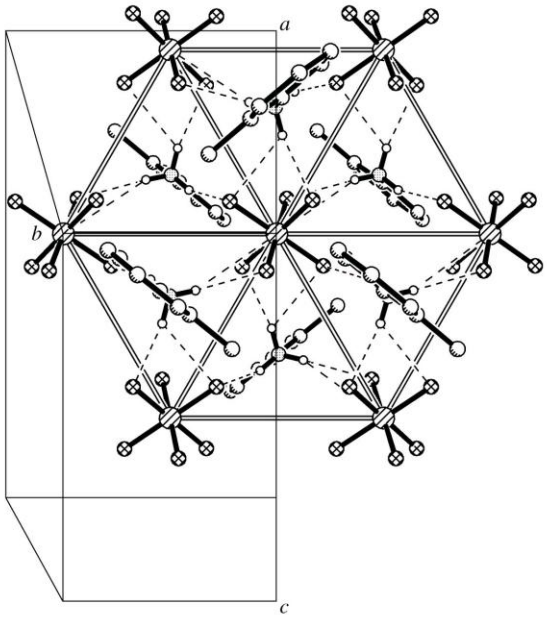

Рис. 3. Ближайшее окружение аниона SiF_6^{2-} в кристалле.

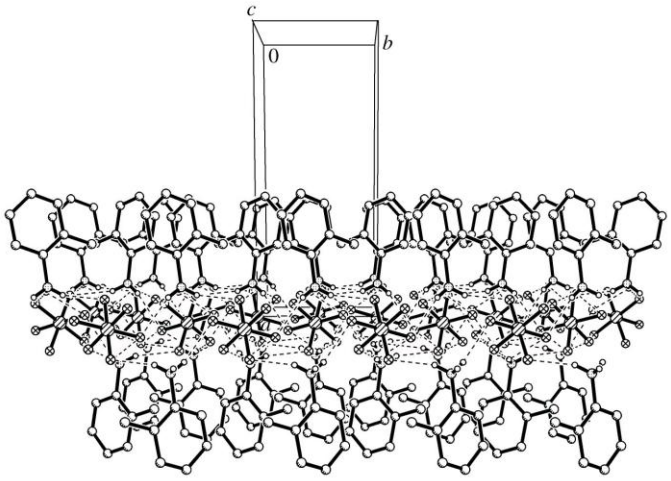

Рис. 4. Фрагмент слоя в кристалле I.

аниона относительно октаэдрической O_h. В структуре I отсутствует антибатная кореляция между прочностью Н-связей NH···F и соответствующих связей SI–F, обнаруженная в структурах многих "ониевых" гексафторсиликатов [1, 2, 6].

СПИСОК ЛИТЕРАТУРЫ

1. *Conley B.D., Yearwood B.C., Parkin S., Atwood D.A.* // J. Fluor. Chem. 2002. V. 115. № 2. P. 155.
2. *Гельмбольдт В.О., Ганин Э.В., Короева Л.В. и др.* // Коорд. химия. 2004. Т. 30. № 3. С. 211.
3. *Эннан А.А., Гаврилова Л.А., Чеботарев А.Н., Борисенко Т.С.* // Журн. неорган. химии. 1977. Т. 22. № 5. С. 1263.
4. Gelmboldt V.O., Ennan A.A., Ganin Ed.V. et al. // J. Fluor. Chem. 2004. V. 215. № 12. P. 1951.
5. *Гельмбольдт В.О., Ганин Э.В., Короева Л.В. и др.* // Журн. неорган. химии. 2006. Т. 51. № 2. С. 237.
6. *Гельмбольдт В.О., Миначева Л.Х., Ганин Э.В., Сергиенко В.С.* // Журн. неорган. химии. 2006. Т. 51. № 10. С. 1661.
7. *Sheldrick G.M.* // SHELXS-97 And SHELXL-97. University of Göttingen, Germany. 1997.

Додаток Г
Копія статті.

“Кристаллические структуры комплексов цис-син-цис изомера дициклогексано-18-краун-6 с гексафтортанталатом оксония и с гексафторниобатом оксония”

ISSN 1063-7745, Crystallography Reports, 2007, Vol. 52, No. 2, pp. 253–259. © Pleiades Publishing, Inc., 2007.
Original Russian Text © M.S. Fonari, O.A. Alekseeva, N.G. Furmanova, K.A. Lysenko, Wen-Jwu Wang, Shang-Wei Tang, É.V. Ganin, V.O. Gel'mbol'dt, Yu.A. Simonov, 2007, published in Kristallografiya, 2007, Vol. 52, No. 2, pp. 271–276.

STRUCTURE
OF ORGANIC COMPOUNDS

Crystal Structures of Complexes of the *cys–syn–cys* Isomer of Dicyclohexano-18-Crown-6 with Oxonium Hexafluorotantalate and Oxonium Hexafluoroniobate

M. S. Fonari[a], O. A. Alekseeva[b], N. G. Furmanova[b], K. A. Lysenko[c], Wen-Jwu Wang[d], Shang-Wei Tang[d], É. V. Ganin[e], V. O. Gel'mbol'dt[f], and Yu. A. Simonov[a]

[a] *Institute of Applied Physics, Academy of Sciences of Moldova, Academiei 5, Chisinau, MD-2028 Moldova*
e-mail: fonari.xray@phys.asm.md

[b] *Shubnikov Institute of Crystallography, Russian Academy of Sciences, Leninskiĭ pr. 59, Moscow, 119333 Russia*
e-mail: furm@ns.crys.ras.ru

[c] *Nesmeyanov Institute of Organoelement Compounds, Russian Academy of Sciences, ul. Vavilova 28, Moscow, 119991 Russia*

[d] *Department of Chemistry, Tamkang University, 151 Ying-Chuan Road, Tamsui, Taipei, 25137 Taiwan*

[e] *Odessa State Environmental University, Ministry of Education and Science and National Academy of Sciences of Ukraine, ul. Lvivska 15, Odessa, 65016 Ukraine*
e-mail:edganin@yahoo.com

[f] *Physicochemical Institute for Human and Environmental Protection, Ministry of Education and Science and National Academy of Sciences of Ukraine, ul. Preobrazhenskaya 2, Odessa, 65026 Ukraine*
e-mail: eksvar@ukr.net

Received July 25, 2006

Abstract—The crystal structures of [(*cys–syn–cys*-dicyclohexano-18-crown-6 · H_3O)][TaF_6] and [(*cys–syn–cys*-dicyclohexano-18-crown-6 · H_3O)][NbF_6] complex compounds are determined using X-ray diffraction analysis. The tantalum complex has two polymorphic modifications, namely, the monoclinic (**I**) and triclinic (**II**) modifications. The unit cell parameters of these compounds are as follows: a = 8.507(4) Å, b = 11.947(5) Å, c = 27.392(12) Å, β = 93.11(1)°, Z = 4, and space group $P2_1/n$ for modification **I**; and a = 10.828(1) Å, b = 11.204(1) Å, c = 12.378(1) Å, α = 72.12(1)°, β = 79.40(1)°, γ = 73.70(1)°, Z = 2, and space group P-1 for modification **II**. The triclinic niobium complex [(*cys–syn–cys*-dicyclohexano-18-crown-6 · H_3O)][NbF_6] (**III**) with the unit cell parameters a = 10.796(3) Å, b = 11.183(3) Å, c = 12.352(3) Å, α = 72.364(5)°, β = 79.577(5)°, γ = 73.773(4)°, Z = 2, and space group P-1 is isostructural with tantalum complex **II**. The structures of all three complexes are ionic in character. The oxonium cation in complexes **I–III** is encapsulated by the crown ether and thus forms one ordinary and two bifurcated hydrogen bonds with the oxygen atoms of the crown ether. This macrocyclic cation is bound to the anions through the C–H···F contacts (H···F, 2.48–2.58 Å). The conformation of the macrocycle in complex **I** differs substantially from that in complex **II** (**III**).

PACS numbers: 61.66.Fn

DOI: 10.1134/S1063774507020150

INTRODUCTION

This study is a continuation of our systematic investigations into the influence of the synthesis conditions and nature of macrocyclic ligands on the composition and structure of the products of the interaction of niobium(V) fluoride and tantalum(V) fluoride complexes with crown ethers (CE) [1, 2]. In our previous studies, it was demonstrated that, in the case of benzo-18-crown-6 [1] and diphenyl-20-crown-6 [2], the sizes of the cavities of their macrocyclic rings appear to be large enough to accommodate one oxonium cation and the composition of the final product in both cases corresponds to the formula [CE · H_3O][MF_6] (M = Nb, Ta). In the case of other biphenyl derivative, namely, [1.5]dibenzo-18-crown-6, the oxonium cation cannot be accommodated in the cavity of the macrocyclic ring because of the decrease in the number of oxygen atoms acceptable for the interaction in the ligand. Therefore, the three-membered aqueous cluster $H_7O_3^+$, which has the form of an $H_2O\cdots H_3O^+\cdots H_2O$ chain linked by the hydrogen bonds, is encapsulated between two crown ether molecules with the formation of a positively charged associate composed of two ether molecules and an $H_7O_3^+$ cation and the composition of the final

product is described by the formula $[(CE)_2 \cdot H_7O_3][MF_6]$.

Using the complex [benzo-18-crown-6 · H_3O][MF_6] as an example, we demonstrated that the technique used for synthesizing the compound affects both the process of crystallization and the structure of the final crystalline product.

This paper reports on the results of investigations into the crystal structure of the complexes [(*cys–syn–cys*-dicyclohexano-18-crown-6 · H_3O)][TaF_6] and [(*cys–syn–cys*-dicyclohexano-18-crown-6 · H_3O)][NbF_6], which are the products of the interaction in the $M_2O_5(MF_5)$–HF–H_2O–CE systems (where M is Nb or Ta and CE is *cys–syn–cys*-dicyclohexano-18-crown-6).

SAMPLE PREPARATION AND EXPERIMENTAL TECHNIQUE

The complex *cys–syn–cys*-dicyclohexano-18-crown-6 · $H_3O^+TaF_6^-$ was synthesized in the form of two polymorphic modifications (**I** and **II**). Crystals of modification **I** were prepared by the reaction of tantalum oxide (0.5 mmol) dissolved in a 45% hydrofluoric acid (6–7 ml) with *cys–syn–cys*-dicyclohexano-18-crown-6 (1 mmol) dissolved in methanol (8–10 ml). The melting temperature of complex **I** is equal to 103–104°C. Crystals of modification **II** and those of the complex *cys–syn–cys*-dicyclohexano-18-crown-6 · $H_3O^+NbF_6^-$ (**III**) were prepared according to the same procedure through the reaction of tantalum fluoride (niobium fluoride for complex **III**) (1 mmol) dissolved in a 45% hydrofluoric acid (6–7 ml) with *cys–syn–cys*-dicyclohexano-18-crown-6 (1 mmol) dissolved in methanol (8–10 ml). The melting temperatures of complexes **II** and **III** are equal to 110–111 and 106–107°C, respectively. Single crystals of compounds **I**–**III** suitable for the X-ray diffraction analysis were obtained through isothermal evaporation of the reaction mixture at a temperature of 18–20°C.

The experimental intensities of 16714 reflections for the crystal of complex **I** were collected at a temperature of 293 K on a Bruker Smart 1000 CCD automated diffractometer (MoK_α radiation, graphite monochromator, ω scan mode, $2\theta_{max} = 58°$), and 6521 observed reflections were used in further calculations. The experimental data were processed and averaged with the SAINT Plus program package [3], and the semiempirical correction for absorption was introduced using the SADABS program package [4]. The structure was solved with the AREN program package [5]. The coordinates of the tantalum atom were determined from the Patterson map. Then, all the non-hydrogen atoms in the structure were located from two successive difference electron-density syntheses. The structure was refined by the full-matrix least-squares procedure in the anisotropic–isotropic approximation on F^2 with the SHELXL97 program package [6]. The analysis of the residual electron-density syntheses revealed that the TaF_6^- anion is disordered over two positions with occupancies of 0.4 and 0.6. The positions of the fluorine atoms with occupancies of 0.6 and 0.4 were refined in the anisotropic and isotropic approximations, respectively. The refinement was performed under the constraint that the Ta–F bond lengths tend to be equal to the mean value of 1.877 Å.

The hydrogen atoms of the crown ether were placed in the calculated positions and refined with the fixed thermal parameters U_j taken to be equal to 1.2 U_j of the carbon atoms bonded to these hydrogen atoms. Since the scatter in the bond lengths in the second cyclohexyl fragment was relatively large, the refinement was performed under the constraint that the bond lengths tend to be 1.54 Å. The oxonium cation was located in the course of the refinement of the structure. The hydrogen atoms of the oxonium cation were located from the difference electron-density syntheses and refined within a riding model.

The experimental intensities of reflections for the crystals of complexes **II** and **III** were collected on a Bruker Smart automated diffractometer equipped with a CCD detector (MoK_α radiation, graphite monochromator, φ-ω scan mode, $2\theta_{max} = 52°$). The structures were solved by direct methods with the SHELXS97 program package [6] and refined by the full-matrix least-squares procedures on F^2 with the SHELXL97 program package [6]. The semiempirical correction for absorption was introduced with the SADABS program package [4]. The analysis of the residual electron-density syntheses revealed that the fluorine atoms in the TaF_6^- (NbF_6^-) anion are disordered over several positions, as can be judged from the final parameters of thermal vibrations. However, only two positions with their equal occupancies were taken into account in the course of the refinement. Both positions were refined in the anisotropic approximation. The refinement was performed under the constraint that the Ta–F bond lengths tend to be equal to the mean value of 1.877 Å and the distances between the fluorine cis atoms tend to be equal to the mean value of 2.653 Å. In the *cys–syn–cys*-dicyclohexano-18-crown-6 molecule, the C(5) atom is disordered over two positions with occupancies of 0.75 and 0.25. The positions of the C(5) atoms with occupancies of 0.75 and 0.25 were refined in the anisotropic and isotropic approximations, respectively. In the course of the refinement, it was revealed that the oxonium cation is disordered over two positions with occupancies of 0.9 and 0.1 and shared hydrogen atoms. The minor component of the oxonium cation was refined in the isotropic approximation.

The hydrogen atoms of the crown ether were placed in the calculated positions and refined with the fixed thermal parameters U_j taken to be equal to 1.2 U_j of the carbon atoms bonded to these hydrogen atoms. The

Table 1. Crystallographic data, experimental details, and parameters of the structure solution and refinement for complexes **I–III**

Compound	I	II	III
Empirical formula	$C_{20}H_{39}F_6O_7Ta$	$C_{20}H_{39}F_6O_7Ta$	$C_{20}H_{39}F_6O_7Nb$
Molecular weight	686.46	686.46	598.42
Crystal system	Monoclinic	Triclinic	Triclinic
Space group, Z	$P2_1/n$, 4	$P\bar{1}$, 2	$P\bar{1}$, 2
Unit cell parameters:			
a, Å	8.507(4)	10.828(1)	10.796(3)
b, Å	11.948(5)	11.204(1)	11.183(3)
c, Å	27.392(12)	12.378(1)	12.352(3)
α, deg	90	72.117(2)	72.364(5)
β, deg	93.110(8)	79.400(2)	79.577(5)
γ, deg	90	73.697(2)	73.773(4)
V, Å^3	2780(2)	1363.8(3)	1357.0(6)
ρ_{calcd}, g/cm^3	1.640	1.672	1.465
μ, mm^{-1}	4.027	4.105	0.519
Crystal size, mm	0.3 × 0.2 × 0.2	0.48 × 0.39 × 0.22	0.63 × 0.52 × 0.48
Index ranges	$-11 \le h \le 11$ $-15 \le k \le 13$ $-33 \le l \le 36$	$-13 \le h \le 13$, $-6 \le k \le 13$, $-15 \le l \le 15$	$-13 \le h \le 12$, $-12 \le k \le 13$, $-10 \le l \le 15$
Number of reflections measured/number of unique reflections/number of reflections with $I > 2\sigma(I)$	16714/6521/3777 [$R(int)$ = 0.0421]	7914/5279/2624 [$R(int)$ = 0.0234]	7682/5244/3990 [$R(int)$ = 0.0128]
S on F^2	1.088	0.861	1.105
Final R factors for reflections with $I > 2\sigma(I)$	$R_1 = 0.0547$, $wR_2 = 0.1127$	$R_1 = 0.0401$, $wR_2 = 0.0867$	$R_1 = 0.0598$, $wR_2 = 0.1821$
Final R factors for all reflections	$R_1 = 0.0910$, $wR_2 = 0.1200$	$R_1 = 0.0826$, $wR_2 = 0.0938$	$R_1 = 0.0739$, $wR_2 = 0.1947$
Extinction coefficient	–	0.0051(4)	0.011(3)
$\Delta\rho_{max}$ and $\Delta\rho_{min}$, e/Å^3	1.266 and –1.205	0.583 and –0.983	0.594 and –0.786

hydrogen atoms of the oxonium cations were located from the difference electron-density syntheses and refined under the constraint that the O–H bond lengths tend to be 0.86 Å (in order to unify the geometry of the oxonium cation in the crystal structures of complexes **II** and **III**) with the fixed thermal parameters U_j taken to be equal to $1.5U_j$ of the oxygen atoms bonded to these hydrogen atoms. The crystallographic data, experimental details, and parameters of the structure solution and refinement for complexes **I–III** are summarized in Table 1.

The crystallographic data for complexes **I–III** have been deposited with the Cambridge Crystallographic Data Centre (CCDC no. 609787 for complex **I**, CCDC no. 609786 for complex **II**, and CCDC no. 609785 for complex **III**).

RESULTS AND DISCUSSION

As was reported earlier in [1], we investigated the monoclinic and orthorhombic polymorphic modifications of the benzo-18-crown-6 complexes with oxonium hexafluorotantalate and oxonium hexafluoroniobate of the general formula [(benzo-18-crown-6) · H_3O][MF_6] (M = Ta, Nb). It was revealed that, in the system under investigation, the oxonium cation H_3O^+ is generated and then encapsulated by the crown ether. The macrocyclic cation and the inorganic anion are held in the crystal through the CH···F hydrogen bonds and π–π interactions between the phenyl substituents in the macrocycle. It was established that the molecular complexes in both polymorphs are organized almost identically. The differences between the monoclinic and orthorhombic modifications are apparently determined by the thermodynamic conditions used for synthesizing the complexes and lie in the slight variations

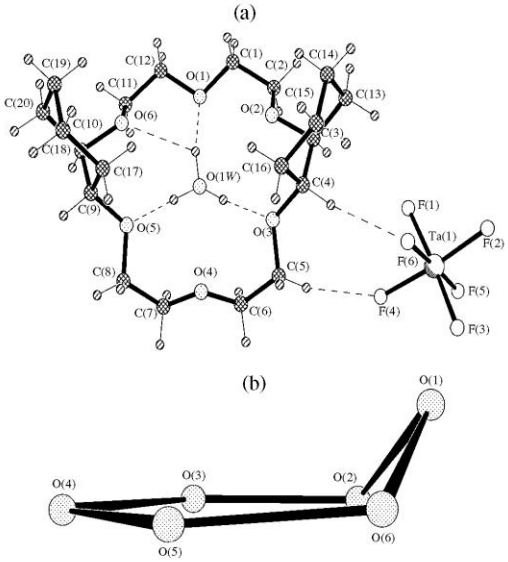

Fig. 1. (a) Structure of complex **I** (only the main positions of the fluorine atoms are shown). (b) Schematic drawing of the conformation of the macrocyclic skeleton of the *cys–syn–cys*-dicyclohexano-18-crown-6 molecule in the crystal structure of complex **I** (only the oxygen atoms are shown).

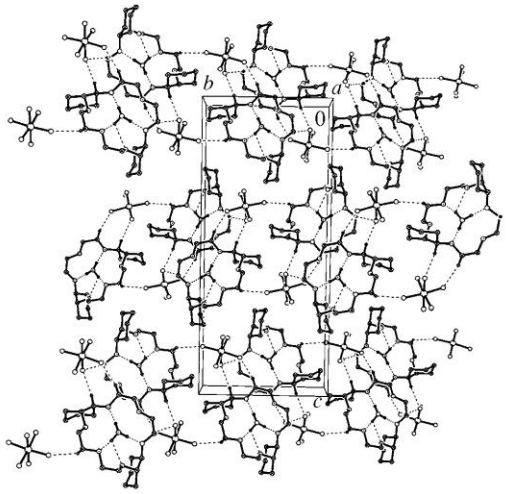

Fig. 2. Packing of complexes **I** in the crystal structure (only the hydrogen atoms involved in hydrogen bonds are shown).

observed in their packings. This manifests itself in different degrees of corrugation of both the organic and inorganic layers in the structure.

The structures of compounds **I**–**III** are ionic in character. They are composed of inorganic anions $[MF_6]^-$ and cations formed by the crown ether and the encapsulated oxonium cation H_3O^+. The structure of complex **I** is depicted in Fig. 1a. In the anion, the tantalum atom has an octahedral coordination. All six fluorine positions are split. The Ta–F and Ta–F' bond lengths in the octahedron fall in the range 1.874(4)–1.891(4) Å. The cis angles at the tantalum atom vary in the range from 81.5(5)° to 95.8(5)°.

In the structure of the crown ether, the C–O and C–C mean bond lengths are equal to 1.428 and 1.479 Å, respectively, and the C–O–C and O–C–C mean bond angles are 113.7° and 108.3°, respectively. The macrocyclic skeleton of the crown ether molecule in the structure of complex **I** has a sofa conformation (Fig. 1b). The five oxygen atoms O(2), O(3), O(4), O(5), and O(6) are coplanar to within 0.0468 Å, and the O(1) oxygen atom deviates from the plane of the aforementioned atoms by 1.249(7) Å. The endocyclic distances O···O in the macrocycle take on values in the range from 5.225(7) to 5.509(6) Å. The torsion angles about the C–C and C–O bonds lie in the ranges 57.7(8)°–67.6(8)° and 142.8(7)°–178.5(8)°, respectively. It is worth noting that the C(3)C(4)O(3)C(5) and C(8)O(5)C(9)C(10) torsion angles in the structure of complex **I** [145.6(6)° and –142.8(7)°, respectively] differ substantially from those in the structure of complex **II** [90.7(8)° and –79.0(7)°, respectively]. The torsion angles characterizing the conformation of the macrocycles in the structures of complexes **I** and **II** are listed in Table 2.

In the structure of complex **I**, the oxygen atom of the oxonium cation deviates by 0.714(5) Å from the plane determined by the five oxygen atoms of the macrocycle. As in the previously investigated structures of the crown ether complexes with oxonium hexafluorotantalate and oxonium hexafluoroniobate [1, 2], the configuration of the oxonium cation has a slightly pyramidal coordination: the oxygen atom deviates from the plane of the hydrogen atoms of this oxonium cation by 0.24 Å. Although the accuracy of the location of the hydrogen atoms was not very high, their positions best correspond to two ordinary hydrogen bonds and one bifurcated hydrogen bond (Table 3).

The interaction between the macrocyclic cation and the inorganic anion occurs through the CH···F contacts, the shortest of which are presented in Fig. 2 and Table 3. Owing to the C–H···F interactions, the hexafluorotantalate anion forms three macrocyclic cations in its environment. In this case, the F(6) atom is bonded to the two cations, thus forming a centrosymmetric dimer. Then, the dimers spaced at a translation along the *b* axis are linked together into chains through the F(1) and F(4) atoms (Fig. 2).

Table 2. Torsion angles in the *cys–syn–cys*-dicyclohexano-18-crown-6 molecule in the structures of complexes **I** and **II**

Angle	τ, deg	
	I	**II**
C(12)O(1)C(1)C(2)	178.5(7)	179.7(4)
O(1)C(1)C(2)O(2)	−62.1(9)	−65.5(6)
C(1)C(2)O(2)C(3)	−173.0(6)	−172.0(5)
C(2)O(2)C(3)C(4)	−157.1(6)	−164.6(5)
O(2)C(3)C(4)O(3)	58.4(7)	60.0(6)
C(3)C(4)O(3)C(5)	145.6(6)	90.7(8)
C(4)O(3)C(5)C(6)	168.0(6)	166.9(7)
O(3)C(5)C(6)O(4)	−67.2(7)	53.7(12)
C(5)C(6)O(4)C(7)	168.4(5)	−172.3(7)
C(6)O(4)C(7)C(8)	−167.6(6)	158.6(6)
O(4)C(7)C(8)O(5)	67.6(8)	−57.7(8)
C(7)C(8)O(5)C(9)	−174.3(7)	−160.9(5)
C(8)O(5)C(9)C(10)	−142.8(7)	−79.0(7)
O(5)C(9)C(10)O(6)	−57.7(8)	−56.4(6)
C(9)C(10)O(6)C(11)	149.5(7)	167.8(5)
C(10)O(6)C(11)C(12)	168.5(7)	177.9(4)
O(6)C(11)C(12)O(1)	64.6(10)	64.2(6)
C(11)C(12)O(1)C(1)	−169.2(8)	170.6(4)

Since complexes **II** and **III** are isostructural to each other and are characterized by close values of the geometric and conformational parameters, the description is given only for complex **II**. The structure of complex **II** is shown in Fig. 3a. In the anion, the tantalum atom has an octahedral coordination. The fluorine atoms in the TaF_6^- anion are disordered over two positions with equal probability. The Ta–F and Ta–F' bond lengths in the octahedron lie in the range from 1.859(4)° to 1.898(4)°. The cis angles at the tantalum atom vary in the range from 84.4(5)° to 95.3(5)°.

The macrocyclic skeleton of the crown ether molecule in the structure of complex **II** exhibits a boat conformation (Fig. 3b) elongated in the direction of the cyclohexane substituents. The endocyclic distances O···O in the macrocycle are as follows: O(1)···O(4), 4.811(5) Å; O(3)···O(6), 5.345(5) Å; and O(2)···O(5), 5.365(5) Å. The four oxygen atoms O(2), O(3), O(5), and O(6), which are bonded to the cyclohexane substituents, are coplanar to within 0.0585 Å, and the two oxygen atoms O(1) and O(4) deviate from the plane of the aforementioned atoms by 0.714(5) and 1.445(6) Å, respectively. The oxygen atom of the oxonium cation deviates by 0.386(5) Å from the plane determined by the four oxygen atoms of the macrocycle. According to the C–C bonds, the macrocycle (symmetry C_m) has the most favorable gauche conformation.

Table 3. Geometric parameters for the hydrogen bonds in the structure of complexes **I** and **II**

D–H···*A* bond	Distances, Å			Angle, deg	Symmetry operations for the acceptor
	D–H	H···*A*	*D*···*A*	*DHA*	
		I			
O(1*W*)–H(1*W*)···O(1)	0.92(2)	1.82(2)	2.599(6)	143(4)	*x, y, z*
O(1*W*)–H(1*W*)···O(6)	0.92(3)	2.39(2)	2.901(7)	116(5)	*x, y, z*
O(1*W*)–H(2*W*)···O(3)	0.90(3)	1.68(2)	2.561(6)	173(5)	*x, y, z*
O(1*W*)–H(3*W*)···O(5)	0.92(2)	1.64(2)	2.553(7)	179(4)	*x, y, z*
C(5)–H(5*B*)···F(4)	0.97	2.42	3.362(11)	165	*x, y, z*
C(4)–H(4*A*)···F(6)	0.98	2.41	3.384(11)	171	*x, y, z*
C(5)–H(5*B*)···F(4')	0.97	2.37	3.269(18)	156	*x, y, z*
C(4)–H(4*A*)···F(6')	0.98	2.44	3.32(2)	151	*x, y, z*
C(1)–H(1*B*)···F(2)	0.97	2.48	3.077(11)	120	−*x*, −*y*, −*z*
C(8)–H(8*B*)···F(6)	0.97	2.56	3.259(13)	129	−*x* + 1, −*y* + 1, −*z*
		II			
O(1*W*)–H(1*W*)···O(1)	0.87(2)	1.84(2)	2.709(6)	176(4)	*x, y, z*
O(1*W*)–H(2*W*)···O(3)	0.86(2)	1.76(2)	2.584(5)	160(5)	*x, y, z*
O(1*W*)–H(2*W*)···O(4)	0.86(2)	2.43(4)	2.949(6)	119(4)	*x, y, z*
O(1*W*)–H(3*W*)···O(5)	0.86(2)	1.77(2)	2.622(5)	175(4)	*x, y, z*
C(1)–H(1*A*)···F(5')	0.97	2.56	3.469(11)	156	*x*, *y*−1, *z*
C(6)–H(6*B*)···F(1')	0.97	2.55	3.421(16)	149	−*x* + 1, −*y* + 1, −*z*
C(18)–H(18*B*)···F(6')	0.97	2.24	2.981(9)	132	−*x*, −*y* + 1, −*z*

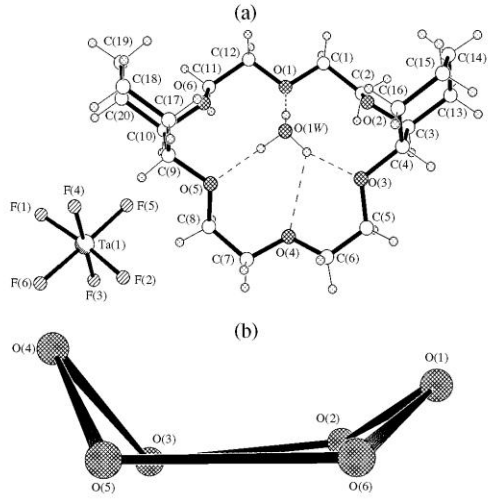

Fig. 3. (a) Structure of complex **II** (the fluorine atoms located in only one position are shown, and the minor components of the C(5) and O(1*W*) atoms are omitted). (b) Schematic drawing of the conformation of the macrocyclic skeleton of the *cys–syn–cys*-dicyclohexano-18-crown-6 molecule in the crystal structure of complex **II** (only the oxygen atoms are shown).

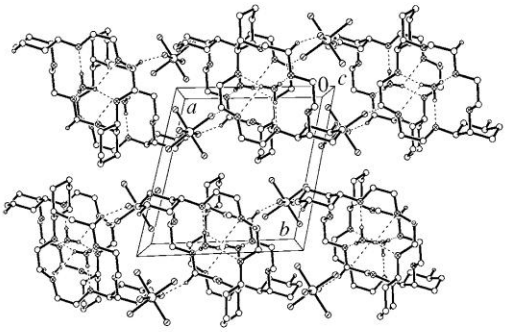

Fig. 4. Packing of complexes **II** in the crystal structure (only the hydrogen atoms involved in hydrogen bonds are shown).

The conformation of the C–O bonds is determined by ten trans and two gauche fragments (Table 2).

A comparison between the conformations of the macrocyclic skeleton of the *cys–syn–cys*-dicyclohexano-18-crown-6 molecule in the structures of complexes **I** and **II** demonstrates that these conformations differ significantly. Quite possibly, the conformational transformation is associated with the redistribution of the OH···O hydrogen bonds with the participation of the oxonium cation, as can be seen from Table 3 and Figs. 1a and 3a.

The interaction between the macrocyclic cation and the inorganic anion in the structure of complex **II** occurs through the CH···F contacts, the shortest of which are presented in Table 3. First and foremost, it should be noted that the number of these interactions in the structure of complex **II** is considerably smaller than that in the structure of complex **I**. Since the fluorine atoms of the anion are disordered with equal probability, the CH···F contacts are formed only in half the complexes in the crystal (with the primed fluorine atoms); in this case, the main packing motif remains similar to the packing motif in the structure of complex **I** (Fig. 4).

Earlier, we studied host–guest complexes of the following compositions: [dicyclohexano-18-crown-6 · H_3O^+][BF_4^-] [7], [dicyclohexano-18-crown-6 · H_3O^+][SiF_5^-] [8], and [dicyclohexano-18-crown-6 · H_3O^+][ClO_4^-] [9]. A comparison of the structural motifs in these three complexes [8] revealed their close similarity: all three compounds (like compound **I**) crystallize in space group $P2_1/n$ with very close values of the unit cell parameters. In the crystal structure, the bulky organic cations [dicyclohexano-18-crown-6 · H_3O^+] form zigzag channels occupied by the BF_4^-, SiF_5^-, and ClO_4^- counterions. A similar structural motif is observed in the crystal structures of complexes **I** and **II** (**III**). Moreover, complex **I** can be the next member of this series, because compound **I** crystallize in the same space group, $P2_1/n$, with the corresponding increase in the unit cell parameters.

It should be noted that, unlike the previously studied system [benzo-18-crown-6 · H_3O][MF_6] (M = Nb, Ta) in which the difference between the polymorphs manifests itself only in their packings, the structures of complexes **I–III** are characterized by conformational changes in the macrocyclic skeleton of the *cys–syn–cys*-dicyclohexano-18-crown-6 molecule in different polymorphs.

ACKNOWLEDGMENTS

We acknowledge the support of the Russian Foundation for Basic Research in the payment of the license for using the Cambridge Structural Database. Wen-Jwu Wang, Shang-Wei Tang, and E.V. Ganin acknowledge the support of the National Council on Science of Taiwan, grant no. 94-2811-M-032.

This study was supported by the Russian Foundation for Basic Research and the Academy of Sciences of Moldova, joint project no. Mol_a 06-03-90894.

REFERENCES

1. M. S. Fonari, N. G. Furmanova, Wen-Jwu Wang, et al., Kristallografiya **51** (5), 856 (2006) [Crystallogr. Rep. **51**, (5), 804 (2006)].

2. Ed. V. Ganin, V. O. Gelmboldt, L. V. Koroeva, et al., J. Inclusion Phenom. Macrocyclic Chem. (in press).
3. *SMART (Version 5.051) and SAINT (Version 5.00): Area Detector Control and Integration Software* (Bruker AXS, Madison, USA, 1998).
4. G. M. Sheldrick, *SADABS: Multi-Scan Absorption Correction Programs* (Bruker AXS, Madison, USA, 1997).
5. V. I. Andrianov, Kristallografiya **32** (1), 228 (1987) [Sov. Phys. Crystallogr. **32** (1), 130 (1987)].
6. G. M. Sheldrick, *SHELXS97 and SHELXL97: Programs for the Solution and Refinement of Crystal Structures* (University of Göttingen, Göttingen, Germany, 1997).
7. V. O. Gel'mbol'dt, É. V. Ganin, Yu. A. Simonov, et al., Zh. Neorg. Khim. **40** (4), 594 (1995).
8. V. O. Gel'mbol'dt, É. V. Ganin, L. V. Ostapchuk, et al., Zh. Neorg. Khim. **44** (7), 1139 (1999) [Russ. J. Inorg. Chem. **44** (7), 1072 (1999)].
9. N. F. Krasnova, Yu. A. Simonov, V. K. Bel'skiĭ, et al., Dokl. Akad. Nauk SSSR **272** (5), 1129 (1983) [Sov. Phys. Dokl. **28**, 823 (1983)].

Translated by O. Borovik-Romanova

Додаток Д
Копія статті.

“Two new "onium" fluorosilicates, the products of interaction of fluorosilicic acid with 12-membered macrocycles: structures and spectroscopic properties”

PAPER www.rsc.org/dalton | Dalton Transactions

Two new "onium" fluorosilicates, the products of interaction of fluorosilicic acid with 12-membered macrocycles: structures and spectroscopic properties

Vladimir O. Gelmboldt,[a] Eduard V. Ganin,[b] Marina S. Fonari,*[c] Yurii A. Simonov,[c] Larisa V. Koroeva,[a] Alim A. Ennan,[a] Stepan S. Basok,[d] Sergiu Shova,[c] Hanspeter Kählig,[e] Vladimir B. Arion[f] and Bernhard K. Keppler[f]

Received 12th March 2007, Accepted 8th May 2007
First published as an Advance Article on the web 9th May 2007
DOI: 10.1039/b703645k

Two novel compounds, $(L^1H)_2[SiF_6]\cdot 2H_2O$ (**1**) and $(L^2H)_2[SiF_5(H_2O)]_2\cdot 3H_2O$ (**2**), resulting from the reactions of H_2SiF_6 with 4′-aminobenzo-12-crown-4 (L^1) and monoaza-12-crown-4 (L^2), respectively, were studied by X-ray diffraction and characterised by IR and ^{19}F NMR spectroscopic methods. Both complexes have ionic structures due to the proton transfer from the fluorosilicic acid to the primary amine group in L^1 and secondary amine group incorporated into the macrocycle L^2. The structure of **1** is composed of $[SiF_6]^{2-}$ centrosymmetric anions, N-protonated cations $(L^1H)^+$, and two water molecules, all components being bound in the layer through a system of NH···F, NH···O and OH···F hydrogen bonds. The $[SiF_6]^{2-}$ anions and water molecules are assembled into inorganic negatively-charged layers *via* OH···F hydrogen bonds. The structure of **2** is a rare example of stabilisation of the complex anion $[SiF_5(H_2O)]^-$, the labile product of hydrolytic transformations of the $[SiF_6]^{2-}$ anion in an aqueous solution. The components of **2**, *i.e.*, $[SiF_5(H_2O)]^-$, $(L^2H)^+$, and water molecules, are linked by a system of NH···F, NH···O, OH···F, OH···O hydrogen bonds. In a way similar to **1**, the $[SiF_5(H_2O)]^-$ anions and water molecules in **2** are combined into an inorganic negatively-charged layer through OH···F and OH···O interactions.

Introduction

The products of reaction of fluorosilicic acid (FSA) with organic bases, the fluorosilicates of the relevant "onium" cations, find application as inorganic–organic hybrid functional materials,[1] ionic liquids[2] and reagents for modified zeolite catalytic agents,[3–5] and in the synthesis of silicon tetrafluoride complexes,[6,7] in the production of fungicides,[8] and in the preparation of herbicide-containing mixtures.[9] In addition, these compounds are of interest for the stabilisation of various fluorido complexes of silicon, the products of the hydrolytic transformations of FSA.[10,11] The equilibria in the FSA solution, and number and composition of the co-existing silicon fluorido complexes, still remain a subject of debate.[10–12] The most effective reagents for the selective stabilisation of certain silicon fluorido complexes still remain 18-membered crown- and azacrown-ethers. In particular, the labile products of hydrolytic transformations of the $[SiF_6]^{2-}$ anion, *viz.* complexes $[SiF_5(H_2O)]^-$, $[SiF_5]^-$ and *trans*-$[SiF_4(H_2O)_2]$, have been stabilised in the solid state and structurally described as host–guest complexes with aza- and 1,10-diaza-18-crown-6,[13] *cis,syn,cis*-dicyclohexyl-18-crown-6[14] and 18-crown-6,[15,16] respectively. It is noteworthy that the smaller 1,7-diaza-15-crown-5[17] and azamacrocycles[18] exclusively form the anhydrous or hydrated ammonium hexafluorosilicates.

It should, however, be noted that the complexing ability of other macrocycles, *e.g.* 12-crown-4 and its substituted derivatives in the reaction with FSA remains practically unexplored. The present study is carried out in continuation of our previous systematic investigations[11,19] and is devoted to the specific features of FSA complex formation with the macrocyclic ligands. We report herein the synthesis, spectroscopic characterisation and structural organisation of compounds resulting from the reaction of FSA with two 12-membered macrocycles, 4′-aminobenzo-12-crown-4 (L^1) and monoaza-12-crown-4 (L^2) (Scheme 1).

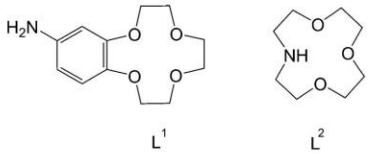

Scheme 1 12-Membered crown ethers used in this study.

Results and discussion

Synthesis

4′-Aminobenzo-12-crown-4 (L^1) was prepared in 3 steps from pyrocatechol following the modified Pedersen procedure.[20]

[a]*Physico-Chemical Institute of Environment and Human Protection, Ministry of Education and Science of Ukraine and National Academy of Sciences of Ukraine, Preobrazhenskaya str., 3, 65026, Odessa, Ukraine. E-mail: eksvar@ukr.net*
[b]*Odessa State Environmental University, Lvovskaya str., 15, 65016, Odessa, Ukraine*
[c]*Institute of Applied Physics, Academy of Sciences of Moldova, Academy str. 5, MD2028, Chisinau, Moldova. E-mail: fonari.xray@phys.asm.md*
[d]*A. V. Bogatsky Physico-Chemical Institute, National Academy of Sciences of Ukraine, Lustdorfskaya doroga 86, 65080, Odessa, Ukraine*
[e]*Institute of Organic Chemistry of the University of Vienna, Währingerstr. 38, A-1090, Vienna, Austria*
[f]*Institute of Inorganic Chemistry of the University of Vienna, Währingerstr. 42, A-1090, Vienna, Austria*

This journal is © The Royal Society of Chemistry 2007

Aza-12-crown-4 (L^2) was obtained following the protocol reported in the literature.[21] Compounds **1** and **2** were synthesised by mixing a methanol solution of the corresponding crown ether and an aqueous solution of fluorosilicic acid in a 1 : 3 molar ratio. Crystals suitable for X-ray study were obtained by slow solvent evaporation at room temperature.

Crystal structures

Compound $(L^1H)_2[SiF_6]\cdot 2H_2O$ (**1**) crystallises in the monoclinic space group $P2_1/c$. The asymmetric unit of **1** consists of one half of the hexafluorosilicate anion in partial position on an inversion center, one ammonium-benzo-12-crown-4 cation and one water molecule, both occupying the general positions (Fig. 1). The FSA molecule protonates the primary amine group of the crown ether molecule. Complex **1** is composed of the $[SiF_6]^{2-}$ anion, two macrocyclic cations and two water molecules.

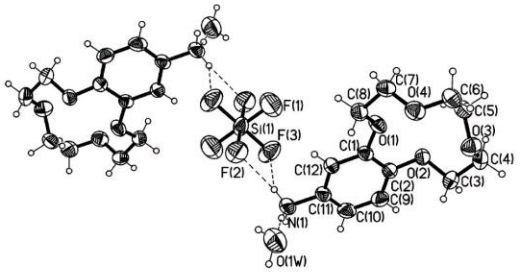

Fig. 1 ORTEP view of **1** with the atom numbering scheme. Displacement ellipsoids are drawn at the 50% probability level. Dashed lines represent the hydrogen bonds.

The components are bound by a network of charge-assisted hydrogen bonds of NH···F, NH···O and OH···F types (Fig. 1). The $[SiF_6]^{2-}$ anion has an usual distorted octahedral geometry with the Si–F distances in the range 1.6588(15)–1.6719(11) Å, F(*cis*)–Si–F(*cis*) bond angles being close to 90° and F(*trans*)–Si–F(*trans*) angles equal to 180°. Each of the $[SiF_6]^{2-}$ octahedra is involved in four bifurcated NH···F hydrogen bonds with ammonium groups of four macrocycles and in four OH···F hydrogen bonds with four water molecules as multi-center acceptors *via* F(2) and F(3) atoms (Fig. 1, Table 1). The water molecules act as H-acceptors towards the ammonium group *via* a single NH···O hydrogen bond, while as H-donors they bridge two symmetry-related $[SiF_6]^{2-}$ anions *via* one single and one bifurcated OH···F hydrogen bond. These latter interactions result in the negatively-charged layer (Fig. 2) that runs perpendicular to the [100] direction in the crystal.

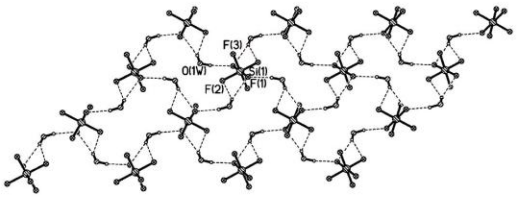

Fig. 2 Fragment of the inorganic negatively-charged layer in **1**.

The macrocyclic ammonium cations are joined *via* NH···F and NH···O hydrogen bonds in a centrosymmetric mode to the both sides of this inorganic sheet, forming its two hydrophobic surfaces (Fig. 3).

The host–guest complex $(L^2H)_2[SiF_5(H_2O)]_2\cdot 3H_2O$ (**2**) is a quite rare example of stabilisation of the complex anion $[SiF_5(H_2O)]^-$,

Table 1 Hydrogen bonding geometry for **1** and **2**

D–H···A	d(D–H)/Å	d(H···A)/Å	d(D···A)/Å	d(DHA)/°	Symmetry transformation for acceptor
Complex **1**					
N(1)–H(1A)···F(3)	0.95(3)	1.86(3)	2.731(2)	151(3)	$x, -y+\frac{1}{2}, z+\frac{1}{2}$
N(1)–H(1A)···F(2)	0.95(3)	2.48(3)	3.235(2)	136(2)	$-x, y-\frac{1}{2}, -z+\frac{3}{2}$
N(1)–H(1B)···F(2)	0.86(3)	2.10(3)	2.903(2)	156(2)	x, y, z
N(1)–H(1B)···F(3)	0.86(3)	2.20(3)	2.883(2)	137(2)	x, y, z
N(1)–H(1C)···O(1W)	0.97(2)	1.74(2)	2.701(3)	174(2)	x, y, z
O(1W)–H(1W1)···F(1)	0.90(4)	1.91(4)	2.790(3)	166(3)	$x, y, z+1$
O(1W)–H(1W1)···F(2)	0.90(4)	2.60(4)	3.280(3)	133(3)	$-x, -y+1, -z+2$
O(1W)–H(2W1)···F(1)	0.80(4)	2.24(4)	2.915(3)	143(3)	$x, -y+\frac{3}{2}, z+\frac{1}{2}$
O(1W)–H(2W1)···F(2)	0.80(4)	2.26(4)	2.949(3)	145(3)	$x, -y+\frac{3}{2}, z+\frac{1}{2}$
Complex **2**					
N(1)–H(1N1)···F(4)	0.83(3)	2.02(3)	2.829(2)	164(2)	x, y, z
N(1)–H(1N1)···F(3)	0.83(3)	2.46(2)	2.982(2)	121(2)	x, y, z
N(1)–H(2N1)···O(2)	0.83(3)	2.09(3)	2.811(2)	146(2)	x, y, z
N(1)–H(2N1)···O(1)	0.83(3)	2.38(3)	2.785(2)	111(2)	x, y, z
N(2)–H(1N2)···O(5)	0.86(3)	2.04(3)	2.786(2)	145(2)	x, y, z
N(2)–H(1N2)···O(6)	0.86(3)	2.38(3)	2.799(2)	111(2)	x, y, z
N(2)–H(2N2)···F(8)	0.86(3)	1.94(3)	2.786(2)	169(2)	x, y, z
N(2)–H(2N2)···F(7)	0.86(3)	2.47(3)	3.079(2)	128(2)	x, y, z
O(1W)–H(1W1)···F(10)	0.85(4)	1.78(4)	2.629(2)	175(3)	$x, -y-\frac{1}{2}, z+\frac{1}{2}$
O(1W)–H(2W1)···O(3W)	0.88(2)	1.72(2)	2.588(2)	171(3)	x, y, z
O(2W)–H(1W2)···O(4W)	0.87(2)	1.71(2)	2.569(2)	169(3)	x, y, z
O(2W)–H(2W2)···F(3)	0.86(3)	1.77(3)	2.626(2)	172(3)	$x, -y+\frac{1}{2}, z-\frac{1}{2}$
O(3W)–H(1W3)···F(7)	0.83(3)	1.97(3)	2.794(2)	172(3)	$x, -y+\frac{1}{2}, z+\frac{1}{2}$
O(3W)–H(2W3)···F(9)	0.79(3)	1.96(4)	2.733(2)	168(3)	$-x+1, y+\frac{1}{2}, -z+\frac{1}{2}$
O(4W)–H(1W4)···F(5)	0.84(4)	1.90(4)	2.744(2)	173(3)	$x, -y-\frac{1}{2}, z-\frac{1}{2}$
O(4W)–H(2W4)···F(1)	0.79(3)	1.98(3)	2.754(2)	167(3)	$-x, y-\frac{1}{2}, -z+\frac{1}{2}$

This journal is © The Royal Society of Chemistry 2007

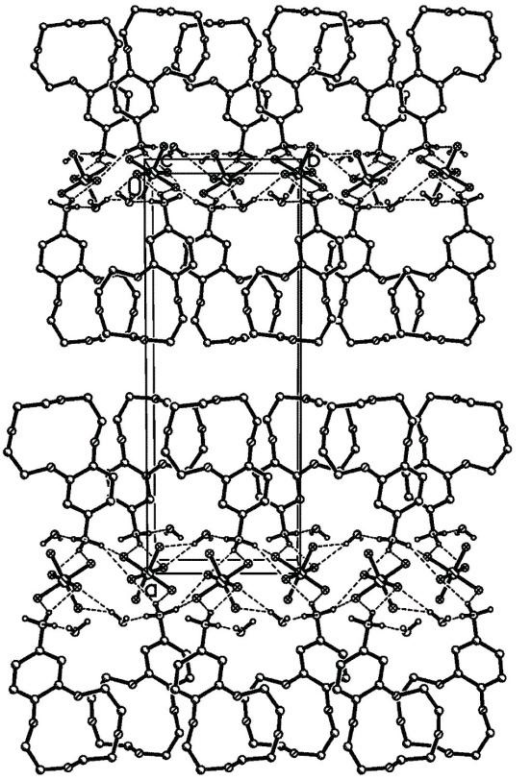

Fig. 3 Packing of the layers in **1**.

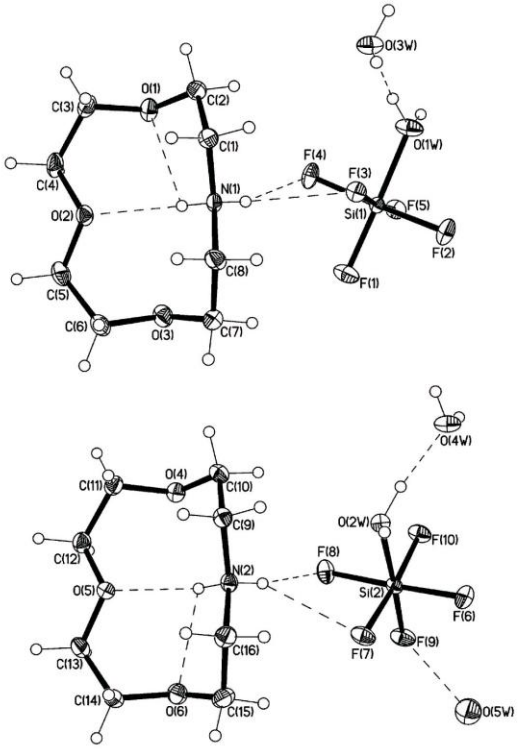

Fig. 4 ORTEP view of two $(L^2H)_2[SiF_5(H_2O)]_2 \cdot 3H_2O$ units in **2** with the atom numbering scheme. Displacement ellipsoids are drawn at the 50% probability level. Dashed lines represent the hydrogen bonds.

the labile product of hydrolytic transformations of $[SiF_6]^{2-}$. The asymmetric unit of **2** consists of two 12-membered macrocyclic cations, two $[SiF_5(H_2O)]^-$ anions and three water molecules, one of which, O(5W), has been found to show 25% occupancy. In the crystal each of two crystallographically independent FSA molecules protonates the NH-binding site of the independent macrocycle and is linked with the latter *via* a bifurcated NH···F hydrogen bond (Fig. 4, Table 1) with formation of two neutral units. The second hydrogen of the crown ether ammonium group is directed inside the cavity and is involved in the bifurcated NH···O hydrogen bond responsible for the folded conformation of both cations. The $[SiF_5(H_2O)]^-$ anion has a distorted octahedral geometry with the Si–F distances in the range 1.6424(12)–1.6979(11) Å. The distances Si–O(H_2O) adopt the values 1.8416(15) and 1.8675(14) Å in two independent anions, the F(*cis*)–Si–F(*cis*) bond angles being 87.32(6)–93.94(6)°, F(*trans*)–Si–F(*trans*) angles being in the range 173.21(6)–176.65(7)°, H_2O(*cis*)–Si–F(*cis*) angles being 85.99(6)–89.10(6)° and H_2O(*trans*)–Si–F(*trans*) angles adopting the values 178.31(7) and 177.89(7)° in two independent anions, respectively (Fig. 4). The geometry of the $[SiF_5(H_2O)]^-$ anion is in agreement with the reported data.[13,19]

As in **1**, the inorganic anions $[SiF_5(H_2O)]^-$ and water molecules in **2** form the negatively-charged layers *via* OH···F and OH···O interactions (Fig. 5). The fluoride ligands of both $[SiF_5(H_2O)]^-$ anions, which are situated in approximately the same plane as those coordinated to the silicon atoms' water molecules, are involved in the intermolecular interactions, and the layer is built up of two alternative ribbons. The first one represents the alteration of five H-bonded unique rings with the following graph set notations:[22] $R_4^4(12)$, $R_3^3(10)$, $R_3^5(12)$ [taking into account non-localised H-atoms of the O(5W) water molecule, the corresponding O(5W)···F(9) and O(5W)···F(9)^i ($i = 1 - x, -1 - y, -z$) separations being 2.664(8) and 2.856(8) Å], $R_4^5(12)$, and $R_3^3(10)$. The next ribbon with the edges shared with the previous one is built up of four unique alternating rings, $R_6^6(16)$, $R_3^3(10)$, $R_4^4(12)$ and $R_3^3(10)$.

As is evident from Fig. 5, the two water molecules coordinated to two silicon atoms [O(1W) and O(2W)] and the two lattice [O(3W) and O(4W)] water molecules use the maximal number of their proton-donor capabilities within the layer: all water molecules act as double donors and all but O(5W) act as single acceptors (*via* coordination or hydrogen bond) within this layer. As we have already noted, this is only the third example of crystal structures that include $[SiF_5(H_2O)]^-$ anions and protonated N,O-containing macrocycles [those previously reported were complexes $(L^3H \cdot H_2O)[SiF_5(H_2O)] \cdot H_2O$ and $(L^4H_2)[SiF_5(H_2O)]_2$, where L^3 = aza-18-crown-6 and L^4 = 1,10-diaza-18-crown-6].[13] The supramolecular architecture of these related compounds reveals an essential difference: the $\{[SiF_5(H_2O)]^-\}_2$ units are joined

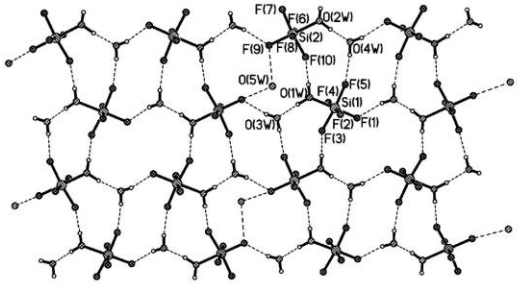

Fig. 5 Fragment of the inorganic negatively-charged layer in **2**.

into centrosymmetric dimers or in chains due to incorporation of lattice water molecules, and the hybrid organic–inorganic layer combines these inorganic motifs and organic cations. Compound **2** is the first example of layer organisation of the negatively-charged species by incorporation of additional lattice water molecules. This leads to different types of anion–anion associations with water molecules mediating the interaction between neighbouring $[SiF_5(H_2O)]^-$ anions.

In a manner similar to **1**, the macrocycles are attached to this inorganic layer using the axial fluoride ligands that are not involved in the intermolecular interactions within the inorganic layer, Fig. 6.

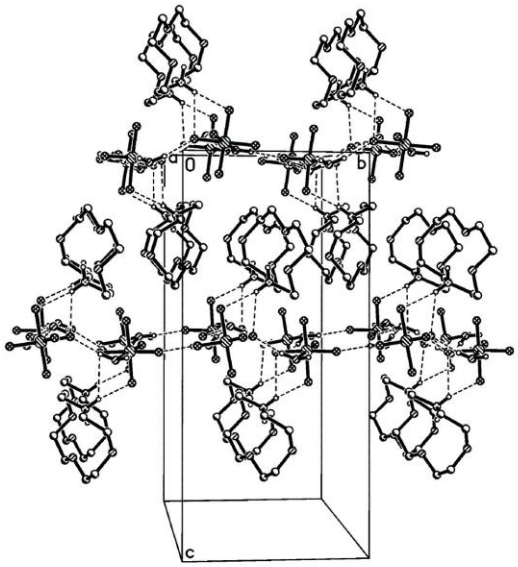

Fig. 6 Packing of the layers in **2**.

It is well known that FSA does not exist as an individual anhydrous compound H_2SiF_6.[23] It crystallises as low-stability hydrates of the general formula $H_2SiF_6{\cdot}nH_2O$ (n = 4, 6, 9.5), which represent the oxonium salts of composition $(H_5O_2)_2SiF_6$, $(H_5O_2)_2[SiF_6]{\cdot}2H_2O$ and $(H_5O_2)_2[SiF_6]{\cdot}4.5H_2O$.[24] Recently, the relatively stable (mp $\geq$60 °C) "simplest hydrate" $H_2SiF_6{\cdot}2H_2O$ was obtained, and its structure was described as an oxonium hexafluorosilicate, $(H_3O)_2[SiF_6]$.[25] Despite its high symmetry (O_h), the hexafluorosilicate anion may be a suitable component for ionic liquids when paired with an appropriate linear or planar base. The family of hexafluorosilicates of aromatic bases is restricted to a few examples[26–29] with different networks of hydrogen bonding in these compounds resulting in different final supramolecular architectures. Thus, in complexes $[o\text{-}CH_3O(O)CC_6H_4NH_3]_2[SiF_6]$[26] and $[o\text{-}C_6H_4(NH_3)_2]_2[SiF_6]$[29] all fluoride ligands of the $[SiF_6]^{2-}$ anions are involved in hydrogen-bonding. In the case of $[o\text{-}CH_3O(O)CC_6H_4NH_3]_2[SiF_6]$ the components form chains, and the chains are involved in stacking interactions *via* benzene rings. The general topology of the structure $[o\text{-}C_6H_4(NH_3)_2]_2SiF_6$ corresponds to a 2D network formed by $[o\text{-}C_6H_4(NH_3)_2]^{2+}$ cations and $[SiF_6]^{2-}$ anions. The hydrates of *p*-bromoanilinium hexafluorosilicate and *p*-toluidinium hexafluorosilicate[28] both also form 2D structures, where the hexagonal H-bonded network built up of $[SiF_6]^{2-}$ anions, ammonium cations and bridging water molecules is surrounded in a centrosymmetric manner by the aromatic rings of the cations arranged perpendicular to the inorganic network and forming two hydrophobic layer surfaces.

The use of 4-aminobenzenesulfonamide or the 4-aminobenzoic acid in the reaction with fluorosilicic acid results in the corresponding ammonium hexafluorosilicates[29] with a complex system of hydrogen bonding that combines the components into a 3D grid. The presence of a tetrahedral ammonium group in L^1 provides the only 2D supramolecular architecture in **1**. In the crystal structure there are no interactions between H-donor groups and oxygen atoms of the polyether ring, indicating that **1** is not a host–guest complex. Instead, it can be categorised as the salt-like adduct of functionalised arylammonium cation. The starting thermolysis temperature, t_0, for compound **1** and for a number of hexafluorosilicates of *ortho*-substituted anilinium hexafluorophosphates[26] (Table 3) has been determined, showing a correlation between the t_0 values and pK_a values of the corresponding arylamines.

It is worth noting that none of the products resulting from reactions of crown ethers or their aza-analogues with FSA are inclusion complexes.[11,19] The interaction between the inorganic "guest" and macrocycle occurs exclusively *via* a net of hydrogen bonds. Therefore the influence of the macrocycle structure on the identity of the extracted from aqueous solution of FSA inorganic species should be considered from the point of view of their ability to form hydrogen bonds. Starting from different macrocycles, we succeeded to stabilise (along with $[SiF_6]^{2-}$) the labile products of its hydrolytic transformations, *viz.*, $[SiF_5(H_2O)]^-$, $[SiF_5]^-$ and $[SiF_4(H_2O)_2]$. In particular, the homoleptic compounds with equivalently sterically-shielded macrocycle sides, *viz.*, 18-crown-6, 15-crown-5 and 12-crown-4, stabilise selectively the *trans*-$[SiF_4(H_2O)_2]$ species, whereas the *cis*,*syn*,*cis*-dicyclohexane-18-crown-6, with non-equivalently shielded macrocycle sides, forms an ionic complex with $[SiF_5]^-$ anion. The observed relationship between the crown-ether structure and the composition of the bound fluoro-containing inorganic complex (molecular or ionic) has also been documented for related "host–guest" systems based on neutral $BF_3{\cdot}H_2O$ and anionic $[BF_4]^-$.[11] Stabilisation of the $[SiF_5(H_2O)]^-$ anion has been observed when azacrown-ethers with the N-to-O ratio in favour of oxygen have been used as "host" molecules and organic bases.

Obviously, in each particular case upon interaction of FSA or similar equilibrium system with the corresponding macrocycle, the species is sequestered from aqueous solution, for which the

 This journal is © The Royal Society of Chemistry 2007

Table 2 Crystal data and structure refinement parameters for **1** and **2**

Compound	1	2
Chemical formula	$C_{24}H_{40}F_6N_2O_{10}Si$	$C_{26}H_{46}F_{10}N_2O_{11}Si_2$
Formula weight	658.67	688.73
Temperature/K	100(2)	100(2)
Wavelength/Å	0.71073	0.71073
Crystal system	Monoclinic	Monoclinic
Space group	$P2_1/c$	$P2_1/c$
a/Å	21.8548(6)	14.8889(7)
b/Å	8.0635(2)	9.3635(5)
c/Å	8.5300(2)	20.3291(9)
β/°	98.599(2)	93.900(3)
V/Å^3	1486.31(7)	2827.6(2)
Z, ρ_{calc}/g cm^{-3}	2, 1.472	4, 1.618
μ/mm^{-1}	0.173	0.247
$F(000)$	692	1448
θ range/°	1.88–30.82	2.35–27.50
Limiting indices	$-31 \le h \le 31$ $-11 \le k \le 11$ $-12 \le l \le 12$	$-19 \le h \le 19$ $-12 \le k \le 12$ $-26 \le l \le 26$
Reflections collected/unique	33020/4660 [R(int) = 0.0296]	88034/6465 [R(int) = 0.0409]
Goodness-of-fit on F^2	1.111	1.063
Final R indices [$I > 2\sigma(I)$]	$R_1 = 0.0493$, $wR_2 = 0.1370$	$R_1 = 0.0410$, $wR_2 = 0.1148$
R indices (all data)	$R_1 = 0.0752$, $wR_2 = 0.1515$	$R_1 = 0.0512$, $wR_2 = 0.1199$
Largest diff. peak and hole, e Å^{-3}	0.380/−0.335	0.594/−0.380

Table 3 Relationship between the pK_a of arylamines and thermolysis temperatures t_0 of the corresponding arylammonium hexafluorosilicates[38]

Amine	pK_a	t_0/°C
L^1	4.63[a]	190[b]
o-$CH_3OC_6H_4NH_2$	4.49	175
o-$CH_3C_6H_4NH_2$	4.39	135
o-$ClC_6H_4NH_2$	2.64	125
o-$BrC_6H_4NH_2$	2.60	125
o-$CH_3O(O)CC_6H_4NH_2$	2.23	115
o-$HO(O)CC_6H_4NH_2$	2.11	140
o-$O_2NC_6H_4NH_2$	−0.29	100

[a] Calculated value. [b] For the anhydrous form.

most effective stabilisation of the host–guest complex by a net of hydrogen bonding interactions is achieved. In addition, lattice water molecules often act as bridging species between "inorganic" and "organic" fragments with formation of supramolecular architecture of the host–guest complex.

Infrared spectra

Broad bands of medium intensity between 3650 and 3030 cm^{-1} in the IR spectrum of **1** (Table 4) have been assigned to the stretching vibrations of the NH_3^+ groups and water molecules involved in the hydrogen bonding network. The deformation vibrations $\delta(NH_3)$ and $\delta(H_2O)$ were registered at 1655 and 1620 cm^{-1}, correspondingly. Absorptions at 705, 465 and 440 cm^{-1} were attributed to the ν(SiF) and $\delta(SiF_2)$ vibrations of the $[SiF_6]^{2-}$ anion, respectively. The character of absorption changes in the range 1145–1095 cm^{-1}, where the bands assigned to the conformationally-sensitive ν_{as}(COC) vibrations of macrocyclic fragment were registered: instead of the observed for L^1 doublet band of medium intensity at 1145 and 1115 cm^{-1}, an intense band at 1130 cm^{-1} with the shoulder at 1100 cm^{-1} is found for **1**, while the band at 1090 cm^{-1} changes its intensity but not the position. In addition, the vibrations ν_s(COC) appear in the spectrum as an intense singlet at *ca.* 1040 cm^{-1}, instead of two bands of medium and weak intensities at 1060 and 1045 cm^{-1} in the spectrum of L^1. We note that the assignment of the skeleton vibrations of the macrocycle in the spectra of L^1 and **1** (Table 4) was made taking into account the data for the related monobenzo-12-crown-4.[30]

The IR spectrum of **2** (Table 4) shows the ν(NH) vibrations of the protonated secondary amine group and the ν(OH) vibrations of coordinated and lattice water molecules as broad bands of medium intensity with weakly pronounced maxima between 3590 and 3110 cm^{-1}. The position of higher frequency components at 3590 and 3550 cm^{-1} is in line with the X-ray data, indicating the presence of outer-sphere water molecules in **2**. The complex band with a maximum at 1585 cm^{-1} and shoulders around 1725, 1655 and 1625 cm^{-1} was assigned to deformation vibrations $\delta(H_2O)$, $\delta(NH_2)$ and δ(CNH). Intraligand vibrations of macrocycle attributed to the fragments NCH_2CH_2O and OCH_2CH_2O [ν_{as}(CNC), ν_{as}(COC) in the range 1170–1050 cm^{-1}, and ν_s(COC), ν_s(CNC) and ν(CC), ν(CN) in the range 1050–940 cm^{-1}] were also observed. A marked difference between the IR spectra for L^2 and **2** in the range of the $\nu_{as,s}$(CNC) and $\nu_{as,s}$(COC) vibrations, as well as in the range typical of valence-deformation vibrations of the ligand (1000–800 cm^{-1}) indicates the change of conformation and macrocycle symmetry upon complex formation.

In accordance with the X-ray data, the interpretation of the vibrations of the SiF_5O polyhedron was carried out using an approximation of point group symmetry C_{4v}. Thus, the most intense component (760 cm^{-1}) of the complex absorption band in the range 800–700 cm^{-1} includes the $\nu(SiF_a)$ (A_1) vibration, and a clearly pronounced shoulder around 720 cm^{-1} – vibrations $\nu(SiF_a)$ (A_1). The band of doubly degenerate vibrations ν(SiF) (E)

Table 4 IR spectral data for **1** and **2** and free organic bases

L^1	**1**	L^2	**2**	
	3560 m	3480 m w	3590 m w	
	3455 m		3550 m w	
3430 m	3415 m w		3400 m w	ν(NH), ν(OH)
3345 m w		3300 m w		
3170 m w	3130 m w		3230 m w	
	3110 sh	3090 m w	3110 sh	
3045 sh	3030 sh			
	1655 m	1655 sh	1725 sh	
	1620 m	1635 m	1655 sh	$\delta(NH_2)$, $\delta(OH_2)$, $\delta(NH_3)$, δ(CNH)
1620 m		1620 m		
			1625 sh	
		1585 sh	1585 s	
1595 s	1585 s			
1555 m	1570 sh			$\nu(CC)_{Ph}$
1510 s	1505 s			
1360 sh	1340 sh	1360 sh	1340 sh	
1320 m	1320 m			$\omega(CH_2)$, $\tau(CH_2)$, $\omega(NH_2)$, δ(CNH), $\omega(NH_3)$, $\nu_s(C_{Ph}\text{-}OC)$, $\nu_{as}(C_{Ph}\text{-}OC)$
1295 m				
1275 m	1275 m	1280 s	1285 m	
1240 m	1240 m	1240 s	1240 sh	
1220 sh	1220 sh	1220 sh	1220 s	
1180 m				
1165 m	1160 sh		1170 sh	
1145 m	1130 s	1130 s	1140 s	$\delta(CCH)_{Ph}$, $\nu_{as}(CNC)$, $\nu_{as}(COC)$, $\nu_s(COC)$, ν(CC), $\rho(NH_2)$
1115 m	1100 sh	1100 s		
1090 sh	1090 m			
1060 m		1070 s	1070 m	
1045 w	1040 m	1055 sh	1050 sh	
1030 s	1025 sh	1020 m	1020 m	
965 m	965 m	930 s	940 m	
915 m	920 s		920 sh	$\nu_s(COC)$, $\nu_s(CNC)$, δ(CCH), $\rho(CH_2)$ + ν(CO) + ν (CC), $\rho(CH_2)$ + ν(CO) + ν(CC) + ν(NC)
900 m	905 sh	900 s	900 sh	
885 sh	890 w			
870 sh	855 m		850 m	
830 m		840 w		
815 sh	800 sh	820 m	820 sh	
765 m	770 sh	780 m	760 s	
750 sh	760 sh	755 m	720 sh	$\nu(SiF_{eq})$, $\nu(SiF_a)$, ν(SiF), $\rho(NH_2)$, $\rho(NH_3)$, $\nu_{puls.}$, $\gamma(H_2O)$
725 sh	705 s	720 sh	680 sh	
620 w	610 sh	620 sh	610 sh	
565 w	565 w		565 sh	δ(CCO), δ(COC), δ(NCC)
530 w	530 w	510 m	510 m	
	465 m		465 m	$\delta(SiF_2)$
	440 sh		420 m	

Abbreviations: w: weak, m: medium, s: strong, sh: shoulder.

is revealed as a shoulder around 680 cm^{-1}. The plane vibrations $\delta(SiF_4)$ (E) were assigned to the band around 465 cm^{-1}; out-of-plane vibrations $\delta(SiF_2)$ (A_1) were registered as a shoulder around 420 cm^{-1}.

^{19}F NMR study on 2

^{19}F NMR spectra for **2** in acetonitrile solution show several signals, some of them being temperature-dependent, typical for systems with fluorine exchange (Fig. 7). Their line widths decrease with decreasing temperature due to the decreased exchange rate. Thus, the spectrum measured at the lowest temperature of 243 K was used for the assignment of the different fluoride complexes (Fig. 8 and Table 5).

The intense singlet at δ −127.86 ppm and a heteronuclear coupling constant $J(^{29}Si,^{19}F) = 108$ Hz corresponds to the $[SiF_6]^{2-}$ anion.[31] Only at 243 K can the silicon satellites be observed, as at higher temperatures the line width exceeds the J coupling. Two signals of equal intensity with chemical shift values of −123.81 and −136.05 ppm can be attributed to *cis*-$SiF_4 \cdot 2H_2O$ (Fig. 8). They appear as poorly resolved triplets due to a rather small fluorine coupling constant $J(^{19}F,^{19}F) = 1.3$ Hz at 243 K, which increases

 This journal is © The Royal Society of Chemistry 2007

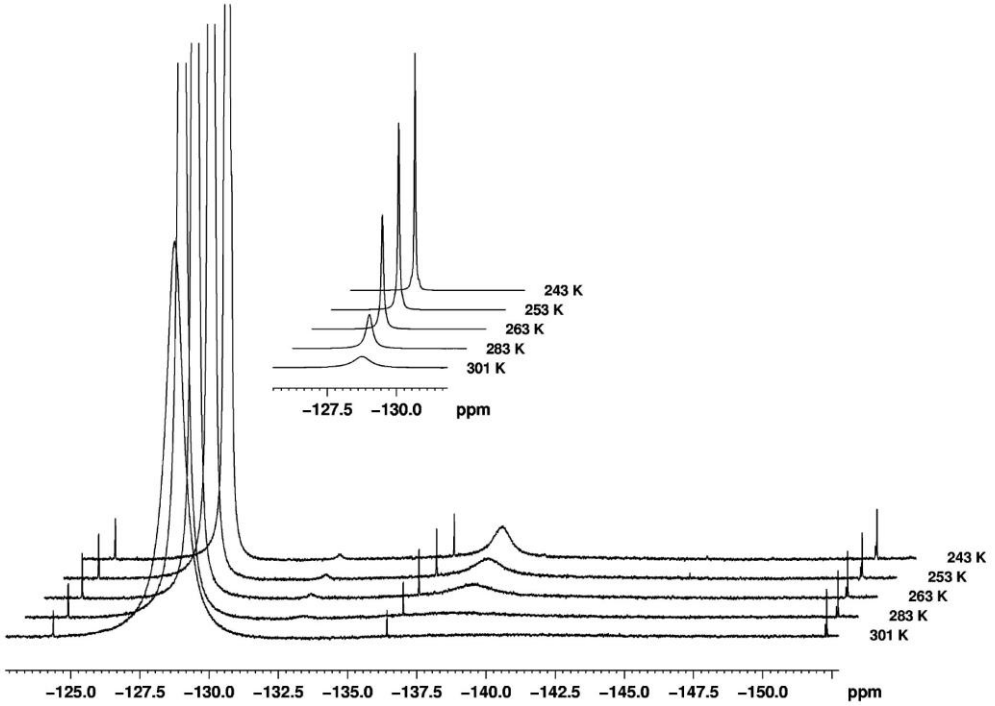

Fig. 7 ^{19}F NMR spectra for **2** at different temperatures (vertical scaling optimised for the minor signals, with the main signal in the inset).

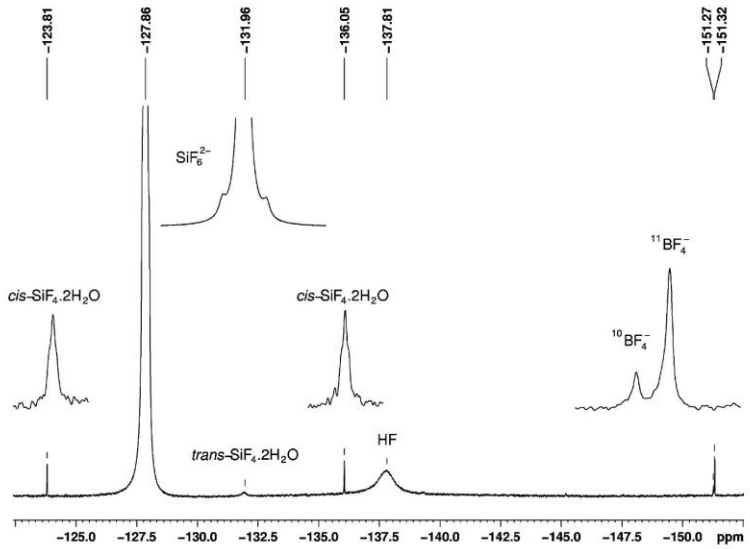

Fig. 8 ^{19}F NMR spectrum of **2** at 243 K.

Table 5 ^{19}F NMR data for complex **2** in CD_3CN at 243 K

Complex	δ(F)/ppm [a]	J/Hz
$[SiF_6]^{2-}$	−127.86	(^{29}Si,^{19}F) 108
trans-$SiF_4 \cdot 2H_2O$	−133.0 (F_c)	
cis-$SiF_4 \cdot 2H_2O$	−123.81[b] (F_c); −136.05[b] (F_t)	(^{19}F,^{19}F) 1.3
HF	−137.81	
BF_4^-	−151.27; −152.32	

[a] F_c, F_t: fluorine atoms *cis* and *trans* to H_2O, respectively. [b] Incompletely resolved triplet.

slightly to 2 Hz upon elevating the temperature to 301 K. In addition, as the only fluorine–silicon species, these signals exhibit the same sharp line over the whole measured temperature range.

The signal with the chemical shift δ(F) around 131.96 ppm can presumably be referred to the *trans*-isomer. The assignment has been made taking into account the closeness of the chemical shifts of *cis*- and *trans*-$SiF_4 \cdot 2H_2O$ with those of isomeric complexes $SiF_4 \cdot 2DMSO$ with an analogous O-donor.[32] The *cis*-isomers of SiF_4 with the molecular N-donors show ^{19}F signals for the vector N–Si–F shifted to higher fields.[33,34] The broad signal with the chemical shift at −137.8 ppm is probably due to HF or exchange interaction between HF, F^- and HF_2^-,[31] formed as a result of hydrolytic transformations of fluorido complexes. The strong field signals at −151.27 and −151.32 ppm with relative intensities of 1 : 4 refer to the anion BF_4^- [35] (resonance $^{10}BF_4^-$ and $^{11}BF_4^-$ correspondingly, with a chemical shift difference between the two signals of about 20 Hz as the sequence of the isotopic shift ^{10}B–^{11}B), which is probably formed as a by-product by reaction of HF with the borosilicate glass of the NMR tube.[34]

The results obtained may be interpreted as follows: the labile anions $[SiF_5(H_2O)]^-$ formed from the weak Lewis acid (SiF_5^-) and weak Lewis base (H_2O) as a result of the first step of the hydrolysis of SiF_6^{2-} anions in solutions of FSA[10] can be stabilised in the solid state as host–guest complexes with the protonated forms of azacrown ethers. The system of charge-assisted hydrogen bonds serves as a stabilising basis for complex **2** and related compounds reported previously, *e.g.* $(L^3H \cdot H_2O)[SiF_5(H_2O)] \cdot H_2O$ and $(L^4H_2)[SiF_5(H_2O)]_2$ (L^3 = aza-18-crown-6, L^4 = 1,10-diaza-18-crown-6). Upon dissolution in the absence of that stabilising factor the anions $[SiF_5(H_2O)]^-$ disproportionate according to eqn (1):

$$2[SiF_5(H_2O)]^- \rightarrow [SiF_6]^{2-} + [SiF_4(H_2O)_2] \quad (1)$$

with the formation of a more stable $[SiF_6]^{2-}$ anion and $[SiF_4(H_2O)_2]$ complex. The last species may undergo further hydrolysis with the participation of the outer-sphere water molecules according to eqn (2):

$$[SiF_4(H_2O)_2] + H_2O \rightarrow SiO_2 \cdot H_2O + 4HF \quad (2)$$

This, together with the volatility of the diaqua-complex, probably explains the rather low content of *cis*- and *trans*-$SiF_4 \cdot 2H_2O$ in acetonitrile solution. We note here that the complex $SiF_4 \cdot 2H_2O$, which is a strong Brønsted acid,[36] is relatively stable only in highly acidic solutions of FSA; the decrease of solution acidity results in the hydrolytic decomposition of the complex.

It should be also noted that ^{19}F NMR spectroscopy data indicate that $[SiF_4(H_2O)_2]$ is present in acetonitrile solution in the form of two geometric isomers. Previously,[15,16] we succeeded to stabilise and describe the crystal structure of the *trans*-$[SiF_4(H_2O)_2]$ isomer isolated in the solid state as a host–guest complex of composition (*trans*-$SiF_4 \cdot 2H_2O$)·18-crown-6·$2H_2O$. The possibility for $SiF_4 \cdot 2H_2O$ to exist as *cis*- and *trans*-isomers has been predicted[37] on the basis of gaseous-phase non-empirical calculations for the products of hydrolysis of silicon tetrafluoride. The theoretical study revealed higher thermodynamic stability (by 5.0 kcal mol^{-1}) for *cis*-$SiF_4 \cdot 2H_2O$ (symmetry C_{2v}) compared to the *trans*-$SiF_4 \cdot 2H_2O$ (symmetry C_i) for the idealised geometries in the gaseous state. The evident influence of the medium (solvation and other factors) on the relative stability of the isomeric forms of $SiF_4 \cdot 2H_2O$ in liquid phase has also been discussed.[37]

Conclusions

A novel 12-membered crown ether, 4′-aminobenzo-12-crown-4 (L^1), has been synthesised using the modified Pedersen procedure. This macrocycle, containing a primary amine group, together with another as-yet poorly exploited 12-membered crown ether, aza-12-crown-4 (L^2), with a secondary amine group incorporated into the macrocyclic framework, were used as ligands in the reaction with fluorosilicic acid. Two novel complexes, $(L^1H)_2[SiF_6] \cdot 2H_2O$ and $(L^2H)_2[SiF_5 \cdot 2(H_2O)]_2 \cdot 3H_2O$, were obtained and studied by IR and ^{19}F NMR spectroscopy and X-ray diffraction methods. In complex **1**, the ligand does not use its macrocyclic function, and the final product belongs to the family of the aromatic ammonium hexafluorosilicates sustained by the plethora of charge-assisted $NH(NH_3^+) \cdots F^-$ and $OH(H_2O) \cdots F^-$ hydrogen bonds. The majority of the bases that belong to various classes of compounds, *e.g.*, arylamines,[26–29] alkylamines,[38,39] propargylamine,[40] nitrogen-containing heterocycles of the piperidine or quinoline type,[39] derivatives of guanine,[41,42] hydrazides, thiosemicarbazides and tetraazamacrocycles,[11] form complexes exclusively with the highly symmetric hexafluorosilicate anion, $[SiF_6]^{2-}$. At the same time, only two examples of stabilisation of the labile complex $[SiF_5(H_2O)]^-$ (present in solutions of FSA) by azacrown ethers have been documented so far.[13] The complex $(L^2H)_2[SiF_5(H_2O)]_2 \cdot 3H_2O$ is only the third example of $[SiF_5(H_2O)]^-$ anion stabilised by complex formation with a protonated N-containing crown ether. The major role in stabilisation of the less symmetric and labile species $[SiF_5(H_2O)]^-$ is played by the multiple H-bonding interactions between "organic" and "inorganic" components of the host–guest complex.

Experimental

General methods

All chemicals were purchased from commercial suppliers and used as received. Elemental analyses were carried out at the Physico-Chemical Institute of Environment and Human Protection, Odessa, Ukraine. EI mass spectra were recorded on an MX-1321 instrument (direct sample injection into the ion source, ionisation voltage 70 eV). Infrared spectra were recorded on a Specord 75IR spectrophotometer (4000–400 cm^{-1}, samples in Nujol mulls, KRS-5 glasses). Thermogravimetric analysis (TGA) and differential thermal analysis were performed simultaneously with an OD-102 Paulik–Paulik–Erdey apparatus, with a 10 °C min^{-1} heating rate in air. All NMR experiments were recorded on Avance spectrometers

This journal is © The Royal Society of Chemistry 2007

(Bruker Biospin GmbH, Rheinstetten, Germany), *i.e.* ^{1}H NMR spectra on a DPX 400 instrument (UltraShield™ Magnet) at a resonance frequency of 400.13 MHz, and ^{19}F NMR spectra on a DRX 400 WB instrument equipped with an ATM-BBO probe (outer coil double tunable for ^{1}H or ^{19}F) at a resonance frequency of 376.5 MHz. Chemical shifts were referenced internally to the residual, non-deuterated solvent signal for ^{1}H, or externally to $CFCl_3$ ($\delta = 0$ ppm) for ^{19}F.

The synthesis of L^1 was performed by catalytic reduction of 4′-nitrobenzo-12-crown-4, resulting from the nitration of the initial benzo-12-crown-4 by 50% nitric acid.

Benzo-12-crown-4 [2,3-benzo-1,4,7,10-tetraoxacyclododeca-2-ene]. The compound was synthesised using the modified Pedersen procedure.[19] To a solution of pyrocatechol (22.0 g, 0.20 mol) in *n*-butanol (300 ml) stirred under inert atmosphere a solution of $LiBr{\cdot}2H_2O$ (61.5 g, 0.50 mol) and $LiOH{\cdot}H_2O$ (17.8 g, 0.42 mol) in water (45 ml) was added. The reaction mixture was brought to reflux and then within 5–10 min 1,8-dichloro-3,6-dioxaoctane (38.5 ml, 0.20 mol) was added. The mixture was allowed to react at this temperature for 28 h. After cooling to room temperature the reaction mixture was acidified by concentrated HCl to pH 3–4, filtered and the filtrate evaporated to dryness. The residue was dissolved in chloroform and washed successively with water, saturated Na_2CO_3 and NaCl solutions. After chloroform removal the resulting product was extracted by boiling heptane (2 × 100 ml). After cooling the combined fractions yielded an oil. The supernatant was decanted. The addition of diethyl ether to the remaining oil produced crystals of dibenzo-24-crown-8, which were filtered off, washed with diethyl ether and dried in air. Yield: 1.2 g (27%), mp 112–113 °C (lit.[20] mp 113–114 °C). The filtrate after evaporation of diethyl ether yielded benzo-12-crown-4, which was purified by distillation *in vacuo*, bp 140–145 °C, mp 43–44 °C. An analytical-grade sample was obtained by re-crystallisation from hexane, mp 44–45 °C, in accordance with the literature data[19] (mp 44–45.5 °C). Yield: 11.7 g (26%).

4′-Nitrobenzo-12-crown-4 [2,3-(4′-nitrobenzo)-1,4,7-tetraoxacyclododeca-2-ene]. To a boiling solution of benzo-12-crown-4 (11.2 g, 0.05 mol) in acetonitrile (15 ml), 56% nitric acid (6.0 ml, 0.075 mol) was carefully added. The reaction mixture was allowed to react at this temperature for 30 min and then poured into the ice–water. The precipitate formed was filtered off, washed with water until neutral pH, dried in air and re-crystallised from ethanol. Yield: 12.4 g (92%), mp 108–109 °C (lit.,[43] mp 105–108 °C).

4′-Aminobenzo-12-crown-4 [2,3-(4′-aminobenzo)-1,4,7,10-tetraoxacyclododeca-2-ene]. In a hydrogenation flask were placed 10% Pd/C (1.0 g) and anhydrous methanol (100 ml). The catalyst was activated by passing a stream of hydrogen through the suspension for 1 h. Then a solution of 4′-nitrobenzo-12-crown-4 in methanol (100 ml) was added and the mixture was hydrogenated for 8–10 h to complete the conversion of the substrate [TLC control, DC-Alufolien Kieselgel 60 F254 "Merck", eluent hexane–acetone (1 : 1) or GC control, DIP, glass column (3 × 1200 mm), 5% SE-30 at Inerton N-Super (0.100–0.125 mm) at 50–250 °C]. The catalyst was filtered off, washed with methanol and the combined methanol fractions were evaporated to dryness. The residue was extracted by boiling *n*-heptane (3 × 200 ml) for 20–25 min. The combined extracts were evaporated to one fourth of the initial volume and cooled to 5–10 °C, producing an oil that crystallised on standing for 12–24 h. The product was thoroughly ground and dried *in vacuo*. Yield: 9.9 g (83%), mp 86–88 °C. ^{1}H NMR ($CDCl_3$) δ 3.6 (s, broad, 2H, NH_2), 3.80 (s, 4H, OCH_2CH_2O), 3.81–3.94 (m, 4H, $ArOCH_2CH_2O$), 4.00–4.16 (m, 4H, $ArOCH_2$), 6.24 (dd, 1H, H6, $J_{2'5'} = 8$ Hz, $J_{5'6'} = 3$ Hz), 6.34 (d, 1H, $H_{6'}$), 6.72 (d, 1H, $H_{2'}$).

Aza-12-crown-4 (L^2). Obtained following the literature protocol.[21]

$(L^1H)_2[SiF_6]{\cdot}2H_2O$ (1). To a solution of L^1 (0.24 g, 1.0 mmol) in methanol (10 ml) was added 45% H_2SiF_6 (molar ratio 1 : 3). The resulting solution was allowed to stand at room temperature. Slow evaporation of methanol resulted in almost quantitative formation of a colourless crystalline product, mp ≥180 °C (decomp.). Anal. Calc. for $C_{24}H_{40}F_6N_2O_{10}Si$: C 43.76, H 6.12, F 17.31, N 4.25, Si 4.26%; Found: C 43.71, H 6.16, F 17.38, N 4.33, Si 4.30%. Mass spectrum: $[ML^1]^+$ ($m/z = 239$, $I = 100\%$), SiF_3^+ ($m/z = 85$, $I = 45\%$).

$(L^2H)_2[SiF_6(H_2O)]_2{\cdot}3H_2O$ (2). L^2 (0.18 g, 1.0 mmol) in methanol (5 ml) was mixed with 45% H_2SiF_6 in a 1 : 3 molar ratio. The resulting solution was allowed to stand at room temperature. Slow evaporation of methanol resulted in almost quantitative formation of a colourless crystalline product, mp ≥110 °C (decomp.); Anal. Calc. for $C_{16}H_{46}F_{10}N_2O_{11}Si_2$: C 27.90, H 6.73, F 27.59, N 4.07, Si 8.16%; Found: C 27.96, H 6.77, F 27.64, N 4.14, Si 8.23%. Mass spectrum: $[ML^2]^+$ ($m/z = 175$, $I = 4\%$), $[ML^2 - CH_2OH]^+$ ($m/z = 144$, $I = 8\%$), SiF_3^+ ($m/z = 85$, $I = 58\%$).

X-Ray diffraction measurements

Diffraction intensities for two complexes were collected at 100 K on a X8APEX II CCD diffractometer with MoKα radiation ($\lambda = 0.71073$ Å) in φ and ω scan modes. The structures were solved by direct methods and refined by full-matrix least-squares method on F^2 using SHELXS97 and SHELXL97 programs, respectively.[44] Non-hydrogen atoms were refined anisotropically. C-bound hydrogen atoms were placed in geometrically calculated positions, N- and O-(water) bound hydrogen atoms were found from difference Fourier maps and refined isotropically. The hydrogen bonding geometries for complexes **1** and **2** are listed in Table 1, and crystallographic data in Table 2. Crystallographic data (CIF files) for the structural analysis of complexes **1** and **2** have been deposited with the Cambridge Crystallographic Data Centre, CCDC reference numbers 635343 and 635344, respectively. For crystallographic data in CIF or other electronic format see DOI: 10.1039/b703645k).

Acknowledgements

We are thankful to Mr A. Roller for the collection of X-ray diffraction data.

References

1 C. Airoldi and R. F. de Farias, *J. Fluorine Chem.*, 2000, **103**, 53.
2 Y. Katayama, M. Yokomizo, T. Miura and T. Kishi, *Electrochemistry*, 2001, **69**, 834.

3 S. Han, D. S. Shihabi and C. D. Chang, *J. Catal.*, 2000, **196**, 375.
4 D. E. Clark, *US Pat.* 4689137, 1987.
5 E. Benazzi, J.-F. Jolly, J. M. Silva and M. F. Ribeiro, *US Pat.* 6245704 B1, 2001.
6 V. O. Gelmboldt, *Russ. J. Gen. Chem.*, 1987, **57**, 709.
7 V. O. Gelmboldt, *Russ. J. Inorg. Chem. (Transl. of Zh. Neorg. Khim.)*, 1989, **34**, 231.
8 R. C. Sheridan, *US Pat.* 112784, 1989.
9 H. Baltruschat and S. Baltruschat, *World Pat.* WO 02/15694 A2, 2002.
10 E. T. Urbansky, *Chem. Rev.*, 2002, **102**, 2837.
11 V. O. Gelmboldt, L. V. Koroeva, Ed. V. Ganin, M. S. Fonari, Yu. A. Simonov, V. Ch. Kravtsov, J. Lipkowski, V. S. Sergienko and A. A. Ennan, *Russ. J. Coord. Chem.*, 2004, **30**, 198.
12 N. N. Golovnev, V. V. Nogteva and I. I. Golovneva, *Russ. J. Gen. Chem.*, 2003, **73**, 1468.
13 V. O. Gelmboldt, Yu. A. Simonov, Ed. V. Ganin, M. S. Fonari, V. Ch. Kravtsov, A. A. Dvorkin, L. V. Ostapchuk and A. A. Ennan, *Russ. J. Coord. Chem.*, 1996, **22**, 21.
14 V. O. Gelmboldt, Ed. V. Ganin, L. V. Ostapchuk, A. A. Ennan, Yu. A. Simonov, V. Ch. Kravtsov, M. S. Fonari and J. Lipkowski, *Russ. J. Inorg. Chem. (Transl. of Zh. Neorg. Khim.)*, 1999, **44**, 1139.
15 Yu. A. Simonov, Ed. V. Ganin, A. A. Dvorkin, M. S. Fonari, V. O. Gelmboldt and A. A. Ennan, *Supramol. Chem.*, 1994, **3**, 185.
16 V. O. Gelmboldt, Ed. V. Ganin, Yu. A. Simonov, L. V. Ostapchuk, M. S. Fonari, J. Lipkowski, A. A. Dvorkin and A. A. Ennan, *Russ. J. Coord. Chem.*, 1995, **21**, 183.
17 V. O. Gelmboldt, Ed. V. Ganin, L. V. Ostapchuk, A. A. Ennan, Yu. A. Simonov, J. Lipkowski, A. A. Dvorkin and M. S. Fonari, *Russ. J. Inorg. Chem. (Transl. of Zh. Neorg. Khim.)*, 1996, **41**, 1041.
18 (*a*) C. A. Ilioudis, D. A. Tocher and J. W. Steed, *J. Am. Chem. Soc.*, 2004, **126**, 12395; (*b*) Yu. A. Simonov, M. S. Fonari, V. Ch. Kravtsov, V. O. Gelmboldt, Ed. V. Ganin, L. V. Ostapchuk, A. A. Ennan, Yu. A. Popkov and J. Lipkowski, *Russ. J. Inorg. Chem. (Transl. of Zh. Neorg. Khim.)*, 1998, **43**, 1982; (*c*) A. N. Chekhlov, *Russ. J. Inorg. Chem. (Transl. of Zh. Neorg. Khim.)*, 2003, **48**, 931; (*d*) M. S. Fonari, Y. A. Simonov, V. Ch. Kravtsov, V. O. Gelmboldt, Ed. V. Ganin, Yu. A. Popkov and L. V. Ostapchuk, *J. Inclusion Phenom. Mol. Recognit. Chem.*, 1998, **30**, 197; (*e*) S. Mason, J. M. Llinares, M. Morton, T. Clifford and K. Bowman-James, *J. Am. Chem. Soc.*, 2000, **122**, 1814; (*f*) J. A. Aguilar, T. Clifford, A. Danby, J. M. Llinares, S. Mason, E. Garcia-Espana and K. Bowman-James, *Supramol. Chem.*, 2001, **13**, 405; (*g*) M. S. Fonari, V. Ch. Kravtsov, Yu. A. Simonov, Ed. V. Ganin and V. O. Gelmboldt, *Zh. Strukt. Khim.*, 1999, **40**, 1002; (*h*) L. Q. Tang, M. S. Dadachov and X. D. Zou, *Z. Kristallogr. – New Cryst. Struct.*, 2001, **216**, 391; (*i*) Md. A. Hossain, J. M. Llinares, S. Mason, P. Morehouse, D. Powell and K. Bowman-James, *Angew. Chem., Int. Ed.*, 2002, **41**, 2335; (*j*) Md. A. Hossain, P. Morehouse, D. Powell and K. Bowman-James, *Inorg. Chem.*, 2005, **44**, 2143; (*k*) M. Szafran, Z. Dega-Szafran, A. Addlagatta and M. Jaskolski, *J. Mol. Struct.*, 2001, **598**, 267; (*l*) G. Rother, H. Worzala and U. Bentrup, *Z. Kristallogr.*, 1997, **212**, 310.
19 Yu. A. Simonov, J. Lipkowski, M. S. Fonari, V. Ch. Kravtsov, ed. V. Ganin, V. O. Gelmboldt and A. A. Ennan, in: *Molecular Recognition and Inclusion* from the Proceedings of the Ninth International Symposium on Molecular Recognition and Inclusion, Lyon, 7–12 September, 1996, ed. A. W. Coleman, Kluwer Academic Publishers, Dordrecht, The Netherlands, 1998, p. 503.
20 C. J. Pedersen, *J. Am. Chem. Soc.*, 1967, **89**, 7017.
21 M. J. Calverley and J. Dale, *Acta Chem. Scand., Ser. B*, 1982, **36**, 241.
22 (*a*) M. C. Etter, *Acc. Chem. Res.*, 1990, **23**, 120; (*b*) J. Bernstein, R. E. Davis, I. Shimoni and N.-L. Chang, *Angew. Chem., Int. Ed. Engl.*, 1995, **34**, 1555.
23 W. W. Wilson and K. O. Christe, *J. Fluorine Chem.*, 1982, **19**, 253.
24 D. Mootz and E.-J. Oellers, *Z. Anorg. Allg. Chem.*, 1988, **559**, 27.
25 V. O. Gelmboldt, Ed. V. Ganin, L. Ch. Minacheva and V. S. Sergienko, *Russ. J. Inorg. Chem. (Transl. of Zh. Neorg. Khim.)*, 2005, **50**, 143.
26 V. O. Gelmboldt, Ed. V. Ganin, L. V. Koroeva, L. Ch. Minacheva, V. S. Sergienko and A. A. Ennan, *Russ. J. Inorg. Chem. (Transl. of Zh. Neorg. Khim.)*, 2006, **51**, 194.
27 V. O. Gelmboldt, L. V. Koroeva and K. V. Domasevich, *Russ. J. Inorg. Chem. (Transl. of Zh. Neorg. Khim.)*, 2006, **51**, 1653.
28 W. A. Denne, A. McL Mathieson and M. F. Mackay, *J. Cryst. Mol. Struct.*, 1971, **1**, 155.
29 V. O. Gelmboldt, A. A. Ennan, Ed. V. Ganin, Yu. A. Simonov, M. S. Fonari and M. M. Botoshansky, *J. Fluorine Chem.*, 2004, **125**, 1949.
30 A. Yu. Tsivadze, A. A. Varnek and V. E. Khutorsky, *Coordination Compounds of Metals with Crown-Ligands* (in Russian), Nauka, Moscow, 1991.
31 K. O. Christe and W. W. Wilson, *J. Fluorine Chem.*, 1990, **46**, 339.
32 V. O. Gelmboldt and S. P. Petrosyants, *Russ. J. Coord. Chem.*, 1989, **15**, 501.
33 V. O. Gelmboldt, S. P. Petrosyants, L. A. Gavrilova and A. A. Ennan, *Russ. J. Coord. Chem.*, 1987, **13**, 1615.
34 T. Q. Nguyen, F. Qu, X. Huang and A. F. Janzen, *Can. J. Chem.*, 1992, **70**, 2089.
35 V. N. Plakhotnyk, R. Schmutzler, L. Ernst, Yu. V. Kovtun and A. V. Plakhotnyk, *J. Fluorine Chem.*, 2002, **116**, 41.
36 K. Kleboth, *Monatsh. Chem.*, 1969, **100**, 1057.
37 S. K. Ignatov, P. G. Sennikov, B. S. Ault, A. A. Bagatur'yants, I. V. Simdyanov, A. G. Razuvaev, E. Ju. Klimov and O. Gropen, *J. Phys. Chem. A*, 1999, **103A**, 8328.
38 G. J. Reiss, *Acta Crystallogr., Sect. C: Cryst. Struct. Commun.*, 1998, **54**, 1489.
39 B. D. Conley, B. C. Yearwood, S. Parkin and D. A. Atwood, *J. Fluorine Chem.*, 2002, **115**, 155.
40 T. Steiner, *J. Chem. Crystallogr.*, 1997, **27**, 673.
41 X. Zhang, R. Bau, J. A. Sheehy and K. O. Christe, *J. Fluorine Chem.*, 1999, **98**, 121.
42 A. Waśkowska, *Acta Crystallogr., Sect. C: Cryst. Struct. Commun.*, 1997, **53**, 128.
43 S. Shinkai, T. Ogawa, Yu. Kusano, O. Manabe, K. Kikukawa, T. Goto and T. Matsuda, *J. Am. Chem. Soc.*, 1982, **104**, 1960.
44 G. M. Sheldrick, *SHELXS97 and SHELXL97, Programs for solution and refinement of crystal structures*, University of Göttingen, Germany, 1997.

This journal is © The Royal Society of Chemistry 2007

Додаток Е
Копія статті.

“Hydrogen bonded frameworks of 2-carboxypyridinium hexafluorosilicate and 2-carboxyquinolinium hexafluorosilicate dihydrate”

Acta C preprint

Submitted to *Acta Cryst. C*

Hydrogen bonded frameworks of 2-carboxypyridinium hexafluorosilicate and 2-carboxyquinolinium hexafluorosilicate dihydrate

Vladimir O. Gelmboldt[a], Eduard V. Ganin[a] and Konstantin V. Domasevitch[b]

[a]Physico-Chemical Instutute of Environmental and Human Protection, Ministry of Education and Science of Ukraine, and National Academy of Sciences of Ukraine, Preobrazhenskaya Str. 3, Odessa 65082, Ukraine, and [b]Inorganic Chemistry Department, Kiev University, Volodimirska Str. 64, Kiev 01033, Ukraine

Correspondence email: dk@univ.kiev.ua

Abstract

In 2-carboxypyridinium hexafluorosilicate, $2[C_6H_6NO_2]^+\cdot SiF_6^{2-}$, (I), and in 2-carboxyquinolinium hexafluorosilicate dihydrate, $2[C_{10}H_8NO_2]^+\cdot SiF_6^{2-}\cdot 2H_2O$, (II), silicon atoms of the anions occupy center of inversion. Primary intermoiety interactions in (I) occur by means of strong NH···F and OH···F hydrogen bonding yielding corrugated layers incorporating SiF_6^{2-} anions as four-connected net nodes and organic cations as simple links between them. In (II), a set of strong hydrogen bonding NH···F, OH···O and OH···F, involving also water molecules, led to three-dimensional heterocoordinated rutile-like framework that integrates SiF_6^{2-} anions as six- and water molecules as three-connected nodes. Carboxylic group of the cation was hydrogen bonded to water molecule (O···O 2.5533 (13) Å), while NH function supports direct bonding to the anion (N···F 2.7061 (12) Å).

Comment

Fluorosilicate salts involving onium cations of N– and O-containing organic bases have a significance for practical applications as high crystallinity ionic liquids (Katayama *et al.*, 2000), dielectrics with cryptocrystalline structure (Kalem, 2004), layered organic-inorganic hybrid materials (Airoldi & De Farias, 2000) and also as chemical reagents (Han *et al.*, 2000; Gelmboldt, 1989). Their structure is commonly dominated by strong directional interactions involving fluorine atoms and convenient hydrogen bond donors, although the relations in such systems could be more complicated due to the presence of competitive OH and NH binding sites, inclusion of solvent molecules and extensive weak CH···F hydrogen bonding, as it occurs for 4-carboxyanilinium hexafluorosilicate hydrate (Gelmboldt *et al.*, 2004). Therefore, heteroaromatic onium cations combining set of typical hydrogen bond donating functions (such as NH^+, COOH, CONH2, *etc*) are especially well suited for examination of hydrogen bonding preferences of hexafluorosilicate and its utility as a rigid building block for designing of framework structures. In this context we have prepared two new hexafluorosilicate salts involving 2-carboxypyridinium [compound (I)] and 2-carboxyquinolinium [compound (II)] cations as ambidentate NH/OH H-bond donors, and report their structures here.

Compounds (I) and (II) adopt complicated framework structures originating in strong hydrogen bonding between the cationic and anionic counterparts. In (I), the hexafluorosilicate anion is centrosymmetric with the silicon atom occupying

a center of inversion (Fig. 1). Each of the 2-carboxypyridinium cations provides pair of strong directional hydrogen bonds (NH···F and OH···F) (Table 2). That is a second known example for direct hydrogen bonding of carboxylic group to hexafluorosilicate and O···F separations in (I) and in *N*-carboxymethyl-N-metylpiperidinium salt (2.58 and 2.56 Å, respectively) (Szafran, *et al.*, 2001) are actually the same. Thus the SiF_6^{2-} anion accepts in total two pairs of such interactions utilizing four fluorine atoms, which are coplanar within the coordination octahedron. Therefore the primary strong hydrogen bond connectivity in the structure may be considered as plane (4,4)-net, with SiF_6^{2-} moieties providing four-connected net nodes and the organic cations as simple links between them (Fig. 2). Such principle is very comparable with eight-connected framework topology of tetrakis(2-carboxypyridinium) octacyanomolybdate(IV) (Basson *et al.*, 1980) and this suggests utility of the bifunctional organic cation for designing of hydrogen bonded frameworks, in combination with suitable counter anions as geometrically rigid acceptors of hydrogen bonds.

Corrugated hydrogen bonded layers are parallel to [−101] plane and they pack with a set of weaker interlayer interactions (Fig. 3), such as CH···F hydrogen bonding (C···F 3.14–3.18 Å, Table 2) and a weak slipped π/π interaction that occurs between a pair of antiparallel organic moieties related by inversion (symmetry code: $1-x, 2-y, -z$). The parameters of such interaction, interplanar and intercentroid distances (3.347 (2) and 3.626 (2) Å, respectively) and slippage angle 22.6 (1)° are typical for π/π contacts of electron-deficient heteroaromatic rings (Janiak, 2000).

Structure of the quinolinium salt (II) [the silicon atom of the anion occupies a center of inversion] is much more complicated due to the incorporation of water molecules, which provide additional donor and acceptor sites for strong hydrogen bonding. That is a first structure involving simple 2-carboxyquinolinium cations, since in the previously reported salts of 3-carboxy-4-hydroxybenzenesulfonate (Smith *et al.*, 2004), iodocuprate (Goher *et al.*, 2001) and tetrabromoaurate (Goher *et al.*, 1994) the 2-carboxyquinolinium cations were typically associated by strong OH···O hydrogen bonding with neutral zwitterionic quinolinium-2-carboxylate moieties.

Carboxyl group donates strong hydrogen bond to O atom of water molecule (Table 4), while NH function retains direct interaction with the SiF_6^{2-} anions, similarly to structure (I). This situation parallels hydrogen bonding preferences of hexafluorosilicate in 4-carboxyanilinium hexafluorosilicate hydrate (Gelmboldt *et al.*, 2004), while in a simpler hydrated quinolinium salt the cation/anion interaction was extended by inclusion of water molecules: NH···OH_2···F (Conley *et al.*, 2002). In the latter case the incorporation of water molecules indicates lack of convenient hydrogen bond donors for the quinolinium/hexafluorosilicate system.

Water molecules form pairs of OH···F bonds with the anions (O···F 2.6711 (13) and 2.7064 (13) Å), in a very characteristic manner found for the aqua/anion dimers (Domasevitch & Boldog, 2005). This yields the aqua/anionic chains along 0x direction in the crystal and the organic cations connect these chains into three-dimensional framework as simple bitopic connectors (through employing OH and NH functions). Thus either fluorine atom of the anions accepts one strong hydrogen bond and the water molecule participates in three such interactions as acceptor of one and donor of two bonds. Therefore, the entire hydrogen bonded structure exists as three-dimensional heterocoordinated framework constituted with 3- (water molecules) and 6-connected (SiF_6^{2-} anions) nodes in a 2:1 proportion [total Schlafli symbol $\{4;6^2\}\{4^2;6^{10};8^3\}$] (Fig. 6). Such topology is commonly related to the heterocoordinated rutile net (rtl) (O Keeffe *et al.*, 2000).

There are a set of weaker hydrogen bonding with CH groups of the aromatic frames, in particular C9H9 center F1F2F3 triangular edge of the [SiF_6] octahedron forming trifurcated hydrogen bond. Stacking interactions were also of significance for the crystal packing. They occur between carbocyclic ring of the cation and two carboxylic groups situated at the both

Acta Crystallographica Section C
Crystal Structure Communications
ISSN 0108-2701

Hydrogen-bonded frameworks of bis(2-carboxypyridinium) hexafluorosilicate and bis(2-carboxyquinolinium) hexafluorosilicate dihydrate

Vladimir O. Gelmboldt,[a] Eduard V. Ganin[b] and Konstantin V. Domasevitch[c]*

[a]Physico-Chemical Instutute of Environmental and Human Protection, Ministry of Education and Science of Ukraine and National Academy of Sciences of Ukraine, Preobrazhens'ka Street 3, Odessa 65082, Ukraine, [b]Odessa State Environmental University, Lvivs'ka Street 15, Odessa 65016, Ukraine, and [c]Inorganic Chemistry Department, Kiev University, Volodimirska Street 64, Kiev 01033, Ukraine
Correspondence e-mail: dk@univ.kiev.ua

Received 26 May 2007
Accepted 19 July 2007
Online 9 August 2007

In bis(2-carboxypyridinium) hexafluorosilicate, $2C_6H_6NO_2^+\cdot SiF_6^{2-}$, (I), and bis(2-carboxyquinolinium) hexafluorosilicate dihydrate, $2C_{10}H_8NO_2^+\cdot SiF_6^{2-}\cdot 2H_2O$, (II), the Si atoms of the anions reside on crystallographic centres of inversion. Primary inter-ion interactions in (I) occur *via* strong N—H···F and O—H···F hydrogen bonds, generating corrugated layers incorporating $[SiF_6]^{2-}$ anions as four-connected net nodes and organic cations as simple links in between. In (II), a set of strong N—H···F, O—H···O and O—H···F hydrogen bonds, involving water molecules, gives a three-dimensional hetero-coordinated rutile-like framework that integrates $[SiF_6]^{2-}$ anions as six-connected and water molecules as three-connected nodes. The carboxyl groups of the cation are hydrogen bonded to the water molecule [O···O = 2.5533 (13) Å], while the N—H group supports direct bonding to the anion [N···F = 2.7061 (12) Å].

Comment

Fluorosilicate salts involving onium cations of N- and O-containing organic bases have practical applications as ionic liquids (Katayama *et al.*, 2001), dielectrics with cryptocrystalline structure (Kalem, 2004), layered organic–inorganic hybrid materials (Airoldi & De Farias, 2000) and chemical reagents (Han *et al.*, 2000; Gelmboldt, 1989). Their structure is commonly dominated by strong directional interactions involving F atoms and convenient hydrogen-bond donors, although the relationships in such systems could be more complicated due to the presence of competitive OH and NH binding sites, inclusion of solvent molecules and extensive weak C—H···F hydrogen bonding, as occurs for 4-carboxyanilinium hexafluorosilicate hydrate (Gelmboldt *et al.*, 2004). Therefore, heteroaromatic onium cations combining sets of typical hydrogen-bond donating functions (such as NH^+, COOH, $CONH_2$, *etc.*) are especially well suited for the examination of the hydrogen-bonding preferences of $[SiF_6]^{2-}$ and are useful as rigid building blocks for the design of framework structures. In this context, we have prepared two new $[SiF_6]^{2-}$ salts involving the cations 2-carboxypyridinium and 2-carboxyquinolinium as ambidentate N—H/O—H hydrogen-bond donors, giving the title compounds, (I) and (II), respectively, and report their structures here.

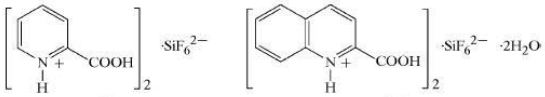

(I) (II)

Compounds (I) and (II) adopt complicated framework structures originating in strong hydrogen bonding between the cationic and anionic counterparts. In (I), the $[SiF_6]^{2-}$ anion is centrosymmetric, with the Si atom occupying a crystallographic centre of inversion (Fig. 1). Each of the 2-carboxypyridinium cations provides a pair of strong directional hydrogen bonds (N—H···F and O—H···F) (Table 2). This is a second known example of direct hydrogen bonding of a carboxyl group to $[SiF_6]^{2-}$; the O···F separations in (I) and in the *N*-carboxymethyl-*N*-methylpiperidinium salt (2.58 and 2.56 Å, respectively; Szafran *et al.*, 2001) are similar. Thus, the $[SiF_6]^{2-}$ anion accepts (in total) two pairs of such interactions utilizing four F atoms, which are coplanar within the coordination octahedron. Therefore, the primary strong hydrogen-bond connectivity in the structure may be considered as a plane (4,4) net, with $[SiF_6]^{2-}$ anions providing four-connected net nodes and with the organic cations as simple links between them (Fig. 2). Such a principle is comparable with the eight-connected framework topology of tetrakis(2-carboxypyridinium)octacyanomolybdate(IV) (Basson *et al.*, 1980) and this suggests the utility of the bifunctional organic cations in the design of hydrogen-bonded frameworks, in combination with suitable counter-anions as geometrically rigid acceptors of hydrogen bonds.

Corrugated hydrogen-bonded layers of (I) are parallel to the $[\bar{1}01]$ plane and pack with a set of weaker interlayer

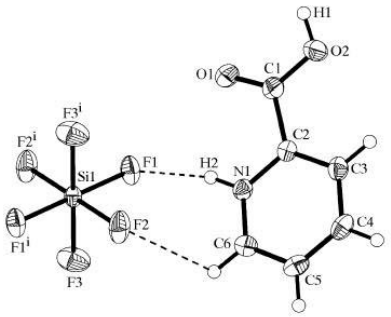

Figure 1
A view of (I), showing the atom-labelling scheme. Displacement ellipsoids are drawn at the 50% probability level and H atoms are shown as small spheres of arbitrary radii. [Symmetry code: (i) $1-x, 2-y, 1-z$.]

 © 2007 International Union of Crystallography DOI: 10.1107/S0108270107035469

electronic reprint

interactions (Fig. 3), such as C—H···F hydrogen bonding (C···F = 3.14–3.18 Å; Table 2) and a weak slipped π–π interaction that occurs between a pair of antiparallel organic moieties related by inversion (symmetry code: $1 - x, 2 - y, -z$). The parameters of such interactions, *i.e.* the interplanar and intercentroid distances [3.347 (2) and 3.626 (1) Å, respectively] and the slippage angle [22.6 (1)°], are typical for π–π contacts between electron-deficient heteroaromatic rings (Janiak, 2000).

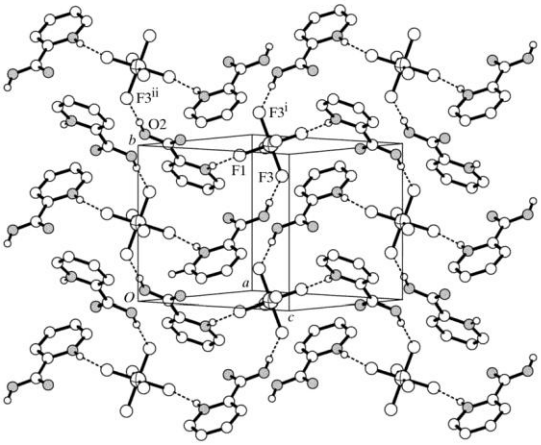

Figure 2
A view of the O—H···F and N—H···F hydrogen-bonded four-connected network in (I). [Symmetry codes: (i) $1 - x, 2 - y, 1 - z$; (ii) $\frac{1}{2} - x, \frac{1}{2} + y, \frac{1}{2} - z$.]

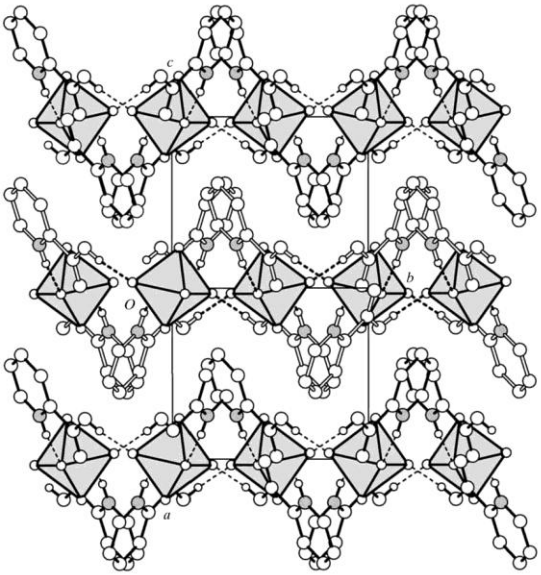

Figure 3
A projection of the structure of (I) on to the [101] plane, showing the packing mode of three successive hydrogen-bonded layers. The $[SiF_6]^{2-}$ anions are represented as shaded polyhedra.

In the quinolinium salt, (II), the Si atom of the anion resides on an inversion centre (Fig. 4). The structure is more complicated due to the incorporation of water molecules, which provide additional donor and acceptor sites for strong hydrogen bonding. This is the first structure involving simple 2-carboxyquinolinium cations, since in the previously reported salts of 3-carboxy-4-hydroxybenzenesulfonate (Smith *et al.*, 2004), iodocuprate (Goher *et al.*, 2001) and tetrabromoaurate (Goher *et al.*, 1994), the 2-carboxyquinolinium cations were typically associated by strong O—H···O hydrogen bonding with neutral zwitterionic quinolinium-2-carboxylate moieties.

The carboxyl group of (II) donates a strong hydrogen bond to the O atom of the water molecule (Table 4), while the N—H function interacts directly with the $[SiF_6]^{2-}$ anions, similar to (I). This situation parallels the hydrogen-bonding preferences of the anion in 4-carboxyanilinium hexafluorosilicate hydrate (Gelmboldt *et al.*, 2004), while in a simpler hydrated quinolinium salt, the cation–anion interaction was extended by inclusion of water molecules (N—H···OH$_2$···F; Conley *et al.*, 2002). Here, the incorporation of water molecules indicates a lack of convenient hydrogen-bond donors for the quinolinium/$[SiF_6]^{2-}$ system in (II).

The water molecules of (II) form pairs of O—H···F bonds with the anions [O···F = 2.6707 (13) and 2.7070 (13) Å], in a very characteristic manner found for aqua–anion dimers (Domasevitch & Boldog, 2005). This generates aqua–anion chains along the *a*-axis direction in the crystal structure (Fig. 5) and the organic cations connect these chains into a three-

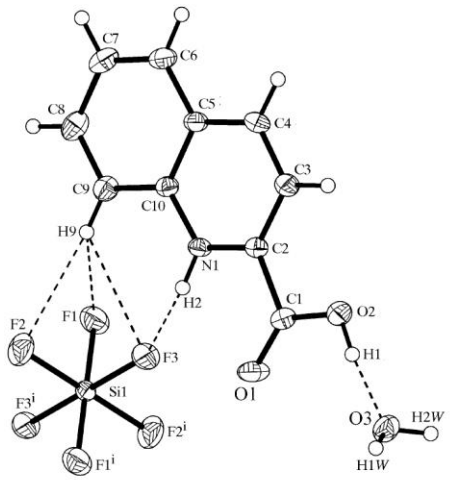

Figure 4
A view of (II), showing the atom-labelling scheme. Displacement ellipsoids are drawn at the 50% probability level and H atoms are shown as small spheres of arbitrary radii. Dashed lines indicate hydrogen bonds. Note the trifurcated hydrogen bonding of the C9—H9 group. [Symmetry code: (i) $-x, 2 - y, -z$.]

electronic reprint

dimensional framework as simple bitopic connectors (using O—H and N—H functions). Thus, either F atom of the anions accepts one strong hydrogen bond and the water molecule participates in three such interactions as an acceptor of one and donor of two bonds. Therefore, the entire hydrogen-bonded structure exists as a three-dimensional hetero-coordinated framework consisting of three- (water molecules) and six-connected ($[SiF_6]^{2-}$ anions) nodes in the ratio 2:1 (total Schlafli symbol $\{4;6^2\}2\{4^2;6^{10};8^3\}$) (Fig. 6). Such topology is commonly related to the heterocoordinated rutile net (rtl) (O'Keeffe *et al.*, 2000).

There are weaker hydrogen bonds involving the aromatic C—H groups of (II), in particular the C9—H9 group directed towards the F1/F2/F3 triangular edge of the $[SiF_6]$ octahedron, forming a trifurcated hydrogen bond (Fig. 4). Stacking interactions are also of significance for the crystal packing. These occur between the carbocyclic ring of the cation and two carboxyl groups situated on both axial sides (Fig. 7). Atoms $O1^{v}$ and $O2^{vi}$ [symmetry codes: (v) $\frac{1}{2}-x, y-\frac{1}{2}, \frac{1}{2}-z$; (vi) $-\frac{1}{2}-x, y-\frac{1}{2}, \frac{1}{2}-z$] are situated almost exactly above the ring centroid with relatively short O···centroid distances (3.22 and 3.30 Å) (Table 5). Such stacking may be compared with recently documented examples of π···anion (heteroatom) interactions, which are characteristic for the most electron-deficient systems of 1,2,4,5-tetrazine (Schottel *et al.*, 2006) and 1,3,5-triazine (Maheswari *et al.*, 2006) [F(O)···π = 2.80–3.20 Å].

In both structures, the organic cations adopt a planar structure [O1—C1—C2—N1 torsion angles do not exceed −3.3 (2)°], with a *trans* orientation of the O—H and N—H groups. The geometric parameters agree well with those of the 2-carboxypyridinium (Smith *et al.*, 1995) and 2-carboxyquinolinium salts (Goher *et al.*, 2001).

The geometry of the $[SiF_6]^{2-}$ anion is sensitive to H···F hydrogen bonding and strong interactions effect an elongation of some Si—F bonds. This is observed in (I) and involves a set of three main bond types (O—H···F3, N—H···F1 and C—H···F2), with a longest Si—F separation corresponding to the F atom interacting with the strongest hydrogen-bond donor [Si—F3 = 1.7003 (9) Å; Table 1]. For (II), there is no such evident differentiation in the strength of the primary hydrogen bonding (N—H···F and O—H···F with water molecules) and all three unique Si—F separations are similar (Table 3).

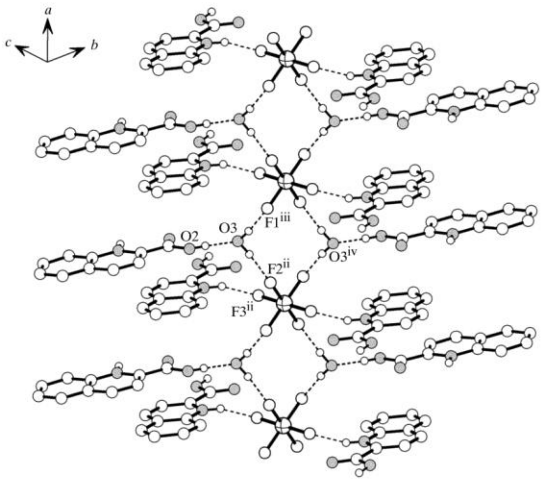

Figure 5
A view of the aqua–$[SiF_6]^{2-}$ chains dominating the connectivity in the structure of (II). The $[SiF_6]^{2-}$ anion (acceptor of six hydrogen bonds) and the water molecules (acceptors of one and donors of two hydrogen bonds) provide six- and three-connected net nodes for the entire three-dimensional framework. [Symmetry codes: (ii) $\frac{1}{2}-x, \frac{1}{2}+y, \frac{1}{2}-z$; (iii) $-\frac{1}{2}-x, \frac{1}{2}+y, \frac{1}{2}-z$; (iv) $-x, 3-y, 1-z$.]

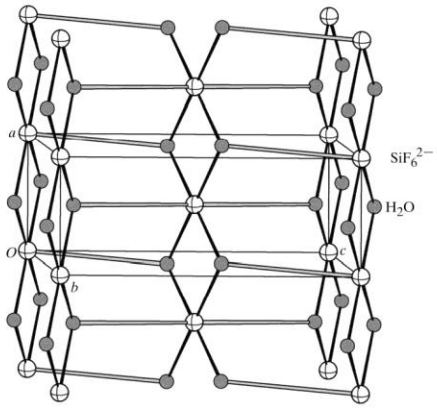

Figure 6
A schematic view of the heterocoordinated three-dimensional rutile-like framework topology in (II). The long grey-shaded links of the net represent 2-carboxyquinolinium bridges between $[SiF_6]^{2-}$ anions (six-connected nodes) and water molecules (three-connected nodes).

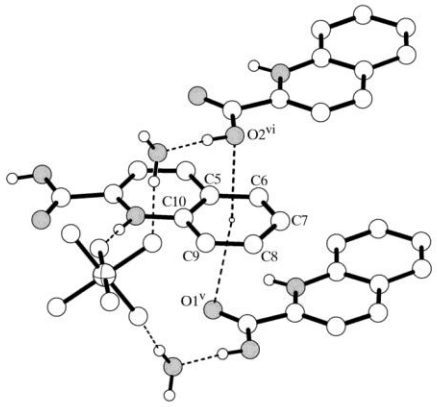

Figure 7
Stacking interactions between the carbocyclic fragment and two carboxyl groups of the 2-carboxyquinolinium cations in (II). [Symmetry codes: (v) $\frac{1}{2}-x, y-\frac{1}{2}, \frac{1}{2}-z$; (vi) $-\frac{1}{2}-x, y-\frac{1}{2}, \frac{1}{2}-z$.]

electronic reprint

In conclusion, both 2-carboxypyridinium and 2-carboxyquinolinium cations reveal potential as singly charged donors of two strong hydrogen bonds and, in combination with $[SiF_6]^{2-}$, they support two- and three-dimensional framework topologies.

Experimental

Compounds (I) and (II) were obtained as large colourless prisms by crystallization of pyridine-2- and quinoline-2-carboxylic acids from aqueous methanolic hexafluorosilicic acid by slow evaporation of the solutions at room temperature. In a typical synthesis, pyridine-2-carboxylic acid (0.123 g, 1 mmol) was dissolved in methanol (3 ml) under reflux and this solution was combined with 45% aqueous H_2SiF_6 (0.9 ml, molar ratio 1:3). The reaction mixture was allowed to stand at room temperature until colourless transparent crystals were deposited (m.p. 455 K, without decomposition).

Compound (I)

Crystal data

$2C_6H_6NO_2^+\cdot SiF_6^{2-}$
M_r = 390.33
Monoclinic, $P2_1/n$
a = 9.3571 (9) Å
b = 7.8717 (6) Å
c = 9.8053 (8) Å
β = 91.943 (7)°
V = 721.81 (11) Å^3
Z = 2
Mo $K\alpha$ radiation
μ = 0.26 mm^{-1}
T = 173 (2) K
0.17 × 0.16 × 0.14 mm

Data collection

Stoe IPDS diffractometer
9005 measured reflections
1935 independent reflections
1646 reflections with $I > 2\sigma(I)$
R_{int} = 0.059

Refinement

$R[F^2 > 2\sigma(F^2)]$ = 0.033
$wR(F^2)$ = 0.092
S = 1.04
1935 reflections
115 parameters
H-atom parameters constrained
$\Delta\rho_{max}$ = 0.39 e Å^{-3}
$\Delta\rho_{min}$ = 0.34 e Å^{-3}

Table 1
Selected geometric parameters (Å, °) for (I).

Si1—F1	1.6866 (8)	O2—C1	1.3147 (17)
Si1—F2	1.6621 (8)	N1—C2	1.3453 (16)
Si1—F3	1.7003 (9)	N1—C6	1.3349 (17)
O1—C1	1.2015 (17)	C1—C2	1.5047 (17)
F1—Si1—F2	90.73 (4)	O1—C1—O2	126.77 (13)
F1—Si1—F3	90.08 (5)	O1—C1—C2	121.01 (12)
F2—Si1—F3	90.15 (6)	O2—C1—C2	112.19 (11)
O2—C1—C2—C3	−1.22 (18)		

Table 2
Hydrogen-bond geometry (Å, °) for (I).

D—H···A	D—H	H···A	D···A	D—H···A
O2—H1···F3^{i}	0.85	1.76	2.5819 (14)	163
N1—H2···F1	0.88	1.85	2.6730 (14)	156
C3—H3···F2^{ii}	0.95	2.37	3.1785 (18)	142
C5—H5···F1^{iii}	0.95	2.36	3.1364 (15)	139
C5—H5···F2^{iv}	0.95	2.56	3.4602 (16)	159
C6—H6···F2	0.95	2.61	3.0416 (17)	108

Symmetry codes: (i) $-x+\frac{1}{2}, y+\frac{1}{2}, -z+\frac{1}{2}$; (ii) $-x+1, -y+2, -z$; (iii) $x+\frac{1}{2}, -y+\frac{3}{2}, z-\frac{1}{2}$; (iv) $-x+\frac{3}{2}, y-\frac{1}{2}, -z+\frac{1}{2}$

Compound (II)

Crystal data

$2C_{10}H_8NO_2^+\cdot SiF_6^{2-}\cdot 2H_2O$
M_r = 526.47
Monoclinic, $P2_1/n$
a = 6.6382 (6) Å
b = 9.4274 (9) Å
c = 17.0668 (14) Å
β = 91.731 (8)°
V = 1067.57 (17) Å^3
Z = 2
Mo $K\alpha$ radiation
μ = 0.21 mm^{-1}
T = 173 (2) K
0.16 × 0.12 × 0.12 mm

Data collection

Stoe IPDS diffractometer
9457 measured reflections
2697 independent reflections
2368 reflections with $I > 2\sigma(I)$
R_{int} = 0.039

Refinement

$R[F^2 > 2\sigma(F^2)]$ = 0.037
$wR(F^2)$ = 0.102
S = 1.05
2697 reflections
160 parameters
H-atom parameters constrained
$\Delta\rho_{max}$ = 0.36 e Å^{-3}
$\Delta\rho_{min}$ = 0.42 e Å^{-3}

Table 3
Selected geometric parameters (Å, °) for (II).

Si1—F1	1.6830 (8)	N1—C10	1.3718 (14)
Si1—F2	1.6861 (8)	O1—C1	1.2061 (15)
Si1—F3	1.6834 (7)	O2—C1	1.3086 (15)
N1—C2	1.3349 (14)	C1—C2	1.5065 (15)
F1—Si1—F2	89.74 (5)	O1—C1—O2	127.59 (11)
F1—Si1—F3	89.59 (4)	O1—C1—C2	120.95 (11)
F2—Si1—F3	90.19 (4)	O2—C1—C2	111.45 (10)
O1—C1—C2—N1	−1.58 (19)		

Table 4
Hydrogen-bond geometry (Å, °) for (II).

D—H···A	D—H	H···A	D···A	D—H···A
N1—H2···F3	0.88	1.86	2.7061 (12)	160
O2—H1···O3	0.85	1.71	2.5531 (13)	171
O3—H1W···F2^{i}	0.85	1.86	2.7070 (13)	175
O3—H2W···F1^{ii}	0.85	1.82	2.6707 (13)	176
C3—H3···F2^{iii}	0.95	2.63	3.2125 (15)	120
C4—H4···O3^{iv}	0.95	2.51	3.3940 (15)	156
C4—H4···F2^{iii}	0.95	2.69	3.2526 (15)	118
C6—H6···O1^{iv}	0.95	2.43	3.1655 (16)	134
C7—H7···F1^{v}	0.95	2.59	3.3463 (16)	137
C9—H9···F1	0.95	2.59	3.3823 (15)	141
C9—H9···F2	0.95	2.57	3.4900 (16)	164
C9—H9···F3	0.95	2.62	3.2907 (15)	128

Symmetry codes: (i) $-x+\frac{1}{2}, y+\frac{1}{2}, -z+\frac{1}{2}$; (ii) $-x-\frac{1}{2}, y+\frac{1}{2}, -z+\frac{1}{2}$; (iii) $x-\frac{1}{2}, -y+\frac{3}{2}, z+\frac{1}{2}$; (iv) $x, y-1, z$; (v) $-x, -y+1, -z$.

Table 5
Carbonyl···π contacts (Å, °) for (II).

For details, see Fig. 7. φ is the angle of the O···π axis with respect to the plane of the aromatic ring.

O atom	C···O range	O···π	O···plane	φ
O1^{v}	3.31–3.71	3.2240 (11)	3.1830 (13)	80.9 (2)
O2^{vi}	3.40–3.77	3.3008 (11)	3.2626 (13)	81.3 (2)

Symmetry codes: (v) $\frac{1}{2}-x, y-\frac{1}{2}, \frac{1}{2}-z$; (vi) $-\frac{1}{2}-x, y-\frac{1}{2}, \frac{1}{2}-z$.

electronic reprint

All H atoms were located in difference maps and then treated as riding, with O H distances constrained to 0.85 Å, N H distances constrained to 0.88 Å and C H distances constrained to 0.95 Å, and with $U_{iso}(H) = 1.2U_{eq}(C)$ or $1.5U_{eq}(N,O)$.

For both compounds, data collection: *IPDS Software* (Stoe & Cie, 2000); cell refinement: *IPDS Software*; data reduction: *IPDS Software*; program(s) used to solve structure: *SHELXS97* (Sheldrick, 1997); program(s) used to refine structure: *SHELXL97* (Sheldrick, 1997); molecular graphics: *DIAMOND* (Brandenburg, 1999); software used to prepare material for publication: *WinGX* (Version 1.700.00; Farrugia, 1999).

The authors acknowledge support from the Deutsche Forschungsgemeinschaft (KVD).

Supplementary data for this paper are available from the IUCr electronic archives (Reference: GG3102). Services for accessing these data are described at the back of the journal.

References

Airoldi, C. & De Farias, R. F. (2000). *J. Fluorine Chem.* **103**, 53–55.

Basson, S. S., Leipoldt, J. G. & van Wyk, A. J. (1980). *Acta Cryst.* **B36**, 2025–2028.

Brandenburg, K. (1999). *DIAMOND*. Release 2.1e. Crystal Impact GbR, Bonn, Germany.

Conley, B. D., Yearwood, B. C., Parkin, S. & Atwood, D. A. (2002). *J. Fluorine Chem.* **115**, 155–160.

Domasevitch, K. V. & Boldog, I. (2005). *Acta Cryst.* **C61**, o373–o376.

Farrugia, L. J. (1999). *J. Appl. Cryst.* **32**, 837–838.

Gelmboldt, V. O. (1989). *Zh. Neorg. Khim.* **34**, 239–240.

Gelmboldt, V. O., Ennan, A. A., Ganin, E. V., Simonov, Yu. A., Fonari, M. S. & Botoshansky, M. M. (2004). *J. Fluorine Chem.* **125**, 1951–1957.

Goher, M. A. S., Hafez, A. K. & Mak, T. C. W. (2001). *Polyhedron*, **20**, 2583–2587.

Goher, M. A. S., Hafez, A. K., Wang, R.-J., Chen, X.-M. & Mak, T. C. W. (1994). *Aust. J. Chem.* **47**, 1423–1430.

Han, S., Shihabi, D. S. & Chang, C. D. (2000). *J. Catal.* **196**, 375–378.

Janiak, C. (2000). *J. Chem. Soc. Dalton Trans.* pp. 3885–3898.

Kalem, S. (2004). *Appl. Surf. Sci.* **236**, 336–341.

Katayama, Y., Yokomizo, M., Miura, T. & Kishi, T. (2001). *Electrochemistry*, **69**, 834–836.

Maheswari, P. U., Modec, B., Pevec, A., Kozlevcar, B., Massera, C., Gamez, P. & Reedijk, J. (2006). *Inorg. Chem.* **45**, 6637–6645.

O'Keeffe, M., Eddaoudi, M., Li, H., Reineke, T. & Yaghi, O. M. (2000). *J. Solid State Chem.* **154**, 3–20.

Schottel, B. L., Chifotides, H. T., Shatruk, M., Chouai, A., Perez, L. M., Bacsa, J. & Dunbar, K. R. (2006). *J. Am. Chem. Soc.* **128**, 5895–5912.

Sheldrick, G. M. (1997). *SHELXS97* and *SHELXL97*. University of Göttingen, Germany.

Smith, G., Byriel, K. A. & Kennard, C. H. L. (1995). *Acta Cryst.* **C51**, 1425–1427.

Smith, G., Wermuth, U. D. & White, J. M. (2004). *Acta Cryst.* **C60**, o575–o581.

Stoe & Cie (2000). *IPDS Software*. Stoe & Cie GmbH, Darmstadt, Germany.

Szafran, M., Dega-Szafran, Z., Addlagata, A. & Jaskolski, M. (2001). *J. Mol. Struct.* **598**, 267–276.

electronic reprint

Додаток Ж
Копія статті.

“Structure of oxonium hexafuoroniobate and hexafuorotantalate complexes with crown ethers of diferent dimensionality”

POLY 6850
14 August 2007 Disk Used
ARTICLE IN PRESS
No. of Pages 10, Model 5+

Available online at www.sciencedirect.com
ScienceDirect
Polyhedron xxx (2007) xxx xxx
POLYHEDRON
www.elsevier.com/locate/poly

Structure of oxonium hexafluoroniobate and hexafluorotantalate complexes with crown ethers of different dimensionality

Marina S. Fonari [a,*], Yurii A. Simonov [a], Wen-Jwu Wang [b], Shang-Wei Tang [b], Eduard V. Ganin [c], Vladimir O. Gelmboldt [d], Tatiana S. Chernaya [e], Olga A. Alekseeva [e], Nina G. Furmanova [e]

Q1 [a] *Institute of Applied Physics, X-ray Laboratory, Academiei str., 5, MD-2028 Chisinau, Moldova*
[b] *Department of Chemistry, Tamkang University, Tamsui, Taipei, Taiwan, ROC*
[c] *Odessa State Environmental University, Odessa, Ukraine*
[d] *Physico-Chemical Institute of Environment and Human Protection, Odessa, Ukraine*
[e] *Institute of Crystallography RAS, Moscow, Russia*

Received 6 July 2007; accepted 16 July 2007

Abstract

Two synthetic pathways, the interaction of Nb_2O_5 or Ta_2O_5 with an aqueous solution of hydrofluoric acid, HF, in the presence of 18-crown-6 (18C6), 15-crown-5 (15C5), benzo-15-crown-5 (B15C5) or benzo-12-crown-4 (B12C4), and the direct interaction of the corresponding pentafluorides, MF_5 (M = Ta, Nb), in the presence of HF with the same crown ethers result in crystalline complexes of the same composition, $[18C6 \cdot H_3O][NbF_6]$ (**1**), $[18C6 \cdot H_3O][TaF_6]$ (**2**), $[15C5 \cdot H_5O_2][TaF_6]$ (**3**), $[(B15C5)_2 \cdot H_5O_2][(B15C5)_2 \cdot H_3O][TaF_6]_2$ (**4**) and $[(B12C4)_2 \cdot H_3O][TaF_6]$ (**5**). Complexes **1–5** were identified by elemental and X-ray structural analysis. Compounds **1** and **2** are isostructural, with the $[H_3O]^+$ oxonium ion embedded in one crown molecule *via* OH···O hydrogen bonds. Complexes **3–5** represent sandwich-like adducts with the $[H_3O]^+$ or $[H_5O_2]^+$ cations encapsulated. A plethora of weak C–H···F interactions with NbF_6 and TaF_6 anions is responsible for the extended supramolecular architectures.
© 2007 Elsevier Ltd. All rights reserved.

Keywords: Hexafluoroniobate and hexafluorotantalate anions; Oxonium ions; Crown ethers; Hydrogen bond; Crystal structure

1. Introduction

The solid-state structures of crown ether (CE) inclusion complexes represent a compromise of interaction energies of as many supramolecular interactions as possible ranging from ion–dipole interactions to strong and weak hydrogen bonds. A significant amount of work on crown ether complexes of the hydrated proton (oxonium ion $[H(H_2O)_n]^+$) revealed the CEs acting as excellent acceptors for strong, charge-assisted hydrogen bonds with oxonium ions, where the choice of CE and counter-ion is of crucial influence. The dimensionality of the CE is a decisive factor that dictates the composition of the stored oxonium species: the 18-membered CEs were shown to be almost entirely selective for the simplest oxonium ion $[H_3O]^+$ (often called the Eigen core), because of the size and symmetry match of $[H_3O]^+$ and the CE cavity [1]. Smaller in size, 12C4 and 15C5 provide sandwich-like cages for $[H_5O_2]^+$ and $[H_7O_3]^+$ oxonium species when $[AuCl_4]^-$ acts as a counter-ion [2].

* Corresponding author. Tel.: +373 22 73 81 54; fax: +373 22 72 58 87.
E-mail addresses: fonari.xray@phys.asm.md (M.S. Fonari), wjw@mail.tku.edu.tw (W.-J. Wang), edganin@yahoo.com (E.V. Ganin), eksvar@ukr.net (V.O. Gelmboldt), furm@ns.crys.ras.ru (N.G. Furmanova).

0277-5387/$ - see front matter © 2007 Elsevier Ltd. All rights reserved.
doi:10.1016/j.poly.2007.07.037

Please cite this article in press as: M.S. Fonari et al., Polyhedron (2007), doi:10.1016/j.poly.2007.07.037

POLY 6850 ARTICLE IN PRESS No. of Pages 10, Model 5+
14 August 2007 Disk Used

On the other hand, an interest in the chemistry of Nb(V) and Ta(V) fluorides is essentially connected with the development of suitable methods for concentration (separation) of these elements, the processes being based on the recrystallization or extraction of the proper complexes from acidic aqueous solutions [3]. Recently, we revealed some interesting features of the "host–guest" complexes formed as a result of the interaction of Nb and Ta pentafluorides with crown ethers. Two synthetic routes were applied: the interaction of the corresponding M_2O_5 oxides with hydrofluoric acid in the presence of the CE, and the direct interaction of MF_5, also in the presence of HF, with the same crown ethers. These two pathways resulted in crystalline complexes of the composition $[CE \cdot H_3O][MF_6]$ for the hexadentate benzo-18-crown-6 [4], *cis-syn-cis*-dicyclohexyl-18-crown-6 [5] and diphenyl-20-crown-6 [6], $[(1.5DB18C6)_2 \cdot H_7O_3][MF_6]$ complexes for 1.5-dibenzo-18C6 [6] and $[TB30C10 \cdot H_5O_2][MF_6]$ for tetrabenzo-30-crown-10 (M = Nb, Ta) [7]. Complexes with B18C6 and *cis-syn-cis*-DCH18C6 provided examples of supramolecular isomers: monoclinic ($P2_1/n$) and orthorhombic ($Pbca$) polymorphs for $[B18C6 \cdot H_3O][TaF_6]$ that are distinct by the subtle packing changes [4], and monoclinic again ($P2_1/n$) and triclinic ($P\bar{1}$) polymorphs for [*cis-syn-cis*-$DCH18C6 \cdot H_3O][TaF_6]$, differing by the pronounced conformational changes in the macrocyclic molecule and in the crystal packing [5]. The occurrence of supramolecular isomerism (SI) [8] implies a superstructural diversity for a given building block. Complexes with conformationally flexible CEs and aza-macrocycles give some examples of supramolecular isomers [9].

The next intriguing feature of the studied complexes is a diversity of the encapsulated oxonium ions [10]. The use of hexadentate B18C6, *cis-syn-cis*-DCH18C6 and DP20C6 resulted in crystalline complexes of the general formula $[CE \cdot H_3O][MF_6]$, where the macrocyclic cavity includes the simplest oxonium cation H_3O^+ (also called an Eigen core [10]), while the use of TB30C10 afforded the opportunity for the extraction of the $[H_5O_2]^+$ Zundel cation, $[H_2O \cdots H \cdots OH_2]^+$ [10] within the complex of the same stoichiometry. The decrease in number of oxygen atoms accessible for interaction with the tripodal oxonium cation in the case of [1.5] DB18C6 resulted in the storage of the three-membered oxonium cluster $[H_7O_3]^+$ within the cage formed by two [1.5] DB18C6 molecules in the complex of composition $[(1.5DB18C6)_2 \cdot H_7O_3][MF_6]$ (M = Nb, Ta) [6].

In this paper, we selected gradually diminishing in size classic 18-crown-6 (18C6), 15-crown-5 (15C5), benzo-15-crown-5 (B15C5) and benzo-12-crown-4 (B12C4) as macrocyclic ligands to react with Nb and Ta pentafluorides. Five new complexes, $[18C6 \cdot H_3O][NbF_6]$ (**1**), $[18C6 \cdot H_3O][TaF_6]$ (**2**), $[15C5 \cdot H_5O_2][TaF_6]$ (**3**), $[(B15C5)_2 \cdot H_5O_2][(B15C5)_2 \cdot H_3O][TaF_6]_2$ (**4**) and $[(B12C4)_2 \cdot H_3O][TaF_6]$ (**5**), were obtained. The crystals were obtained by the two above described synthetic routes, resulting in both cases (four crown ethers used) in crystallographically identical complexes. The details of their synthesis and structure are reported.

2. Experimental

2.1. Materials and apparatus

Caution! Hydrofluoric acid should be treated as an extremely aggressive liquid. All crown ethers were purchased from ACROS, Ta_2O_5/Nb_2O_5 and TaF_5/NbF_5 were purchased from Aldrich and were used without further purification. Complexes $[18C6 \cdot H_3O][NbF_6]$ (**1**), $[18C6 \cdot H_3O][TaF_6]$ (**2**), $[15C5 \cdot H_5O_2][TaF_6]$ (**3**), $[(B15C5)_2 \cdot H_5O_2][TaF_6]$ $[(B15C5)_2 \cdot H_3O][TaF_6]$ (**4**) and $[(B12C4)_2 \cdot H_3O][TaF_6]$ (**5**) were obtained by two synthetic pathways: by an interaction of the corresponding oxides with 40% aqueous HF followed by treatment of the resulting solution with the corresponding crown ether, and by the interaction of the initial corresponding metal pentafluoride, NbF_5/TaF_5, with the CE in a medium of 40% HF. All the complexes were analyzed for C, H and F in a Perkin–Elmer 240 °C instrument. The X-ray structural analysis revealed the identity of the complexes obtained under the different synthetic conditions, the best crystallographic results are discussed in this paper.

2.2. Synthesis

I route: To Nb_2O_5/Ta_2O_5 (0.5 mmol) dissolved in 45% HF (6–7 ml), the corresponding CE (1 mmol) dissolved in 8–10 ml methanol was added. The resulting solution was stored at 20–25 °C in a Teflon exsiccator for a low evaporation of solvent to a volume of 5–6 ml over several days.

II route: To solution of CE (1 mmol) was added a solution of NbF_5/TaF_5 (1 mmol) in 10–12 ml of 45% hydrofluoric acid. The resulting solution was stored at 20–25 °C in a Teflon exsiccator for a low evaporation of solvent to a volume of 5–6 ml over several days.

2.2.1. $[18C6 \cdot H_3O][NbF_6]$ (1)

Crystals of complex **1** separated in a yield of 72% (0.350 g), and are colorless transparent prisms, soluble in methanol, ethanol; m.p.: >220 °C (decomp). *Anal.* Calc. for $C_{12}H_{27}F_6NbO_7$: C, 29.40; H, 5.55; F, 23.25. Found: C, 29.33; H, 5.58; F, 23.45%.

2.2.2. $[18C6 \cdot H_3O][TaF_6]$ (2)

Crystals of **2** separated in a yield of 75% (0.430 g), and are colorless transparent prisms, soluble in methanol, ethanol; m.p.: >195 °C (decomp). *Anal.* Calc. for $C_{12}H_{27}F_6TaO_7$: C, 29.42; H, 4.71; F, 19.71. Found: C, 24.87; H, 4.68; F, 19.70%.

2.2.3. $[15C5 \cdot H_5O_2][TaF_6]$ (3)

Crystals of **3** separated in a yield of 74% (0.280 g), and are colorless transparent prisms, soluble in methanol, ethanol; m.p.: 124–125 °C (decomp). *Anal.* Calc. for

Please cite this article in press as: M.S. Fonari et al., Polyhedron (2007), doi:10.1016/j.poly.2007.07.037

POLY 6850 ARTICLE IN PRESS No. of Pages 10, Model 5+
14 August 2007 Disk Used

$C_{10}H_{25}F_6O_7Ta$: C, 31.10; H, 5.87; F, 14.76. Found: C, 31.13; H, 5.92; F, 14.82%.

2.2.4. $\{(B15C5)_2 \cdot H_5O_2\}\{TaF_6\}\{(B15C5)_2 \cdot H_3O\}\{TaF_6\}$ (4)

Crystals of **4** were separated in a yield of 82% (0.350 g), and are colorless transparent crystals, soluble in methanol, ethanol; m.p.: 126–127 °C (decomp). *Anal.* Calc. for $C_{56}H_{88}F_{12}O_{23}Ta_2$: C, 39.12; H, 5.16; F, 13.26. Found: C, 39.59; H, 5.17; F, 13.34%.

2.2.5. $\{(B12C4)_2 \cdot H_3O\}\{TaF_6\}$ (5)

Crystals of **5** were separated in a yield of 95% (0.360 g), and are colorless transparent crystals, soluble in methanol, ethanol; m.p.: >180 °C (decomp). *Anal.* Calc. for $C_{24}H_{35}F_6O_9Ta$: C, 37.81; H, 4.63; F, 14.95. Found: C, 37.78; H, 4.67; F, 14.91%.

2.3. X-ray diffraction determination

The X-ray intensity data for complexes **1**, **2**, **4** and **5** were recorded at 123 K on a Bruker SMART 1000 CCD area detector diffractometer employing graphite monochromatized Mo Kα radiation ($\lambda = 0.71073$ Å) in the ϕ and ω scan mode. Final unit cell dimensions and positional data were obtained and refined on the entire data set. Integration and scaling resulted in a data set corrected for Lorentz and polarization effects using DENZO [11]. The scaling as well as the global refinement of the crystal parameters were performed by SCALEPACK [11]. The experimental data for complex **3** were recorded at ambient temperature (295 K) on an Xcalibur S with a CCD detector (Mo-Kα radiation, graphite monochromator, ω scan mode). The absorption correction for **2–5** was applied using SADABS [12]. The structure solution and refinement proceeded similarly using the SHELX-97 program package [13] for all the structures. Direct methods yielded all non-hydrogen atoms of the asymmetric unit. These atoms were treated anisotropically (full-matrix least squares method on F^2). In complexes **1** and **2** the macrocycle and oxonium cation occupy the special position 2/*m*, that makes it impossible to localize the oxonium hydrogen atoms, and in the next section only O···O distances will be discussed. In complex **3** the mirror plane *m* bisects the macrocycle through the O(1) atom and the C(5)–C(5′) valent bond, both oxygen atoms and one hydrogen atom of the $(H_5O_2)^+$ oxonium cation. The crown oxygen atom O(3) is disordered over two positions with equal occupancies. In complexes **4** and **5** the oxonium ion occupies a position on a two-fold axis, being equally disordered. C-bound H atoms were placed in calculated positions, with C–H distances of 0.93 or 0.97 Å, and were treated using a riding-model approximation with $U_{iso}(H) = 1.2\ U_{eq}(C)$. H atoms of water molecules and oxonium ions were determined from difference Fourier maps and were then allowed to refine isotropically with $U_{iso}(H) = 1.5U_{eq}(O)$ and O–H distances subjected to DFIX restraints.

The X-ray data and details of the refinement for **1–5** are summarized in Table 1, selected geometric parameters are given in Table 2 and the hydrogen bonding geometries for **3–5** are given in Table 3.

3. Results and discussion

3.1. Description of the structures

Complexes **1** and **2** are isostructural (Table 1), so only complex **2** is further discussed. Both complexes crystallize in the orthorhombic space group *Pbam*. The NbF_6^- anion in complex **1** resides on an inversion centre and is characterized by an octahedral core with Nb–F distances ranging from 1.844(2) up to 1.876(2) Å and F–Nb–F valent angles between *cis*-fluorine atoms practically being equal to 90°. The geometry of the NbF_6^- anion is close to that found in 3-chloro-1,3,4,2,5-thiadiselenadiazolium hexafluoroniobium [14] and in bis(pyrazine)dicopper bis(hexafluoroniobium) piperazine solvate [15]. The TaF_6^- anions in complexes **2–5** also adopt the usual octahedral geometry with Ta–F distances ranging from 1.854(5) to 1.877(7) Å in **2**, from 1.868(8) to 1.887(7) Å in **3**, from 1.845(4) to 1.874(4) Å in **4**, and from 1.881(3) to 1.888(2) Å in **5**, the maximal deviation for the F–Ta–F valent angle between *cis*-fluorine atoms from a right angle being 1.5°. This geometry is close to that found in catena-[(μ-chloro)-bis(μ-fluoro)tetrafluoro-hexamethyltantalum)] ditin [16] and in methyltriphenylphosphonium hexafluorotantalate [17].

3.1.1. $\{18C6 \cdot H_3O\}\{TaF_6\}$ (2)

The ORTEP view for complex **2** is shown in Fig. 1. The 18C6 molecule and oxonium cation $(H_3O)^+$ are situated in the 2/*m* position: the *m* plane passes through the O(1) and O(1′) atoms, and the twofold axis bisects the C(3)–C(3′) bond. The arrangement of both macrocycle and oxonium ion on a special position explains the availability of only two different O(oxonium)···O(crown) distances, being equal to 2.777(6) Å [to O(1) and its symmetry-related counterpart], and 2.708(5) Å [to O(2) and its three symmetry-related counterparts]. The 18C6 molecule is characterized by the idealized D_{3d} symmetry with the *trans-gauche-trans*-sequence of torsion angles and ±0.171(5) Å deviation of oxygen atoms from the mean plane.

3.1.2. $\{15C5 \cdot H_5O_2\}\{TaF_6\}$ (3)

Complex **3**, of the composition $[15C5 \cdot H_5O_2][TaF_6]$, crystallises in the orthorhombic crystal system, space group *Pnma*. The ORTEP view for complex **3** is shown in Fig. 2. The asymmetric unit of **3** comprises of one half of the TaF_6^- anion, one half of the 15C5 molecule and one half of the $(H_5O_2)^+$ Zundel cation, all these species residing on a mirror plane. Within the Zundel cation, the water molecule and oxonium ion are held together *via* a strong OH···O hydrogen bond, the O···O separation being 2.462(12) Å. Its interaction with two neighboring crown molecules related by the glide plane occurs in such a way

Please cite this article in press as: M.S. Fonari et al., Polyhedron (2007), doi:10.1016/j.poly.2007.07.037

POLY 6850 ARTICLE IN PRESS No. of Pages 10, Model 5+
14 August 2007 Disk Used

Table 1
Crystal data and structure refinement parameters for complexes 1–5

	1	2	3	4	5
Composition	$C_{12}H_{27}F_6NbO_7$	$C_{12}H_{27}F_6O_7Ta$	$C_{18}H_{25}F_6O_7Ta$	$C_{56}H_{88}F_{12}O_{23}Ta_2$	$C_{24}H_{35}F_6O_9Ta$
CCDC number	652989	652990	652991	652992	652993
Formula weight	490.25	578.29	552.25	1719.16	762.47
Crystal system	orthorhombic	orthorhombic	orthorhombic	monoclinic	triclinic
Space group	*Pbam*	*Pbam*	*Pnma*	*C2/c*	*P*1
a (Å)	9.0639(8)	9.0655(13)	12.2350(16)	28.293(5)	8.7701(15)
b (Å)	10.1656(9)	10.1316(14)	12.6607(16)	16.023(3)	8.8881(15)
c (Å)	10.9854(13)	10.9474(16)	11.9124(16)	15.943(3)	10.0280(17)
α (°)	90.0	90.0	90.0	90.0	72.114(3)
β (°)	90.0	90.0	90.0	106.05(3)	83.909(3)
γ (°)	90.0	90.0	90.0	90.0	73.275(3)
V (Å^3)	1012.19(17)	1005.5(2)	1845.3(4)	6946(2)	712.3(2)
Z	2	2	4	8	1
D_{calc} (Mg/m^3)	1.609	1.910	1.988	1.644	1.778
μ (mm^{-1})	0.676	5.548	6.041	3.252	3.945
F(000)	500	564	1072	3448	378
Reflections collected/unique	942/942	5421/1054	14070/1791	15382/6162	3978/2730
Reflections with $I > 2\sigma(I)$	677	733	1423	4730	2730
Goodness-of-fit	1.064	1.055	1.170	1.022	1.075
R_1, wR_2 [$I > 2\sigma(I)$]	0.0517, 0.1441	0.0289, 0.0862	0.0566, 0.1099	0.0378, 0.0783	0.0227, 0.0604

that the $(H_3O)^+$ oxonium part is involved in two equal OH···O bifurcated hydrogen bonds to the O(2) and O(3A) atoms, the O···O separations being 2.646 and 2.945 Å, while the 'water part' *via* O(4) is involved in the O(4)···O(3) interaction, the O···O separation being 2.995(15) Å (Table 3). The crown molecules and $(H_5O_2)^+$ cations alternate in the infinite chain. The atom O(4) deviates by 1.692(4) Å from the mean plane of crown oxygen atoms that are coplanar to within ±0.28 Å, while atom O(5) deviates by 1.692(4) Å from the same atoms of the next crown molecule. In the macrocyclic framework all the C–O–C–C torsion angles are *anti*-, four O–C(sp^3)–C(sp^3)–O angles are *gauche*-and the O(3)–C(5)–C5′–O3′ angle is 0.0° due to the mirror symmetry (Table 2).

3.1.3. $[(B15C5)_2 \cdot H_5O_2]$ $[(B15C5)_2 \cdot H_3O][TaF_6]_2$ (4)

Complex 4, of the composition $[(B15C5)_2 \cdot H_5O_2][(B15C5)_2 \cdot H_3O][TaF_6]_2$, crystallises in the monoclinic crystal system, space group *C2/c*. It is built of two different in composition sandwich cations (associated with A and B macrocycles) and two TaF_6^- anions. The ORTEP view for complex 4 is shown in Fig. 3. The asymmetric unit of 4 comprises two halves of the TaF_6^- anions, (one is situated on an inversion center and the other is situated on a two-fold axis), two B15C5 molecules (designated A and B) in general positions, and two oxonium oxygen atoms O(6A) and O(6B) (associated with the similarly labelled macrocycles), the former being located on a twofold axis, the latter being located in a general position in the vicinity of an inversion center and forming a $(H_5O_2)^+$ Zundel cation. In sandwich **A** the oxonium ion is equally disordered over the inversion center, forming correspondingly two and one hydrogen bonds to two crown molecules in the sandwich, the O(oxonium)···O(crown) separations falling in the range 2.742(3)–3.031(3) Å. The O(6A) oxygen atom deviates by 1.811(2) Å from the mean plane of the crown oxygen atoms that are coplanar to within ±0.28 Å. In molecule **A** the dihedral angle between the plane through the phenyl ring and 5 oxygens is equal to 26.2(1)°. Along the 15-membered heterocyclic framework all O–C(sp^3)–C(sp^3)–O torsion angles are *gauche*-, while O–C(sp^2)–C(sp^2)–O that belongs to the phenyl ring is *cis*, of 10 C–C–O–C torsions 8 are *anti*- and two adopt the *gauche*-conformation, giving rise to the sequence of two *gauche*-torsion angles meeting at C(3A) and C(6A) atoms (Table 2). In sandwich **B**, having the composition $[(B15C5)_2 \cdot H_5O_2]$, the O···O separation of 2.409 Å within the Zundel cation is the shortest among the corresponding O···O distances that are of concern in the cited data [9]. The other O···O distances to crown oxygens range from 2.651 to 3.012 Å (Table 3). The atom O(6B) deviates by 1.692(4) Å from the mean plane of crown oxygen atoms that are coplanar to within ±0.28 Å. In molecule **B** the dihedral angle between the planes through the phenyl ring and 5 oxygens is equal to 17.5(1)°, all C–O–C–C torsion angles are *anti*-, all O–C(sp^3)–C(sp^3)–O angles are *gauche*-, and the O–C(sp^2)–C(sp^2)–O angle is *cis* (Table 2). The dependence of the hydrogen bonding on the system is evident on changing the crown ether conformation.

3.1.4. $[(B12C4)_2 \cdot H_3O][TaF_6]$ (5)

Complex **5**, of the composition $[(B12C4)_2 \cdot H_3O][TaF_6]$, crystallises in the triclinic space group $P\bar{1}$. The ORTEP view for this complex is shown in Fig. 4. The TaF_6^- anion occupies a position on an inversion center. The macrocyclic cation has a typical B12C4 sandwich-like structure with the oxonium ion enclosed between two inversion-related macrocycles with three main O···O separations to crown oxygens equal to 2.652(3), 2.819(3) and 2.881(3) Å. The oxonium cation O(5) deviates by 1.953(2) Å from the mean

Please cite this article in press as: M.S. Fonari et al., Polyhedron (2007), doi:10.1016/j.poly.2007.07.037

POLY 6850
14 August 2007 Disk Used
ARTICLE IN PRESS
No. of Pages 10, Model 5+

Table 2
Selected bond distances (Å) and angles (°) for complexes **2–5**

Complex **2**			
Ta(1)–F(2)	1.856(5)	Ta(1)–F(1)	1.877(7)
Ta(1)–F(3)	1.854(5)		
F(2)–Ta(1)–F(3)	89.5(3)	F(2)–Ta(1)–F(1)	90.0(1)
F(3)–Ta(1)–F(1)	90.0(1)		
C(2)#1–C(1)#1–O(1)–C(1)	179.3(5)	C(1)–C(2)–O(2)–C(3)	174.4(8)
C(1)#1–O(1)–C(1)–C(2)	179.3(5)	C(2)–O(2)–C(3)–C(3)#2	178.4(13)
O(1)–C(1)–C(2)–O(2)	64.0(8)	O(2)–C(3)–C(3)#2–O(2)#2	52(2)
Complex **3**			
Ta(1)–F(1)	1.868(8)	Ta(1)–F(3)	1.883(6)
Ta(1)–F(4)	1.877(8)	Ta(1)–F(2)	1.887(7)
F(1)–Ta(1)–F(4)	179.8(4)	F(1)–Ta(1)–F(2)	90.4(3)
F(1)–Ta(1)–F(3)	90.1(3)	F(4)–Ta(1)–F(2)	89.7(3)
F(4)–Ta(1)–F(3)	89.7(3)	F(3)–Ta(1)–F(2)	90.2(4)
F(3)–Ta(1)–F(3)#3	88.6(4)	F(2)#3–Ta(1)–F(2)	91.0(6)
F(3)–Ta(1)–F(2)#3	178.7(3)		
C(1)#4–O(1)–C(1)–C(2)	168.2(6)	O(2)–C(3)–C(4)–O(3)	45(3)
O(1)–C(1)–C(2)–O(2)	64(1)	C(3)–C(4)–O(3)–C(5)	170(2)
C(1)–C(2)–O(2)–C(3)	168(1)	C(4)–O(3)–C(5)–C(5)#4	151(1)
C(2)–O(2)–C(3)–C(4)	141(2)		
Complex **4**			
Ta(1)–F(3)	1.853(3)	Ta(2)–F(6)	1.845(4)
Ta(1)–F(2)	1.864(3)	Ta(2)–F(5)	1.866(3)
Ta(1)–F(1)	1.866(3)	Ta(2)–F(4)	1.874(4)
F(3)–Ta(1)–F(2)	89.0(2)	F(5)#5–Ta(2)–F(5)	91.1(3)
F(3)–Ta(1)–F(1)	90.0(2)	F(6)#5–Ta(2)–F(4)	90.0(2)
F(2)–Ta(1)–F(1)	91.5(2)	F(5)#5–Ta(2)–F(4)	179.7(2)
F(6)–Ta(2)–F(6)#5	175.2(3)	F(5)–Ta(2)–F(4)	89.0(2)
F(6)–Ta(2)–F(5)#5	93.1(2)	F(4)–Ta(2)–F(4)#5	90.8(3)
F(6)–Ta(2)–F(5)	90.3(2)	F(6)–Ta(2)–F(4)	86.7(2)
O(1A)–C(1A)–C(2A)–O(2A)	69.4(5)	O(1B)–C(1B)–C(2B)–O(2B)	64.3(6)
C(1A)–C(2A)–O(2A)–C(3A)	167.2(4)	C(1B)–C(2B)–O(2B)–C(3B)	167.4(5)
C(2A)–O(2A)–C(3A)–C(4A)	91.4(5)	C(2B)–O(2B)–C(3B)–C(4B)	163.9(5)
O(2A)–C(3A)–C(4A)–O(3A)	63.6(5)	O(2B)–C(3B)–C(4B)–O(3B)	68.0(6)
C(3A)–C(4A)–O(3A)–C(5A)	179.8(4)	C(3B)–C(4B)–O(3B)–C(5B)	165.0(4)
C(4A)–O(3A)–C(5A)–C(6 A)	172.8(4)	C(4B)–O(3B)–C(5B)–C(6B)	170.0(4)
O(3A)–C(5A)–C(6A)–O(4A)	60.9(5)	O(3B)–C(5B)–C(6B)–O(4B)	70.9(6)
C(5A)–C(6A)–O(4A)–C(7A)	82.2(5)	C(5B)–C(6B)–O(4B)–C(7B)	158.0(5)
C(6A)–O(4A)–C(7A)–C(8A)	170.3(4)	C(6B)–O(4B)–C(7B)–C(8B)	169.5(4)
O(4A)–C(7A)–C(8A)–O(5A)	66.3(5)	O(4B)–C(7B)–C(8B)–O(5B)	60.9(5)
C(7A)–C(8A)–O(5A)–C(9A)	175.6(3)	C(7B)–C(8B)–O(5B)–C(9B)	178.2(3)
C(8A)–O(5A)–C(9A)–C(10A)	176.3(3)	C(8B)–O(5B)–C(9B)–C(10B)	171.8(4)
O(5A)–C(9A)–C(10A)–O(1A)	0.8(5)	O(5B)–C(9B)–C(10B)–O(1B)	1.1(5)
C(9A)–C(10A)–O(1A)–C(1A)	158.8(3)	C(9B)–C(10B)–O(1B)–C(1B)	156.1(3)
C(10A)–O(1A)–C(1A)–C(2A)	171.1(4)	C(10B)–O(1B)–C(1B)–C(2B)	176.9(4)
Complex **5**			
Ta(1)–F(3)	1.881(3)	Ta(1)–F(2)	1.888(2)
Ta(1)–F(1)	1.885(2)		
F(3)–Ta(1)–F(1)	90.5(1)	F(1)–Ta(1)–F(2)	90.7(1)
F(3)–Ta(1)–F(2)	90.3(1)		
O(1)–C(1)–C(2)–O(2)	61.2(4)	O(3)–C(5)–C(6)–O(4)	63.5(5)
C(1)–C(2)–O(2)–C(3)	136.0(3)	C(5)–C(6)–O(4)–C(7)	157.0(3)
C(2)–O(2)–C(3)–C(4)	75.5(4)	C(6)–O(4)–C(7)–C(12)	73.3(4)
O(2)–C(3)–C(4)–O(3)	65.8(4)	O(4)–C(7)–C(12)–O(1)	9.3(4)
C(3)–C(4)–O(3)–C(5)	171.0(4)	C(7)–C(12)–O(1)–C(1)	157.0(3)
C(4)–O(3)–C(5)–C(6)	84.7(5)	C(12)–O(1)–C(1)–C(2)	172.7(3)

Symmetry transformations used to generate equivalent atoms: (#1) x, y, z; (#2) $x, y+1, z$ for **2**; (#3) $x, y+3/2, z$; (#4) $x, 1/2 \quad y, z$ for **3** and (#5) $x+1, y, z+3/2$ for **4**.

plane of the four crown oxygens, which are coplanar to within ±0.294 Å. The dihedral angle between the plane through the phenyl ring and the 4 oxygens is equal to 17.2(2)°. Within the 12-membered heterocyclic framework three O–C–C–O torsion angles are *gauche* and the one that belongs to the phenyl ring is *cis*-; of 8 C–O torsion angles

UNCORRECTED PROOF

Please cite this article in press as: M.S. Fonari et al., Polyhedron (2007), doi:10.1016/j.poly.2007.07.037

POLY 6850
14 August 2007 Disk Used
ARTICLE IN PRESS
No. of Pages 10, Model 5+

Table 3
Hydrtogen bond distances (Å) and angles (°) for complexes **3** **5**

D H···A	d(D H)	d(H···A)	d(D···A)	∠(DHA)	Symmetry transformation for acceptor
Complex **3**					
O(4) H(1O4)···O(3)	0.90(1)	2.24(2)	2.995(15)	142(2)	x, y, z
O(5) H(1O5)···O(4)	0.86(2)	1.61(3)	2.462(12)	171(14)	x, y, z
O(5) H(2O5)···O(2)	0.85(2)	1.84(4)	2.646(9)	156(9)	$x-1/2, y, -z+1/2$
O(5) H(2O5)···O(3A)	0.85(2)	2.41(8)	2.945(15)	121(7)	$x-1/2, y, -z+1/2$
Complex **4**					
O(6A) H(61)···O(4A)	0.87(2)	1.95(6)	2.740(3)	150(10)	$-x+1, y, -z+3/2$
O(6A) H(61)···O(5A)	0.87(2)	2.44(8)	3.031(3)	126(8)	$-x+1, y, -z+3/2$
O(6A) H(62)···O(2A)	0.87(2)	2.09(6)	2.868(3)	150(10)	x, y, z
O(6A) H(62)···O(3A)	0.87(2)	2.28(9)	2.866(4)	125(9)	x, y, z
O(6A) H(63)···O(2A)	0.87(2)	2.05(4)	2.868(3)	159(10)	$-x+1, y, -z+3/2$
O(6B) H(16)···O(2B)	0.84(2)	1.81(2)	2.648(5)	179(6)	x, y, z
O(6B) H(26)···O(6B)	0.85(2)	1.55(3)	2.402(5)	173(15)	$-x+3/2, -y+1/2, -z+1$
O(6B) H(36)···O(4B)	0.83(2)	1.92(3)	2.710(4)	158(5)	x, y, z
O(6B) H(36)···O(5B)	0.83(2)	2.50(4)	3.014(4)	121(4)	x, y, z
Complex **5**					
O(5) H(51)···O(4)	0.88(2)	1.95(3)	2.819(3)	172(12)	x, y, z
O(5) H(52)···O(2)	0.88(2)	1.79(3)	2.652(3)	167(12)	x, y, z
O(5) H(53)···O(1)	0.88(2)	2.17(9)	2.881(3)	138(11)	$-x+1, -y+1, -z+1$

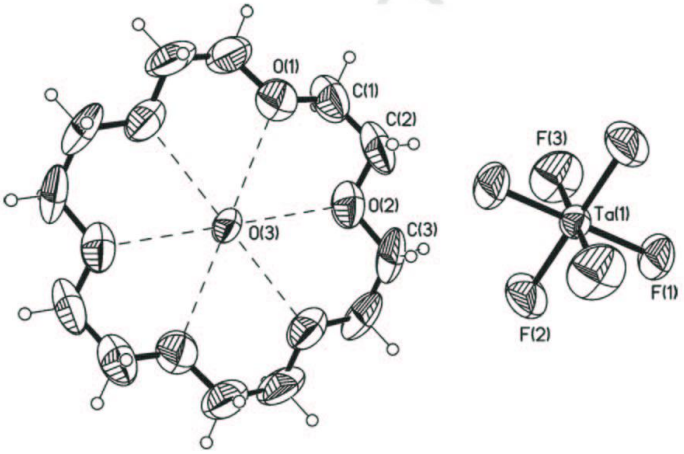

Fig. 1. ORTEP drawing of **2** with the numbering scheme and the shortest O···O distances shown by dashed lines. Thermal ellipsoids are shown at the 50% probability level.

three adopt a *gauche*-conformation and give rise to two corner fragments with a sequence of two *gauche*-torsion angles at the C(3) and C(5) atoms and meets with a *cis*-torsion angle at the C(7) atom (Table 2).

Analysis of CSD [18] data for oxonium-containing crown complexes of the composition $[CE \cdot H(H_2O)_n{}^{+} \cdot An]$ (where CE – crown ether, An – halogen-containing anion) reveals that 18C6 and its benzo-, dicyclohexano- and tetracarboxylic derivatives are highly selective for H_3O^+ because of the size and symmetry fit between them, allowing the inclusion of the oxonium ion within the 18-membered crown ether cavity with the formation of three strong OH···O hydrogen bonds [19]. However, both larger and smaller in size macrocycles are capable of accommodating the Eigen core as well. As examples, dibenzo-30C10 simultaneously contains two H_3O^+ cations within the cavity [20], two B15C5 molecules enclose the oxonium cation in a sandwich structure [21] similar to complex **4**, two dibromo-15C5 molecules incapsulate two H_3O^+ cations within sandwich structure [22]. Smaller in size, benzo-15C5 and 12C4 are also capable of fixing the oxonium ion either in a sandwich mode [23] or through an additional contact with the anion [24]. The next in size $[H_2O \cdots H \cdots OH_2]^+$Zundel cation is perfectly displayed on one side of the DB18C6 macrocycle in the DB18C6 oxonium perchlorate trihydrate [25], within 24- and 30-

Please cite this article in press as: M.S. Fonari et al., Polyhedron (2007), doi:10.1016/j.poly.2007.07.037

POLY 6850
14 August 2007 Disk Used
ARTICLE IN PRESS
No. of Pages 10, Model 5+

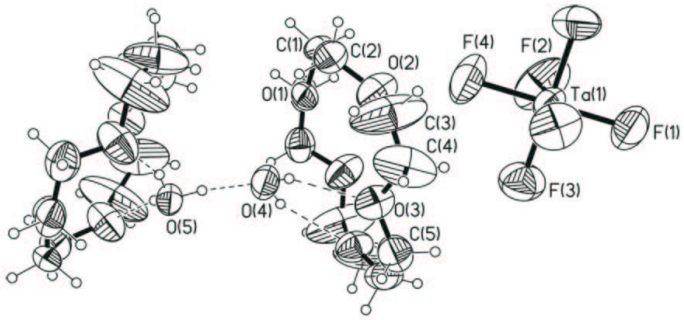

Fig. 2. ORTEP drawing of **3** with the numbering scheme and the shortest O···O distances shown by dashed lines. Thermal ellipsoids are shown at the 50% probability level.

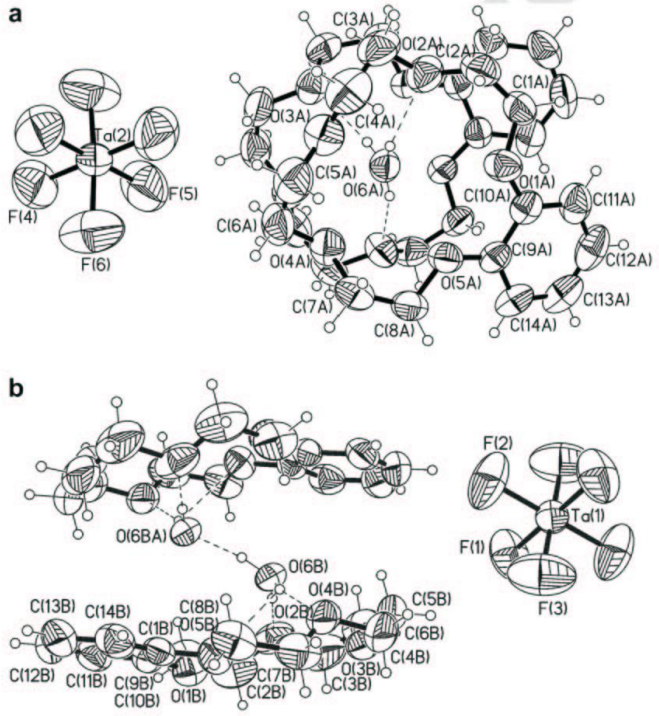

Fig. 3. ORTEP drawing of **4** with the partial numbering scheme and hydrogen bonding shown by dashed lines. Thermal ellipsoids are shown at the 50% probability level.

membered macrocycles [19u] or between two molecules of B15C5, as in bis(B15C5) tetrachloro-aurate(III) oxonium monohydrate [2] and in our complex **3**, while tetrabenzo30C10 excellently stores the Zundel cation within one cavity [7]. On the contrary, the fixation of the $[H_7O_3]^+$ cation by crown ethers is relatively uncommon and only few examples are known so far where $[H_7O_3]^+$ oxonium cations alternate with crown ether in hydrogen-bonded chains with long-range interactions to the anions [2,26] or are encapsulated within the cage formed by two crown molecules [6]. A comparison of novel compounds with the known literary examples shows the reproducibility of the crown ether–oxonium ion supramolecular architecture for 18C6, 15C5 and B15C5. A reliable comparison of subtle effects (hydrogen bond lengths and angles) for these units cannot be made due to the location of the oxonium species on the crystallographic symmetry elements.

Please cite this article in press as: M.S. Fonari et al., Polyhedron (2007), doi:10.1016/j.poly.2007.07.037

POLY 6850
14 August 2007 Disk Used
ARTICLE IN PRESS
No. of Pages 10, Model 5+

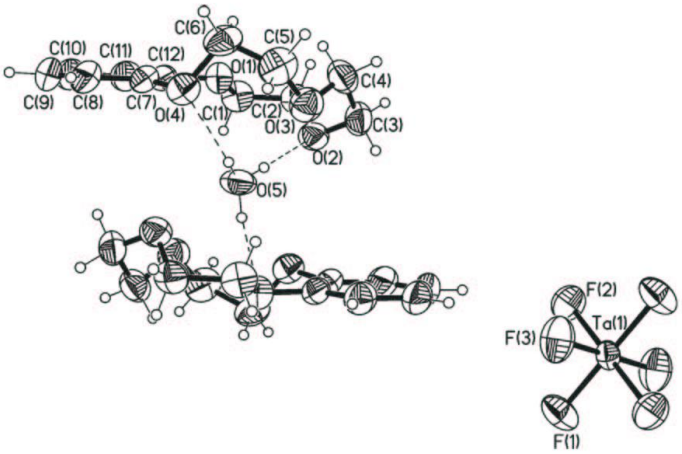

Fig. 4. ORTEP drawing of **5** with the numbering scheme and hydrogen bonding shown by dashed lines. Thermal ellipsoids are shown at the 50% probability level.

The crystal packing in **1–5** exhibits common structural features. The all H-bonding coordination abilities of the $[H_3O]^+$ or $[H_5O_2]^+$ cations are used to interact with the crown ether oxygen atoms since both NbF_6^- and TaF_6^- behave as very non-coordinating anions, being much poorer hydrogen bond acceptors than for example $AuCl_4^-$ which contributes to the interactions with oxonium species [2]. The decisive factor in the supramolecular organization are weak CH(crown)···F interactions. Similar to all previously reported complexes of this family [4–7], the crystal packing in **1–5** represents an alternation of rows of organic (macrocyclic cations in **1–2**, or macrocyclic sandwiches in **3–5**) and inorganic (Nb_6^-/TaF_6^- anions) components (Fig. 5), being held together by CH···F interactions. The simplest case of crystal packing is evident for **1–2**. For the perfectly regular structure **2**, shown in Fig. 4a, the C(3)H···F(2) contact (H···F 2.61, C···F 3.394(15) Å, CHF angle 138° slightly exceeds the accepted limit (H···Acceptor = 2.6 Å). In **5**, due to the shortest C(1)H···F(1) contact (H···F 2.52, C···F 3.211(5) Å, CHF angle 128°, charged components alternate in the chain. In the layer structure **4** two independent TaF_6^- anions fulfill different structural functions: the $Ta(1)F_6$ anion is located on an inversion center and acts as a bridge between two different macrocyclic sandwiches (**A** and **B**) *via* the F(1) atom, [C(7A)–H(7A1)···F(1)(x, $1-y$, $0.5+z$) 2.55, C···F 3.250(6) Å, CHF angle 129° and C(5B)–H(5B2)···F(1) 2.55, C···F 3.343(6) Å, CHF angle 140°], while the second anion, $Ta(2)F_6$, located on a two-fold axis, bridges only **B** sandwiches *via* C(14B)···F(5) interactions [C(14B)–H(14B)···F(5)($3/2-x$, $-0.5+y$, $3/2-z$) 2.54, C···F 3.312(6) Å, CHF angle 141°].

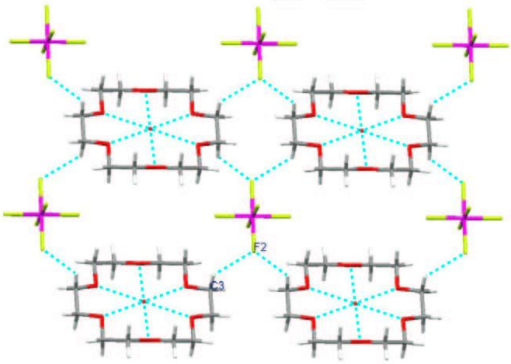

Fig. 5. Fragment of the crystal packing for **2**. Only atoms responsible for short CH···F contacts are labelled.

4. Conclusion

The interaction of Nb_2O_5/Ta_2O_5 or NbF_5/TaF_5 with 18-,15- and 12-membered CEs in the presence of hydrofluoric acid results in complexes of the compositions $[18C6 \cdot H_3O][NbF_6]$ (**1**), $[18C6 \cdot H_3O][TaF_6]$ (**2**), $[15C5 \cdot H_5O_2][TaF_6]$ (**3**) $[(B15C5)_2 \cdot H_5O_2]$ $[(B15C5)_2 \cdot H_3O][TaF_6]_2$ (**4**) and $[(B12C4)_2 \cdot H_3O][TaF_6]$ (**5**). All compounds represent ionic species with direct interactions between the oxonium ion and oxygen atoms of the macrocyclic molecule and a lack of any interactions between the oxonium ion and the anion. According to the X-ray data, the $[H_3O]^+$ oxonium cation centers the 18-membered crown cavity in isostructural complexes **1–2**, and bridges two smaller 12-membered macrocycles in **5**. Compound **5** is the first example of an oxonium ion direct interaction with the small B12C4 macrocycle. The crystal **3** contains the $[H_5O_2]^+$ dioxonium cation and alternates with 15C5 molecules in the infinite chains, whereas complex **4** represents a unique example

Please cite this article in press as: M.S. Fonari et al., Polyhedron (2007), doi:10.1016/j.poly.2007.07.037

of the co-existence of both the $[H_3O]^+$ Eigen core and $[H_2O\cdots H\cdots OH_2]^+$ Zundel cations within one structure, both being incorporated in two sandwich-type organized macrocyclic cations. The B15C5 molecules that form these sandwiches differ by their conformations.

Acknowledgements

This work was supported by the Russian Foundation for Basic Research and the Academy of Sciences of Moldova (Project No. 06-03-90894-Mol-a). W.J.W. and E.V.G. acknowledge the support of the National Council of Science of Taiwan (Grant No. 94-2811-M-032).

Appendix A. Supplementary material

CCDC 652989, 652990, 652991, 652992 and 652993 contains the supplementary crystallographic data for **1**, **2**, **3**, **4** and **5**. These data can be obtained free of charge via http://www.ccdc.cam.ac.uk/conts/retrieving.html, or from the Cambridge Crystallographic Data Centre, 12 Union Road, Cambridge CB2 1EZ, UK; fax: (+44) 1223 336 033; or e-mail: deposit@ccdc.cam.ac.uk. Supplementary data associated with this article can be found, in the online version, at doi:10.1016/j.poly.2007.07.037.

References

[1] J.L. Atwood, S.G. Bott, P.C. Junk, M.T. May, J. Coord. Chem. 37 (1996) 89.
[2] (a) M. Calleja, K. Johnson, W.J. Belcher, J.W. Steed, Inorg. Chem. 40 (2001) 4978, and references cited therein;
(b) M. Calleja, S.A. Mason, P.D. Prince, J.W. Steed, C. Wilkinson, New J. Chem. 25 (2001) 1475.
[3] A.G. Babkin, V.G. Maiorov, A.I. Nikolaev, Nauka 224 (1988).
[4] M.S. Fonari, N.G. Furmanova, W.-J. Wang, E.V. Ganin, I.A. Verin, Yu.A. Simonov, V.O. Gelmboldt, Kristallografiya (Russ.) 51 (2006) 856.
[5] M.S. Fonari, O.A. Alekseeva, N.G. Furmanova, K.A. Lysenko, W.-J. Wang, S.-W. Tang, E.V. Ganin, V.O. Gelmboldt, Yu.A. Simonov, Kristallografiya (Russ.) 52 (2007) 271.
[6] Ed.V. Ganin, V.O. Gelmboldt, L.V. Koroeva, M.S. Fonari, Yu.A. Simonov, J. Lipkowski, S.A. Kotlyar, G.L. Kamalov, J. Incl. Phenom. 56 (2006) 345.
[7] N.G. Furmanova, M.X. Rabadanov, T.S. Chernaya, M.S. Fonari, Yu.A. Simonov, Ed.V. Ganin, V.O. Gelmboldt, R.Ya. Grygorash, S.A. Kotlyar, G.L.Kamalov, Kristallografiya, submitted for publication. Q2
[8] (a) B. Moulton, M.J. Zaworotko, Chem. Rev. 101 (2001) 1629;
(b) G.R. Desiraju, Science 278 (1997) 404.
[9] (a) M.A. Xiang Hao, S. Siegler, C. Parkin, P. Brock, Cryst. Growth Des. 5 (2005) 2225;
(b) L.-Q. Kong, J.-M. Dou, Da-C. Li, Da-Qi Wan, J. Mol. Struct. 785 (2006) 186;
(c) M.S. Fonari, V.Ch. Kravtsov, Yu.A. Simonov, E.V. Ganin, V.O. Gelmboldt, Russ. J. Struct. Chem. 40 (1999) 1002;
(d) M.S. Fonari, Yu.A. Simonov, Yu.M. Chumakov, G. Bocelli, E.V. Ganin, V.O. Gelmboldt, Acta Crystallogr., Sect. C 59 (2003) m168.
[10] (a) M. Eigen, Angew. Chem., Int. Ed. Engl. 3 (1964) 1;
(b) G. Zundel, in: Sandorfy (Ed.), The Hydrogen Bond – Recent Developments in Theory and Experiments, North-Holland, Amsterdam, 1976, p. 683;
(c) J. Xu, M.A. Sharpe, L. Qin, S. Ferguson-Miller, G.A. Voth, J. Am. Chem. Soc. 129 (10) (2007) 2910;
(d) F. Garczarek, K. Gerwert, Nature 439 (2006) 109.
[11] Z. Otwinowski, W. Minor, in: C.W. Carter, R.M. Sweet (Eds.), Methods. Enzymol., Macromolecular Crystallography, Part A, vol. 276, Academic Press, London, 1996, p. 307.
[12] G.M. Sheldrick, SADABS, Bruker AXS Inc., Madison, WI-53719, USA, 1997.
[13] G.M. Sheldrick: SHELXS97 and shelxl97, Programs for Crystal Structure Solution and Refinement, University of Göttingen, Germany, 1997.
[14] A. Haas, J. Kasprowski, K. Angermund, P. Betz, C. Kruger, Yi-Hung Tsay, S. Werner, Chem. Ber. 124 (1991) 1895.
[15] P. Halasyamani, K.R. Heier, M.J. Willis, C.L. Stern, K.R. Poeppelmeier, Z. Anorg. Allg. Chem. 622 (1996) 479.
[16] O.I. Guzyr, M. Schormann, J. Schimkowiak, H.W. Roesky, C. Lehmann, M.G. Walawalkar, R. Murugavel, H.-G. Schmidt, M. Noltemeyer, Organometallics 18 (1999) 832.
[17] M.A. McLoughlin, N.L. Keder, W.C. Kaska, Acta Crystallogr., Sect. C 48 (1992) 1098.
[18] F.N. Allen, Acta Crystallogr., Sect. B 58 (2002) 380.
[19] (a) B.M. Bulychev, V.K. Bel'sky, Zh. Neorg. Khim. (Russ.) (Russ. J. Inorg. Chem.) 40 (1995) 1834;
(b) H. Feinberg, I. Columbus, S. Cohen, M. Rabinovitz, H. Selig, G. Shoham, Polyhedron 12 (1993) 1811;
(c) L.J. Barbour, L.R. MacGillivray, J.L. Atwood, J. Chem. Cryst. 26 (1996) 59;
(d) B. Neumuller, M. Plate, K. Dehnicke, Z. Kristallogr. 209 (1994) 92;
(e) V.S. Sergienko, L.Kh. Minacheva, N.Kh. Ashurova, M.A. Porai-Koshits, K.G. Yakubov, V.G. Sakharova, Russ. J. Inorg. Chem. 36 (1991) 381;
(f) V.S. Sergienko, L.Kh. Minacheva, G.G. Sadikov, N.Kh. Ashurova, V.V. Minin, K.G. Yakubov, V.M. Sherbakov, Russ. J. Inorg. Chem. 37 (1992) 346;
(g) H. Feinberg, I. Columbus, S. Cohen, M. Rabinovitz, H. Selig, G. Shoham, Polyhedron 12 (1993) 2913;
(h) P.C. Junk, J.L. Atwood, J. Chem. Cryst. 24 (1994) 247;
(i) R. Chenevert, D. Chamberland, M. Simard, F. Brisse, Can. J. Chem. 68 (1990) 797;
(j) J.L. Atwood, S.G. Bott, P.C. Junk, M.T. May, J. Organomet. Chem. 487 (1995) 7;
(k) J.L. Atwood, S.G. Bott, C.M. Means, A.W. Coleman, Hongming Zhang, M.T. May, Inorg. Chem. 29 (1990) 467;
(l) P.C. Junk, L.R. MacGillivray, M.T. May, K.D. Robinson, J.L. Atwood, Inorg. Chem. 34 (1995) 5395;
(m) S.A. El Khalik, M. El Essawi, I. Dombrowski, K.-F. Tebbe, Z. Naturforsch. B54 (1999) 136;
(n) J.L. Atwood, P.C. Junk, M.T. May, K.D. Robinson, J. Chem. Cryst. 24 (1994) 243;
(o) Yu.A. Simonov, N.F. Krasnova, A.A. Dvorkin, V.V. Yakshin, V.M. Abashkin, B.N. Laskorin, Dokl. Akad. Nauk SSSR (Russ.) (Proc. Natl. Acad. Sci. USSR) 272 (1983) 1129;
(p) V.O. Gel'mbol'dt, E.V. Ganin, L.V. Ostapchuk, A.A. Ennan, Yu.A. Simonov, V.Kh. Kravtsov, M.S. Fonari, J. Lipkowski, Russ. J. Inorg. Chem. 44 (1999) 1139;
(q) V.O. Gelmboldt, E.V. Ganin, Yu.A. Simonov, J. Lipkowski, M.S. Fonari, V.Kh. Kravtsov, Russ. J. Inorg. Chem. 40 (1995) 594;
(r) J.-P. Behr, P. Dumas, D. Moras, J. Am. Chem. Soc. 104 (1982) 4540;
(s) A. Hammerschmidt, S. Bonmann, M. Lage, B. Krebs, Z. Anorg. Allg. Chem. 630 (2004) 2035.
[20] P.C. Junk, J.L. Atwood, J. Chem. Soc., Dalton Trans. (1997) 4393.
[21] M.I. Saleh, E. Kusrini, N. Ngah, B.M. Yamin, Acta Crystallogr., Sect. E 62 (2006) o1654.
[22] A. Hammerschmidt, I. Beckmann, M. Lage, B. Krebs, Z. Anorg. Allg. Chem. 631 (2005) 393.

UNCORRECTED PROOF

POLY 6850
14 August 2007 Disk Used
ARTICLE IN PRESS
No. of Pages 10, Model 5+

[23] S.P. Petrosyants, A.M. Shpirt, A.B. Ilyukhin, Russ. J. Inorg. Chem. 45 (2000) 954.
[24] J.L. Atwood, P.C. Junk, J. Coord. Chem. 51 (2000) 379.
[25] A.N. Chekhlov, Russ. J. Inorg. Chem. 51 (2006) 569.
[26] D. Braga, M. Gandolfi, M. Lusi, M. Polito, K. Rubini, F. Grepioni, Cryst. Growth Des. 7 (2007) 919.

UNCORRECTED PROOF

Please cite this article in press as: M.S. Fonari et al., Polyhedron (2007), doi:10.1016/j.poly.2007.07.037

Додаток 3.

Копія статті. “Crystal Structure of Bis(3-carboxypyridinium) Hexafluorosilicate”

ISSN 0036-0236, Russian Journal of Inorganic Chemistry, 2008, Vol. 53, No. 6, pp. 875–878. © Pleiades Publishing, Ltd., 2008.
Original Russian Text © V.O. Gel'mbol'dt, L.Kh. Minacheva, E.V. Ganin, V.S. Sergienko, 2008, published in Zhurnal Neorganicheskoi Khimii, 2008, Vol. 53, No. 6, pp. 947–950.

COORDINATION COMPOUNDS

Crystal Structure of Bis(3-carboxypyridinium) Hexafluorosilicate

V. O. Gel'mbol'dt[a], L. Kh. Minacheva[b], E. V. Ganin[c], and V. S. Sergienko[b]

[a] *Physicochemical Institute of Environmental and Human Protection, Ministry of Education and Science of Ukraine and National Academy of Sciences of Ukraine, Preobrazhenskaya ul. 3, Odessa, 65082 Ukraine*

[b] *Kurnakov Institute of General and Inorganic Chemistry, Russian Academy of Sciences, Leninskii pr. 31, Moscow, 119991 Russia*

[c] *Odessa State Ecological University, Ministry of Education and Science of Ukraine, Lvovskaya ul. 15, Odessa, 65016 Ukraine*

Received May 17, 2007

Abstract—Complex $[3\text{-HO(O)CC}_5\text{H}_4\text{NH}]_2\text{SiF}_6$ is synthesized, and its structure is determined by single-crystal X-ray diffraction. In its ionic structure, the centrosymmetric SiF_6^{2-} anions (the Si–F bond lengths are 1.6658(15)–1.7033(17) Å) and $[3\text{-HO(O)CC}_5\text{H}_4\text{NH}]^+$ cations are linked through interionic H-bonds NH···F, NH···O, and OH···F (the N···F, N···O, and O···F distances are 2.752(3), 2.935(3), and 2.596(2) Å, respectively).

DOI: 10.1134/S0036023608060107

"Onium" fluorosilicates are the products of reactions of N- and O-containing organic bases with fluorosilicic acid. They find use as chemical reagents and functional materials [1]. In this respect, it is of interest to reveal some relation between the structure and physicochemical characteristics of these compounds. Hexafluorosilicates of functionalized anilinium [2–4] and pyridinium derivatives are convenient models for this analysis. In this work, bis(3-carboxypyridinium) hexafluorosilicate, $[3\text{-HO(O)CC}_5\text{H}_4\text{NH}]_2\text{SiF}_6$ (**I**), has been synthesized and structurally studied.

EXPERIMENTAL

Synthesis. Pyridine-3-carboxylic acid (123 mg, 1 mmol) was dissolved in methanol (10 mL) at 64 °C, and water (2 ml) and 45% H_2SiF_6 (pure for analysis grade) (0.9 mL) were added. The reaction mixture was concentrated at room temperature. Colorless crystals of compound **I** were obtained; mp = 248–250°C.

For $[3\text{-HO(O)CC}_5\text{H}_4\text{NH}]_2\text{SiF}_6$ anal. calcd. (%): Si, 7.20; N, 7.18.

Found (%): Si, 7.37; N, 7.03.

Mass spectrum of compound I (MX-1321 spectrometer, direct injection, energy of ionizing electrons 70 eV): $[ML]^+$ (m/z = 123, I = 52%), $[ML–H_2O]^+$ (m/z = 105, I = 26%), $[ML–COOH]^+$ (m/z = 78, I = 25%), SiF_3^+ (m/z = 85, I = 100%).

Single-crystal X-ray diffraction analysis. The crystals of compound **I** are monoclinic, a = 11.707(2) Å, b = 9.6003(19) Å, c = 13.077(3) Å, b = 103.54(3)°, V = 1429.0(5) Å^3, ρ_{calcd} = 1.814 g/cm^3, $\mu(\text{Mo}K_\alpha)$ = 2.409 mm^{-1}, $F(000)$ = 792, Z = 4, space group $C2/c$.

The experimental material was obtained from a needle-like single crystal 0.42 × 0.21 × 0.21 mm in size at 293(2) K on an Enraf-Nonius CAD4 automated four-circle diffractometer ($\lambda\text{Cu}K_\alpha$, λ radiation, 1.54178 Å, graphite monochromator, ω scan mode, 6.03°–76.07° θ range). The total number of measured reflections was 2210 ($-2 \le h \le 14$, $-2 \le k \le 12$, $-15 \le l \le 16$); 1476 of them were independent (R_{int} = 0.0486, 98.3% θ coverage). Absorption anisotropy was ignored.

The structure was determined by direct methods (SHELXS86 [5]) and refined by the least-squares method for F^2 (SHELXL97 [6]) in the full-matrix anisotropic approximation for non-hydrogen atoms. Positions of all hydrogen atoms of the 3-carboxypyridinium cation LH^+ were determined from the difference Fourier synthesis and refined isotropically.

The final refinement results are $R1$ = 0.0574, $wR2$ = 0.1536, GOOF = 1.085 for 1321 reflections with $I > 2\sigma(I)$; $R1$ = 0.0614, $wR2$ = 0.1584 for all reflections; 140 refined parameters. The molar absorption coefficient was 0.0025(5); $\Delta\rho_{max}$ and $\Delta\rho_{min}$ were 0.466 and –0.585 Å^{-3}, respectively.

The coordinates and temperature factors of the atoms in the structure of compound **I** are presented in Table 1. The interatomic distances and bond angles are listed in Table 2.

Table 1. Coordinates of atoms ($\times 10^4$, $\times 10^3$ for H atoms) and their thermal parameters U_{eq}/U_{iso} ($\times 10^3$, Å^2) in the structure of compound **I**

Atom	x	y	z	U_{eq}/U_{iso}
Si(1)	2500	2500	5000	39(1)
F(1)	3439(1)	1199(2)	4949(1)	55(1)
F(2)	1656(1)	1424(2)	5501(2)	56(1)
F(3)	1720(1)	2095(2)	3766(1)	62(1)
O(2)	4159(2)	–949(2)	3315(2)	57(1)
O(1)	4476(2)	–3234(2)	3559(2)	53(1)
C(1)	2596(2)	–2400(2)	3525(2)	41(1)
C(2)	2202(2)	–3748(3)	3565(2)	49(1)
N	1116(2)	–3958(2)	3704(2)	52(1)
C(4)	394(2)	–2932(3)	3832(2)	51(1)
C(5)	756(2)	–1578(3)	3802(2)	54(1)
C(6)	1865(2)	–1305(3)	3638(2)	49(1)
C(7)	3826(2)	–2108(3)	3442(2)	44(1)
H(1)	524(4)	–300(4)	353(4)	88(13)
H(2)	267(3)	–456(3)	343(3)	57(8)
H(3)	90(3)	–478(4)	378(3)	67(10)
H(4)	–37(3)	–314(3)	400(3)	60(9)
H(5)	28(4)	–93(4)	386(3)	73(11)
H(6)	207(3)	–36(3)	365(2)	52(8)

Table 2. Selected bond lengths (d) and bond angles (ω) in structure **I**

Bond	d, Å
Si(1)–F(2)	1.6658(15)
Si(1)–F(1)	1.6756(14)
Si(1)–F(3)	1.7033(17)
O(2)–C(7)	1.203(3)
O(1)–C(7)	1.310(3)
C(1)–C(2)	1.380(3)
C(1)–C(6)	1.385(3)
C(1)–C(7)	1.497(3)
C(2)–N	1.341(3)
N–C(4)	1.334(4)
C(4)–C(5)	1.371(4)
C(5)–C(6)	1.389(4)
Angle	**ω, deg**
F(2)Si(1)F(1)	90.45(8)
F(2)Si(1)F(3)	89.71(9)
F(1)Si(1)F(3)	90.20(9)
C(2)C(1)C(6)	119.2(2)
C(2)C(1)C(7)	121.0(2)
C(6)C(1)C(7)	119.7(2)
NC(2)C(1)	118.8(2)
C(4)NC(2)	123.7(2)
NC(4)C(5)	119.2(2)
C(4)C(5)C(6)	119.3(3)
C(1)C(6)C(5)	119.7(2)
O(2)C(7)O(1)	125.6(2)
O(2)C(7)C(1)	122.1(2)
O(1)C(7)C(1)	112.3(2)

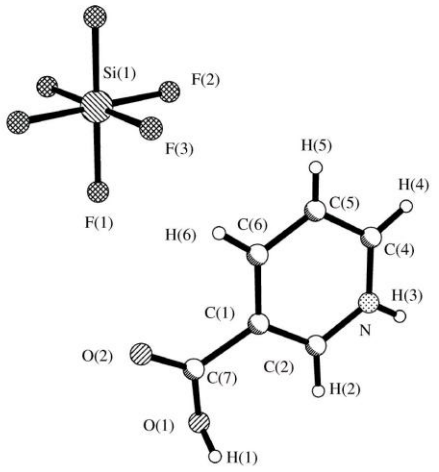

Fig. 1. Structural units in a crystal of compound **I**: the SiF_6^{2-} anion and LH^+ cation.

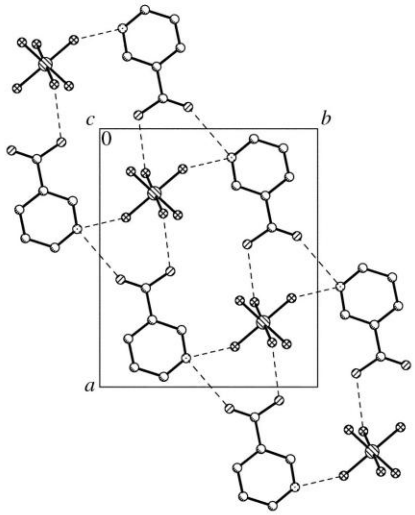

Fig. 2. Packing of structural units in a crystal of compound **I** (projection along the *c* axis).

RESULTS AND DISCUSSION

The structural units of a crystal of compound **I** are the hexafluorosilicate anions and 3-carboxypyridinium cations (Fig. 1). In the centrosymmetric SiF_6^{2-} anion, the silicon atom has an insignificantly distorted octahedral coordination (the average Si–F bond length is 1.682 ± 0.021 Å, and the FSiF bond angles range from 89.71(9)° to 90.45(8)°). The interatomic distances and bond angles in the LH^+ cation take standard values.

In the crystal one can distinguish ribbons consisting of two symmetrically linked chains of the LH^+ cations between which the SiF_6^{2-} anions are arranged (Fig. 2). The protonated nitrogen atom of the organic cation forms rather weak bifurcate interionic H-bonds, one of which, N–H(3)···O(2), links the cations into chains. The second H-bond, N–H(3)···F(1), as well as O(1)–H(1)···F(3), links the chains of the cations and anions into a ribbon. The translationally related ribbons form a layer lying parallel to the *ab* plane. The layers are stabilized due to the stacking interaction of the pyridinium rings from different ribbons, which are related through the inversion center (Fig. 3), the distance between the pyridinium rings being 3.56 Å.

Three independent interatomic Si–F distances correlate with the relative strength of the interionic con-

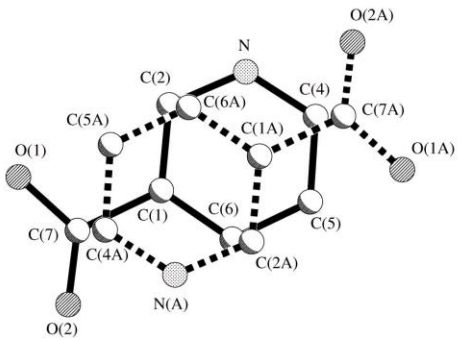

Fig. 3. Stacking interaction of the LH^+ cations in a crystal compound **I**.

tacts. The longest Si–F(3) bond is formed by the fluorine atom involved in the stable O(1)–H(1)···F(3) H-bond (1.7033(17) Å). The weak bifurcate H-bond N–H(3)···F(1) corresponds to the intermediate (in length) Si–F(1) bond (1.6756(14) Å). The fluorine atom of the strongest Si–F(2) bond (1.6658(15) Å) is not involved in short interionic contacts (the shortest F(2)···C(2) contact is 3.019 Å). A similar inverse correlation between Si–F distances and the strengths of the H-bonds formed by the corresponding fluorine atoms is characteristic of the structures of "onium" hexafluorosilicates [2, 7].

REFERENCES

1. V. O. Gel'mbol'dt and A. A. Ennan, Ekotekhnol. Resursosberezhenie, No. 5, 33 (2007).
2. V. O. Gel'mbol'dt, E. V. Ganin, L. V. Koroeva, et al., Zh. Neorg. Khim. **51** (2), 237 (2006) [Russ. J. Inorg. Chem. **51** (2), 194 (2006)].
3. V. O. Gel'mbol'dt, L. Kh. Minacheva, E. V. Ganin, and V. S. Sergienko, Zh. Neorg. Khim. **51** (10), 1661 (2006) [Russ. J. Inorg. Chem. **51** (10), 1561 (2006)].
4. V. O. Gel'mbol'dt, L. V. Koroeva, and K. V. Domasevich, Zh. Neorg. Khim. **51** (10), 1757 (2006) [Russ. J. Inorg. Chem. **51** (10), 1653 (2006)].
5. G. M. Sheldrick, Acta Crystallogr. **46A** (5), 467 (1990).
6. G. M. Sheldrick, *SHELXL97. Program for the Refinement of Crystal Structures* (Univ. of Göttingen, Göttingen, 1997).
7. B. D. Conley, B. C. Yearwood, S. Parkin, and D. A. Atwood, J. Fluorine Chem. **115** (2), 155 (2002).

Додаток I.

Копія статті. “Structure of Benzo- and Dibenzocrown Ethers and Their H-Bonded Adducts. 4.§ Structural Motifs in the 2,4-Dithiouracil Complexes with 4-Bromo- and 4-Nitrobenzo-18-crown-6, [2.4]Dibenzo- and Thia[1.5]dibenzo-18-crown-6 ”

J Incl Phenom Macrocycl Chem (2008) 61:367–375
DOI 10.1007/s10847-008-9431-7

ORIGINAL ARTICLE

Structure of benzo- and dibenzocrown ethers and their H-bonded adducts. 4. Structural motifs in the 2,4-dithiouracil complexes with 4-bromo- and 4-nitrobenzo-18-crown-6, [2.4]dibenzo- and thia[1.5]dibenzo-18-crown-6

Marina S. Fonari · Yurii A. Simonov · Gabriele Bocelli · Eduard V. Ganin · Wen-Jwu Wang · Sergei M. Pluzhnik-Gladyr · Vyacheslav V. Tkachyuk · Sergei A. Kotlyar · Gerbert L. Kamalov

Received: 9 October 2007 / Accepted: 26 February 2008 / Published online: 1 April 2008
© Springer Science+Business Media B.V. 2008

Abstract Four novel complexes of 2,4-dithiouracil (pyrimidine-2,4(1*H*,3*H*)-dithione, DTU) with 18-membered benzo- and dibenzo-crown ethers were synthesized in approximately the same conditions and studied by single crystal diffraction. Hydrogen bonding was observed to be the most important for the complexation in the solid state but π–π interactions also contribute to it. The crystalline monohydrates of the 1:1:1 stoichiometry are recorded for 4-bromo- and 4-nitrobenzo-18-crown-6 (complexes **1** and **2**), while complexes with [2.4]dibenzo- and thia[1.5]dibenzo-18-crown-6 (complexes **3** and **4**) represent anhydrous adducts of the 2:2 ratio. The crystal structures reveal three supramolecular structural motifs: the alternative chain for the ternary complex **1** and two types of capsules for complexes **2**–**4** where the DTU dimers are encapsulated inside the space restricted by two crown molecules.

Keywords Benzo- and dibenzocrown ethers · Complexes · 2,4-Dithiouracil · Hydrogen bonding · Synthesis · Crystal structure

For part 3 see *JIPh.*, **56**, 345 (2006).

M. S. Fonari (✉) · Y. A. Simonov
Institute of Applied Physics, Academy of Sciences of Moldova, Academy str., 5, MD2028 Chisinau, Moldova
e-mail: fonari.xray@phys.asm.md

G. Bocelli
IMEM-CNR, Parma, Italy

E. V. Ganin
Odessa State Environmental University, Ministry of Education and Science of Ukraine, Lvovskaya str., 15, 65016 Odessa, Ukraine

W.-J. Wang
Department of Chemistry, Tamkang University, 151 Ying-Chuan Road, Tamsui, Taipei 25137, Taiwan, ROC

S. M. Pluzhnik-Gladyr · V. V. Tkachyuk · S. A. Kotlyar · G. L. Kamalov
A.V. Bogatsky Physico-Chemical Institute, National Academy of Sciences of Ukraine, Lustdorfskaya doroga 86, 650080 Odessa, Ukraine

Introduction

In 2007 the chemical scientific community marked the fortieth anniversary of the publication in the Journal of the American Chemical Society of the synthesis and cation binding properties of crown ethers by Charles J. Pedersen [1, 2]. The fields of anionic synthetic reagents, phase-transfer catalysis, biological ion transport, enzyme mimics, molecular devices and machines and other emerging disciplines benefited profoundly from the discovery of crown ethers. Enormous excellent reviews describe thousands of crown structures and crown applications in chemistry [3]. The deep analysis of the hydrogen bond formation and understanding of factors controlling the formation of complexes are still required.

For the last two decades along with the others we were involved in the host–guest chemistry of the crown ethers with an accent on their interaction with biologically important molecules (drugs, heterocyclic bases etc.). These studies have been developed in two directions: construction of extended supramolecular networks sustained by conventional hydrogen bonds using the unique property of classic crown ethers to serve as the double-face spacers for the organic molecules with the variety of H-donor groups (NH_2, $C(=S)NH_2$, $C(=O)NH_2$ etc.) that serve as the linkers [4], and the structural study of the host–guest complexes on the base of the novel crown ethers [5].

Heterocyclic bases such as pyrimidine, imidazole and purine and their derivatives are of great importance in biological systems due to their proton acceptor and hydrogen bonding abilities. Pursiainen et al. [6] thoroughly studied the complexation of tropylium, pyridinium derivatives and five-membered N-heteroatomic cations with crown ethers. In our turn we have demonstrated the formation of ionic complexes between pyrimidine derivatives and aza-crown ethers with the proton transfer from the pyrimidine molecule to the macrocyclic nitrogen atom [7]. Alongside with uracil, its sulfur substituted analogues 2-thiouracil, 2,4-dithiouracil (DTU) are intensively studying both by the computational [8] and crystallographic methods [9] with an emphasis on the preferable forms of the DTU existence in the solid and gas phases, the estimation of the comparative affinity of the DTU binding sites for the protonation and participation in the metal complexation and hydrogen bonding. Our investigations [5a, 10] appeared to be the pioneering ones in the preparation and X-ray study of the genuine molecular complexes of the DTU with classic crown ethers (18C6, *cis*-isomers of dicyclohexano-18C6, benzo-18C6 and [1.5]dibenzo-18C6). By that study we showed that of six possible isomers namely dithione isomer actually forms the crystalline complexes, and the CE···DTU interactions occur via one NH···O hydrogen bond through the nitrogen atom being in the position "2" of the DTU ring (see Scheme 1 for the numbering in the DTU molecule) and the subsidiary CH···O interaction through one additional carbon atom of the DTU ring. The coupling of two DTU molecules via $R_2^2(8)$ homosynthon [11] built on two NH···S hydrogen bonds has been registered in the complexes with dicyclohexyl-18C6 and [1.5]dibenzo-18C6, while the incorporation of water molecule that blocks the nitrogen atom in the position "1" of the DTU ring and completely destroys the hydrogen bonding network typical for the pure DTU [9a] results in the reproducible 1D supramolecular motif for 18C6, B18C6 or *cis-syn-cis*-DCH18C6 with the alternation of the CE, DTU and water molecules in the chain. These three earlier reported supramolecular motifs are reproduced in Fig. 1.

In continuation of this research we report here the synthesis and crystal structures of four complexes of DTU with benzo-crown ethers. Four monomers used in this study are shown in Scheme 1. They are two mono- and two dibenzo-derivatives of 18C6, namely 4-bromo-, 4-nitrobenzo-18C6, [2.4]dibenzo- and thia[1.5]dibenzo-18C6. Four novel complexes were characterised by elemental analysis, ^{1}H NMR and X-ray investigation.

It is known [3b] that an attachment of the benzene ring to the crown ether framework influences the flexibility of the oxyethylene chain and decreases the accessibility of the oxygen atoms relative to it for the hydrogen bonding

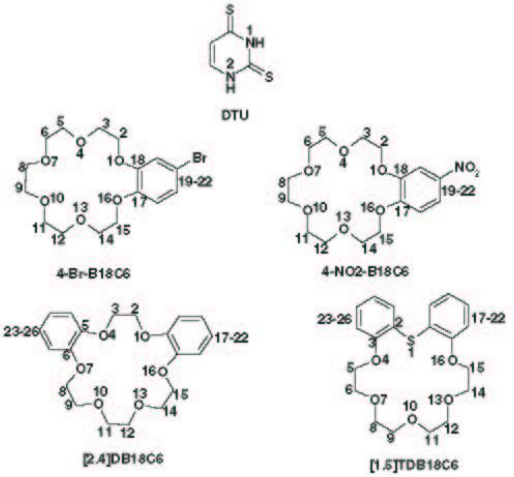

Scheme 1 Structural formulas and crystallographic numbering for studied compounds

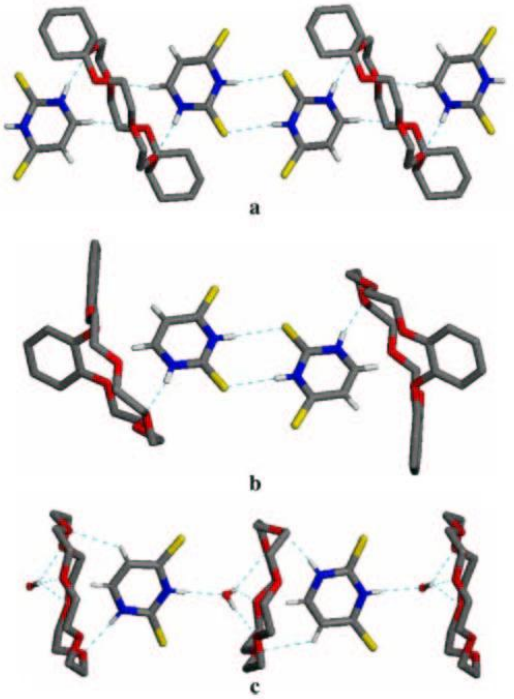

Fig. 1 Structural motifs in the DTU complexes with crown ethers: (**a**) fragment of the chain in the complex *cis-anti-cis*-DCH18C6·2DTU [10], refcode CATCIK in CSD [12]); (**b**) molecular capsule in the complex [1.5]DB18C6·DTU [5a], refcode YAXNAN in CSD; (**c**) fragment of the chain in the complex 18C6·DTU·H_2O [12], refcode CATCEG in CSD

interaction, the second aromatic ring arranged in a close proximity to the first one in the macrocyclic molecule is expected to make additional impediments for the macrocyclic oxygens for intermolecular interactions. On the other hand, the availability of the aromatic units in the macrocyclic molecule enhances the contribution of the π–π interactions in the overall system of the crown ether–DTU interactions. This study aims to register the preferable modes of DTU interactions with benzo-crown ethers with the estimation of the contribution of π–π component in an overall system of interactions. The divalent sulfur atoms are significantly larger than oxygen. Being incorporated in the macrocyclic framework, the sulfurs prefer an exocyclic conformation [13]. It seems to be interesting to compare the structural peculiarities of the previously reported DTU—[1.5]dibenzo-18C6 complex [5a] with its thia-analogue, thia[1.5]dibenzo-18C6.

Experimental

Synthesis

4-Bromo-B18C6 and 4-nitro-B18C6 were obtained as described in [14] and [15] respectively, and [2.4]DB18C6 as reported in [16]. Thia[1.5]DB18C6 was synthesized by us according to the originally developed procedure. Commercially available DTU (Aldrich Chemical Co) was used in its initial state. The thin layer chromatographic control of the substances purity was performed on Silufol UV-254 plates. Complexes **1**–**4** were obtained in a similar way by mixing of the methanol solutions of DTU and the corresponding crown ether. The ratio of the components varied from 1:1 till 1:3 (excess of the crown ether). Only four complexes described in this article were obtained. Complexes were analyzed for C, H, Br, N and S in a Perkin Elmer 240C instrument. Crystals suitable for the X-ray diffraction experiments were isolated from the mass of the crystals obtained. Suitable microanalyses were obtained for all compounds. ^{1}H NMR spectra were recorded in $DMSO_{d6}$ (99.9%) and $CDCl_3$ (99.8%) on the 299.95 MHz Varian WXP-300 instrument using TMS as internal standard. ^{1}H NMR spectra recorded only the peaks typical for the separate components (crown ether and DTU), no solution studies were fulfilled. Mass spectrum was obtained with a MX-1321 spectrometer equipped with a direct inlet; ionization voltage 70 eV, ionization chamber temperature 200 °C.

Synthesis of thia[1.5]DB18C6

Sodium hydroxide (4.0 g, 100 mmol) was added with an effective stirring to the solution of 2,2^{I}-dihydroxydiphenyl sulfide (10.91 g, 50 mmol) and tetraethyleneglycol ditosylate (19.10 g, 51 mmol) in dry 1,4-dioxane (150 ml). The resulting mixture was stirred during 20 h at 100 °C, then cooled and acidified by concentrated hydrochloric acid to pH 3–4. The residue was filtered, washed by cool 1,4-dioxane (2 × 10 ml) and filtrate was treated by activated charcoal. The solvent was evaporated at reduced pressure. The residue was extracted by boiling *n*-heptane (4 × 150 ml) and combined extracts were cooled to 5–10 °C and filtered off. The residue was washed by boiling *n*-heptane (2 × 30 ml) and crystallized from *iso*-propanol. White crystals M.P. 107–108 °C were obtained with the yield 3.76 g (20%). Found, C, 63.72; H, 6.50; S, 8.46 for $C_{20}H_{24}O_5S$. Calculated, %: C, 63.81; H, 6.43; S; 8.52. ^{1}H NMR ($CDCl_3$, 299.95 MHz): 3.57, m; 3.67, m; 4.08, m (16H, CH_2); 6.72, t; 6.78–6.99, m; 7.09 t (8H, CH_{Ar}). Mass spectra, *m/z* (I%): 377 (20.8), 376 (100.0), 218 (34.2), 200 (10.7), 171 (10.6), 151 (47.6), 137 (81.8), 120 (14.6), 96 (13.6), 94 (25.1), 91 (20.1), 45 (73.8), 43 (38.7).

Synthesis of 4-bromo-B18C6 · DTU · H_2O (1)

DTU (36 mg, 0.25 mmol) and 4-bromo-B18C6 (98 mg, 0.25 mmol) were dissolved in methanol (20 ml) at 64 °C. Ethyl acetate (30 ml) was added, and the mixture was remained to crystallize at room temperature and spontaneous evaporation of solvents. Yellow transparent crystals M.P. 260–262 °C (with decomposition) suitable for X-ray analysis were obtained with the yield 117 mg (85%). Found, C, 43.44; H, 5.25; Br, 14.49; N, 5.13; S, 11.64 for $C_{20}H_{29}BrN_2O_7S_2$. Calculated, %: C, 43.40; H, 5.28; Br, 14.44; N, 5.06, S; 11.59. ^{1}H NMR ($DMSO_{d6}$, 299.95 MHz): 3.55 m, 3.59 m, 3.73 m, 4.07 m (20H, CH_2) and 7.05 d, 7.10 s (3H, CH_{Ar})—crown ether; 6.50 d, 7.25 d (2H, CH)—pyrimidine-2,4(1*H*,3*H*)-dithione.

Synthesis of 4-nitro-B18C6 · DTU · H_2O (2)

DTU (36 mg, 0.25 mmol) and 4-nitro-B18C6 (89 mg, 0.25 mmol) were dissolved in methanol (3 ml) at 64 °C. Ethyl acetate (6 ml) was added, and the mixture was remained to crystallize at room temperature and spontaneous evaporation of solvents. Yellow transparent crystals, M.P. 253–254 °C (with decomposition) suitable for X-ray analysis were obtained with the yield 118 mg (91%). Found, C, 46.18; H, 5.67; N, 8.13; S, 12.39 for $C_{20}H_{29}N_3O_9S_2$. Calculated, %: C, 46.23; H, 5.63; N, 8.09; S, 12.34. ^{1}H NMR ($DMSO_{d6}$, 299.95 MHz): 3.57 m, 3.62 m, 3.76 m, 4.23 m (20H, CH_2) and 7.25 d, 7.73 s (3H, CH_{Ar})—crown ether; 6.50 d, 7.25 d (2H, CH)—pyrimidine-2,4(1*H*,3*H*)-dithione.

Synthesis of [2.4]DB18C6 · DTU (3)

A solution of [2.4]DB18C6 (360 mg, 1 mmol) and DTU (144 mg, 1 mmol) in the methanol:ethyl acetate mixture (20 ml:40 ml) was stored during 3–4 days at 20–25 °C in an open flask. The resulting transparent yellow crystals, suitable for X-ray analysis, M.P. 236–238 °C (with decomposition) were separated with the yield of 80% (400 mg). Found, C, 57.08; H, 5.63; N, 5.58; S, 12.75 for $C_{24}H_{28}N_2O_6S_2$. Calculated, %: C, 57.12; H, 5.59; N, 5.55; S, 12.71. ^{1}H NMR ($DMSO_{d6}$, 300 MHz): 3.59 m, 3.72 m, 4.07 m, 4.28 m (16H, CH_2) and 6.96 m (8H, CH_{Ar})—crown ether; 6.49 d, 7.25 d (2H, CH)—pyrimidine-2,4(1*H*,3*H*)-dithione.

Synthesis of thia[1.5]DB18C6 · DTU (4)

DTU (36 mg, 0.25 mmol) and thia[1.5]DB18C6 (94 mg, 0.25 mmol) were dissolved in methanol (2 ml) at 64 °C. Ethyl acetate (2 ml) and *n*-butanol (1 ml) were added, and the mixture was remained to crystallize at room temperature and spontaneous evaporation of solvents. Yellow transparent crystals M.P. 250–252 °C (with decomposition) suitable for X-ray analysis were obtained with the yield 114 mg (88%). Found, C, 55.53; H, 5.38; N, 5.43; S, 18.52 for $C_{24}H_{28}N_2O_5S_3$. Calculated, %: C, 55.36; H, 5.42; N, 5.38; S, 18.48. ^{1}H NMR ($DMSO_{d6}$, 299.95 MHz): 3.59 m, 3.66 m, 4.12 m (16H, CH_2) and 6.99 m, 7.25 m (8H, CH_{Ar})—crown ether; 6.50 d, 7.25 d (2H, CH)—pyrimidine-2,4(1*H*,3*H*)-dithione.

Data collection and structure refinement

Unit cell dimensions and intensity data collection were performed at a room temperature on a Philips PW1100 diffractometer equipped with graphite monochromated MoKα radiation for **1**, **2**, **4** and CuKα radiation for **3**. All the data sets were collected by ω-2θ scan mode. There was no significant intensity decay. Structure solutions were performed by direct methods (SHELXS-97) and refined by full-matrix least-squares methods on F^2 (SHELXL-97) [17]. All non-disordered non-hydrogen atoms were refined anisotropically. In all structures H atoms attached to carbons were included in idealized positions in a riding model with isotropic temperature factors (1.2 times the carbon temperature factor), whereas those on N and O (water) atoms were found from difference Fourier maps at an intermediate stage of the refinement and refined with isotropic temperature factors (1.5 times the parent N(O) temperature factor) subjected to the geometrical restraints for the distance (N–H and O–H = 0.86 Å). In complex **2** the 4-Br-1,2-phenylene moiety is disordered over two positions with the occupancies equal to 0.811(3) and 0.189(3), correspondingly, the minor component being refined in an approximation of the rigid group with all but Br atom being isotropic. In complex **4** two atoms of the oxyethylene chain, O10 and C9 were found to be disordered over two positions with the occupancies equal to 0.723(1) and 0.277(1), correspondingly, the minor component being refined in an isotropic approximation.

The X-ray data and details of the refinement for **1–4** are summarized in Table 1, hydrogen bonding geometry—in Table 2, torsion angles—in Table 3.

Results and discussion

DTU–CE complex organisation

The retrieval of CSD (CSD version 5.28, November 2006, three updates 2007) [12] reveals only very few examples of the crystalline complexes of the CEs shown in Scheme 1 [18]. Moreover, among them only 1:1 adduct of thia[1.5]DB18C6 with antimony trifluoride represents a genuine host–guest complex where the components are held together through electronic interactions [18f]. We present here the single crystal structures for the molecular complexes **1–4**. All compounds crystallize in the centric space groups, triclinic $P-1$ for complexes **1** and **2** and monoclinic $P2_1/n$ and $P2_1/c$ for complexes **3** and **4**, correspondingly. Complexes **1** and **2** represent the monohydrates of the 1:1:1 ratio, while complexes **3** and **4** represent the binary adducts of the 2:2 ratio. The formula units for **1–4** are shown in Fig. 2. The asymmetric unit contains one ternary complex for **1** (Fig. 2a) and **2** (Fig. 2b), one binary complex for **3** (Fig. 2c) and one half of the binary complex for **4** (Fig. 2d). Below we summarize the differences in the complex organisation dictated by the structure of the corresponding CE.

The common feature for **1–4** is a weakness of intermolecular hydrogen bonding. Similar to the earlier discussed DTU complexes [5a, 10] in the complexes **1–4** the DTU-CE units are held together via an NH···O hydrogen bond with the sterically non-hindered N2 nitrogen atom of the DTU ring and by the subsidiary weak CH···O interaction with the neighboring CH-group (Table 2). The π–π stacking interactions between the pyrimidine ring of DTU molecule and the aromatic moieties in the macrocyclic molecules (varying number of phenylene rings) and the nature of the substituents (Br, NO_2) influence the mutual arrangement of the components in the complexes **1–4**. The mutual arrangement of the DTU and CE molecules is completely described by two dihedral angles, the first one (angle 1) is between the planes through the heterocyclic pyrimidine ring in the DTU molecule and the plane through six oxygen atoms in the macrocyclic

Table 1 Crystallographic data for complexes **1–4**

Complex	**1**	**2**	**3**	**4**
Composition	$C_{20}H_{29}BrN_2O_7S_2$	$C_{20}H_{29}N_3O_9S_2$	$C_{24}H_{28}N_2O_6S_2$	$C_{24}H_{28}N_2O_5S_3$
CCDC numbers	663173	663172	663170	663171
Formula weight	553.48	519.58	504.60	520.66
Wavelength (Å)	0.71073	0.71073	1.54180	0.71073
Space group	*P*-1	*P*-1	$P2_1/n$	$P2_1/c$
a (Å)	8.8461(18)	7.2210(14)	21.739(4)	9.0864(18)
b (Å)	9.4941(19)	11.535(2)	9.1700(18)	17.611(4)
c (Å)	15.663(3)	15.025(3)	25.360(5)	16.400(4)
α (°)	104.21(3)	91.14(3)	90.0	90.0
β° (°)	90.10(3)	95.94(3)	90.11(3)	99.04(3)
γ (°)	101.47(3)	92.81(3)	90.0	90.0
V ($Å^3$)	1248.0(4)	1242.9(4)	5055.4(17)	2591.7(9)
Z	2	2	8	4
*D*calc (g cm^{-3})	1.473	1.388	1.326	1.334
μ (mm^{-1})	1.856	0.268	2.261	0.323
F(000)	572	548	2128	1096
Reflections collected/unique	11272/4852	4877/4877	9815/9602	22203/5049
Reflections with $I > 2\sigma(I)$	2307	2602	6047	5049
Refinement method	Full-matrix least-squares on F^2	Full-matrix least-squares on F^2	Full-matrix least-squares on F^2	Full-matrix least-squares on F^2
Data/restraints/parameters	4852/6/323	4877/2/315	9602/4/630	5049/2/323
Goodness-of-fit on F^2	1.021	1.009	0.998	1.016
R_1, wR_2 [$I > 2\sigma(I)$]	0.0647, 0.1913	0.0662, 0.1608	0.0429, 0.1029	0.0541, 0.1227
R_1, wR_2 (all data)	0.1396, 0.2092	0.1291, 0.1786	0.0746, 0.1146	0.0707, 0.1297
Largest diff. peak and hole e· $Å^{-3}$	0.302/−0.426	0.450/−0.457	0.499/−0.451	0.281/−0.364

molecule in complexes **1–3** and S_1O_5 set in complex **4**; and the second angle (angle 2) is between the same plane of the DTU molecule and the plane through the 1,2-phenylene ring in the CE molecule (it is one such angle for complexes **1** and **2** and two angles for complexes **3** and **4**, further they will be designated as angles 2/3, correspondingly). The angle 1 is equal to 50.7(2)° in **1**, 57.0(1)° in **2**, 77.3(1)/74.1(1)° for units A and B in complex **3** and 83.4(2)° in complex **4**, respectively. The gradual increase of this torsion angle with the approaching to the practically perpendicular arrangement of the DTU molecule towards the least-square plane of S_1O_5 atom set in the complex **4** is observed. The dihedral angle 2 has the values of 50.8(3)° and 9.8(1)° in complexes **1** and **2**, respectively. The dihedral angles 2/3 in complexes **3** and **4** adopt the values 44.8(1)/80.5(1)° and 45.4(1)/70.1(1)° for units A and B in **3**, and 57.2(3)/75.6(3)° in **4**. The inspection of these values evidently reveals the most pronounced contribution of stacking component in complex **2**, where the planar moieties of the DTU and CE molecules are displayed in practically parallel planes with the distance between the centroids of the DTU and benzene rings equal 3.811 Å. It is concerted with the typical π–π interactions and demonstrates the function of the electron-seeking nitro-group in the phenylene ring of CE that increases the planar π-electronic system and the π–π component of the intermolecular interaction. Contrary, the electron-withdrawing Br substituent in the 4-Br-B18C6 molecule in complex **1** impoverishes the π-electronic system of the crown that results in the lack of π–π stacking and instead demonstrates the close to the T-shape mode arrangement of the phenyl and DTU rings in the complex. In both complexes **1** and **2** the DTU arrangement occurs on the concave side of the macrocycle with the water molecule displayed on its convex side. The 4-Br-B18C6 and 4-NO_2-B18C6 molecules provide both sides of the molecule for the hydrogen bonding interactions. In contrary, arranged in a close proximity phenylene rings in the dibenzocrown ethers in complexes **3** and **4** preclude any interaction on one side of the macrocycle.

In the 4-Br-B18C6 and 4-NO_2-B18C6 molecules the oxygen atoms of the macrocyclic ring adopt a half-boat shape with five oxygen atoms that define its bottom being coplanar within ±0.12 and ±0.16 Å, correspondingly and the O7 atom deviating from this plane at 0.97 and 0.70 Å, correspondingly. The macrocyclic conformation is

Table 2 Hydrogen bonds for complexes **1–4** [Å and °]

D–H···A	d(D–H), Å	d(H···A), Å	d(D···A), Å	∠(DHA), [°]	Symmetry transformation for acceptor
1					
N(1)–H(1N1)···O(1W)	0.90(2)	1.97(3)	2.814(6)	156(6)	$x + 1, y, z$
N(2)–H(1N2)···O(10)	0.91(2)	2.02(4)	2.835(6)	148(6)	$-x + 1, -y + 1, -z + 1$
C(25)–H(25)···O(13)	0.93	2.58	3.458(8)	157	x, y, z
O(1W)–H(1W)···O(7)	0.85(2)	2.41(8)	2.971(6)	124(7)	$-x + 1, -y + 1, -z + 1$
O(1W)–H(2W)···O(1)	0.86(2)	2.51(2)	3.283(6)	151(4)	$-x + 1, -y + 1, -z + 1$
2					
N(1)–H(1N)···S(1)	0.86(2)	2.49(2)	3.340(3)	170(3)	$-x, -y + 2, -z + 1$
N(2)–H(2N)···O(13)	0.86(2)	2.20(3)	2.953(4)	144(4)	$x-1, y, z$
N(2)–H(2N)···O(10)	0.86(2)	2.53(3)	3.137(4)	127(3)	$x-1, y, z$
O(1W)–H(1W)···O(7)	0.84	2.26	2.937(5)	137	x, y, z
O(1W)–H(2W)···O(13)	0.92	2.52	3.425(5)	168	x, y, z
C(25)–H(25)···O(7)	0.93	2.45	3.369(4)	168	$x-1, y, z$
3					
N(2A)–H(2NA)···O(16A)	0.82(2)	2.49(2)	3.074(3)	129(2)	x, y, z
N(2A)–H(2NA)···O(1A)	0.82(2)	2.18(2)	2.946(2)	156(2)	x, y, z
C(28A)–H(28A)···O(10A)	0.93	2.44	3.133(3)	131	x, y, z
N(1A)–H(1NA)···S(1B)	0.83(2)	2.49(2)	3.305(2)	172(2)	$x + 1/2, -y + 3/2, z + 1/2$
N(1B)–H(1NB)···S(1A)	0.81(1)	2.62(1)	3.425(2)	174(2)	$x-1/2, -y + 3/2, z-1/2$
N(2B)–H(2NB)···O(7B)	0.82(2)	2.57(2)	3.181(2)	132(2)	x, y, z
N(2B)–H(2NB)···O(4B)	0.82(2)	2.22(2)	2.984(2)	155(2)	x, y, z
C(28B)–H(28B)···O(13B)	0.93	2.29	3.052(3)	139	x, y, z
4					
N(1)–H(1)···S(2)	0.86(2)	2.47(2)	3.297(2)	161(3)	$-x + 1, -y + 1, -z$
N(2)–H(2)···O(10)	0.86(2)	1.93(3)	2.789(3)	172(3)	x, y, z

Table 3 Torsion angles along the macrocyclic framework in crown molecules in complexes **1–4**

Complex	**1**	**2**	**3** (A)	**3** (B)	**4**
C(18)–O(S)(1)–C(2)–C(3)	−177.3(5)	−171.7(4)	−179.6(2)	−162.8(2)	−166.1(2)
O(1)–C(2)–C(3)–O(4)	−71.0(7)	73.9(5)	67.5(3)	−64.9(2)	−0.1(3)
C(2)–C(3)–O(4)–C(5)	−176.5(5)	−179.0(4)	167.1(2)	178.0(2)	160.1(2)
C(3)–O(4)–C(5)–C(6)	−172.2(6)	165.7(4)	179.7(2)	−170.2(2)	−167.9(2)
O(4)–C(5)–C(6)–O(7)	68.8(7)	−68.9(4)	−3.0(3)	−0.1(3)	66.6(3)
C(5)–C(6)–O(7)–C(8)	178.6(6)	−175.2(3)	−172.8(2)	176.1(2)	−168.7(3)
C(6)–O(7)–C(8)–C(9)	169.9(5)	173.6(3)	170.8(2)	−162.7(2)	160.1(4)
O(7)–C(8)–C(9)–O(10)	−75.0(6)	77.1(5)	−63.3(2)	68.4(2)	55.2(7)
C(8)–C(9)–O(10)–C(11)	176.5(5)	−177.0(3)	−174.2(2)	173.5(2)	175.4(4)
C(9)–O(10)–C(11)–C(12)	−82.0(6)	89.7(4)	−172.2(2)	172.9(2)	73.7(6)
O(10)–C(11)–C(12)–O(13)	−77.6(6)	65.7(4)	74.9(2)	−72.4(2)	49.0(5)
C(11)–C(12)–O(13)–C(14)	−179.1(5)	179.7(3)	−171.8(2)	168.3(2)	166.6(3)
C(12)–O(13)–C(14)–C(15)	−178.1(5)	−179.1(3)	−166.5(2)	166.3(2)	175.8(3)
O(13)–C(14)–C(15)–O(16)	72.5(6)	−75.5(4)	−67.8(2)	63.2(3)	−70.3(3)
C(14)–C(15)–O(16)–C(17)	−179.8(5)	167.3(3)	153.7(2)	−171.6(2)	−86.2(3)
C(15)–O(16)–C(17)–C(18)	−179.6(5)	−178.5(3)	−166.0(2)	169.2(2)	163.2(2)
O(16)–C(17)–C(18)–O(1)	1.5(8)	−2.1(5)	−2.5(3)	6.4(3)	−9.4(3)
C(17)–C(18)–O(S)(1)–C(2)	−169.6(6)	179.9(4)	174.9(2)	176.9(2)	85.1(2)

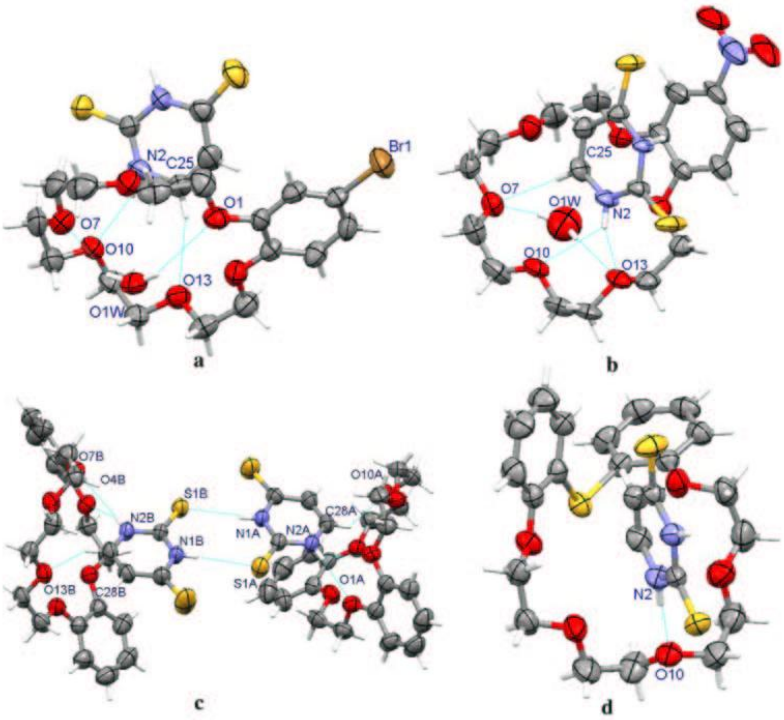

Fig. 2 ORTEP view for complexes **1**–**4**: (**a**) complex **1**; (**b**) complex **2**; (**c**) complex **3**; (**d**) complex **4**. Ellipsoids for non-hydrogen atoms are drawn at the 50% probability level. Only atoms involved in hydrogen bonding (and Br1 in complex **1**) are labeled

described by five *gauche*- and one *cis*- C–C torsion angles and 11 *anti*- and one *gauche*- C–O torsion angles (Table 3). Two DB18C6 macrocycles in complex **3** (A and B) adopt very close conformations with six oxygen atoms being coplanar within ±0.16 Å, all C–O bonds being in *anti*-conformation, two C–C bonds that belong to the 1,2-phenylene rings being in *cis*-conformation, four other C–C bonds being *gauche*. The dihedral angle between two phenylene rings in the molecule A is equal to 57.1(1)°, in the molecule B—60.2(1)°. In the thia[1.5]DB18C6 molecule in complex **4** five oxygen atoms are coplanar within ±0.05 Å, and sulfur atom deviates from this plane at 1.52 Å. In the macrocyclic framework one C–S bond is in *anti*-, and one—in *gauche*-conformation, of ten C–O bonds 8 being in *anti*- and 2—in *gauche*-conformation, of 6 C–C bonds two that belong to the phenylene rings are *cis*- and four others—are *gauche* (Table 3). The dihedral angle between the phenylene rings in the molecule adopts the value 88.1(3)°.

Supramolecular organisation

As we noted in Introduction, three different modes of supramolecular organisation of the DTU–CE units have been found so far (Fig. 1): for the ternary complexes which incorporate water molecules it is a chain organisation with the alternation of the components; for the binary complexes it is a chain organization again with the alternation of the CE molecules and the dimers of the inversion-related DTU molecules and the capsule organisation with the incorporation of the DTU dimer inside two CE molecules. Complex **1** reveals the first type of supramolecular organization, whilst complexes **2**–**4** reveal the different modes of capsules (Figs. 2c, 3).

In the complex **1** the O(1W) water molecule is situated on the convex face of the crown ether with the O(1W)···O(crown) distances being in the range 2.971(6) (till O7)–3.905(7) Å (till O10) (Table 2) and at the distance of 1.815(6) Å from the least-square plane of six oxygen atoms. It is weakly bound with the macrocycle. The water molecule blocks the second amino group of the DTU ring, thus precluding the typical nucleic bases pairing [9, 19] via $R_2^2(8)$ NH···S synthon [11]. The strong intermolecular H-bonding, N(1)–H(1)···O(1W) is described by the N(1)···O(1W) separation of 2.819(7) Å and N(1)–H(1)···O(1w) angle of 157(4)°. The components are organized in the chain running along *c* axis in the crystal (Fig. 3a).

In the ternary complex **2**, similar to **1**, water molecule is displayed on the convex face of the macrocyclic cavity at the distances 2.937(5)–3.864(5) Å from the crown oxygen atoms being weakly bounded with the macrocycle via only

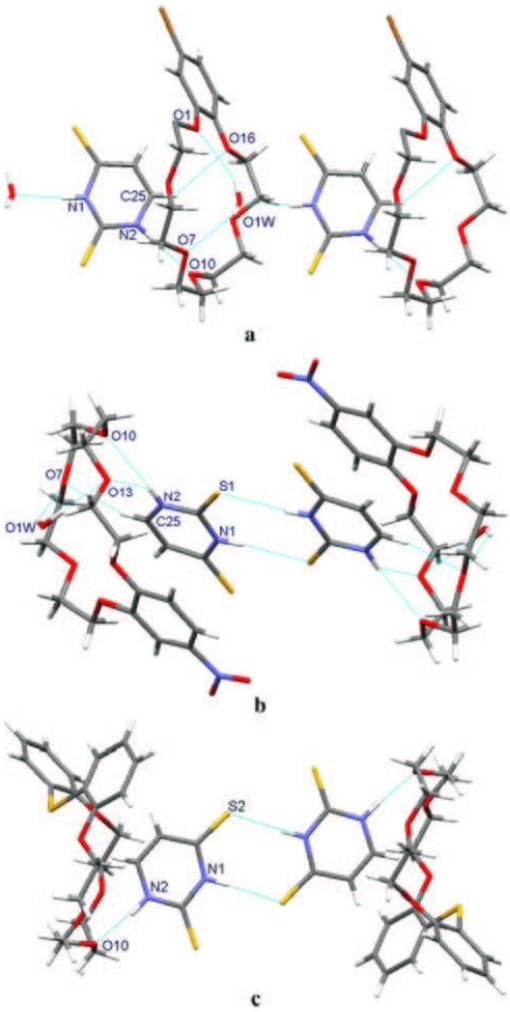

Fig. 3 Supramolecular organisation for **1**, **2**, **4**: (**a**) the chain fragment for **1**; (**b**) supramolecular capsule for **2**; (**c**) supramolecular capsule for **4**

one OH···O hydrogen bond (Table 2). The water molecule deviates at 1.802(4) Å from the least-square plane of six oxygen atoms of the CE, which are coplanar within ±0.262 Å. In this complex the water molecule does not exhibit its typical bridging function, and does not have any direct contacts with the DTU molecule. We observe here the novel six-membered type of the capsule (Fig. 3b).

The binary complexes **3** and **4** represent the fine examples of the four-membered capsules relative to that one previously reported for the [1.5]DB18C6 [5a]. The unusual feature of **3** is a lack of the inversion center within the capsule. The N···S distances are slightly different, the dihedral angle between two planar S1/C27/N2/H2N moieties in the eight-membered H-bonded ring is equal to 9.9(3)°, and this deviation from the planarity confirms the P1 capsule symmetry (Fig. 2c).

Conclusion

Four novel complexes of 2,4-dithiouracil (DTU) with 18-membered benzo- and dibenzo-crown ethers (CE) were synthesized in approximately the same conditions and characterized by X-ray diffraction analysis. From six possible tautomeric forms of DTU, only 2,4-dithione form was registered in all crystalline products. The crystal structures revealed the three structural motifs: 1D chain ···***CE***···***water***···***DTU***···***CE***···, and two types of capsules ***CE***···$(\boldsymbol{DTU})_2$···***CE*** and ***water***···***CE***··· $(\boldsymbol{DTU})_2$···***CE***···***water***. These supramolecular motifs are sustained by the diverse hydrogen bonding. In the first motif *all* hydrogen bonding interactions typical for the pure DTU were substituted by the interactions with the oxygen atoms of the water and crown ether molecules as the stronger hydrogen acceptors. In the two types of capsules the only $R_2^2(8)$ NH···S base-pairing supramolecular synthon responsible for the coupling of the DTU molecules remains as a part of the DTU self-assembling in the pure form.

Supplementary material

Crystallographic data (excluding structure factors) for the structures in this article have been deposited with the Cambridge Crystallographic Data Center, deposition numbers CCDC 663173 (**1**), CCDC 663172 (**2**), CCDC 663170 (**3**), CCDC 663171 (**4**). Copies of this information may be obtained free of charge from The Director, CCDC, 12 Union Road, Cambridge, CB2 1EZ, UK (Fax: +44-1233-336-033; E-mail: deposit@ccdc.cam.ac.uk or www: http://www.ccdc.cam.ac.uk).

References

1. Pedersen, C.J.: Cyclic polyethers and their complexes with metal salts. J. Am. Chem. Soc. **89**, 7017 7036 (1967)
2. Pedersen, C.J.: The discovery of crown ethers (noble lecture). Angew. Chem. Int. Ed. Engl. **27**, 1021 1027 (1988)
3. (a) Bradshaw, J.S., Krakowiak, K.E., Izatt, R.M.: Aza-Crown Compounds, vol. 51, 885 pp. Wiley, New York (1993); (b) Gokel, G.W., Leevy, W.M., Weber, M.E.: Crown ethers: sensors for ions and molecular scaffolds for materials and biological models. Chem. Rev. **104**, 2723 2750 (2004); (c) Gokel, G.W., Carasel, I.A.: Biologically active, synthetic ion transporters. Chem. Soc. Rev. **36**, 378 389 (2007); (d) Steed, J.W.: First- and second-sphere coordination chemistry of alkali metal crown ether complexes. Coord. Chem. Rev. **215**, 171 221 (2001); (e) Bond, A.H.,

Dietz, M.L., Chiarizia, R.: Incorporating size selectivity into synergistic solvent extraction: a review of crown ether-containing systems. Ind. Eng. Chem. Res. **39**(10), 3442–3464 (2000); (f) Cusack, P.A., Smith, P.J.: Crown ethers in tin chemistry. Appl. Organometal. Chem. **4**, 311–317 (1990)

4. (a) Simonov, Yu.A., Fonari, M.S., Zaworotko, M.J., Abourahma, H., Lipkowski, J., Ganin, E.V., Yavolovskii, A.A.: From 1D strands to extended supramolecular assemblies in the binary compounds of dithiooxamide and dithiobiurea with crown ethers. Org. Biomol. Chem. **1**, 2922–2929 (2003); (b) Fonari, M.S., Simonov, Yu.A., Kravtsov, V.Ch., Lipkowski, J., Ganin, E.V., Yavolovskii, A.A.: Hydrogen bonding assemblies in the host-guest complexes with 18-crown-6. J. Mol. Struct. **647**(1–3), 129–140 (2003)
5. (a) Ganin, E.V., Fonari, M.S., Simonov, Yu.A., Bocelli, G., Basok, S.S., Tkachuk, V.V., Kotlyar, S.A., Kamalov, G.L.: Structure of dibenzocrown ethers and their H-bonded adducts. 2. [1.5]Dibenzo-18-crown-6, a suitable building block to modulate the supramolecular assemblages sustained by conventional and weak hydrogen bonds. J. Incl. Phenom. **52**, 63–74 (2005); (b) Kotlyar, S.A., Fonari, M.S., Simonov, Yu.A., Bocelli, G., Shishkin, O.V., Shishkina, S.V., Tkachuk, V.V., Grigorash, R.Ya., Kamalov, G.L.: Structure of dibenzocrownethers and their H-bonded adducts. 1. [1.5]Dibenzo-18-crown-6 and biphenyl-20-crown-6: complexes with amidosulfuric acid. J. Incl. Phenom. **52**, 75–84 (2005)
6. Kiviniemi, S., Nissinen, M., Kolli, T., Jalonen, J., Rissanen, K., Pursiainen, J.: Crown ether complexes of six-membered N-heteroaromatic cations. J. Incl. Phenom. **40**, 153–159 (2001)
7. (a) Simonov, Yu.A., Fonari, M.S., Lipkowski, J., Yavolovskii, A.A., Ganin, E.V.: Preparation and X-ray study of inclusion complexes of (4*Z*,5*E*)-pyrimidine-2,4,5,6(1*H*, 3*H*)-tetraone 4,5-dioxime and the product of its cyclization, (1,2,5)-oxadiazolo(3,4-*d*)-pyrimidine-5,7(4*H*,6*H*)-dione with two 18-membered macrocycles. J. Incl. Phenom. **46**(1–2), 27–36 (2003); (b) Fonari, M.S., Simonov, Yu.A., Chumakov, Yu.M., Bocelli, G., Ganin, Ed.V., Yavolovskii, A.A.: The dihydropyrimidine-2,4-(1H,3H)-dione functionality: a suitable module for novel crown-containing hydrogen-bonded supramolecular assemblies. Supramol. Chem. **16**(1), 23–30 (2004)
8. (a) Rostkowska, H., Szczepaniak, K., Nowak, M.J., Leszczynski, J., KuBulat, K., Person, W.B.: Thiouracils. 2. Tautomerism and infrared spectra of thiouracils. Matrix-isolation and ab initio studies. J. Am. Chem. Soc. **112**, 2147–2160 (1990); (b) Leszczynski, J., Lammertsma, K.: 2,4-Dithiouracil tautomers: structures and energies. J. Phys. Chem. **95**, 3128–3132 (1991); (c) Leš, A., Adamowicz, L.: Tautomerism of 2- and 4-thiouracil. Ab initio theoretical study. J. Am. Chem. Soc. **112**, 1504–1509 (1990); (d) Lapinski, L., Rostkowska, H., Nowak, M., Kwiatkowski, J., Leszczynski, J.: Infrared spectra of thiouracils: experimental matrix isolation and ab initio Hartree-Fock, post-Hartree-Fock and density functional theory studies. Vib. Spectrosc. **13**, 23–40 (1996); (e) Yekeler, H.: Ab initio study on tautomerism of 2-thiouracil in the gas phase and in solution. J. Comput. Aided Mol. Des. **14**, 243–250 (2000); (f) Wang, H., Meng, F., Xu, W., Liu, C.: The effects of incorporating 2,4-dithiouracil into uracil tetrad: a theoretical study. J. Mol. Struct. THEOCHEM **716**, 137–141 (2005); (g) Gomzi, V., Herak, J.N.: Ionization potentials of nucleobase analogs using partial third-order electron propagator method. J. Mol. Struct. THEOCHEM **683**, 155–157 (2004); (h) Yang, Z., Rodgers, M.T.: Influence of thioketo substitution on the properties of uracil and its noncovalent interactions with alkali metal ions: threshold collision-induced dissociation and theoretical studies. J. Phys. Chem. A **110**(4), 1455–1468 (2006)
9. (a) Shefter, E. Mautner, H.G.: The crystal and molecular structure of 2,4-dithiouracil. J. Am. Chem. Soc. **89**, 1249–1253 (1967); (b) Tiekink, E.R.T.: Crystal structure of 2-thiouracil. Z. Kristallogr. **187**, 79–84 (1989); (c) Fonari, M.S., Simonov, Yu.A., Ganin, E.V., Yavolowski, A.A., Luboradzki, R.: Crystal and molecular structures of the 1:2 "host-guest" complex between *cis-anti-cis* isomer of dicyclohexano-18-crown-6 and 2-thiouracil. Crystallogr. Rep. **44**, 1006–1009 (1999)
10. Wang, W.-J., Ganin, E.V., Fonari, M.S., Simonov, Yu.A., Bocelli, G.: 2,4-Dithiouracil: the reproducible H-bonded structural motifs in the complexes with 18-membered crown ethers. Org. Biomol. Chem. **3**, 3054–3058 (2005)
11. Etter, M.C., Frankenbach, G.A.: Hydrogen-bond directed co-crystallization as a tool for designing acentric organic solids. Chem. Mater. **1**, 10–12 (1989)
12. Allen, F.N.: The Cambridge Structural Database: a quarter of a million crystal structures and rising. Acta Crystallogr. **B58**, 380–388 (2002)
13. (a) Goldberg, I.: Geometry of the ether, sulphide and hydroxyl Groups and structural chemistry of macrocyclic and non-cyclic polyether compounds. In: Patai, S., Rappaport, Z. (eds.) Crown Ethers and Analogs, pp. 359–476. Wiley (1989); (b) Abramson, S., Berkovich-Berger, D., Dagan, S., Goldberg, I., Golender, L., Grabarnik, M., Lemcoff, N.G., Weinman, S., Fuchs, B.: Polythiacrown macro- and gigantocycles with chiral diacetal cores. Eur. J. Org. Chem. 1957–1975 (2007)
14. Kotlyar, S.A., Pluzhnik-Gladyr, S.M.: The development of convenient synthesis methods of halogenosubstituted benzo- and dibenzocrown ethers. In: Monomers for Thermotolerant Polymers (Russ.). Moscow. NIITECHIM, 74–80 (1990)
15. Ivanov, O.V., Markovich, I.S., Blokhina, L.I., Nikolaenko, S.P., Filatova, M.P.: The method of nitration of benzocrown ethers. Patent USSR, № 1544754 (1990). Bull. 1990, №7
16. Gorodnuyk, V.P., Ivanov, O.V., Kotlyar, S.A.: Simple synthesis of unsymmetrical dibenzocrown ethers. Chem. Heterocycl. Comp. (Russ.). **26**, 1414–1415 (1990) (translated from Khimiya Geterotsiklicheskikh Soedinenii, No. 12, pp. 1697–1698, 1990)
17. Sheldrick, G.M.: SHELXS97 and SHELXL97. Programs for Crystal Structure Solution and Refinement. University of Göttingen, Germany (1997)
18. (a) Kotlyar, S.A., Shishkina, S.V., Shishkin, O.V., Pluzhnik-Gladyr, S.M., Kiriyak, A.V., Chuprin, G.N., Kamalov, G.L.: (4-Bromobenzo-18-crown-6)potassium chlorochromate. Acta Crystallogr. **E62**, m120–m122 (2006); (b) Hlavata, D., Hasek, J., Huml, K.: The crystal and molecular structure of 4-nitrobenzo-1,4,7,10,13,16-hexaoxacyclooctadecane. RbSCN, $C_{17}H_{23}O_8N_2SRb$. Acta Crystallogr. **B34**, 416–420 (1978); (c) Hasek, J., Hlavata, D., Huml, K.: Crystal and molecular structure of a complex formed by caesium thiocyanate and 4-nitrobenzo-1,4,7,10,13,16-hexaoxacyclooctadecane (4-nitrobenzo-18-crown-6). Acta Crystallogr. **B33**, 3372–3376 (1977); (d) Calleja, M., Johnson, K., Belcher, W.J., Steed, J.W.: Oxonium ions from aqua regia: isolation by hydrogen bonding to crown ethers. Inorg. Chem. **40**, 4978–4985, (2001); (e) Talanova, G.G., Elkarim, N.S.A., Talanov, V.S., Hanes Junior, R.E., Hwang, H.-S., Bartsch, R.A., Rogers, R.D.: The "picrate effect" on extraction selectivities of aromatic group-containing crown ethers for alkali metal cations. J. Am. Chem. Soc. **121**, 11281–11290 (1999); (f) Fonari, M.S., Ganin, E.V., Gelmboldt, V.O., Lipkowski, J., Kotlyar, S.A., Kamalov, G.L.: The 1:1 adduct of antimony trifluoride with [1.5]dibenzothia-18-crown-6. Acta Crystallogr. **E62**, m1021–m1023 (2006)
19. (a) Brewer, A.D., Ferguson, G., Parvez, M.: Triethylammonium salt of 1,2,3,4-tetrahydro-6-hydroxy-4-oxo-N-phenyl-2-thio-5-pyrimidinecarboxamide, ethanol solvate. Acta Crystallogr. **C43**, 144–147 (1987); (b) Tiekink, E.R.T.: Crystal and molecular structure of 5-carboxy-2-thiouracil monohydrate. Z. Kristallogr. **216**, 122–125 (2001)

Додаток Й.

Копія статті. “Crystal Structures of Dioxonium Hexafluorotantalate and Dioxonium Hexafluoroniobate Complexes with Tetrabenzo-30-Crown-10”

ISSN 1063-7745, Crystallography Reports, 2008, Vol. 53, No. 2, pp. 246–252. © Pleiades Publishing, Inc., 2008.
Original Russian Text © N.G. Furmanova, M.Kh. Rabadanov, T.S. Chernaya, M.S. Fonari, Yu.A. Simonov, É.V. Ganin, V.O. Gelmboldt, R.Ya. Grigorash, S.A. Kotlyar, G.L. Kamalov, 2008, published in Kristallografiya, 2008, Vol. 53, No. 2, pp. 273–278.

STRUCTURE OF ORGANIC COMPOUNDS

Crystal Structures of Dioxonium Hexafluorotantalate and Dioxonium Hexafluoroniobate Complexes with Tetrabenzo-30-Crown-10

N. G. Furmanova[a], M. Kh. Rabadanov[a], T. S. Chernaya[a], M. S. Fonari[b], Yu. A. Simonov[b], É. V. Ganin[c], V. O. Gelmboldt[d], R. Ya. Grigorash[e], S. A. Kotlyar[e], and G. L. Kamalov[e]

[a] *Shubnikov Institute of Crystallography, Russian Academy of Sciences, Leninskiĭ pr. 59, Moscow, 119333 Russia*
e-mail: furm@ns.crys.ras.ru

[b] *Institute of Applied Physics, Academy of Sciences of Moldova, Academiei 5, Chisinau, MD-2028 Moldova*
e-mail: fonari.xray@phys.asm.md

[c] *Odessa State Environmental University, Ministry of Education and Science and National Academy of Sciences of Ukraine, ul. Lvivska 15, Odessa, 65016 Ukraine*
e-mail:edganin@yahoo.com

[d] *Physicochemical Institute for Human and Environmental Protection, Ministry of Education and Science and National Academy of Sciences of Ukraine, ul. Preobrazhenskaya, Odessa, 65026 Ukraine*
e-mail: eksvar@ukr.net

[e] *Bogatsky Physicochemical Institute, National Academy of Sciences of Ukraine, Lyustdorfskaya dor. 86, Odessa, 65080 Ukraine*
e-mail: kamalov@ukr.net.ua

Received April 24, 2007

Abstract—Two isostructural complexes of dioxonium $[H_5O_2]^+$ with tetrabenzo-30-crown-10 of the compositions $[(\text{tetrabenzo-30-crown-10} \cdot H_5O_2)][TaF_6]$ (**I**) and $[(\text{tetrabenzo-30-crown-10} \cdot H_5O_2)][NbF_6]$ (**II**) are studied using X-ray diffraction. The complexes crystallize in the monoclinic crystal system (space group $C2/c$, $Z = 4$). The unit cell parameters of these compounds are as follows: $a = 15.6583(12)$ Å, $b = 15.2259(13)$ Å, $c = 16.4473(13)$ Å, and $\beta = 99.398(6)°$ for complex **I** and $a = 15.7117(12)$ Å, $b = 15.2785(15)$ Å, $c = 16.5247(15)$ Å, and $\beta = 99.398(7)°$ for complex **II**. These complexes belong to the ionic type. The dioxonium cation $[H_5O_2]^+$ in the form of the two-unit cluster $[H_3O \cdot H_2O]^+$ is stabilized by the strong hydrogen bond OH···O [O···O, 2.353(4) Å] and encapsulated by the crown ether. Each oxygen atom of the dioxonium cation also forms two oxygen bonds O···O(crown). The crown ether adopts an unusual two-level (pocket-like) conformation, which provides a complete encapsulation of the oxonium associate. The interaction of the cationic complex with the anion in the crystal occurs through contacts of the C–H···F type.

PACS numbers: 61.66.Hq

DOI: 10.1134/S1063774508020120

INTRODUCTION

As is known, crown ethers (CEs) have been used in the processes of extraction concentration and separation of different metals from acidic aqueous solutions. In this respect, information on the composition and structure of the corresponding extracted forms, i.e., host–guest complexes of crown ethers with metal or hydroxonium cations, is of particular interest [1–3]. In the latter case, the anionic metal complex acts an outer-sphere counterion. The selectivity of the complex formation in the host–guest system is an important characteristic from the viewpoint of the practical technology. This characteristic is determined by the stereochemical features, as well as by the structure and composition (including the denticity) of the crown ether, or, more specifically, by the size and conformation lability of the macroheterocycle cavity (which, in turn, depends on the character and position of the substituents in the macrocycle), the number and nature of donor centers, their mutual arrangement, and other factors.

In the course of our investigations of the reaction products in the M_2O_5–HF–H_2O–CE systems (where M is Nb or Ta, and CE is 18-membered or 20-membered aliphatic, cycloaliphatic, and aromatic crown ethers), which were used as model extraction systems [4–6], we have demonstrated the influence of the composition, the structure, and the configuration of crown ethers on the stoichiometry and structural organization of the host–guest complexes formed in the experiments. For example, it was revealed that, in the case of classical hexadentate crown ethers, such as benzo-18-crown-6 [4], biphenyl-20-crown-6 [5], and *cis–syn–cis*-dicyclo-

hexano-18-crown-6 [6], the sizes of their macrocyclic cavities appear to be large enough to accommodate one oxonium cation $[H_3O]^+$ and that the complexes formed in all the above cases have the composition $[CE \cdot H_3O][MF_6]$. Furthermore, it was found that, in the case of the asymmetric [1.5]dibenzo-18-crown-6, which is isomeric to the symmetric [3.3]dibenzo-18-crown-6, the tripodal oxonium ion cannot be accommodated in the cavity of [1.5]dibenzo-18-crown-6 because of the actual decrease in the number of oxygen atoms accessible for hydrogen bonding in this crown ether. Consequently, the oxonium dihydrate $[H_7O_3]^+$ (trioxonium), which has the form of an $H_2O\cdots H_3O^+\cdots H_2O$ chain linked by the hydrogen bonds, is encapsulated by two [1.5]dibenzo-18-crown-6 molecules with the formation of the $[(CE)_2 \cdot H_7O_3][MF_6]$ complex [5]. As a result, owing to the presence of closely spaced phenylene fragments and the conjugate diphenyloxide oxygen atom, [1.5]dibenzo-18-crown-6 simulates the corresponding cyclic polyether (for example, 15-crown-5) with five oxygen atoms accessible for the participation in the formation of hydrogen bonds. The above explanation is confirmed by the composition and the structure of the well-known oxonium complex of 15-crown-5 [7] with the aurate anion acting as a counterion. This complex has a sandwich structure with the oxonium cluster $[H_7O_3]^+$ encapsulated between two rings. Crown ethers in which the number of oxygen atoms is larger than six can potentially accommodate hydrated oxonium ions inside the macrocyclic cavity. An example is provided by the complex of dioxonium tetrachloroaurate with dibenzo-24-crown-8 of the composition [dibenzo-24-crown-8 $\cdot H_5O_2][AuCl_4]$ [7].

This study is a continuation of our systematic investigations. We report here the results of our investigations into the specific features of the crystal structure of the complexes [tetrabenzo-30-crown-10 $\cdot H_5O_2][TaF_6]$ (**I**) and [tetrabenzo-30-crown-10 $\cdot H_5O_2][NbF_6]$ (**II**), which are the products of the reaction in the $M_2O_5(MF_5)$–HF–H_2O–CE system (where M is Nb or Ta and CE is tetrabenzo-30-crown-10).

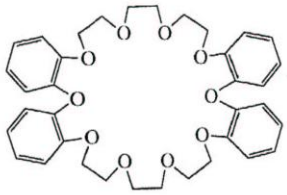

11,12,14,15,17,18,30,31,33,34,36,37-Dodecahydrotetraabenzo[*b,e,q,t*]
[1,4,7,10,13,16,19,22,25,28]decaoxacyclotriacontine (tetrabenzo-30-crown-10)

It can be seen that, unlike [1.5]dibenzo-18-crown-6, tetrabenzo-30-crown-10 contains two diphenyl oxide fragments, which are symmetrically located in the macrocycle with respect to each other. It should also be noted that tetrabenzo-30-crown-10 is formed in small amounts as a by-product of the [2 + 2] dimerization in the course of the synthesis of [1.4]dibenzo-15-crown-5 and can be separated using column chromatography [8, 9]. We developed a convenient technique that makes it possible to prepare tetrabenzo-30-crown-10 with a high yield and to easily separate a pure sample of this crown ether with the use of conventional crystallization.

SAMPLE PREPARATION AND EXPERIMENTAL TECHNIQUE

Tetrabenzo-30-crown-10 was synthesized by the reaction of 2,2'-dihydroxydiphenyl oxide with triethylene glycol ditosylate in dioxane in the presence of potassium hydroxide.

Solid KOH (20.4 g, 0.31 mol) was added to a solution of 2,2'-dihydroxydiphenyl oxide (30.0 g, 0.15 mol) and triethylene glycol ditosylate (68.8 g, 0.15 mol) in dry dioxane (500 ml) with vigorous stirring. The mixture was stirred at a temperature of ~100°C for one day, cooled, and acidified with a concentrated hydrochloric acid to pH 3–4. The precipitate was filtered off, washed with a cold dioxane (2 × 150 ml), and evaporated at a reduced pressure. The residue was dissolved in chloroform (300 ml) and washed sequentially in 5% NaOH (2 × 100 ml) and water (2 × 100 ml). The organic layer was dried with $MgSO_4$ and evaporated to dryness. The product was crystallized sequentially from ethyl acetate and an acetone–water (4 : 1) mixture. The yield of the crown ether was 8.25 g (12%). The melting temperature was equal to 95–97°C.

For $C_{36}H_{40}O_{10}$ anal. calcd. (%): C, 68.48; H, 6.43.

Found (%): C, 68.34; H, 6.37.

Thin-layer chromatography (eluent: acetone–hexane, 3 : 7) was performed on Silufol UV-254 plates (Kavalier) with development in the ultraviolet light (R_f = 0.2). ^{1}H NMR spectrum (0.1 M solution in $CDCl_3$;

Table 1. Crystallographic data, experimental details, and parameters of the structure solution and refinement for complexes **I** and **II**

Compound	I	II
Empirical formula	$C_{36}H_{45}F_6O_{12}Ta$	$C_{36}H_{45}F_6O_{12}Nb$
Molecular weight, M	964.67	876.63
Temperature T, K	293	293
Crystal system	Monoclinic	Monoclinic
Space group, Z	$C2/c$, 4	$C2/c$, 4
a, Å	15.6583(12)	15.7117(12)
b, Å	15.2259(13)	15.2785(15)
c, Å	16.4473(13)	16.5247(15)
β, deg	99.398(6)	99.398(7)
V, Å^3	3868.6(5)	3913.5(6)
Density ρ_{calcd}, g/cm^3	1.656	1.488
Absorption coefficient μ, mm^{-1}	2.930	0.396
Crystal size, mm	0.31 × 0.22 × 0.20	0.35 × 0.25 × 0.22
$F(000)$	1936	1808
Index range	$-19 \le h \le 19$ $-18 \le k \le 18$ $-20 \le l \le 20$	$-19 \le h \le 19$ $-18 \le k \le 18$ $-20 \le l \le 20$
Number of reflections measured/Number of unique reflections/Number of reflections with $I > 2\sigma(I)$	16994/3799/3423 [R_{int} = 0.0731]	18533/3844/3231 [R_{int} = 0.0225]
S on F^2	1.026	1.076
Final R factors for reflections with $I > 2\sigma(I)$	R_1 = 0.0286, wR_2 = 0.0692	R_1 = 0.0289, wR_2 = 0.0764
Final R factors for all reflections	R_1 = 0.0326, wR_2 = 0.0705	R_1 = 0.0374, wR_2 = 0.0791
Residual electron density $\Delta\rho_{max}$, $\Delta\rho_{min}$, e Å^{-3}	0.802, −0.909	0.319, −0.487

T = 298 K; Varian WXP-300; 299.95 MHz; TMS; δ, ppm): CH_2O, 3.44 (s, 8H), 3.62–3.57 (m, 8H), 4.08–4.00 (m, 8H); H_{Ar}, 6.78–6.73 (d, 4H), 6.89–6.82 (m, 4H), 7.03–6.99 (m, 8H). Mass spectrum (MX-1321; direct injection; ionizing voltage, 70 eV; temperature of the ionization chamber, 473 K) m/z (I %): 632 (35.6), 316 (14.4), 229 (11.2), 147 (16.5), 121 (100.0), 120 (27.5), 119 (10.0), 109 (14.3), 108 (14.8), 94 (11.2), 91 (23.2), 45 (38.9), 43 (28.9).

Crystals of complexes **I** and **II** were prepared according to the same procedure.

Tantalum(V) or niobium(V) oxide (0.5 mmol) was dissolved in a 45% hydrofluoric acid (10 ml), and the solution thus obtained was evaporated to 2 ml. Then, a solution of tetrabenzo-30-crown-10 (316 mg, 0.5 mmol) in methanol (5 ml) was added to the 2-ml solution, and the resulting solution was left to crystallize with spontaneous evaporation of the solvents at room temperature. The yield of complex **I** (colorless transparent crystals) was 409 mg (85%). The melting (decomposition) temperature was higher than 210°C.

For $C_{36}H_{45}F_6O_{12}Ta$ anal. calcd. (%): C, 44.82; H, 4.70; F, 11.82.

Found (%): C, 44.80; H, 4.61; F, 11.87.

The yield of complex **II** (colorless transparent crystals) was 351 mg (80%). The melting (decomposition) temperature was higher than 200°C.

For $C_{36}H_{45}F_6O_{12}Nb$ anal. calcd. (%): C, 49.32; H, 5.17; F, 13.00.

Found (%): C, 49.41; H, 5.13; F, 13.07.

The experimental X-ray diffraction data for the crystals of complexes **I** and **II** were collected on an Xcalibur S automated diffractometer equipped with a CCD detector (MoK_α radiation; graphite monochromator; ω scan mode; scan step, 1°; $2\theta_{max}$ = 52°). All the calculations in the processing of the experimental data, including the absorption correction, were carried out with the CrysAlis program package [10]. The structures were solved by direct methods with the SHELXS97 program package [11]. The structures were refined by the full-matrix least-squares procedure on F^2 with the SHELXL97 program package [11]. The analysis of the residual electron-density syntheses revealed that the fluorine atoms of the TaF_6^- (NbF_6^-) anion located at a special position on the twofold axis are disordered over two positions with an equal occupancy. Both positions were refined in the anisotropic approximation. The refinement was performed under the constraint that the

Table 2. Selected interatomic distances d (Å), bond angles ω (deg), and torsion angles φ (deg) in the structure of complex **I**

Atom	d	Atom	d
Ta(1)–F(1)	1.900(12) × 2	O(2)–C(3)	1.415(4)
Ta(1)–F(2)	1.838(12)	O(3)–C(4)	1.410(4)
Ta(1)–F(3)	1.921(8) × 2	O(3)–C(5)	1.404(4)
Ta(1)–F(4)	1.896(14)	O(4)–C(6)	1.411(4)
O(1)–C(1)	1.380(3)	O(4)–C(7)	1.404(4)
O(1)–C(10)^{ii}	1.380(3)	O(5)–C(8)	1.434(3)
O(2)–C(2)	1.359(3)	O(5)–C(9)	1.360(3)
	ω		ω
F(1)–Ta(1)–F(2)	92.2(6)	F(3)–Ta(1)–F(4)	85.1(3)
F(1)–Ta(1)–F(1)^{i}	175.6(11)	F(3)–Ta(1)–F(3)^{i}	170.1(6)
F(1)–Ta(1)–F(3)	93.6(6)	C(1)–O(1)–C(10)^{ii}	119.0(2)
F(1)–Ta(1)–F(3)^{i}	86.3(6)	C(2)–O(2)–C(3)	116.6(2)
F(1)–Ta(1)–F(4)	87.8(6)	C(4)–O(3)–C(5)	112.6(2)
F(2)–Ta(1)–F(3)	94.9(3)	C(6)–O(4)–C(7)	113.7(3)
		C(8)–O(5)–C(9)	117.3(2)
	φ		φ
O(1)C(1)C(2)O(2)	−6.0(4)	C(6)O(4)C(7)C(8)	175.7(3)
C(1)C(2)O(2)C(3)	−172.7(3)	O(4)C(7)C(8)O(5)	−64.4(3)
C(2)O(2)C(3)C(4)	164.1(3)	C(7)C(8)O(5)C(9)	−177.2(2)
O(2)C(3)C(4)O(3)	66.1(4)	C(8)O(5)C(9)C(10)	−178.0(2)
C(3)C(4)O(3)C(5)	178.3(3)	O(5)C(9)C(10)O(1)^{ii}	−2.4(3)
C(4)O(3)C(5)C(6)	178.5(3)	C(9)C(10)O(1)^{ii}C(1)^{ii}	143.8(2)
O(3)C(5)C(6)O(4)	63.7(4)	C(10)O(1)^{ii}C(1)^{ii}C(2)^{ii}	140.6(3)
C(5)C(6)O(4)C(7)	−167.4(3)		

Note: Symmetry operations: (i) $-x, y, -z + 1/2$ and (ii) $-x + 1, y, -z + 1/2$.

Ta–F bond lengths tend to be equal to the average value of 1.877 Å.

The hydrogen atoms of the crown ether were placed in the calculated positions and refined with the fixed thermal parameters U_j, which were taken to be equal to $1.2U_j$ of the atoms bonded to these hydrogen atoms. The hydrogen atoms of the oxonium cation were located from the difference electron-density syntheses: the central hydrogen atom is located on the twofold axis, and the other two independent atoms occupy the general positions. The latter atoms were refined under the constraint that the O–H bond lengths tend to be equal to 0.86 Å with the fixed thermal parameters U_j, which were taken to be equal to $1.5U_j$ of the oxygen atoms bonded to these hydrogen atoms. The crystallographic data, experimental details, and parameters of the structure solution and refinement for crystals of complexes **I** and **II** are summarized in Table 1. The selected geometric characteristics of complex **I** are presented in Table 2. The parameters of the hydrogen bonds in the structure of complex **I** are listed in Table 3.

The crystallographic data for complexes **I** and **II** have been deposited with the Cambridge Crystallographic Data Centre (CCDC no. 637004 for complex **I** and CCDC no. 637005 for complex **II**).

RESULTS AND DISCUSSION

Our crystallographic investigations have revealed that complexes **I** and **II** are isostructural to each other. In the system under consideration, the oxonium cation $[H_3O]^+$ in the monohydrate (dioxonium) form $[H_5O_2]^+$ is encapsulated by the crown ether, as is the case with many crown ether complexes synthesized in an acidic medium from aqueous or water–alcohol solutions. As a consequence, compounds **I** and **II** are complex salts consisting of [tetrabenzo-30-crown-10 · H_5O_2]$^+$ cations and $[TaF_6]^-$ anions (compound **I**) or $[NbF_6]^-$ anions (compound **II**). Since the performed investigations have not revealed significant differences in the structures of complexes **I** and **II** or in the geometric param-

Table 3. Geometric parameters for the hydrogen bonds in the structure of complex **I**

D–H···*A* bond	Distances, Å			Angle, deg	Symmetry operations for the acceptor
	D–H	H···*A*	*D*···*A*	*DHA*	
O(1*W*)–H(1*W*)···O(3)	0.85(2)	1.86(2)	2.676(3)	169(5)	*x*, *y*, *z*
O(1*W*)–H(2*W*)···O(5)	0.83(2)	2.36(4)	3.042(3)	140(5)	*x*, *y*, *z*
O(1*W*)–H(2*W*)···O(1)	0.83(2)	2.12(4)	2.861(3)	149(6)	$-x+1, y, -z+1/2$
O(1*W*)–H(3*W*)···O(1*W*)	1.18(2)	1.18(1)	2.349(5)	170(8)	$-x+1, y, -z+1/2$

eters of both the macrocyclic cations and the anions, we report a detailed description only for complex **I**.

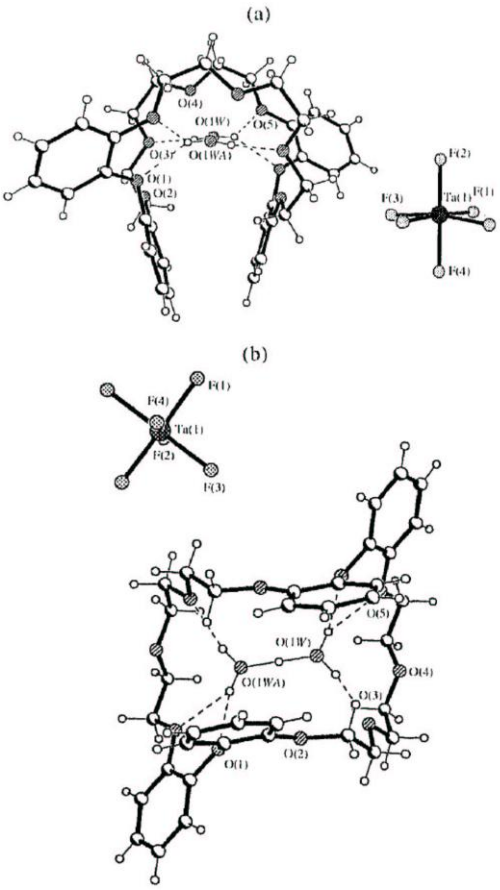

Fig. 1. Structure of complex **I**: (a) side view and (b) projection onto the plane of the oxygen atoms of the macrocycle. The index *A* indicates the oxygen atom related to the basis atom by the symmetry operation $-x+1, y, -z+1/2$.

The crystal structure of complex **I** is shown in Fig. 1. In the crystal structure (space group $C2/c$, $Z=4$), the macrocycle, the MF_6^- anion, and the oxonium cation of the composition $[H_5O_2]^+$ are located along the twofold axis. In the anion, the tantalum atom has an octahedral coordination. The Ta–F bond lengths in the anion lie in the range from 1.834(13) to 1.919(8) Å. The *cis* angles at the tantalum atom vary in the range from 85.1(3)° to 94.9(3)°.

Since the cavity of the 30-membered macrocycle of tetrabenzo-30-crown-10 is large enough for the accommodation of one oxonium cation $[H_3O]^+$, the crown ether encapsulates the oxonium hydrate $[H_5O_2]^+$ (dioxonium), in which the distance between the oxygen atoms is equal to 2.353(5) Å. A similar decrease in the O···O distance equal to 2.360 Å was observed in the structure of the $[(H_5O_2)^+_{0.5}(H_3O)^+_{0.5}][MoOCl_4(H_2O)\cdot(12\text{-crown-}4)]\cdot H_2O$ compound [12]. In the crystal structure of complex **I**, the O–H distances to the H(3*W*) atom located on the twofold axis are equal to 1.18(1) Å. The two other hydrogen atoms of each oxonium oxygen atom form hydrogen bonds with the oxygen atoms of the crown ether, namely, one ordinary hydrogen bond and one bifurcated hydrogen bond. This phenomenon is characteristic of the oxonium cation $[H_3O]^+$.

The analysis of the Cambridge Structural Database [13] has revealed approximately 50 compounds with the crystal structures containing a similar dioxonium cation $[H_5O_2]^+$. Among them, the compounds involving oxygen-containing macrocycles represent the largest group (13 compounds). In the structure of the complex with the smallest ring 1,4-dioxane (which can be considered as a specific 6-crown-2), the $[H_5O_2]^+$ associate (the O···O distance is equal to 2.530 Å) is coordinated from the side of the plane of the six-membered ring [14]. In the sandwich complexes with small-sized rings, such as 12-crown-4 [16], benzo-15-crown-5, and 4,5-dinitrobenzo-15-crown-5 [7, 15], the dioxonium cluster is encapsulated between the two neighboring macrocycles. A somewhat unexpected thing is as follows. In the complex $[18\text{-crown-}6\cdot H_3O](H_5O_2)[2Cl]$ [16], the ligand is traditionally centered by the oxonium cation $[H_3O]^+$ and the dioxonium ion occupies the outer-sphere position with respect to the macrocycle. In

the other complex, namely, [18-crown-6 · $(H_5O_2)_2$][UO_2Cl_4] [15], 18-crown-6 occupies the position at the inversion center and two symmetrically related dioxonium cations are located on both sides of the macrocyclic cavity. The formation of this structure is clearly affected by the anion containing a strong hydrogen acceptor, such as the chloride anion. Owing to the interaction of the chloride anion with one of the hydrogen atoms of the dioxonium cation $[H_5O_2]^+$, the two-unit oxonium cluster forms the tripodal hydrogen bond (typical of the $[H_3O]^+$ cation) with the oxygen atoms of 18-crown-6. As was noted above, the sizes of the cavity of dibenzo-24-crown-8 turn out to be large enough to accommodate the dioxonium cation $[H_5O_2]^+$. In the two previously studied complexes, the dibenzo-24-crown-8 molecule exhibits somewhat different conformations, i.e., a slightly corrugated conformation in the [(dibenzo-24-crown-8 · $H_5O_2)_2$][$(\mu_2\text{-Br})_2Te_2Br_8$] complex [17] and an S-shaped conformation in the [dibenzo-24-crown-8 · H_5O_2][$AuCl_4$] complex [7].

Among the 30-membered crown ethers (30-crown-10 and its aromatic derivatives), dibenzo-30-crown-10 has been investigated the most thoroughly. The cavity of this crown ether can accommodate two metal cations or one cation with a larger coordination number or an incomplete coordination by the oxygen atoms of the macrocycle. According to the crystallographic data obtained by Bheda et al. [18], the structure of the tetrahydrate of this dibenzo-30-crown-10 contains two water dimers located on both sides of the macrocyclic cavity. It is interesting to note that dibenzo-30-crown-10 can coordinate two oxonium cations $[H_3O]^+$ inside one cavity (thus almost completely simulating the behavior of 18-crown-6 [19]) or the three-unit oxonium cluster $[H_7O_3]^+$ in the complexes [(2,3,19,20-Br_4-dibenzo-30-crown-10 · $H_7O_3)_2$] [$(\mu_2\text{-Br})_2Se_2Br_7$] · $1.5CH_2Cl_2$ [18] (the O···O distances in the chain are equal to 2.479 and 2.491 Å) and [$(O_2N)_2$(dibenzo-30-crown-10) · H_7O_3][$AuCl_4$] [7] (the O···O distances in the chain are equal to 2.529 and 2.436 Å).

An inference suggests itself that the *ortho*-phenylene fragments, which are fairly distant from one another, do not substantially affect the formation of OH···O(crown) bonds in the structure of dibenzo-30-crown-10. However, the introduction of two diphenyl oxide fragments into the tetrabenzo-30-crown-10 molecule has a profound effect on its complexing ability, as can be judged from the composition and structure of compounds **I** and **II**.

In these complexes, tetrabenzo-30-crown-10 is characterized by interatomic distances and bond angles that are typical of cyclic polyethers and its conformation undergoes a substantial change as compared to an *S*-shaped conformation of the initial tetrabenzo-30-crown-10 molecule [9]. The torsion angles characterizing the conformation of the macrocycle in the structure of complex **I** are presented in Table 2. In the asymmetric part of the tetrabenzo-30-crown-10 molecule, all the torsion angles about the C–O bonds correspond to the *trans* conformation, whereas the torsion angles about the C–C bonds in the oxyethylene chain correspond to the *gauche* conformation. The macrocycle adopts a saddle shape with a "many-level" arrangement of the oxygen atoms. The dihedral angle between the planes of the phenylene rings in the asymmetric part of the crown ether molecule is equal to 53.1(1)°. The interaction between the cationic complex and the anion occurs through contacts of the CH···F type, among which the shortest contacts C(12)1)···F(1) ($-x$, $1 - y$, $-z$) and H(12)···F(1) ($-x$, $1 - y$, $-z$) are equal to 3.353 and 2.55 Å, respectively.

In conclusion, we should note that, before our investigation, there were no data available in the literature on the structure of the complexes based on tetrabenzo-30-crown-10. In this paper, the encapsulation of the dioxonium cation $[H_5O_2]^+$ by one tetrabenzocrown ether molecule has been analyzed for the first time.

ACKNOWLEDGMENTS

This study was supported by the Russian Foundation for Basic Research and the Academy of Sciences of Moldova (joint project no. Mol_a 06-03-90894), as well as the National Academy of Sciences of Ukraine. The authors also acknowledge the support of the Russian Foundation for Basic Research in the payment of the license for using the Cambridge Structural Database.

REFERENCES

1. Yu. A. Zolotov and N. M. Kuz'min, *Macrocyclic Compounds in Analytical Chemistry* (Nauka, Moscow, 1993) [in Russian].
2. S. V. Nesterov, Usp. Khim. **69** (9), 840 (2000).
3. V. V. Yakshin, Koord. Khim. **28** (10), 742 (2002) [Russ. J. Coord. Chem. **28** (10), 697 (2002)].
4. M. S. Fonari, N. G. Furmanova, Wen-Jwu Wang, et al., Kristallografiya **51** (5), 856 (2006) [Crystallogr. Rep. **51** (5), 804 (2006)].
5. Ed. V. Ganin, V. O. Gelmboldt, L. V. Koroeva, et al., J. Inclusion Phenom. Macrocyclic. Chem. **56**, 345 (2006).
6. M. S. Fonari, O. A. Alekseeva, N. G. Furmanova, et al., Kristallografiya **52** (2), 271 (2007) [Crystallogr. Rep. **52** (2), 253 (2007)].
7. M. Calleja, K. Johnson, W. J. Belcher, and J. W. Steed, Inorg. Chem. **40**, 4978 (2001).
8. K. Torizuka and T. Sato, Org. Magn. Reson. **12** (4), 190 (1979).
9. G. W. Buchanan, A. Rodrigue, K. Bourque, et al., Can. J. Chem. **72**, 1218 (1994).
10. *CrysAlis: Software for Automated Data Collection and Reduction* (Oxford Diffraction, Oxford, United Kingdom, 2006).

11. G. M. Sheldrick, *SHELXS97 and SHELXL97: Programs for the Solution and Refinement of Crystal Structures* (University of Göttingen, Göttingen, Germany, 1997).
12. V. S. Sergienko, A. B. Ilyukhin, A. V. Luzikova, and M. A. Poraĭ-Koshits, Koord. Khim. **17**, 1489 (1991).
13. F. H. Allen, Acta Crystallogr., Sect. B: Struct. Sci. **58**, 380 (2002).
14. O. Reich, S. Hasche, S. Bonmann, and B. Krebs, Z. Anorg. Allg. Chem. **624**, 411 (1998).
15. R. D. Rogers, A. H. Bond, W. G. Hipple, et al., Inorg. Chem. **30**, 2671 (1991).
16. J. L. Atwood, S. G. Bott, K. D. Robinson, et al., J. Crystallogr. Spectrosc. Res. **21**, 459 (1991).
17. A. Hammerschmidt, S. Bonmann, M. Lage, and B. Krebs, Z. Anorg. Allg. Chem. **630**, 2035 (2004).
18. M. C. Bheda, J. S. Merola, W. A. Woodward, et al., J. Org. Chem. **59**, 694 (1994).
19. P. C. Junk and J. L. Atwood, J. Chem. Soc., Dalton Trans. (1972–1999), 4393 (1997).

Translated by O. Borovik-Romanova

Додаток К.

Копія статті. “Binding of fluoro-containing anions to hexaazamacrocyclic ligand: competitive interactions of fluoride and tetrafluoroborate anions with hexaprotonated [18]aneN6”

Provided for non-commercial research and education use.
Not for reproduction, distribution or commercial use.

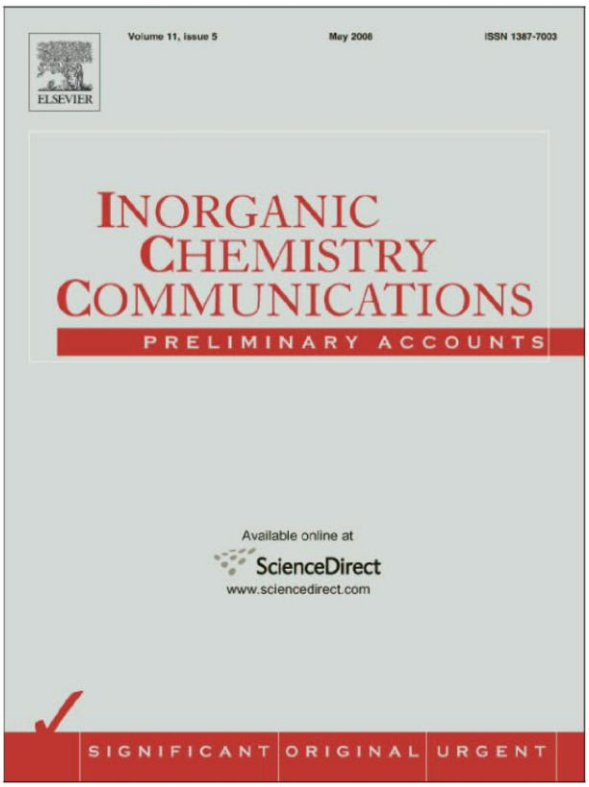

This article appeared in a journal published by Elsevier. The attached copy is furnished to the author for internal non-commercial research and education use, including for instruction at the authors institution and sharing with colleagues.

Other uses, including reproduction and distribution, or selling or licensing copies, or posting to personal, institutional or third party websites are prohibited.

In most cases authors are permitted to post their version of the article (e.g. in Word or Tex form) to their personal website or institutional repository. Authors requiring further information regarding Elsevier's archiving and manuscript policies are encouraged to visit:

http://www.elsevier.com/copyright

Author's personal copy

ELSEVIER

Available online at www.sciencedirect.com

ScienceDirect

Inorganic Chemistry Communications 11 (2008) 497–501

INORGANIC CHEMISTRY COMMUNICATIONS

www.elsevier.com/locate/inoche

Binding of fluoro-containing anions to hexaazamacrocyclic ligand: Competitive interactions of fluoride and tetrafluoroborate anions with hexaprotonated [18]aneN$_6$

Marina S. Fonari [a,*], Eduard V. Ganin [b], Vladimir O. Gelmboldt [c], Stepan S. Basok [d], Brian S. Luisi [e], Brian Moulton [e]

[a] *Institute of Applied Physics, Academy of Sciences of Moldova, Academiei Street, 5 MD-2028 Chişinău, Republic of Moldova*
[b] *Odessa State Environmental University, Lvovskaya Street, 15, 65016 Odessa, Ukraine*
[c] *Physico-Chemical Institute of Environment and Human Protection, Preobrazhenskaya Street, 3, 65082 Odessa, Ukraine*
[d] *A.V.Bogatsky Physico-Chemical Institute, Lustdorfskaya doroga, 86, 65080 Odessa, Ukraine*
[e] *Brown University Chemistry, 324 Brook Street Box H Providence, RI 02912 401-863-3773, United States*

Received 31 October 2007; accepted 26 January 2008
Available online 9 February 2008

Abstract

Reaction of hexaazamacrocycle, 1,4,7,10,13,16-hexaazacyclooctadecane (L = [18]aneN$_6$) with boron trifluoride etherate in an aqueous solution of hydrofluoric acid yields the proton-transfer complex of the composition $[H_6L(F)(BF_4)_5] \cdot 3H_2O$ (**1**). X-ray crystallographic analysis shows that the macrocyclic cation adopts an unusual conformation to accommodate the fluoride anion and to keep the tetrafluoroborate anions in a close proximity. The tetrafluoroborate anions and water molecules participate in NH···F, NH···O and OH···F hydrogen bonding responsible for the 3D supramolecular architecture.
© 2008 Elsevier B.V. All rights reserved.

Keywords: Anion binding; Hexaazamacrocycle; Fluoro-containing anions; 3D network

Anion co-ordination, or recognition, is an area that has been receiving increased attention in the past two decades [1,2] with particular emphasis on the thermodynamics of interactions between the anions and a wide variety of synthetic hosts where preorganization and cooperative effects play a critical role [3]. The hot reviews [4,5] cover the wide range of recently developed anion receptors that employ amides and thioamides, pyrroles and indoles, ureas and thioureas, ammonium, guanidinium, imidazolium, and receptors containing hydroxyl groups [4] and describe the 'supramolecular chemistry of environmentally relevant anions' [5]. In general halides, and in particular fluoride ion as the smallest spherical anion, occupy the special place within the family of inorganic anions, and as it is evident from the outlining the recent findings in this topic, the search of the effective receptors for their binding is still in progress [6].

Having a long-standing interest to the fluoro-containing anions (SiF_5^-, $[SiF_5 \cdot H_2O]^-$, SiF_6^{2-}, GeF_6^{2-}, BF_4^-) we have studied the ways of their binding by the macrocyclic molecules [7] and alongside with the others [8] have estimated the possibilities of O-, O,N-crown ethers and azamacrocycles to elicit either the neutral ($BF_3 \cdot H_2O$, $SiF_4 \cdot 2H_2O$, $GeF_4 \cdot 2H_2O$) or the aforementioned charged species from aqueous solutions. Particularly for the N,O-containing crown ethers and azamacrocycles easily protonating in the reaction medium the interaction with the anionic species has been demonstrated [9–11].

For the naked halides the host containing NH moieties has been known as good binding agent and as Mascal has

* Corresponding author. Tel.: +373 22 73 81 54; fax: +373 22 72 58 87.
E-mail addresses: fonari.xray@phys.asm.md, fonari.xray@gmail.com (M.S. Fonari).

1387-7003/$ - see front matter © 2008 Elsevier B.V. All rights reserved.
doi:10.1016/j.inoche.2008.01.028

Author's personal copy

underlined [12] the most effective H-bond donor is the $[N–H]^+$ functionality that promotes interactions with halides through a combination of electrostatic interactions and hydrogen bonding. The systematically studied by the Warden's group the hexaazamacrocycle, 1,4,7,10,13,16-hexaazacyclooctadecane ([18]aneN$_6$, L, sometimes referred to as hexacyclen or 18-azacrown-6), is easily protonated in an acidic medium and demonstrates its high efficacy both towards the biologically relevant oxoanions, such as sulfate [13], phosphate [14], oxalate, nitrate, pyrophosphate, etc. [15], and halide ions.

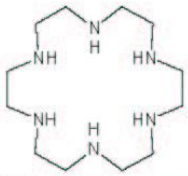

L, [18]aneN$_6$, 1,4,7,10,13,16-hexaazacyclooctadecane

Apart from the equally met in its complexes the $[H_4L]^{4+}$ tetra- [13–16] and $[H_6L]^{6+}$ hexaprotonated [17] forms, only very few occurrences of $[H_2L]^{2+}$di-, [(4,7,13,16-tetraaza-1,10-diazoniacyclooctadecane bis(picolinate) pentahydrate] and $[H_3L]^{3+}$ triprotonated forms, [(4,10,16-triaza-1,7,13-triazoniacyclooctadecane tris(bis(4-nitrophenyl)phosphate) pentahydrate] [15], were found for this macrocycle in the CSD [18]. The investigations into the halide binding properties of [12]aneN$_4$ and [18]aneN$_6$ (L) have resulted in the determination of the molecular structure of five compounds, $[H_4[12]aneN_4(Br)_4] \cdot 2H_2O$, $[H_2[12]aneN_4(I_3)_2] \cdot 2I_2 \cdot 2CH_3CN$, $[H_6L(Cl)_6] \cdot 4H_2O$, $[H_4L(Br)_4] \cdot 2H_2O$ and $[H_4L(I)_2(I_3)_2]$ with the perching arrangement of the anions in a symmetry-related mode on the both sides of the centrosymmetric macrocyclic cavity. All three investigated halides (Cl^-, Br^-, I^-) have appeared to be big enough for the nesting inside the 12- or 18-membered cavities [17b].

This contribution is the first successful attempt of [18]aneN$_6$ application to bind the fluoride anion and it also provides a rather rare example of the competitive interaction of the F^-/BF_4^- anions with the macrocyclic NH_2^+-binding sites of the [18]aneN$_6$ hexaazamacrocycle [19].

Compound **1** of the composition $[H_6L(F)(BF_4)_5] \cdot 3H_2O$ crystallises in the orthorhombic space group $C222_1$. The complex cation $[H_6L(F)]^{5+}$ resides on a two-fold axis, and the fluoride anion surrounded by all six $>NH_2^+$ macrocyclic groups is held tightly inside the cavity (Fig. 1). The N–H···F hydrogen bonds are characterized by an average N···F separation of 2.793(3) Å and N–H···F angle of 164°.

The hexaprotonated cation has a distorted geometry with six nitrogens N1, N2(x, y, $z+1$), N3 and their symmetry-related congeners equally distributed between two practically parallel planes with the mean-plane dis-

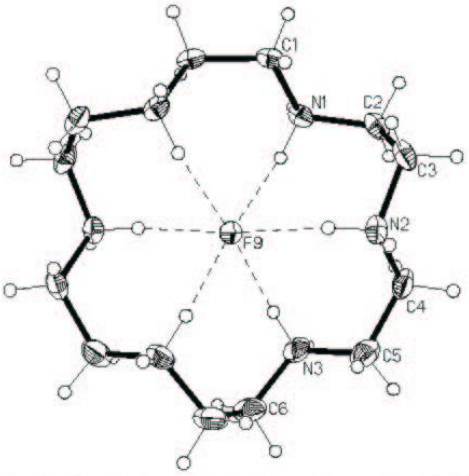

Fig. 1. ORTEP plot (which 30%) for complex cation $[H_6L(F)]^{5+}$. Hydrogen bonds shown by dotted lines are: N3···F9 2.763(3), H···F9 1.88(2) Å, N3–H···F9 angle 168(3)°; N2···F9 2.815(3), H···F9 1.94(2) Å, N2–H···F9 angle 165(2)°; N1···F9 2.798(3), H···F9 1.92(2) Å, N1–H···F9 angle 159(3)°.

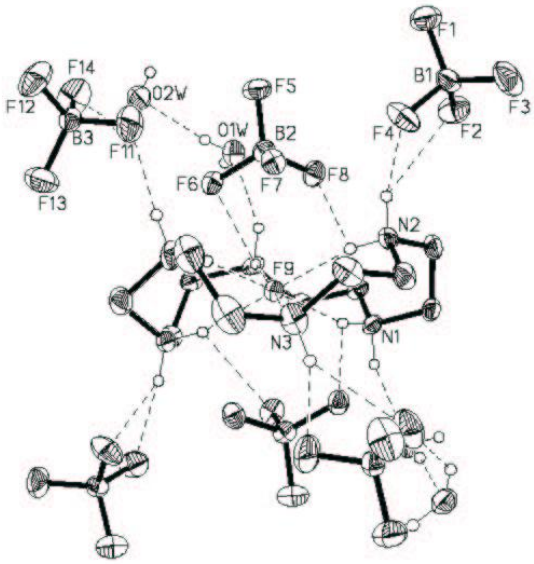

Fig. 2. ORTEP plot for the closest environment of the complex cation $[H_6L(F)]^{5+}$ in **1**. C-bound H-atoms are omitted for clarity. For the hydrogen bonds shown by dotted lines the N···F, H···F distances and NHF angle are given: N3–H···F13 ($x+1$, y, $z+1/2$) 3.156(5), 2.52(2) Å, 127(2)°; N3–H···F12 3.216(5), 2.42(2) Å, 146(3)°; N3–H2···F11 2.853(3), 2.01(2) Å, 153(3)°; N2–H···F2 3.144(3), 2.49(2) Å, 129(2)°; N2–H···F4 2.834(3), 1.98(2) Å, 155(3)°; N2–H···F8(x 1/2, $y+1/2$, $z+1$) 2.828(3), 2.38(2) Å, 111(2)°; N1–H···F8(x 1/2, y 1/2, z) 2.988(3), 2.52(3) Å, 112(2)°; N1–H···F6 (x 1/2, y 1/2, z) 2.843(3), 2.29(3) Å, 118(2)°; N1–H···O1W(x 1, y, z) 2.816(3), 1.96(2) Å, 155(3)°; O1W-H···O2W($x+1/2$, $y+1/2$, $z+1$) 2.765(3), 1.94(3) Å, 172(3)°.

Author's personal copy

tance of 1.64 Å and a fluoride anion being equally displaced (at 0.82 Å) from each of them. The survive of CSD [18] reveals that in the majority of the salt-like adducts either the *tetracationic* $[H_4L]^{4+}$ or *hexacationic* $[H_6L]^{6+}$ macrocycle commonly resides on an inversion center in the centrosymmetric space groups ($P\bar{1}$, $P2_1/c$, $P2_1/n$, $C2/m$) with the bulky anions perching in a symmetry-related mode on the both sides of the macrocyclic cavity, and only in complex $[H_6L]^{6+} \cdot 4(HSO_4)^{1-}(SO_4)^{2-} \cdot H_2O$ [13] the non-symmetric environment of the macrocycle explains its C_1 symmetry in the non-centrosymmetric space group $Pca2_1$. The conformational flexibility of the neutral ligand provides its octahedral coordination around large metals such as Co(III), Cr(III), Hg(II), Ni(II) [20], and can explain the hosting of two smaller metal ions, such as Cu(II) and Pd(II) [21]. Moreover as we have recently showed [20j] in the complexes $[Cu([18]aneN_6)]Cl_2 \cdot H_2O$ and $[Cu_2([18]aneN_6)Cl_2]Cl_2 \cdot 4H_2O$ Cu(II) centers the $[18]aneN_6$ cavity in a mononuclear and in a binuclear mode, correspondingly. In spite of the type of the metal coordination, no examples of the cycle residing on a two-fold axis have been found so far. The C_2 macrocyclic symmetry in **1** facilitates the most suitable access of all macrocyclic $>NH_2^+$ groups for the hydrogen bonding with the fluoride anion.

Of three crystallographically unique BF_4^- anions in **1** two (defined by B1 and B2 atoms) occupy general positions, and one BF_4^- anion (defined by B3 atom) resides on a two-fold axis being equally disordered. Of two crystallographically unique water molecules O1W resides on a two-fold axis, and O2W is situated in a general position. The BF_4^- anions have a geometry of a distorted tetrahedron with the B–F distances ranging from 1.374(4) to 1.407(4) Å and F–B–F angles ranging from 108.5(2) to 110.7(3)°, correspondingly. The twelve macrocyclic ammonium hydrogens are equally distributed between *endo*- and *exo*-co-ordination. The *endo*-oriented hydrogens are shared between the fluoride anion (the major component of the hydrogen bonding) and $B(2)F_4^-$ anion (*via* minor component of the hydrogen bonding, taking into account the H···F distances less than 2.6 Å and NHF angle higher than 110°), that is arranged in a chelate mode above (and below) the macrocyclic cavity. Besides these rather weak, the same anion and $[H_6L]^{6+}$ cation are predominantly held together

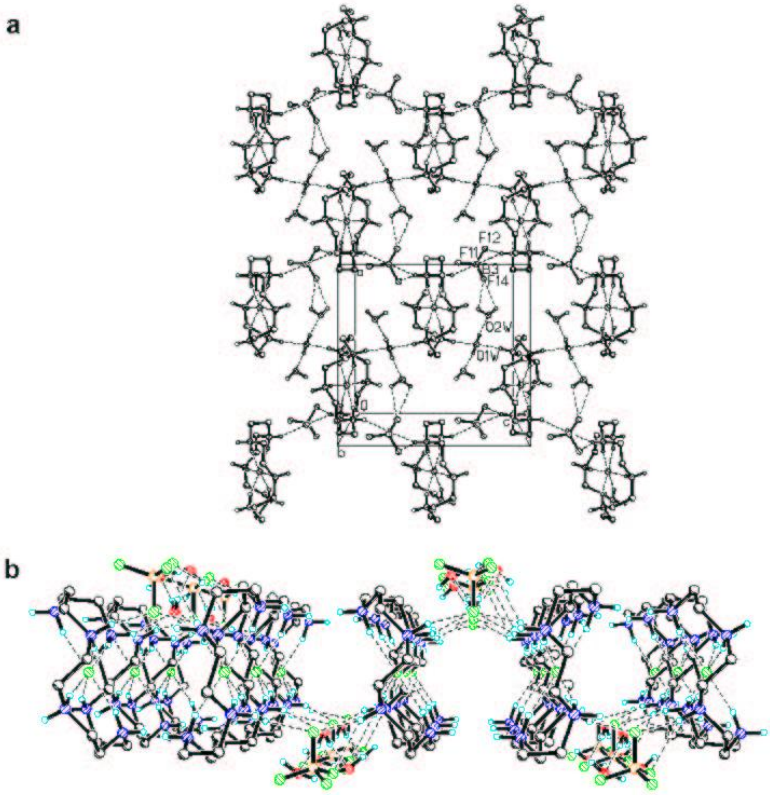

Fig. 3. Top (a) and side (b) view of the hydrogen bonding motif organisation parallel to the *ac* plane in **1**. The BF_4^- anions defined by B1 and B2 atoms, are not shown, for the disordered $B(3)F_4^-$ anion only one occupancy is shown.

Author's personal copy

via stronger NH···F interactions with the *exo*-oriented ammonium hydrogens. Furthermore, the *exo*-oriented ammonium hydrogens are involved into NH···F interactions with two other BF_4^- anions (defined by B1 and B3 atoms) situated in a 'side' mode alongside the cavity and in NH···O interactions with O1W water molecules. In general, excluding fluoride anion that centers the cavity, the nearest environment of the macrocyclic cation comprises of six BF_4^- anions and two water molecules (Fig. 2).

The 3D supramolecular network in **1** is formulated with the aid of two water molecules and BF_4^- anions. The O1W molecule, acting as a double acceptor, and the $B(3)F_4^-$ anion, *via* F11 atom, both bridge in a symmetric mode two translated along *c* direction macrocyclic cations giving rise to the layer (Fig. 3), N3···F11 separation being 2.853(3) Å, N1···O1W separation being 2.816(3) Å. In an approximately perpendicular direction, the same O1W molecule acting as a double donor, interacts with the O2W water molecule, giving rise to the O2W···O1W···O2W three-membered water cluster with the O···O separation being 2.765(3) Å, which in its turn *via* short OH···F contacts combine these 'conditional layers' into 3D network.

In conclusion, **1** represents the first example of the coordination of fluoride anion inside the cavity of the hexacationic [18]aneN_6 due to the cooperative effect of six $NH^{+}\cdots F^-$ hydrogen bonds in the anion binding, and a rather rare example of the self-organisation of multi-component system in the form of the tightly-bound mixed-anion complex.

Acknowledgement

The work is supported by MRDA(Moldova) – CRDF(US) award No. MRDA-008: BGP-III, MOC2-3063-CS-03 and joint award of Russian Foundation for Basic Research and Academy of Sciences of Moldova (Grant 06-03-90,894-Mol_a).

Appendix A. Supplementary material

CCDC 665685 contains the supplementary crystallographic data for this paper. These data can be obtained free of charge from The Cambridge Crystallographic Data Centre via www.ccdc.cam.ac.uk/data_request/cif. Supplementary data associated with this article can be found, in the online version, at doi:10.1016/j.inoche.2008.01.028.

References

[1] J.M. Lehn, Supramolecular Chemistry, VCH, Weinheim, 1995.
[2] A. Bianchi, K. Bowman-James, E. Garcia-Espana (Eds.), Supramolecular Chemistry of Anions, Wiley-VCH, New York, 1997.
[3] G.A. Jeffrey, W. Saenger, Hydrogen Bonding in Biological Structures, Springer, Berlin, 1991.
[4] P.A. Gale, S.E. García-Garrido, J. Garric, Chem. Soc. Rev. 37 (2008) 151.
[5] B.A. Moyer, L.H. Delmau, C.J. Fowler, A. Ruas, D.A. Bostick, J.L. Sessler, E. Katayev, G.D. Pantos, J.M. Llinares, M.A. Hossain, S.O. Kang, K. Bowman-James, in: R. Eldik, K. Bowman-James (Eds.), Advanced Inorganic Chemistry, Academic Press, 59, 2006, p. 175.
[6] (a) T. Clifford, S. Mason, J.M. Llinares, K. Bowman-James, J. Am. Chem. Soc. 122 (2000) 1814;
(b) J.A. Aguilar, T. Clifford, A. Danby, J.M. Llinares, S. Mason, E. Garcia-Espana, K. Bowman-James, Supramol. Chem. 13 (2001) 405;
(c) M.A. Hossain, J.M. Llinares, C.A. Miller, L. Seib, K. Bowman-James, Chem. Commun. (2000) 2269;
(d) J.L. Sessler, H. Maeda, T. Mizuno, V.M. Lynch, H. Furuta, Chem. Commun. (2002) 862;
(e) S. Camiolo, P.A. Gale, Chem. Commun. (2000) 1129;
(f) B. Zhang, P. Cai, C. Duan, R. Miao, L. Zhu, T. Niitsu, H. Inoue, Chem. Commun. (2004) 2206;
(g) E.R. Libra, M.J. Scott, Chem. Commun. (2006) 1485;
(h) C. Bazzicalupi, A. Bencini, A. Bianchi, A. Danesi, C. Giorgi, M.A.M. Lorente, B. Valtancoli, New J. Chem. 30 (2006) 959;
(i) M.A. Hossain, J.M. Llinares, N.W. Alcock, D. Powell, K. Bowman-James, J. Supramol. Chem. 2 (2002) 143;
(j) K. Ghosh, S. Adhikaria, Tetrahedron. Lett. 47 (2006) 8165;
(k) S.H. Lee, H.J. Kim, Y.O. Lee, J. Vicens, J.S. Kim, Tetrahedron Lett. 47 (2006) 4373;
(l) S. Camiolo, S.J. Coles, P.A. Gale, M.B. Hursthouse, J.L. Sessler, Acta Crystallogr. E57 (2001) o816.
[7] V.O. Gelmboldt, E.V. Ganin, M.S. Fonari, Yu.A. Simonov, L.V. Koroeva, A.A. Ennan, S.S. Basok, S. Shova, H. Kählig, V.B. Arion, B.K. Keppler, Dalton Trans. 27 (2007) 2915, and the references cited herein.
[8] (a) Y.A. Simonov, V.O. Gelmboldt, E.V. Ganin, A.A. Dvorkin, M.S. Fonari, L.V. Ostapchuk, J. Lipkowski, Koord. Khim. (Russ. Coord. Chem.) 21 (1995) 760;
(b) H. Feinberg, I. Columbus, S. Cohen, M. Rabinovitz, H. Selig, G. Shoham, Polyhedron 12 (1993) 2913;
(c) S.G. Bott, A. Alvanipour, J.L. Atwood, J. Inclusion Phenom. Mol. Recog. Chem. 10 (1991) 153;
(d) M.S. Fonari, Yu.A. Simonov, M.D. Mazus, E.V. Ganin, V.O. Gelmboldt, Kristallografiya (Russ. Crystallogr. Rep.) 42 (1997) 858.
[9] V.O. Gelmboldt, E.V. Ganin, Yu.A. Simonov, J. Lipkowski, M.S. Fonari, V.Ch. Kravtsov, Zh. Neorg. Khim. (Russ. J. Inorg. Chem.) 40 (1995) 594.
[10] S.S. Basok, L. Croitoru, M.S. Fonari, E.V. Ganin, V.O. Gelmboldt, J. Lipkowski, Y.A. Simonov, Acta Crystallogr. C 61 (2005) o188.
[11] (a) M.S. Fonari, Yu.A. Simonov, M.D. Mazus, E.V. Ganin, V.O. Gelmboldt, Zh. Strukt. Khim. (Russ. J. Struct. Chem.) 40 (1999) 1016;
(b) J. Lipkowski, Yu.A. Simonov, M.S. Fonari, E.V. Ganin, V.O. Gelmboldt, Yu.A. Popkov, Zh. Strukt. Khim. (Russ. J. Struct. Chem.) 42 (2001) 997.
[12] M. Mascal, J. Chem. Soc. Perkin Trans. 2 (1999) 1997.
[13] A.C. Warden, M. Warren, M.T.W. Hearn, L. Spiccia, New J. Chem. (Nouv. J. Chim.) 28 (2004) 1301.
[14] A.C. Warden, M. Warren, M.T.W. Hearn, L. Spiccia, Inorg. Chem. 43 (2004) 6936.
[15] A.C. Warden, M. Warren, M.T.W. Hearn, L. Spiccia, Cryst. Growth Des. 5 (2005) 713.
[16] (a) J. Cullinane, R.I. Gelb, T.N. Margulis, L.J. Zompa, J. Am. Chem. Soc. 104 (1982) 3048;
(b) P. Thuery, N. Keller, M. Lance, J.-D. Vigner, M. Nierlich, Acta Crystallogr. C 51 (1995) 1407;
(c) C. Bazzicalupi, A. Bencini, A. Bianchi, M. Cecchi, B. Escuder, V. Fusi, E. Garcia-Espana, C. Giorgi, S.V. Luis, G. Maccagni, V. Marcelino, P. Paoletti, B. Valtancoli, J. Am. Chem. Soc. 121 (1999) 6807.
[17] (a) T.N. Margulis, L.J. Zompa, J. Heterocycl. Chem. 20 (1983) 975;
(b) A.C. Warden, M. Warren, M.T.W. Hearn, L. Spiccia, New J. Chem. (Nouv. J. Chim.) 28 (2004) 1160;
(c) A.C. Warden, M. Warren, M.T.W. Hearn, L. Spiccia, Inorg. Chem. 43 (2004) 6936;
(d) T.N. Margulis, L.J. Zompa, Acta Crystallogr. B 37 (1981) 1426.

Author's personal copy

[18] F.N. Allen, Acta Crystallogr. B 58 (2002) 380.

[19] Synthesis $[H_6L(F)(BF_4)_5] \cdot 3H_2O$ (1). All reagents were purchased from commercial suppliers and used as supplied. L (77 mg, 0.3 mmol) dissolved in ethanol (5 ml) was added to the boron trifluoride etherate, $BF_3 \cdot O(C_2H_5)_2$ (0.8 ml) in 1 ml of 45% HF. The solution was left to evaporate in an open flask and after several days colorless transparent crystals were precipitated. Yield is close to the quantitative one. M.p. > **300** °C (dec.). Microanalysis: Calcd for $C_{12}H_{42}B_5F_{21}N_6O_3$: C, 18.68; H, 5.49; B, 7.01; F, 51.71; N, 10.89. Found, % C, 18.65; H, 5.53; B, 6.97; F, 51.79; N, 10.94. Crystal data for 1: $C_{12}H_{42}B_5F_{21}N_6O_3$, $M_r = 771.57$, orthorhombic, $C222_1$, $T = 90(2)$ K, $\lambda = 0.71073$ Å, $a = 11.695(2)$, $b = 20.540(4)$, $c = 12.439(3)$ Å, $U = 2988.0(10)$ Å^3, $Z = 4$, $D_c = 1.715$ g cm^{-3}, $\mu = 0.200$ mm^{-1}, θ range 1.98–26.00°, GOF = 1.018, $R_1 = 0.0393$, $wR_2 = 0.0882$ for 2607 reflections with $I > 2\sigma(I)$, $R_1 = 0.0470$, $wR_2 = 0.0923$ for all 2943 unique reflections. X-ray data were collected on a Bruker SMART-APEX CCD diffractometer by ω and ϕ-scan mode at 90 K using graphite-monochromated Mo-$K\alpha$ radiation. There was no intensity decay. Structure solution was performed by direct methods (SHELXS-97) and refined by full-matrix least-squares methods on F^2 (SHELXL-97) (Sheldrick, G.M. SHELXS and SHELXL97 Programs for structure refinement and solution, Göttingen, Germany, 1997). Lorentz and polarization corrections were applied for diffracted reflections. In addition, the data were corrected for absorption using SADABS (Sheldrick, G.M., SADABS, Program for the Empirical Absorption Correction of Area Detector Data, University of Göttingen, Germany, 1996). Non–hydrogen atoms were refined anisotropically. H-atoms attached to carbons were included in idealized positions in a riding model with isotropic temperature factors (1.2 times the parent carbon atom temperature factor), whereas those on N and O(water) atoms were found from difference Fourier maps and refined isotropically. Absolute configuration was not defined.

[20] (a) D.J. Royer, G.J. Grant, D.G. VanDerveer, M.J. Castillo, Inorg. Chem. 21 (1982) 1902;
(b) Y. Yoshikawa, K. Toriumi, T. Ito, H. Yamatera, Bull. Chem. Soc. Jpn. 55 (1982) 1422;
(c) M. Morooka, S. Ohba, Acta Crystallogr. B 48 (1992) 459;
(d) M.A.A.F. De, C.T. Carrondo, V. Felix, M.T. Duarte, M.A. Santos, Polyhedron 12 (1993) 931;
(e) X.-He Bu, S.-L. Lu, R.-H. Zhang, H.-G. Wang, X.-K. Yao, Polyhedron 16 (1997) 3247;
(f) M. Nierlich, J.-M. Sabattie, N. Keller, M. Lance, J.-D. Vigner, Acta Crystallogr. C 50 (1994) 52;
(g) R.E. Marsh, Acta Crystallogr. B 60 (2004) 252;
(h) R.-Y. Wang, J.-J. Zhao, T.-Z. Jin, G.-X. Xu, Z.-Y. Zhou, X.-Ge. Zhou, Polyhedron 17 (1998) 43;
(i) S. Chandrasekhar, D.G. Fortier, A. McAuley, Inorg. Chem. 32 (1993) 1424;
(j) L. Ballester, A. Gutierrez, M.F. Perpinan, A.E. Sanchez, M. Fonari, M. Gdaniec, Inorg. Chem. 46 (2007) 3946.

[21] (a) J.E. Barker, Yu. Liu, N.D. Martin, Tong Ren, J. Am. Chem. Soc. 125 (2003) 13332;
(b) J.E. Barker, Yu. Liu, G.T. Yee, W.-Z. Chen, G. Wang, V.M. Rivera, T. Ren, Inorg. Chem. 45 (2006) 7973;
(c) G. Yang, R. Miao, Y. Li, J. Hong, C. Zhao, Z. Guo, L. Zhu, Dalton Trans. (2005) 1613;
(d) A. Bencini, A. Bianchi, P. Dapporto, E. Garcia-Espana, M. Micheloni, P. Paoletti, P. Paoli, Chem. Commun. (1990) 1382;
(e) A. Bencini, A. Bianchi, M. Micheloni, P. Paoletti, P. Dapporto, P. Paoli, E. Garcia-Espana, J. Inclusion Phenom. Mol. Recog. Chem. 12 (1992) 291;
(f) A. McAuley, T.W. Whitcombe, M.J. Zaworotko, Inorg. Chem. 30 (1991) 3513.

Додаток Л.

Копія статті. “From clusters to coordination polymers in the crown-templated system ZrO_2/HfO_2 (Nb_2O_5/Ta_2O_5) – HF – H_2O – azacrown ether Rarely Observed Metal Oxide Fluoride Anions $[(TaF_5)_2O]^{2-}$ and $[(H_2O)NbF_4O NbF_5]^{2-}$ in the Complexes with Azacrown Ethers”

Provided for non-commercial research and education use.
Not for reproduction, distribution or commercial use.

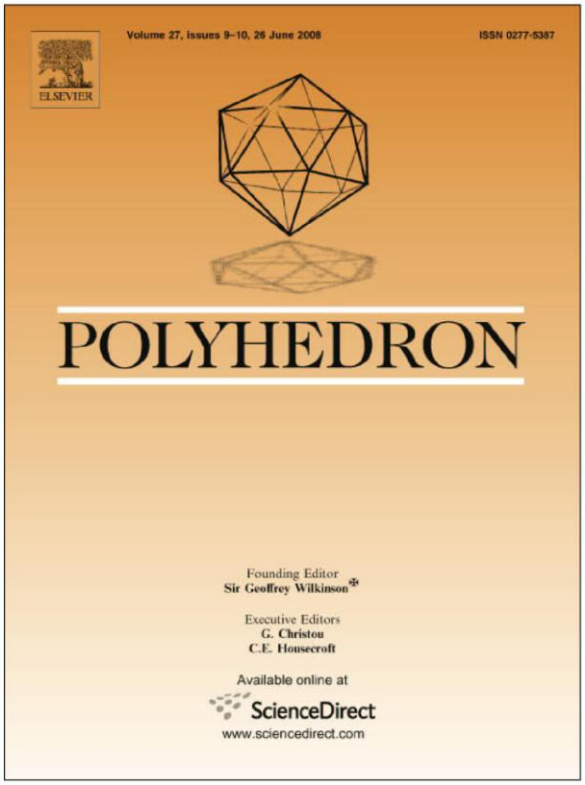

This article appeared in a journal published by Elsevier. The attached copy is furnished to the author for internal non-commercial research and education use, including for instruction at the authors institution and sharing with colleagues.

Other uses, including reproduction and distribution, or selling or licensing copies, or posting to personal, institutional or third party websites are prohibited.

In most cases authors are permitted to post their version of the article (e.g. in Word or Tex form) to their personal website or institutional repository. Authors requiring further information regarding Elsevier's archiving and manuscript policies are encouraged to visit:

http://www.elsevier.com/copyright

Author's personal copy

Polyhedron 27 (2008) 2049–2058

Contents lists available at ScienceDirect

Polyhedron

journal homepage: www.elsevier.com/locate/poly

Crown-templated assembling of the inorganic binuclear fluoro-containing anions in the system ZrO_2/HfO_2 (Nb_2O_5/Ta_2O_5)–HF–H_2O-azacrown ether

Marina S. Fonari [a,*], Victor Ch. Kravtsov [a], Yurii A. Simonov [a], Stepan S. Basok [b], Eduard V. Ganin [c,d], Vladimir O. Gelmboldt [d], Kinga Suwinska [e], Janusz Lipkowski [e], Olga A. Alekseeva [f], Nina G. Furmanova [f]

[a] Institute of Applied Physics, Academy of Sciences of R. Moldova, Academiei Str., 5 MD-2028 Chisinau, Republic of Moldova
[b] A.V. Bogatsky Physico-Chemical Institute, National Academy of Sciences of Ukraine, Lustdorfskaya Doroga 86, 650080 Odessa, Ukraine
[c] Odessa State Environmental University, Odessa, Ukraine
[d] Physico-Chemical Institute of Environment and Human Protection, Odessa, Ukraine
[e] Institute of Physical Chemistry Polish Academy of Sciences, Warszawa, Poland
[f] Institute of Crystallography RAS, Moscow, Russia

ARTICLE INFO

Article history:
Received 29 December 2007
Accepted 20 March 2008
Available online 9 May 2008

Keywords:
Rarely observed metal oxide fluoride anions
Aza crown ethers
Hydrogen bond
Crystal structure

ABSTRACT

The interaction of ZrO_2/HfO_2 or Nb_2O_5/Ta_2O_5 with an aqueous solution of hydrofluoric acid in the presence of aza-crown ether resulted in novel organically templated metal oxyfluorides of the compositions $[(HA15C5)_2][Ta_2F_{10}O]$ (**1**), $[(HA18C6 \cdot H_2O)(A18C6 \cdot H_2O)][(H_2O)Nb_2F_9O] \cdot H_2O$ (**2**), $[(HA18C6 \cdot H_2O)(M_2F_{10} \cdot 2H_2O) \cdot (H_3O) \cdot H_2O]$ (**3**, **4**) and $[(H_2DA18C6)(M_2F_{10} \cdot 2H_2O) \cdot 2H_2O]$ (**5**, **6**) (M = Zr, Hf, A15C5 = aza-15-crown-5, A18C6 = aza-18-crown-6, DA18C6 = diaza-18-crown-6). Complexes **1**–**6** were identified by single crystal X-ray diffraction. In **1**, the negative charge of the $[(TaF_5)_2O]^{2-}$ centrosymmetric dianion is balanced by two azonia-15C5 cations, while in **2** the charge of asymmetric $[(H_2O)NbF_4ONbF_5]^-$ monoanion is compensated by azonia-18C6 cation. The crystal of **2** revealed an extensive hydrogen bonding between the anions, protonated and neutral macrocycles and water molecules that combine the components into 2D sheet. Complexes **3**–**4** and **5**–**6** are isostructural in pairs; in all of them the rigid 2D inorganic motif is formed through the association of the $[(M_2F_{10} \cdot 2H_2O)]^{2-}$ anions by means of OH···F hydrogen bonds. The similar 3D supramolecular architecture in **3**–**6** represents an alternation of the negatively-charged inorganic sheets and the columns of $(HA18C6)^+$ or $(DA18C6)^{2+}$ organic cations glued by oxonium cations or water molecules.

© 2008 Elsevier Ltd. All rights reserved.

1. Introduction

The successful efforts undertaken by Atwood to stabilize the Lewis acidic species by the complexation with crown ethers [1], initiated our long-standing interest to the fluoro-containing Lewis acids (BF_3, SiF_4, GeF_4, SbF_3, etc.) and the products of their transformations in aqueous solutions in the presence of crown ether macrocyclic molecules as organic-templating species. Following to Atwood and Selig [1,2], we have discovered the possibility to retain the rather unstable neutral adducts of the composition $BF_3 \cdot H_2O$ [3] and $SiF_4 \cdot 2H_2O$ [4] in the complexes with *classic all O-containing crown ethers* (18-crown-6, *cis–anti–cis*-dicyclohexyl-18-crown-6) stabilised by the OH···O hydrogen bonding between the intermediate water molecule and crown oxygen atoms. In the case of SbF_3 interaction with the macrocyclic molecule (18C6, B18C6, *cis*-isomers of DCH18C6, thia-[1.5]DB18C6) [5], the electronic effects are crucial, and the anhydrous adducts of the 1:1 ratio are held together through the interaction of the antimony atom lone pair with O-collective electronic system.

The interaction of the fluorosilicic acid (H_2SiF_6, FSA) solution with aza-containing macrocycles has resulted in ionic crystalline complexes of the compositions $(HA18C6 \cdot H_2O)$ $[SiF_5(H_2O)] \cdot H_2O$, $(H_2DA18C6)[SiF_5(H_2O)]_2$, $(HA12C4)_2[SiF_5(H_2O)]_2 \cdot 3H_2O$ [6], (A18C6, aza-18-crown-6; DA18C6, diaza-18-crown-6; A12C4, aza-12-crown-4), which have represented the structural evidence for the existence in the solid state of the $[SiF_5(H_2O)]^-$ anion, the labile product of the hydrolytic transformations of $[SiF_6]^{2-}$ anion. So far these three complexes remain the only known examples of the crystallographically proven existence of the $[SiF_5(H_2O)]^-$ anion in the solid state. The major role in stabilisation of the asymmetric and labile $[SiF_5(H_2O)]^-$ species plays the multiple H-bonding interactions between 'organic' and 'inorganic' components.

The problem of concentration and extraction of such elements as Zr, Hf, Nb, Ta encouraged us to apply the macrocyclic molecules

* Corresponding author. Tel.: +373 22 73 81 54; fax: +373 22 72 58 87.
E-mail addresses: fonari.xray@phys.asm.md (M.S. Fonari), edganin@yahoo.com (E.V. Ganin), eksvar@ukr.net (V.O. Gelmboldt), klatrat@ichf.edu.pl (K. Suwinska), furm@ns.crys.ras.ru (N.G. Furmanova)

0277-5387/$ - see front matter © 2008 Elsevier Ltd. All rights reserved.
doi:10.1016/j.poly.2008.03.023

Author's personal copy

with the aim to obtain new supramolecular complexes involving these elements in the form of neutral or anionic fluoro-containing species and crown ethers. In the previously reported system ZrO_2/HfO_2–HF–H_2O–18C6, the crystals suitable for X-ray diffraction have been obtained only for Hf, and the crystalline complex of the composition $[(18C6)(H_3O)_2(Hf_2O_{10}\cdot 2H_2O)\cdot 4H_2O]$ has been studied [7]. Although the *neutral* 18C6 molecule has been used in synthesis, the resulting supramolecular complex combines both neutral and ionic species. The $(Hf_2O_{10}\cdot 2H_2O)^{2-}$ anions form inorganic 2D sheet through the OH···F hydrogen bonds and is adjusted to the 18C6 molecules *via* oxonium clusters of the composition $(H_7O_3)^+$. The 3D supramolecular architecture represents an alternation of the inorganic sheets and columns of H-bonded crown-ethers and water molecules.

Our recent study of the systems Nb_2O_5/Ta_2O_5 (NbF_5/TaF_5)–HF–H_2O–CE for a wide range of oxygen-containing crown ethers showed that in the crystalline ionic complexes of the compositions $[CE\cdot H_3O][MF_6]$ for 18C6, B18C6, *cis–syn–cis*-DCH18C6 and diphenyl-20C6, $[(CE)_2\cdot H_7O_3][MF_6]$ for [1.5]DB18C6 [6], $[CE\cdot H_5O_2][MF_6]$ for 15C5 and tetrabenzo-30C10, $[(CE)_2\cdot H_5O_2][(CE)_2\cdot H_3O][MF_6]_2$ for B15C5 and $[(CE)_2\cdot H_3O][MF_6]$ for B12C4, the negative charge of NbF_6^-/TaF_6^- anions is balanced by the oxonium ions [8]. Thus, the general feature for these complexes is a retention of metal-containing *anionic species* by neutral O-containing crown molecules due to the acidity of the reaction medium introduced by the presence of hydrofluoric acid. We also showed that in spite of either the MF_5 pentafluorides or the corresponding M_2O_5 oxides were used as starting materials, all-O-containing CEs extract NbF_6^-/TaF_6^- hexafluoroniobate/hexafluorotantalate anions in the form of crystalline complexes.

Keeping in mind the disclosed ability of aza-containing crown ethers to extract the hydrolytically unstable species from FSA solutions [7], we have used the aza-containing crown ethers, A15C5, A18C6 and DA18C6 with the aim to extract the products of interaction of ZrO_2/HfO_2 and Nb_2O_5/Ta_2O_5 with an aqueous solution of hydrofluoric acid. Six new complexes, $[(HA15C5)_2][Ta_2F_{10}O]$ (**1**), $[(HA18C6\cdot H_2O)(A18C6\cdot H_2O)][(H_2O)\ Nb_2F_9O]\cdot H_2O$ (**2**), $[(HA18C6\cdot H_2O)(Zr_2F_{10}\cdot 2H_2O)\cdot(H_3O)\cdot H_2O]$ (**3**), $[(HA18C6\cdot H_2O)(Hf_2F_{10}\cdot 2H_2O)\cdot(H_3O)\cdot H_2O]$ (**4**), $[(H_2DA18C6)(Zr_2F_{10}\cdot 2H_2O)\cdot 2H_2O]$ (**5**), $[(H_2DA18C6)(Hf_2F_{10}\cdot 2H_2O)\cdot 2H_2O]$ (**6**) were obtained and studied by single crystal X-ray diffraction.

2. Experimental

2.1. Materials and apparatus

Caution! Hydrofluoric acid is toxic and corrosive, and must be handled with extreme caution and the appropriate protective gear! If contact with the liquid or vapor occurs, proper treatment procedures should immediately be followed [9]. Crown ethers were purchased from ACROS, ZrO_2, HfO_2, Nb_2O_5 and Ta_2O_5 were purchased from Aldrich and were used without further purification. Complexes **1–6** were obtained by an interaction of the corresponding oxides with the 40% aqueous HF followed by treatment of the resulting solution with the corresponding crown ether and were analyzed for C, H and N in a Perkin Elmer 240 °C instrument.

2.2. Synthesis

2.2.1. $[(HA15C5)_2][Ta_2F_{10}O]$ (1)

Crystals of complex **1** separated in a quantitative yield, and are colorless transparent prisms, soluble in methanol, ethanol; m.p. 152–153 °C. *Anal.* Calc. for $C_{20}H_{44}F_{10}N_2O_9Ta_2$: C, 23.82; H, 4.40; F, 18.84; N, 2.78. Found: C, 23.80; H, 4.43; F, 18.86; N, 2.81%.

2.2.2. $[(HA18C6\cdot H_2O)(A18C6\cdot H_2O)][(H_2O)Nb_2F_9O]\cdot H_2O$ (2)

Crystals of complex **2** separated in a quantitative yield, and are colorless transparent prisms, soluble in methanol, ethanol; m.p. 115–117 °C. *Anal.* Calc. for $C_{24}H_{59}F_9N_2Nb_2O_{15}$: C, 29.64; H, 6.11; F, 17.58; N, 2.88. Found: C, 29.69; H, 6.13; F, 17.63; N, 2.84%.

2.2.3. $[(HA18C6\cdot H_2O)(Zr_2F_{10}\cdot 2H_2O)\cdot(H_3O)\cdot H_2O]$ (3)

Crystals of complex **3** separated in an approximately quantitative yield, and are colorless transparent prisms, soluble in methanol; m.p. ≫250 °C. *Anal.* Calc. for $C_{12}H_{37}F_{10}NO_{10}Zr_2$: C, 19.80; H, 5.12; F, 26.10; N, 1.92. Found: C, 19.7; H, 5.15; F, 26.14; N, 1.90%.

2.2.4. $[(HA18C6\cdot H_2O)(Hf_2F_{10}\cdot 2H_2O)\cdot(H_3O)\cdot H_2O]$ (4)

Crystals of complex **4** separated in an approximately quantitative yield, and are colorless transparent prisms, soluble in methanol; m.p. ≫250 °C. *Anal.* Calc. for $C_{12}H_{37}F_{10}Hf_2NO_{10}$: C, 15.97; H, 4.13; F, 21.05; N, 1.55. Found: C, 15.94; H, 4.15; F, 21.08; N, 1.57%.

Table 1
Crystal data and structure refinement parameters for complexes 1–6

	1	2	3	4	5	6
Composition	$C_{20}H_{44}F_{10}N_2O_9Ta_2$	$C_{24}H_{59}F_9N_2Nb_2O_{15}$	$C_{12}H_{37}F_{10}NO_{10}Zr_2$	$C_{12}H_{37}F_{10}Hf_2NO_{10}$	$C_{12}H_{36}F_{10}N_2O_8Zr_2$	$C_{12}H_{36}F_{10}Hf_2N_2O_8$
CCDC number	671858	671860	671862	671859	671863	671861
Formula weight	1008.47	972.55	727.87	907.38	708.87	883.41
Crystal system	triclinic	orthorhombic	orthorhombic	orthorhombic	triclinic	triclinic
Space group	$P\bar{1}$	$Pna2_1$	$Pca2_1$	$Pca2_1$	$P\bar{1}$	$P\bar{1}$
a (Å)	8.995(4)	19.734(4)	15.651(3)	15.637(3)	8.9617(6)	8.915(2)
b (Å)	9.021(3)	10.303(2)	11.487(2)	11.495(2)	10.5137(7)	10.530(2)
c (Å)	11.965(5)	19.618(4)	15.923(3)	15.814(3)	14.3368(11)	14.295(3)
α (°)	86.12(3)	90.0	90.0	90.0	108.059(3)	107.94(2)
β (°)	69.26(2)	90.0	90.0	90.0	98.930(3)	98.70(2)
γ (°)	66.50(2)	90.0	90.0	90.0	96.118(5)	96.18(2)
V (Å³)	829.6(5)	3988.7(14)	2862.7(9)	2842.5(10)	1251.38(15)	1244.9 (2)
Z	1	4	4	4	2	2
D_{calc} (Mg/m³)	2.019	1.620	1.689	2.109	1.881	2.357
μ (mm⁻¹)	6.690	0.678	0.833	7.405	0.945	8.446
F(000)	486	2000	1464	1720	712	840
Reflections collected/unique	10006/2927	37300/7821	5377/5377	3212/3212	5441/5441	5701/5701
Reflections with $I > 2\sigma(I)$	2499	7014	3386	2358	3861	5221
Goodness-of-fit	1.001	1.019	1.002	1.000	1.003	1.004
R_1, wR_2 [$I > 2\sigma(I)$]	0.0223, 0.0337	0.0329, 0.0760	0.0397, 0.0934	0.0395, 0.1024	0.0853, 0.2212	0.0565, 0.1664

Author's personal copy

Table 2
Selected bond distances (Å) and angles (°) for complexes **1–6**

Complex **1**			
Ta(1)–F(2)	1.847(3)	Ta(1)–O(1M)	1.8869(7)
Ta(1)–F(4)	1.861(3)	Ta(1)–F(3)	1.898(2)
Ta(1)–F(1)	1.865(3)	Ta(1)–F(5)	1.908(2)
F(2)–Ta(1)–F(4)	175.90(12)	F(1)–Ta(1)–F(3)	174.17(10)
F(2)–Ta(1)–F(1)	89.59(15)	O(1M)–Ta(1)–F(3)	91.72(7)
F(4)–Ta(1)–F(1)	92.02(16)	F(2)–Ta(1)–F(5)	87.56(12)
F(2)–Ta(1)–O(1M)	93.76(9)	F(4)–Ta(1)–F(5)	88.71(12)
F(4)–Ta(1)–O(1M)	89.90(9)	F(1)–Ta(1)–F(5)	88.66(12)
F(1)–Ta(1)–O(1M)	93.59(9)	O(1M)–Ta(1)–F(5)	177.40(9)
F(2)–Ta(1)–F(3)	87.64(12)	F(3)–Ta(1)–F(5)	86.09(11)
F(4)–Ta(1)–F(3)	90.41(13)		
O(1)–C(1)–C(2)–N(1)	44.6(5)	C(6)–O(3)–C(7)–C(8)	177.1(4)
C(1)–C(2)–N(1)–C(3)	61.8(5)	O(3)–C(7)–C(8)–O(4)	66.1(5)
C(2)–N(1)–C(3)–C(4)	178.6(3)	C(7)–C(8)–O(4)–C(9)	179.2(4)
N(1)–C(3)–C(4)–O(2)	59.2(4)	C(8)–O(4)–C(9)–C(10)	170.1(4)
C(3)–C(4)–O(2)–C(5)	146.1(4)	O(4)–C(9)–C(10)–O(1)	64.0(5)
C(4)–O(2)–C(5)–C(6)	93.4(5)	C(9)–C(10)–O(1)–C(1)	136.5(4)
O(2)–C(5)–C(6)–O(3)	63.1(5)	C(10)–O(1)–C(1)–C(2)	77.8(5)
C(5)–C(6)–O(3)–C(7)	171.0(4)		
Complex **2**			
Nb(1)–O(1M)	1.734(3)	Nb(2)–F(9)	1.710(3)
Nb(1)–F(1)	1.884(3)	Nb(2)–F(5)	1.890(2)
Nb(1)–F(2)	1.911(2)	Nb(2)–F(6)	1.919(2)
Nb(1)–F(4)	1.929(2)	Nb(2)–F(7)	1.919(3)
Nb(1)–F(3)	1.930(3)	Nb(2)–F(8)	1.958(2)
Nb(1)–O(1W)	2.311(3)	Nb(2)–O(1M)	2.344(3)
O(1M)–Nb(1)–F(1)	100.03(16)	F(9)–Nb(2)–F(5)	99.02(17)
O(1M)–Nb(1)–F(2)	99.66(12)	F(9)–Nb(2)–F(6)	98.80(13)
F(1)–Nb(1)–F(2)	90.31(11)	F(5)–Nb(2)–F(6)	91.66(13)
O(1M)–Nb(1)–F(4)	97.92(11)	F(9)–Nb(2)–F(7)	98.95(17)
F(1)–Nb(1)–F(4)	90.22(14)	F(5)–Nb(2)–F(7)	161.60(12)
F(2)–Nb(1)–F(4)	162.03(11)	F(6)–Nb(2)–F(7)	89.45(15)
O(1M)–Nb(1)–F(3)	98.99(16)	F(9)–Nb(2)–F(8)	96.77(13)
F(1)–Nb(1)–F(3)	160.96(11)	F(5)–Nb(2)–F(8)	88.28(14)
F(2)–Nb(1)–F(3)	87.22(13)	F(6)–Nb(2)–F(8)	164.24(10)
F(4)–Nb(1)–F(3)	86.44(15)	F(7)–Nb(2)–F(8)	85.74(15)
O(1M)–Nb(1)–O(1W)	176.82(13)	F(9)–Nb(2)–O(1M)	179.04(14)
F(1)–Nb(1)–O(1W)	79.47(12)	F(5)–Nb(2)–O(1M)	80.93(13)
F(2)–Nb(1)–O(1W)	83.49(13)	F(6)–Nb(2)–O(1M)	82.16(10)
F(4)–Nb(1)–O(1W)	78.96(12)	F(7)–Nb(2)–O(1M)	81.03(13)
F(3)–Nb(1)–O(1W)	81.50(13)	F(8)–Nb(2)–O(1M)	82.28(11)
	A	B	
O(1)–C(1)–C(2)–N(1)	67.9(5)	41.9(11)	
C(1)–C(2)–N(1)–C(3)	176.4(4)	175.1(7)	
C(2)–N(1)–C(3)–C(4)	174.6(4)	171.3(7)	
N(1)–C(3)–C(4)–O(2)	67.8(5)	49.7(10)	
C(3)–C(4)–O(2)–C(5)	176.3(4)	102.7(6)	
C(4)–O(2)–C(5)–C(6)	177.8(4)	176.6(5)	
O(2)–C(5)–C(6)–O(3)	64.2(5)	74.0(5)	
C(5)–C(6)–O(3)–C(7)	178.9(4)	175.3(4)	
C(6)–O(3)–C(7)–C(8)	178.3(4)	166.3(3)	
O(3)–C(7)–C(8)–O(4)	64.7(5)	70.1(4)	
C(7)–C(8)–O(4)–C(9)	178.6(4)	166.1(3)	
C(8)–O(4)–C(9)–C(10)	179.5(3)	176.9(3)	
O(4)–C(9)–C(10)–O(5)	67.3(4)	69.9(4)	
C(9)–C(10)–O(5)–C(11)	179.9(3)	174.5(4)	
C(10)–O(5)–C(11)–C(12)	179.6(4)	174.4(4)	
O(5)–C(11)–C(12)–O(1)	66.4(5)	69.7(5)	
C(11)–C(12)–O(1)–C(1)	175.2(3)	178.5(5)	
C(12)–O(1)–C(1)–C(2)	178.2(4)	114.4(7)	
Complex **3**			
Zr(1)–F(4)	1.959(7)	Zr(2)–F(6)	1.984(6)
Zr(1)–F(2)	1.968(5)	Zr(2)–F(8)	1.982(6)
Zr(1)–F(1)	1.999(6)	Zr(2)–F(7)	1.994(5)
Zr(1)–F(3)	2.033(7)	Zr(2)–F(5)	2.006(6)
Zr(1)–F(1m)	2.147(8)	Zr(2)–F(1m)	2.135(7)
Zr(1)–F(2m)	2.150(7)	Zr(2)–F(2m)	2.142(7)
Zr(1)–O(1w)	2.207(6)	Zr(2)–O(2w)	2.208(8)
Zr(1)–Zr(2)	3.6039(8)		
F(4)–Zr(1)–F(2)	174.8(3)	F(6)–Zr(2)–F(8)	176.6(3)
F(4)–Zr(1)–F(1)	91.8(3)	F(6)–Zr(2)–F(7)	87.6(3)
F(2)–Zr(1)–F(1)	91.8(3)	F(8)–Zr(2)–F(7)	90.1(3)

Table 2 (*continued*)

F(4)–Zr(1)–F(3)	89.0(3)	F(6)–Zr(2)–F(5)	93.7(3)
F(2)–Zr(1)–F(3)	90.2(3)	F(8)–Zr(2)–F(5)	89.6(3)
F(1)–Zr(1)–F(3)	144.9(3)	F(7)–Zr(2)–F(5)	143.8(3)
F(4)–Zr(1)–F(1m)	89.5(2)	F(6)–Zr(2)–F(1m)	89.7(2)
F(2)–Zr(1)–F(1m)	87.8(2)	F(8)–Zr(2)–F(1m)	90.4(2)
F(1)–Zr(1)–F(1m)	75.0(3)	F(7)–Zr(2)–F(1m)	141.10(19)
F(3)–Zr(1)–F(1m)	140.1(2)	F(5)–Zr(2)–F(1m)	75.1(2)
F(4)–Zr(1)–F(2m)	88.8(3)	F(6)–Zr(2)–F(2m)	87.3(2)
F(2)–Zr(1)–F(2m)	86.00(18)	F(8)–Zr(2)–F(2m)	89.7(2)
F(1)–Zr(1)–F(2m)	140.1(2)	F(7)–Zr(2)–F(2m)	75.6(2)
F(3)–Zr(1)–F(2m)	75.0(3)	F(5)–Zr(2)–F(2m)	140.57(18)
F(1m)–Zr(1)–F(2m)	65.2(2)	F(1M)–Zr(2)–F(2m)	65.5(2)
F(4)–Zr(1)–O(1w)	93.4(3)	F(6)–Zr(2)–O(2w)	89.7(4)
F(2)–Zr(1)–O(1w)	91.3(3)	F(8)–Zr(2)–O(2w)	92.0(3)
F(1)–Zr(1)–O(1w)	72.0(3)	F(7)–Zr(2)–O(2w)	71.8(3)
F(3)–Zr(1)–O(1w)	72.9(3)	F(5)–Zr(2)–O(2w)	72.0(2)
F(1m)–Zr(1)–O(1w)	146.9(2)	F(1m)–Zr(2)–O(2w)	147.0(2)
F(2m)–Zr(1)–O(1w)	147.8(2)	F(2m)–Zr(2)–O(2w)	147.4(2)
Zr(2)–F(1m)–Zr(1)	114.64(10)	Zr(2)–F(2m)–Zr(1)	114.20(10)
	A	B	
O(1)–C(1)–C(2)–N(1)	72(3)	66(2)	
C(1)–C(2)–N(1)–C(3)	179(2)	176(2)	
C(2)–N(1)–C(3)–C(4)	173(3)	161(4)	
N(1)–C(3)–C(4)–O(2)	53(5)	53(5)	
C(3)–C(4)–O(2)–C(5)	166(4)	171(3)	
C(4)–O(2)–C(5)–C(6)	170(3)	164(2)	
O(2)–C(5)–C(6)–O(3)	63(2)	69(3)	
C(5)–C(6)–O(3)–C(7)	172(2)	179.2(19)	
C(6)–O(3)–C(7)–C(8)	170.4(18)	174(2)	
O(3)–C(7)–C(8)–O(4)	72(3)	43(3)	
C(7)–C(8)–O(4)–C(9)	164(2)	156(2)	
C(8)–O(4)–C(9)–C(10)	174(2)	166(3)	
O(4)–C(9)–C(10)–O(5)	76(3)	64(4)	
C(9)–C(10)–O(5)–C(11)	179(3)	174(3)	
C(10)–O(5)–C(11)–C(12)	173(2)	176(3)	
O(5)–C(11)–C(12)–O(1)	69(2)	58(3)	
C(11)–C(12)–O(1)–C(1)	178.4(19)	175.0(19)	
Complex **4**			
Hf(1)–F(4)	1.939(11)	Hf(2)–F(6)	1.974(11)
Hf(1)–F(2)	1.987(9)	Hf(2)–F(8)	1.977(8)
Hf(1)–F(3)	2.003(9)	Hf(2)–F(5)	1.996(7)
Hf(1)–F(1)	2.011(10)	Hf(2)–F(7)	2.014(9)
Hf(1)–F(1m)	2.161(15)	Hf(2)–F(1m)	2.104(16)
Hf(1)–F(2m)	2.171(14)	Hf(2)–F(2m)	2.110(16)
Hf(1)–O(1w)	2.202(10)	Hf(2)–O(2w)	2.184(12)
Hf(1)–Hf(2)	3.5840(9)		
F(4)–Hf(1)–F(2)	172.5(7)	F(6)–Hf(2)–F(5)	91.5(6)
F(4)–Hf(1)–F(3)	89.8(6)	F(8)–Hf(2)–F(5)	90.2(6)
F(2)–Hf(1)–F(3)	87.4(6)	F(6)–Hf(2)–F(7)	89.2(7)
F(4)–Hf(1)–F(1)	91.5(5)	F(8)–Hf(2)–F(7)	89.9(7)
F(2)–Hf(1)–F(1)	94.6(5)	F(5)–Hf(2)–F(7)	143.0(8)
F(3)–Hf(1)–F(1)	147.6(10)	F(6)–Hf(2)–F(1m)	88.9(6)
F(4)–Hf(1)–F(1m)	88.5(5)	F(8)–Hf(2)–F(1m)	90.8(5)
F(2)–Hf(1)–F(1m)	89.0(5)	F(5)–Hf(2)–F(1m)	75.3(5)
F(3)–Hf(1)–F(1m)	138.6(6)	F(7)–Hf(2)–F(1m)	141.7(6)
F(1)–Hf(1)–F(1m)	73.7(6)	F(6)–Hf(2)–F(2m)	87.4(5)
F(4)–Hf(1)–F(2m)	87.1(5)	F(8)–Hf(2)–F(2m)	90.7(5)
F(2)–Hf(1)–F(2m)	85.4(5)	F(5)–Hf(2)–F(2m)	142.1(5)
F(3)–Hf(1)–F(2m)	73.9(6)	F(7)–Hf(2)–F(2m)	74.9(5)
F(1)–Hf(1)–F(2m)	138.5(6)	F(1m)–Hf(2)–F(2m)	66.8(4)
F(1M)–Hf(1)–F(2m)	64.7(5)	F(6)–Hf(2)–O(2w)	90.4(8)
F(4)–Hf(1)–O(1w)	95.3(8)	F(8)–Hf(2)–O(2w)	91.0(8)
F(2)–Hf(1)–O(1w)	90.7(8)	F(5)–Hf(2)–O(2w)	71.6(5)
F(3)–Hf(1)–O(1w)	74.7(7)	F(7)–Hf(2)–O(2w)	71.4(6)
F(1)–Hf(1)–O(1w)	72.9(6)	F(1m)–Hf(2)–O(2w)	146.9(4)
F(1m)–Hf(1)–O(1w)	146.5(5)	F(2m)–Hf(2)–O(2w)	146.2(4)
F(2m)–Hf(1)–O(1w)	148.5(5)	Hf(2)–F(1M)–Hf(1)	114.3(2)
F(6)–Hf(2)–F(8)	178.0(7)	Hf(2)–F(2M)–Hf(1)	113.7(3)
Complex **5**			
Zr(1)–F(4)	1.970(6)	Zr(2)–F(8)	1.980(6)
Zr(1)–F(2)	1.990(6)	Zr(2)–F(6)	1.988(6)
Zr(1)–F(3)	2.012(5)	Zr(2)–F(7)	2.012(5)
Zr(1)–F(1)	2.029(5)	Zr(2)–F(5)	2.018(5)
Zr(1)–F(2m)	2.141(5)	Zr(2)–F(1m)	2.151(5)

(*continued on next page*)

Author's personal copy

Table 2 (*continued*)

Zr(1)–F(1m)	2.162(5)	Zr(2)–F(2m)	2.158(5)
Zr(1)–O(1w)	2.231(6)	Zr(2)–O(2w)	2.212(7)
Zr(1)–Zr(2)	3.6159(11)		
F(4)–Zr(1)–F(2)	175.4(3)	F(8)–Zr(2)–F(6)	173.6(3)
F(4)–Zr(1)–F(3)	88.4(3)	F(8)–Zr(2)–F(7)	89.3(3)
F(2)–Zr(1)–F(3)	95.2(3)	F(6)–Zr(2)–F(7)	89.8(3)
F(4)–Zr(1)–F(1)	90.4(3)	F(8)–Zr(2)–F(5)	92.4(3)
F(2)–Zr(1)–F(1)	88.4(3)	F(6)–Zr(2)–F(5)	92.1(3)
F(3)–Zr(1)–F(1)	143.1(2)	F(7)–Zr(2)–F(5)	144.2(2)
F(4)–Zr(1)–F(2m)	90.2(2)	F(8)–Zr(2)–F(1m)	87.9(3)
F(2)–Zr(1)–F(2m)	88.0(2)	F(6)–Zr(2)–F(1m)	88.8(2)
F(3)–Zr(1)–F(2m)	75.0(2)	F(7)–Zr(2)–F(1m)	141.2(2)
F(1)–Zr(1)–F(2m)	141.9(2)	F(5)–Zr(2)–F(1m)	74.7(2)
F(4)–Zr(1)–F(1m)	89.3(3)	F(8)–Zr(2)–F(2m)	88.4(3)
F(2)–Zr(1)–F(1m)	86.1(2)	F(6)–Zr(2)–F(2m)	85.3(2)
F(3)–Zr(1)–F(1m)	140.7(2)	F(7)–Zr(2)–F(2m)	75.54(19)
F(1)–Zr(1)–F(1m)	76.2(2)	F(5)–Zr(2)–F(2m)	140.3(2)
F(2m)–Zr(1)–F(1m)	65.78(18)	F(1m)–Zr(2)–F(2m)	65.68(18)
F(4)–Zr(1)–O(1w)	95.1(3)	F(8)–Zr(2)–O(2w)	93.1(3)
F(2)–Zr(1)–O(1w)	88.7(3)	F(6)–Zr(2)–O(2w)	92.6(3)
F(3)–Zr(1)–O(1w)	72.0(2)	F(7)–Zr(2)–O(2w)	71.6(2)
F(1)–Zr(1)–O(1w)	71.3(2)	F(5)–Zr(2)–O(2w)	72.6(2)
F(2m)–Zr(1)–O(1w)	146.4(2)	F(1m)–Zr(2)–O(2w)	147.2(2)
F(1m)–Zr(1)–O(1w)	147.2(2)	F(2m)–Zr(2)–O(2w)	147.1(2)
Zr(2)–F(1m)–Zr(1)	114.0(2)	Zr(2)–F(1m)–Zr(1)	114.5(2)
	A	B	
O(1)–C(1)–C(2)–N(1)	55.5(14)	69.2(15)	
C(1)–C(2)–N(1)–C(3)	54.9(14)	174.7(12)	
C(2)–N(1)–C(3)–C(4)	171.4(10)	167.4(13)	
N(1)–C(3)–C(4)–O(2)	57.1(15)	51.7(19)	
C(3)–C(4)–O(2)–C(5)	81.3(14)	174.7(14)	
C(4)–O(2)–C(5)–C(6)	167.7(10)	68(3)	
O(2)–C(5)–C(6)–O(1)	175.1(10)	61(3)	
C(5)–C(6)–O(1)–C(1)	177.1(10)	178(2)	
C(6)–O(1)–C(1)–C(2)	167.0(10)	175.4(15)	
Complex 6			
Hf(1)–F(4)	1.963(8)	Hf(2)–F(8)	1.967(8)
Hf(1)–F(2)	1.983(7)	Hf(2)–F(6)	1.972(8)
Hf(1)–F(3)	1.997(6)	Hf(2)–F(7)	2.003(6)
Hf(1)–F(1)	2.021(6)	Hf(2)–F(5)	2.015(6)
Hf(1)–F(2m)	2.133(5)	Hf(2)–F(2m)	2.134(5)
Hf(1)–F(1m)	2.207(5)	Hf(2)–F(1m)	2.146(5)
Hf(1)–O(1w)	2.215(7)	Hf(2)–O(2w)	2.191(7)
Hf(1)–Hf(2)	3.5970(9)		
F(4)–Hf(1)–F(2)	175.7(3)	F(8)–Hf(2)–F(6)	173.3(3)
F(4)–Hf(1)–F(3)	88.0(4)	F(8)–Hf(2)–F(7)	88.9(4)
F(2)–Hf(1)–F(3)	95.2(3)	F(6)–Hf(2)–F(7)	89.5(3)
F(4)–Hf(1)–F(1)	90.5(3)	F(8)–Hf(2)–F(5)	93.1(4)
F(2)–Hf(1)–F(1)	88.6(3)	F(6)–Hf(2)–F(5)	92.0(3)
F(3)–Hf(1)–F(1)	143.8(3)	F(7)–Hf(2)–F(5)	144.4(3)
F(4)–Hf(1)–F(2m)	90.1(3)	F(8)–Hf(2)–F(2m)	87.7(3)
F(2)–Hf(1)–F(2m)	88.0(3)	F(6)–Hf(2)–F(2m)	85.6(3)
F(3)–Hf(1)–F(2m)	75.0(2)	F(7)–Hf(2)–F(2m)	75.2(2)
F(1)–Hf(1)–F(2m)	141.2(2)	F(5)–Hf(2)–F(2m)	140.3(2)
F(4)–Hf(1)–F(1m)	90.4(3)	F(8)–Hf(2)–F(1m)	88.7(3)
F(2)–Hf(1)–F(1m)	85.3(3)	F(6)–Hf(2)–F(1m)	88.6(3)
F(3)–Hf(1)–F(1m)	141.2(2)	F(7)–Hf(2)–F(1m)	142.6(2)
F(1)–Hf(1)–F(1m)	74.9(2)	F(5)–Hf(2)–F(1m)	73.0(2)
F(2m)–Hf(1)–F(1m)	66.3(2)	F(2M)–Hf(2)–F(1m)	67.4(2)
F(4)–Hf(1)–O(1w)	95.0(4)	F(8)–Hf(2)–O(2w)	93.6(4)
F(2)–Hf(1)–O(1w)	88.7(3)	F(6)–Hf(2)–O(2w)	92.1(4)
F(3)–Hf(1)–O(1w)	72.6(3)	F(7)–Hf(2)–O(2w)	71.6(3)
F(1)–Hf(1)–O(1w)	71.5(3)	F(5)–Hf(2)–O(2w)	72.8(3)
F(2m)–Hf(1)–O(1w)	147.0(3)	F(2m)–Hf(2)–O(2w)	146.8(2)
F(1m)–Hf(1)–O(1w)	146.0(2)	F(1m)–Hf(2)–O(2w)	145.8(2)
Hf(2)–F(1m)–Hf(1)	111.5(2)	Hf(1)–F(2m)–Hf(2)	114.9(2)

2.2.5. $\{(H_2DA18C6)(Zr_2F_{10}\cdot 2H_2O)\cdot 2H_2O\}$ (5)

Crystals of complex **5** separated in an approximately quantitative yield, and are colorless transparent prisms, soluble in methanol; m.p. ≫250 °C. *Anal.* Calc. for $C_{12}H_{36}F_{10}N_2O_8Zr_2$: C, 20.33; H, 5.12; F, 26.80; N, 3.95. Found: C, 20.37; H, 5.10; F, 26.84; N, 3.98%.

2.2.6. $\{(H_2DA18C6)(Hf_2F_{10}\cdot 2H_2O)\cdot 2H_2O\}$ (6)

Crystals of complex **6** separated in an approximately quantitative yield, and are colorless transparent prisms, soluble in methanol; m.p. ≫250 °C. *Anal.* Calc. for $C_{12}H_{36}F_{10}Hf_2N_2O_8$: C, 16.32; H, 4.11; F, 21.51, N, 3.17.Found: C, 16.30; H, 4.15; F, 21.54, N, 3.15

2.3. X-ray diffraction study

The experimental data for complexes **1**, **2** were recorded on a Xcalibur S with a CCD detector (Mo Kα radiation (λ = 0.71073 Å), graphite monochromator, ω scan mode). The X-ray intensity data for complexes **3**–**6** were recorded on a Nonius CCD area detector diffractometer employing graphite monochromatized Mo Kα radiation in ϕ and ω scan mode. Final unit cell dimensions were obtained and refined on the entire data set. Integration and scaling resulted in a data set corrected for Lorentz and polarization effects using DENZO [10]. The scaling as well as the global refinement of crystal parameters were performed by SCALEPACK [10]. The absorption correction for **1**–**6** was applied using SADABS [11] The structure solution and refinement proceeded similarly using SHELX-97 program package [12] for all structures. The non-hydrogen atoms were treated anisotropically (full-matrix least-squares method on F^2). In complexes **3** and **4**, the macrocycle, water molecules and oxonium ions are disordered over two positions with equal occupancies. In **3**–**4**, the H–O atoms of the disordered water molecules and oxonium ions were not localized. N–H atoms were found from geometric considerations. The X-ray study for complexes **5**–**6** revealed their lamellar structure and the disorder due to the shift of the layers being parallel to the crystallographic plane (101). The major crystal component corresponds to 86% and 85% in the crystals of **5** and **6**, correspondingly. Two minor shifted components with the contributions of 11% and 2% for **5** and 11% and 3 % for **6** were detected. For minor components only position of inorganic anions were localized. The crown and water molecules were refined with the occupancies that correspond to the major component. In all complexes, C-bound H atoms were placed in calculated positions, with C–H distances of 0.97 Å, and were treated using a riding-model approximation, with $U_{iso}(H) = 1.2U_{eq}(C)$. In **2**, H-atoms of water molecules and NH-groups were determined from a difference Fourier map and were then allowed to refine isotropically with $U_{iso}(H) = 1.5U_{eq}(O)$ and O–H and N–H distances subjected to DFIX restraints. The X-ray data and the details of the refinement for **1**–**6** are summarized in Table 1, the selected geometric parameters are given in Table 2, the hydrogen bonding geometry is given in Table 3.

3. Results and discussion

3.1. Description of the structures

3.1.1. $\{(HA15C5)_2\}[Ta_2F_{10}O]$ (1)

The ORTEP view for complex **1** is shown in Fig. 1. Compound **1** crystallises in the triclinic space group *P*1. The formula unit comprises of the $[(TaF_5)_2O]^{2-}$ dianion which resides on an inversion center, and two azonia-15C5 monocations which compensate the negative charge and are bound with the anion *via* NH···F hydrogen bond, N(1)–H(1N1)···F(3) ($x+1$, y, z), H···F 2.07(4), N···F 2.886(4) Å, NHF angle 165(3)°. The Ta(1) atom has a distorted octahedron surrounding (Table 2) with the Ta–F distances falling in the range 1.847(3)–1.908(2) Å, the maximal deviations of the F–Ta–F bond angles from the straight and right angles being 5.83(10)° and 3.9(10)°, correspondingly, and the deviation for the O–Ta–F angle from the right angle being 3.76(8)°. The geometry of the $[(TaF_5)_2O]^{2-}$ dianion coincides with that in the structure of bis(tetraethylammonium)μ-oxo-bis(pentafluorotantalum(v)) [13]. The

Author's personal copy

Table 3
Hydrogen bond distances (Å) and angles (°) for complexes **1**, **2**, **3**, **5**

D–H···A	d(D–H)	d(H···A)	d(D···A)	∠(DHA)	Symmetry transformation for acceptor
Complex **1**					
N(1)–H(1)···F(3)	0.83(3)	2.07(4)	2.886(4)	165(3)	$-x+1, y, z$
N(1)–H(2)···O(4)	0.94(5)	1.94(5)	2.835(5)	159(4)	x, y, z
Complex **2**					
N(1A)–H(1A)···O(2wa)	0.90	1.93	2.785(5)	157	x, y, z
N(1A)–H(2A)···F(8)	0.90	1.96	2.804(4)	156	x, y, z
N(1B)–H(1B)···O(2wb)	0.89(2)	1.78(2)	2.663(5)	171(6)	x, y, z
O(1w)–H(1w1)···O(3w)	0.86(2)	1.84(2)	2.686(5)	171(6)	$x, y-1, z$
O(1w)–H(2w1)···F(9)	0.83(2)	1.89(3)	2.690(4)	162(5)	$x, y-1, z$
O(2wa)–H(2wa)···O(3A)	0.88(2)	2.02(2)	2.894(4)	168(6)	x, y, z
O(2wa)–H(1wa)···O(5A)	0.92(2)	2.04(2)	2.923(4)	161(5)	x, y, z
O(2wb)–H(2wb)···O(5B)	0.86(2)	1.94(3)	2.762(4)	159(6)	x, y, z
O(2wb)–H(1wb)···O(3B)	0.85(2)	2.01(3)	2.822(4)	160(6)	
O(3w)–H(1w3)···O(4A)	0.84(2)	1.96(3)	2.774(4)	162(8)	$-x+3/2, y+1/2, z+1/2$
O(3w)–H(2w3)···O(4B)	0.86(2)	2.22(2)	2.886(4)	134(3)	$-x+3/2, y-1/2, z+1/2$
Complex **3**					
O(1w)–H(1w1)···F(5)	0.94	1.63	2.567(8)	176	$-x+1/2, y, z-1/2$
O(1w)–H(2w1)···F(7)	0.93	1.65	2.584(8)	178	$-x, -y, z-1/2$
O(2w)–H(1w2)···F(1)	0.93	1.66	2.592(10)	178	$-x+1/2, y, z+1/2$
O(2w)–H(2w2)···F(3)	0.91	1.65	2.556(10)	179	$-x, -y, z+1/2$
N(1a)–H(1A1)···F(6)	0.90	2.14	2.98(2)	154	$x+1/2, -y+1, z$
N(1a)–H(1A2)···O(3w)	0.90	2.10	2.900(15)	148	x, y, z
N(1b)–H(1B1)···O(3w)	0.90	1.96	2.839(13)	164	x, y, z
N(1b)–H(1B2)···F(2)	0.90	1.99	2.888(18)	173	$x+1/2, -y+1, z$
Complex **5**					
O(1w)–H(1w)···F(1)	0.95	1.66	2.612(8)	175	$-x+1, -y+1, -z+1$
O(1w)–H(2w)···F(5)	0.95	1.64	2.590(8)	172	$x-1, y, z$
O(2w)–H(3w)···F(3)	0.94	1.64	2.576(8)	178	$x+1, y, z$
O(2w)–H(4w)···F(7)	0.98	1.66	2.620(9)	163	$-x+2, -y+1, -z$
N(1A)–H(1A1)···F(2)	0.90	1.98	2.812(12)	153	$-x+1, -y+1, -z+1$
N(1A)–H(1A2)···O(3W)	0.90	2.06	2.900(13)	153	$-x+1, -y+2, -z+1$
N(1B)–H(1B1)···O(4W)	0.90	2.48	3.037(13)	120	$-x+1, -y, -z+1$
N(1B)–H(1B2)···O(4W)	0.90	2.01	2.899(14)	169	$x, y, z+1$
O(3w)–H(1w3)···F(4)	0.92	1.91	2.759(10)	152	x, y, z
O(3w)–H(2w3)···F(8)	0.95	1.94	2.881(10)	172	x, y, z
O(4w)–H(1w4)···F(2)	0.93	1.92	2.789(9)	156	x, y, z
O(4w)–H(2w4)···F(6)	0.93	1.82	2.709(9)	159	x, y, z

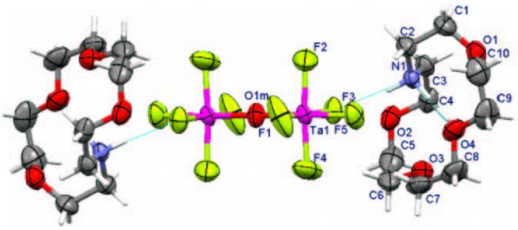

Fig. 1. ORTEP drawing of **1** with the numbering scheme and hydrogen bonding distances shown by dashed lines. Thermal ellipsoids are shown at the 50% probability level.

$(HA15C5)^+$ cation has a distorted shape fixed by the intramolecular N(1)–H(2N1)···O(4) hydrogen bond, H···O 1.94(5), N···O 2.835(5) Å, NHO angle 159(4)°. The similar macrocycle conformation (N···O 2.858 Å) was found in the structure of N-(2-methoxy-4-((4-nitrophenyl)azo)phenyl)-1,4,7,10-tetraoxa-13-azoniacyclopentadecane hexafluorophosphate [14]. It is noteworthy that **1** represents the only second after [13] known example of the organically templated tantalum oxofluoride and the first compound where the macrocycle is used in this function.

3.1.2. $[(HA18C6 \cdot H_2O)(A18C6 \cdot H_2O)][(H_2O)Nb_2F_9O] \cdot H_2O$ (**2**)

Compound **2** crystallizes in the space group $Pna2_1$. The content of the asymmetric unit is shown in Fig. 2. It comprises of $[(H_2O)NbF_4O\ NbF_5]^-$ anion, two macrocycles (designated A and B; cycle A represents monocation, cycle B represents neutral molecule) centered by two water molecules, and bridging water molecule O(3w). The X-ray data unambiguously showed that $[(H_2O)NbF_4ONbF_5]^-$ is built of $(H_2O)NbF_4O$ and $ONbF_5$ moieties joined *via* common oxygen atom. Complex **2** is the first known example of non-symmetric binuclear aqua niobium oxofluoride and only the second example after bis(ethylenediaminium) μ-oxo-bis[tetrafluorooxoniobium(V)], $(C_2H_{10}N_2)_2[(NbF_5O)_2O]$ [15] dimeric unit. The anion has an angular shape with the Nb(1)–O(1)–Nb(2) angle equal to 158.4(2)° and the Nb(1)···Nb(2) distance of 4.008 Å. The geometry of two octahedral units is rather similar: the longest Nb(1)–O(1w) distance of 2.310(3) Å corresponds to the longest Nb(2)–O(1m) distance of 2.346(3) Å in the second octahedron, while the shortest Nb(1)–O(1m) distance of 1.732(3) Å corresponds to the shortest Nb(2)–F(9) distance of 1.709(3) Å in the second octahedron, etc. The conclusions made by Poeppelmeier et al. [16] about out-of-center distortions observed in Group 5 and 6 metal oxide fluoride octahedra with the general formula of $[MO_xF_{6-x}]^{n-}$ ($x = 1$, M = V^{5+}, Nb^{5+}, Ta^{5+}, $n = 2$) that arise from the inherent differences between M=O and M–F bonding and allow for the strong dπ–pπ metal–oxide orbital interactions, are manifested themselves either in purely inorganic niobium oxyfluorides, e.g., Li_2NbOF_5, $Rb_5Nb_3OF_{18}$ [17] or in mixed inorganic–organic compounds, $[4\text{-apyH}]_2[Cu(4\text{-apy})_4(NbOF_5)_2]$ (4-apy = 4-aminopyridine), $Cd(3\text{-apy})_4(NbOF_5)$ (3-apy = 3-aminopyridine), $Cd(py)_4NbOF_5$ (py = pyridine) [16], $[NEt_3H][NbOF_4(H_2O)]$ [18] and can be extrapolated to the reported here new anion, $[(H_2O)NbF_4ONbF_5]^-$ (Table 3).

Author's personal copy

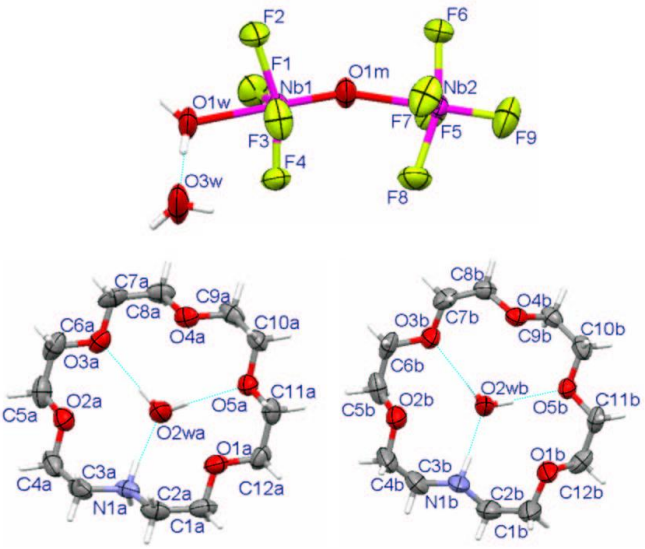

Fig. 2. ORTEP drawing of **2** with the numbering scheme and hydrogen bonding distances shown by dashed lines. Thermal ellipsoids are shown at the 50% probability level.

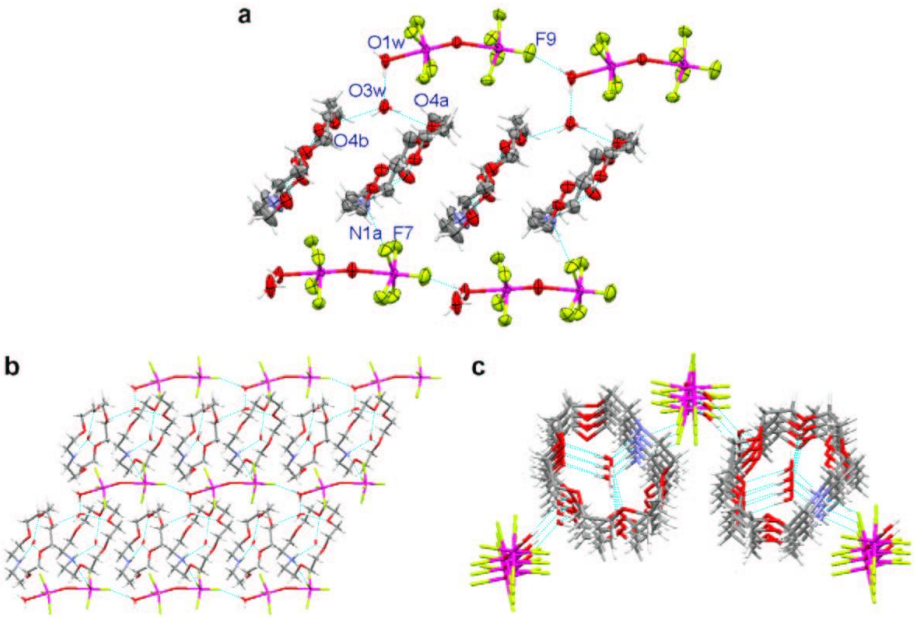

Fig. 3. View of the layer in **2**. (a) Fragment of layer with the numbering of the atoms participating in hydrogen bonding. (b) View along *a* direction. (c) View along *b* direction.

The specific feature of this anion is a *trans*-arrangement of water molecule referring to μ-oxoatom. As it is known, in the hetero-ligand metal complexes with the d^0 configuration of the central atom the mutual ligand influence is manifested in the form of *trans*-effect [19], while the relative stabilization of either *cis*- or *trans*-isomers of the complexes MF_4XO is dictated by the difference in σ- and π-donor characteristics of X and Y ligands [20]. For the oxo-bridge and water molecule arranged in the opposite points of the row of static trans-influence and being essentially different by their σ-, π-donor properties, the approaches [20] indicate the stabilization of the *trans*-form that is agreed with experimental data. It is interesting to note that in formally similar dimeric anion $[Nb_2F_8O_3]^{4-}$ [15] the double-bonded oxygen atoms are arranged in a *cis*-position to the oxo-bridge that is typical for the octahedral

Author's personal copy

fluorocomplexes of d^0-metals with multiple-bound ligands [20].

In the crystal, the anions translated along *a* direction form OH···F hydrogen bond chain (Fig. 3, Table 3). The analysis of the system of hydrogen bonding as well as the pronounced distinctions in A and B crown ethers' conformations (see Table 2) permit to conclude that in the crystal both monoprotonated and neutral forms of A18C6 co-exist. Water molecules center both macrocycles and act in a similar way, as a double H-donor towards two crown oxygen atoms and as a single H-acceptor towards nitrogen atom (Fig. 2, Table 3). In molecule A, the hydrogens of $>H_2N^+$ group are *endo*,*exo*-oriented that facilitates for the *exo*-oriented hydrogen atom its participation in NH^+···F hydrogen bonding with the anion. Water molecule O(3w) occupies an intermediate position between the negatively charged inorganic chain and rows of macrocyclic molecules and bridges A and B crown molecules *via* OH···O hydrogen bonds. Thus, the supramolecular architecture in **2** represents a 2D sheet built of the alternating negatively-charged inorganic chains and rows of crown molecules, where A and B macrocyclic molecules arranged in approximately parallel planes (the dihedral angle between the planes (A/B) of NO_5 atom set is equal to 13.8(1)°) alternate (Fig. 3).

3.1.3. $[(HA18C6 \cdot H_2O)(M_2O_{10} \cdot 2H_2O) \cdot (H_3O) \cdot (H_2O)]$ (M = Zr, Hf) (**3**, **4**)

The system ZrO_2/HfO_2–HF–H_2O–aza18C6 resulted in two isostructural crystalline complexes of the composition $[(HA18C6 \cdot H_2O)(M_2O_{10} \cdot 2H_2O) \cdot (H_3O) \cdot (H_2O)]$ (**3**, **4**), so the only complex **3** is further discussed. Complexes crystallize in the orthorhombic space group $Pca2_1$. The asymmetric unit for **3** is shown in Fig. 4. It comprises of the $(Zr_2F_{10} \cdot 2H_2O)^{2-}$ dianion, azonia-18C6 cation, oxonium ion, and two water molecules. In the dimeric $(Zr_2F_{10} \cdot 2H_2O)^{2-}$ anion, the coordination environment of each Zr atom represents a pentagonal bipyramid. In the equatorial plane of the anion, the bridging F(1m) and F(2m) atoms form a double bridge, with the Zr–F distances being in the range 2.135(7)–2.150(7) Å, and coordinated to Zr water molecules located along the Zr(1)···Zr(2) line, Zr···O distances being 2.207(6) and 2.208(7) Å, Zr(1)···Zr(2) separation being 3.604(1) Å. Our survey of the CSD [21] revealed no examples of such organically templated zirconate anion. The only known relative example with the same Brutto formula of the anion is a tetramethylammonium pentafluoro-zirconium monohydrate, $(C_4H_{12}N)_2(Zr_2F_{10} \cdot 2H_2O)$ [22], where the coordinated to Zr water molecules are arranged perpendicular to the Zr...Zr line.

The monoprotonated macrocyclic molecule in the complex is disordered over two positions (A and B) with equal probabilities. Similar to complex **2**, water molecule O(3w) centers the macrocyclic cation and acts as a double H-donor towards two crown oxygens and as a single H-acceptor towards *endo*-oriented H-atom of NH_2-group. It was impossible to unambiguously find the positions of hydrogen atoms in water molecule due to the severe disorder of the macrocycle and the proposition of the possible hydrogen bonding was assumed from consideration of the shortest O(3w)···N(O) crown distances which adopt the following values in two (A and B) systems: 2.91(2), 2.97(2) and 2.74(2) Å to atoms O(1A), O(3A) and O(5A), respectively and 2.86(3), 3.03(2) and 2.72(2) Å to atoms O(1B), O(2B) and O(5B), respectively.

The anions form in the crystal an inorganic layer due to OH···F hydrogen bonds between the coordinated to Zr water molecules and four equatorial fluorine atoms (Fig. 5, Table 3), in such a way, that every anion is surrounded by four closest neighbors, the association of the anions occurs *via* alternation of $R_2^2(8)$ and $R_4^4(16)$ hydrogen-bonded rings. The similar inorganic sheet is generated in structures containing $(Hf_2F_{10} \cdot 2H_2O)^{2-}$ anion, hexamethyldiammonium pentafluorohafnate tetrahydrate $(C_6N_2H_{18})[Hf_2F_{10}(H_2O)_2] \cdot 4H_2O$, tetramethylenediammonium pentafluorohafnate hexahydrate $(C_4N_2H_{14})[Hf_2F_{10}(H_2O)_2] \cdot 4H_2O$ [23] as well as in the complex $[(18C6)(H_3O)_2(Hf_2O_{10} \cdot 2H_2O) \cdot 4H_2O]$ [7].

The disorder of the macrocycle causes the disordering of the oxonium ion labelled O5o(a,b) and solvated water molecule O4w(a,b) which are bound in a slightly different mode with the macrocycle and inorganic layer (Fig. 4). The 3D supramolecular architecture in **3** is formed *via* alternation of the inorganic layers and rows of macrocyclic molecules held together via oxonium

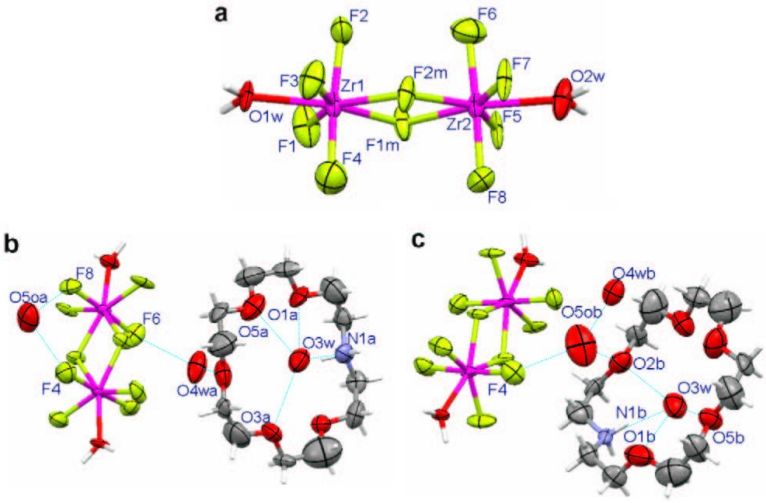

Fig. 4. ORTEP drawing of **3**. (a) View of the $(Zr_2F_{10} \cdot 2H_2O)^{2-}$ anion with the numbering scheme. (b) View of the crown molecule in position A, water molecules and oxonium ion O(5oa) that participate in hydrogen bonds in this system. (c) View of the crown molecule in position B, water molecules and oxonium ion O(5ob) that participate in hydrogen bonds in this system with partial numbering scheme. Complete numbering scheme in crown molecule is the same as in **2** (Fig. 2). Hydrogen bonding distances shown by dashed lines. Thermal ellipsoids are shown at the 50% probability level.

Author's personal copy

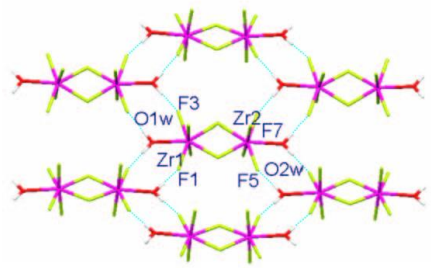

Fig. 5. Fragment of inorganic layer in **3**.

and water molecules. Besides these indirect interactions, the direct $NH^+\cdots F^-$ contacts between charged units also exist (Table 3, Fig. 6).

*3.1.4. [(H₂DA18C6)(M₂O₁₀ · 2H₂O) · 2H₂O] (M = Zr, Hf) (**5**, **6**)*

The interaction in the system ZrO_2/HfO_2–HF–H_2O–1,10-diaza18C6 resulted in two isostructural complexes $[(H_2DA18C6)(M_2O_{10}\cdot 2H_2O)\cdot 2H_2O]$ (**5**, **6**), and only complex **5** is further discussed. Complexes crystallize in the triclinic space group $P\bar{1}$. The content of the asymmetric unit is shown in Fig. 7. It comprises of the $(Zr_2F_{10}\cdot 2H_2O)^{2-}$ anion and two water molecules in general

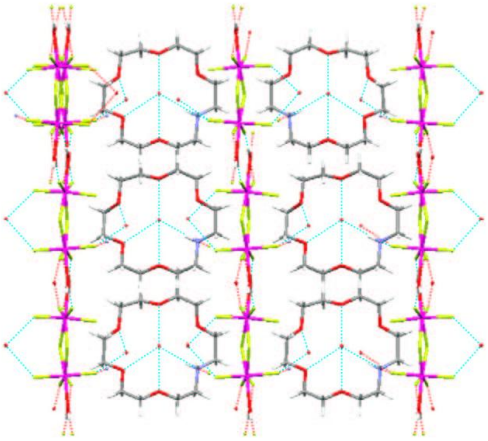

Fig. 6. Fragment of the crystal packing in **3**.

positions and two halves of two crystallographically different diazonia-18C6 cations (A and B), which reside on inversion centers. The structure of the dimeric anion is the same as in **3** and in its Hf analogue in **4** and **6**, the coordination environment of each Zr atom represents a pentagonal bipyramid (Table 2).

Similar to **3**, the anions in **5** formulate a rigid inorganic negatively charged 2D sheet sustained by OH···F hydrogen bonds (Table 3). Two water molecules O(3w) and O(4w) in an identical mode are bridging two pairs of the anion's axial fluorine atoms (Table 3). Further, these two water molecules in different modes act as intermediates between the inorganic anion and macrocyclic cations. Fig. 8a demonstrates interactions between the components in the complex. Water molecule O(3w) acts in a 'side' mode, and as a single H-acceptor forms N(1a)H···O(3w) hydrogen bond with the A macrocycle, while the second H-atom of the same $>NH_2^+$ group is involved in a single charged-assisted N(1a)H···F(2) hydrogen bond, it is a unique such contact (between the charged species) in this structure. Water molecule O(4w) is situated above the macrocyclic cation B and, acting as a double H-acceptor across the cavity, binds both protons of $>N(1b)H_2$ ammonia group. It explains, why this macrocycle does not have any direct contacts with the anionic layer. The different modes of water inclusion as well as the distinctions in the interaction with the anionic component, determine the different conformations of A and B macrocyclic cations (Fig. 7, Table 2). Nevertheless, the 3D supramolecular architecture still remains very similar to that one described for **3** (**4**) and for the aforementioned complex $[(18C6)(H_3O)_2(Hf_2O_{10}\cdot 2H_2O)\cdot 4H_2O]$ [7] (Fig. 8b) and represents the alternation of inorganic layers and rows of macrocyclic cations attached, where the A and B macrocycles alternate.

Summarizing these two sections, the following general remarks can be given. Complexes **3–6** have enriched a rather restricted family of the aqua, fluoro-containing zirconates [22] and hafnates [23]. For the compounds containing the anions of the similar composition $(M_2O_{10}\cdot 2H_2O)^{2-}$ (M = Zr, Hf), the different arrangement of the coordinated to the central atom water molecules is observed: they are always displayed in the equatorial plane and either lie along the M–M line (complexes **3–6**, $[(18C6)(H_3O)_2(Hf_2O_{10}\cdot 2H_2O)\cdot 4H_2O]$ [7]) or perpendicular to it. Besides the discussed here crown-templated complexes, the similar inorganic 2D motif also has been recorded in hexamethyldiammonium pentafluorohafnate tetrahydrate, tetramethylenediammonium pentafluorohafnate hexahydrate [23] and can be considered as a reproducible supramolecular motif. The type of bridging of axial fluorine atoms *via* coordinated or solvated water molecule or oxonium ion found in **3–4**, and **5–6**, was also registered in Refs. [22,23]. Moreover, this bridge can also represent two-membered H_5O_2 oxonium cluster as in $[(18C6)(H_3O)_2(Hf_2O_{10}\cdot 2H_2O)\cdot 4H_2O]$

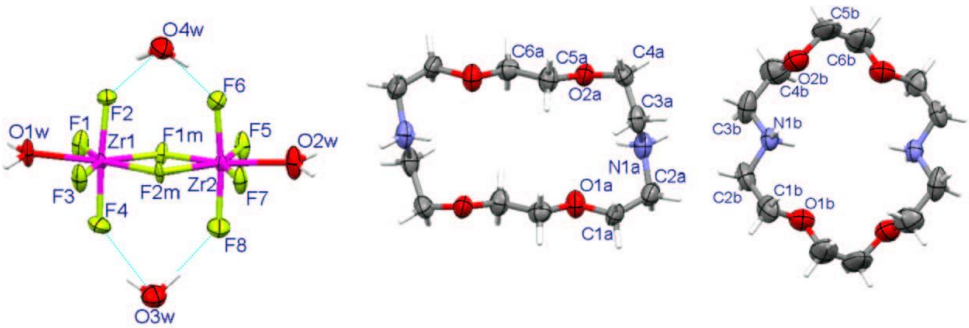

Fig. 7. ORTEP drawing of **5** with the numbering scheme and hydrogen bonding distances shown by dashed lines. Thermal ellipsoids are shown at the 50% probability level.

Author's personal copy

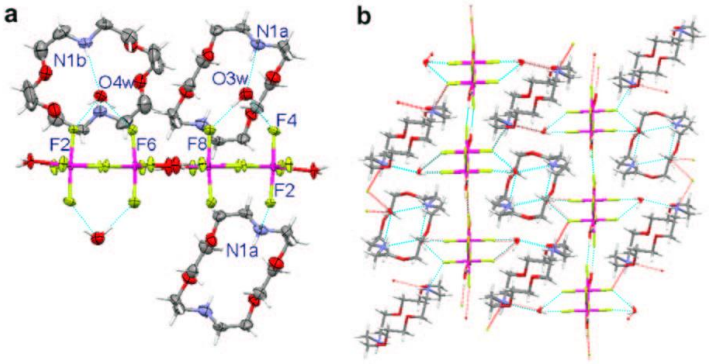

Fig. 8. Fragment of crystal packing in **5**. (a) Fragment of the structure demonstrating the interactions between the inorganic layer and macrocyclic cations, only atoms participating in hydrogen bonding are labeled. (b) 3D network in **5**.

[7] or association of water molecule and ammonium group of templated amine. For **3–6**, we conclude the reproduction of 3D supramolecular architecture, which represents the alternation of 2D inorganic sheets and columns of 18-membered crown ethers glued by the different number of water molecules. We also observe the gradual decrease of water content in the complexes with the increase of the positive charge of the macrocyclic cation.

4. Conclusion

The interaction of ZrO_2/HfO_2 or Nb_2O_5/Ta_2O_5 with an aqueous solution of hydrofluoric acid in the presence of aza-crown ether resulted in novel organically templated metal oxofluorides of the compositions $[(HA15C5)_2][Ta_2F_{10}O]$ (**1**), $[(HA18C6 \cdot H_2O)(A18C6 \cdot H_2O)][(H_2O)\ Nb_2F_9O] \cdot H_2O$ (**2**), $[(HA18C6 \cdot H_2O)(M_2F_{10} \cdot 2H_2O) \cdot (H_3O) \cdot H_2O]$ (**3**, **4**) and $[(H_2DA18C6)(M_2F_{10} \cdot 2H_2O) \cdot 2H_2O]$ (**5**, **6**) (M = Zr, Hf, A15C5 = aza-15-crown-5, A18C6 = aza-18-crown-6, DA18C6 = diaza-18-crown-6). The unique ability of crown macrocyclic molecules to form the complexes with novel or rarely observed anions has been demonstrated. So far **1–6** represent the exclusive examples of *crown-templated* mixed O,F-containing anions for Zr, Hf, Nb and Ta. The Ta complex **1** represents the second example of such organically templated anion alongside with [9] and the first example of the macrocyclic molecule used in this function. For the first time, the structural information has been obtained for the anion $[(H_2O)NbF_4ONbF_5]^-$ in the complex with macrocyclic molecule. Complex **2** represents a perspective example of the non-centrosymmetric solid with the local ordered anion, thus being crystallized in an acentric space group with an ordered inorganic unit, it might give rise to the new NLO materials. Complexes **3–6** give bright examples of the reproducible supramolecular motifs where the factors of domination of inorganic framework and dimensionality of crown molecule are decisive ones. We concluded, that the substitution of one or two oxygen atoms in 18C6 molecule by nitrogen atom did not crucially change the composition of the negatively-charged framework for Zr and Hf in particular and the 3D supramolecular architecture in a whole in the row 18C6–A18C6–DA18C6. The isostructural products have been obtained for Zr and Hf.

Acknowledgement

This work was supported by the Russian Foundation for Basic Research and the Academy of Sciences of R. Moldova (Project No. 06-03-90894-Mol-a).

Appendix A. Supplementary data

CCDC 671858, 671860, 671862, 671859, 671863 and 671861 contains the supplementary crystallographic data for **1**, **2**, **3**, **4**, **5** and **6**. These data can be obtained free of charge via http://www.ccdc.cam.ac.uk/conts/retrieving.html, or from the Cambridge Crystallographic Data Centre, 12 Union Road, Cambridge CB2 1EZ, UK; fax: (+44) 1223-336-033; or e-mail: deposit@ccdc.cam.ac.uk. Supplementary data associated with this article can be found, in the online version, at doi:10.1016/j.poly.2008.03.023.

References

[1] S.G. Bott, A. Alvanipour, J.L. Atwood, J. Incl. Phenom. Mol. Recog. Chem. 10 (1991) 153.
[2] H. Feinberg, I. Columbus, S. Cohen, M. Rabinovitz, H. Selig, G. Shoham, Polyhedron 12 (1993) 2913.
[3] (a) Y.A. Simonov, V.O. Gelmboldt, E.V. Ganin, A.A. Dvorkin, M.S. Fonari, L.V. Ostapchuk, J. Lipkowski, Koord. Khim. (Russ.) (Coord.Chem.) 21 (1995) 760;
(b) M.S. Fonari, Yu.A. Simonov, M.D. Mazus, E.V. Ganin, V.O. Gelmboldt, Kristallografiya (Russ.) (Crystallogr. Rep.) 42 (1997) 858.
[4] Yu.A. Simonov, Ed.V. Ganin, A.A. Dvorkin, M.S. Fonari, V.O. Gelmboldt, A.A. Ennan, Supramol. Chem. 3 (1994) 185.
[5] (a) J. Lipkowski, M.S. Fonari, V.Ch. Kravtsov, V.O. Gelmboldt, E.V. Ganin, Yu.A. Simonov, J. Chem. Cryst. 26 (1996) 823;
(b) M.S. Fonari, E.V. Ganin, V.O. Gelmboldt, J. Lipkowski, S.A. Kotlyar, G.L. Kamalov, Acta Crystallogr., Sect. 62 (2006) m1021.
[6] (a) V.O. Gelmboldt, Yu.A. Simonov, E.V. Ganin, M.S. Fonari, V.Ch. Kravtsov, A.A. Dvorkin, L.V. Ostapchuk, A.A. Ennan, Koord. Khim. 22 (1996) 21;
(b) V.O. Gelmboldt, E.V. Ganin, M.S. Fonari, Yu.A. Simonov, L.V. Koroeva, A.A. Ennan, S.S. Basok, S. Shova, H. Kählig, V.B. Arion, B.K. Keppler, Dalton Trans. 27 (2007) 2915.
[7] V.O. Gelmboldt, E.V. Ganin, L.V. Koroeva, M.S. Fonari, Yu.A. Simonov, V.Ch. Kravtsov, J. Lipkowski, Zh. Neorg. Khim. (Russ. J. Inorg. Chem.) 46 (2001) 1833.
[8] (a) M.S. Fonari, N.G. Furmanova, W.-J. Wang, E.V. Ganin, I.A. Verin, Yu.A. Simonov, V.O. Gelmboldt, Kristallografiya (Russ. Crystallogr. Rep.) 51 (2006) 856;
(b) M.S. Fonari, O.A. Alekseeva, N.G. Furmanova, K.A. Lysenko, W.-J. Wang, S.-W. Tang, E.V. Ganin, V.O. Gelmboldt, Yu.A. Simonov, Kristallografiya (Russ. Crystallogr. Rep.) 52 (2007) 271;
(c) M.S. Fonari, Yu.A. Simonov, W.-J. Wang, S.-W. Tang, E.V. Ganin, V.O. Gelmboldt, T.S. Chernaya, O.A. Alekseeva, N.G. Furmanova, Polyhedron 26 (2007) 5193;
(d) E.V. Ganin, V.O. Gelmboldt, L.V. Koroeva, M.S. Fonari, Yu.A. Simonov, J. Lipkowski, S.A. Kotlyar, G.L. Kamalov, J. Incl. Phenom. 56 (2006) 345;
(e) N.G. Furmanova, M.X. Rabadanov, T.S. Chernaya, M.S. Fonari, Yu.A. Simonov, E.V. Ganin, V.O. Gelmboldt, R.Ya. Grygorash, S.A. Kotlyar, G.L. Kamalov, Kristallografiya (Russ. Crystallogr. Rep.) 53 (2008) 273.
[9] (a) J.C. Bertolini, J. Emerg. Med. 10 (1992) 163;
(b) D. Peters, R. Miethchen, J. Fluorine Chem. 79 (1996) 161;
(c) E.B. Segal, Chem. Health Saf. 7 (2000) 18.
[10] Z. Otwinowski, W. Minor, in: C.W. Carter, R.M. Sweet (Eds.), Methods in Enzymology, Macromolecular Crystallography, Part A, vol. 276, Academic Press, London, 1996, p. 307.
[11] G.M. Sheldrick, SADABS, Bruker AXS Inc., Madison, WI, USA, 1997.

Author's personal copy

[12] G.M. Sheldrick, SHELXS 97 and SHELXL 97, Programs for Crystal Structure Solution and Refinement, University of Göttingen, Germany, 1997.
[13] J.C. Dewan, A.J. Edwards, J.Y. Calves, J.E. Guerchais, J. Chem. Soc., Dalton Trans. (1977) 978.
[14] T. Gunnlaugsson, M. Nieuwenhuyzen, L. Richard, V. Thoss, J. Chem. Soc., Perkin Trans. 2 (2002) 141.
[15] N.F. Stephens, P. Lightfoot, Acta Crystallogr., Sect. C 61 (2005) m344.
[16] (a) M.E. Welk, A.J. Norquist, F.P. Arnold, C.L. Stern, K.R. Poeppelmeier, Inorg. Chem. 41 (2002) 5119;
(b) P.A. Maggard, A.L. Kopf, C.L. Stern, K.R. Poeppelmeier, CrystEngComm 6 (2004) 451;
(c) H.K. Izumi, J.E. Kirsch, C.L. Stern, K.R. Poeppelmeier, Inorg. Chem. 44 (2005) 884;
(d) P.C.R. Guillory, J.E. Kirsch, H.K. Izumi, C.L. Stern, K.R. Poeppelmeier, Cryst. Growth Des. 6 (2) (2006) 382.
[17] (a) J. Galy, S. Andersson, J. Portier, Acta Chem. Scand. 23 (1969) 2949;
(b) A.I. Agulyanskii, V.E. Zavodnik, V.Ya. Kuznetsov, N.V. Sidorov, S.Yu. Stefanovich, D.V. Tsikaeva, V.T. Kalinnikov, Izv. Akad. Nauk SSSR Neorg. Mater. 27 (1991) 1055.
[18] N.G. Furmanova, I.A. Verin, A.N. Zozulin, E.G. Il'in, Kristallografiya 37 (1) (1992) 136.
[19] A.A. Levin, P.N. Diyachkov, Èlektronnoe stroenie, struktura i prevrasenia geteroligandnyh molekul [BOOK] (1990) 256.
[20] Yu.A. Buslaev, E.G. Ilin, Interligand interactions and stereochemistry of octahedral different ligand complexes (Mezhligandnyie vzaimodeistviya I stereokhimiya oktaedricheskikh raznoligandnyx kompleksov, Russ.) Itogi nauki i tekhniki. Ser. neorgan. khimiya. T. 16. M.: VINITI, 1987. 98s.
[21] F.N. Allen, Acta Crystallogr., Sect. B 58 (2002) 380.
[22] B.V. Bukvetskii, A.V. Gerasimenko, R.L. Davidovich, M.A. Medkov, Koord. Khim. (Russ. Coord. Chem.) 11 (1985) 77.
[23] (a) A.V. Gerasimenko, R.L. Davidovich, V.V. Tkachev, S.W. Ng, Acta Crystallogr., Sect. E 62 (2006) m196;
(b) V.V. Tkachev, L.O. Atovmyan, V.B. Logvinova, R.L. Davidovich, Koord. Khim. (Russ. Coord. Chem.) 22 (1996) 234;
(c) V.V. Tkachev, L.O. Atovmyan, V.B. Logvinova, R.L. Davidovich, Koord. Khim. (Russ. Coord. Chem.) 22 (1996) 7727.

Додаток М.

Копія статті. “Hexafluorosilicates of bis(carboxypyridinium) and bis(2-carboxyquinolinium)”

Provided for non-commercial research and education use.
Not for reproduction, distribution or commercial use.

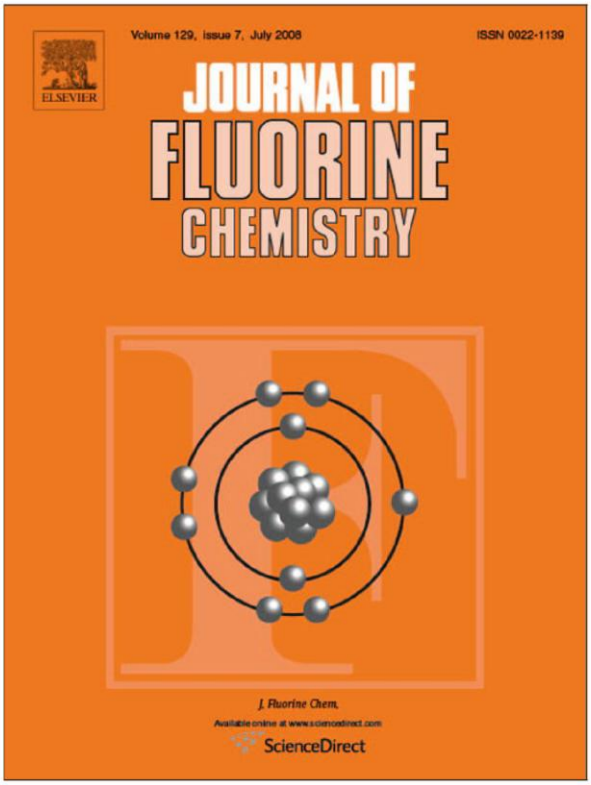

This article appeared in a journal published by Elsevier. The attached copy is furnished to the author for internal non-commercial research and education use, including for instruction at the authors institution and sharing with colleagues.

Other uses, including reproduction and distribution, or selling or licensing copies, or posting to personal, institutional or third party websites are prohibited.

In most cases authors are permitted to post their version of the article (e.g. in Word or Tex form) to their personal website or institutional repository. Authors requiring further information regarding Elsevier's archiving and manuscript policies are encouraged to visit:

http://www.elsevier.com/copyright

Author's personal copy

Journal of Fluorine Chemistry 129 (2008) 632–636

Contents lists available at ScienceDirect

Journal of Fluorine Chemistry

journal homepage: www.elsevier.com/locate/fluor

Hexafluorosilicates of bis(carboxypyridinium) and bis(2-carboxyquinolinium)

Vladimir O. Gelmboldt [a,1], Larisa V. Koroeva [a], Eduard V. Ganin [b], Marina S. Fonari [c,*], Mark M. Botoshansky [d], Alim A. Ennan [a]

[a] Physico-Chemical Institute of Environment and Human Protection of Ministry of Education and Science of Ukraine and National Academy of Sciences of Ukraine, Preobrazhenskaya Street 3, 65082 Odessa, Ukraine
[b] Odessa State Environmental University of Ministry of Education and Science of Ukraine, Lvovskaya Street 15, 65016 Odessa, Ukraine
[c] Institute of Applied Physics, Academy of Sciences of Moldova, Academy Street 5, MD2028 Chisinau, Republic of Moldova
[d] Schulich Faculty of Chemistry, Technion-Israel Institute of Technology, Technion City, 32000 Haifa, Israel

ARTICLE INFO

Article history:
Received 24 March 2008
Received in revised form 30 April 2008
Accepted 3 May 2008
Available online 13 May 2008

Keywords:
Hexafluorosilicate
Heterocyclic amines
Solubility
Hydrogen bonding
Crystal structure

ABSTRACT

The preparation and characterization of three isomeric carboxypyridinium and carboxyquinolinium hexafluorosilicate salts is described. The salts of the general formulas $(LH)_2[SiF_6]$ (**I–III**, L = 2-carboxypyridine, 3-carboxypyridine, 4-carboxypyridine) and $(LH)_2[SiF_6]\cdot 2H_2O$ (IV, L = 2-carboxyquinoline) were prepared from the protonation reaction of the corresponding pyridine carbonic acid by the fluorosilicic acid. The compounds were characterized by IR, mass-spectrometry, thermogravimetric analysis, solubility data, and in the case of III by X-ray crystallography. The relationship between the salts solubility and the H-bonding system was analysed.

© 2008 Elsevier B.V. All rights reserved.

1. Introduction

"Onium" hexafluorosilicates $(LH)_2[SiF_6]$ (L = ammonia, N-,O-containing organic bases) find application as chemical reagents [1–3], herbicides and fungicides [4,5], functional materials [6,7], and also can be utilised as the models for estimation of influence of interionic H-bonds on structure and physicochemical properties of the complexes [8]. In continuation of our previous examinations on relationship between structure and properties of "onium" hexafluorosilicates the preparation, spectral data, thermochemical transformations and solubility of salts of three isomeric bis(carboxypyridinium) hexafluorosilicates (**I–III**) and bis(2-carboxyquinolinium) hexafluorosilicate (**IV**) are described alongside with the crystal structure of bis(4-carboxypyridinium) hexafluorosilicate (**III**). The structural characteristics for hexafluorosilicates of the general formula $(LH)_2[SiF_6]\cdot nH_2O$ (L = 2-, 3-carboxypyridine, $n = 0$; L = 2-carboxyquinoline, $n = 2$) have been reported earlier [9,10].

2. Results and discussion

Compound **III** crystallizes in the monoclinic crystal system (space group $P2_1/n$) with $Z = 2$. Crystal structure and refinement data is given in Table 1. Selected bond distances and angles are given in Table 2. The asymmetric unit of **III** comprises a half of a hexafluorosilicate anion that resides on an inversion center and one 4-carboxypyridinium cation in general position (Fig. 1). The positions of pyridinium and carboxylic hydrogen atoms were found in the difference Fourier map.

In the $[SiF_6]^{2-}$ anion the Si–F bond lengths are between 1.666(1) and 1.692(1) Å. The fluorine atoms in the longer Si–F bond participates in the strongest hydrogen bond (Table 3). The F(*trans*)–Si–F(*trans*) angles are 180°, the F(*cis*)–Si–F(*cis*) angles deviate at 1.08(5)° from the right angle. Such a slightly distorted octahedral geometry is typical for $[SiF_6]^{2-}$ anion involved in the system of hydrogen bonding. The relationship between Si–F bond length and hydrogen bonding is also observed in bis(piperidinium) hexafluorosilicate, bis(quinolinium) hexafluorosilicate monohydrate, and in *N*-methylpiperidine betaine hexafluorosilicate [11,12] and surprisingly is not observed in bis(methylammonium) hexafluorosilicate [11]. The 4-carboxypyridinium cation in **III** has a practically planar skeleton with the twisted angle between the pyridinium ring and the carboxylic group equal to 23.7°. The C–O

* Corresponding author. Tel.: +373 22 73 81 54; fax: +373 22 72 58 87.
E-mail addresses: edganin@yahoo.com (E.V. Ganin), fonari.xray@phys.asm.md, fonari.xray@gmail.com (M.S. Fonari), botoshan@tx.technion.ac.il (M.M. Botoshansky).
[1] eksvar@ukr.net.

0022-1139/$ – see front matter © 2008 Elsevier B.V. All rights reserved.
doi:10.1016/j.jfluchem.2008.05.006

Author's personal copy

Table 1
Crystal data and structure refinement parameters for **III**

Empirical formula	$C_{12}H_{12}F_6N_2O_4Si$
Formula weight	390.33
Crystal system	Monoclinic
Space group	$P2_1/n$
Unit cell dimensions	
a (Å)	7.384(2)
b (Å)	12.981(3)
c (Å)	7.738(2)
β (°)	99.24(3)
Cell volume (Å^3)	732.1(3)
Z	2
D_{calc} (g/cm^3)	1.771
μ (mm^{-1})	0.255
F(0 0 0)	396
θ range for data collection (°)	3.21–25.02
Limiting indices	$0 < h < 8$ $0 < k < 15$ $-9 < l < 9$
Reflections collected	1243
Reflections with $I > 2\sigma(I)$	1162
Refinement method	Full-matrix least-squares on F^2
Data/restraints/parameters	1243/0/123
Goodness-of-fit on F^2	1.107
Final R indices [$I > 2\sigma(I)$]	$R_1 = 0.0308, wR_2 = 0.0750$
R indices (all data)	$R_1 = 0.0333, wR_2 = 0.0761$
Largest diff. peak and hole (e Å^{-3})	0.207/−0.154

Table 2
Selected intermolecular distances (Å) and angles (°) for **III**

Si(1)–F(1)	1.666(1)	F(1)–Si(1)–F(2)	91.08(5)
Si(1)–F(2)	1.683(1)	F(1)–Si(1)–F(3)	89.57(6)
Si(1)–F(3)	1.692(1)	F(2)–Si(1)–F(3)	90.33(6)
O(1)–C(6)	1.317(2)	O(2)–C(6)–O(1)	125.0(2)
O(2)–C(6)	1.202(2)	O(2)–C(6)–C(3)	122.6(2)
N(1)–C(5)	1.330(2)	O(1)–C(6)–C(3)	112.4(1)
N(1)–C(1)	1.331(3)	C(5)–N(1)–C(1)	123.1(2)
C(1)–C(2)	1.379(3)	N(1)–C(1)–C(2)	119.7(2)
C(2)–C(3)	1.382(2)	N(1)–C(5)–C(4)	119.6(2)

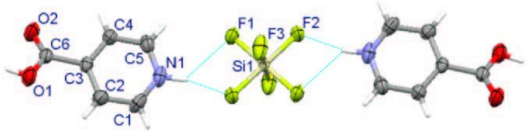

Fig. 1. ORTEP drawing for **III** showing hydrogen bonding. Only asymmetric unit is numbered.

distances essentially differ (Table 2) and are in agreement with the neutral form of carboxylic group.

Two effects are crucial for crystal packing: the hydrogen bonding between the charged species and π–π stacking interactions between the cationic units. Both pyridinium and carboxylic hydrogens participate in H-bonding with the $[SiF_6]^{2-}$ anion, each anion being connected with four closest cations. In their turn, the adjacent cations related by inversion are arranged in parallel planes with the centroid–centroid distance of 3.765 Å that is in agreement with the value typical for π–π stacking interactions. These concerted interactions combine the charged species in the chain running along c direction. The fragment of this chain showing the environment of the $[SiF_6]^{2-}$ anion is given in Fig. 2.

The IR data for hexafluorosilicates **I–IV** are summarized in Table 4. The IR spectra for **I–III** exhibit stretching vibrations $\nu(N^+H)$ in the form of fuzzy bands of average intensity in the range 3210–3085 cm^{-1}. In spectrum for **IV** the complicated bands in the range 3420–3125 cm^{-1} can be assigned to the ν(OH) vibrations of water molecules involved in the system of H-bonding (upfield components 3420, 3310, 3205 cm^{-1}), and $\nu(N^+H)$ vibrations for protonated quinoline-2-carbonic acid (preferred contribution in the downfield component at 3125 cm^{-1}). The presence of fuzzy absorption bands in the spectra **I–IV** in the field of 2720–2525 cm^{-1} can be assigned to strong interionic OH···F hydrogen bonds [9,10]. In the field of 800–650 cm^{-1} (Table 4) was registered the superposition of vibration bands ν(SiF) for $[SiF_6]^{2-}$ anions and deformation vibrations for the N^+H, CCH moieties (for **IV**, the vibrations for water molecule). Deformation vibrations $\delta(SiF_2)$ for the anions in the form of triplets (**I**, **II**, **IV**) or doublets of average intensity are registered in the range 490–435 cm^{-1} free of natural oscillations of the cations. The multiple character of the $\delta(SiF_2)$ vibrations is in agreement with the X-ray data indicating the distortion of the octahedral geometry of the $[SiF_6]^{2-}$ anion in **I–IV** due to interionic hydrogen bonds.

The results of thermogravimetric analysis for hexafluorosilicates **I–IV** are summarized in Table 5. As it follows from Table 5, the thermolysis of compounds **I** and **III** is accompanied by a stage of elimination of hydrogen fluoride and silicon tetrafluoride with the subsequent decomposition of the ligands:

$$(L^{1,3}H)_2[SiF_6] \rightarrow SiF_4 + 2HF + 2L^{1,3} \quad (1)$$

$$L^{1,3} \rightarrow \text{decomposition products} \quad (2)$$

The thermal decomposition for **IV** is implemented with consecutive elimination in a gas phase of two moles H_2O, two moles HF, one mole SiF_4 and decomposition products for L^4:

$$(L^4H)_2[SiF_6] \cdot 2H_2O \rightarrow (L^4H)_2[SiF_6] + 2H_2O \quad (3)$$

$$(L^4H)_2[SiF_6] \rightarrow SiF_4 \cdot 2L^4 + 2HF \quad (4)$$

$$SiF_4 \cdot 2L^4 \rightarrow SiF_4 + 2L^4 \quad (5)$$

$$L^4 \rightarrow \text{decomposition products} \quad (6)$$

The thermolysis of compound **II** proceeds similarly to decomposition of the anhydrous phase **IV**. It is interesting to note, that in their thermal stability which in the first approximation is characterized by the values t_0 for the first endothermic effect, compounds **I–III** somewhat surpass the hexafluorosilicates $(C_5H_5NH)_2[SiF_6]$ and $(n\text{-}CH_3C_5H_4NH)_2[SiF_6]$; ($n$ = 2, 3, 4; t_0 = 120–140 °C) [13], despite of higher values of basicity for pyridine and isomeric picolines (pK_a L^1–L^3 4.81–5.32; pK_a C_5H_5N 5.23; pK_a n-$CH_3C_5H_4N$ 5.68–6.02) [14,15]. Apparently, the relative stabilization of salts **I–III** in comparison with the hexafluorosilicates $(C_5H_5NH)_2[SiF_6]$ and $(n\text{-}CH_3C_5H_4NH)_2[SiF_6]$ is dictated by the extra

Table 3
Geometry of hydrogen bonds for **III**

D–H···A	d(D–H) Å	d(H···A) Å	d(D···A) Å	∠(DHA) (°)	Symmetry transformation for acceptor
O(1)–H(1O1)···F(3)	0.82(3)	1.77(3)	2.5869(17)	168(2)	$-x+2, -y+1, -z$
N(1)–H(1N1)···F(2)	0.90(3)	1.85(3)	2.7278(19)	164(2)	$-x+1, -y+1, -z+1$
N(1)–H(1N1)···F(1)	0.90(3)	2.37(3)	3.014(2)	129(2)	x, y, z

Author's personal copy

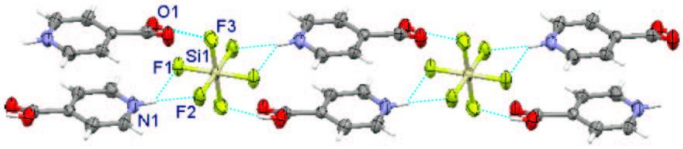

Fig. 2. Fragment of chain in **III**.

Table 4
IR spectral data (cm $^{-1}$) for **I–IV**

	ν(N$^+$H), ν(OH)	ν(OH···F)	ν(C = O), δ(N$^+$H), δ(H$_2$O)	ν_{ring}	ν(SiF), ρ(N$^+$H), δ(CCH), γ(H$_2$O)	δ(SiF$_2$)
I	3135 m,br	2710 m,br	1720 m	1610 m	767 sh	490 sh
		2590 m,br	1670 sh	1560 m	720 s	475 m
			1645 sh	1535 m	685 s	435 m
				1055 m		
II	3170 m,br	2720 m,br	1715 v,s	1580 s	745 v,s	490 sh
	3085 m,br		1690 sh	1545 m	720 sh	465 m
			1625 m	1040 m	680 m	435 sh
III	3210 m,br	2655 m,br	1725 sh	1610 m	745 sh	475 m
	3150 m,br		1700 m	1550 m	720 v,s	435 m
			1635 m	1040 m	690 sh	
IV	3420 sh	2525 sh	1720 sh	1590 s	770 s	465 m
	3310 m,br		1670 m	1560 m	725 s,br	450 sh
	3205 m,br		1645 sh	1500 m		435 sh
	3125 m,br		1630 m	1065 c		
				1050 sh		

Note: w = weak, m = medium, s = strong, v = very, sh = shoulder, br = broad.

Table 5
Thermogravimetric data for **I–IV**

Compound	Effect (°C)			Mass loss (%)		Assignment
	Type	t_0	t_M	Found	Calcd	
$(L^1H)_2[SiF_6]$	*endo*	145	200	37.1	36.9	Elimination of 2 mol HF + 1 mol SiF_4
	endo	205	223	97.0	100	Decomposition of L^1
$(L^2H)_2[SiF_6]$	*endo*	175	207	–	10.3	Elimination of 2 mol HF
	endo	–	220	35.0	36.9	Elimination of 1 mol SiF_4
	endo	225	235	–	–	Melting of L^2
	endo	258	270	96.0	100	Decomposition of L^2
$(L^3H)_2[SiF_6]$	*endo*	185	241	37.4	36.9	Elimination of 2 mol HF + 1 mol SiF_4
	endo	257	308	98.0	100	Decomposition of L^3
$(L^4H)_2[SiF_6]\cdot 2H_2O$	*endo*	100	130	9.0	6.8	Elimination of 2 mol H_2O
	endo	145	170	14.0	14.4	Elimination of 2 mol HF
	endo	176	195	29,0	27,4	Elimination of 1 mol SiF_4
	endo	211	450	96,0	100	Decomposition of L^4

intermolecular OH···F hydrogen bonds which are absent in the structures of pyridinium and pycolinium salts.

Solubility data for **I–IV** as well as for hexafluorosilicates of pyridinium, 2-methylpyridinium and several functionalized derivatives of carboxypyridinium and 2-carboxyquinolinium are summarized in Table 6. The introduction in the pyridinium cation of H-donor functional groups, -COOH, –CONHNH$_2$, –CONH$_2$, –CSNH$_2$ essentially (in some cases more than by order of magnitude) decreases the solubility of the relevant hexafluorosilicates. The observed differences in the solubility of the hexafluorosilicates can be explained by the specificity of H-bonding in the discussed compounds. So, quite apparently, that pyridinium (2-methylpyridinium) cation can function as a single H-donor (one H-bond from NH$^+$-group), whereas basing on the X-ray data in the salts the carboxypyridinium (2-carboxyquinolinium) cations donate two strong H-bonds, OH···F and NH···F (COOH and NH$^+$–groups). The embodying of auxilary interionic NH···F H-bonds (besides that formed by NH$^+$-group) with participation of NHNH$_3^+$ fragment is structurally confirmed also for the hexafluorosilicate [4-H$_3$NHN(O)CC$_5$H$_4$NH][SiF$_6$] [16]. Thus, cation functionalization by introduction of substituents with H-donor properties is accompanied by amplification of interionic H-interactions and results in a lower solubility of the relevant hexafluorosilicates. It is interesting to note, that from the point of

Table 6
Solubility of pyridinium hexafluorosilicates and its substituted derivates in water

Compound	Solubility (mol%) 25 °C
$(C_5H_5NH)_2[SiF_6]$	19.6
$(2\text{-}CH_3C_5H_4NH)_2[SiF_6]$	11.6
$[2\text{-}HO(O)CC_5H_4NH]_2[SiF_6]$	5.33
$[3\text{-}HO(O)CC_5H_4NH]_2[SiF_6]$	3.33
$[4\text{-}HO(O)CC_5H_4NH]_2[SiF_6]$	0.80
$[2\text{-}HO(O)CC_9H_6NH]_2[SiF_6]\cdot 2H_2O$	1.75
$[4\text{-}H_3NHN(O)CC_5H_4NH][SiF_6]$	0.87
$[2\text{-}H_3NHN(O)CC_9H_6NH][SiF_6]$	0.24
$[3\text{-}H_2N(O)CC_5H_4NH]_2[SiF_6]$	0.39
$[2\text{-}C_2H_5\text{-}4\text{-}H_2N(S)CC_5H_3NH]_2[SiF_6]$	0.10

Author's personal copy

view of Davies's group numbers conception [17] used for a qualitative estimation of the hydrophilic–lipophilic balance (HLB) in a series of complexes of a similar composition and structure and not taking into account the effects of H-bonding, compounds $[n\text{-HO(O)CC}_5\text{H}_4\text{NH}]_2[\text{SiF}_6]$ (n = 2, 3, 4) should differ by greater solubility in comparison with salts $(\text{RC}_5\text{H}_4\text{NH})_2[\text{SiF}_6]$ (R = H, CH_3) (within the framework of model [17] the COOH-group provides the hydrophilic contribution to the HLB of the complex against to the lipophilic contribution of CH, CH_3 groups). Besides, the account of effects of H-bonding allows to explain the differences in the solubility of the pyridinium $(\text{RC}_5\text{H}_4\text{NH})_2[\text{SiF}_6]$ and phenylammonium $(\text{RC}_6\text{H}_4\text{NH}_3)_2[\text{SiF}_6]$ salts [18]: in spite of the formal concurrence of the HLB characteristics, the $(\text{RC}_6\text{H}_4\text{NH}_3)_2[\text{SiF}_6]$ salts exhibit a lower solubility. It can be provoked by the ability of the $\text{RC}_6\text{H}_4\text{NH}_3^+$ cation to donate three H-bonds (without the account of effects of the substituent R) [8,18], while for the $\text{RC}_5\text{H}_4\text{NH}^+$ cation—only one hydrogen bond.

It is possible to ascertain, that in the carboxypyridinium (2-carboxyquinolinium) hexafluorosilicates the interionic H-bonds carry out the structural and stabilizing functions and noticeably influence the structural characteristics of the anions and salts properties. The sensitivity of the geometry of $[\text{SiF}_6]^{2-}$ anion to the effects of XH···F (X = N, O) H-bonds is manifested in **I–III** as an antibate relationship of the Si–F and X···F distances, and as a consequence, as an essential redistribution of the Si–F bond distances in the anion. At the same time the solubility of the pyridinium salts $(\text{RC}_5\text{H}_4\text{NH})_2[\text{SiF}_6]$ depends on a number of short interionic H-contacts and decreases with their increase upon introduction in the cation of the H-donor substituents. It might be concluded, that the cation functionalization can serve as a convenient tool for directional change of physicochemical properties of "onium" hexafluorosilicates.

3. Experimental

The IR-absorption spectra were recorded on a spectrophotometer Specord 75IR (range 4000–400 cm^{-1}, samples as suspension in Nujol mulls between KRS-5 windows). The mass spectra were registered on a spectrometer MX-1321 (direct input of a sample in a source, energy of ionizing electrons 70 eV). The thermogravimetric experiments were carried out on a OD-102 derivatograph of a system F. Paulik–J. Paulik–L. Erdey in ambient conditions (Al_2O_3 internal standard, heating rate of a sample 5°/min, sensitivity of DTA and DTG—1/10 or 1/5 from maximal, samples 150–200 mg). The isothermal conditions of experiments on detection of a solubility of hexafluorosilicates (t = 25 ± 0.2 °C) were provided with the help of an ultra thermostat U15.

3.1. Synthesis of bis(2-carboxypyridinium) hexafluorosilicate (I)

Pyridine-2-carbonic acid (L^1; 0.123 g, 1 mmol) was dissolved in boiling methanol (3 mL) and to the obtained solution the fluorosilicic acid (FSA, 0.9 mL, molar ratio L^1: FSA = 1:3) was added. A reaction mixture stored at ambient conditions prior to the beginning of crystallization of the reaction product, which was obtained in an approximately qualitative yield. Colourless transparent crystals of the composition $(L^1H)_2SiF_6$ (**I**) with mp 180–182 °C. Anal. found, %: Si 6,33, N 7,41, F 25,11. Calcd for $C_{12}H_{12}F_6N_2O_4Si$, Si 6,83, N 6,81, F 27,72. Mass spectrum: $[ML^1]^+$ (m/z = 123, I = 100%), SiF_3^+ (m/z = 85, I = 41%).

3.2. Synthesis of bis(3-carboxypyridinium) hexafluorosilicate (II)

Pyridine-3-carbonic acid (L^2, 0.123 g, 1 mmol) was dissolved in boiling ethanol (10 mL) and to obtained solution water (2 mL) and 45% FSA (0.9 mL) were added. A reaction mixture subjected to isothermal evaporation at ambient conditions. Colourless transparent crystals of composition $(L^2H)_2SiF_6$ and mp 248–250 °C were obtained in an approximately qualitative yield. Anal. found, %: Si 7,11, N 6,09, F 29,31. Calcd for $C_{12}H_{12}F_6N_2O_4Si$, Si 6,83, N 6,81, F 27,72. Mass spectrum: $[ML^2]^+$ (m/z = 123, I = 52%); SiF_3^+ (m/z = 85, I = 100%); $[ML^2\text{–COOH}]^+$ (m/z = 78, I = 26%).

3.3. Synthesis of bis(4-carboxypyridinium) hexafluorosilicate (III)

Pyridine-4-carbonic acid (L^3, 0.123 g, 1 mmol) was dissolved in boiling water (10 mL) and to obtained solution 45% FSA (0.9 mL) was added. A reaction mixture subjected to isothermal evaporation at ambient conditions. Colourless transparent crystals of composition $(L^3H)_2SiF_6$ with mp >220 °C (sublimation) were obtained in an approximately qualitative yield. Anal. found, %: Si 6,67, N 7,09, F 28,85. Calcd for $C_{12}H_{12}F_6N_2O_4Si$, Si 6,83, N 6,81, F 27,72. Mass spectrum: $[ML^3]^+$ (m/z = 123, I = 100%); SiF_3^+ (m/z = 85, I = 48%); $[ML^3\text{–COOH}]^+$ (m/z = 78, I = 41%).

3.4. Synthesis of bis(2-carboxyquinolinium) hexafluorosilicate dihydrate (IV)

Quinoline-2-carbonic acid (L^2, 1.73 g, 10 mmol) was dissolved in boiling methanol (20 mL) and to obtained solution 45% FSA (9 mL, molar ratio L^4: FSA = 1: 3) was added. A reaction mixture stored at ambient conditions prior to the beginning crystallization of the reaction product, colourless transparent crystals of composition $(L^4H)_2SiF_6{\cdot}2H_2O$ with mp >200 °C (with decomposition) were obtained in an approximately qualitative yield. Anal. found, %: Si 5,62, N 5,48, F 23,51. Calcd for $C_{20}H_{20}F_6N_2O_6Si$, Si 5,34, N 5,32, F 21,65. Mass spectrum: $[ML^4]^+$ (m/z = 173, I = 44%); $[ML^4\text{–COOH}]^+$ (m/z = 129, I = 100%); SiF_3^+ (m/z = 85, I = 69%).

3.5. Structure determination

The X-ray intensity data were collected at a room temperature on a Nonius Kappa CCD diffractometer equipped with graphite monochromated Mo Kα radiation using ϕ–ω rotation. Unit cell parameters were obtained and refined using the whole data set. Experimental data reduction and cell refinement were performed using DENZO [19] package. The structure solution and refinement proceeded using SHELX-97 program package [20]. Direct methods yielded all non-hydrogen atoms of the asymmetric unit which were treated anisotropically. C-bound hydrogen atoms were placed in calculated positions with their isotropic displacement parameters riding on those of the parent atoms, while the N-bound and O-bound H-atoms were found from differential Fourier maps at an intermediate stage of the refinement and were treated isotropically. Crystallographic data (cif file) for the structural analysis of compound **III** has been deposited with the Cambridge Crystallographic Data Center, CCDC No. 682042. Copies of this information may be obtained free of charge from The Director, CCDC, 12 Union Road, Cambridge, CB2 1EZ, UK (Fax: +44 1233 336 033; E-mail: deposit@ccdc.cam.ac.uk or http://www.ccdc.cam.ac.uk).

Acknowledgement

The diffraction data were collected at the Schulich Faculty of Chemistry, Technion, The Haifa, through the cooperation of Professor Menahem Kaftory whom we would like to acknowledge.

Author's personal copy

References

[1] S. Han, D.S. Shihabi, C.D. Chang, J. Catal. 196 (2000) 375–378.
[2] D.E. Clark, Patent 4,689,137 USA (1987).
[3] V.O. Gelmboldt, Russ. J. Inorg. Chem. 34 (1989) 231–232.
[4] R.C. Sheridan, Patent 112,784 USA (1989).
[5] H.S. Baltruschat, A. Brandt, Patent WO 02/15694 A2 (2002).
[6] Y. Katayama, M. Yokomizo, T. Miura, T. Kishi, Electrochemistry 69 (2001) 834–836.
[7] C. Airoldi, R.F. de Farias, J. Fluor. Chem. 103 (2000) 53–55.
[8] V.O. Gelmboldt, L.Kh. Minacheva, E.V. Ganin, V.S. Sergienko, Russ. J. Inorg. Chem. 51 (2006) 1561–1564.
[9] V.O. Gelmboldt, E.V. Ganin, K.V. Domasevitch, Acta Crystallogr. C63 (2007) o530–o534.
[10] V.O. Gelmboldt, L.Kh. Minacheva, E.V. Ganin, V.S. Sergienko, Russ. J. Inorg. Chem. 53 (2008) 873–876.
[11] B.D. Conley, B.C. Yearwood, S. Parkin, D.A. Atwood, J. Fluorine Chem. 115 (2002) 155–160.
[12] M. Szafran, Z.D. Szafran, A. Addlagatta, M. Jaskolski, J. Mol. Struct. 589 (2001) 267–272.
[13] V.P. Petrosyan, A.A. Ennan, Russ. J. Inorg. Chem. 24 (1979) 1562–1565.
[14] A. Albert, E. Sergeant, Ionization Constants of Acids and Bases, Wiley, New York, 1962.
[15] A.R. Katritzky (Ed.), Physical Methods in Heterocyclic Chemistry, vol. 3, Academic Press, New York, 1971.
[16] V.O. Gelmboldt, V.N. Davydov, L.V. Koroeva, E.V. Ganin, Russ. J. Inorg. Chem. 47 (2002) 1094–1101.
[17] V.Yu. Kukushkin, Yu.N. Kukushkin, Teoriya i Praktika Sinteza Koordinatsionnykh Soedinenii (Theory and Practice of Synthesis of Coordination Compounds), Nauka, Leningrad, 1990, p. 260s.
[18] V.O. Gelmboldt, E.V. Ganin, L.V. Koroeva, L.Kh. Minacheva, V.S. Sergienko, A.A. Ennan, Russ. J. Inorg. Chem. 51 (2006) 194–201.
[19] Z. Otwinowski, W. Minor, in: C.W. Carter, R.M. Sweet (Eds.), Methods in Enzymology, 276, Academic Press, London, 1996, p. 307.
[20] G.M. Sheldrick, SHELXS97 and SHELXL97, University of Göttingen, Germany, 1997.

Додаток Н.

Копія статті. “Inclusion of triphenylmethane derivatives by crown and linear O-containing molecules : selective interactions and crystal structure”

PAPER www.rsc.org/crystengcomm | CrystEngComm

Inclusion of triphenylmethane derivatives by crown and linear O-containing molecules : selective interactions and crystal structures†

Marina S. Fonari,*[a] Yurii A. Simonov,[a] Wen-Jwu Wang,[b] Shang-Wei Tang[b] and Eduard V. Ganin[c]

Received 13th June 2008, Accepted 12th August 2008
First published as an Advance Article on the web 8th October 2008
DOI: 10.1039/b810076d

The sulfamide derivative of triphenylmethanol, 3-[hydroxy(diphenyl)methyl]benzenesulfonamide $(H_2NSO_2Ph)Ph_2COH$ was synthesized and, alongside with the parent triphenylmethanol and triphenylmethylamine, was investigated for selective interactions with crown ethers of different dimensionality (12-18-membered cycles). The molecule of 12-crown-4 (12C4) appeared to be the best candidate for Ph_3COH, Ph_3CNH_2 and $Ph_3CNH_3 \cdot NCS$, while $(H_2NSO_2Ph)Ph_2COH$ forms the complex exclusively with 18-crown-6 (18C6). The triphenylammonia trifluoroacetate, $Ph_3CNH_3 \cdot CF_3COO$, selectively forms the complex only with 2-methoxyethanol. The crystalline products of the compositions $(Ph_3COH)_2 \cdot 12C4$, $(Ph_3CNH_2)_2 \cdot 12C4$, $(Ph_3CNH_3 \cdot NCS)_2 \cdot 12C4$, $[(H_2NSO_2Ph)Ph_2COH]_2 \cdot 18C6$ and $Ph_3CNH_3 \cdot CF_3COO\ CH_3OCH_2CH_2OH$ were obtained and studied by X-ray single crystal diffraction.

Introduction

Publication by Charles J. Pedersen of the synthesis of crown ethers and their property to form host guest complexes with cations and comparatively small neutral guest molecules[1,2] has initiated the search and investigation of new, functionally isomorphous to crown ethers host molecules,[3–11] like cyclic cryptands, calixarenes and calixcrowns, cyclodextrines,[12] and acyclic molecules like aromatic diols,[8] arylureas,[13,14] derivatives of triphenylmethane (tritane)[7,9,14] *etc.* The numerous studies revealed the low selectivity of triphenylmethanol (tritanol, Ph_3COH) which binds in supramolecular complexes methanol, acetone, dimethyl formamide, dimethylsulfoxide, 1,4-dioxane, morpholine, piperidine, N-methylpiperazine, phenoxine,[9,15] tetrahydrofurane.[16] Triphenylsilanol Ph_3SiOH, the precise analogue of triphenylmethanol, in its turn forms stable adducts with dimethylsulfoxide and 1,4-dioxane due to O H···O and C H···π(arene) interactions.[17,18] Similarly, triphenylmethanaminium chloride forms an inclusion compound with acetone.[19] Now we are witnesses to the growing numbers of successful application of bulky host molecules. Thus, using excellent inclusion properties of bulky bisphenols Csöregh and co-workers[20] have stabilized carboxylic acid and ester molecules in a monomeric state for spectroscopic investigation. The recent research of Tohnai *et al.*[21] has demonstrated the triphenymethylamine ability for an efficient and robust fabrication of [4 + 4] ion-pair clusters consisting of a wide range of sulfonic acids with an emphasis on the efficiency of the combination of sterically hindered triphenylmethylamine and sulfonate ions (complementarity in hydrogen bonding, steric effects of the substituents, acidity of the sulfonic acids). In 1998 Hayashi *et al.*[22] showed on fluorosubstituted triphenylmethanol derivatives that the C H··· F(-C) interactions control the packing motif as well as the thermal stability of the crystal, in continuation in the hot *CrystEngComm* article Schollmeyer *et al.*[23] demonstrated that the trityl alcohols bearing three bromine or three iodine atoms at the *para*-positions of the aromatic units, as well as the fluorosubstituted derivatives of triphenylmethanol may be a very useful platform for analysing OH···π and halogen π interactions as driving forces in crystal packing.

Surprisingly, apart from the two known examples of Ph_3SiOH[24] and Ph_3CSH[25] inclusion by 12-crown-4 (12C4), no systematic study of crown inclusion into the network of these bulky molecules has been carried out so far. This has motivated us to synthesize and study by X-ray diffraction the crystalline inclusion complexes of tritane derivatives with crown ethers of different dimensionality with an emphasis on the selectivity of interactions in these binary systems.

Experimental

Preparation of the crystalline inclusion compounds

It has been stated that spontaneous evaporation of solvents from the mixture of coronands **I–III** with triphenylmethanol (**IVa**), 1,1,1-triphenylmethanamine (**IVb**) and 1,1,1-triphenylmethanaminium thiocyanate (**IVc**) results in the crystalline molecular complexes of compositions $(\mathbf{IVa})_2.\mathbf{I}$ (complex **VI**), $(\mathbf{IVb})_2.\mathbf{I}$ (complex **VII**), $(\mathbf{IVc})_2.\mathbf{I}$ (complex **VIII**), respectively (Scheme 1).

The precipitation of **VI** from methanol solution indicates its higher stability in comparison with the triphenylmethanol complex with methanol.[9,15] The incorporation of the H-donor sulfamide group in the phenyl ring of **IVa** molecule yielding the

[a]*Institute of Applied Physics Academy of Sciences of Moldova, Academiei str., 5, MD-2028 Chisinau, R. Moldova. E-mail: fonari.xray@phys.asm.md; Fax: +373 22 72 58 87; Tel: +373 22 73 81 54*
[b]*Department of Chemistry Tamkang University, 151 Ying-Chuan Road, Tamsui, Taipei, 25137, Taiwan (ROC). E-mail: wjw@mail.tku.edu.tw; Fax: +886-2-2620-9924; Tel: +886-2-26215656(2530)*
[c]*Odessa State Environmental University, Ministry of Education and Sciences of Ukraine, Lvovskaya str. 15, Odessa, 65016, Ukraine. E-mail: edganin@yahoo.com; Tel: +38-048-7852711*

† CCDC reference numbers 690773–690777. For crystallographic data in CIF or other electronic format see DOI : 10.1039/b810076d

 This journal is © The Royal Society of Chemistry 2009

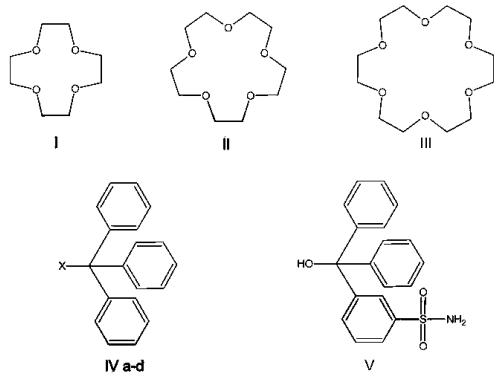

IV: X = OH (a), NH_2 (b), NH_3SCN (c), NH_3CF_3COO (d).

Scheme 1 Formulae of the substances used.

3-[hydroxy(diphenyl)methyl]benzenesulfonamide **V** drastically changes the mode of intermolecular recognition and results in the extraction of the largest 18C6 from the reaction mixture of **I, II, III** with the formation of the crystalline molecular complex of the composition $(\mathbf{V})_2.\mathbf{III}$ (complex **IX**). In previously reported studies no selectivity in the interaction of neutral molecules with the titled crown ethers was registered.[4] Moreover, the bulky di(benzenesulfonyl)amine $HN(SO_2C_6H_5)_2$ yields crystalline molecular complexes both with **I**[26] and **III**.[27–29] The replacement of the thiocyanate anion (**IVc**) by trifluoroacetate (**IVd**) dramatically changes the complexation process. From the methanolic mixture of **I, II, III**, compound **IVd** is reverted in an invariable form, while from the solution **IVd**–**I**–methanol–2-methoxyethanol the crystalline complex of triphenylmethanaminium trifluoroacetate with 2-methoxyethanol (compound **X**) is precipitated selectively. Thus, herein for the first time the selective interaction of bulky triphenylmethane derivatives with crown ethers is described with an emphasis on the possibility of crown ethers' separation[30] similar to the procedure described earlier.[31,32]

The initial chemicals were used as received from Aldrich without further purification. The ^{1}H NMR spectra were recorded with a Bruker AC 300 instrument at 300 MHz using tetramethylsilane as an internal reference. Thin-layer chromatography was conducted on Silufol plates with 1 : 8 methanol–chloroform as eluent and ninhydrin as developer. The crown ethers appeared as gray spots against a pink background.

Compound **V**, 3-[hydroxy(diphenyl)methyl]benzenesulfonamide: a mixture of 1,1′,1″-(chloromethanetriyl)tribenzene (2.788 g, 10 mmol) and chlorosulfonic acid (2.35 g, 20 mmol) was heated for 8 h at 150 °C and then cooled and poured onto 50 g of ice. The crystals were separated, placed into 40 ml of 25% aqueous ammonia, and heated with stirring for 12 h. The crystals that formed at 20 °C were washed with water, dried in air, and recrystallized from acetone–hexane (1 : 1). Yield: 1.80 g (53%), mp 188–190 °C, found, %: C 67.21; H 5.09; N 4.19; S 9.55, required for $C_{19}H_{17}NO_3S$: C 67.24; H 5.05; N 4.13; S 9.45. ^{1}H NMR ($CDCl_3$), δ, ppm: 7.27m, 7.44m (14H, CH).

Compound **VI**, triphenylmethanol–1,4,7,10-tetraoxacyclododecane, 2 : 1 : triphenylmethanol (260 mg, 1 mmol) and a mixture of 1,4,7,10-tetraoxacyclododecane (176 mg, 1 mmol), 1,4,7,10,13-pentaoxacyclopentadecane (220 mg, 1 mmol) and 1,4,7,10,13,16-hexaoxacyclooctadecane (264 mg, 1 mmol) were dissolved in methanol (10 ml) The colorless, transparent crystals were obtained by slow evaporation of solvents at room temperature for several days. Yield: 593 mg (85%), mp 147–148 °C, found, %: C 79.28; H 6.94, required for $C_{46}H_{48}O_6$: C 79.33; H 6.90. ^{1}H NMR ($CDCl_3$), δ, ppm: 1.62 (s 2H, OH), 3.70 (s, 16H, CH_2), 7.24–7.35 (m, 30H, CH).

Compound **VII**, 1,1,1-triphenylmethanamine–1,4,7,10-tetraoxacyclododecane, 2 : 1 : 1,1,1-triphenylmethanamine (259 mg, 1 mmol) and a mixture of 1,4,7,10-tetraoxacyclododecane (176 mg, 1 mmol), 1,4,7,10,13-pentaoxacyclopentadecane (220 mg, 1 mmol) and 1,4,7,10,13,16-hexaoxacyclooctadecane (264 mg, 1 mmol) were dissolved in a mixture of benzene/diethyl ether (1 : 2, 5 ml). The colorless, transparent crystals were obtained by slow evaporation of solvents at room temperature for several days. Yield: 495 mg (71%), mp 94–95 °C, found, %: C 79.51; H 7.25; N 4.03, required for $C_{46}H_{50}N_2O_4$: C 79.53; H 7.24; N 4.05. ^{1}H NMR ($CDCl_3$), δ, ppm: 1.86 (s, 4H, NH), 3.70 (s, 16H, CH_2), 7.20–7.32 (m, 30H, CH).

Compound **VIII**, triphenylmethanaminium thiocyanate–1,4,7,10-tetraoxacyclododecane, 2 : 1 : triphenylmethanaminium thiocyanate (318 mg, 1 mmol) and a mixture of 1,4,7,10-tetraoxacyclododecane (176 mg, 1 mmol), 1,4,7,10,13-pentaoxacyclopentadecane (220 mg, 1 mmol) and 1,4,7,10,13,16-hexaoxacyclooctadecane (264 mg, 1 mmol) were dissolved in methanol (15 ml). The colorless, transparent crystals were obtained by slow evaporation of solvents at room temperature for several days. Yield: 650 mg (80%), mp 170–172 °C, found, %: C 70.85; H 6.48; N 6.93; S 7.89, required for $C_{48}H_{52}N_4O_4S_2$: C 70.90; H 6.45; N 6.89; S 7.93. ^{1}H NMR ($CDCl_3$), δ, ppm: 3.70 (s, 16H, CH_2), 7.09–7.45 (m, 30H, CH).

Compound **IX**, 3-[hydroxy(diphenyl)methyl]benzenesulfonamide–1,4,7,10,13,16-hexaoxacyclooctadecane, 2 : 1 : 3-[hydroxy(diphenyl)methyl]benzenesulfonamide (340 mg, 1 mmol) and a mixture of 1,4,7,10-tetraoxacyclododecane (176 mg, 1 mmol), 1,4,7,10,13-pentaoxacyclopentadecane (220 mg, 1 mmol) and 1,4,7,10,13,16-hexaoxacyclooctadecane (264 mg, 1 mmol) were dissolved in a mixture of acetone/hexane (1 : 1, 15 ml). The colorless, transparent crystals were obtained by slow evaporation of solvents at room temperature for several days. Yield: 835 mg (98%), mp 174–176 °C, found, %: C 63.71; H 6.24; N 2.99; S 6.85, required for $C_{50}H_{58}N_2O_{12}S_2$: %: C 63.67; H 6.20; N 2.97; S 6.85. ^{1}H NMR (CD_3OD), δ, ppm: 3.62 (s, 24H, CH_2), 7.27–7.44 (m, 28H, CH).

Compound **X**, triphenylmethanaminium trifluoroacetate–2-methoxyethanol, 1 : 1 : triphenylmethanaminium trifluoroacetate (373 mg, 1 mmol) (373 mg, 1 mmol)) and 1,4,7,10-tetraoxacyclododecane (176 mg, 1 mmol) were dissolved in a mixture of methanol/2-methoxyethanol (1 : 1, 10 ml). The colorless, transparent crystals were obtained by slow evaporation of solvents at room temperature for several days. Yield: 380 mg (85%), mp 155–156 °C, found, %: C 64.13; H 5.80; N 3.19; F 12.64, required for $C_{24}H_{26}F_3NO_4$: %: C 64.18; H 5.83; N 3.12; F 12.68. ^{1}H NMR (DMSO), δ, ppm: 2.49 (s, 3H, CH_3), 3.49 (s, 4H, CH_2), 7.05–7.44 (m, 30H, CH).

Crystallographic studies

The X-ray intensity data for **VI–X** were recorded at room temperature on a Bruker SMART 1000 CCD area detector diffractometer employing graphite monochromatized Mo Kα radiation ($\lambda = 0.71073$ Å) in ϕ and ω scan mode. Final unit cell dimensions and positional data were obtained and refined on an entire data set. Integration and scaling resulted in a data set corrected for Lorentz and polarization effects using DENZO.[33] The scaling as well as global refinement of the crystal parameters were performed by SCALEPACK.[33] The absorption correction for **VI**, **VIII**, **IX** was applied using SADABS.[34] The structure solution and refinement proceeded similarly using SHELX-97 program package[35] for all structures. Direct methods yielded all non-hydrogen atoms of the asymmetric unit. Some disorder was found in **IX** and **X**: in **IX** the O6 and C24 atoms of the macrocyclic ring are disordered over two positions with partial occupancies of 0.90(1) and 0.10(1), and only the major component was refined in an anisotropic approximation. In **X** the triflate anion, CF_3COO^- and 2-methoxyethanol molecule were modeled in such a way that anionic F and O atoms and CH_3 O CH_2 CH_2– fragment of the 2-methoxyethanol molecule were disordered over two positions with partial occupancies of 0.58(1) and 0.42(1), respectively; both positions were refined in an anisotropic approximation. In all structures C bound H atoms were placed in calculated positions and were treated using a riding-model approximation, with $U_{iso}(H) = 1.2U_{eq}(C)$. The O- and N-bound H-atoms were determined from a difference Fourier map and were then allowed to refine isotropically with $U_{iso}(H) = 1.5U_{eq}(O,N)$. DFIX restraints were applied to the N H distances ($d = 0.86$ Å) in **VII** and **VIII**. Crystal data together with further details of data collections and refinement calculations are given in Table 1. CCDC reference numbers 690773 690777.

Results and discussion

Crystallographic description of the complexes

Compounds **VI** and **VII** crystallize in the same triclinic space group *P*1 and have close unit cell dimensions, as is evident from Table 1. For both compounds the asymmetric unit comprises one half of the 12C4 molecule that resides on an inversion center and one Ph_3COH or Ph_3CNH_2 molecule in general position (Fig. 1). The geometry of the Ph_3COH (Ph_3CNH_2) and 12C4 molecules is in agreement with the literature data.[24,25,36–38] The components are associated in the 1 : 2 molecular complexes *via* two single OH···O (NH···O) hydrogen bonds (Table 2).

The crystal packing in **VI** and **VII** is dictated by the combination of conventional OH···O (NH···O) hydrogen bonds that combine the molecules in the 1 : 2 complex, weak CH(arene)···O(crown) interactions that combine the complexes in the tape with the hydrophobic exterior formed by the phenyl rings (Fig. 2), and the concerted sextuple phenyl embrace (SPE)[39] between the Ph_3COH (Ph_3CNH_2) molecules in the neighboring tapes. Four host molecules surround each 12C4 molecule in the tape. The packing in **VII** is characterized by slightly increased distances analogous to those shown in Fig. 2a for **VI** with the second hydrogen of the amino group being free of any involvement in hydrogen bonding (very similar to the pure phase of Ph_3CNH_2).[37]

This ordering function of 12C4 molecule in **VI** and **VII** is looking very amazing in confrontation with the relative although rather restrictive examples available in CSD:[40] thus, inclusion of a dioxane molecule in the network of isostructural Ph_3COH[36] or Ph_3SiOH[17] molecules results in the 1 : 1 adduct in the first case and 1 : 2 adduct in the second one with pronounced changes in the crystal packing, although both compounds crystallize in the same triclinic crystal system. On the other hand, the same hosts yield the isostructural 2 : 1 aggregates with dimethylsulfoxide, both being crystallized in the same *C*2/*c* space group with close

Table 1 Summary of the crystal data of the five studied compounds, **VI–X**, and structure refinement parameters

Compound	VI	VII	VIII	IX	X
Composition	$2C_{19}H_{16}O \cdot C_8H_{16}O_4$	$2C_{19}H_{17}N\ C_8H_{16}O_4$	$2(C_{19}H_{18}N \cdot NCS) \cdot C_8H_{16}O_4$	$2C_{19}H_{17}NO_3S \cdot C_{12}H_{24}O_6$	$C_{19}H_{18}N \cdot C_2F_3O_2\ C_3H_8O_2$
CCDC number	690773	690777	690776	690775	690774
Formula weight	696.84	694.88	813.06	943.10	449.46
Crystal system	Triclinic	Triclinic	Monoclinic	Triclinic	Monoclinic
Space group	*P*1	*P*1	$P2_1/c$	*P*1	*C*2/*c*
a /Å	8.3614(7)	8.4675(8)	14.7301(15)	8.4707(6)	17.069(4)
b /Å	10.4963(9)	10.2973(13)	16.1984(16)	12.4699(9)	10.694(3)
c /Å	11.710(1)	11.943(2)	9.729(1)	12.8600(9)	26.520(7)
α/°	82.114(2)	84.058(9)	90.0	115.372(1)	90.0
β/°	86.716(2)	88.008(12)	103.97(2)	97.929(1)	107.367(5)
γ/°	66.740(2)	67.966(8)	90.0	99.540(1)	90.0
V /Å^3	935.25(14)	960.1(2)	2252.7(4)	1176.63(14)	4620(2)
Z	1	1	2	1	8
D_c /Mg m^{-3}	1.237	1.202	1.199	1.331	1.292
μ(MoKα)/mm^{-1}	0.081	0.076	0.165	0.179	0.103
F(000)	372	372	864	500	1888
Reflections collected / unique	5310/ 3605 [*R*(int) = 0.020]	3625 / 3373 [*R*(int) = 0.026]	12820 / 4413 [*R*(int) = 0.043]	6829 / 4541 [*R*(int) = 0.015]	12877 / 4554 [*R*(int) = 0.024]
Reflections with $I>2\sigma(I)$	2978	2622	1462	3154	3066
Goodness-of-fit	1.060	1.042	0.831	0.925	1.011
R, *wR* [$I>2\sigma(I)$]	0.048, 0.138	0.041, 0.111	0.054, 0.117	0.039, 0.096	0.043, 0.121

 This journal is © The Royal Society of Chemistry 2009

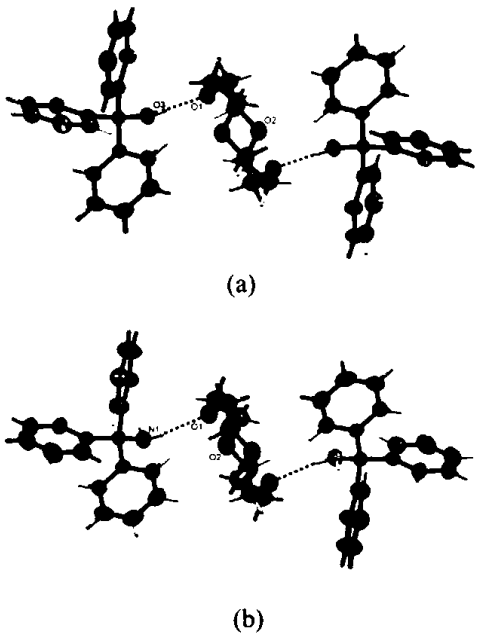

Fig. 1 ORTEP drawing (a) for **VI**, (b) for **VII** with a partial numbering scheme. Thermal ellipsoids are drawn at 50% probability level.

unit cell dimensions.[15-17] Ferguson and co-workers[36] analysing the series of the group 14 Ph_3MOH molecules (M = C, Si, Ge, Sn, Pb) revealed for them different crystal packing motifs: the C-, Si- and Ge-[17,41] derivatives represent hydrogen-bonded tetramers with the O-atoms in a flatten tetrahedral arrangement, while Sn- and Pb-containing molecules have structures consisting of zigzag chains of planar Ph_3M (M = Sn, Pb) groups joined by OH groups giving trigonal bipyramidal geometry at M,[42] whilst in Ph_3CSH,[43] a precise analogue of Ph_3COH as well as in $PhCNH_2$,[37] being isoelectronic with Ph_3COH, there are no intermolecular hydrogen bonding despite the availability of potential H-donors (SH, NH_2 groups) and H-acceptors (S, N-lone pair), and the structures consist of isolated molecules with no indication that the H-atoms take part in any hydrogen bonding. Concluding this section, the row of the relative crown-containing binary systems $(Ph_3COH)_2$.12C4 (**VI**), $(Ph_3CNH_2)_2$.12C4 (**VII**) (present work), $(Ph_3SiOH)_2$.12C4,[24] and $(Ph_3CSH)_2$.12C4[25] represents the isomorphous aggregates with close unit cell dimensions and a common structural motif. It permits to conclude the ordering and leveling function of the 12C4 molecule upon its inclusion.

The view of complex **VIII** is shown in Fig. 3. The ternary salt-like adduct **VIII** crystallizes in the centrosymmetric space group $P2_1/c$ and, similar to **VI** and **VII**, the 12C4 molecule resides on an inversion center. The components in the crystal are held together *via* the diverse system of charge-assisted hydrogen bonds, $NH^+\cdots$O(crown), $NH^+\cdots N^-(NCS^-)$ and $NH^+\cdots S^-(NCS^-)$ (Fig. 3, Table 2).

The tetrahedral ammonia group provides one hydrogen for the $NH^+\cdots$O interaction with a crown molecule and two hydrogens for interionic $NH^+\cdots N^-(NCS^-)$ and $NH^+\cdots S(NCS^-)$ interactions with two inversion-related NCS^- anions. Just as in the two

Table 2 Hydrogen bond distances (Å) and angles (°) for **VI–X**

D–H···A	d(D–H)	d(H···A)	d(D···A)	∠(DHA)	Symmetry transformation for acceptor
VI					
O(3)–H(3A)···O(1)	0.89(2)	1.94(2)	2.814(2)	169(2)	*x, y, z*
C(19)-H(19A)···O(2)	0.93	2.61	3.380(2)	141	*x, y, z*
C(8)-H(8A)···O(2)	0.93	2.59	3.482(2)	162	*x, y* − 1, *z*
VII					
N(1)–H(1N)···O(1)	0.89(2)	2.22(2)	3.087(2)	168(2)	*x, y, z*
C(19)-H(19A)···O(2)	0.93	2.66	3.426(2)	140	*x, y, z*
C(8)-H(8A)···O(2)	0.93	2.65	3.493(2)	152	*x, y* − 1, *z*
VIII					
N(1)–H(2N)···O(1)	0.89(2)	1.92(2)	2.790(3)	166(3)	*x, y, z*
N(1)–H(3N)···N(2)	0.90(2)	2.01(2)	2.892(4)	166(3)	*x, y, z*
N(1)–H(1N)···S(1)	0.90(2)	2.35(2)	3.246(3)	170(3)	−*x* + 1, −*y* + 2, −*z* + 1
IX					
O(3)–H(1O)···O(2)	0.77(2)	2.16(2)	2.917(2)	169(2)	*x*, −*y*, *z*
N(1)–H(1N)···O(5)	0.82(2)	2.37(2)	3.029(2)	138(2)	*x, y* − 1, *z*
N(1)–H(1N)···O(6)	0.82(2)	2.51(2)	3.086(2)	129(2)	*x, y* − 1, *z*
N(1)–H(2N)···O(4)	0.88(2)	2.25(2)	3.013(2)	145(2)	*x*, −*y*, *z*
N(1)–H(2N)···O(5)	0.88(2)	2.41(2)	3.135(2)	140(2)	*x*, −*y*, *z*
X					
N1–H(2N)···O(1)	0.94(2)	1.95(2)	2.877(5)	174(2)	*x, y, z*
N1–H(2N)···O(1′)	0.94(2)	1.98(2)	2.886(6)	162(2)	*x, y, z*
N1–H(1N)···O(2)	0.93(2)	1.93(2)	2.862(2)	177(2)	−*x, y*, −*z* + 1/2
N1–H(3N)···O(3)	0.95(2)	1.80(2)	2.752(11)	179(2)	*x, y, z*
N1–H(3N)···O(3′)	0.95(2)	1.82(2)	2.766(14)	174(2)	*x, y, z*
O(2)–H(2B)···O(4)	0.95(2)	1.71(3)	2.658(10)	173(2)	*x, y, z*
O(2)–H(2B)···O(4′)	0.95(2)	1.69(3)	2.640(10)	171(2)	*x, y, z*

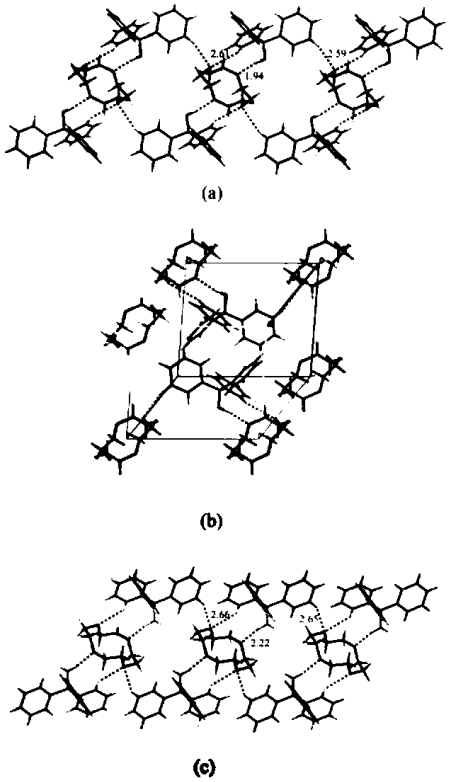

Fig. 2 Crystal packing for **VI** and **VII**, (a) fragment of tape in **VI** with the shortest C H···O distances shown by dashed lines, (b) fragments of adjacent tapes with SPE between two Ph_3COH molecules, (c) fragment of tape in **VII** with the shortest N H···O and C H···O distances shown by dashed lines.

previous structures, these concerted interactions combine the components in the tape propagated along the *c* axis in the crystal (Fig. 4). The neighboring tapes are packed in an antiparallel

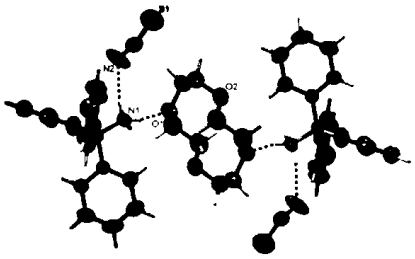

Fig. 3 ORTEP drawing for **VIII** with a partial numbering scheme. Thermal ellipsoids are drawn at 50% probability level.

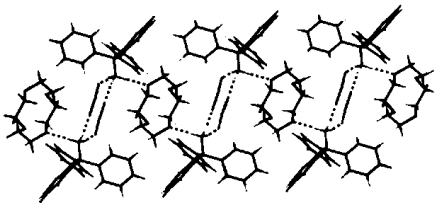

Fig. 4 Fragment of tape in **VIII**.

arrangement to maximize the SPE. The crystal architecture of **VIII** is very close to structure organization in tritylammonium chloride 1,4-dioxane solvate, $Ph_3CNH_3Cl.(CH_2CH_2O)_2$ (YAGSIJ refcode in CSD).[44]

As was stressed above, incorporation of the amidosulfoxide group into the phenyl ring of **IVa** results in competition between the two donor groups (SO_2NH_2 and OH) of **V** for the crown's oxygens and following the Etter's rule[45] in a preferable interaction of the stronger H-donor, SO_2NH_2 group with the macrocyclic oxygens *via* two bifurcated NH···O hydrogen bonds with the formation of 1 : 2 molecular complex **IX** (Fig. 5, Table 2). **IX** crystallizes in triclinic space group *P*1 where the 18C6 molecule resides on an inversion center. The hydroxyl group seeking for the next H-acceptor is responsible for the association of these complexes into tapes *via* OH···O(SO_2) hydrogen bonds (Fig. 6, Table 2). Similar to the previous examples, the tape in **IX** is characterized by the hydrophilic interior saturated by hydrogen bonds and two external hydrophobic sides formed by the phenyl rings. Compound **IX** represents the first known example of the inclusion of spacious 18C6 molecule in the lattice of triphenylmethanol derivative. The common feature of the crystal packing for **VI**–**IX** is a ribbon motif with crown inclusion within the ribbon and the SPE formulated between the neighboring ribbons.

Compound **X** of the 1 : 1 : 1 stoichiometry is formed as a result of the interaction of **IVd** with a linear 2-methoxyetanol molecule. **X** crystallizes in monoclinic space group *C*2/*c*. The content of the asymmetric unit is shown in Fig. 7. Similar to **VIII** it is a ternary complex where two hydrogens of the same ammonia group are involved in the NH^+···O(COO^-) and NH^+···O(2-methoxyethanol) contacts (Table 2). Furthermore, inside the complex the terminal hydroxyl group of the 2-methoxyethanol molecule participates in OH···O^-(COO^-) interaction with the second carboxyl oxygen. These three hydrogen bonds close the eleven-membered ring, $R_3^3(11)$ using a graph set notation.[45]

Contrary to **VIII** where each ammonia group interacts with two anions and one neutral crown molecule, in **X** the third ammonia hydrogen is involved into NH^+···O interaction with the second 2-methoxyethanol molecule related by the two-fold axis with the basic one. These concerted interactions combine two complexes into a six-membered calix-like capsule stabilized by 8 charge-assisted hydrogen bonds within the hydrophilic core that is covered by the hydrophobic exterior formed by six phenyl rings of two tritylammonia cations and two terminal methyl groups of 2-methoxyethanol molecules (Fig. 8). The CH···F interactions[22,23,46] between triflate anion and 2-methoxyethanol

 This journal is © The Royal Society of Chemistry 2009

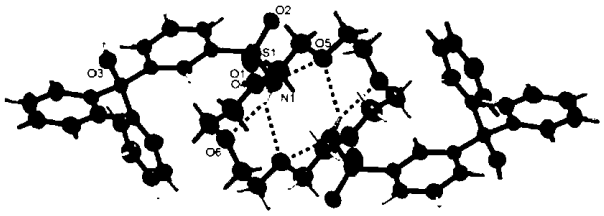

Fig. 5 ORTEP drawing for **IX** with a partial numbering scheme. Thermal ellipsoids are drawn at 50% probability level.

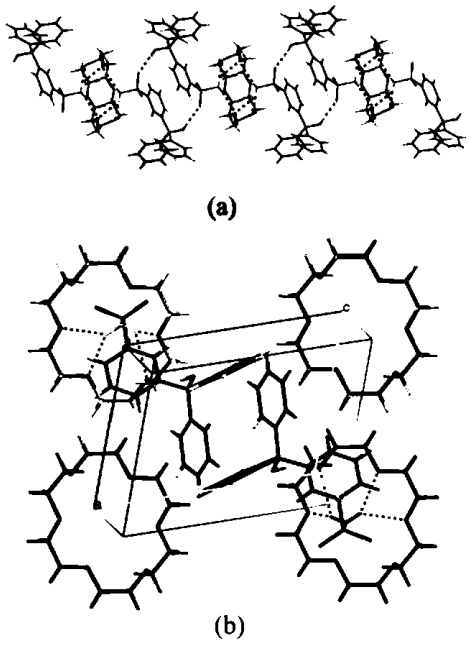

Fig. 6 Packing diagram for **IX** (a), fragment of tape (b), fragments of adjacent tapes with SPE between two **V** molecules.

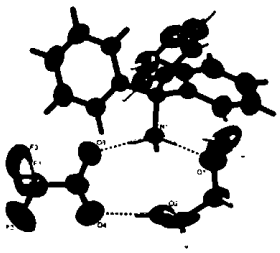

Fig. 7 ORTEP drawing for **X** with the partial numbering scheme. Thermal ellipsoids are drawn at 50% probability level.

molecule are responsible for the association of the 6-membered globules into tape running along the *b* direction in the crystal.

Thus, the present study amplifies the scanty family of trytilammonia salts by two novel representatives. Contrary to the trytile sulfonates studied so far[21] all of which represent binary adducts and formulate the well-defined [4 + 4] ion-pair clusters, **VIII** and **X** alongside the tritylammonium chloride acetone and tritylammonium chloride dioxane solvates [19,44] belong to the ternary compounds with the inclusion of the different O-containing neutral molecules (acetone, dioxane, 12C4, 2-methoxyethanol) in the ionic crystal lattice of the parent salt. The size and topology of these guests appear to be crucial for the final aggregates: linear acetone and 2-methoxyethanol molecules facilitate the formation of the isolated 6-membered clusters while the cyclic double-face 1,4-dioxane and 12C4 molecules provide extended 1D structures. In any closest environment [three anions,[21] two anions and one neutral molecule[19,44] or one anion and two neutral molecules (present work)] all three ammonium hydrogens are involved in the hydrogen bonding system.

Conclusions

For the first time the approaches of supramolecular chemistry were used to estimate the preferable in size crown ethers (in the order of 12–18-membered CEs) for interaction with triphenylmethane derivatives. The 12C4 molecule has proven to be the best candidate as it is selectively included in the crystal lattice of neutral Ph_3COH and Ph_3CNH_2 in the 1 : 2 ratio and in the ionic network of Ph_3CNH_3NCS in the 1 : 1 : 1 ratio. Contrary to the pure forms of Ph_3COH, Ph_3SiOH, Ph_3CSH, and Ph_3CNH_2 which differ essentially by the crystal packing, the corresponding binary aggregates with 12C4 appear to be isomorphous and ordered with each macrocyclic molecule entrapping by four bulky host molecules. The functionalization of one of the phenyl rings in the Ph_3COH molecule by the H_2NSO_2-group provides its involvement in the interaction with 18C6 in a traditional manner and excludes the hydroxyl group from the host–guest interactions. The supramolecular architecture of the studied tritylammonium salts is dictated by the concerted effect of the topology of the anion and the included neutral molecule, being 1D structure for $Ph_3CNH_3 \cdot NCS$ assimilating cyclic 12C4 molecule and the isolated six-membered capsule upon inclusion of linear 2-methoxyethanol molecules in the ionic lattice of $Ph_3NH_3 \cdot CF_3COO$. In all cases the common packing motif maximizes the SPE arrangement of the host molecules.

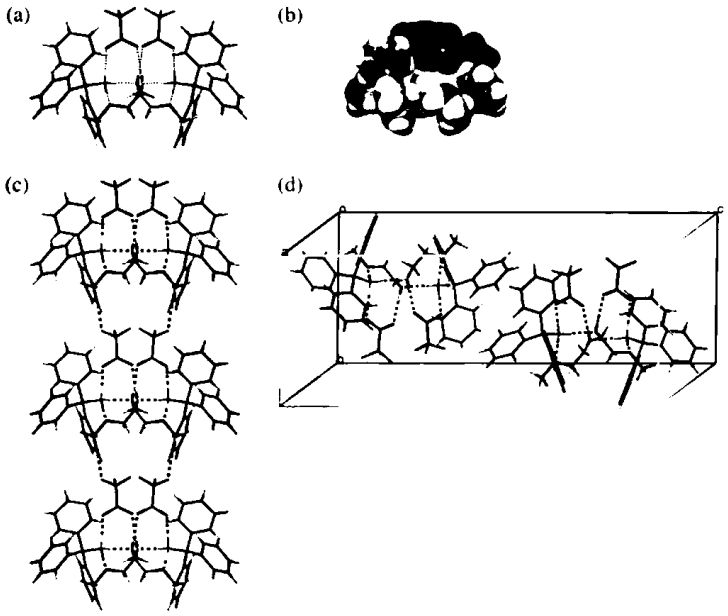

Fig. 8 Packing diagram for X· (a) network of hydrogen bonds shown by dashed lines within the six-membered cluster, (b) space-filling representation of the cluster, (c) column of clusters sustained by CH···F interactions, (d) the SPE between adjacent clusters.

Acknowledgements

E.V.G. and W.J.W. are indebted to the National Science Council of Taiwan 94-2811-M-032 project for financial support.

References

1 C. J. Pedersen, *J. Am. Chem. Soc.*, 1967, **89**, 7017.
2 C. J. Pedersen, *Angew. Chem., Int. Ed. Engl.*, 1988, **27**, 1021.
3 *Inclusion Compounds. Structural Aspects of Inclusion Compounds formed by Organic Host Lattices*, ed. J. L. Atwood, J. E. D. Davies and D. D. MacNicol, Academic Press, London, Orlando, San Diego, San Francisco, New York, Toronto, Montreal, Sydney, Tokyo, San Paulo, 1984, vol. 2, 499 pp.
4 *Host Guest Complex Chemistry. Macrocycles. Synthesis, Structure, Applications*, ed. A. Vogtle and E. Weber,Springer, Berlin, 1985, 511 pp.
5 J.-M. Lehn, *Supramolecular Chemistry/ Concepts and Perspectives*, VCH Verlagsgesellschaft mbH, Weinheim; New York; Basel; Cambridge; Tokyo, 1995, 334 p.
6 G. R. Desiraju, in *Comprehensive Supramolecular Chemistry*, ed. J-M. Lehn, J. L. Atwood, J. E. D. Davies, D. D. MacNicol and F. Wogtle, Pergamon, Oxford, New York, Tokyo, 1996, vol. 6, pp 1–22.
7 P. Dastidar andI. Goldberg, in *Comprehensive Supramolecular Chemistry*, ed. J-M. Lehn, J. L. Atwood, J. E. D. Davies, D. D. MacNicol and F. Wogtle, Pergamon, Oxford, New York, Tokyo, 1996, vol. 6, pp 305–350.
8 (*a*) F. Toda, in *Comprehensive Supramolecular Chemistry*, ed. J-M. Lehn, J. L. Atwood, J. E. D. Davies, D. D. MacNicol and F. Wogtle, Pergamon, Oxford, New York, Tokyo, 1996, vol. 6, pp 465–516; (*b*) E. Weber, N. Dörpinghaus and I. Goldberg, *J. Chem. Soc., Chem. Commun.*, 1988, 1566; (*c*) S. A. Bourne, L. R. Nassimbeni, M. L. Niven, E. Weber and A. Wierig, *J. Chem. Soc., Perkin Trans.*, 1994, **2**, 1215; (*d*) M. R. Caira, L. R. Nassimbeni, M. L. Niven, W.-D. Schubert, E. Weber and N. Dörpinghaus, *J. Chem. Soc., Perkin Trans.*, 1990, **2**, 2129; (*e*) A. Jacobs, N. L. Z. Masuku, L. R. Nassimbeni and J. H. Taljaard, *CrystEngComm*, 2008, **10**, 322.
9 E. Weber, in *Comprehensive Supramolecular Chemistry*, ed. J-M. Lehn, J. L. Atwood, J. E. D. Davies, D. D. MacNicol and F. Wogtle, Pergamon, Oxford, New York, Tokyo, 1996, vol. 6, pp 535–592.
10 M. R. Caira and L. R. Nassimbeni, in *Comprehensive Supramolecular Chemistry*, ed. J-M. Lehn, J. L. Atwood, J. E. D. Davies, D. D. MacNicol and F. Wogtle, Pergamon, Oxford, New York, Tokyo, 1996, vol. 6, pp 825–850.
11 A. Reichert, H. Ringsdorf and P. Schuhmacher, in *Comprehensive Supramolecular Chemistry*, ed. J-M. Lehn, J. L. Atwood, J. E. D. Davies, D. D. MacNicol and F. Wogtle, Pergamon, Oxford, New York, Tokyo, 1996, vol. 9, pp 313–350.
12 G. W. Gokel, W. M. Leevy and M. E. Weber, *Chem. Rev.*, 2004, **104**, 2723.
13 M. C. Etter, Z. Urbanczyk-Lipkowska, M. Zia-Ebrahimi and T. Panunto, *J. Am. Chem. Soc.*, 1990, **112**, 8415.
14 (*a*) K.-K. D. Ng and H. Hart, *Tetrahedron*, 1995, **51**, 7883; (*b*) E. Weber, N. Dörpinghaus and I. Csöregh., *J. Chem. Soc., Perkin Trans. 2*, 1990, 2167; (*c*) K. Eckardt, H. Paulus, H. Fuess, N. Onoda-Yamamuro and R. Ikeda, *J. Incl. Phenom.*, 1999, **35**(3), 431.
15 E. Weber, K. Skobridis and I. Goldberg, *J. Chem. Soc., Chem. Commun.*, 1989, 1195.
16 R. West, R. H. Baney and D. L. Powell, *J. Am. Chem. Soc.*, 1960, **82**, 6269.
17 K. F. Bowes, C. Glidewell and J. N. Low, *Acta Crystallogr., Sect. C: Cryst. Struct. Commun.*, 2002, **58**, o409.
18 S. A. Bourne, L. Johnson, C. Marais, L. R. Nassimbeni, E. Weber, K. Skobridis and F. Toda, *J. Chem. Soc., Perkin Trans. 2*, 1991, 1707.
19 M. Canle L, W. Clegg, I. Demirtas, M. R. J. Elsegood and H. Maskill, *J. Chem. Soc., Perkin Trans. 2*, 2000, 85.

 This journal is © The Royal Society of Chemistry 2009

20 I. Csöregh, S. Hirano, S. Toyota, P. Bombisz and F. Toda, *CrystEngComm*, 2004, **6**, 60.
21 N. Tohnai, Y. Mizobe, M. Doi, S. Sukata, T. Hinoue, T. Yuge, I. Hisaki, Y. Matsukawa and M. Miyata, *Angew. Chem., Int. Ed.*, 2007, **46**, 2220.
22 N. Hayashi, T. Mori and K. Matsumoto, *Chem. Commun.*, 1998, 1905.
23 D. Schollmeyer, O. V. Shishkin, T. Rühl and M. O. Vysotsky, *CrystEngComm*, 2008, **10**, 715.
24 E. A. Babaian, M. Huff, F. A. Tibbals and D. C. Hrncir, *J. Chem. Soc., Chem. Commun.*, 1990, 306.
25 M. S. Fonari, E. V. Ganin and W.-J. Wang, *Acta Crystallogr., Sect. C: Cryst. Struct. Commun.*, 2005, **61**, o431.
26 K. Wijaya, O. Moers, P. G. Jones and A. Blaschette, *Acta Crystallogr., Sect. C: Cryst. Struct. Commun.*, 1998, **54**, 818.
27 D. Henschel, A. Blaschette and P. G. Jones, *Z. Naturforsch*, 1995, **50b**, 128.
28 D. Henschel, A. Blaschette and P. G. Jones, *Z. Naturforsch.*, 1995, **50b**, 229.
29 D. Henschel, M. Naveke, T. Hamann, A. Blaschette and P. G. Jones, *Z. Naturforsch.*, 1995, **50b**, 913.
30 J. Dale and K. J. Daasvatn, *J. Chem. Soc., Chem. Commun.*, 1976, 295.
31 E. V. Ganin, V. F. Makarov, S. A. Kotlyar, N. G. Lukyanenko, M. S. Fonari, A. A. Dvorkin and A. YuSimonov, *Russ. Khim. Geterotsikl. Soedin.*, 1988, 1190.
32 A. A. Dvorkin, M. S. Fonari, S. T. Malinovskii, E. V. Ganin, A. YuSimonov, V. F. Makarov, S. A. Kotlyar and N. G. Lukyanenko, *Russ. Zh. Strukt. Khim.*, 1989, **30**, 96.
33 Z. Otwinowski and W. Minor, in *Methods in Enzymology, Macromolecular Crystallography, Part A*, ed. C. W. Carter and R. M. Sweet, Academic Press, London, 1996, vol. 276, p 307.
34 G. M. Sheldrick, *SADABS*, 1997, Bruker AXS Inc., Madison, WI-53719, USA.
35 G. M. Sheldrick: SHELXS97 and SHELXL97, *Programs for Crystal Structure Solution and Refinement*. University of Göttingen, Germany, 1997.
36 G. Ferguson, J. F. Gallagher, C. Glidewell, J. N. Low and S. N. Scrimgeour, *Acta Crystallogr., Sect. C: Cryst. Struct. Commun.*, 1992, **48**, 1272.
37 C. Glidewell and G. Ferguson, *Acta Crystallogr., Sect. C: Cryst. Struct. Commun.*, 1994, **C50**, 924.
38 A. Michalides, D. Henschel, A. Blaschette and P. G. Jones, *Z. Naturforsch.*, 1995, **50b**, 1018.
39 (*a*) A. I. Kitaigorodsky, *Molecular Crystals and Molecules*, Academic Press, New York, 1973; (*b*) I. Dance and M. Scudder, *J. Chem. Soc., Chem. Commun.*, 1995, 1039; (*c*) R. Thaimattam, F. Xue, J. A. R. P. Sarma, C. W. Mak and G. R. Desiraju, *J. Am. Chem. Soc.*, 2001, **123**, 4432; (*d*) J. J. Perry, G. J. McManus and M. J. Zaworotko, *Chem. Commun.*, 2004, 2534.
40 F. N. Allen, *Acta Crystallogr., Sect. B: Struct. Sci.*, 2002, **58**, 380.
41 (*a*) H. Puff, K. Braun and H. Reuter, *J. Organomet. Chem.*, 1991, **409**, 119; (*b*) G. Ferguson, J. F. Gallagher, D. Murphy, T. R. Spalding, C. Glidewell and H. D. Holden, *Acta Crystallogr., Sect. C: Cryst. Struct. Commun.*, 1992, **48**, 1228.
42 C. Glidewell and D. C. Liles, *Acta Crystallogr., Sect. B: Struct. Crystallogr. Cryst. Chem.*, 1978, **34**, 129.
43 G. Bernardinelli, M. Geoffroy and R. Franzi, *Z. Kristallogr.*, 1991, **195**, 147.
44 S. Parsons, K. Borisenko, D. Rankin and P. Wood, *private communication*, 2004.
45 (*a*) M. Etter, *J. Phys. Chem.*, 1991, **95**, 4601; (*b*) M. Etter, *Acc. Chem. Res.*, 1990, **23**, 120.
46 E. D'Oria and J. J. Novoa, *CrystEngComm*, 2008, **10**, 423.

Додаток О.

Копія статті. “Hexafuorosilicates of bis(aminopyridinium). The relationship between H-bonding system and solubility of salts ”

Provided for non-commercial research and education use.
Not for reproduction, distribution or commercial use.

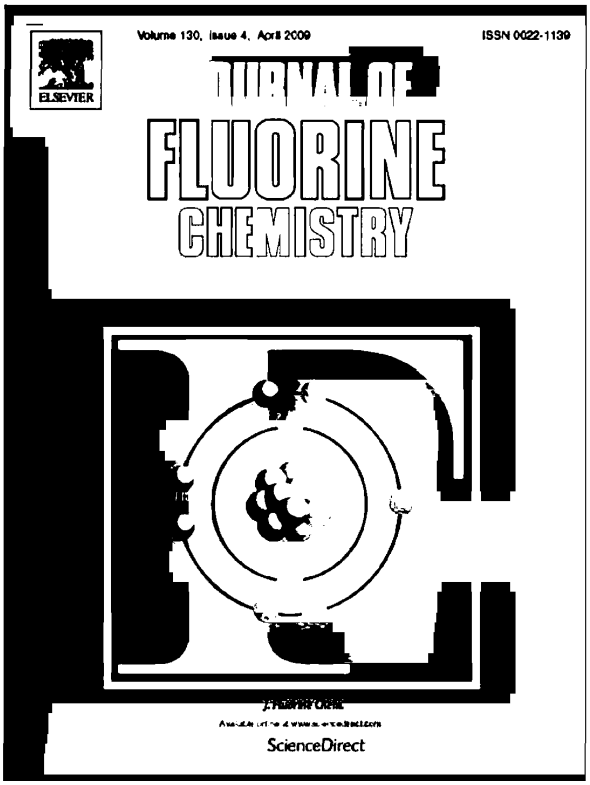

This article appeared in a journal published by Elsevier. The attached copy is furnished to the author for internal non-commercial research and education use, including for instruction at the authors institution and sharing with colleagues.

Journal of Fluorine Chemistry 130 (2009) 428–433

Contents lists available at ScienceDirect

Journal of Fluorine Chemistry

journal homepage: www.elsevier.com/locate/fluor

Hexafluorosilicates of *bis*(aminopyridinium). The relationship between H-bonding system and solubility of salts

Vladimir O. Gelmboldt [a], Eduard V. Ganin [b], Marina S. Fonari [c,*], Larisa V. Koroeva [a], Yurii Ed. Ivanov [d], Mark M. Botoshansky [e]

[a] Physico-Chemical Institute of Environment and Human Protection of Ministry of Education and Science of Ukraine and National Academy of Sciences of Ukraine, Preobrazhenskaya str., 3, 65082, Odessa, Ukraine
[b] Odessa State Environmental University of Ministry of Education and Science of Ukraine, Lvovskaya str., 15, 65016, Odessa, Ukraine
[c] Institute of Applied Physics, Academy of Sciences of Moldova, Academy str., 5, MD2028 Chisinau, Republic of Moldova
[d] A.V. Bogatsky Physico-Chemical Institute of National Academy of Sciences of Ukraine, Lustdorfskaya Doroga, 86, 65080, Odessa, Ukraine
[e] Schulich Faculty of Chemistry, Technion-Israel Institute of Technology, Technion City, 32000 Haifa, Israel

ARTICLE INFO

Article history:
Received 16 December 2008
Received in revised form 27 January 2009
Accepted 27 January 2009
Available online 5 February 2009

Keywords:
Hexafluorosilicate
Heterocyclic amine
Solubility
Hydrogen bonding
Crystal structure

ABSTRACT

Pyridinium hexafluorosilicates of the composition $(LH)_2[SiF_6]$ (I, II, IV, L = 2-aminopyridine, 3-aminopyridine, and 2,6-diaminopyridine) and $(LH)_2[SiF_6]\cdot H_2O$ (III, L = 4-aminopyridine) were separated as crystalline products of interaction of fluorosilicic acid with relevant aminopyridines. The compounds were characterized by IR, mass-spectrometry, potentiometry, solubility data, and in the case of I and IV by X-ray crystallography. The relationship between the salts structure and some physical properties is discussed.

© 2009 Elsevier B.V. All rights reserved.

1. Introduction

Anion co-ordination or recognition is an area that has been receiving increased attention in the past two decades [1,2] with particular emphasis on the thermodynamics of interactions between the anions and a wide variety of synthetic hosts where pre-organization and cooperative effects are of a crucial importance [3]. Contrary to the "classic" complexes of transition metals generated due to coordinative covalent bonds the coordination chemistry of anions [4] is based on interionic H-bonds with synthetic organic receptors. The wide range of recently developed anion receptors include amides and thioamides, pyrroles and indoles, ureas and thioureas, ammonium, guanidinium, imidazolium, as well as the receptors with hydroxyl groups [5,6]. Apparently, H-bonds should definitely influence on the geometry of anion (in the case of complex anion) and on physicochemical properties of complex in a whole; moreover, the effects of H-bonds have appeared to be decisive in synthetic chemistry, for example, for the stabilization of the poor stable anions of the type $[H_{n-1}F_n]^-$ (n = 3–5) [7–9], $[SiF_5(H_2O)]^-$ [10] and $[GeF_5(H_2O)]^-$ [11]. The high H-acceptor affinity of fluoride-anion [12], which is substantially preserved also by a covalently bound fluorine in complex fluoro-containing anions such as $[SiF_6]^{2-}$ [13], makes "onium" hexafluorosilicates attractive models to clarify the features that influence on the interionic H-bonds and on the structural properties of the complexes. For the naked halides the host containing NH moieties has been known as good binding agent and as Mascal has underlined [14] the most effective H-bond donor is the $[N-H]^+$ functionality that promotes interactions with halides through a combination of electrostatic interactions and hydrogen bonding. Earlier we have demonstrated the ways of binding of $[SiF_6]^{2-}$ anions by protonated aza-macrocycles [10] as well as by aromatic molecules, derivatives of benzoic or pyridinecarbonic acids [15,16]. The present communication continues the previous investigations and is devoted to the study of relationship between the composition and some properties of aminopyridinium hexafluorosilicates. Both 2-aminopyridine and 2,6-diaminopyridine are very popular co-crystal formers in supramolecular chemistry of anions [17,18]. In contrast to *para*-aminopyridine, it is found that *ortho*-aminopyridines (2-aminopyridine and 2,6-diaminopyridine)

* Corresponding author. Tel.: +373 22 73 81 54; fax: +373 22 72 58 87.
E-mail addresses: eksvar@ukr.net (V.O. Gelmboldt), edganin@yahoo.com (E.V. Ganin), fonari xray@phys asm.md, fonari xray@gmail.com (M.S. Fonari), ivanov yu@ukr.net (Y.Ed. Ivanov), botoshan@tx.technion.ac.il (M.M. Botoshansky).

0022-1139/$ – see front matter © 2009 Elsevier B.V. All rights reserved.
doi:10.1016/j.jfluchem.2009.01.007

Author's personal copy

Table 1
Crystal data and structure refinement parameters for **I** and **IV**

	I	IV
Empirical formula	$(C_6H_7N_2)_2[SiF_6]$	$(C_5H_8N_3)_2[SiF_6]$
Formula weight	332.34	362.38
Crystal system	Monoclinic	Triclinic
Space group	$C2/c$	$P\bar{1}$
Unit cell dimensions		
a (Å)	13.916(3)	6.841(1)
b (Å)	10.623(2)	7.473(1)
c (Å)	9.833(2)	7.670(2)
α (°)	90.0	97.65(3)
β (°)	111.46(3)	105.86(3)
γ (°)	90.0	102.35(3)
Cell volume (Å^3)	1352.6(5)	380.72(12)
Z	4	1
D_{calc} (g/cm^3)	1.632	1.658
μ (mm^{-1})	0.243	0.239
$F(000)$	680	186
θ range for data collection (°)	2.48–25.91	2.82–25.02
Limiting indices	$0 \le h \le 16$ $0 \le k \le 12$ $-11 \le l \le 10$	$0 \le h \le 8$ $-8 \le k \le 8$ $-9 \le l \le 8$
Reflections collected	1258	1261
Reflections with $I > 2\sigma(I)$	964	1059
Refinement method	Full-matrix least-squares on F^2	Full-matrix least-squares on F^2
Data/restraints/parameters	1243/0/123	1261/0/126
Goodness-of-fit on F^2	1.096	1.037
Final R indices [$I > 2\sigma(I)$]		
R_1	0.0484	0.0380
wR_2	0.1351	0.1003
R indices (all data)		
R_1	0.0646	0.0463
wR_2	0.1433	0.1032
Largest diff. peak and hole (e Å^{-3})	0.423/−0.275	0.268/−0.308

support bent pathways of supramolecular assembly through H-bond formation as the amino and pyridinium groups together form a kind of "angle joint" [17] and serve as an efficient molecular tecton for the intermolecular assembly supported by hydrogen bonding and in some cases can lead to noncentric cocrystalline salts.

The crystal structures of hexafluorosilicate salts presented herein demonstrate the influence of subtle modification of the cation that induces distinctive lattice structure formation. The preparation, spectral data and solubility data for four aminopyridinium hexafluorosilicates $(LH)_2[SiF_6]$ (**I**, **II**, **IV**, L = 2-aminopyridine, 3-aminopyridine, and 2,6-diaminopyridine) and $(LH)_2[SiF_6]\cdot H_2O$ (**III**, L = 4-aminopyridine) alongside with the crystal structures for **I** and **IV** are described.

Table 2
Selected intermolecular distances (Å) and angles (°) for **I** and **IV**.

	I	IV		I	IV
Si(1)–F(1)	1.689(1)	1.684(1)	[illegible]	90.23(8)	90.28(7)
Si(1)–F(2)	1.666(2)	1.669(1)	[illegible]	89.28(9)	89.79(9)
Si(1)–F(3)	1.655(2)	1.655(1)	[illegible]	89.09(11)	90.14(8)
N(1)–C(4)	1.348(3)	1.358(3)	[illegible]	122.6(3)	124.2(2)
N(1)–C(5)	1.356(3)	1.359(3)	C(5)–C(1)–C(2)	119.3(3)	119.2(2)
N(2)–C(4)	1.326(4)	1.331(3)	C(3)–C(2)–C(1)	120.3(3)	121.8(2)
C(1)–C(5)	1.344(5)	1.382(3)	C(2)–C(3)–C(4)	120.1(3)	118.8(2)
C(1)–C(2)	1.393(4)	1.381(4)	N(2)–C(4)–N(1)	119.1(3)	117.3(2)
C(2)–C(3)	1.352(4)	1.374(4)	N(2)–C(4)–C(3)	123.2(3)	124.6(2)
C(3)–C(4)	1.403(4)	1.383(3)	N(1)–C(4)–C(3)	117.6(2)	118.1(2)
N(3)–C(5)	–	1.350(3)	C(1)–C(5)–N(1)	120.1(3)	118.0(2)
			N(3)–C(5)–N(1)	–	116.5(2)

2. Results and discussion

All compounds were obtained by interaction of the proper aminopyridine with an aqueous solution of fluorosilicic acid. Binary compounds **I** and **IV** crystallize in monoclinic (space group $C2/c$ with $Z = 4$) and triclinic (space group $P\bar{1}$ with $Z = 1$) crystal systems, respectively. Crystal structure and refinement data for **I** and **IV** is given in Table 1. Selected bond distances and angles are given in Table 2, hydrogen bonding geometry is summarized in Table 3. The asymmetric units of **I** and **IV** reveal half of the hexafluorosilicate anion and the 2-aminopyridinium or 2,6-diaminopyridinium cation. Both structures are built from the hydrogen-bonded units consisting of the anion and two cations (Fig. 1). The positions of N-bound hydrogen atoms were found in the difference Fourier map. Proton transfer to the pyridine nitrogen atom is clearly revealed by the widened C–N–C bond angle in the aromatic ring (Table 2). In **I** two donor centers of 2-aminopyridinium cation act in a chelate mode resulting in a non-planar $R_2^2(8)$ hydrogen-bonding ring [19], with the twisted angle between the planes of equatorial fluorine atoms (F1 and F2) and planar H1N–N1–C4–N2–H2N2 fragment of the aromatic cation equal to 28.4°. In **IV** the H-donor area of the cation enriched by the additional aminogroup provides the set of four short NH…F contacts (two single and one bifurcated H-bonds) that formulate three shared H-bonded rings, $R_2^1(6)$, $R_1^2(4)$, $R_2^1(6)$ sequence in graph set notation. The twisted angle between two six-membered H-bonded rings is equal to 15.3°.

The second hydrogen atom of amino-group in **I** is involved in bifurcated NH…F hydrogen bonding with apical F3 and equatorial F1 atoms of the anion. Thus, each $[SiF_6]^{2-}$ anion in the crystal is

Table 3
Geometry of hydrogen bonds for **I** and **IV**

D–H…A	d(D–H)/Å	d(H…A)/Å	d(D…A)/Å	∠(DHA)/°	Symmetry transformation for acceptor
I					
N(1)–H(1N)…F(1)	0.80(3)	1.81(3)	2.700(3)	173(3)	$x+1/2,\ y+1/2,\ z+1$
N(2)–H(1N2)…F(3)	0.89(3)	2.00(4)	2.856(3)	163(3)	$x,\ y,\ z-1/2$
N(2)–H(1N2)…F(1)	0.89(4)	2.49(3)	3.165(3)	133(3)	$x,\ y,\ z-1/2$
N(2)–H(2N2)…F(2)	0.82(4)	2.05(4)	2.846(4)	164(3)	$x,\ y,\ z$
IV					
N(1)–H(1N1)…F(1)	0.87(3)	1.92(3)	2.760(3)	161(2)	$x,\ y,\ z$
N(1)–H(1N1)…F(2)	0.87(3)	2.63(3)	3.322(3)	138(2)	$x,\ y,\ z$
N(2)–H(1N2)…F(3)	0.86(3)	1.98(3)	2.835(3)	174(3)	$x,\ y+1,\ z$
N(2)–H(2N2)…F(2)	0.84(4)	2.07(3)	2.881(3)	165(3)	$x,\ y,\ z$
N(3)–H(1N3)…F(1)	0.88(3)	2.25(3)	3.028(3)	147(3)	$x,\ y,\ z$
N(3)–H(2N3)…F(2)	0.84(3)	2.12(3)	2.955(3)	173(3)	$x,\ y,\ z+1$
N(3)–H(2N3)…F(1)	0.84(3)	2.57(3)	3.050(3)	117(2)	$x,\ y,\ z+1$

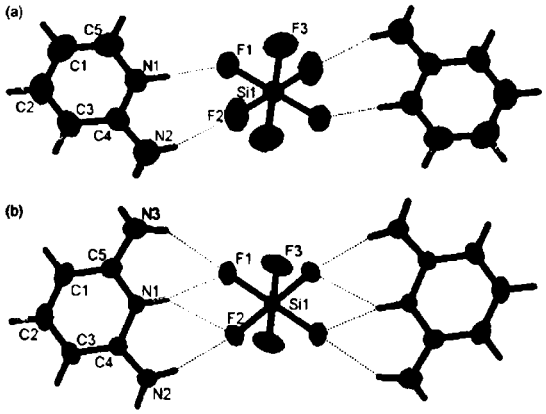

Fig. 1. ORTEP drawing for **I** (a) and **IV** (b) showing hydrogen bonding. Only asymmetric unit is numbered.

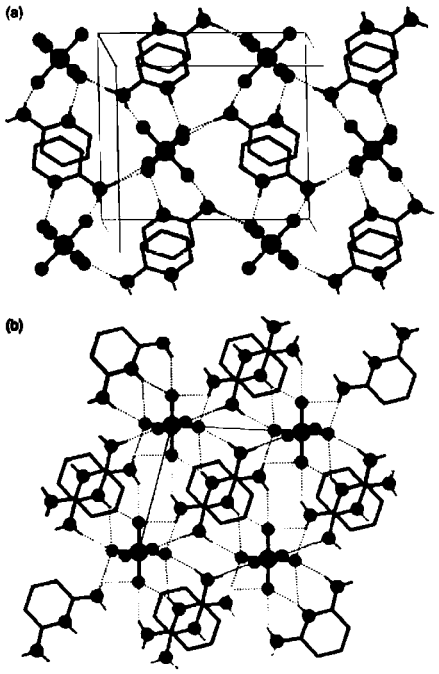

Fig. 2. Fragment of the layer in **I** (a) and **IV** (b). Axes: a – red, b – green, c – blue. C-bound H-atoms are omitted for clarity.

surrounded by four cations (Fig. 2a) being involved in eight hydrogen bonds, each cation bridging two $[SiF_6]^{2-}$ anions. In **IV** due to the second amino-group we observe the more extended system of hydrogen bonding where each $[SiF_6]^{2-}$ anion is surrounded by six cations being involved in 14 hydrogen bonds, each cation being bound with 3 closest anions (Fig. 2b). In both cases these concerted hydrogen-bonding interactions majority of which include the equatorial (F1 and F2) fluorine atoms join the charged species into two-dimensional layers which develop in the bc plane.

In both structures all fluorine atoms are involved in the hydrogen-bonding system. The structures exhibit the same effect marked earlier: the longest Si–F bond length corresponds to the shortest hydrogen bond and vice versa. Following [20] in spite of distribution in Si–F distances we do not observe the pronounced distortion in F–Si–F angles which remain close to the right and open values. Packing of the layers in **I** and **IV** also demonstrates the common features: the π–π stacking interactions between the cationic units is observed both within and between the layers. Fig. 3 shows the packing of the layers and distances between the centroids of the overlapping pyridinium rings, which are in an agreement with the values typical for π–π stacking interactions.

The IR data for **I–IV** are summarized in Table 4. The protonation of the heterocyclic nitrogen atom of aminopyridines proved by X-ray data in the case of complexes **I** and **IV**, is concerted with the IR data, in particular, with high-frequency shift of the bands ν(CC), ν(CN) (ν_{ring}) and pulsating vibrations of a cycle (ν_{puls}) in comparison with positions of these bands in the spectra of initial ligands [21]. The spectra **I–IV** in the region 800–650 cm^{-1} are complicated by superposition of vibration bands of cations and ν(SiF) vibrations of $[SiF_6]^{2-}$ anion, that impedes the assignment of the last ones. The $\delta(SiF_2)$ vibrations in a disclosed area of spectra are registered by a band of an average intensity and a shoulder at 470 ± 5 cm^{-1} for **I**, by two shoulders for **III** and **IV**, and by a doublet band at 450 and 475 cm^{-1} for **II**. The multiple character of $\delta(SiF_2)$ vibrations indicates the decrease of symmetry of $[SiF_6]^{2-}$ anion with regard to O_h and is concerted with the X-ray data.

Table 5 summarises the solubility data and pH values for 0.001 M solutions of **I–IV** in comparison with other hexafluorosilicates of

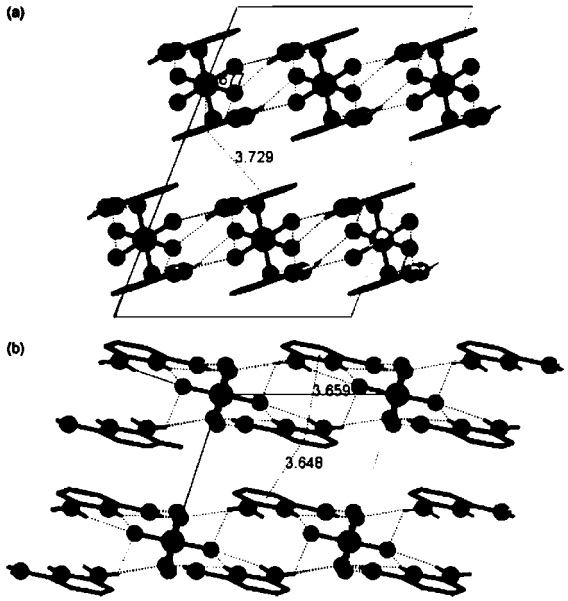

Fig. 3. Packing of the layers in **I** (a) and **IV** (b). View along *b* axis. Axes: *a* – red, *c* – blue. C-bound H-atoms are omitted for clarity.

functionalized pyridinium cations. As it has been previously noted [16], the tendencies in change of solubility of pyridinium hexafluorosilicates cannot be interpreted within the Davies's group numbers conception [25] that operates by characteristics of the hydrophilic–lipophilic balance (HLB) of compounds (in our case of pyridinium cations). In particular, a transition from $[HO(O)CC_5H_4NH]_2[SiF_6]$ to $[(HOOC)_2C_5H_3NH]_2[SiF_6]$ should be accompanied by increase in solubility due to increase of the number of hydrophilic carboxylic groups in the final salt. The opposite effect (Table 5) is actually observed. The similar situation is also observed for compounds $[H_2NC_5H_4NH]_2[SiF_6]$ and $[(H_2N)_2C_5H_3NH]_2[SiF_6]$. At the same time attention has been drawn [16] to a relationship between the solubility of pyridinium hexafluorosilicates and a number of interionic H-bonds in the salt structure: the propagation of a number of short interionic contacts of a XH F (X = N, O) type is accompanied, as a rule, by a diminution of solubility of relevant hexafluorosilicates. To estimate the effects of interionic H-bonds on the solubility of salts we have suggested utilizing the

Table 4
IR spectral data (cm^{-1}) for hexafluorosilicates **I–IV**.

Complex	ν(N⁺H), ν(NH₂), ν(OH)	ν(CC), ν(CN), δ(N⁺H) δ(NH₂) δ(H₂O)	ν$_{as}$(SiF)	ν(SiF), μ(N⁺H), δ(CCH), δ(CNC), γ(H₂O)	δ(SiF₂)
I	3370 m. 3340 m. 3190 m.br. 3080 sh.	1655 m. 1620 s. 1565 m. 1500 s.	1000 m.	770 sh. 745 v.s.br.	470 m. 425 sh.
II	3370 m.br. 3190 m.br. 3080 m.	1640 m. 1590 s. 1500 s.	1015 m.	740 v.s.br.	475 m 450 m
III	3400 sh. 3380 m. 3305 m. 3220 m. 3130 m. 3080 sh.	1650 m. 1635 m. 1620 s. 1560 s. 1505 s.	1010 m.	765 sh. 740 v.s. 670 sh.	490 sh. 475 m. 425 sh.
IV	3375 m.br. 3315 m.br. 3070 sh.	1630 v.s. 1550 sh. 1500 s.	1010 m.	750 v.s.br.	465 m. 440 sh. 420 sh.

Note: w = weak, m = medium, s = strong, v = very, sh = shoulder, br = broad.

Table 5
Solubility of pyridinium hexafluorosilicates in water and pH of salts solutions.

Compound	Solubility/mol.%, 25 °C	h/Å^{-1}	pH of 0.001 M solutions	Reference
$[C_5H_5NH]_2[SiF_6]$	19.60[a]	-	3.20	
$[2\text{-}CH_3C_5H_4NH]_2[SiF_6]$[b]	11.60[a]	0.71	3.27	[20]
$[2\text{-}HO(O)CC_5H_4NH]_2[SiF_6]$[b]	5.33[a]	0.76	-	[22]
$[3\text{-}HO(O)CC_5H_4NH]_2[SiF_6]$[b]	3.33[a]	1.09	-	[23]
$[4\text{-}HO(O)CC_5H_4NH]_2[SiF_6]$[b]	0.80[a]	1.08	-	[16]
$[2,5\text{-}(HOOC)_2C_5H_3NH]_2[SiF_6]$	0.07	-	-	
$[2,6\text{-}(HOOC)_2C_5H_3NH]_2[SiF_6]$	0.02	-	-	
$[2\text{-}H_2NC_5H_4NH]_2[SiF_6]$[b]	5.60	1.38	3.30	
$[3\text{-}H_2NC_5H_4NH]_2[SiF_6]$	1.86	-	3.35	
$[4\text{-}H_2NC_5H_4NH]_2[SiF_6]H_2O$	3.88	-	3.09	
$[2,6\text{-}(H_2N)_2C_5H_3NH]_2[SiF_6]$[b]	0.06	2.35	3.33	
$[4\text{-}H_3NHN(O)CC_5H_4NH][SiF_6]$[b]	0.87[a]	1.80	3.23	[24]

[a] Data [9].
[b] X-ray characterized compounds.

parameter **h** (Eq. (1)):

$$h = \frac{n}{d(D\cdots A)_{av.}} \quad (1)$$

where **n** is a number of short interionic contacts (D...A ≤ 3.2 Å, strong and moderate H-bonds following the classification [13]), $d(D\ldots A)_{av.}$ is an average donor–acceptor distance in the complex structure. The calculated **h** values for the structurally characterized compounds are given in Table 5, and the graphical dependence of solubility values C upon parameter **h** is given in Fig. 4. As it follows from these data the propagation of **h** values, reflecting the magnification of intensity of interionic H-interactions, results in exponential diminution of solubility of the relevant hexafluorosilicates. The potentiometric data given in Table 5, confirm the repeatedly marked fact of hydrolytic instability of "onium" hexafluorosilicates. The pH values of solutions of pyridinium hexafluorosilicates are close to the similar values for anilinium hexafluorosilicates [26], however, against to anilinium analogs, for pyridinium salts the relationship between the pH of salt solutions and pK_a of the relevant pyridine ligands is not observed. The aptitude of hydrolytic equilibrium expressed by Eq. (2) can be promoted by a weakening of a number of Si–F bonds of $[SiF_6]^{2-}$ anions due to the participation of relevant fluoroligands in strong interionic H-bonds.

$$(LH)_2[SiF_6] + 2H_2O \rightarrow 2LH^+ + SiO_2 + 2HF_2^- + 2HF \quad (2)$$

The known X-ray data, including presented herein, are adjusted with such opportunity. Concluding, we should stress that the interionic H-bonds in pyridinium hexafluorosilicates result in a disproportionation of Si–F bond lengths of anion that is affected on the salt properties. In particular, quite probable the relationship between the hydrolytic instability of salts and weakening of a part of Si–F bond lengths in the studied structures is demonstrated. On the other hand, the effects of H-bonds essentially influence the salt solubility: functionalization of pyridinium cation by introduction of the H-donor groups allows directionally varying (to decrease) a solubility of relevant hexafluorosilicates. Thus the solubility values can serve as a simple test for a qualitative estimation of a degree of interionic H-bonding in pyridinium hexafluorosilicates.

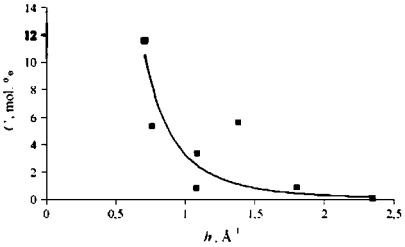

Fig. 4. Relationship between C and h values.

3. Experimental

The IR-absorption spectra were recorded on a spectrophotometer Specord 75IR (range 4000–400 cm^{-1}, samples as suspension in Nujol mulls between KRS-5 windows). The mass spectra were registered on a spectrometer MX-1321 (direct input of a sample in a source, energy of ionizing electrons 70 eV). The isothermal conditions of experiments on detection of a solubility and hydrolysis of hexafluorosilicates (t = 25 ± 0.2 °C) were provided with the help of an ultra thermostat U15.

3.1. Synthesis of bis(2-aminopyridinium) hexafluorosilicate (I)

Pyridine-2-amine (0.094 g, 1 mmol) was dissolved in boiling methanol (5 mL) and to the obtained solution the fluorosilicic acid (FSA, 45%, 9 mL, molar ratio L^1:FSA = 1:3) was added. A reaction mixture stored at ambient conditions prior to the beginning of crystallization of the reaction product, which was obtained in an approximately quantitative yield. Colorless transparent crystals of the composition $(L^1H)_2SiF_6$ (**I**) with m.p. > 240 °C (with decomposition). Anal. found, %: Si 8.28, N 16.31, F 35.11. Calcd for $C_{10}H_{14}F_6N_4Si$, Si 8.45, N 16.86, F 34.30. Mass spectrum: $[ML^1]^+$ (m/z = 94, I = 100%), $[ML^1-HCN]^+$ (m/z = 67, I = 69%), SiF_3^+ (m/z = 85, I = 11%).

3.2. Synthesis of bis(3-aminopyridinium) hexafluorosilicate (II)

Pyridine-3-amine (0.094 g, 1 mmol) was dissolved in boiling methanol (5 mL) and to the obtained solution the fluorosilicic acid (FSA, 45%, 9 mL, molar ratio L^2:FSA = 1:3) was added. A reaction mixture stored at ambient conditions prior to the beginning of crystallization of the reaction product, which was obtained in an approximately quantitative yield. Colorless transparent crystals of the composition $(L^2H)_2SiF_6$ (**II**) with m.p. > 210 °C (with decomposition). Anal. found, %: Si 8.16, N 17.02, F 34.57. Calcd for $C_{10}H_{14}F_6N_4Si$, Si 8.45, N 16.86, F 34.30. Mass spectrum: $[ML^2]^+$ (m/z = 94, I = 100%), $[ML^2-HCN]^+$ (m/z = 67, I = 31%), SiF_3^+ (m/z = 85, I = 4%).

Author's personal copy

3.3. Synthesis of bis(4-aminopyridinium) hexafluorosilicate monohydrate (III)

Pyridine-4-amine (0.094 g, 1 mmol) was dissolved in boiling methanol (5 mL) and to the obtained solution the fluorosilicic acid (FSA, 45%, 9 mL, molar ratio L^3:FSA = 1:3) was added. A reaction mixture stored at ambient conditions prior to the beginning of crystallization of the reaction product, which was obtained in an approximately quantitative yield. Colorless transparent crystals of the composition $(L^3H)_2SiF_6 \cdot H_2O$ (**III**) with m.p. > 210 °C (with decomposition). Anal. found, %: Si 8.02, N 15.71, F 33.10. Calcd for $C_{10}H_{16}F_6N_4OSi$, Si 8.02, N 15.99, F 32.54. Mass spectrum: $[ML^3]^+$ (m/z = 94, I = 100%), $[ML^3 \cdot HCN]^+$ (m/z = 67, I = 37%), SiF_3^+ (m/z = 85, I = 7%).

3.4. Synthesis of bis(2,6-diaminopyridinium) hexafluorosilicate (IV)

Pyridine-2,6-diamine (0.109 g, 1 mmol) was dissolved in boiling methanol (15 mL) and to the obtained solution the fluorosilicic acid (FSA, 45%, 9 mL, molar ratio L^4:FSA = 1:3) was added. A reaction mixture stored at ambient conditions prior to the beginning of crystallization of the reaction product, which was obtained in an approximately quantitative yield. Colorless transparent crystals of the composition $(L^4H)_2SiF_6$ (**IV**) with m.p. > 230 °C (with decomposition). Anal. found, %: Si 7.92, N 23.38, F 33.19. Calcd for $C_{10}H_{16}F_6N_6Si$, Si 7.75, N 23.19, F 31.46. Mass spectrum: $[ML^4]^+$ (m/z = 109, I = 100%), $[ML^4 \cdot HCN]^+$ (m/z = 82, I = 36%), SiF_3^+ (m/z = 85, I = 9%).

3.5. Structure determination

The X-ray intensity data were collected at a room temperature on a Nonius Kappa CCD diffractometer equipped with graphite monochromated Mo-Kα radiation using ϕ–ω rotation. Unit cell parameters were obtained and refined using the whole data set. Experimental data reduction and cell refinement were performed using DENZO [27] package. The structure solution and refinement proceeded using SHELX-97 program package [28]. Direct methods yielded all non-hydrogen atoms of the asymmetric unit which were treated anisotropically. C-bound hydrogen atoms were placed in calculated positions with their isotropic displacement parameters riding on those of the parent atoms, while the N-bound H-atoms were found from differential Fourier maps at an intermediate stage of the refinement and were treated isotropically. Crystallographic data (cif files) for **I** and **IV** have been deposited with the Cambridge Crystallographic Data Center, CCDC Nos 713403 and 713404. Copies of this information may be obtained free of charge from The Director, CCDC, 12 Union Road, Cambridge, CB2 1EZ, UK (Fax: +44-1233-336-033; E-mail: deposit@ccdc.cam.ac.uk or www: http://www.ccdc.cam.ac.uk).

Acknowledgements

The diffraction data were collected at the Schulich Faculty of Chemistry, Technion, The Haifa, through the cooperation of Professor Menahem Kaftory whom we would like to acknowledge.

References

[1] J.M. Lehn, Supramolecular Chemistry, VCH, Weinheim, 1995.
[2] A. Bianchi, K. Bowman-James, E. Garcia-Espana (Eds.), Supramolecular Chemistry of Anions, Wiley-VCH, New York, 1997.
[3] G.A. Jeffrey, W. Saenger, Hydrogen Bonding in Biological Structures, Springer, Berlin, 1991.
[4] K. Bowman-James, Acc. Chem. Res. 38 (2005) 671–678.
[5] P.A. Gale, S.E. Garcia-Garrido, J. Garric, Chem. Soc. Rev. 37 (2008) 151–190.
[6] B.A. Moyer, L.H. Delmau, C.J. Fowler, A. Ruas, D.A. Bonnett, J.L. Sessler, E. Katayev, G.D. Pantos, J.M. Llinares, M.A. Hossain, S.O. Kang, K. Bowman-James, in: R. Eldik, K. Bowman-James (Eds.), Adv. Inorg. Chem., vol. 59, Academic Press, 2006, pp. 175–204.
[7] I. Gessick, K.M. Harmon, M.M. Poovia, Inorg. Chem. 16 (1977) 2033–2040.
[8] D. Boenigk, D. Mootz, J. Am. Chem. Soc. 110 (1988) 2135–2139.
[9] D. Wiechert, D. Mootz, R. Franz, G. Siegemund, Chem. Eur. J. 4 (1998) 1043–1047.
[10] V.D. Gelmboldt, Ed.V. Ganin, M.S. Fonari, Yu.A. Simonov, L.V. Koroeva, A.A. Ennan, S.S. Basok, S. Shova, H. Kahlig, V.B. Arion, B.K. Keppler, Dalton Trans. (2007) 2915–2924.
[11] V.D. Gelmboldt, Ed.V. Ganin, L.V. Ostapchuk, J. Lipkowski, A.A. Dvorkin, Yu.A. Simonov, M.S. Fonari, J. Incl. Phenom. 24 (1996) 287–299.
[12] J. Emsley, Chem. Soc. Rev. 9 (1980) 91–124.
[13] T. Steiner, Angew. Chem. Int. Ed. 41 (2002) 48–76.
[14] M. Mascal, J. Chem. Soc. Perkin Trans. 2 (1997) 1999–2001.
[15] V.D. Gelmboldt, A.A. Ennan, Ed.V. Ganin, Yu.A. Simonov, M.S. Fonari, M.M. Botoshansky, J. Fluor. Chem. 125 (2004) 1951–1957.
[16] V.D. Gelmboldt, L.V. Koroeva, Ed.V. Ganin, M.S. Fonari, M.M. Botoshansky, A.A. Ennan, J. Fluor. Chem. 129 (2008) 632–636.
[17] M.J. Prakash, T.P. Radhakrishnan, Cryst. Growth Des. 5 (2005) 721–725.
[18] J.A. Bis, M.J. Zaworotko, Cryst. Growth Des. 5 (2005) 1169–1179.
[19] M.C. Etter, Acc. Chem. Res. 23 (1990) 120–126.
[20] A. Pevec, A. Demšar, J. Fluor. Chem. 129 (2008) 707–712.
[21] A.R. Katritzky, Physical Methods in Heterocyclic Chemistry, vol. 3, Academic Press, New York, 1971.
[22] V.D. Gelmboldt, E.V. Ganin, K.V. Domasevitch, Acta Crystallogr. C 63 (2007) o530–o534.
[23] V.D. Gelmboldt, E.Kh. Minacheva, E.V. Ganin, V.S. Sergienko, Rus. J. Inorg. Chem. 53 (2008) 947–950.
[24] V.D. Gelmboldt, V.N. Davydov, L.V. Koroeva, Ed.V. Ganin, Rus. J. Inorg. Chem. 47 (2002) 987–994.
[25] V.Yu. Kukushkin, N.Yu. Kukushkin, Theory and Practice of Synthesis of Coordination Compounds (Russ.), Nauka, Leningrad, 1990, p. 280.
[26] V.D. Gelmboldt, Ed.V. Ganin, L.V. Koroeva, L.Kh. Minacheva, V.S. Sergienko, A.A. Ennan, Rus. J. Inorg. Chem. 51 (2006) 184–201.
[27] Z. Otwinowski, W. Minor, in: C.W. Carter, R.M. Sweet (Eds.), Methods in Enzymology, 276, Academic Press, London, 1996, p. 307.
[28] G.M. Sheldrick, SHELXS97 and SHELXL97, University of Göttingen, Germany, 1997.

Додаток П.

Копія статті. “Синтез и кристаллическая структура гексафторосиликата N,N-диметилбигуанидиния”

ЖУРНАЛ НЕОРГАНИЧЕСКОЙ ХИМИИ, 2009, том 54, № 12, с. 1–4

КООРДИНАЦИОННЫЕ СОЕДИНЕНИЯ

УДК 541.49:546.284.161–32:547.551

СИНТЕЗ И КРИСТАЛЛИЧЕСКАЯ СТРУКТУРА ГЕКСАФТОРОСИЛИКАТА N,N-ДИМЕТИЛБИГУАНИДИНИЯ

© 2009 г. В. О. Гельмбольдт*, Л. Х. Миначева, Э. В. Ганин***, В. С. Сергиенко**, М. М. Ботошанский******

**Физико-химический институт защиты окружающей среды и человека Министерства образования и науки Украины и НАН Украины, Одесса*

** *Учреждение Российской академии наук Институт общей и неорганической химии им. Н.С. Курнакова РАН, Москва*

****Одесский государственный экологический университет, Украина*

*****Израильский технологический институт, Хайфа*

Поступила в редакцию 10.02.2009 г.

Синтезирован комплекс $[(CH_3)_2NC(NH_2)NHC(NH_2)NH_2]SiF_6$ (**I**) и методом РСА установлено его строение. Кристаллы моноклинные, a = 7.4346(10), b = 12.7628(10), c = 11.0828(10) Å, β = 104.080(10)°, V = 1020.01(18) Å^3, $\rho_{выч}$ = 1.780 г/см^3, μ(MoK_α) = 0.302 мм$^{-1}$, Z = 4, пр. гр. $P2_1/c$. Структурные единицы кристалла I – анионы SiF_6^{2-} – (Si–F 1.657(2)–1.699(2) Å) и катионы N,N-диметилбигуанидиния (H_2L^{2+}) – объединены межионными Н-связями NH···F в каркас. В катионах центрами протонирования являются концевые имидные группы.

Соединения минеральных кислот с полидентатными органическими лигандами, содержащими N-донорные центры различной природы, представляют интерес как модели для выяснения особенностей "жестко-жесткой" конкурентной H/N-координации [1] и влияния межионных Н-связей на строение и свойства комплексов [2, 3]. Проявления эффектов Н-связей в системах "катион–анион" должны быть особенно заметны в случае соединений комплексных фторокислот, в частности, кремнефтороводородной кислоты (**КФК**), чьи фтролиганды обладают достаточно высокой протоноакцепторной способностью [4]. В настоящей работе, выполненной в продолжение начатых ранее исследований взаимосвязи строения и свойств "ониевых" гексафторосиликатов [2, 3], изучена кристаллическая структура гексафторосиликата N,N-диметилбигуанидиния.

ЭКСПЕРИМЕНТАЛЬНАЯ ЧАСТЬ

Синтез. Гидрохлорид $(CH_3)_2NC(NH)_2C(NH)NH_2XHCl$ (500 мг) растворяли в 10 мл воды, полученный раствор фильтровали, к фильтрату добавляли 5 мл 45%-ной КФК и 1 мл 40%-ной фтороводородной кислоты. Реакционную смесь подвергали самопроизвольному испарению при комнатной температуре до начала кристаллизации продукта реакции в виде бесцветных прозрачных кристаллов; $t_{пл}$ = 268–270°C (с разложением).

	Si	N
Найдено,%:	10.13;	26.09.
Для $[(CH_3)_2NC(NH_2)NHC(NH_2)NH_2]SiF_6$ (**I**)		
вычислено,%:	0.28;	25.63.

Масс-спектр I (спектрометр МХ-1321, прямой ввод образца в источник, энергия ионизирующих электронов 70 эВ): $[ML]^+$ (m/z = 129, I = 29%), $[ML–NH_2]^+$ (m/z = 113, I = 8%), SiF_3^+ (m/z = 85, I = = 100%).

ИК-спектр I (см$^{-1}$, область 4000–400 см$^{-1}$, спектрофотометр Specord 75IR, стекла KRS-5, образец в виде суспензии в вазелиновом масле): 3400, 3370, 3145, 3090 (ν(NH)), 1765, 1730, 1695, 1640, 1582, 1550, 1530, 1490 (δ(NH_2), δ(CHN)); 970 (ν(CN)); 785, 720, 670 (ν(SiF), ρ(NH_2)); 640, 550, 535 (δ(CNC), δ(NCN)); 478, 455 (δ(SiF_2)).

РСА. Кристаллы I ($C_4H_{13}F_6N_5Si$, M = 273.28) моноклинные: a = 7.4346(10), b = 12.7628(10), c = = 11.0828(10) Å, β = 104.080(10)°, V = 1020.01(18) Å^3, $\rho_{выч}$ = 1.780 г/см^3, μ(MoK_α) = 0.302 мм$^{-1}$, Z = 4, пр. гр. $P2_1/c$.

Экспериментальный материал получен с бесцветного монокристалла размером 0.35 × 0.14 × 0.11 мм при 293(2) K на автоматическом четырехкружном дифрактометре Enraf-Nonius CAD-4 (MoK_α, λ = = 0.71073 Å, графитовый монохроматор, ω-сканирование, $2\theta_{max}$ = 24.97°). Всего снято 2770 отражений ($-2 \le -h \le 8$, $-1 \le k \le 15$, $-13 \le l \le 13$, заполнение

Таблица 1. Координаты атомов ($\times 10^4$, для атомов H $\times 10^3$) и их тепловые параметры $U_{экв}/U_{изо}$ (Å^2, $\times 10^3$) в структуре I*

Атом	x	y	z	$U_{экв}/U_{изо}$
Si(1)	6198(1)	9008(1)	2817(1)	25(1)
F(1)	5291(3)	9092(2)	4044(2)	46(1)
F(2)	5382(3)	7803(2)	2518(2)	47(1)
F(3)	7181(4)	8975(2)	1608(2)	72(1)
F(4)	7085(3)	10228(2)	3162(2)	55(1)
F(5)	8192(3)	8523(2)	3716(2)	47(1)
F(6)	4259(3)	9502(2)	1910(2)	41(1)
N(1)	8746(5)	10116(3)	6000(3)	32(1)
N(2)	7057(5)	8788(3)	6542(3)	33(1)
N(3)	9812(5)	9322(3)	7883(3)	32(1)
N(4)	8061(4)	8971(3)	9278(3)	33(1)
N(5)	11053(4)	8341(2)	9647(2)	26(1)
C(6)	8474(5)	9404(3)	6796(3)	25(1)
C(7)	9637(5)	8849(2)	8965(3)	24(1)
C(8)	12733(5)	8111(4)	9237(3)	46(1)
C(9)	10953(5)	7895(3)	10852(3)	37(1)
H(1A)	975(6)	1050(3)	620(3)	34(11)
H(2A)	624(6)	887(3)	582(4)	51(13)
H(2B)	693(5)	840(3)	699(3)	23(12)
H(3)	1072(5)	959(3)	793(3)	19(11)
H(4A)	790(5)	871(3)	990(3)	28(11)
H(4B)	728(5)	943(3)	885(3)	39(12)

* Приведены координаты атомов водорода, участвующих в H-связях.

по θ = 99.9%), из них 1798 независимых (R(int) = = 0.0396). Полный набор экспериментальных данных депонирован в Кэмбриджском банке структурных данных (регистрационный № для соединения I – CCDC 720313).

Структура определена прямыми методами (SHELXS-86 [5]) и уточнена методом наименьших квадратов по F^2 (SHELXL-97 [6]) в полноматричном анизотропном приближении для всех неводородных атомов. Позиции всех атомов водорода катиона N,N-диметилбигуанидиния определены из разностного синтеза Фурье и уточнены в изотропном приближении, кроме атомов H концевых метильных групп. Последние уточнены по методу "наездника".

Окончательные результаты уточнения: $R1$ = = 0.0338, $wR2$ = 0.0775, $GOOF$ = 0.967 по 884 отражениям с $I > 2\sigma(I)$; $R1$ = 0.1400, $wR2$ = 0.1016 по всем рефлексам; 174 уточняемых параметра. Коэффициент экстинкции равен 0.012(2), значения $\Delta\rho_{max}$ и $\Delta\rho_{min}$ составляют соответственно 0.374 и –0.251 e.Å^{-3}.

Координаты и температурные факторы атомов структуры I приведены в табл. 1, межатомные расстояния и валентные углы – в табл. 2.

Таблица 2. Основные длины связей (d) и валентные углы (ω) в структуре I

Связь	d, Å
Si(1)–F(2)	1.658(2)
Si(1)–F(1)	1.661(2)
Si(1)–F(6)	1.667(2)
Si(1)–F(3)	1.675(2)
Si(1)–F(5)	1.690(2)
Si(1)–F(4)	1.698(2)
N(1)–C(6)	1.316(4)
N(2)–C(6)	1.289(5)
N(3)–C(6)	1.367(5)
N(3)–C(7)	1.377(4)
N(4)–C(7)	1.310(4)
N(5)–C(7)	1.309(4)
N(5)–C(8)	1.460(4)
N(5)–C(9)	1.470(4)
Угол	**ω, град**
F(2)Si(1)F(1)	91.24(12)
F(2)Si(1)F(6)	90.56(12)
F(1)Si(1)F(6)	90.34(12)
F(2)Si(1)F(3)	91.50(14)
F(1)Si(1)F(3)	177.13(15)
F(6)Si(1)F(3)	90.51(12)
F(2)Si(1)F(5)	90.18(12)
F(1)Si(1)F(5)	90.79(12)
F(6)Si(1)F(5)	178.64(13)
F(3)Si(1)F(5)	88.33(13)
F(2)Si(1)F(4)	178.17(13)
F(1)Si(1)F(4)	88.24(13)
F(6)Si(1)F(4)	91.19(12)
F(3)Si(1)F(4)	89.00(14)
F(5)Si(1)F(4)	88.07(11)
C(6)N(1)H(1A)	118(2)
C(6)N(1)H(1B)	113(3)
H(1A)N(1)H(1B)	128(3)
C(6)N(2)H(2A)	118(3)
C(6)N(2)H(2B)	120(3)
H(2A)N(2)H(2B)	122(4)
C(6)N(3)C(7)	126.8(3)
C(6)N(3)H(3)	119(3)
C(7)N(3)H(3)	114(3)
C(7)N(4)H(4A)	120(3)
C(7)N(4)H(4B)	117(2)
H(4A)N(4)H(4B)	122(4)
C(7)N(5)C(8)	123.3(3)
C(7)N(5)C(9)	120.4(3)
C(8)N(5)C(9)	116.2(3)
N(2)C(6)N(1)	121.7(4)
N(2)C(6)N(3)	121.8(3)
N(1)C(6)N(3)	116.5(3)
N(5)C(7)N(4)	123.5(3)
N(5)C(7)N(3)	119.2(3)
N(4)C(7)N(3)	117.3(3)

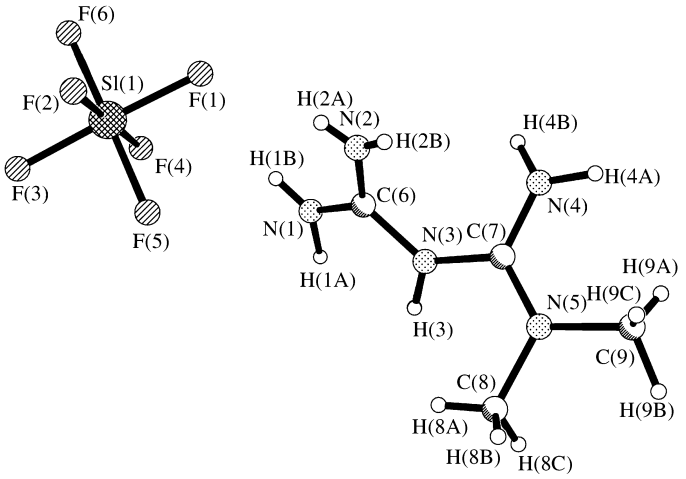

Рис. 1. Структурные единицы кристалла I – анион SiF_6^{2-} и катион LH_2^{2+}.

РЕЗУЛЬТАТЫ И ИХ ОБСУЖДЕНИЕ

Структурные единицы кристалла I – гексафторосиликатные анионы SiF_6^{2-} и катионы N,N-диметилбигуанидиния (H_2L^{2+}) (рис. 1).

Гексафторосиликатный анион имеет слегка искаженное октаэдрическое строение: длины связей Si–F лежат в интервале 1.657(2)–1.699(2) Å (средн. 1.675 ± 0.002 Å), углы FSiF изменяются в пределах 88.07(11)° – 91.24(12)° и 177.13(15)° –178.64(13)°. В целом параметры аниона в I типичны для аналогичных соединений [7].

Катион N,N-диметилбигуанидиния в I, протонированный по двум концевым имидным группам, неплоский. В нем можно выделить два практически плоских фрагмента N(1)C(6)N(2)N(3) (А, среднее отклонение атомов от плоскости – Δ – 0.007 Å) и N(4)C(7)N(5)N(3) (Б, Δ = 0.007 Å), двугранный угол А/Б 51.5°. В плоских фрагментах А и Б расстояния углерод–азот с протонированной имидной (N(2)–C(6) и N(4)–C(7)) и аминной группами (N(1)–C(6) и N(5)–C(7)) практически выравнены (средн. C–N 1.306(4) ± 0.017 Å). Все атомы азота в катионе характеризуются практически плоской конфигурацией (сумма углов при атомах N(1)–N(5) 359°–360°). По-видимому, все это может свидетельствовать о делокализации двойных связей N(2)–C(6) и N(4)–C(7) в каждом из плоских фрагментов. Аналогичное строение катиона H_2L^{2+}, также протонированного по концевым имидным группам, обнаружено в гидрате оксалата N,N-диметилгуанидиния (II) и гидрате сульфата N,N-диметилгуанидиния (III) [8] (угол А/Б равен 52.8° и 56.1°, средн. длина соответствующих связей C–N 1.312 и 1.310 Å в II и III).

В структуре I комплексные анионы SiF_6^{2-} и катионы H_2L^{2+} объединены системой водородных связей (**ВС**) N–H···F с образованием каркаса (табл. 3, рис. 2). Акцепторами ВС являются все шесть атомов фтора, донорами – все атомы водорода амин-

Таблица 3. Геометрические параметры водородных связей в структуре I

№№	Контакт D–H···A	Расстояния, A			Углы DHA, град	Координаты атома A
		D–H	A···H	D···A		
1	N(1)–H(1A)···F(5)	0.87(4)	1.96(4)	2.820(4)	167(3)	$-x + 2, -y + 2, -z + 1$
2	N(2)–H(2A)···F(1)	0.89(4)	1.94(4)	2.788(4)	159(4)	x, y, z
3	N(3)–H(3)···F(4)	0.75(4)	2.27(3)	2.880(4)	140(3)	$-x + 2, -y + 2, -z + 1$
4	N(4)–H(4A)···F(3)	0.80(4)	2.12(4)	2.814(4)	145(3)	$x, y, z + 1$
5	N(4)–H(4B)···F(6)	0.87(4)	1.85(4)	2.721(4)	174(3)	$-x + 1, -y + 2, -z + 1$
6	N(2)–H(2B)···F(2)	0.72(3)	2.09(4)	2.738(4)	150(4)	$x, -y + 3/2, z + 1/2$

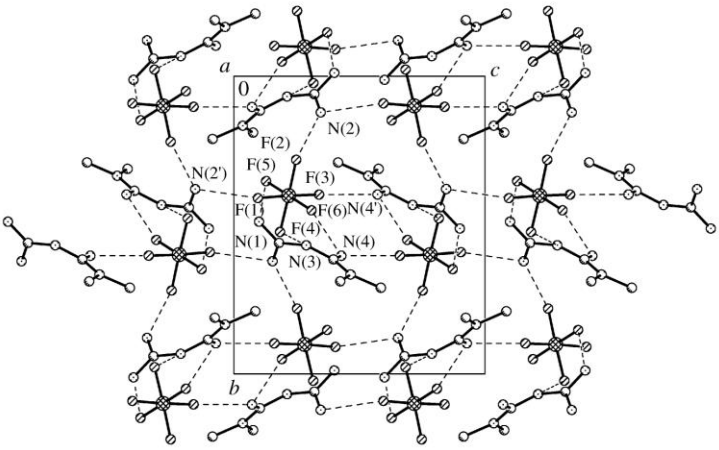

Рис. 2. Упаковка структурных единиц в кристалле I (проекция вдоль оси *a*).

ных и имидных групп катиона, за исключением атома H(1B). В каркасе можно выделить слои, образованные за счет ВС 1–5, параллельные плоскости *ac*. Слои объединены ВС 6.

Следует отметить, что в соединении I отсутствует четкая корреляция между расстояниями Si–F и прочностью соответствующих H-связей, как это обычно наблюдается в структуре гексафторосиликатов с "ониевыми" катионами различных типов [2, 3, 9, 10].

СПИСОК ЛИТЕРАТУРЫ

1. *Бородкина И.Г., Анцышкина А.С., Садиков Г.Г. и др.* // Коорд. химия. 2003. Т. 29. № 3. С. 555.
2. *Gelmboldt V.O., Koroeva L.V., Ganin Ed.V. et al.* // J. Fluor. Chem. 2008. V. 129. № 7. P. 632.
3. *Gelmboldt V.O., Ganin Ed.V., Fonari M.S. et al.* // J. Fluor. Chem. 2009 (in press).
4. *Steiner T.* // Angew. Chem. Int. Ed. 2002. V. 41. № 1. P. 48.
5. *Sheldrick G.M.* // Acta Crystallogr. 1990. V. 46A. № 5. P. 467.
6. *Sheldrick G.M.* // SHELXL-97. Program for the Refinement of Crystal Structures. University of Göttingen, Germany. 1997.
7. *Tandura S.N., Voronkov M.G., Alekseev N.V.* // Top. Curr. Chem. 1986. V. 131. P. 99.
8. *Li-Ping Lu, Hong-Mei Zhang, Miao-Li Zhu* // Acta Crystallogr. 2004. V. 60C. P. 740.
9. *Conley B.D., Yearwood B.C., Parkin S., Atwood D.A.* // J. Fluor. Chem. 2002. V. 115. № 2. P. 155.
10. *Гельмбольдт В.О., Миначева Л.Х., Ганин Э.В. и др.* // Журн. неорган. химии. 2008. Т. 53. № 6. С. 947.

Додаток Р.

Копія статті. “Conformational Mobility of 7,16-Bis(4-methoxybenzyl)-1,4,10,13-tetraoxa-7,16-diazacyclooctadecane in Molecular and Proton Transfer Complexes: X-ray and DFT Study”

NJC

New Journal of Chemistry

An international journal of the chemical sciences

www.rsc.org/njc

Volume 33 | Number 8 | August 2009 | Pages 1621–1792

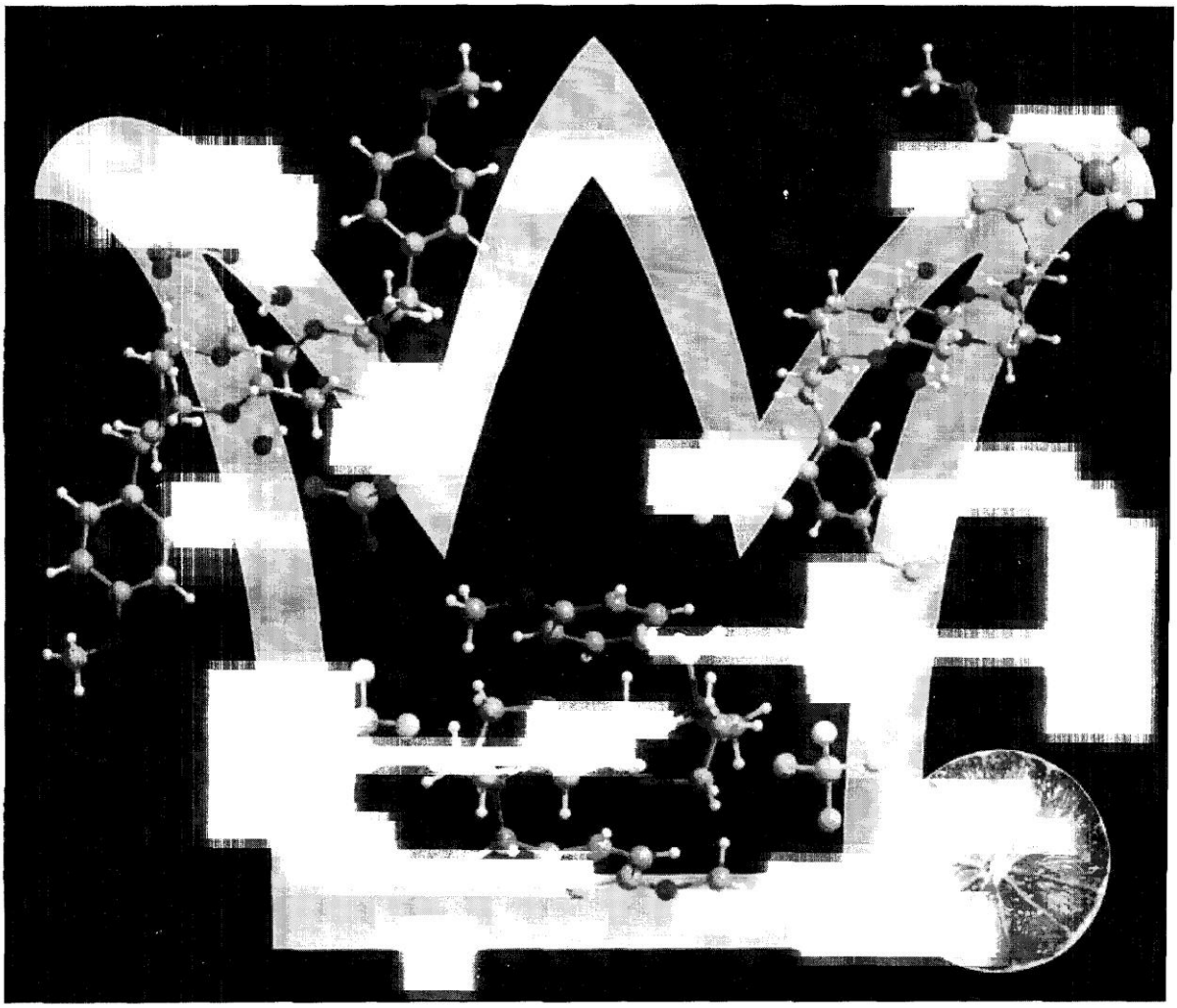

ISSN 1144-0546

RSC Publishing

PAPER

Marina S. Fonari *et al.*

Conformational mobility of 7,16-bis(4-methoxybenzyl)-1,4,10,13-tetraoxa-7,16-diazacyclooctadecane in molecular and proton-transfer complexes

1144-0546(2009)33:8;1-W

PAPER www.rsc.org/njc | New Journal of Chemistry

Conformational mobility of 7,16-bis(4-methoxybenzyl)-1,4,10,13-tetraoxa-7,16-diazacyclooctadecane in molecular and proton-transfer complexes: X-ray and DFT studies†

Marina S. Fonari,*[a] Eduard V. Ganin,[b] Yurii M. Chumakov,[a] Mark M. Botoshansky,[c] Kinga Suwinska,[d] Stepan S. Basok[e] and Yurii A. Simonov[a]

Received (in Victoria, Australia) 12th February 2009, Accepted 22nd April 2009
First published as an Advance Article on the web 28th May 2009
DOI: 10.1039/b902953b

For the first time the bibracchial-crown ether 7,16-bis(4-methoxybenzyl)-1,4,10,13-tetraoxa-7,16-diazacyclooctadecane (**1**) and its molecular and proton-transfer complexes were isolated and characterized by X-ray single-crystal diffraction. Hydrogen bonding between the neutral molecules is present in the binary complex **1**·$(H_2NCS)_2$ (**3**) giving rise to a tape structure. The proton migration from an inorganic acid to a macrocyclic molecule results in doubly protonated cations $(\mathbf{1}\text{-}H_2)^{2+}$ and $(\mathbf{2}\text{-}H_2)^{2+}$ (where **2** is the parent 7,16-dibenzyl-1,4,10,13-tetraoxo-7,16-diazacyclooctadecane) giving rise to the ionic complexes $(\mathbf{1}\text{-}H_2)\cdot[ClO_4]_2\cdot 2H_2O$ (**4**), $(\mathbf{1}\text{-}H_2)\cdot[NbF_6]_2\cdot 2H_2O$ (**5**), $(\mathbf{1}\text{-}H_2)\cdot[TaF_6]_2\cdot 2H_2O$ (**6**), $(\mathbf{1}\text{-}H_2)\cdot[BF_4]_2$ (**7**) and $(\mathbf{2}\text{-}H_2)\cdot[ClO_4]_2\cdot 2H_2O$ (**8**) sustained by a system of charge-assisted hydrogen bonding. The macrocyclic entities in **1–8** differ by the conformation of the crown ring and the arrangement of the pendant arms. To rationalize the different conformations of **1** in comparison with the relative compounds based on **2**, the theoretical quantum chemical calculations on the DFT (B3LYP) level were performed. The contribution of the methoxy group that provides the C–H···O(OCH_3) hydrogen bonding to the overall system of intermolecular interactions has been estimated by comparison with the complexes based on **2**.

Introduction

The crown ether family of macrocyclic compounds has attracted a huge amount of interest since its discovery in 1967,[1,2] especially in the fields of host–guest and coordination chemistry. The metal ion complexing abilities of crown ethers can be improved significantly by their functionalization with ligating side arms that enhance the cation selectivity and transport through liquid membranes.[3] The C- or N-pivot, bibracchial (two arms) lariat ethers (BiBLEs)[4,5] were modeled on valinomycin complexation and designed to be flexible and dynamic when unbound and enveloping when a guest is complexed.[6] The historically first synthesized *N,N'*-dibenzyl-1,7,10,16-tetraoxo-4,13-diazacyclooctadecane (*N,N'*-dibenzyl-diaza-18-crown-6, **2**)[4,5,7] has been studied in detail, and it has manifested itself as a good complexing agent for a wide range of metals, both inside the cavity acting in its neutral form and in an outer-sphere coordination. Evans and co-workers[8] have indicated that the alkaline and lighter lanthanoid species (La–Sm) tend to form inclusion-type compounds with a metal salt incorporated into the macrocyclic cavity. It results in different crown conformations: an asymmetric 'basket-like' shape with two phenyl substituents situated on the same side of the macrocyclic cavity as in the cases of NaI·**2**[8] and $Ln(NCS)_3\cdot\mathbf{2}$ (Ln = La, Nd, Eu),[9] a T-shaped arrangement of two phenyl substituents in the complex $AgPF_6\cdot\mathbf{2}$,[10] and a more symmetric conformation with benzyl arms splayed up from the both sides of the macrocyclic ring in *catena*-((μ_2-isothiocyanato-*N,S*)-(μ_2-thiocyanato-*N,S*)-bis(**2**)-di-potassium).[5] In contrast, protonation of the aza-crown ether inhibits inclusion of the lanthanoid species, affording complex metal anion species interspersed between the network of crown dications.[8] In a similar way, the recently reported metal-free structures of $(\mathbf{2}\text{-}H_2)\cdot[BF_4]_2\cdot H_2O$[11] and $(\mathbf{2}\text{-}H_2)\cdot I_8$[12] as well as $[Na\cdot N,N'\text{-dipyridyl-bis-aza-18C6}]_2[(H^+)_2N,N'\text{-dipyridyl-bis-aza-18C6}][ClO_4]\cdot 2H_2O$[13] revealed unusual C–H···π interactions between the phenyl substituents and two macrocyclic methylene protons that effectively anchor the ring into the folded conformation and inhibit flexing, typical for macrocycles of this type. Extended studies were devoted to the modification of

[a] *Institute of Applied Physics, Academy of Sciences of Moldova, Academy str., 5 MD2028 Chisinau R., Moldova. E-mail: fonari.xray@phys.asm.md; Fax: +373 22 72 58 87; Tel: +373 22 73 81 54*
[b] *Odessa State Environmental University of Ministry of Education and Science of Ukraine, Lvovskaya str.15, 65016 Odessa, Ukraine. E-mail: edganin@yahoo.com*
[c] *Schulich Faculty of Chemistry, Technion-Israel Institute of Technology, Technion City, 32000 Haifa, Israel. E-mail: botoshan@tx.technion.ac.il*
[d] *Institute of Physical Chemistry Polish Academy of Science, Kasprzaka, 44/52, Warsaw, Poland. E-mail: kinga@ichf.edu.pl*
[e] *A.V. Bogatsky Physico-Chemical Institute, National Academy of Science of Ukraine, Lustdorfskaya doroga 86, 650080 Odessa, Ukraine*

† Electronic supplementary information (ESI) available: Overlapping diagram (Fig. S1) for **1** and **2** in the relative complexes, table of torsion angles (Table S1) along with the macrocyclic framework of **2** in the complexes parent to those discussed herein. The coordinates for all optimized conformers are available from the authors. CCDC reference numbers 717101–717107. For ESI and crystallographic data in CIF or other electronic format see DOI: 10.1039/b902953b

 This journal is © The Royal Society of Chemistry and the Centre National de la Recherche Scientifique 2009

the pendant side arm by the introduction of the fluorescent or redox switched moieties in the molecule.[14] Lariat ethers appear to be good candidates to analyze the cation–π interactions with the participation of the pendant arm. The fruitful conclusion made by Gokel's group that the arenes should be placed two carbons from the macrocyclic nitrogen rather than one permitted them to prove the contribution of one and two arms to the metal complexation.[15] Special attention has been drawn to the substituents mimicking the function of the four amino acids possessing aromatic side chains capable of complexing alkali metal cations, phenylalanine (benzene), tyrosine (phenol), tryptophan (indole), as these aromatic residues are generally regarded as π-donors, and histidine, (imidazole) as a σ-donor.

For decades, the high flexibility of crown ethers (CEs) has impeded their conformational analysis. However, nowadays we are witnesses of the growing number of calculated approaches for analyzing the conformational mobility of CEs in general and lariat-crown ethers (LCEs) in particular. Theoretically, different conformers of CEs can be obtained through a conformational search with molecular dynamics (MD) or molecular mechanics (MM) techniques, while the actual conformer(s) may be retrieved from the Cambridge Structural Database (CSD) when their crystal structures are known. The latter provides a good starting point for a conformational search. For example, Reedijk *et al.*[16] used the computational facilities (MM3, PM3) to estimate the conformational and electronic properties of N,S,O-mixed donor CEs in nucleophilic coupling of their secondary nitrogen atoms to an epoxide. The conformational analysis of *N*-tosyl-substituted diaza-crown ethers theoretically studied by empirical and semi-empirical methods using MSI/DISCOVER97 (ESFF force field) and MOPAC (PM3) permitted the authors to estimate the preferred conformations.[17] C-pivot LCEs were the subject of the DFT calculations by the Chinese group to estimate the side arm remote controlling effect.[18] Through the cooperation of the crown ring and the side arm the LCEs often exhibit different cation-binding properties when compared with their parent CEs. Because the functional groups of side arm LCEs are key components in the formation of metal–CE complexes and in molecular recognition, detailed information about the conformational energies of LCE is important for the understanding of the binding affinities of the crownophanes with guest molecules and for the design of artificial host molecules. Platas-Iglesias and co-workers have carried out a systematic investigation of the electronic structure and changes in conformations on lariat ethers in the complexes, starting from the X-ray data using DFT facilities.[19]

The aza-crown ethers bearing the phenolic side arms are very attractive targets and their synthesis has been reported.[14b] For a wide range of metals, a strong affinity was found for the mono- and diaza-crown ethers containing a phenolic group. The advantage of phenol-containing LCEs might refer to the possibility of forming covalent complexes as well as complexes with ion-pair binding between the phenoxide oxygen and metal cation; moreover, the selective cation coordination by these lariats is pH-dependent. It might be expected that the replacement of a phenoxy hydrogen by a methyl group, resulting in the methoxy-substituted analog of *N,N'*-dibenzyldiaza-18C6

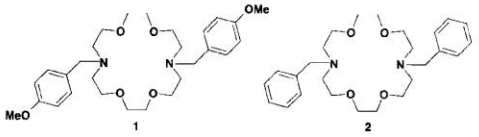

Scheme 1 Structure of lariat crown ethers.

(**2**), *N,N'*-dimethoxydibenzyldiaza-18C6 (**1**),[20] may enhance the liphophilicity in two directions—the methyl group will provide the higher solubility in lipids, while the oxygen atom of the methoxy group will enhance the water solubility. Furthermore, the oxygen atom of the methoxy group will provide an additional acceptor for hydrogen bonding. Apart from the synthesis[20] no data dealing with the complexing ability of **1** are known so far.

Being involved in the host–guest chemistry based on the CEs and crowncyclophanes,[21] we, alongside others, have studied the complexation of *N,N'*-dibenzyldiaza-18-crown-6 (**2**) with neutral molecules.[22] In contrast to the well-developed field of metal complexation by lariat ethers only single examples of their genuine host–guest complexes are available.[23] This gap is explained by the weakness of the arising hydrogen bonding with the LCEs bearing the bulky pendant arms. This has provoked us to study the methoxy-substituted analog of **2**, *N,N'*-bis(4-methoxybenzyl)-1,7,10,16-tetraoxo-4,13-diazacyclo-octadecane (**1**),[20] in the host–guest interactions, and compare this with the data available for **2**. For the first time the bibracchial-crown ether, 7,16-bis(4-methoxybenzyl)-1,4,10,13-tetraoxa-7,16-diazacyclooctadecane (**1**), and its molecular complex **1**·$(H_2NCS)_2$ (**3**) and proton-transfer complexes (**1**-H_2)·$[ClO_4]_2$·$2H_2O$ (**4**), (**1**-H_2)·$[NbF_6]_2$·$2H_2O$ (**5**), (**1**-H_2)·$[TaF_6]_2$·$2H_2O$ (**6**), (**1**-H_2)·$[BF_4]_2$ (**7**) and (**2**-H_2)·$[ClO_4]_2$·$2H_2O$ (**8**) were isolated and characterized by X-ray single-crystal diffraction. We intend to comparatively study the conformations of these two LCEs by computational methods in order to obtain a better insight into the conformational behavior of these kinds of compounds, and we will also try to estimate the preferable conformations for **1** and **2** depending on the degree of their protonation and the surrounding environment. We offer these results as a proof that the computational technique has now advanced to the point where calculated geometries and conformational energies of relatively complicated crown–ethers complexes are in agreement with the experimental findings (Scheme 1).

Results and discussion

X-Ray crystallography

Free macrocycle **1** crystallizes in the centrosymmetric monoclinic space group *C*2/*c* with the macrocyclic molecule residing on an inversion center giving half a molecule in the asymmetric unit. Molecule **1** with the numbering scheme is shown in Fig. 1. The same numbering is used both for **1** in **3–7** and for **2** (except for the missing methoxy group) in **8**.

In **1** the oxygen atoms are arranged in an *endo*-dentate mode typical for most crowns, while the nitrogen atoms flip to an *exo*-dentate mode to incorporate binding of the methoxybenzyl

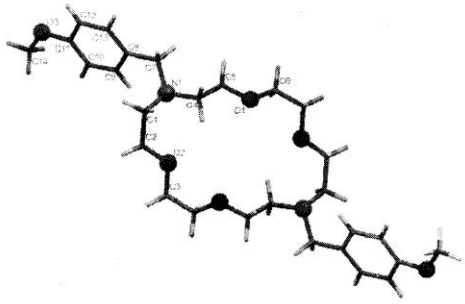

Fig. 1 Compound **1**: view with the numbering scheme.

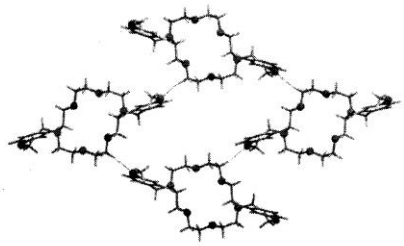

Fig. 2 Fragment of crystal packing in **1** showing the association of the molecules in a sheet *via* CH···O hydrogen bond, H···O 2.46, C···O 3.417(3) Å, CHO angle 169°.

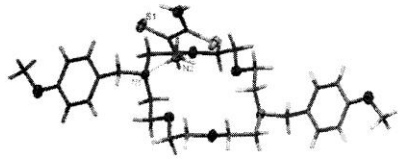

Fig. 3 View of **3** with the partial numbering scheme. Hydrogen bonding is shown by dotted lines.

groups. The molecule adopts a typical elliptical shape (Fig. 1) with two inversion-related methylene hydrogens turned inward toward the center of the ring. The two nitrogen atoms extend out in a *trans*-fashion, deviating from the plane of four oxygen atoms at ±0.884(3) Å. The conformation of the asymmetric part of the crown molecule is described by the sequence of four consecutive bonds in *trans*-conformation, followed by the *gauche*, *gauche*, *trans*, *trans*, *gauche* sequence (Table 1). The comparison with the pure phases of other bibracchial diaza-18C6 derivatives[24] as well as with the 18-membered crown ethers, 18C6, *cis*-transoid-*cis*-dicyclohexano-18C6[25] shows similarities in the shape of the macrocyclic cavity and in the pattern of the torsion angles. The methoxybenzyl side arms in **1** splay out from the crown rather than being below and above the macrocyclic plane; the dihedral angle between the planes of the N_2O_4 macrocyclic heteroatoms and the phenyl ring of the side arm is equal to 66.35(6)°.

The crystal packing for **1** clearly demonstrates the contribution of the methoxy group to the whole system of intermolecular interactions (Fig. 2). The molecules *via* weak CH···O hydrogen bonds are associated in tetramers giving rise to the H-bonded sheets. Due to the *C*2/*c* crystal symmetry these sheets interpenetrate in such a way that the methyl group of the pendant arm is arranged at 2.75 Å above (and below) the macrocyclic cavity of the nearest symmetry-related molecule of **1**. Such an arrangement is very common for the complexes of 18C6 with the CH_3 group containing guests,[26] although in our case the cavity is closed by the cross-cavity interactions and no CH (methyl)···O (crown) short contacts typical for the actual host–guest complexes were found.

Fig. 3 depicts the molecular complex **3** in a 1 : 1 ratio that crystallizes in the centrosymmetric monoclinic space group *C*2/*c*. Both **1** and dithiooxamide (**dtox**) molecules reside on inversion centers. They are held together *via* a single hydrogen bond, N2···N1 = 3.096(3) Å (Table 2). The planar **dtox** molecule is inclined at an angle of 76.46(7)° to the mean plane of six N_2O_4 heteroatoms of **1**, N2 atom deviating at 2.254(2) Å from the same plane.

Two **dtox** molecules are arranged on both sides of the centrosymmetric macrocyclic cavity. The arising host–guest interactions essentially influence the conformation of the macrocyclic molecule, which in **3** has a more flat and a more circular shape (Table 4) than in the free molecule **1**, characterized by the deviation of nitrogen atoms from the plane of four macrocyclic oxygens equal to ±0.473(3) Å and transition of two C–C bonds from *trans*-conformation to the preferable

Table 1 Torsion angles (°) along the macrocyclic framework in **1**, **3–5**, **7**

Angle	1	3	4	5	7A	7B
C(6)–O(1)–C(5)–C(4)	−179.6(2)	−173.0(2)	−171.6(3)	−179.7(4)	−173.5(1)	−171.7(1)
O(1)–C(5)–C(4)–N(1)	−161.0(2)	−67.7(2)	53.8(3)	58.4(5)	43.7(1)	45.5(1)
C(5)–C(4)–N(1)–C(1)	168.2(2)	171.8(2)	56.3(3)	59.9(4)	−172.5(1)	−169.2(1)
C(4)–N(1)–C(1)–C(2)	−81.0(2)	−55.3(3)	175.6(3)	−176.0(3)	86.6(1)	89.8(1)
N(1)–C(1)–C(2)–O(2)	76.7(2)	−53.8(3)	60.4(3)	53.6(4)	55.6(1)	58.1(1)
C(1)–C(2)–O(2)–C(3)	−179.8(2)	175.6(2)	−175.1(3)	−178.9(4)	71.5(1)	73.9(1)
C(2)–O(2)–C(3)–C(6)[a]	178.0(2)	173.2(2)	−179.3(3)	177.3(4)	163.3(1)	158.3(1)
O(2)–C(3)–C(6)[a]–O(1)[a]	−71.4(2)	73.8(3)	63.8(3)	64.0(5)	63.5(1)	61.2(1)
C(3)–C(6)[a]–O(1)[a]–C(5)[a]	−178.2(2)	172.3(2)	173.8(3)	170.5(4)	177.1(1)	−178.6(1)
C(1)–N(1)–C(7)–C(8)	−66.7(2)	−65.7(3)	164.6(3)	−163.9(3)	67.35(1)	166.9(1)
C(4)–N(1)–C(7)–C(8)	169.3(2)	60.6(3)	40.1(3)	70.2(4)	166.31(1)	−67.4(1)

[a] Symmetry transformations used to generate equivalent atoms: $a - x + 1/2, -y + 3/2, -z + 1$ (**1**); $-x + 1, -y + 1, -z$ (**3**); $-x + 1, -y + 1, -z + 1$ (**4**); $-x + 2, -y + 1, -z + 2$ (**5**); $-x + 1, -y + 1, -z$ (**7A**); $-x + 2, -y + 2, -z + 1$ (**7B**).

 This journal is © The Royal Society of Chemistry and the Centre National de la Recherche Scientifique 2009

Table 2 Hydrogen bond distances (Å) and angles (°) in **3–5**, **7**, **8**

D–H···A	d(D–H)	d(H···A)	d(D···A)	∠(DHA)	Symmetry transformation for acceptor
3					
N(2)–H(2N)···N(1)	0.94(2)	2.16(3)	3.096(3)	179(2)	x, y, z
4					
N(1)–H(1N)···O(1W)	0.89(1)	1.92(3)	2.805(3)	169(2)	x, y, z
O(1W)–H(1W)···O(4)	1.00(4)	1.87(4)	2.818(6)	158(3)	x, y, z
O(1W)–H(1W)···O(4′)	1.00(4)	2.15(6)	2.84(5)	125(3)	x, y, z
O(1W)–H(2W)···O(2)	0.83(4)	2.17(5)	2.995(4)	172(4)	$1 - x, 1 - y, 1 - z$
5					
N(1)–H(1N1)···O(1W)	0.88	2.00	2.874(5)	174	x, y, z
O(1W)–H(2W)···O(2)	0.91	2.03	2.928(5)	170	$2 - x, 1 - y, 2 - z$
O(1W)–H(1W)···F(6)	1.04	2.12	3.043(6)	147	$1 - x, 1 - y, 1 - z$
7					
N(1A)–H(1A)···O(2A)	0.91(2)	2.35(1)	2.864(1)	116(1)	x, y, z
N(1B)–H(1B)···O(2B)	0.92(2)	2.40(1)	2.889(1)	114(1)	x, y, z
8					
N(1)–H(1N)···O(1W)	0.90(3)	1.90(3)	2.792(3)	171(3)	$-x, -y, 1 - z$
O(1W)–H(1W)···O(1)	0.73(5)	2.27(5)	2.989(3)	173(5)	x, y, z
O(1W)–H(2W)···O(6′)	0.89(5)	2.01(5)	2.90(1)	173(4)	x, y, z
O(1W)–H(2W)···O(6)	0.89(5)	2.02(5)	2.893(7)	167(4)	x, y, z

Table 3 Comparison of calculated structures of neutral **1** and **2** with experimental solid-state structures[a]

	1	Calculated structure **1**			Calculated structure **2**	
	Experimental structure	Vacuum	Methanol	Experimental structure, XESSUJ01	Vacuum	Methanol
N···N′	7.696	7.925	7.926	7.298	7.925	7.920
O1···O1′	4.565	**4.690**	4.754	4.578	4.678	4.747
O2···O2′	6.124	**6.388**	6.403	6.809	6.386	6.412
i-C···*i*-C′	12.518	12.727	12.729	12.207	12.715	12.719
C1–N1–CH_2–C_{ipso}	−66.65	−68.66	−70.43	−74.40	−69.21	−70.09
C4–N1–CH_2–C_{ipso}	169.31	160.01	159.42	167.84	159.06	159.46

[a] The coordinates for **2** were taken from CSD (ref. code XESSUJ01).

gauche-conformation (Table 1). In spite of these pronounced changes, the macrocycle in **3** retains its extended conformation with the twisting angle between the planes of the macrocyclic N_2O_4 heteroatoms and phenyl ring of the side arm equal to 33.78(7)°. The recently described complex **2**·$(H_2NCS)_2$[22], similarly to **3**, crystallizes as a 1 : 1 tape where the components alternate. Similar to all previously reported **dtox** complexes with CEs including complex **2**·$(H_2NCS)_2$ no short contact **dtox**···**dtox** were found in **3**. Similar to **1**, the contribution of the methoxy oxygen atom to the intermolecular CH···O interactions is essential although the H···O distance slightly exceeds the parameter typical for the conventional hydrogen bond. Due to these interactions, the tapes are packed in a zipper-like mode providing their partial interpenetration and giving rise to the layer. Following the recent investigation by Gdaniec and co-workers,[27] we can also mention here the multiple CH···S interactions, which contribute to the stability of the layer in **3** (Fig. 4).

A search of the CSD[28] and our own efforts to expand this family of complexes led us to conclude that the genuine molecular host–guest complexes are rather rare for LCEs. The most preferable guest for them is a water molecule that, due to its small size, is easily accommodated on both sides of the macrocyclic cavity.[23] In the complexes with **dtox**, 4-nitrophenylsulfonamide,[22] and malononitrile,[23a] the components are held together *via* conventional NH(CH)···O(N)$_{crown}$ hydrogen bonds.

Compounds **4–8** represent the proton-transfer complexes built up of doubly protonated macrocyclic cations, $(\mathbf{1}\text{-}H_2)^{2+}$ in **4–7** or $(\mathbf{2}\text{-}H_2)^{2+}$ in **8** and inorganic anions. The N-bound H-atoms were objectively localized in the difference Fourier maps. All except **7** represent the crystal hydrates with the water molecules incorporated between the charged species; complexes **4** and **8**, which differ by the LCE used, have a similar composition and structure and will be discussed in a sequential order, while complexes **5** and **6** are isomorphous, and so only **5** will be discussed in detail. All compounds crystallize in centrosymmetric space groups, and the macrocyclic cations $(\mathbf{1}\text{-}H_2)^{2+}$ and $(\mathbf{2}\text{-}H_2)$ exhibit a crystallographically imposed C_i symmetry. The protonation of the macrocyclic nitrogen atoms causes dramatic changes in the macrocyclic shape and in the arrangement of the pendant arms in comparison with the neutral molecules (Table 5). Complexes **4** (Fig. 5) and **8** (Fig. 6) crystallize in triclinic space group $P\bar{1}$, with similar unit cell dimensions (Table 6). The macrocyclic cations reside on an inversion center. The water molecule and the $[ClO_4]^-$ anion occupy general positions, with the latter being disordered over two sites; hence, only its major component is shown in Fig. 5 and 6. Two water molecules are located on either side of the macrocyclic cavity and reside at

Table 4 Comparison of calculated equilibrium structures of neutral **1** and **2** in **3** and **2**·$(H_2NCS)_2$[a] with experimental solid-state structures

	3	Calculated structure		**2**·$(H_2NCS)_2$ (**A**)	Calculated structure **2A**		**2**·$(H_2NCS)_2$ (**B**)	Calculated structure **2B**	
	Experimental structure	Vacuum	Methanol	Experimental structure	Vacuum	Methanol	Experimental structure	Vacuum	Methanol
N···N′	7.014	6.688	7.074	6.707	6.819	6.687	6.326	6.699	6.784
O1···O1′	4.388	5.172	4.920	5.537	5.818	5.958	5.299	5.554	5.491
O2···O2′	5.673	6.033	5.831	6.216	6.380	6.463	7.192	6.921	7.062
i-C···*i*-C′	11.879	11.178	12.013	11.370	11.575	11.487	11.343	11.803	10.671
C1–N1–CH_2–C_{pso}	−60.61	−66.32	−64.53	−58.55	−69.67	−66.01	−62.14	−64.43	−66.21
C4–N1–CH_2–C_{pso}	65.69	74.61	68.91	69.04	70.74	68.42	64.10	74.02	67.48

[a] In **2**·$(H_2NCS)_2$ **2** is present in two conformations, both of them were optimized.

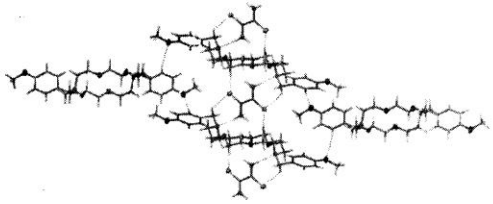

Fig. 4 Fragment of crystal packing in **3** showing the association of molecular complexes in the layer *via* NH···N hydrogen bond and weak CH···O and CH···S interactions, H···O 2.65, C···O 3.533(3) Å, CHO angle 159°, H···S 2.93 and 2.98, C···S 3.551(3) and 3.684(3) Å, CHS angles 120° and 135°.

1.805(3) Å (**4**) and 1.678(3) Å (**8**), respectively, above the macrocyclic plane in a twin pseudo-perched orientation. In both complexes, the nitrogen atom adopts an *endo*-orientation, with their hydrogen atom being involved in NH···O hydrogen bonding with the lone pair of the water molecule. In turn, the water molecule, acting as a H-donor, provides both of its hydrogens for the OH···O interactions with one oxygen atom of the crown molecule and one oxygen atom of the $[ClO_4]^-$ anion (Table 2). Thus, the water molecule exhibits its traditional mediating function between the charged species.[29] A very similar example gives *N*,*N*′-dibenzyl-4,13-diazonia-18-crown-6 tetrachloro-dioxo-uranium dihydrate (**2**-H_2)(UCl_4O_2)·$2H_2O$,[8] where two water molecules bind to the inner cavity of the crown ether in a symmetry-related mode. For both protonated macrocycles, we observe the further tendency toward more circular (Tables 4 and 5) and more planar shapes in comparison with the neutral molecules; the deviation of the nitrogen atoms from the plane through the macrocyclic oxygens is equal to ±0.606(4) Å and ±0.629(3) Å in (**1**-H_2)$^{2+}$ and (**2**-H_2)$^{2+}$, respectively. The twisting angle between the N_2O_4 and C8–···–C13 planes is equal to 62.76(9) in **4** and 77.45(8) in **8**, respectively.

The distinction in the twisting angle values is most probably dictated by the involvement of the methoxy group in the intermolecular interactions with the inversion-related macrocyclic cations with the formation of R_2^2(**8**) planar supramolecular synthon (Fig. 7a), while in **8** the aryl substituents are displayed in parallel planes with an interplane distance of 3.330 Å (Fig. 7b).

Recently,[30a] we have succeeded in using aza-CEs, namely aza-15C5 and aza-18C6, under synthetic conditions identical to those described in the Experimental part of this article to elicit the rather unusual anionic forms for Nb and Ta, $[(H_2O)NbF_4ONbF_5]^-$ and $[(TaF_5)_2O]^{2-}$, respectively. However, the use of **1** yielded two isomorphous complexes **5** and **6** (Table 3), with the $[NbF_6]^-$ and $[TaF_6]^-$ hexafluorometallate anions as the counter-ions being typical for the oxonium complexes of O-containing CEs.[30b] In **5** and **6** both $[NbF_6]^-$ and $[TaF_6]^-$ have an octahedral geometry, with the Nb–F and Ta–F distances being in the range 1.852(4)–1.879(2) and 1.856(8)–1.885(8) Å, respectively. In **5** the (**1**-H_2)$^{2+}$ cation and the two crystallographically unique $[NbF_6]^-$ anions reside on inversion centers, while the water molecule occupies the general position (Fig. 8). Similar to **4** and **8**, the water molecule

 This journal is © The Royal Society of Chemistry and the Centre National de la Recherche Scientifique 2009

Table 5 Comparison of calculated equilibrium structures of doubly protonated macrocycles $(\mathbf{1}\text{-}H_2)^{2+}$ and $(\mathbf{2}\text{-}H_2)^{2+}$ in **4–8** with experimental solid-state structures

	4			**8**			**5**		
	Experimental structure	Vacuum	Methanol	Experimental structure	Vacuum	Methanol	Experimental structure	Vacuum	Methanol
N···N′	6.357	6.623	6.394	6.242	6.630	6.529	6.432	6.626	
O1···O1′	4.443	4.907	4.770	4.797	4.868	4.857	4.697	4.858	
O2···O2′	5.789	5.328	5.515	5.744	5.361	5.425	5.547	5.418	
i-C···*i*-C′	10.405	9.498	8.972	9.722	9.677	9.114	9.550	9.911	
C1–N1–CH_2–C_{ipso}	−40.10	−59.98	−66.09	−62.67	−58.00	−65.46	−70.22	−53.85	
C4–N1–CH_2–C_{ipso}	164.61	174.01	168.03	174.09	176.05	169.20	163.83	179.79	
	7(A)			**7(B)**			**$(\mathbf{2}\text{-}H_2)[BF_4]_2\cdot H_2O$**		
	Experimental structure	Vacuum	Methanol	Experimental structure	Vacuum	Methanol	Experimental structure	Vacuum	Methanol
N···N′	5.641	6.351	6.197	5.684	6.363	6.138	5.841	6.306	6.121
O1···O1′	5.088	4.558	4.564	4.792	4.533	4.604	4.469	4.471	4.633
O2···O2′	5.106	5.265	5.323	5.324	5.262	5.321	5.449	5.301	5.341
i-C···*i*-C′	6.619	8.438	7.714	6.660	8.376	7.626	6.995	7.932	7.658
C1–N1–CH_2–C_{ipso}	−67.35	−60.79	−68.90	−67.40	−62.23	−67.40	−69.62	−66.32	−65.86

Fig. 5 View of **4** with the partial numbering scheme. Only the major position for the disordered anion is shown. Hydrogen bonding is shown by dotted lines. The atom with the suffix A is at the symmetry position $(1 - x, 1 - y, 1 - z)$.

Fig. 6 View of **8** with the partial numbering scheme. Only the major position for the disordered anion is shown. Hydrogen bonding is shown by dotted lines. Atoms with the suffix A are at the symmetry position $(-x, -y, 1 - z)$.

mediates charged species as a single acceptor with the crown's NH^+ group *via* an $NH^+\cdots O$ (water) hydrogen bond and as a double donor *via* OH (water)···O and OH (water)···F hydrogen bonds with one oxygen atom of the macrocycle and one fluorine atom of the anion (Table 2). It is located at 1.577(5) Å (1.678(3) Å in **6**) above the mean plane of the N_2O_4 set of heteroatoms. Only one anion, $[Nb(2)F_6]^-$, makes contact with the intermediate water molecule, while the other, $[Nb(1)F_6]^-$, is involved in the CH···F intermolecular interactions, thus being interspersed between a network of crown molecules (Fig. 9). The *trans-annular* N···N and O···O distances across the cavity and the sequence of torsion angles along the macrocyclic framework in the $(\mathbf{1}\text{-}H_2)^{2+}$ cation are very close to those of **4**, while the orientation of the side arms differs as indicated by the twisting angle of 75.03(9)° between the planes through the N_2O_4 set and the phenyl ring.

The explanation for the different turn of the pendant arms in **4** and **5** may follow from slightly different interactions between the pendant arms of neighboring complexes, since the lone pair of the methoxy-group oxygen atom in **5(6)** is not involved in the H-bonding self-assembling interactions, and the pendant arms of inversion-related macrocycles are

Table 6 Crystal data and structure refinement parameters for **1**, **3–8**

	1	**3**	**4**	**5**	**6**	**7**	**8**
Formula	$C_{28}H_{42}N_2O_6$	$C_{28}H_{42}N_2O_6 \cdot C_2H_4N_2S_2$	$C_{28}H_{44}N_2O_6 \cdot [ClO_4]_2 \cdot 2H_2O$	$C_{28}H_{44}N_2O_6 \cdot [NbF_6]_2 \cdot 2H_2O$	$C_{28}H_{44}N_2O_6 \cdot [TaF_6]_2 \cdot 2H_2O$	$C_{28}H_{44}N_2O_6 \cdot [BF_4]_2$	$C_{26}H_{40}N_2O_4 \cdot [ClO_4]_2 \cdot 2H_2O$
Formula weight	502.64	622.83	739.58	954.50	1130.58	678.27	679.53
Crystal system	Monoclinic	Monoclinic	Triclinic	Triclinic	Triclinic	Triclinic	Triclinic
Space group	$C2/c$	$C2/c$	$P\bar{1}$	$P\bar{1}$	$P\bar{1}$	$P\bar{1}$	$P\bar{1}$
a/Å	21.436(4)	17.2050(5)	7.322(1)	6.8821(3)	6.8062(11)	11.933(2)	7.592(2)
b/Å	11.050(2)	8.4590(3)	10.757(2)	11.3041(5)	11.3381(18)	12.120(2)	10.458(2)
c/Å	12.701(3)	23.3120(9)	12.450(2)	14.0931(5)	14.098(2)	12.404(2)	10.976(2)
α/°	90.0	90.0	91.67(2)	106.232(2)	105.873(9)	94.820(1)	98.11(3)
β/°	108.86(3)	104.260(12)	104.92(3)	101.770(2)	101.336(9)	111.714(1)	94.67(2)
γ/°	90.0	90.0	109.41(3)	106.118(2)	106.175(6)	100.392(1)	108.51(3)
V/Å^3	2846.9(10)	3288.2(2)	886.6(2)	963.03(7)	960.2(3)	1616.86(5)	810.7(3)
Z	4	4	1	1	1	2	1
ρ_{calc}/g cm^{-3}	1.173	1.258	1.385	1.646	1.955	1.393	1.392
μ/mm^{-1}	0.082	0.208	0.256	0.699	5.797	0.125	0.268
F(000)	1088	1336	392	484	548	712	
Reflections collected/unique	10373/2525	8339/2905	9404/3296	6316/3763	5444/3640	11815/6275	3162/3162
Reflections with $I > 2\sigma(I)$ (R_{int})	1661 [R_{int} = 0.042]	1947 [R_{int} = 0.0655]	2039 [R_{int} = 0.041]	2854 [R_{int} = 0.0212]	2021 [R_{int} = 0.0371]	5547 [R_{int} = 0.0139]	2361 [R_{int} = 0.031]
Goodness-of-fit	1.055	0.953	1.106	1.068	0.924	1.046	1.030
R_1, wR_2 [$I > 2\sigma(I)$]	0.0456, 0.1210	0.0568, 0.1474	0.0574, 0.1599	0.0550, 0.1658	0.0546, 0.1571	0.0338, 0.0914	0.0585, 0.1668
R_1, wR_2 (all data)	0.0784, 0.1331	0.0838, 0.1595	0.1009, 0.1747	0.0688, 0.1788	0.0971, 0.1870	0.0387, 0.0943	0.0793, 0.1781

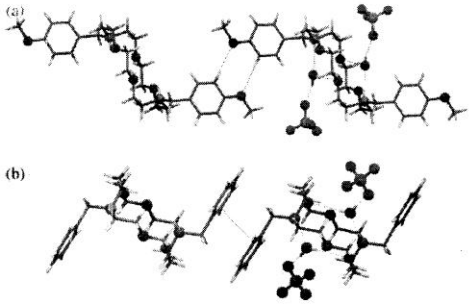

Fig. 7 (a) Self-assembling of adjacent macrocycles in **4** *via* C–H···O hydrogen bonds, H···O 2.56, C···O 3.491(4) Å, CHO angle 179°. (b) An arrangement of adjacent macrocycles in **8** with the interplane distance of 3.330 Å. The shortest intermolecular contacts are shown by dotted lines.

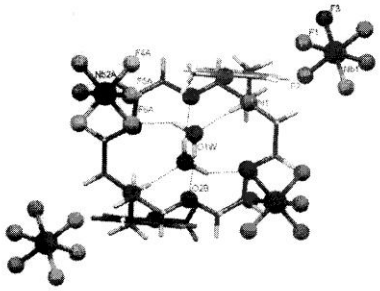

Fig. 8 View of **5** with the partial numbering scheme. Hydrogen bonding is shown by dotted lines. Atoms with the suffixes A and B are at the symmetry positions (1 − x, 1 − y, 1 − z) and (2 − x, 1 − y, 2 − z), respectively.

arranged in parallel planes with a partial overlap typical for the π–π interactions (Fig. 9).

Compound **7** of the 1 : 2 ratio crystallizes in the triclinic space group $P\bar{1}$. The asymmetric unit contains two halves of two macrocyclic cations (labeled **A** and **B**) that reside on two different inversion centers and two $[BF_4]^-$ anions (also labeled **A** and **B**) in general positions. The conformations of the two macrocycles (Tables 1 and 5) and the geometry of the two $[BF_4]^-$ anions are very similar, and so only the components labeled **A** are shown in Fig. 10.

Of the proton-transfer complexes discussed herein, only **7** represents a water-free compound. The protonated macrocyclic nitrogen atoms adopt an *endo*-orientation that is stabilized by the short-cut intramolecular N–H···O distance (Table 2). The macrocyclic cavity adopts a chair conformation with the deviation of nitrogen atoms at ±1.507(1) Å (±1.511(1) Å in

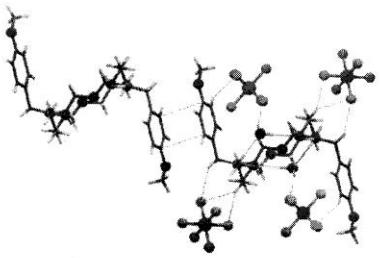

Fig. 9 Fragment of crystal packing in **5** showing the association of the adjacent macrocycles. The interplane separation between the aromatic units is equal to 3.389 Å. The shortest CH···F intermolecular contacts H···F 2.52–2.64, C···F 3.308(3)–3.461(3) Å, CHF angle 136°–154° are shown by dotted lines.

 This journal is © The Royal Society of Chemistry and the Centre National de la Recherche Scientifique 2009

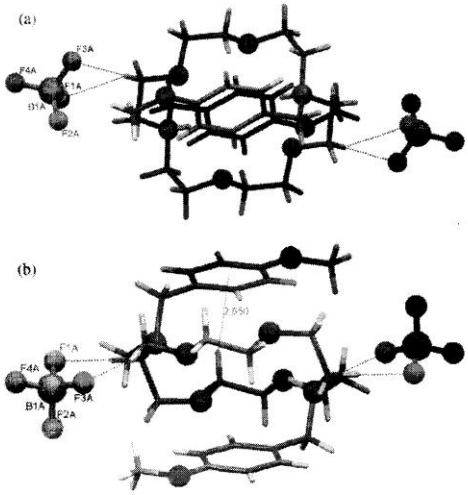

Fig. 10 Top (a) and side (b) views of complex **7A** with the partial numbering scheme. The shortest CH···F intermolecular contacts H···F 2.54 and 2.59, C···F 3.485(4) and 3.130(4) Å, CHF angle 164° and 115° are shown by dotted lines. (b) C–H···π interaction is shown by a dotted line.

cation **B**) from the plane of four oxygen atoms, the value being maximal among all the complexes described here. The C–H···π interactions between two methylene hydrogens and aromatic subunits effectively turn the phenyl groups of the side arms above and below the macrocycle (Fig. 10b) in such a way that the dihedral angle between the plane of the aromatic ring and the plane of the crown oxygen atoms is 43.17(4)° (45.46(4)° for cation **B**). Both of these types of intramolecular interactions were previously noted in the parent $(\mathbf{2}\text{-}H_2)^{2+}$ in the series of lanthanoid complexes,[8] in $(\mathbf{2}\text{-}H_2)I_8$,[12] and in $(\mathbf{2}\text{-}H_2)[BF_4]_2\cdot H_2O$.[11] Inspection of torsion angles (Table 1) reveals that the macrocycle is characterized by the energetically preferable *gauche*- and *trans*-conformations along the C–C and C–O bonds, while N–C bonds are equally distributed between *gauche*- and *trans*-conformations. The pendant arms of the symmetry-related macrocycles demonstrate the same type of self-association as in **5** (Fig. 11).

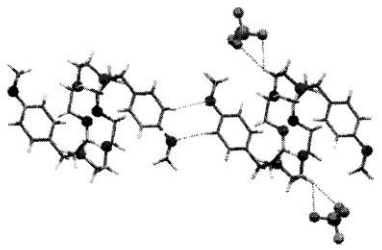

Fig. 11 Fragment of crystal packing in **7**. Self-assembling of adjacent macrocycles (labeled **A**) *via* C–H···O hydrogen bond, H···O 2.57, C···O 3.452(4) Å, CHO angle 160°. The shortest intermolecular contacts are shown by dotted lines.

The reported data represent three types of complexes: the genuine host–guest complex **3** with the conventional hydrogen bonds as the main interactions between the components, the proton-transfer ternary complexes **4–6**, **8** with the water molecule incorporated between the charged species, and the binary water-free complex **7**. Our own results and recent literature data providing the structural information make it possible to compare the conformations of **1** and **2** with the related structure complexes and to estimate the influence of minor changes in the macrocycle (the methoxy group incorporated into the pendant arm) on the conformation of the macrocycle and the overall system of interactions.

Quantum chemical calculations

Herein we have completed the X-ray data by quantum chemical calculations on the DFT level of theory that provide in-depth details on the conformations of **1** and **2** macrocycles, and especially on the positions of the pendant arms. Calculations were performed in the gas phase and in methanol to simulate the solvation effects. Since the relevant experimental structures exhibited crystallographically imposed inversion symmetry, all quantum chemical calculations were also performed with that symmetry restriction. For all structures, the optimization of the geometry of the macrocycle in vacuum and in methanol solution has been carried out and the results are summarized in Tables 3–5. All the calculated conformers are very close to the parent X-ray structures. In general, for all optimized structures, the shape of the macrocycle (measured by the distances of opposite facing heteroatoms) and the position of the pendant arms measured by the distance of two *ipso*-C atoms (atom C7 and its symmetry-related counterpart in Fig. 1) are close to the experimental solid-state structures (see Tables 3–5). The comparison of two sets of optimization carried out in vacuum and in methanol reveals the best fit of crystalline data with the vacuum structure for free **1**, while for the complexed macrocycle the best fit was obtained when the solvation effects were taken into consideration, *i.e.* for the optimization made in methanol. Fig. 12 summarizes the equilibrium structures for **1** and $(\mathbf{1}\text{-}H_2)^{2+}$ in **1**, **3–7**.

Ab initio HF/6-31+G quantum chemical calculations have been performed for the complexation energy for pairs of compounds $\mathbf{1}\cdot(H_2NCS)_2$, (**3**) and $\mathbf{2}\cdot(H_2NCS)_2$, and

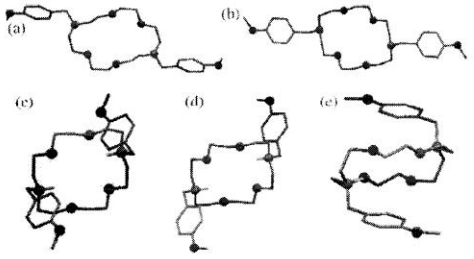

Fig. 12 Calculated equilibrium structures for neutral **1** and $(\mathbf{1}\text{-}H_2)^{2+}$ cation from **1**, **3–7**. All C-bound H-atoms are omitted for clarity. (a) free **1** (vacuum); (b) neutral **1** from **3** (methanol); (c) $(\mathbf{1}\text{-}H_2)^{2+}$ from **4** (methanol); (d) $(\mathbf{1}\text{-}H_2)^{2+}$ from **5** (vacuum); (e) $(L^1H_2)^{2+}$ from **7** (methanol).

[redacted]

$(\mathbf{1}\text{-}H_2)\cdot[BF_4]_2$ (**7**) and $(\mathbf{2}\text{-}H_2)\cdot[BF_4]_2\cdot H_2O$, where the water molecules are not incorporated between the host and guest molecules. The complexation energy was estimated as $\Delta E = E_{Complex} - E_{Host} - E_{Guest}$. The complexation energies of -724.844 kcal mol^{-1} for complex **7** and -762.558 kcal mol^{-1} for $(\mathbf{2}\text{-}H_2)\cdot[BF_4]_2\cdot H_2O$ show a better complexation efficiency for the proton-transfer complexes than for the molecular complexes, -16.996 kcal mol^{-1} for $\mathbf{1}\cdot(H_2NCS)_2$, (**3**), and -12.408 kcal mol^{-1} for $\mathbf{2}\cdot(H_2NCS)_2$.

Conclusion

We have reported the synthesis, and X-ray and DFT studies for the molecular and proton-transfer complexes based on unexplored bibracchial-crown ether, *N,N'*-dimethoxydibenzyl-1,7,10,16-tetraoxo-4,13-diazacyclooctadecane (**1**). The available data demonstrate the pronounced conformational mobility of macrocyclic cavity and distinctions in the orientation of pendant arms. Moreover, the nature of the anion strongly influences the twisting of the pendant group, making it orient in opposite directions. To rationalize different conformations of **1** in comparison with the parent *N,N'*-bis(4-methoxybenzyl)-1,7,10,16-tetraoxo-4,13-diazacyclooctadecane (**2**), theoretical quantum chemical calculations on the DFT (B3LYP) level were performed. All calculated conformers are close to the initial X-ray structures. The investigation shows that the computational approach correlates with the structural findings. We can conclude that we can emulate in the calculations the weak force interactions that we observe in the solid-state structures. The methoxy group that contributes by the C–H···O(OCH_3) hydrogen bonding to the overall system of intermolecular interactions imposes distinctions both in the orientation of pendant arms in particular and in the crystal packing as a whole.

Experimental

General

Caution! Although we have experienced no difficulties with the perchloric and hydrofluoric acids, these should be regarded as potentially dangerous substances and handled with care. Commercially available reagents were used as received. Compounds **3–8** were analyzed for C, H, and N in a Perkin Elmer 240C. The thin layer chromatographic control of the purity of substances was performed on Silufol UV-254 plates. All compounds were synthesized by an addition of the corresponding 'guest' species directly to a stirred solution of the LCE. Moderate heating was required to complete full dissolution. The composition of all compounds was confirmed by routine elemental analysis.

(1). The initial ligand was synthesized following the procedure described earlier.[20]

$\mathbf{1}\cdot(H_2NCS)_2$ (3). **1** (125 mg, 0.25 mmol) and ethanedithioamide (30 mg, 0.25 mmol) were dissolved in methanol (3 ml) at 64 °C, followed by the addition of ethyl acetate (3 ml) and *n*-butanol (1 ml). The resulting clear solution was slowly reduced in volume by evaporating the solvents at room temperature. Red transparent crystals were obtained, mp 108–110 °C. Analysis: found: C, 57.81, H, 7.49, N, 9.06, S, 10.33%; $C_{30}H_{46}N_4O_6S_2$: calc.: C, 57.85, H, 7.44, N, 9.00, S, 10.30%.

$(\mathbf{1}\text{-}H_2)\cdot[ClO_4]_2\cdot 2H_2O$ (4). To **1** (50 mg, 0.1 mmol) dissolved in methanol (5 ml) was added 70% perchloric acid (0.7 ml) dissolved in methanol (2 ml) at 64 °C, followed by the addition of ethyl acetate (4 ml). The resulting clear solution was slowly reduced in volume by evaporating the solvents at room temperature. Colorless transparent crystals were obtained, mp 132–134 °C. $C_{28}H_{48}Cl_2N_2O_{16}$: calc.: C, 45.47; H, 6.54; N, 3.79%. Found: C, 45.43; H, 6.57; N, 3.82%.

$(\mathbf{1}\text{-}H_2)\cdot[NbF_6]_2\cdot 2H_2O$ (5). To niobium oxide (v) (133 mg, 0.5 mmol) was added 45% hydrofluoric acid (10 ml). The resulting solution was boiled till the volume of 4–5 ml was reached. To the obtained acidic solution was added a solution of **1** (251 mg, 0.5 mmol) in methanol (10 ml). The resulting crystals were removed from the solution before the solvent had completely evaporated. Colorless transparent crystals of the complex were obtained, mp 185–187 °C (dec.). The yield is almost quantitative. $C_{28}H_{48}F_{12}N_2Nb_2O_8$: calc.: C, 35.23; H, 5.07%; F, 23.89; N, 2.93%. Found: C, 35.28; H, 5.02; F, 23.86; N, 2.96%.

$(\mathbf{1}\text{-}H_2)\cdot[TaF_6]_2\cdot 2H_2O$ (6). To tantalum oxide (v) (221 mg, 0.5 mmol) was added 45% hydrofluoric acid (10 ml). The resulting solution was boiled till the volume of 4–5 ml was reached. To the obtained acidic solution was added a solution of L^1 (251 mg, 0.5 mmol) in methanol (10 ml). The resulting crystals were removed from the solution before the solvent had completely evaporated. Colorless transparent crystals of the complex were obtained, mp 185–187 °C (dec.). The yield was almost quantitative. $C_{28}H_{48}F_{12}N_2O_8Ta_2$: calc.: C, 29.75; H, 4.28; F, 20.17; N, 2.48%. Found: C, 29.71; H, 4.25; F, 20.21; N, 2.44%.

$(\mathbf{1}\text{-}H_2)\cdot[BF_4]_2$ (7). To L^1 (50 mg, 0.1 mmol) dissolved in methanol (5 ml) boron trifluoride etherate (0.35 ml) was added. The resulting clear solution was slowly reduced in volume by evaporating the solvents at room temperature. Colorless transparent crystals were obtained by recrystallization from a methanol–ethyl acetate mixture (1 : 2), mp 132–134 °C. $C_{28}H_{44}B_2F_8N_2O_6$: calc.: C, 49.58; H, 6.54; F, 22.41; N, 4.13%. Found: C, 49.54; H, 6.59; F, 22.47; N, 4.15%.

$(\mathbf{2}\text{-}H_2)\cdot[ClO_4]_2\cdot 2H_2O$ (8). To **2** (44 mg, 0.1 mmol) dissolved in a mixture of methanol (5 ml) and *n*-BuOH (0.5 ml) was added 70% perchloric acid (0.3 ml). The resulting clear solution was slowly reduced in volume by evaporating the solvents at room temperature. Colorless transparent crystals were obtained, mp 154–155 °C. $C_{26}H_{44}Cl_2N_2O_{14}$: calc.: C, 45.95; H, 6.53; N, 4.12%. Found: C, 45.92; H, 6.57; N, 4.10%.

X-Ray crystallographic data for 1, 3–8. The X-ray data and the details of the refinement for **1**, **3–8** are given in Table 6; the torsion angles and H-bonding data are summarized in Tables 1 and 2, respectively. Tables 3–5 contain the geometric parameters for **1**, **2** and their protonated forms for the experimental solid-state and calculated structures. The X-ray intensity data for **1**, **3–5** and **8** were collected at

 This journal is © The Royal Society of Chemistry and the Centre National de la Recherche Scientifique 2009

room temperature on a Nonius Kappa CCD diffractometer[31] while for **6** and **7** they were collected on a Bruker CCD diffractometer—both diffractometers were equipped with graphite monochromated Mo-Kα radiation. Unit cell parameters were obtained and refined using the whole data set. Frames were integrated and corrected for Lorentz and polarization effects using DENZO.[32] The scaling and the global refinement of the crystal parameters were performed by SCALEPACK.[32] For **5** and **6**, the absorption correction using SADABS was applied.[33] The structure solution and refinement proceeded similarly for all structures using the SHELX-97 program package.[34] Direct methods yielded all non-hydrogen atoms of the asymmetric unit. These atoms were treated anisotropically (full-matrix least squares method on F^2). In **4** the oxygen atoms of the $[ClO_4]^-$ anion are disordered over two positions with occupancies of 0.86(1) and 0.14(1), respectively, and only the major component was treated anisotropically. In **7** the oxygen atom of the water molecule was refined with the partial occupancy of 0.17(2) in an isotropic approximation. Hydrogen atoms in the water molecule were not localized. In **8** three oxygen atoms O4, O5, and O6 of the $[ClO_4]^-$ anion are disordered over two positions with occupancies of 0.75(1) and 0.25(1), respectively; the major component was treated anisotropically and the minor position was treated in an isotropic approximation. In all structures, C-bound H atoms were placed in the calculated positions and were treated using a riding-model approximation, with $U_{iso}(H) = 1.2\ U_{eq}(C)$ for methylene and $U_{iso}(H) = 1.5\ U_{eq}(C)$ for methyl groups, respectively, while the N- and O-bound H-atoms were found from differential Fourier maps at an intermediate stage of the refinement and were treated isotropically. All images were produced using Mercury.[35]

Computational details. *Ab initio* calculations were carried out using density functional theory with the Gaussian03 package at the B3LYP/6-31+G and HF/6-31+G levels of theory.[36] To avoid SCF convergence problems, a quadratic convergence procedure was applied during the geometry optimizations. Full geometry optimizations of the studied compounds were performed both in solution and in the gas phase. The polarizable continuum model (PCM) was included in the SCF procedure for the description of the methanol solutions with the exception of **4**. The dielectric constant was set at 32.63. All calculations were carried out using the restricted spin formalism (closed-shell).

Acknowledgements

The diffraction data for **1**, **4** and **8** were collected at the Schulich Faculty of Chemistry, Technion, Haifa, through the cooperation of Prof. Menahem Kaftory, whom we would like to acknowledge. The authors thank Prof. A. S. Dimoglo for the computational facility.

References

1 C. J. Pedersen, *J. Am. Chem. Soc.*, 1967, **89**, 7017.
2 C. J. Pedersen, *J. Am. Chem. Soc.*, 1967, **89**, 2495.
3 M. E. Weber, E. K. Elliott and G. W. Gokel, *Org. Biomol. Chem.*, 2006, **4**, 83.
4 V. J. Gatto and G. W. Gokel, *J. Am. Chem. Soc.*, 1984, **106**, 8240.
5 K. A. Arnold, A. M. Viscariello, M. Kim, R. D. Gandour, F. R. Fronczek and G. W. Gokel, *Tetrahedron Lett.*, 1988, **29**, 3025.
6 (*a*) G. W. Gokel, W. M. Leevy and M. E. Weber, *Chem. Rev.*, 2004, **104**, 2723; (*b*) G. W. Gokel, *Chem. Soc. Rev.*, 1992, **21**, 39.
7 K. R. Fewings and P. C. Junk, *Aust. J. Chem.*, 1999, **52**, 1109.
8 D. J. Evans, P. C. Junk and M. K. Smith, *New J. Chem.*, 2002, **26**, 1043.
9 M. I. Saleh, A. Salhin, B. Saad and H.-K. Fun, *J. Mol. Struct.*, 1999, **475**, 93.
10 T. W. Hambley, L. F. Lindoy, J. R. Reimers, P. Turner, G. Wei and A. N. Widmer-Cooper, *J. Chem. Soc., Dalton Trans.*, 2001, 614.
11 S. S. Basok, L. Croitoru, M. S. Fonari, E. V. Ganin, V. O. Gelmboldt, J. Lipkowski and Yu. A. Simonov, *Acta Crystallogr., Sect. C: Cryst. Struct. Commun.*, 2005, **61**, o188.
12 A. S. Gaballa, S. M. Teleb, E. Rusanov and D. Steinborn, *Inorg. Chim. Acta*, 2005, **357**, 4144.
13 P. C. Junk and M. K. Smith, *Inorg. Chem. Commun.*, 2002, **5**, 1082.
14 (*a*) E. K. Elliott, J. Hu and G. W. Gokel, *Supramol. Chem.*, 2007, **19**, 175; (*b*) A. V. Bordunov, J. S. Bradshaw, X. X. Zhang, N. K. Dalley, X. Kou and R. M. Izatt, *Inorg. Chem.*, 1996, **35**, 7229; (*c*) A. Awasthy, M. Bhatnagar, J. Tomar and U. Sharma, *Bioinorg. Chem. Appl.*, 2006, **2006**, 1.
15 (*a*) J. Hu, L. J. Barbour, R. Ferdani and G. W. Gokel, *Chem. Commun.*, 2002, 1806; (*b*) J. Hu, L. J. Barbour and G. W. Gokel, *Chem. Commun.*, 2002, 1808; (*c*) J. Hu, L. J. Barbour, R. Ferdani and G. W. Gokel, *Chem. Commun.*, 2002, 1810.
16 L. G. A. van de Water, W. Buijs, W. L. Driessen and J. Reedijk, *New J. Chem.*, 2001, **25**, 243.
17 M. Grotjahn and E. Kleinpeter, *J. Mol. Model*, 1999, **5**, 296.
18 (*a*) C.-C. Su and L.-H. Lu, *J. Mol. Struct.*, 2004, **702**, 23; (*b*) C.-C. Su, L.-H. Lu and T.-J. Hsieh, *J. Mol. Struct.*, 2007, **831**, 151.
19 (*a*) C. Platas-Iglesias, D. Esteban-Gómez, T. Enríquez-Pérez, F. Avecilla, A. de Blas and T. Rodríguez-Blas, *Inorg. Chem.*, 2005, **44**, 2224; (*b*) C. Platas-Iglesias, D. Esteban, V. Ojea, F. Avecilla, A. de Blas and T. Rodríguez-Blas, *Inorg. Chem.*, 2003, **42**, 4299; (*c*) M. González-Lorenzo, C. Platas-Iglesias, F. Avecilla, S. Faulkner, S. J. A. Pope, A. de Blas and T. Rodríguez-Blas, *Inorg. Chem.*, 2005, **44**, 4254.
20 N. G. Lukyanenko, S. S. Basok, E. Yu. Kulygina and V. I. Vetrogon, *Russ. J. Gen. Chem.*, 2003, **73**, 1919.
21 (*a*) M. S. Fonari, Yu. A. Simonov, Yu. M. Chumakov, G. Bocelli, E. V. Ganin and A. A Yavolovskii, *Supramol. Chem.*, 2004, **16**, 23; (*b*) N. G. Lukyanenko, T. I. Kirichenko, A. Yu. Lyapunov, C. Yu. Kulygina, Yu. A. Simonov, M. S. Fonari and M. M. Botoshansky, *Tetrahedron Lett.*, 2004, **45**, 2927; (*c*) M. S. Fonari, Yu. A. Simonov, G. Bocelli, M. M. Botoshansky and E. V. Ganin, *J. Mol. Struct.*, 2005, **738**, 85; (*d*) Yu. A. Simonov, M. S. Fonari, Gh. Duca, M. V. Gonta, E. V. Ganin, A. A. Yavolovskii, M. Gdaniec and J. Lipkowski, *Tetrahedron*, 2005, **61**, 6596; (*e*) N. G. Lukyanenko, T. I. Kirichenko, A. Yu. Lyapunov, A. V. Mazepa, Yu. A. Simonov, M. S. Fonari and M. M. Botoshansky, *Chem.–Eur. J.*, 2005, **11**, 262; (*f*) E. V. Ganin, M. S. Fonari, Yu. A. Simonov, G. Bocelli, S. S. Basok, V. V. Tkachuk, S. A. Kotlyar and G. L. Kamalov, *J. Inclusion Phenom. Macrocyclic Chem.*, 2005, **52**, 63; (*g*) W.-J. Wang, E. V. Ganin, M. S. Fonari, Yu. A. Simonov and G. Bocelli, *Org. Biomol. Chem.*, 2005, **3**, 3054; (*h*) M. S. Fonari, E. V. Ganin, S.-W. Tang, W.-J. Wang and Yu. A. Simonov, *J. Mol. Struct.*, 2007, **826**, 89; (*i*) B. Moulton, B. S. Luisi, M. S. Fonari, S. S. Basok, E. V. Ganin and V. Ch. Kravtsov, *New J. Chem.*, 2007, **31**, 561.
22 M. S. Fonari, Yu. A. Simonov, L. Croitoru, S. S. Basok, E. V. Ganin and J. Lipkowski, *J. Mol. Struct.*, 2006, **794**, 110.
23 For lariat ethers host–guest molecular complexes see: (*a*) K. von Deuten, A. Knochel, J. Kopf, J. Oehler and G. Rudolph, *J. Chem. Res.*, 1979, **358**, 4035; (*b*) Y. Habata and S. Akabori, *J. Chem. Soc., Dalton Trans.*, 1995, 3871; (*c*) R. E. Gawley, S. Pinet, C. M. Cardona, P. K. Datta, T. Ren, W. C. Guida, J. Nydick and R. M. Leblanc, *J. Am. Chem. Soc.*, 2002, **124**, 13448; (*d*) Y. Habata, T. Saeki and S. Akabori, *J. Heterocycl. Chem.*, 2001, **38**, 585; (*e*) K. A. Arnold, A. M. Viscariello, M. Kim,

R. D. Gandour, F. R. Fronczek and G. W. Gokel, *Tetrahedron Lett.*, 1988, **29**, 3025.

24 (*a*) S. L. De Wall, E. S. Meadows, L. J. Barbour and G. W. Gokel, *J. Am. Chem. Soc.*, 1999, **121**, 5613; (*b*) L. Kh. Minacheva, I. S. Ivanova, E. N. Pyatova, V. S. Sergienko, A. Yu. Tsivadze, G. A. Artamkina and I. P. Beletskaya, *Russ. Proc. Natl. Acad. Sci. USSR*, 2003, **389**, 58; (*c*) L. Kh. Minacheva, I. S. Ivanova, E. N. Pyatova, V. S. Sergienko, G. A. Artamkina, I. P. Beletskaya and A. Yu. Tsivadze, *Crystallogr. Rep.*, 2004, **49**, 982; (*d*) K. Kubo, R. Ishige, N. Kato, E. Yamamoto and T. Sakurai, *Heterocycles*, 1997, **45**, 2365; (*e*) E. S. Meadows, S. L. De Wall, L. J. Barbour and G. W. Gokel, *J. Am. Chem. Soc.*, 2001, **123**, 3092; (*f*) E. S. Meadows, S. L. De Wall, L. J. Barbour, F. R. Fronczek, M.-S. Kim and G. W. Gokel, *J. Am. Chem. Soc.*, 2000, **122**, 3325; (*g*) S. Suarez, O. Mamula, R. Scopelliti, B. Donnio, D. Guillon, E. Terazzi, C. Piguet and J.-C. G. Bunzli, *New J. Chem.*, 2005, **29**, 1323; (*h*) G. Ulrich, P. Turek, R. Ziessel, A. De Cian and J. Fischer, *Chem. Commun.*, 1996, 2461; (*i*) D. Esteban, F. Avecilla, C. Platas-Iglesias, J. Mahia, A. de Blas and T. Rodriguez-Blas, *Inorg. Chem.*, 2002, **41**, 4337; (*j*) T. Gunnlaugsson, H. Q. N. Gunaratne, M. Nieuwenhuyzen and J. P. Leonard, *J. Chem. Soc., Perkin Trans. 1*, 2002, 1954; (*k*) G. McSkimming, J. H. R. Tucker, H. Bouas-Laurent, J.-P. Desvergne, S. J. Coles, M. B. Hursthouse and M. E. Light, *Chem.–Eur. J.*, 2002, **8**, 3331.

25 (*a*) E. Maverick, P. Seiler, W. B. Schweizer and J. D. Dunitz, *Acta Crystallogr., Sect. B: Struct. Crystallogr. Cryst. Chem.*, 1980, **36**, 615; (*b*) V. Ch. Kravtsov, M. S. Fonari, M. J. Zaworotko and J. Lipkowski, *Acta Crystallogr., Sect. C: Cryst. Struct. Commun.*, 2002, **58**, o683.

26 (*a*) R. D. Rogers and P. D. Richards, *J. Inclusion Phenom.*, 1987, **5**, 631; (*b*) G. Weber, *J. Mol. Struct.*, 1983, **98**, 333; (*c*) G. Weber, *Acta Crystallogr., Sect. C: Cryst. Struct. Commun.*, 1983, **39**, 896; (*d*) B. L. Allwood, S. E. Fuller, P. C. Y. K. Ning, A. M. Z. Slawin, J. F. Stoddart and D. J. Williams, *J. Chem. Soc., Chem. Commun.*, 1984, 1356; (*e*) J. A. Bandy, M. R. Truter and F. Vogtle, *Acta Crystallogr., Sect. B: Struct. Crystallogr. Cryst. Chem.*, 1981, **37**, 1568; (*f*) R. D. Rogers, P. D. Richards and E. J. Voss, *J. Inclusion Phenom.*, 1988, **6**, 65; (*g*) D. Henschel, K. Wijaya, O. Moers, A. Blaschette and P. G. Jones, *Z. Naturforsch., B: Chem. Sci.*, 2000, **55**, 299; (*h*) A. Albert and D. Mootz, *Z. Naturforsch., B: Chem. Sci.*, 1998, **53**, 242.

27 B. Piotrkowska, A. Wasilewska, M. Gdaniec and T. Polonski, *CrystEngComm*, 2008, **10**, 1421.

28 F. N. Allen, *Acta Crystallogr., Sect. B: Struct. Sci.*, 2002, **58**, 380.

29 (*a*) Y. Levy and J. N. Onuchic, *Annu. Rev. Biophys. Biomol. Struct.*, 2006, **35**, 389; (*b*) J. B. Pritchard and D. S. Miller, *Physiol. Rev.*, 1993, **73**, 765; (*c*) P. L. Geissler, C. Dellago and D. Chandler, *J. Phys. Chem. B*, 1999, **103**, 3706.

30 (*a*) M. S. Fonari, V. Ch. Kravtsov, Yu. A. Simonov, S. S. Basok, E. V. Ganin, V. O. Gelmboldt, K. Suwinska, J. Lipkowski, O. A. Alekseeva and N. G. Furmanova, *Polyhedron*, 2008, **27**, 2049; (*b*) M. S. Fonari, Yu. A. Simonov, W.-J. Wang, S.-W. Tang, E. V. Ganin, V. O. Gelmboldt, T. S. Chernaya, O. A. Alekseeva and N. G. Furmanova, *Polyhedron*, 2007, **26**, 5193.

31 *COLLECT*, Nonius BV, Delft, The Netherlands, 1998.

32 Z. Otwinowski and W. Minor, in *Methods in Enzymology Macromolecular Crystallography, Part A*, ed. C. W. Carter and R. M. Sweet, Academic Press, London, 1996, vol. 276, p. 307.

33 G. M. Sheldrick, *SADABS*, Bruker AXS Inc., Madison, WI-53719, USA, 1997.

34 G. M. Sheldrick, *SHELXS97 and SHELXL97. Programs for Crystal Structure Solution and Refinement*, University of Göttingen, Germany, 1997.

35 C. F. Macrae, P. R. Edgington, P. McCabe, E. Pidcock, G. P. Shields, R. Taylor, M. Towler and J. van de Streek, *J. Appl. Crystallogr.*, 2006, **39**, 453.

36 M. J. Frisch, G. W. Trucks, H. B. Schlegel, G. E. Scuseria, M. A. Robb, J. R. Cheeseman, J. A. Montgomery, Jr, T. Vreven, K. N. Kudin, J. C. Burant, J. M. Millam, S. S. Iyengar, J. Tomasi, V. Barone, B. Mennucci, M. Cossi, G. Scalmani, N. Rega, G. A. Petersson, H. Nakatsuji, M. Hada, M. Ehara, K. Toyota, R. Fukuda, J. Hasegawa, M. Ishida, T. Nakajima, Y. Honda, O. Kitao, H. Nakai, M. Klene, X. Li, J. E. Knox, H. P. Hratchian, J. B. Cross, C. Adamo, J. Jaramillo, R. Gomperts, R. E. Stratmann, O. Yazyev, A. J. Austin, R. Cammi, C. Pomelli, J. W. Ochterski, P. Y. Ayala, K. Morokuma, G. A. Voth, P. Salvador, J. J. Dannenberg, V. G. Zakrzewski, S. Dapprich, A. D. Daniels, M. C. Strain, O. Farkas, D. K. Malick, D. Rabuck, K. Raghavachari, J. B. Foresman, J. V. Ortiz, Q. Cui, A. G. Baboul, S. Clifford, J. Cioslowski, B. B. Stefanov, G. Liu, A. Liashenko, P. Piskorz, I. Komaromi, R. L. Martin, D. J. Fox, T. Keith, M. A. Al-Laham, C. Y. Peng, A. Nanayakkara, M. Challacombe, P. M. W. Gill, B. Johnson, W. Chen, M. W. Wong, C. Gonzalez and J. A. Pople, *GAUSSIAN 03 (Revision B.01)*, Gaussian, Inc., Pittsburgh, PA, 2003.

 This journal is © The Royal Society of Chemistry and the Centre National de la Recherche Scientifique 2009

Додаток С.

Копія статті. “Особенности структуры производных 1,3-дигидропиримидин-2,4-дионов в комплексах с макроциклическими поли– и азаполиэфирами ”

ЖУРНАЛ СТРУКТУРНОЙ ХИМИИ

2009. Том 50 *Приложение* *S143 – S149*

УДК 548.736:547.7/8

ОСОБЕННОСТИ СТРУКТУРЫ ПРОИЗВОДНЫХ 1,3-ДИГИДРОПИРИМИДИН-2,4-ДИОНОВ В КОМПЛЕКСАХ С МАКРОЦИКЛИЧЕСКИМИ ПОЛИ- И АЗАПОЛИЭФИРАМИ

© 2009 **Ю.А. Симонов[1]*, М.С. Фонарь[1], Я. Липковский[2], Э.В. Ганин[3], А.А. Яволовский[4], Г.Л. Камалов[4]**

[1]*Институт прикладной физики АН Республики Молдова, Кишинев*
[2]*Институт физической химии ПАН, Варшава*
[3]*Одесский государственный экологический университет, Украина*
[4]*Физико-химический институт им. А.В. Богатского НАНУ, Одесса*

Статья поступила 9 декабря 2008 г.

Обобщены результаты исследований структуры органических комплексов производных 1,3-дигидропиримидин-2,4-дионов и их структурных аналогов с макроциклическими поли- и азаполиэфирами.

Ключевые слова: 1,3-дигидропиримидин-2,4-дионы, макроциклические полиэфиры, водородные связи.

Способность производных пиримидинов к селективному межмолекулярному взаимодействию посредством водородных связей (Н-связи) определяет их роль в биологических процессах и является уникальным примером распознавания субстрата рецептором. Подобным образом формируются димеры из пар азотистых оснований нуклеиновых кислот, комплементарное взаимодействие которых осуществляется за счет системы водородных связей [1]. Согласно существующим представлениям, биологическая активность некоторых природных пуринов и пиримидинов, а также их синтетических аналогов обусловлена способностью функционировать в составе стабильных ди-, три и тетрамолекулярных комплексов [2]. Такие ассоциаты удается зафиксировать и исследовать различными способами, основным среди которых является рентгеноструктурный анализ (РСА). Несмотря на многочисленные публикации о системах межмолекулярных взаимодействий, нам не известен универсальный рецептор для связывания нейтральных молекул посредством водородных связей. Тем не менее, на роль Н-акцепторов, способных образовывать с Н-донорами кристаллические соединения с простой целочисленной стехиометрией, могут претендовать краун-эфиры (КЭ) и их аналоги [3]. Такие комплексы изучаются, в основном, с целью получения информации, необходимой для понимания вклада слабых взаимодействий в общую систему стабилизации супрамолекулярных ассоциатов. Следует отметить, что с момента появления термина " комплекс хозяин—гость" применительно к комплексам КЭ с нейтральными органическими молекулами [4] представления о роли его компонентов претерпели существенные изменения, и теперь нередко макроциклическая молекула рассматривается как "гость", внедряющийся в матрицу молекул "хозяина". В качестве таких примеров можно привести молекулярные комплексы дитиобимочевины и трифенилметановых производных с различными по размерности КЭ [5, 6]. С другой стороны, современная химия нуклеиновых оснований и их синтетических аналогов дает яркие примеры самоорганизации таких систем в присутствии различных темплатов, в качестве которых нередко выступают катионы металлов [7].

* E-mail: simonov.xray@phys.asm.md

В настоящем сообщении авторы намерены продемонстрировать достоинства макроциклических полиэфиров и их аза-аналогов как перспективных темплатов, обеспечивающих перераспределение межмолекулярных водородных связей в кристаллической структуре урацильного производного (хозяина) при внедрении в такую систему макроциклической молекулы (гостя). Наличие в молекуле хозяина подобного рода нескольких Н-донорных (амидные, оксимные, сульфо- и аминогруппы) и Н-акцепторных центров (=O, =S, =N-) планарной и тетраэдрической геометрии позволяет осуществить комплексообразование с КЭ вследствие "высвобождения" из взаимодействий хозяин—хозяин сильных Н-доноров при частичном сохранении самоорганизации исходной структуры. Кроме того, выделение кристаллических комплексов с макрогетероциклами позволило нам идентифицировать и изучить особенности ряда новых 1,3-дигидропиримидин-2,4-дионов, качество кристаллов которых не соответствовало требованиям рентгеноструктурного эксперимента. На схеме 1 представлены производные пиримидина и макрогетероциклы, комплексы которых явились объектами исследований, обобщенных в настоящей публикации.

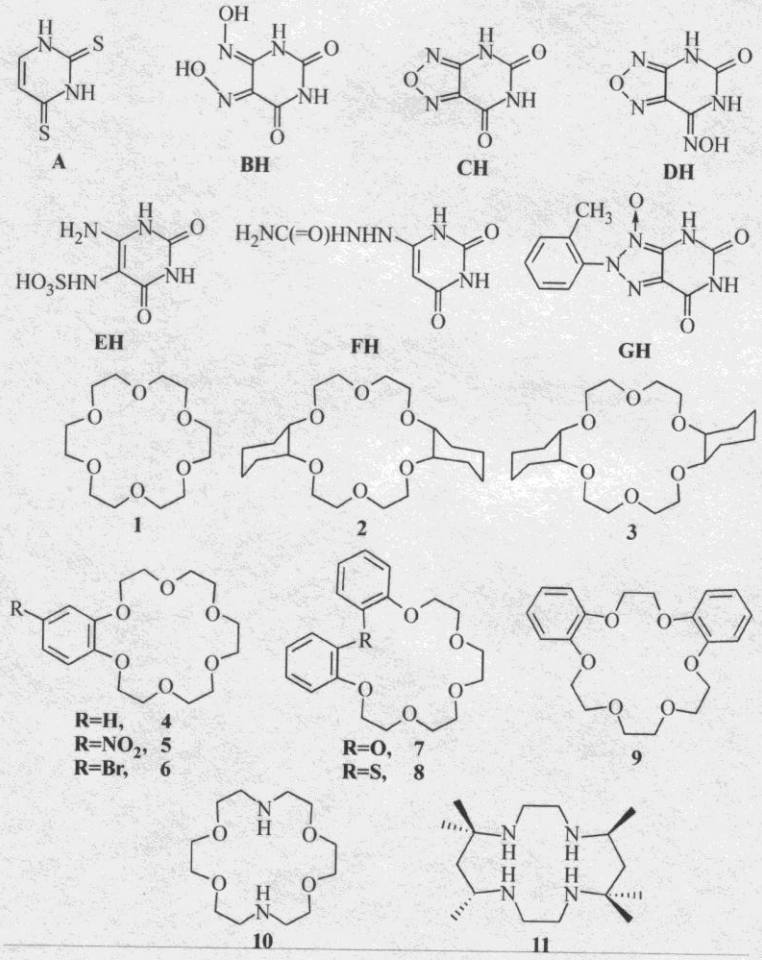

Схема 1

Интерес к 2,4-дитиоурацилу (**A**), простейшему представителю ряда урацилов, обусловлен возможностью изучения различных типов межмолекулярных взаимодействий, характерных для имеющихся в молекуле **A** функциональных групп, а также для определения наиболее легко гидратирующихся фрагментов этой молекулы [8, 9]. Известно, что теоретически для соединения **A** воз-

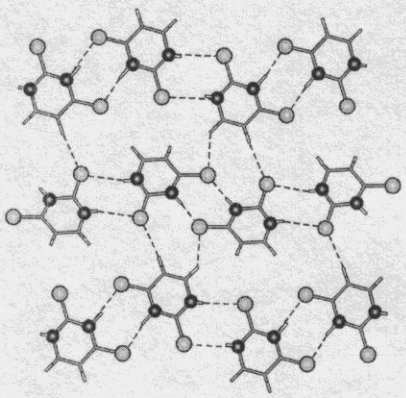

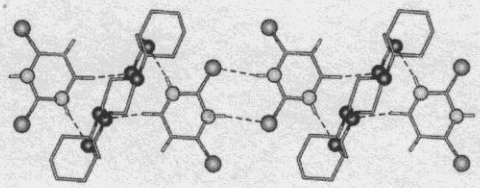

Рис. 1 (*слева*). Кристаллическая структура 2,4-дитиоурацила (**A**). Расстояния N···S в синтонах $R_2^2(8)$ 3,314 и 3,334 Å, кратчайшие расстояния C···S в CH···S контактах 3,487 и 3,828 Å

Рис. 2 (*справа*). Фрагмент полимерной цепочки в кристалле комплекса $\mathbf{2}\cdot(\mathbf{A})_2$

можно шесть тиол-тионных таутомеров. Многочисленные теоретические расчеты оценивали предпочтительность таутомерных форм **A** с энергетической точки зрения в зависимости от агрегатного состояния вещества. Установлено, что в кристалле молекулы **A** присутствуют в дитионной форме и объединены в линейные цепочки за счет чередования двух одинаковых $R_2^2(8)$ супрамолекулярных синтонов с участием NH-группы и одного из тионных атомов серы. Более слабые взаимодействия типа CH···S обусловливают объединение этих цепочек в слои (рис. 1) [10].

Исследованные молекулярные комплексы **1—9** соединения **A** с макрогетероциклами представляют собой двухкомпонентные и трехкомпонентные (гидраты) системы и демонстрируют несколько типов структурной организации [11, 12]. Двухкомпонентные системы $\mathbf{2}\cdot(\mathbf{A})_2$, $(\mathbf{7}\cdot\mathbf{A})_2$, $(\mathbf{8}\cdot\mathbf{A})_2$, $(\mathbf{9}\cdot\mathbf{A})_2$ характеризуются стехиометрией 2:1 или 1:1. Во всех комплексах сохраняется объединение молекул **A** в димер за счет супрамолекулярного гомосинтона $R_2^2(8)$. Супрамолекулярная организация диктуется геометрией макроциклической молекулы: в случае КЭ **2**, являющегося структурным аналогом КЭ **1**, равноценность двух сторон макроцикла обусловливает цепочечную структуру с чередованием димеров **A** и макроциклических молекул (рис. 2).

Три других комплекса этой группы представляют собой молекулярные капсулы с расположением димерного ассоциата $(\mathbf{A})_2$ между двумя молекулами КЭ (рис. 3). Все трехкомпонентные системы демонстрируют стехиометрию 1:1:1. Комплекс $\mathbf{5}\cdot(\mathbf{A})_2\cdot 2H_2O$, единственный в этой группе, является шестичленным ассоциатом, в котором димер $(\mathbf{A})_2$ заключен между двумя молекулами КЭ, а молекулы воды слабо удерживаются на внешней стороне полости макроцикла (см. рис. 3, *б*).

В комплексах $\mathbf{1}\cdot\mathbf{A}\cdot H_2O$, $\mathbf{2}\cdot\mathbf{A}\cdot H_2O$, $\mathbf{4}\cdot\mathbf{A}\cdot H_2O$ молекула воды внедряется между макроциклической молекулой и молекулой **A**, акцептируя протон NH-группы и действуя как H-донор для КЭ. Это приводит к цепочечному мотиву с чередованием компонентов. Интересным в этом плане представляется комплекс $\mathbf{1}\cdot(\mathbf{A})\cdot H_2O$ (рис. 4), в котором макроцикл находится в нехарактерном несимметричном окружении и его конформация описывается симметрией C_1.

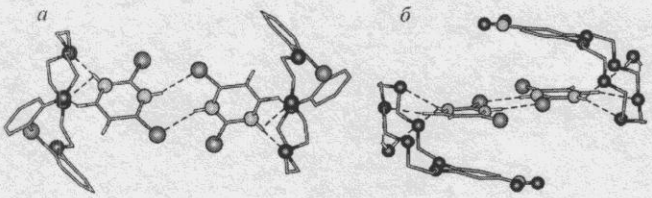

Рис. 3. Примеры молекулярных капсул комплекс $(\mathbf{8}\cdot\mathbf{A})_2$, расстояния N···S 3,297, N···O 2,790, C···O 3,102 Å (*а*); комплекс $\mathbf{5}\cdot(\mathbf{A})_2\cdot 2H_2O$, расстояния N···S 3,340, N···O 2,953 и 3,137, C···O 3,369 Å, расстояния O(вода)···O(краун) 2,937 и 3,425 Å (*б*)

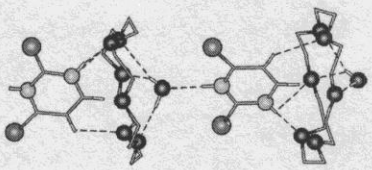

Рис. 4. Фрагмент полимерной цепочки в кристалле комплекса $\mathbf{1}\cdot\mathbf{A}\cdot H_2O$

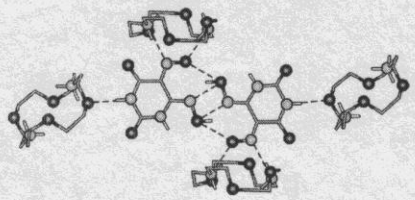

Рис. 5. Ближайшее окружение димера $(\mathbf{B}^-)_2$ в комплексе $(H_2\text{-}\mathbf{10})(\mathbf{B})_2$

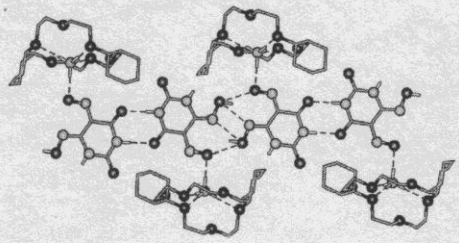

Рис. 6. Фрагмент ленточной структуры в $(\mathbf{2}\cdot NH_4)(\mathbf{B})$

Взаимное расположение компонентов в комплексах представляет собой компромисс между наилучшей направленностью водородных связей и наиболее благоприятным расположением циклических π-ароматических систем. В случае **1**—**3** и **6**, с обедненной π-электронной системой, молекула **A** расположена практически перпендикулярно к макроциклической полости, что обеспечивает максимальное участие как NH-, так и CH-протонов в общей системе межмолекулярных взаимодействий. Комплексы с **4** и **5** демонстрируют существенный вклад ароматической составляющей макроциклического кольца, что проявляется в ориентации молекулы **A** практически параллельно плоскости бензольного кольца КЭ (см. рис. 3, *б*). За исключением КЭ **7** и **8**, все изученные макроциклы ведут себя как "двусторонние" молекулы, что обеспечивает вовлечение максимального числа атомов кислорода КЭ в комплексообразование.

Наличие в молекулах **BH**—**GH** H-донорных групп, способных не только к H-связыванию, но и депротонированию, приводит к усложнению супрамолекулярной архитектуры соответствующих комплексов. Так, замещением аминогруппы в пиримидинах под действием гидроксиламина мы получили разнообразные ди-, три- и тетраоксимы, особенности строения которых (в частности, бициклических соединений **CH** и **DH**, а также таутомерной формы диоксима **BH**) выявлены в кристаллических продуктах их взаимодействия с КЭ и аза-КЭ [13, 14]. Из четырех таутомерных форм, возможных для диоксима **BH**, в кристаллах его комплексов с макроциклами **2** и **10** зафиксирован (4*Z*,5*E*)-изомер (см. схему 1), а кристаллические продукты состава $(H_2\text{-}\mathbf{10})(\mathbf{B})_2$ и $(\mathbf{2}\cdot NH_4)(\mathbf{B})$ являются солями вследствие переноса протона от одной из оксимных групп молекулы **BH** на атом азота макроцикла или аммиака соответственно. В структурах обеих солей сохраняется самоорганизация анионов — планарный димер за счет оксим-оксиматного синтона $R_2^2(6)$ в $(H_2\text{-}\mathbf{10})(\mathbf{B})_2$ (рис. 5) и цепь за счет комбинации синтонов $R_2^2(6)$ и $R_2^2(8)$ в $(\mathbf{2}\cdot NH_4)(\mathbf{B})$ (рис. 6). При этом дикатион $(H_2\text{-}\mathbf{10})^{2+}$ образует H-связи не только посредством взаимодействия протонодонорных групп $>NH_2^+$ с оксимат-анионом, но и H-акцепторов макроцикла, участвующих во взаимодействии NH···(краун) с амидной группой анионов $\mathbf{B}^-$, что, по всей вероятности, и является причиной "обрыва" цепочечного мотива последних в комплексе $(H_2\text{-}\mathbf{10})(\mathbf{B})_2$.

В составе молекулярных комплексов $(\mathbf{10})(\mathbf{CH})_2\cdot 2H_2O$ и $(\mathbf{10})(\mathbf{DH})_2$ определены также структуры продуктов циклизации соответствующих ди- и триоксимов (см. схему 1). Молекулы **CH** и **DH** в этих комплексах имеют планарную геометрию. Оба соединения характеризуются цепочечной структурой. Наличие у таких аннелированных азолоурацилов лишь двух >NH-донорных центров компенсируется в случае комплекса $(\mathbf{10})(\mathbf{CH})_2\cdot 2H_2O$ за счет молекулы воды, способность которой образовывать максимально четыре H-связи в сочетании с малым объемом позволяет увеличить число межмолекулярных водородных связей (рис. 7), тем самым благоприятствуя топологическому соответствию.

В комплексе $(\mathbf{10})(\mathbf{DH})_2$ оксимная группа, будучи вовлеченной во взаимодействия OH···O(краун) и NH(краун)···N (рис. 8), выполняет как H-донорную, так и H-акцепторную функции [14]. Подобно двум предыдущим структурам, в данном случае также сохраняется карбамидный гомосинтон $R_2^2(8)$ димера молекулы **DH**.

Под действием достаточно сильного основания, каковым является диаза-КЭ **10**, происходит депротонирование сульфогруппы 6-амино-2,4-диоксо-1,2,3,4-тетрагидропиримидин-5-суль-

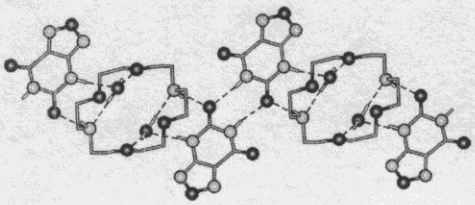

Рис. 7. Фрагмент полимерной цепочки в кристалле комплекса (**10**)(**CH**)$_2\cdot 2H_2O$

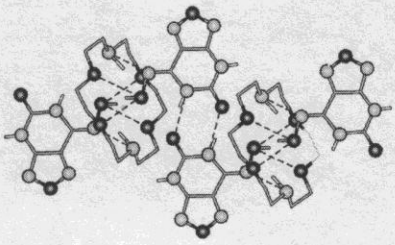

Рис. 8. Фрагмент полимерной цепочки в кристалле комплекса (**10**)(**DH**)$_2$. Расстояния O(H)···O(краун) 2,906 и 3,000, N(H)(краун)···N 3,001 Å, расстояние N···O в карбамидном гомосинтоне 2,834 Å

фамовой кислоты (**EH**) с образованием дигидрата соли (H_2-**10**)(**E**)$_2\cdot 2H_2O$ [15]. Богатый протонодонорными центрами анион формирует отрицательно заряженный слой, стабилизированный традиционными взаимодействиями NH···O(=C) в составе супрамолекулярного гомосинтона $R_2^2(8)$ и перекрестными водородными связями NH···(SO_3^-) (рис. 9). Каждый анион вовлечен во взаимодействие с тремя ближайшими соседями с формированием "двойного" слоя, что определяется тетраэдрической геометрией атома азота сульфамидной группы и тригональным строением сульфогруппы. Макроциклический катион связан с анионной сеткой взаимодействиями NH^+···O. В кристалле осуществляется "боковой" способ координации макроцикла, оба атома водорода NH_2-группы имеют *экзо*-ориентацию. Молекулы воды, присутствующие в структуре, наряду с макроциклическими катионами выполняют мостиковую функцию между соседними отрицательно заряженными слоями.

В присутствии аза-макроциклов возможно депротонирование и гетероциклического атома азота молекулы урацила. Так, мы обнаружили, что при взаимодействии соединений **GH** с **10** и **FH** с **11** образуются соли, в которых, подобно предыдущему комплексу, макроциклический дикатион и два урацильных аниона образуют тесную ионную пару, и в комплексообразование вовлечены функциональные группы пиримидинового цикла [14, 15]. В структуре комплекса (H_2-**10**)(**G**)$_2\cdot 4H_2O$ (рис. 10, *а*), помимо характерного для пуринов стэкинга симметрически связанных анионов, отсутствуют какие-либо супрамолекулярные гомосинтоны, типичные для пиримидинов. Это связано с внедрением в кристаллическую решетку молекул воды, которые в качестве H-доноров блокируют карбонильные атомы кислорода, а в качестве H-акцепторов — амидный атом водорода (см. рис. 10, *а*). Совокупность этих факторов приводит к слоистой структуре, в кото-

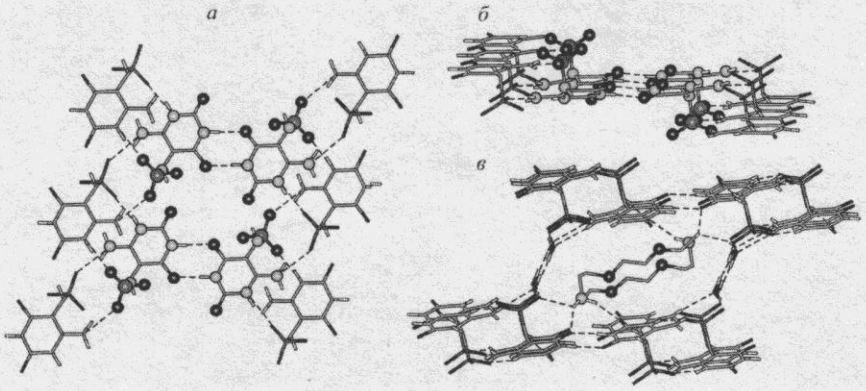

Рис. 9. Строение комплекса (H_2-**10**)(**E**)$_2\cdot 2H_2O$, фрагмент отрицательно заряженного слоя: *а* — вид сверху, *б* — вид сбоку, *в* — ближайшее окружение макроциклического катиона в кристалле

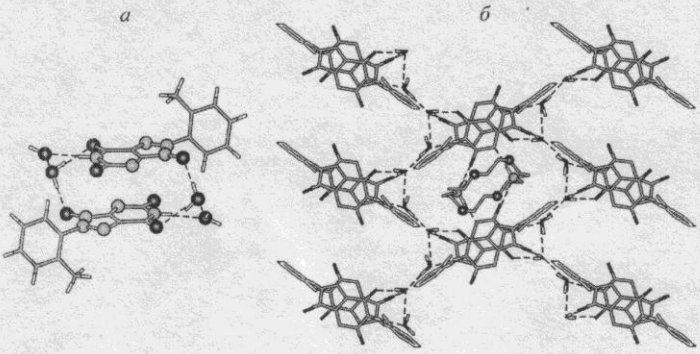

Рис. 10. Строение комплекса $(H_2\text{-}\mathbf{10})(\mathbf{G})_2 \cdot 4H_2O$: *а* — восьмичленный дианион $[(\mathbf{G})_2 \cdot 4H_2O]^{2-}$, *б* — фрагмент слоя в структуре

рой макроциклический катион является фрагментом слоя и занимает положение в ячейке, сформированной 8 анионами и 12 молекулами воды, выполняющими в данном случае важную структурообразующую функцию, формируя непрерывные цепочки (см. рис. 10, *б*).

Подобно комплексу $(H_2\text{-}\mathbf{10})(\mathbf{G})_2 \cdot 4H_2O$, атом азота в положении 1 пиримидинового цикла 2-(2,6-диоксо-1,2,3,6-тетрагидропиримидин-4-ил)гидразинокарбоксамида (**FH**) в составе комплекса $(H_2\text{-}\mathbf{11})(\mathbf{F})_2 \cdot 2H_2O$ депротонирован [16]. Дикатион $(H_2\text{-}\mathbf{11})^{2+}$ образует с двумя анионами урацила две пары водородных связей, $N—H^+\cdots N^-$ и $N—H\cdots O{=}C$, с участием атомов азота и кислорода депротонированного лактамного фрагмента урацила (рис. 11). Анионы формируют отрицательно заряженный слой, стабилизированный комбинацией супрамолекулярных гомосинтонов — двух центросимметричных карбамидных синтонов $R_2^2(8)$ с участием урацильного цикла и периферийной аминогруппы и несимметричного синтона $R_2^1(6)$, характерного для мочевины.

В кристалле комплекса $(H_2\text{-}\mathbf{11})(\mathbf{F})_2 \cdot 2H_2O$ гофрированные слои стыкуются через мостиковые молекулы воды, формируя трехмерную структуру. Молекулы воды являются двойными Н-донорами (образуют с атомами кислорода двух карбонильных групп практически идеальный ромб) и акцепторами одного протона — взаимодействуют с гидразидной NH-группой.

В заключение подчеркнем, что макрогетероциклы **10** и **11** являются азаполиэфирами и обладают собственным центром инверсии. Первое обусловливает предпочтительность образования ионных соединений с потенциальными Н-донорами, а второе — симметричность супрамолекулярного мотива в образующихся комплексах. Нам представляется, что приведенные примеры

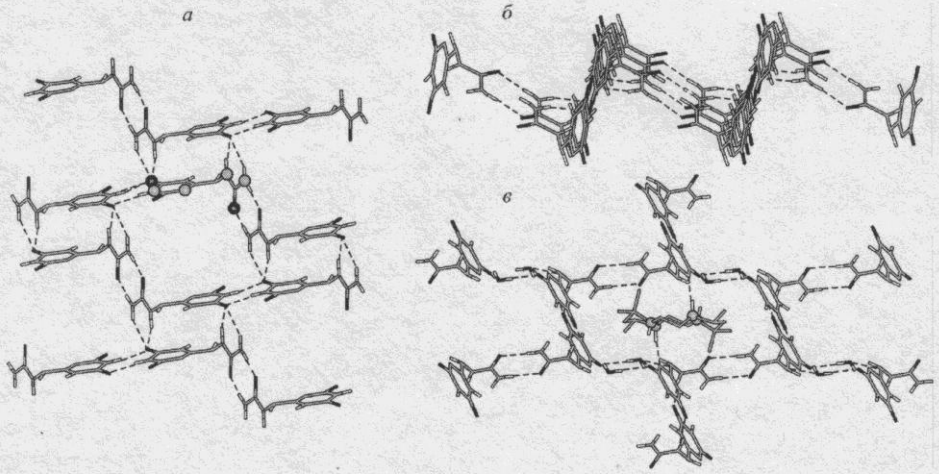

Рис. 11. Строение комплекса $(H_2\text{-}\mathbf{11})(\mathbf{F})_2 \cdot 2H_2O$, фрагмент отрицательно заряженного слоя: *а* — вид сверху, *б* — вид сбоку, *в* — ближайшее окружение макроциклического дикатиона в кристалле

демонстрируют очевидную перспективность макрогетероциклических темплатов (КЭ и аза-КЭ) для изучения супрамолекулярной организации комплексов с такими биомолекулами, как производные пиримидинов, а также для выявления различных факторов активации молекул подобного рода гетероциклов в условиях супрамолекулярного катализа.

СПИСОК ЛИТЕРАТУРЫ

1. (*а*) *Meyer E.A., Castellano R.K., Diederich F.* // Angew. Chem. Int. Ed. – 2003. – **42**. – P. 1210 – 1250. (*б*) *Tsuzuki S., Dhonda K., Uchimaru T. et al.* // J. Amer. Chem. Soc. – 2002. – **124**. – P. 104 – 112. (*в*) *Desiraju G.R., Steiner T.* // The Weak Hydrogen Bond in Structural Chemistry and Biology. – Oxford: Oxford University Press, 1999. – P. 29 – 121.
2. (*а*) *Gallant M., Viet M.T.P., Wuest J.D.* // J. Amer. Chem. Soc. – 1991. – **113**. – P. 721 – 723. (*б*) *Zerkowski J.A., Seto C.T., Whitesides G.M.* // Ibid. – 1992. – **114**. – P. 5473 – 5475. (*в*) *Boucher E., Simard M., Wuest J.D.* // J. Org. Chem. – 1995. – **60**. – P. 1408 – 1412. (*г*) *Chen H., Meena, McLaughlin L.W.* // J. Amer. Chem. Soc. – 2008. – **130**. – P. 13190 – 13191. (*д*) *Drewe W.C., Neidle S.* // Chem. Comm. – 2008. – P. 5295 – 5297.
3. (a) *Liu Y., Yang Y.-W., Li L., Chen Y.* // Org. Biomol. Chem. – 2004. – **2**. – P. 1542 – 1548. (*б*) *Chang S.-K., Van Engen D., Fan E., Hamilton A.D.* // J. Amer. Chem. Soc. – 1991. – **113**. – P. 7640 – 7645.
4. (*а*) *Elbasyouny A., Brugge H.J., Deuten K. et al.* // Ibid. – 1983. – **105**. – P. 6568 – 6577. (*б*) *Симонов Ю.А., Фонарь М.С., Дворкин А.А., Малиновский Т.И.* // Структурная кристаллография. К 100-летию со дня рождения акад. Н.В. Белова. – М.. Наука, 1992. – С. 221 – 250.
5. *Simonov Y.A., Fonari M.S., Zaworotko M.J. et al.*// Org. Biomol. Chem. – 2003. – **1**. – P. 2922 – 2929.
6. *Fonari M.S., Simonov Y.A., Wang W.-J. et al.* // CrystEngComm – 2009. – DOI: 10.1039/b810076d
7. (*а*) *Burrows A.D., Mingos M.P., White A.J.P., Williams D.J.* // J. Chem. Soc. Dalton Trans. – 1996. – P. 3805 – 3812. (*б*) *Aoki S., Shiro M., Koike T., Kimura E.* // J. Amer. Chem. Soc. – 2000. – **122**. – P. 576 – 584. (*в*) *Papaefstathiou G.S., Manessi S., Raptopoulou C.P. et al.* // Inorg. Chem. Commun. – 2004. – **7**. – P. 69 – 72. (*г*) *Davis J.T., Spada G.P.* // Chem. Soc. Rev. – 2007. – **36**. – P. 296 – 313. (*д*) *Sessler J.L., Lawrence C.M., Jayawickramarajah J.* // Ibid. – P. 314 – 325.
8. (*а*) *Rostkowska H., Szczepaniak K., Nowak M.J. et al.* // J. Amer. Chem. Soc. – 1990. – **112**. – P. 2147 – 2160. (*б*) *Leszczynski J., Lammertsma K.* // J. Phys. Chem. – 1991. – **95**. – P. 3128 – 3132. (*в*) *Leš A., Adamowicz L.* // J. Amer. Chem. Soc. – 1990. – **112**. – P. 1504 – 1509. (*г*) *Yekeler H.* // J. Comp.-Aided Molec. Design. – 2000. – **14**. – P. 243 – 250. (*д*) *Wang H., Meng F., Xu W., Liu C.* // J. Mol. Struct. THEOCHEM. – 2005. – **716**. – P. 137 – 141. (*е*) *Yang Z., Rodgers M.T.* // J. Phys. Chem. – 2006. – **A110**, N 4. – P. 1455 – 1468.
9. *Zielenkiewicz W.* // Pure Appl. Chem. – 1999. – **71**, N 7. – P. 1285 – 1290.
10. (*а*) *Shefter E., Mautner H.G.* // J. Amer. Chem. Soc. – 1967. – **89**. – P. 1249 – 1253. (*б*) *Tiekink E.R.T.* // Z. Kristallogr. – 1989. – **187**. – S. 79 – 84.
11. *Wang W.-J., Ganin E.V., Fonari M.S. et al.* // Org. Biomol. Chem. – 2005. – **3**. – P. 3054 – 3058.
12. (*а*) *Ganin E.V., Fonari M.S., Simonov Yu.A. et al.* // J. Incl. Phenom. Macrocycl. Chem. – 2005. – **52**. – P. 63 – 74. (*б*) *Fonari M.S., Simonov Yu.A., Bocelli G. et al.* // Ibid. – 2008. – **61**. – P. 367 – 375.
13. *Simonov Y.A., Fonari M.S., Lipkowski J. et al.* // Ibid. – 2003. – **46**, N 1-2. – P. 27 – 35.
14. *Набор* экспериментальных данных получен в дифрактометре CCD Bruker с единственного пригодного к съемке тонкого пластинчатого кристалла с линейными размерами 0,06×0,14×0,21 мм. $C_{20}H_{32}N_{12}O_{10}$ $M = 600,58$, триклинный, пр. гр. P-1, $a = 7,3954(3)$, $b = 9,7519(4)$, $c = 10,5260(5)$ Å, $\alpha = 71,91(3)$, $\beta = 78,07(2)$, $\gamma = 67,80(2)°$, $V = 664,7(14)$ Å^3, $Z = 1$, $D_c = 1,500$ гсм$^{-3}$, $\mu = 0,122$ мм$^{-1}$. Число независимых рефлексов 1956, число рефлексов с $[I > 2\sigma(I)]$ 763, добротность уточнения 0,995, заключительный R фактор для $[I > 2\sigma(I)]$ $R_1 = 0,1122$, $wR_2 = 0,2090$. Cif-файл депонирован в Кембриджской базе структурных данных, номер регистрации CCDC 710152.
15. *Fonari M.S., Simonov Y.A., Chumakov Y.M. et al.* // Supramolec. Chem. – 2004. – **16**, N 1. – P. 23 – 30.
16. *Fonari M.S., Simonov Y.A., Chumakov Y.M. et al.* // Журн. структур. химии. – 2005. – **46**. – С. 95 – 101.

Додаток Т.

Копія статті. “Синтез краун-эфиров и их взаимодействие с кремнефтороводородной кислотой ”

Випуск 8 2009

ВІСНИК

ОДЕСЬКОГО ДЕРЖАВНОГО ЕКОЛОГІЧНОГО УНІВЕРСИТЕТУ

УДК 547.89 545.737

М.Г. Васильева, М.Г. Горличенко, *к.пед.н.*, **С.В. Шевченко, О.Н. Ласовская, Э.В. Ганин,** *д.х.н.*
Одесский государственный экологический университет

СИНТЕЗ КРАУН-ЭФИРОВ И ИХ ВЗАИМОДЕЙСТВИЕ С КРЕМНЕФТОРОВОДОРОДНОЙ КИСЛОТОЙ

Инвариантность стабилизации диакватетрафторосиликата 18-краун-6 и синтез комплекса пентафторсиликата гидроксония с цис-син-цис-изомером дициклогексано-18-краун-6 при взаимодействии краун-эфиров с растворами диоксида кремния во фтороводородной кислоте выявляют определяющее влияние пространственного строения краун-эфиров на способ комплексообразования.

Ключевые слова: *краун-эфиры, кремнефтороводородная кислота, комплексы.*

Введение.

С момента первой публикации Ч. Перерсена (1967 г.) по краун-эфирам – синтетическим макроциклическим полиэфирам получено огромное структурное многообразие этих необычных комплексонов, найдены многочисленные возможные области их практического применения [1]. Одна их таких областей – использование как краун-эфиров, так и соединений включения на их основе при моделировании биоорганических реакций и природных процессов [2]. Конец прошлого и первая декада XXI века демонстрирует подлинный Ренессанс химии краун-эфиров в том числе в направлении поиска удобных методов синтеза краун-эфиров, а также их изучения в плане «структура – свойства», в частности, влияния строения краун-эфиров на результат комплексообразования [3].

Материалы и методы их исследования.

18-К-6

18-краун-6 (18-К-6). 3,3 г (0,022 моль) триэтиленгликоля и 4,6 г (0,024 моля) *п*-то-луолсульфохлорида растворяли в 40 мл диоксана и полученный раствор по каплям прибавляли за 1 ч в перемешиваемую суспензию растертой в пудру смеси 5,8 г (0,088 моля) 85%-ного гидроксида калия и 10 г оксида бария (или 7,5 г карбоната калия) в 30 мл диоксана при 40±5°С. Реакционную смесь выдерживали при этой температуре 1 ч, затем нагревали до 65±5°С и в горячем виде фильтровали. Фильтрат упаривали досуха, а полученный белый твердый остаток нагревали при 0,1 мм рт. ст. до 275°С, собирая отгоняющуюся жидкость. К ней добавляли смесь 0,2 г гидроксида натрия и 0,5 г оксида бария, полученную массу нагревали при 0,05 мм рт. ст. до 200°, собирая отгоняющийся 18-краун-6. Выход 1,2—1,3 г (41—46%), т. пл. 38—39°, что соответствует данным работ [1]. Хроматографический контроль чистоты 18-краун-6 осуществляли на приборе ЛХМ-8М (катарометр, 250-275°С, 5 % «Верзамид-900» на

«Инертоне», длина колонки 3 м, скорость гелия 25 мл/мин). Синтез позволяет избежать многократных перекристаллизаций целевого продукта из ацетонитрила.

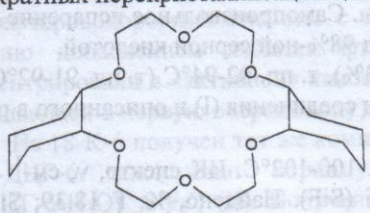

А-ДЦГ-6

В-ДЦГ-6

Разделение диастереомеров цис-син-цис- и цис-анти-цис-изомерами дициклогексано-18-краун-6 (А- и В-ДЦГ-6 соответственно). 20.6 г (0.12 моль) 4-аминобензолсульфамида растворяли при 78 °С в 160 мл этанола, к раствору добавляли 37.2 г (0.1 моль) смеси диастереомеров А- и В-ДЦГ-6, кристаллизовали, затем фильтровали. Выделенные кристаллы комплекса диастереомера В-ДЦГ-6 с 4-аминобензолсульфамидом нагревали с 50 мл 2-пропанола при 82 °С 10 мин, охлаждали до 0 °С, фильтровали, очищенные кристаллы растворяли в 100 мл 5%-ной соляной кислоты при 40 °С и экстрагировали 80 мл хлороформа. Экстракт промывали 100 мл 5%-ной соляной кислоты, затем 2х100 мл воды, хлороформ упаривали, остаток кристаллизовали из 20 мл гексана и получали 18 г (48 %) диастереомера В-ДЦГ-6, т. пл. 69-70 °С. Маточный раствор, оставшийся после фильтрации комплекса, упаривали, добавляли 100 мл хлороформа, фильтровали, фильтрат промывали 100 мл 5%-ной соляной кислоты, 2х100 мл воды, хлороформ упаривали, остаток кристаллизовали из 15 мл диэтилового эфира и получали 12 г (32 %) диастереомера А-ДЦГ-6, т. пл. 61-62 °С.

По литературным данным [1], т. пл. диастереомера В-ДЦГ-6 составляет 69-70 °С, диастереомера А-ДЦГ-6 – 61-62.5 °С. ИК спектры индивидуальных диастереомеров идентичны приведенным в работе [1]. ИК спектры регистрировали на спектрофотометре ИКС 29 в таблетках с бромистым калием. В спектрах ПМР комплексов химические сдвиги (δ) алифатических протонов диастереомеров находятся в области 3,57-3.33 и 1.37-0.90 м. д. Соотношение интенсивностей оксиметиленовых и метиленовых групп протонов А-ДЦГ-6 и В-ДЦГ-6 соответствует приведенным формулам. Спектры ПМР снимали на приборе Tesla BS-467, в дейтероацетоне и трифторуксусной кислоте, внутренний стандарт – ГМДС. ТСХ проводили на пластинах Silufol UV-254 в системе метанол-хлороформ, 1 : 8, с проявлением в УФ свете (для ароматических «гостевых» соединений – гашение) и нингидрином [для аминосоединений – круглые пятна от светло-розового до красного цвета, для диастереомеров А-ДЦГ-6 и В-ДЦГ-6 – удлиненные пятна с Rf 0.41 и 0.49 соответственно]. Синтез исключает использование взрывоопасной хлорной кислоты и перхлоратов тяжелых металлов.

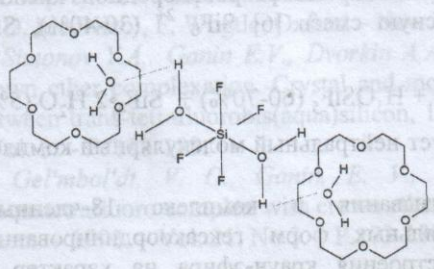

I

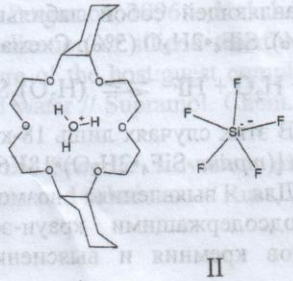

II

Комплексы краун-эфиров с кремнефтороводородной кислотой.

К растворам 264 мг (1 ммоль) 18-К-6, 372 мг (1 ммоль) А- или 372 мг (1 ммоль) В-ДЦГ-6 в 5 мл метанола добавляли 2 г 45%-ной кремнефтороводородной кислоты, добавляли 2 г 48%-ной фтороводородной кислоты. Самопроизвольное испарение смеси проводили при 20°С в тефлоновом эксикаторе над 98%-ной серной кислотой.

Выход комплекса (I) составляет 320 мг (73%), т. пл. 92-94°С (т. пл. 91-92°С [4]); ИК спектр и термогравиграмма полученного нами соединения (I) и описанного в работе [5] идентичны.

Выход комплекса (II) 330 мг (64%), т. пл. 100-102°С. ИК спектр, ν, см-^{1}: 3600-3500, 1650 [$\delta(H_3O^+)$], 1165-1000 (СОС), 875, 785 (SiF). Найдено, %: F 18.39; Si 5.75. $C_{20}H_{36}F_5O_7Si$. Вычислено, %: F 18.78; Si 5.49. Потеря комплексом (II) при термодеструкции фрагментов H_3OSiF_5 с переходом их в газовую фазу происходит в интервале температур 80–145 °С и сопровождается эндотермическим эффектом.

ИК спектры зарегистрированы на приборе Specord M-80 в вазелиновом масле, стекла KPS-5. Термогравиаграммы комплексов (I) и (II) записаны на дериватографе QD-1000 в интервале температур 20–500 °С, чувствительность записи ДТА и ДТГ – 1/5 от максимальной, скорость нагрева 10 град/мин, навески 120 и 30 мг соответственно. ТСХ проводили на пластинах Silufol с элюированием смесью метанол—хлороформ, 1:5, проявление нингидрином. Комплексы (I) и (II) при ТСХ разлагаются на компоненты со значениями Rf 0 (красные пятна кремнийфторидов) ~ 0.53 и 0.70 (белые пятна краун-эфиров) соответственно.

По данным рентгеноструктурного анализа уточненная (при 200 К) кристаллическая структура (I) соединения SiF4•I8K6•4H_2O представляет собой молекулярный комплекс [(*транс*-SiF_4•2H_2O)• 8K6•2H_2O], в котором молекулы воды и *транс*-SiF_4•2H_2O связаны между собой и молекулами краун-эфира в полимерную цепь системой водородных связей OH…O.

Структура комплекса (II) образована из катионов [А-ДЦГ-6•H_3O]$^+$ и анионов SiF_5^-, связанных электростатическими взаимодействиями, В катионе реализуются три Н-связи типа OH…O между ионом H_3O^+ и каждым вторым атомом кислорода А-ДЦГ-6. Тригонально-бипирамидальный анион SiF_5^- разупорядочен: атом кремния занимает одну, а атомы фтора – две равновероятные позиции.

CIF – файлы, исчерпывающе описывающие структуры: (I) – YORRIG, YORRIG01 и (II) – LITNAD депонированы в Cambridge Crystallographic Data Centre < http://www.ccdc.cam.ac.uk/products/csd/deposit/ >.

Авторы признательны Ю.А. Симонову и М.С. Фонарь (Кишинев, Молдова) за помощь в расшифровке структур.

Результаты исследования и их анализ.

Взаимодействие тетрафторида кремния в присутствии влаги воздуха 18-краун-6 (18-К-6), *цис-син-цис-* и *цис-анти-цис*-изомерами дициклогексано-18-краун-6 (А- и В-ДЦГ-6 соответственно) было исследовано в работе [4]. В работе [5] в атмосфере воздуха изучены аналогичные реакции 45%-ной кремнефтороводородной кислоты, представляющей собой лабильную, равновесную смесь [6] SiF_6^{2+} (30-40%), SiF_5^- (60-70%), SiF_4•2H_2O (5%). Схематично:

$$SiO_2 + H_2O + HF \rightleftharpoons (H_3O)_2SiF_6\ (30\text{-}40\%) + H_3OSiF_5\ (60\text{-}70\%) + SiF_4{\bullet}2\,H_2O\ (5\%)$$

В этих случаях лишь 18-краун-6 образует нейтральный молекулярный комплекс состава [(*транс*-SiF_4•2H_2O)•18K6•2H_2O] (I).

Для выявления возможности связывания в комплекс 18-членными кислородсодержащими краун-эфирами лабильных форм гексакоординированных фторидов кремния и выяснения влияния строения краун-эфира на характер их

стабилизации мы провели взаимодействие 18-К-6, А-, В-ДЦГ-6 и 45%-ной кремнефтороводородной кислоты с повышением атомарного соотношения фтора к кремнию добавлением избытка фтороводородной кислоты. Реакционные смеси сконцентрировали в «активной» атмосфере (тефлоновый эксикатор с серной кислотой, поглощающей в первую очередь воду).

Из 18-К-6 получен тот же комплекс (I), В-ДЦГ-6 во взаимодействие не вступил, с А-ДЦГ-6 аналогично борному [7] выделен ионный комплекс состава $\{[А\text{-}ДЦГ\text{-}6 \bullet H_3O]^+ SiF_5^-\}$ (II). Получение того же продукта (I), что и в работах [4,5], и образование нового комплекса (II) с А-ДЦГ-6 подтверждают существенное влияние пространственного окружения электронодонорной макроциклической полости «хозяина», отмеченное в работе [8], и топологической соразмерности компонентов [9] при образовании комплексов типа «гость–хозяин».

Видно, что комплекс (I), на основе пространственно не затрудненного 18-К-6 образуется вне зависимости от окружающей атмосферы, а комплекс (II) лишь в «активной» атмосфере, поглощающей воду.

В рамках моделей самоорганизации естественных равновесных систем [2,3] образование комплекса (II) иллюстрирует то, что катион гидроксония (H_3O^+) может быть стабилизирован водородными связями «тесной» стороной А-ДЦГ-6 в соединение включения из обратимой равновесной «гостевой» системы – SiF_6^{2-} (30-40%), SiF_5^- (60-70%), $SiF_4 \bullet 2\ H_2O$ (5%) – в «засушливой» атмосфере. Результаты могут быть учтены в качестве химической основы при моделировании природных взаимодействий кислотных жидких фаз с большими протоноакцепторными полостями.

Выводы:

Исследования подтверждают инвариантность стабилизации катиона гидроксония (H_3O^+) водородными связями А-ДЦГ-6 в соединение включения в систему «гость-хазяин».

Перспективой дальнейшего исследования в данном направлении есть использование в качестве химической основы при моделировании природных взаимодействий кислотных жидких фаз с протоноакцепторными полостями больших размеров.

Список литературы

1. *Хираока М.* Краун-соединения. Свойства и применение. – М.: Мир, 1986. – 363 с.
2. *Химия* комплексов «гость-хозяин» / под. ред. Ф. Фегтле, Э. Вебера. – М.: Мир, 1988. –512 с.
3. *Comprehensive* supramolecular chemistry / eds.: J-M. Lehn, J. L. Atwood, J. E. D. Davies, D. D. MacNicol, F. Wogtle, Oxford – New York – Tokyo: Pergamon, 1996. – Vol. 1-11.
4. *Simonov Y.A.. Ganin E.V., Dvorkin A.A., et al.* Stabilization of silicon tetrafluoride by crown ether complexation. Crystal and molecular structure of the host:guest complex 1:1:2 between trans-tetrafluorobis(aqua)silicon, 18-crown-6 and water // Supramol. Chem. – 1994. –Vol. 3. – P. 185-189.
5. *Gel'mbol'dt, V. O., Ganin, E. V., Simonov, et al.* Specific solvation of silicon diaquatetrafluoro complex with crown ethers in fluorosilicic acid solutions // Russ. J. Coord. Chem. – 1995. – Vol. 21, No 3. – P.173-180.

6. *Буслаев Ю.А., Петросянц С.П.* О составе фторокомплексов алюминия и кремнефтороводородной кислоты в водных расторвах // Коорд. химия. – 1979. – Т.5, № 2. – С.163-170.
7. *Gel'mbol'dt, V. O., Ganin, E. V., Simonov, Yu. A., et al.* Synthesis, crystal and molecular structure of a hydroxonium tetrafluoroborate complex with the cis-syn-cis isomer of dicyclohexane-18-crown-6 // Zh. Neorg. Khim. – 1995. – Vol. 40, No 4. – P. 594-600.
8. *Ganin, E. V., Makarov, V. F., Kotlyar, S. A., Luk'yanenko, N. G.* Isolation and separation of *cis-syn-cis* and *cis-anti-cis* diastereomers of dicyclohexano-18-crown-6 complexes with organic NH-acids // Zh. Obshch. Khim. – 1988. – Vol. 58, No 6. – P. 1309-1313.
9. *Simonov, Yu. A., Ganin, E. V., Fonar, M. S., et al.* Crystal and molecular structure of a 1:2 complex of cis-anti-cis diastereomer of dicyclohexano-18-crown-6 with 4-acetylaminobenzenesulfamide // Zh. Strukt. Khim. – 1990. – Vol. 31, No 4. – P. 106-110.

Синтез краун-этерів і їхня взаємодія з кремнійфлуороводневою кислотою

Васильєва М.Г., Горліченко М.Г., Шевченко С.В., Ласовська О.М., Ганін Е.В.

Інваріантість стабілізації діакватетрафлуоросилікату 18-краун-6 і синтез комплексу пентафлуоросилікату гідроксонію з цис-син-цис-ізомером дициклогексано-18-краун-6 при взаємодії краун-этерів з розчинами діоксиду кремнію в флуороводневій кислоті виявляють визначальний вплив просторової будови краун-этерів на спосіб комплексоутворення.

***Ключові слова**: краун-этери, кремнійфлуороводнева кислота, комплекси.*

Synthesis of crown- ethers and their interaction with fluorosilicic acid

Vasileva M.G., Gorlichenko M.G., Shevchenko S.V., Lasovskaya O.N., Ganin E.V.

Invariance of stabilization diaquafluorosilicate by 18-crown-6 and synthesis of a complex pentafluorosilicate of hydroxonium with cis-syn-cis isomer dicyclohehane-18-crown-6 at interaction of crown-ethers with solutions of dioxide of silicon in fluorhydric acid reveal dominant influence of a spatial constitution of crown -ethers on an expedient of a complexing.

***Key words**: crown-ethers, fluorosilicic acid , complexes.*

Додаток У.

Копія статті. “Особенности образования комплексов «хозяин-гость» краун-эфиров с HN-протонодонорными молекулами ”

Випуск 8 2009

ВІСНИК

ОДЕСЬКОГО ДЕРЖАВНОГО ЕКОЛОГІЧНОГО УНІВЕРСИТЕТУ

УДК 547.89

М.Г. Васильева , М.Г. Горличенко, *к.пед.н.*, **С.В. Шевченко, С.И.Шепелина, Э.В. Ганин,** *д.х.н.*
Одесский государственный экологический университет

ОСОБЕННОСТИ ОБРАЗОВАНИЯ КОМПЛЕКСОВ «ХОЗЯИН-ГОСТЬ» КРАУН-ЭФИРОВ С HN-ПРОТОНОДОНОРНЫМИ МОЛЕКУЛАМИ

Взаимодействием краун-эфиров с HN-протонодонорными молекулами получены кристаллические молекулярные комплексы "хозяин-гость" и установлено, что в зависимости от линейных размеров и способа стерического экранирования активных центров протонодонорных молекул в комплексы связываются краун-эфиры различного строения.

Ключевые слова: *краун-эфиры, HN-протонодонорные молекулы, комплексы "хозяин-гость".*

Введение.

Выяснение особенностей образования комплексов на основе межмолекулярных связывающих взаимодействий краун-эфиров («хозяев») с «гостевыми» молекулами, моделирующих распространенные природные процессы, – одна из приоритетных задач супрамолекулярной химии [1-3]. Согласно работе [4], сформулировавшей требования к «гостевым» молекулам, последние должны обладать заметным дипольным моментом и невысокой молекулярной массой.

Материалы и методы их исследования.

Спектры ЯМР ^{1}H регистрировали на приборе Varian VXR-300 (300 МГц), внутренний стандарт – ТМС. Краун-эфиры (III-IV, XIIIв) получены соответственно [5], соединения (I-IX, XI-XIIIа) использовали в виде коммерческих образцов, (фирмы Aldrich) без дополнительной очистки.

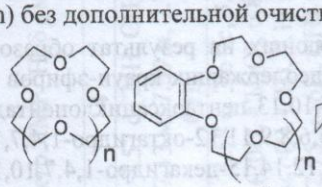

Iа-в IIа-б

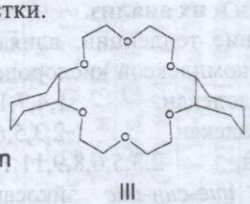

III

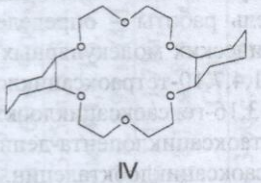

IV

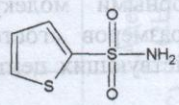

V

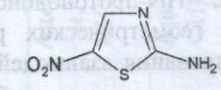

VI

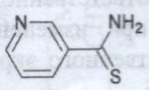

VII

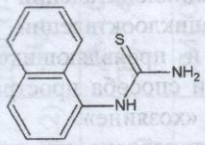

VIII

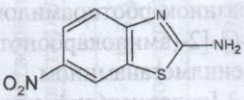

IX

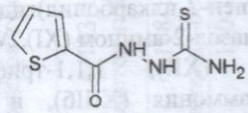

X

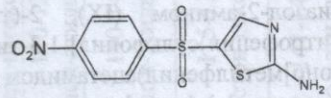

XI

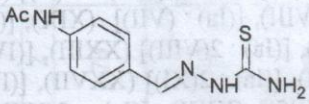

XII

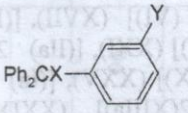

XIIIа-в

I, n = 1 (а), n = 2 (б), n = 3 (в); II, n = 1 (а), n = 2 (б); XIII, X = NH_2, Y = H (а), X = NH_3^+ SCN^-, Y = H (б), X = OH, Y = SO_2NH_2 (в)

2-(Тиен-2-илкарбонил)гидразинокарботиоамид (X). Раствор 1 ммоля тиофен-2-карбогидразида, 10 ммолей тиоцианата калия в смеси 5 мл воды, 10 мл метанола и 0.3 мл 36%-ной соляной кислоты нагревали при температуре кипения реакционной смеси (~ 64 °C) 12 ч. Метанол отгоняли и к остатку добавляли 10 мл воды. Выпавший при 20 °C осадок отфильтровывали и перекристаллизовывали из 40 мл метанола, выход соединения (X) 98 %, т. пл. 234-236 °C. Спектр ЯМР ^{1}H, ДМСО-d_6, δ, м. д.: 7.20 м, 7.63 с, 9.35 с, 10.40 с (4H, NH), 7.80 с (3H, CH). Найдено, %: C 35.89; H 3.54; N 20.93. $C_6H_7N_3OS_2$. Вычислено, %: C 35.81; H 3.51; N 20.93.

Тиоцианат 1,1,1-трифенилметанаммония (XIIIб). Раствор 5 ммолей 1,1,1-трифенилметан-амина, 5 ммолей тиоцианата калия в смеси 5 мл воды, 15 мл метанола и 0.7 мл уксусной кислоты нагревали при температуре кипения реакционной смеси (~ 64 °C) 4 ч. Метанол отгоняли и к остатку добавляли 20 мл воды. Выпавший при 20 °C осадок отфильтровывали и перекристаллизовывали из 40 мл бензола, выход соединения (XIIIб) 69 %, т. пл. 194-196 °C. Спектр ЯМР ^{1}H, $CDCl_3$, δ, м. д.: 7.29 м (30H, CH). Найдено, %: 75.41; H 5.75; N 8.84. $C_{20}H_{18}N_2S$. Вычислено, %: C 75.44; H 5.70; N 8.80.

Молекулярные комплексы (XIV-XXXI). К 1 ммолю краун-эфира (I-IV) добавляли раствор 1 ммоля соединений (V-XIII) в смеси растворителей указанных в таблице, и растворители испаряли при 20 °C. Выделившиеся монокристаллы комплексов (XIV-XXXI) промывали той же смесью растворителей и сушили на воздухе (см. таблицу 1).

Результаты исследования и их анализ.

Цель работы – определение тенденций, влияющих на результат образования кристаллических молекулярных комплексов кислородсодержащих краун-эфиров (I-IV) – 1,4,7,10-тетраоксациклододекан, 1,4,7,10,13-пентаоксациклопентадекан, 1,4,7,10,13,16-гексаоксациклооктадекан, 2,3,5,6,8,9,11,12-октагидро-1,4,7,10,13-бензопентаоксациклопента-децин, 2,3,5,6,8,9,11,12,14,15-декагидро-1,4,7,10,13,16-бензогексаоксациклооктадецин, *цис-син-цис* эйкосагидродибензо[b,k][1,4,7,10,13,16] гексаоксациклооктадецин и *цис-анти-цис* эйкосагидродибензо[b,k][1,4,7,10,13,16] гексаоксациклооктадецин соответственно, с HN-протонодонорными молекулами (V-XIII) и проявляющихся при изменении геометрических размеров «гостевых» молекул и способа пространственного экранирования взаимодействующих центров в «госте» и «хозяине».

Установлено, что при самопроизвольном испарении растворителей из растворов краун-эфиров (I-IV) с тиофен-2-сульфамидом (V), 5-нитро-1,3-тиазол-2-амином (VI), пиридино-3-карботиоамидом (VII), *N*-1-нафтилтиомочевиной (VIII), 6-нитро-1,3-бензотиазол-2-амином (IX), 2-(тиен-2-илкарбонил)гидразинокарботиоамидом (X), 5-[(4-нитрофенил)сульфонил]-1,3-тиазол-2-амином (XI), *N*-(4-[2-(аминокарбонотиоил) гидразоно]метилфенил)ацетамидом (XII), 1,1,1-трифенилметанамином (XIIIа), тиоцианатом 1,1,1-трифенилметанаммония (XIIIб), и 3-[гидрокси(дифенил)метил] бензолсульфамидом (XIIIв) образуются кристаллические молекулярные комплексы. Приведены состав комплекса и его номер: [(Iв) · (V)] (XIV), [(IIb) · 2 (V)] (XV), [(IV) · (V)] (XVI), [(Iв) · (VI)] (XVII), [(IV) · 2(VI)] (XVIII), [(Iв) · (VII)] (XIX), [(IIб) · (VII)] (XX), [(IV) · 2(VII)] (XXI), [(IIа) · 2(VIII)] (XXII), [(Iв) · 2(VIII)] (XXIII), [(IV) · 2(VIII)] (XXIV), [(Iв) · 2(IX)] (XXV), [(Iв) · 2(X)] (XXVI), [(Iв) · 2(XI)] (XXVII), [(IV) · 2(XII)] (XXVIII), [(Iа) · 2(XIIIа)] (XXIX), [(Iа) · 2(XIIIб)] (XXX), [(Iв) · 2(XIIIв)] (XXXI) соответственно.

Таблица 1- Выходы, температуры плавления, спектры ЯМР ^{1}H и данные элементного анализа комплексов (XIV – XXXI)

№	Выход, %	Т. пл., ^{o}C (растворители для кристаллизации)	Спектр ЯМР ^{1}H, δ , м.д.	Найдено, %			Формула	Вычислено, %		
				C	H	N		C	H	N
1	**2**	**3**	**4**	**5**	**6**	**7**	**8**	**9**	**10**	**11**
XIV	79	115-116 (метанол-этилацетат, 1:2)	Ацетон-d_6: 3.57 с (24H, CH_2O), 6.80 с (2H, NH), 7.13 м, 7.59 м, 7.75 м (3H, CH)	44.82	6.80	3.32	$C_{16}H_{29}NO_8S_2$	44.95	6.84	3.28
XV	67	119-121 (ацетон-гексан, 1:1)	Ацетон-d_6: 3.58 с, 3.61 с, 3.68 с, 3.82 м, 4.11 м (20H, CH_2O), 6.82 с (4H, NH), 6.87 м (4H, CH), 7.11 м, 7.59 м, 7.75 м (6H, CH)	45.17	5.33	4.43	$C_{24}H_{34}N_2O_{10}S_4$	45.13	5.36	4.39
XVI	88	103-104 (ацетон-гексан, 1:2)	Ацетон-d_6: 1.25-1.78 м, 3.59 м (36H, CH), 6.81 с (2H, NH), 7.12 м, 7.59 м, 7.75 м (3H, CH)	53.87	7.66	2.64	$C_{24}H_{41}NO_8S_2$	53.81	7.71	2.62
XVII	96	168-170 (метанол-бензол, 1:2)	ДМСО-d_6: 3.50 с, (24H, CH_2O), 8.22 с (1H, CH), 8.74 с (2H, NH)	44.09	6.57	10.34	$C_{15}H_{27}N_3O_8S$	44.00	6.65	10.26
XVIII	93	190-192 (ацетон-гексан, 1:2)	ДМСО-d_6: 1.19-1.46 м, 3.53 м (36H, CH), 8.22 с (2H, CH), 8.74 с (4H, NH)	47.19	6.32	12.75	$C_{26}H_{42}N_6O_{10}S_2$	47.12	6.39	12.68
XIX	91	120-122 (метанол-этилацетат, 1:3)	Метанол-d_4: 3.60 с (24H, CH_2O), 7.45 м, 8.26 м, 8.60 м, 9.00 м (4H, CH)	53.68	7.54	6.93	$C_{18}H_{30}N_2O_6S$	53.71	7.51	6.96
XX	96	140-142 (метанол-этилацетат, 1:2)	ДМСО-d_6: 3.55 м, 3.73 м, 4.05 м (20H, CH_2), 6.90 м (4H, CH), 7.43 м, 8.18 м, 8.64 м, 8.99 м (4H, CH)	58.59	6.83	6.31	$C_{22}H_{30}N_2O_6S$	58.65	6.71	6.22
XXI	71	115-116 (ацетон-гексан, 1:4)	ДМСО-d_6: 1.19-1.71м, 3.55 м (36H, CH), 7.44 м, 8.19 м, 8.65 м, 8.99 м (8H, CH)	57.61	7.59	8.38	$C_{32}H_{50}N_4O_7S_2$	57.63	7.56	8.40
XXII	83	141-143 (метанол-этилацетат, 1:1)	ДМСО-d_6: 3.60 с, 3.75 т, 4.02 т (16H, CH_2), 6.86 м, 6.93 м (4H, CH), 7.53 м, 7.90 м (14H, CH)	64.32	6.06	8.31	$C_{36}H_{40}N_4O_5S_2$	64.26	5.99	8.33

Продолжение таблицы 1

1	2	3	4	5	6	7	8	9	10	11
XXIII	83	188-190 (метанол-этилацетат,1:1)	ДМСО-d_6: 3.50 с, (24H, CH_2O), 7.53 с, 7.90 м (14H, CH)	61.14	6.57	8.41	$C_{34}H_{44}N_4O_6S_2$	61.05	6.63	8.38
XXIV	88	186-188 (метанол-этилацетат,1:1)	ДМСО-d_6: 1.22-1.68 м, 3.52 м (36H, CH), 7.53 м, 7.93 м (14H, CH)	64.94	7.29	7.31	$C_{42}H_{56}N_4O_6S_2$	64.92	7.26	7.21
XXV	80	258-260 (ацетон-гексан, 1:2)	ДМСО-d_6: (24H, CH_2), 7.40 д, 8.09 д, 8.66 с (6H, CH), 8.21 с (4H, NH)	47.74	5.27	12.94	$C_{26}H_{34}N_6O_{10}S_2$	47.70	5.23	12.84
XXVI	80	184-186 (метанол-бензол, 1:3)	ДМСО-d_6: 3.50 с (24H, CH_2O), 7.16 м, 7.63 с, 9.34 с, 10.39 с (4H, NH), 7.80 м (2H, CH)	43.19	5.70	12.63	$C_{24}H_{38}N_6O_8S_4$	43.23	5.74	12.60
XXVII	89	154-156 (ацетон-гексан, 1:2)	ДМСО-d_6: 3.50 м (24H, CH_2O), 7.78 с (2H, CH), 8.21 с (4H, NH), 8.12 д, 8.38 д (8H, CH)	43.19	4.64	10.11	$C_{30}H_{38}N_6O_{14}S_4$	43.16	4.59	10.07
XXVIII	81	240-244 (метанол-этилацетат,1:4)	ДМСО-d_6: 2.04 с (6H, CH_3), 1.22-1.71 м и 3.55 м (36H, CH), 7.58 д, 7.69 д (8H, CH), 7.97 с, 10.05 с, 11.31 с (8H, HN)	56.85	7.16	13.26	$C_{40}H_{60}N_8O_8S_2$	56.64	7.25	13.07
XXIX	81	94-95 (метанол)	$CDCl_3$: 1.86 с (4H, NH), 3.70 с(16H, CH_2O), 7.20-7.32 м (30H, CH)	79.53	7.24	4.05	$C_{46}H_{50}N_2O_4$	79.51	7.25	4.03
XXXI	98	174-176 (ацетон-гексан,1:2)	Метанол-d_4: 3.62 с (24H, CH_2O), 7.27 м, 7.44 м (28H, CH)	63.71	6.24	2.99	$C_{50}H_{58}N_2O_{12}S_2$	63.66	6.20	2.97

Примечание. Указано объемное соотношение растворителей для кристаллизации

Видно (см. таблицу), что при образовании кристаллических молекулярных комплексов типа «хозяин-гость» с нейтральными ароматическими HN-протонодонорными молекулами (V-VIII) наиболее эффективными являются 18-членные краун-эфиры, имеющие эквивалентно пространственно экранированные стороны полости макроцикла (Iв, IV), что не противоречит данным работ [5-7].

Установлено, что с ростом протяженности «гостевой» HN-протонодонорной молекулы, соединения (IX-XI, XIIIв), более эффективным лигандом является краун-эфир (Iв).

Дальнейшее увеличение протяженности «гостевой» молекулы (XI), [максимальный размер «гостевой» молекулы согласно "Advanced Chemistry Development 5.11" [8] составляет > 13.5 Å] приводит к образованию кристаллического молекулярного комплекса с краун-эфиром (IV). Это связано, по видимому, с необходимостью пространственной соразмерности молекул «гостя» и «хозяина». Экранирование HN-протонодонорного центра в «гостевых» молекулах (XIIIа,б) объемным трифенилметильным заместителем позволило при использовании молекул (XIIIа,б) зафиксировать в кристаллических комплексах «хозяин-гость» (XXIX, XXX) краун-эфир (Iа), для которого известны лишь несколько примеров подобного связывания [9-11].

Выводы:

Описанные особенности взаимодействия краун-эфиров (I-IV) с различно пространственно экранированными HN-протонодонорными молекулами (V-XIII), приводящие к образованию кристаллических молекулярных комплексов «хозяин-гость» (XIV-XXXI), могут быть учтены как составная часть при моделировании молекулярных взаимодействий сравнительно крупных природных молекул [1-3], а также явиться химической основой разделения смесей краун-эфиров аналогично изложенному в работах [5-6].

Перспективой последующих исследований в данном направлении научных исследований является определение зависимости таких комплексов от линейных размеров и способов стерического экранирования активных центров NH-протонодонорных молекул в комплексы различного строения.

Список литературы

1. *Химия* комплексов «гость-хозяин» / под. ред. Ф. Фегтле, Э. Вебера. – М.: Мир, 1988. –512 с.
2. *Comprehensive* supramolecular chemistry / eds.: J-M. Lehn, J. L. Atwood, J. E. D. Davies, D. D. MacNicol, F. Wogtle, Oxford – New York – Tokyo: Pergamon, 1996. – Vol. 1-11.
3. *Лен Ж-М.* Супрамолекулярная химия: Концепции и перспективы. – Новосибирск: Наука, 1998. – 334 с.
4. *Elbasyony A.,* Brugge H.J., Deuten K., et al. Host-guest complexes of 18-crown-6 with neutral molecules possessing the structure element XH_2 (X = O, N, C) // J. Am. Chem. Soc. – 1983. – V.105, N 22. – P.6568-6577.
5. *Ganin, E. V.*, Makarov, V. F., Kotlyar, S. A., Luk'yanenko, N. G. Isolation and separation of *cis-syn-cis* and *cis-anti-cis* diastereomers of dicyclohexano-18-crown-6 complexes with organic NH-acids // Zh. Obshch. Khim. – 1988. – Vol. 58, No 6. – P. 1309-1313.
6. *Ганин Э.В.,* Макаров В.Ф., Никитин В.И. Различная способность цис-син-цис (А) и *цис-анти-цис*-диастереомеров (В) дициклогексано-18-краун-6 к образованию комплексов с нитроанилинами // Укр. хим. журн. – 1988. – Т.54, № 3. – С.308-310.
7. *Ганин Э.В.* Реакционная способность макрогетероциклов во взаимодействии с амидосульфокислотой // Химия гетероцикл. соедин. – 1997. – № 11. – С.1571-1573.

8. *Комплекс* программ "Advanced Chemistry Development Inc.", Version 5.11 (Free). Toronto, Ontario M5H 3V9, Canada, 2001. http://acdlabs.com.
9. *Babaian E.A.*, Huff M., Tibbals F.A., Hencir D.C. Synthesis and Structural Characterization of $(Ph_3SiOH)_2$-12-c-4. A Model for Chemistry occurring at the Sediment-Water Interface in Natural Waters // J. Chem. Soc., Chem. Commun. – 1990. – No 4. – P. 306-307.
10. *Y.A.Simonov*, M.S.Fonari, A.A.Dvorkin et al. An X-ray study of a 12-crown-4 host-guest complex. Crystal structure of 4:6 complex between 12-crown-4 and amidosulfuric acid // J. Inclusion phenomena. – 1993. – Vol.16. – P.315-327.
11. *Michalides A.*, Henschel D., Blaschette A., Jones P.G. Supramolecules of Crown Ethers with Geminal Sulfones: Synthesis of Four Binary Complexes and Crystal Structure of $(CH_2CH_2O)_4$-$2H_2C(SO_2C_2H_5)_2$ // Z. Naturforsch. – 1995. – Bd. 50b. – S. 1018-1024.

Особливості утворення комплексів "хазяїн-гість" краун-етерів з HN-протондонорними молекулами.

Васильева М.Г., Горліченко М.Г., Шевченко С.В., Шепеліна С.І., Ганін Е.В.

Взаємодією краун-етерів з HN-протонодонорними молекулами отримані кристалічні молекулярні комплекси "хазяїн-гість" і встановлено, що в залежності від лінійних розмірів і способу стеричного екранування активних центрів протонодонорних молекул у комплекси зв'язуються краун-етери різної будови.

Ключові слова: *краун-етери, HN-протонодонорні молекули, комплекси "хазяїн-гість".".*

Characteristics of formation of complexes "host-guest" of crown-ethers with HN-protondonor moleculas

Vasileva M.G., Gorlichenko M.G., Shevchenko S.V., Shepelina S.I., Ganin E.V.

The interaction of crown-ethers with HN-protondonor molecules obtained crystalline molecular complexes "host-guest" and found, that depending on linear dimensions and method of steric masking of active centres HN-protondonor molecules various structures crown-ethers can be combined in complexes.

Key words: *crown-ethers, HN-protondonor molecules, complexes "host-guest".*

Додаток Ф.

Копія статті. “Селективные взаимодействия краун-эфиров с фторокомплексными кислотами бора, кремния, германия, олова и сурьмы в присутствии воды ”

Випуск 8 2009

ВІСНИК

ОДЕСЬКОГО ДЕРЖАВНОГО ЕКОЛОГІЧНОГО УНІВЕРСИТЕТУ

УДК 541.49:547.89:548.736

М.Г. Васильева, Г.И. Герасименко, *к.х.н.*, **В.Ф. Шевченко,** *к.т.н.*, **Э.В. Ганин,** *д.х.н.*
Одесский государственный экологический университет

СЕЛЕКТИВНЫЕ ВЗАИМОДЕЙСТВИЯ КРАУН-ЭФИРОВ С ФТОРОКОМПЛЕКСНЫМИ КИСЛОТАМИ БОРА, КРЕМНИЯ, ГЕРМАНИЯ, ОЛОВА И СУРЬМЫ В ПРИСУТСТВИИ ВОДЫ

Природа протонодопорных молекул, стабилизированных в кристаллические комплексы краун-эфирами из равновесных водных растворов фторидов бора, кремния, германия, олова, контролируется строением краун-эфиров.

Ключевые слова: *краун-эфиры, фторокомплексные кислоты, комплексы.*

Введение.

В работе [1] показано, что в нормальных условиях контакт катионов металлов (матриц) с окисью этилена приводит к ее циклоолигомеризации с селективным образованием краун-эфиров в составе кристаллических комплексов. В качестве матриц используют также катион гидроксония $[H_3O]^+$ [2] и нейтральную форму воды – H_2O [3]. Возможность функциональной перестановки элементов пары катион краун-эфир не рассматривалась.

Материалы и методы их исследования.

Все исходные соединения использовали в виде коммерческих образцов (фирм: Acros, Aldrich) без дополнительной очистки.

ИК спектры зарегистрированы на приборе Specord IR-75 в вазелиновом масле, стекла KRS-5. Термогравиаграммы комплексов (II–V, VIa, VIII) записаны на дериватографе (QD-102 в температурном интервале 20–500°С, чувствительность записи ДТА и ДТГ – 1/5 от максимальной, скорость нагрева 10 град/мин, платиновые тигли, навески 80–130 мг. Анализ методом ТСХ проводили на пластинах Silufol с элюированием смесью метанол–хлороформ, 1:5, проявление нингидрином. Комплексы при анализе методом ТСХ разлагаются на компоненты со значениями Rf 0 (красно-бурые пятна «гостевых» фторидов) и 0.53, 0.70, 0.82 (белые пятна 18-К-6, А-ДЦГ-6, В-ДЦГ-6) соответственно.

К 264 мг 18-К-6, 372 мг В- или 372 мг А-ДЦГ-6 добавляли соответственно 0.8, 1.5 и 1.5 мл эфирата трифторида бора. Смеси оставляли при 20°С в не защищенной от влаги атмосфере. Образовавшиеся кристаллы комплексов (II, III, VIII) отделяли и перекристаллизовывали. Выходы комплексов составляют: (II) – 350 мг (74%), т. пл. 73–75 °С (из этилацетата); (III) – 370 мг (68%), т. пл. 138–139°С (из этилацетата), т. пл. 137 –139°С [4]; (VIII) – 450 мг (83%), т. пл. 139–140°С (из смеси ацетон–гексан).

Взаимодействие 264 мг 18-К-6 и 1.5 мл эфирата трифторида бора в условиях синтеза ионного комплекса (VIII) [5] при 126°С дает нейтральный комплекс (II) с выходом 330 мг (70%). ИК спектры и термогравиаграммы полученных нами соединений (II, III, VIII) и описанных в работах [4 – 6] идентичны.

К раствору 264 мг 18-К-6 в 10 мл метанола добавляли растворы 105 мг диоксида германия, 179 мг трифторида сурьмы или 195 мг тетрафторида олова в 5, 2 и 2 мл 50%-ной фтористоводородной кислоты соответственно. Полученные смеси оставляли самопроизвольно кристаллизоваться при 20°С: в первом случае – в эксикаторе над 98%-ной серной кислотой, в остальных – на воздухе. Выход комплекса (IV) составлял 460 мг (95%), т. пл. 199–200°С(т. пл. 198-199°С [7]), комплекса (У1а) – 350 мг (84%), т. пл. 215-216°С (т. пл. 215-216°С [8]); ИК спектры и термогравиграммы полученных нами соединений (IV, VIa) и описанных в работах [7, 8] идентичны. Выход комплекса

(V) 410 мг (77%), т. пл. 65-67°С. ИК спектр, ν, см$^{-1}$: 3400-3250, 1640 [δ(H_2O)], 1165-1100 (СОС). Найдено, %: С 26.91; Н 6.22; F 15.32. $C_{12}H_{32}F_4O_{10}Sn$. Вычислено, %: С 27.14; Н 6.07; F 15.06. Потеря комплексом (V) 2 молей внешнесферной воды с переходом ее в газовую фазу происходит в интервале температур 65–90°С и сопровождается эндотермическим эффектом.

Результаты исследования и их анализ.

В работе [1] показано, что в нормальных условиях контакт катионов металлов (матриц) с окисью этилена приводит к ее олигомеризации с селективным образованием краун-эфиров в составе кристаллических комплексов. В качестве матриц используют также катион гидроксония $[H_3O]^+$ [2,3] и нейтральную форму воды – H_2O [4,9,10]. Возможность функциональной перестановки элементов пары катион краун-эфир не рассматривалась.

Для выявления возможности применения краун-эфиров («хозяев») в качестве матриц для селективной стабилизации протонодонорных молекул («гостей») в составе комплексов «гость–хозяин» [11] мы использовали гидролитически нестабильные фториды ряда *p*-элементов, генерирующих в присутствии воды равновесные смеси нейтральных и заряженных двух- и трех-протонодонорных «гостевых» молекул соответственно [12], способных к образованию кристаллических молекулярных комплексов с краун-эфирами [13]. В работе [14] установлено, что характер стабилизации «гостевых» компонентов из равновесного водного раствора тетра-, пента- и гексафторидов кремния (кремнийфтороводородной кислоты) в составе кристаллических молекулярных комплексов (I) [14-16], (VII) [14] контролируется строением кислородсодержащих краун-эфиров. Этот вывод подтверждается взаимодействием этих же краун-эфиров (18-К-6, А- и В-ДЦГ-6) с эфиратом трифторида бора, последовательно генерирующим в присутствии влаги воздуха следующие протонодонорные компоненты: BF_3Et_2O, H_3O^+ $[BF4]^-$, H_3BO_3 [12]. Так, согласно данным работы [14], краун-эфиры 18-К-6 и В-ДЦГ-6, имеющие эквивалентно стерически-экранированные стороны плоскости гетероцикла, стабилизируют нейтральный гидрат трифторида бора с образованием комплексов (II) [6], (III) [4], а неэквивалентно стерически-экранированная полость гетероцикла А-ДЦГ-6 «тесной» стороной связывает в комплекс тетрафтороборат гидроксония, образуя комплекс (VIII) [5]. Инвариантность образования комплексов (II, VIII) при 20 и 100°С дополнительно подтверждает вывод работы [14]. Зависимость имеет более общий характер, что подтверждается данными о составе и строении продукта взаимодействия 18-К-6 с равновесным водным раствором тетра-, пента- и гексафторидов германия (раствором диоксида германия в 50%-ной фтороводородной кислоте) [соединение (IV)] [7] и согласуется с результатами, полученными при взаимодействии названного краун-эфира с раствором тетрафторида олова во фтороводородной кислоте [комплекс (V)]. Видно, что комплексы (IV,V) являются полными аналогами диакватетрафторсиликатного комплекса (I). Отметим, что германатный комплекс (IV) аналогично силикатному комплексу (I) получается как при самопроизвольном испарении реакционной смеси 18-К-6 с раствором диоксида германия во фтороводородной кислоте при нормальных условиях по методике [7], так и при повышении атомарного соотношения фтора к германию добавлением в реакционную смесь избытка фтороводородной кислоты с последующим ее концентрированием. Гидролитически более стабильный трифторид сурьмы при взаимодействии с кислородсодержащими краун-эфирами не претерпевает существенных изменений и как в метаноле [8], так и в 50%-ной фтороводородной кислоте дает негидратные комплексы (VIа–в). Ниже приведено строение исследованных комплексов «гость–хозяин».

Нейтральные комплексы. [$SiF_4 \cdot 2H_2O \cdot$18-K-6$\cdot$2 H_2O] (I) [14-16], [$(BF_3 \cdot H_2O)_2 \cdot$18-K-6$\cdot$2 H_2O] (II) [6], [$(BF_3 \cdot H_2O)_2 \cdot$B-ДЦГ-6] (III) [4], [$GeF_4 \cdot$2 $H_2O \cdot$18-K-6$\cdot$2 H_2O] (IV) [7], [$SnF_4 \cdot 2H_2O \cdot$18-K-6$\cdot 2H_2O$] (V), [SbF_3КЭ] (VIa–в) [8] (КЭ = 18-K-6 (а), A-ДЦГ-6$\cdot$ CH_3OH (б), B-ДЦГ-6 (в)].

Ионные комплексы. {[A-ДЦГ-6$\cdot H_3O]^+$ $[SiF_5]^-$} (VII) [14], {[A-ДЦГ-6$\cdot H_3O]^+[BF_4]^-$} (VIII) [5], {[A18-K-6H$\cdot H_2O]^+$ $[SiF_5 \cdot H_2O]^-$ $\cdot H_2O$} (IX) [17], {$[ДA18\text{-}K\text{-}6H_2]^{2+}[SiF_5 \cdot H_2O]^{2-}$} (X) [17], {$[ДA15\text{-}K\text{-}5H_2]^{2+}[SiF_6]^{2-}$} (XI) [18], {$[ДA18\text{-}K\text{-}6H_2]^{2+}[GeF_5 \cdot H_2O]^{2-}$} (XII) [7].

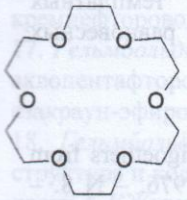

18-K-6

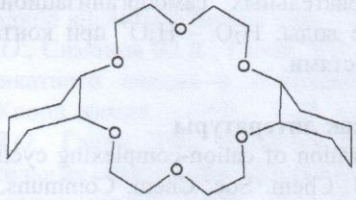

A-ДЦГ-6

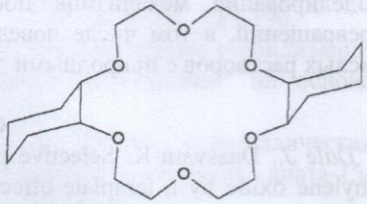

B-ДЦГ-6

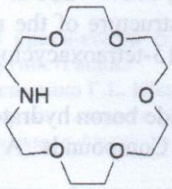

A18-K-6H

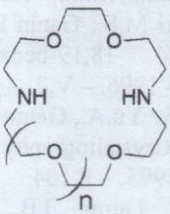

ДA15-K-5
ДA18-K-6

18-K-6 – 18-краун-6, A-ДЦГ-6 – *цис-син-цис*-изомер дициклогексано-18-краун-6, B-ДЦГ-6 – *цис-анти-цис*-изомер дициклогексано-18-краун-6, A18-K-6 – аза-18-краун-6, ДA15-K-5 – диаза-15-краун-5 (n = 1), ДA18-K-6 – диаза-18-краун-6 (n = 2).

Наличие в азакраун-эфирах основного атома азота предопределяет его протонирование в рассматриваемых взаимодействиях и стабилизацию «гостевой» компоненты в комплексы «гость–хозяин» в ионной форме. Однако и в этих случаях прослеживается контролирующее влияние строения полости краун-эфира в выборе протонодонорной «гостевой» молекулы. Так, при взаимодействии 45%-ной кремнийфтороводородной кислоты с A18-K-6, ДA18-K-6 и ДA15-K-5 в первых двух случаях в комплексе «гость– хозяин» стабилизированы аквапентафторосиликатные анионы – комплексы (IX, X) [17], в последнем – гексафторосиликатный анион – соединение (XI) [18]. Это дополнительно подтверждается стабилизацией ДA18-K-6 аквапентафторогерманатного аниона из раствора диоксида германия во фтористоводородной кислоте в составе комплекса «гость–хозяин» (XII) [7], изоструктурного кремниевому комплексу (X) [17].

Изложенное подчеркивает детерминирующую, матричную роль строения краун-эфиров при взаимодействии с равновесными водными растворами перечисленных фторидов р-элементов с образованием комплексов «гость—хозяин». Видно, что по критерию «стабилизация аниона» комплексы (VII, VIII) демонстрируют то, что шесть малоосновных простых эфирных групп, структурно организованных макроциклической полостью A-ДЦГ-6 (в присутствии воды), функционально аналогичны высокоосновному атому азота в азакраун-эфирах (A18-K-6 и ДA18-K-6). В рамках принятой концепции моделирования краун-эфирами макрополостей природных

молекул [11] стабилизация нейтральной, гидратной воды [комплексы (I–V)] и катиона гидроксония [соединения (VII, VIII)] из растворов, содержащих альтернативные ее формы, подчеркивает контролирующее влияние молекулярных макрополостей на механизм вовлечения заряженных и нейтральных форм воды в природные процессы.

Вывод

Принципиальная допустимость функциональных перестановок элементов пары краун-эфир – катион, т.е. использования их как в виде матриц, так и продуктов синтеза, позволяет рассматривать пару в качестве возможной перспективы химической основы моделирования механизмов последовательных самоорганизационных темплатных превращений, в том числе поведение воды: H_2O – H_3O^+ при контакте равновесных кислых растворов с природными полостями.

Список литературы

1. *Dale J.,* Daasvatn K. Selective preparation of cation-complexing cyclic oligoethers from ethylene oxide by a template effect // J. Chem. Soc. Chem. Communs. – 1976. – N 8. – P.295-296.

2. *Яцимирский К. Б.*, Колъчинский А. Г., Павлищук В.В., Таланова Г.Г. Синтез макроциклических соединений. – Киев: Наукова думка, 1987. – 280 с.

3. *Simonov Y.A.,* Fonari M.S., Ganin E.V. et al. Crystal structure of the molecular complex between water and 18,19-benz-1,16-diaza-4,7,10,13-tetraoxacycloeicosa-17,20-dione // Supramolec. Chem. – 1996. – V.7. – P.101-105.

4. *Fonari M.S.,* Simonov Yu.A., Ganin E.V. et al. Trifluoride boron hydrates: Stabilization by the crown ethers / // Crystallography of Supramoleculr Compounds. A NATO Advanced Study Institute. Erice, 1995. – P.104

5. *Гельмбольдт В.О.,* Ганин Э.В., Симонов Ю.А.и др. Синтез, кристаллическая и молекулярная структура комплекса тетрафторобората гидроксония с цис-син-цис-изомером дициклогексано-18-краун-6 // Журн. неорганич. химии. – 1995. – Т.40, № 4. – С. 594-600.

6. *Симонов Ю.А.*, Гельмбольдт В.О., Ганин Э.В., и др. Новый пример стабилизации аквакомплекса $BF_3{\cdot}H_2O$ в соединении типа "гость-хозяин" $[(BF_3{\cdot}H_2O)_2{\cdot}18$-краун-$6{\cdot}2H_2O]$ // Коорд. хим. – 1995. – Т. 21, № 10. – С. 760-765.

7. *Gelmboldt V.O., Ganin E.V., Ostapchuk L.V.,* et al. Stabilization of Germanium (IV) aquafluorocompounds in host-guest type complexes with crown ethers. Synthesis, crystal structure and IR spectra of the complexes $[(GeF_5{\cdot}H_2O)_2{\cdot}H_2$-1,10-diaza-18-crown-6] and $[(trans\text{-}GeF_4{\cdot}\ {\cdot}2H_2O){\cdot}18$-crown-$6{\cdot}2H_2O]$ // J. Inclusion Phenomena. – 1996. – V. 24. – P. 287-299.

8. *Lipkowski J.*, Fonar' M.S., Kravtsou V.Ch., et al. Antimonu (III) fluoride: inclusion complexes with crown-ethers // J. Chem. Cryst. – 1996. – V. 26, N 12. – P. 823-833.

9. *Аникин В.Ф.,* Ганин Э.В., Розынов Б.В. и др. Об особенностях взаимодействия N,N'-замещенных дифталимида с аминами // Химия гетероцикл. соединений. – 1982. – № 2. – С. 246-249.

10. *Simonov Y.A.,* Fonar' M.S., Ganin E.V., et al. Crystal structure of the 1:1 molecular complex between water and 18,19-benz-1,16-diaza-4,7,10,13-tetraoxacycloeicosa-17,20-dione //Supramol. Chem. – 1996. – V. 7. – P. 101-105.

11. *Химия* комплексов «гость-хозяин» / под. ред. Ф. Фегтле, Э. Вебера. – М.: Мир, 1988. – 512 с.

12. *Раков Э.Г.* Химия и технология неорганических фторидов. – М.: Изд. МХТИ, 1990. – 161 с.

13. *Ганин Э.В.* Комплексы краун-эфиров "гость-хозяин". Требования к протонодонорной молекуле // Журн. общей химии. – 1997. – Т. 67, № 6. – С. 891-892.

14. *Ганин Э.В.* Взаимодействие 18-членных краун-эфиров с кремнефтористоводородной кислотой // Журн. общей химии. – 1997. – Т.67, № 6. – С. 889-890.
15. *Simonov Y.A.,* Ganin E.V., Dvorkin A.A., et al. Stabilization of silicon tetrafluoride by crown ether complexation. Crystal and molecular structure of host:guest complex 1:1:2 between *trans*-tetrafluoro-bis(aqua)silicon, 18-crown-6, and water // Supramolec. Chem. – 1994. – V.3. – P.185-189.
16. *Гельмбольдт В.О.,* Ганин Э.В., Симонов Ю.А., и др. Специфическая сольватация диаквотетрафторокомплекса кремния краун-эфирами в растворах кремнефтороводородной кислоты // Коорд. хим. – 1995. – Т.21, № 3. – С. 183-190.
17. *Гельмбольдт В.О.*, Симонов Ю.А., Ганин Э.В., и др. Первый пример стабилизации аквопентафторосиликатного аниона в комплексах типа "гость-хозяин" на основе азакраун-эфиров // Коорд. химия. – 1996. – Т.22, № 1. – С.21-32.
18. *Гельмбольдт В.О.,* Ганин Э.В., Остапчук Л.В., и др. Синтез, кристаллическая структура и колебательные спектры гексафторосиликата дипротонированного диаза-15-краун-5 // Журн. неорганич. химии. – 1996. – Т.41, № 6. – С.1041-1046.

Селективні взаємодії краун-етерів із фторокомплексними кислотами бора, кремнію, германія, олова й сурми в присутності води.

Васильєва М.Г., Герасименко Г.І., Шевченко В.Ф., Ганін Е.В.

Природа протонодопорних молекул, стабілізованих у кристалічні комплекси краун-етерами з рівноважних водяних розчинів флуоридів бора, кремнію, германія, олова, контролюється будовою краун-етерів.

***Ключові слова**: краун-етери, флуорокомплексні кислоти, комплекси.*

Selective interactions of crown-ethers with a acids of fluorinecomplex of boron, silicon, germanium, tin and antimony at the presence of water.

Vasileva M.G., Gerasimenko G.I., Shevchenko V.F., Ganin E.V.

The structure of protonodonor moleculas stabilized in crystalline complexes by crown-ethers from equilibrium water solutions of fluorides of boron, silicon, germanium, tin, is determined by a structure of crown-ethers.

***Key words:** crown-ethers, acids of fluorinecomplex, complexes.*

Додаток Х.

Копія статті. “ Interaction of hexafluorosilicic acid with sulfa drugs. Bis(sulfathiazolium)hexafluorosilicate: Spectral data and crystal structure ”

Provided for non-commercial research and education use.
Not for reproduction, distribution or commercial use.

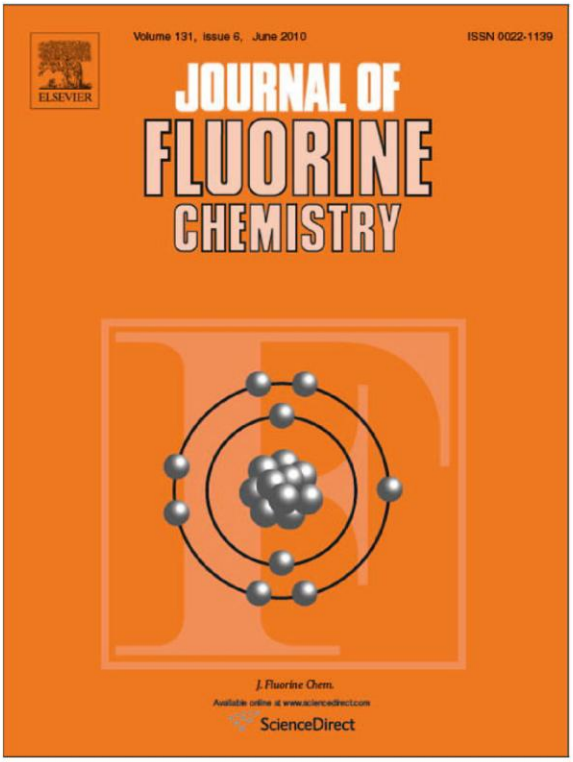

This article appeared in a journal published by Elsevier. The attached copy is furnished to the author for internal non-commercial research and education use, including for instruction at the authors institution and sharing with colleagues.

Other uses, including reproduction and distribution, or selling or licensing copies, or posting to personal, institutional or third party websites are prohibited.

In most cases authors are permitted to post their version of the article (e.g. in Word or Tex form) to their personal website or institutional repository. Authors requiring further information regarding Elsevier's archiving and manuscript policies are encouraged to visit:

http://www.elsevier.com/copyright

Author's personal copy

Journal of Fluorine Chemistry 131 (2010) 719–723

Contents lists available at ScienceDirect

Journal of Fluorine Chemistry

journal homepage: www.elsevier.com/locate/fluor

Interaction of hexafluorosilicic acid with sulfa drugs. Bis(sulfathiazolium) hexafluorosilicate: Spectral data and crystal structure

Vladimir O. Gelmboldt [a], Eduard V. Ganin [b], Larisa V. Koroeva [c], Mark M. Botoshansky [d], Marina S. Fonari [e,*]

[a] Odessa State Medical University of Ministry of Health of Ukraine, Valikhovskiy lane, 2, 65026, Odessa, Ukraine
[b] Odessa State Environmental University of Ministry of Education and Science of Ukraine, Lvovskaya str., 15, 65016, Odessa, Ukraine
[c] Physico-Chemical Institute of Environment and Human Protection of Ministry of Education and Science of Ukraine and National Academy of Sciences of Ukraine, Preobrazhenskaya str., 3, 65082, Odessa, Ukraine
[d] Schulich Faculty of Chemistry, Technion-Israel Institute of Technology, Technion City, 32000 Haifa, Israel
[e] Institute of Applied Physics, Academy of Sciences of Moldova, Academy str., 5, MD2028 Chisinau, Republic of Moldova

ARTICLE INFO

Article history:
Received 27 December 2009
Received in revised form 10 March 2010
Accepted 12 March 2010
Available online 23 March 2010

Keywords:
Hexafluorosilicate
Sulfa drugs
Solubility
Hydrogen bonding
Crystal structure

ABSTRACT

Interaction of hexafluorosilicic acid with sulfa drugs sulfathiazole (**stz**) and sulfalen (2-sulfanilamido-3-methoxypyrazine, **sl**) results in the crystalline salts of the compositions [**stz**H]$_2$[SiF$_6$] (**I**) and [4-H$_2$NO$_2$SPhNH$_3$]$_2$[SiF$_6$] (**II**). Complex **I** is characterized by IR, mass spectrometry data and single crystal X-ray diffraction. The crystal structure of **I** is stabilized by a network of charge-assisted hydrogen bonding. The relationship between the solubility and H-bonding system in **I**, **II** and related "onium" hexafluorosilicates is discussed. The formation of complex **II**, previously reported as an interaction product of hexafluorosilicic acid with 4-aminobenzenesulfonamide (sulfanilamide), is the result of cleavage of the C–N bond in sulfalen in acidic medium.

© 2010 Elsevier B.V. All rights reserved.

1. Introduction

The products of interaction of hexafluorosilicic acid with N-, O-containing organic bases, "onium" fluorosilicates, mainly hexafluorosilicates are of inextinguishable interest as chemical reagents and functional materials for various purposes [1]. As it has been previously noted [1], the system of interionic XH···F (X = N, O) H-bonds in the solid "onium" fluorosilicates has a significant impact on the structural characteristics and properties of the final salts. In particular, the observed inverse-proportional relationship [2,3] between the pyridinium hexafluorosilicates' water solubility and a number of short interionic H-bonds in the crystalline salts has an exponential character. The functionalization of the "onium" cation by the H-donor substituents, differing in the number and nature of the H-donor centers, might serve as a convenient method to detect the directional changes in physico-chemical characteristics of the "onium" hexafluorosilicates.

This work continues the previous research on the correlations between the structure and properties of "onium" hexafluorosilicates [2,3] and is devoted to the interaction products formed by the sulfa drugs sulfathiazole (**stz**) and sulfalen (**sl**) with hexafluorosilicic acid. This choice is explained by our interest to the co-crystals of sulfa drugs, products of their transformations or other active pharmaceutical ingredients (APIs) [4] possessing H-donor/H-acceptor functions with co-crystal partners of different nature [5,6]. In recent years, this topic has received increased attention [7,8]. Sulfa drugs of sulfonamides are a group of antibiotics used as agricultural herbicides and in the treatment of infections of respiratory and urinary tracts in humans. These antibiotics were repeatedly found in aquatic media at concentrations ranging from 0.13 to 1.9 μg/L [9,10]. Members of this class of compounds differ in the N-bound substituent of the sulfonamide linkage. Numerous methods of free-radical-induced oxidative and reductive degradation of sulfa drugs containing heterocyclic five- and six-membered rings have been studied and the authors concluded that the degradation occurs through cleavage at various positions with the formation of sulfanilic acid 4-H$_2$NPhSO$_3$H, sulfanilamide 4-H$_2$NPhSO$_2$NH$_2$, and aniline PhNH$_2$ as the possible degradation products. On the other hand, it is known that, in acidic media, the sulfa drugs are easily protonated with the formation of cationic forms [9].

* Corresponding author. Tel.: +373 22 73 81 54; fax: +373 22 72 58 87.
E-mail addresses: vgelmboldt@te.net.ua (V.O. Gelmboldt), edganin@gmail.com (E.V. Ganin), botoshan@tx.technion.ac.il (M.M. Botoshansky), fonari.xray@phys.asm.md, fonari.xray@gmail.com (M.S. Fonari).

0022-1139/$ – see front matter © 2010 Elsevier B.V. All rights reserved.
doi: 10.1016/j.jfluchem.2010.03.007

Author's personal copy

The interaction of hexafluorosilicic acid with sulfa drugs sulfathiazole **stz** and sulfalen **sl** [11] results in the crystalline salts of the compositions $[\mathbf{stz}H]_2[SiF_6]$ (**I**) and $[4\text{-}H_2NO_2SPhNH_3]_2[SiF_6]$ (**II**) [12]. The preparation, spectral and solubility data alongside with the crystal structure for **I** are reported herein.

2. Results and discussion

We have previously shown that interaction of hexafluorosilicic acid with *p*-aminobenzoic acid, sulfanilamide and 5-amino-1-benzyl-1,2,3-triazol-4-carbonic acid yielded the corresponding hexafluorosilicates with the aromatic cations formed due to protonation of the terminal amino group [6,12,13]. In a similar way, we expected the formation of the corresponding hexafluorosilicates starting from the sulfa drugs sulfathiazole and sulfalen. However, according to the data of elemental analysis and XRD, the crystalline compound isolated from the reaction solution of hexafluorosilicic acid – **sl** – H_2O appeared to be a hexafluorosilicate with the composition $[4\text{-}H_2NO_2SC_6H_4NH_3]_2[SiF_6]$ (**II**). The formation of **II**, previously reported in [12], can be considered as the result of hydrolytic transformation of sulfalen molecule in the acidic medium due to the cleavage of C–N covalent bond [14] (Scheme 1). The possible reaction by-product with the pyrazine cycle or the product of its degradation does not form a crystalline compound in the reaction conditions and has not been identified.

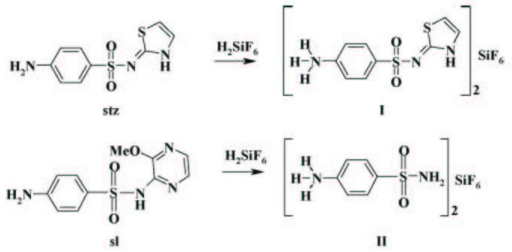

Scheme 1. Schematic pathway to the formation of crystalline salts **I** and **II**.

Sulfathiazolium hexafluorosilicate (**I**) was obtained by interaction of **stz** with an aqueous solution of hexafluorosilicic acid. Table 1 summarizes the IR spectroscopic characteristics for **I**. Vibrations ν(NH) of the secondary amino group are registered near 3525 and 3445 cm^{-1}, whereas the vibrations of $-N^+H_3$ group and –NH fragment of the thiazole ring are identified as a series of bands of average intensity in the range 3260–2630 cm^{-1}. The bands registered at 1320 and 1150 cm^{-1} are assigned to the $\nu_{as,s}(SO_2)$ vibrations, respectively, and their positions are close to the corresponding absorption bands in the IR spectrum of **II** (1320 and 1175 cm^{-1}) [12]. The deformation vibrations of the cation are also visible in the range of the stretching vibrations of the phenyl and thiazole rings ν_{ring} (1650–1505 cm^{-1}) and in the range of 750–680 cm^{-1} of the ν(SiF) vibrations of the anion (Table 1). At the same time, the region of the $\delta(SiF_2)$ vibrations is free of the other types of vibrations: a triplet structure of the $\delta(SiF_2)$ band indicates in favor of the decrease of symmetry of $[SiF_6]^{2-}$ anion with regard to O_h that is explained by the resulting interionic H-interactions.

Being one of the most important physical and chemical properties of the pharmaceuticals, the water solubility is crucial for solving the problems of chemical technology, ecology, and pharmacology [15]. As we have recently shown [3] the water solubility (**C**) of a number of pyridinium hexafluorosilicates correlates with the parameter $\mathbf{h} = \mathbf{n}/\mathbf{d}(\mathbf{D}\cdots\mathbf{A})_{\mathbf{av.}}$, where **n** is a number of short interionic contacts (H-bonds) and $\mathbf{d}(\mathbf{D}\cdots\mathbf{A})_{\mathbf{av.}}$ is an average donor(D)–acceptor(A) distance in the salt crystal structure (taking into account contacts with $D\cdots A \leq 3.2$ Å, $(D)\text{–}H\cdots A \leq 2.6$ Å that correspond to strong and moderate H-bonds following the classification suggested by Steiner [16]). The functional dependence of **C** against *h* has an exponential character. Table 2 demonstrates the water solubility data for **I**, **II**, and some other heterocyclic "onium" hexafluorosilicates. As it follows from Table 2, the solubility of **I**, **II**, and $[C_2H_6N_5]_2[SiF_6]$ (where $C_2H_6N_5$ is a 3,5-diamino-1,2,4-triazolium cation) fits well within the specified dependency, reflecting the decrease in solubility of compounds with the increasing number of short interionic H-bonds. We do not exclude that the observed relationship between **C** and **h** may be of a common character for the "onium" hexafluorosilicates with the "onium" aromatic cations.

Sulfathiazole has a remarkable solvate-forming ability. Many solvent-containing sulfathiazoles are known and their structures

Table 1
IR spectral data (cm^{-1}) for hexafluorosilicate **I**.

ν(NH)	$\nu(N^+H_n)$	ν_{ring}*	$\nu_{as,s}(SO_2)$	$\nu_{puts.}$	ν(SN)	ν(SiF)**	$\delta(SiF_2)$
3525 m.	3260 m.	1650 sh.	1320 m.	1085 s.	915 m.	750 s.	480 sh.
3445 m.	3050 m.	1630 sh.	1150 m.	1015 m.		720 v.s.	455 m.
	2710 m.	1595 m.				680 s.	445 m.
	2630 m.	1570 s.					
		1525 sh.					
		1505 sh.					

m. = medium, s. = strong, v.s. = very strong, sh. = shoulder.
* Also include deformation vibrations δ(HNC), $\delta(N^+H_3)$.
** Also may include deformation vibrations $r(N^+H_3)$, r(CNH), δ(CCH).

Table 2
Solubility of **I**, **II** and related onium hexafluorosilicates in water.

Compound	Solubility/mol.%, 25 °C	Standard deviation, *S*	h/Å^{-1}	References
I	0.10 ± 0.0007	0.0008	2.03	Present work
II	0.06 ± 0.004	0.004	2.10	[12]
$[2,6\text{-}(H_2N)_2C_5H_3NH]_2[SiF_6]$	0.06 ± 0.003	0.004	2.35	[3]
$[C_2H_6N_5]_2[SiF_6]$*	0.28 ± 0.016	0.019	1.78	[17]
$[3\text{-}HO(O)CC_5H_4NH]_2[SiF_6]$	3.33 ± 0.121	0.138	1.09	[3,18]
$[2\text{-}HO(O)CC_5H_4NH]_2[SiF_6]$	5.33 ± 0.251	0.286	0.76	[3]
$[2\text{-}CH_3C_5H_4NH]_2\ [SiF_6]$	11.60 ± 0.82	0.93	0.71	[3,19]

* $C_2H_5N_5$ = 3,5-diamino-1,2,4-triazole.

Author's personal copy

have been previously reported [20,21]. Besides, Caira et al. [22] reported the crystal structure of the 1:1 complex of sulfathiazole and cyclodextrin, in which the molecules are hydrogen bonded with each other. In the sulfathiazolium nitrate monohydrate [23] the drug molecule is protonated on its terminal amino group. The planes of the benzene and thiazole rings are inclined in a *gauche* conformation about the S–N bond with a dihedral angle of 87.63(6)°. The crystal structure is stabilized by a network of hydrogen bonding.

Bis(sulfathiazolium) hexafluorosilicate **I** crystallizes in a monoclinic crystal system (space group $C2/c$ with $Z = 4$). The crystal structure and refinement data for **I** is given in Table 3. Selected bond distances and angles are given in Table 4, while hydrogen-bonding geometry is summarized in Table 5. The formula unit comprises two **[stz**H]$^+$ cations that occupy general positions and one hexafluorosilicate anion that resides on the twofold axis (Fig. 1).

The positions of the N-bound hydrogen atoms were found in the difference Fourier map. The cation is characterized by the common geometry with the S1–O1, S1–O2 and N2–C7 bond distances being in agreement with the double-bond character for sulfoxide and imine groups, respectively. In the sulfathiazolium cation the planes of the benzene and thiazole rings are inclined in a *gauche* conformation about the S–N bond with a C7–N2–S1–C4 dihedral angle of 95.8(2)°. Only major position for the disordered $[SiF_6]^{2-}$ anion is further discussed. The $[SiF_6]^{2-}$ anion has a geometry of a slightly distorted octahedron with the Si–F bond distances range of 1.654(2)–1.679(2) Å and maximal deviation of the *cis*-F–Si–F angle from the right one equal to 1.3°. The crystal structure is stabilized by the network of hydrogen bonding. All fluorine atoms are involved in the hydrogen-bonding system (Table 5). Each $[SiF_6]^{2-}$ anion has NH···F contacts with eight closest **[stz**H]$^+$ cations, while each cation bridges two $[SiF_6]^{2-}$ anions *via* terminal ammonia group and binds one more $[SiF_6]^{2-}$ anion *via* the imine NH– site (Fig. 2(a)). The self-assembling of the **[stz**H]$^+$ cations occurs *via* a couple of the inversion-related N1···N2 hydrogen bonds; N···N separation being 2.925(3) Å (Fig. 2(b)).

The crystal packing represents the alternation of the H-bonded rows of $[SiF_6]^{2-}$ anions and **[stz**H]$^+$ cations. Thus, the interaction of hexafluorosilicic acid with sulfathiazole results in the formation of bis(sulfathiazolium) hexafluorosilicate, whereas the reaction involving sulfalen leads to its hydrolysis with the cleavage of the C–N bond and formation of bis[(4-aminosulfonyl)benzeneammonia] hexafluorosilicate. The solubility of the studied salts, as for the previously studied hexafluorosilicates with functionalized pyridinium cations [2,3], correlates with the number of short interionic H-bonds in their structures.

3. Experimental

Commercially available reagents were used as received. Compounds **I–II** were analysed for C, H, N and S in a Perkin Elmer 240C. The IR-absorption spectra were recorded on a spectrophotometer Specord 75IR (range 4000–400 cm^{-1}, samples as

Table 3
Crystal data and structure refinement parameters for **I**.

	I
Empirical formula	$(C_9H_{10}N_3O_2S_2)_2[SiF_6]$
Formula weight	654.73
Crystal system	Monoclinic
Space group	$C2/c$
Unit cell dimensions	
a (Å)	17.723(3)
b (Å)	11.684(2)
c (Å)	11.938(2)
β (°)	91.78(3)
Cell volume (Å^3)	2470.9(7)
Z	4
D_{calc} (g/cm^3)	1.760
μ (mm^{-1})	0.520
$F(000)$	1336
θ range for data collection (°)	2.30–25.02
Limiting indices	$21 \le h \le 20$ $13 \le k \le 13$ $14 \le l \le 12$
Reflections collected	10,129
Reflections with $I > 2\sigma(I)$	1908
Refinement method	Full-matrix least-squares on F^2
Data/restraints/parameters	2175/87/218
Goodness-of-fit on $F2$	1.021
Final R indices [$I > 2\sigma(I)$]	$R_1 = 0.0389$ $wR_2 = 0.1054$
R indices (all data)	$R_1 = 0.0448$ $wR_2 = 0.1086$
Largest diff. peak and hole (e Å^{-3})	0.431/−0.269

Table 4
Selected intermolecular distances (Å) and angles (°) for **I**.

I		**I**	
Si(1)–F(1)	1.675(4)	Si(1)–F(3)	1.679(2)
Si(1)–F(2)	1.664(4)	Si(1)–F(4)	1.654(2)
F(1)–Si(1)–F(2)	180.00(1)	F(2)–Si(1)–F(3)	89.77(12)
F(1)–Si(1)–F(3)	90.23(12)	F(2)–Si(1)–F(4)	89.09(14)
F(1)–Si(1)–F(4)	90.91(14)	F(3)–Si(1)–F(4)	91.31(12)
S(1)–O(1)	1.435(2)	S(1)–O(2)	1.430(2)
S(1)–N(2)	1.598(2)	S(1)–C(4)	1.781(2)
S(2)–C(8)	1.725(4)	S(2)–C(7)	1.726(3)
N(1)–C(1)	1.469(3)	N(2)–C(7)	1.333(3)
N(3)–C(7)	1.341(3)	N(3)–C(9)	1.375(4)
C(8)–C(9)	1.313(5)		
O(2)–S(1)–O(1)	119.18(14)	C(2)–C(1)–N(1)	120.28(19)
O(2)–S(1)–N(2)	111.82(12)	C(6)–C(1)–N(1)	118.1(2)
O(1)–S(1)–N(2)	106.16(12)	C(5)–C(4)–S(1)	118.69(16)
O(2)–S(1)–C(4)	107.10(11)	C(3)–C(4)–S(1)	120.57(18)
O(1)–S(1)–C(4)	105.30(11)	N(2)–C(7)–N(3)	119.7(2)
N(2)–S(1)–C(4)	106.46(10)	N(2)–C(7)–S(2)	130.7(2)
C(8)–S(2)–C(7)	90.54(17)	N(3)–C(7)–S(2)	109.53(19)
C(7)–N(2)–S(1)	121.53(18)	C(9)–C(8)–S(2)	112.1(2)
C(7)–N(3)–C(9)	115.1(3)	C(8)–C(9)–N(3)	112.8(3)
C(2)–C(1)–C(6)	121.6(2)		

Note: The data are given only for the major position of $[SiF_6]^{2-}$ anion.

Table 5
Geometry of hydrogen bonds for **I**.

D–H···A	d(D–H)/Å	d(H···A)/Å	d(D···A)/Å	∠(DHA)/°	Symmetry transformation for acceptor
N(1)–H(1C)···F(3)	0.85(3)	2.04(2)	2.884(3)	170(2)	$x, 1-y, 1/2+z$
N(1)–H(1A)···F(1)	0.88(2)	2.09(2)	2.936(2)	159(2)	x, y, z
N(1)–H(1A)···F(3)	0.88(2)	2.29(3)	2.869(3)	123(2)	$x, y, 1/2-z$
N(1)–H(1B)···N(2)	0.89(2)	2.07(2)	2.925(3)	159(3)	$x, -y, 1-z$
N(3)–H(3A)···F(4)	0.90(4)	2.06(4)	2.931(4)	163(3)	$x, y-1, z$
N(3)–H(3A)···F(2)	0.90(3)	2.47(4)	3.177(3)	135(3)	$x, y-1, z$

Note: The data are given only for the major position of $[SiF_6]^{2-}$ anion.

Author's personal copy

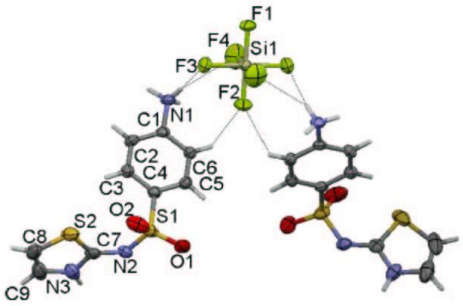

Fig. 1. ORTEP drawing for **I** showing hydrogen bonding. Only the asymmetric unit is numbered and only one position for the disordered $[SiF_6]^{2}$ anion is shown. Thermal ellipsoids are drawn for 50% probabilities.

suspension in Nujol mulls between KRS-5 windows). The mass spectra were registered on a spectrometer MX-1321 (direct input of a sample in a source, energy of ionizing electrons 70 eV). The isothermal conditions of experiments for detection of the solubility of hexafluorosilicates ($t = 25 \pm 0.2$ °C) were provided with the help of an ultra thermostat U15.

3.1. Synthesis of 4-amino-N-(1,3-thiazol-2-ium)benzenesulfonamide hexafluorosilicate (I)

4-Amino-*N*-(1,3-thiazol-2-yl)benzenesulfonamide (0.255 g, 1 mmol) was dissolved in methanol (15 mL) and hexafluorosilicic acid (45%, 2 mL) was then added to the solution. The reaction mixture was stored under ambient conditions prior to the beginning of crystallization of the reaction product, which was obtained with a quantitative yield. The reaction product was a colorless transparent crystals of the composition (**stz**H)$_2$[SiF$_6$] (**I**) with m.p. 232–234 °C (with decomposition). Anal. found, %: Si 4.11, N 12.93, F 19.18. Calcd. for $C_{18}H_{20}F_6N_6O_4S_4Si$, Si 4.29, N 12.84, F 17.41. Mass spectrum: [M**stz**]$^+$ ($m/z = 255$, $I = 14\%$), [M**stz**–SO$_2$]$^+$ ($m/z = 191$, $I = 66\%$), [C$_6$H$_5$NH]$^+$ ($m/z = 90$, $I = 100\%$).

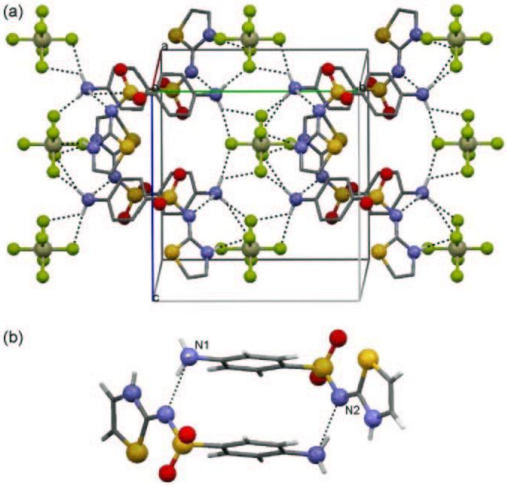

Fig. 2. Fragment of crystal packing in **I**, view along *a*-axis. C-bound H atoms are omitted for clarity (a); self-association pattern of [**stz**H]$^+$ cations in **I** (b).

3.2. Synthesis of the product of interaction of hexafluorosilicic acid with the 4-amino-N-(3-methoxypyrazin-2-yl)benzenesulfonamide, bis(4-ammoniumbenzenesulfonamide) hexafluorosilicate (II)

4-Amino-N-(3-methoxypyrazin-2-yl)benzenesulfonamide (0.280 g, 1 mmol) was dissolved in methanol (7 mL) and hexafluorosilicic acid (45%, 2 mL) was then added to the solution. The reaction mixture was stored under ambient conditions prior to the beginning of crystallization of the reaction product which was obtained with a quantitative yield. The reaction product was a colorless transparent crystals of the composition $(C_6H_9N_2O_2S)_2[SiF_6]$ (**II**) with m.p. 230–232 °C (with decomposition). Anal. found, %: Si 5.49, N 11.61, F 24.01. Calcd. for $C_{12}H_{18}F_6N_4O_4S_2Si$, Si 5.75, N 11.47, F 23.33.

3.3. Structure determination

The X-ray intensity data were collected at room temperature on a Nonius Kappa CCD diffractometer equipped with graphite monochromated Mo Kα radiation using ϕ–ω rotation. Unit cell parameters were obtained and refined using the whole data set. The structure solution and refinement were processed using SHELX-97 program package [24]. Direct methods yielded all non-hydrogen atoms of the asymmetric unit that were treated anisotropically. The $[SiF_6]^{2-}$ anion was disordered over two positions with the occupancies of 0.829(6) and 0.171(6), respectively, and only the major position was refined in anisotropic approximation. The C-bound hydrogen atoms were placed in calculated positions with their isotropic displacement parameters riding on those of the parent atoms, while the N-bound H-atoms were found from differential Fourier maps at an intermediate stage of the refinement and were treated isotropically. Crystallographic data (cif file) for **I** have been deposited with the Cambridge Crystallographic Data Center, CCDC No. 713403. Copies of this information may be obtained free of charge from The Director, CCDC, 12 Union Road, Cambridge, CB2 1EZ, UK (fax: +44 1233 336 033; e-mail: deposit@ccdc.cam.ac.uk or www: http://www.ccdc.cam.ac.uk).

Acknowledgements

The diffraction data were collected at the Schulich Faculty of Chemistry, Technion, The Haifa (Israel) through the cooperation of Professor Menahem Kaftory whom we would like to acknowledge.

This work was supported by the Russian Foundation for Basic Research and the Academy of Sciences of the Republic of Moldova (project number 08.820.05.037RF).

References

[1] V.O. Gelmboldt, Russ. J. Inorg. Chem. 54 (2009) 916–921.
[2] V.O. Gelmboldt, L.V. Koroeva, Ed.V. Ganin, M.S. Fonari, M.M. Botoshansky, A.A. Ennan, J. Fluorine Chem. 129 (2008) 632–636.
[3] V.O. Gelmboldt, Ed.V. Ganin, M.S. Fonari, L.V. Koroeva, Yu.Ed. Ivanov, M.M. Botoshansky, J. Fluorine Chem. 130 (2009) 428–433.
[4] (a) N. Blagden, M. de Matas, P.T. Gavan, P. York, Adv. Drug Del. Rev. 59 (2007) 617–630;
(b) K.R. Morris, U.J. Griesser, C.J. Eckhardt, J.G. Stowell, Adv. Drug Del. Rev. 48 (2001) 91–114;
(c) S. Byrn, R. Pfeiffer, M. Ganey, C. Hoiberg, G. Poochikian, Pharm. Res. 12 (1995) 945–954;
(d) P. Vishweshwar, J.A. McMahon, M.L. Peterson, M.B. Hickey, T.R. Shattock, M.J. Zaworotko, Chem. Commun. (2005) 4601–4603;
(e) N. Shan, M.J. Zaworotko, Drug Discov. Today 13 (2008) 440–446;
(f) P. Vishweshwar, J.A. McMahon, J.A. Bis, M.J. Zaworotko, J. Pharmaceut. Sci. 95 (2006) 499–516.
[5] (a) M.S. Fonari, Ed.V. Ganin, Yu.A. Simonov, W.-J. Wang, Acta Cryst. E62 (2006) o911–o913;
(b) Yu.A. Simonov, M.S. Fonari, G.G. Duca, M.V. Gonta, Ed.V. Ganin, A.A. Yavolovskii, M. Gdaniec, J. Lipkowski, Tetrahedron 61 (2005) 6596–6601.

Author's personal copy

[6] B. Moulton, B.S. Luisi, M.S. Fonari, S.S. Basok, Ed.V. Ganin, V.Ch. Kravtsov, New J. Chem. 31 (2007) 561–568.
[7] M.R. Caira, Mol. Pharmaceut. 4 (2007) 310–316.
[8] (a) C.B. Aakeroy, M.E. Fasulo, J. Desper, Mol. Pharmaceut. 4 (2007) 317–322; (b) J.A. McMahon, J.A. Bis, P. Vishweshwar, T.R. Shattock, O.L. McLaughlin, M.J. Zaworotko, Z. Kristallogr. 220 (2005) 340–350.
[9] A.L. Boreen, W.A. Arnold, K. Mcneill, Environ. Sci. Technol. 38 (2004) 3933–3940.
[10] S.P. Mezyk, T.J. Neubauer, W.J. Cooper, J.R. Peller, J. Phys. Chem. A 111 (2007) 9019–9024.
[11] E.N. Padeiskaya, L.M. Polulkhina, Pharmaceut. Chem. J. 11 (1977) 139–143.
[12] V.O. Gelmboldt, A.A. Ennan, Ed.V. Ganin, Yu.A. Simonov, M.S. Fonari, M.M. Botoshansky, J. Fluorine Chem. 125 (2004) 1951–1957.
[13] M.S. Fonari, Yu.A. Simonov, J. Lipkowski, V.O. Gelmboldt, Ed.V. Ganin, A.A. Yavolovski, Crystallogr. Rep. 48 (2003) 630–637.
[14] D.N. Jones (Ed.), Comprehensive Organic Chemistry, Vol. 3. Sulfur Compounds, Pergamon Press, Oxford, 1979.
[15] (a) S.H. Yalkowsky, Y. He, Handbook of Aqueous Solubility Data, CRC, Boca Raton, FL, USA, 2003; (b) R. O'Shea, H.E. Moser, J. Med. Chem. 51 (2008) 2871–2878; (c) G.P. Stahly, Cryst. Growth Des. 9 (2009) 4212–4229.
[16] T. Steiner, Angew. Chem. Int. Ed. 41 (2002) 48–76.
[17] E. Goreshnik, V.O. Gelmboldt, L.V. Koroeva, Ed.V. Ganin, Abstr. Int. Conf. ded. to the 50th anniversary from the Foundation of the Institute of Chemistry of the Academy of Sciences of Moldova, Chisinau, Moldova, 2009, p. 32.
[18] V.O. Gelmboldt, L.Kh. Minacheva, Ed.V. Ganin, V.S. Sergienko, Russ. J. Inorg. Chem. 53 (2008) 875–878.
[19] A. Pevec, A. Demšar, J. Fluorine Chem. 129 (2008) 707–712.
[20] A.L. Bingham, D.S. Hughes, M.B. Hursthouse, R.W. Lancaster, S. Tavener, T.L. Threlfall, Chem. Commun. (2001) 603–604.
[21] N. Blagden, R.J. Davey, H.F. Lieberman, L. Williams, R. Payne, R. Roberts, R. Rowe, R. Docherty, J. Chem. Soc., Faraday Trans. 94 (1998) 1035–1044.
[22] M.R. Caira, V.J. Griffith, L.R. Nassimbeni, R. Luigi, B.V. Oudtshoorn, J. Incl. Phenom. 17 (1994) 187–201.
[23] A. Banu, G.M.G. Hossain, Acta Crystallogr. E62 (2006) o1573–o1574.
[24] G.M. Sheldrick, Acta Crystallogr. A64 (2008) 112–122.

Додаток Ц.

Копія статті. “ Гексафторосиликаты бис(2-алкилтиокарбамоил-4-пиридиния) ”

ЖУРНАЛ НЕОРГАНИЧЕСКОЙ ХИМИИ, 2010, том 55, № 8, с. 1284–1290

КООРДИНАЦИОННЫЕ СОЕДИНЕНИЯ

УДК 541.49:546.284'161-32:547.826.1

ГЕКСАФТОРОСИЛИКАТЫ *БИС*(2-АЛКИЛ-4-ТИОКАРБАМОИЛ-4-ПИРИДИНИЯ)

© 2010 г. В. О. Гельмбольдт*, Э. В. Ганин**, Л. Х. Миначева***, Л. В. Короева*, В. С. Сергиенко***

*Физико-химический институт защиты окружающей среды и человека Министерства образования и науки Украины и НАН Украины, Одесса
E-mail: eksvar@ukr.net

**Одесский государственный экологический университет, Украина

***Учреждение Российской академии наук Институт общей и неорганической химии им. Н.С. Курнакова РАН, Москва

Поступила в редакцию 27.02.2009 г.

Взаимодействие 45%-ной кремнефтороводородной кислоты (КФК) с 2-этил-4-тиокарбамоил-4-пиридином (L1) и 2-пропил-4-тиокарбамоил-4-пиридином (L2) приводит к получению гексафторосиликатов (L1H)2SiF6 и (L2H)2SiF6, охарактеризованных данными ИК-, масс-спектроскопии, потенциометрии, растворимости. Строение соединения (L1H)2SiF6 установлено методом РСА. В ионной структуре комплекса катионы L1H+ (центр протонирования – пиридиновый атом N) и анионы SiF_6^{2-} (Si–F 1.657(2)–1.699(2) Е) объединены системой межионных Н-связей NH···F. Обсуждена зависимость характеристик межионных Н-связей и растворимости гексафторосиликатов.

Ранее было показано [1, 2], что гексафторосиликаты пиридиния с функционализированными катионами являются удобными модельными соединениями для изучения влияния межионных Н-связей на структурные характеристики и свойства комплексов. В продолжение исследований [1, 2] осуществлен синтез, изучены ИК-, масс-спектральные характеристики, строение и некоторые свойства гексафторосиликатов *бис*(2-алкил-4-тиокарбамоил-4-пиридиния).

ЭКСПЕРИМЕНТАЛЬНАЯ ЧАСТЬ

Синтез. Этил-4-тиокарбамоил-4-пиридин (L^1, 166 мг, 1 ммоль) растворяли в 5 мл метанола, добавляли 0.9 мл 45%-ной **КФК**, полученную смесь подвергали самопроизвольному испарению при комнатной температуре. Продукт реакции выделяется в виде желто-оранжевых кристаллов, $t_{пл}$ 222–224°С (с разложением).

	Si	N
Найдено, %:	6.13;	11.54.
Для $[2\text{-}C_2H_5\text{-}4\text{-}H_2N(S)CC_5H_3NH]_2SiF_6$ (**I**)		
вычислено, %:	5.87;	11.71.

По аналогичной методике получали продукт взаимодействия пропил-4-тиокарбамоил-4-пиридина (L^2, 180 мг, 1 ммоль) и **КФК** (0.9 мл) – желто-оранжевые кристаллы, $t_{пл}$ 182–184°С (с разложением).

	Si	N
Найдено, %:	5.29;	11.38.
Для $[2\text{-}C_3H_7\text{-}4\text{-}H_2N(S)CC_5H_3NH]_2SiF_6$ (**II**)		
вычислено, %:	5.54;	11.06.

Масс-спектры регистрировали на спектрометре МХ-1321 (прямой ввод образца в источник, энергия ионизирующих электронов 70 эВ).

Для **I**: $[ML^1]^+$ (m/z = 166, I = 100%), $[ML^1–H_2CN]^+$ (m/z = 138, I = 15%), $[ML^1–HS]^+$ (m/z = 133, I = 11%), SiF_3^+ (m/z = 85, I = 20%).

Для **II**: $[ML^2]^+$ (m/z = 180, I = 27%), $[ML^2–H_2CN]^+$ (m/z = 152, I = 100%), SiF_3^+ (m/z = 85, I = 23%).

ИК-спектры снимали на спектрофотометре Specord 75IR (стекла KRS-5, образцы в виде суспензии в вазелиновом масле).

pH водных 0.001 М растворов гексафторосиликатов определяли с использованием иономера ЭВ-74. Изотермические условия экспериментов по определению растворимости гексафторосиликатов (t = 25 ± 0.2°С) обеспечивали с помощью ультратермостата U15.

РСА. Кристаллы **I**, $C_{16}H_{22}F_6N_4S_2Si$ (M = 476.59), моноклинные, a = 13.9736(9), b = 14.3798(10), c = 11.3334(8) Å, β = 113.703(1)°, V = 2085.2(2) Å^3,

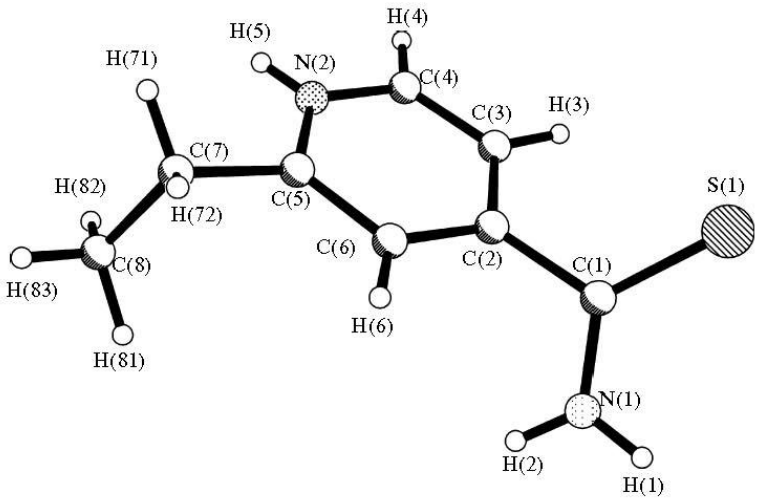

Строение комплексного катиона L^1H^+ в структуре I.

$\rho_{выч}$ = 1.518 г/см^3, μ(MoK_α) = 0.376 мм$^{-1}$, F(000) = = 984, Z = 4, пр. гр. $C2/c$.

Экспериментальный материал (11456 отражений, из них 3130 независимых, R(int) 0.0238) получен при 298 K с кристалла размером 0.40 × 0.35 × 0.26 мм на автоматическом дифрактометре Bruker SMART APEX II (MoK_α, λ 0.71073 Å, графитовый монохроматор, ψ-сканирование). Отражения собраны в интервале индексов $-19 \le h \le 19$, $-20 \le k \le 19$, $-16 \le l \le 16$ ($2.13° \le \theta \le 30.61°$, заполнение по θ = 97.3%). Поглощение введено по измерениям интенсивностей эквивалентных отражений (SADABS) [3]. Полный набор экспериментальных данных депонирован в Кембриджском банке структурных данных (регистрационный № для соединения I – CCDC 723032).

Структура решена прямым методом (SHELXS-93 [4]) и уточнена методом наименьших квадратов по F^2 (SHELXL-97 [5]) в полноматричном анизотропном приближении для всех неводородных упорядоченных атомов. В структуре три кристаллографически независимых атома фтора статистически разупорядочены по 27 позициям, две из которых на оси 2, остальные – в общем положении. Факторы заселенности (ФЗ) всех атомов фтора уточнены при фиксированных значениях U_f. Затем все неупорядоченные атомы F уточняли изотропно с фиксированными ФЗ. Положения большинства атомов водорода в катионе найдены экспериментально и уточнены изотропно. Атомы водорода концевой метильной группы уточнены по методу "наездника" с изотропными температурными факторами U_H, в 1.2 раза бóльшими фактора U_C атома углерода C(8), с которым связаны данные атомы H.

Окончательные результаты уточнения: $R1$ = = 0.0650, $wR2$ = 0.1577, $GOOF$ = 1.075 по 2467 отражениям с $I > 2\sigma(I)$; $R1$ = 0.0823, $wR2$ = 0.1723 по всем рефлексам; 242 уточняемых параметра. Коэффициент экстинкции 0.0109(13), значения $\Delta\rho_{max}$ и $\Delta\rho_{min}$ составляют соответственно 0.464 и –0.471 e Å^{-3}.

Координаты, температурные факторы всех атомов структуры I и параметры ФЗ приведены в табл. 1, межатомные расстояния и валентные углы в катионе – в табл. 2.

РЕЗУЛЬТАТЫ И ИХ ОБСУЖДЕНИЕ

Структурные единицы кристалла I – гексафторосиликатные анионы SiF_6^{2-}, расположенные на оси 2, и катионы 2-этил-4-тиокарбомоилпиридиния (L^1H^+) (рисунок).

Разупорядоченность атомов фтора, не позволившая выделить отдельные фиксированные положения октаэдров SiF_6^{2-}, делает невозможным обсуждение деталей строения кристалла I. Можно лишь отметить, что интервал длин связей Si–F (1.641(8)–1.744(5) Å) и ее средняя длина (1.683 Å) обычны [6].

Катион HL^+ протонирован по пиридиновому атому азота. Его геометрические параметры отвечают стандартным значениям и близки к найденным в структуре гидрохлорида [7] и гидробромида 2-этил-4-тиокарбомоилпиридиния [8].

В структуре I анионы SiF_6^{2-} и катионы L^1H^+ объединены системой межионных водородных

Таблица 1. Координаты атомов ($\times 10^4$, для атомов H $\times 10^3$), их тепловые параметры $U_{экв}/U_{изо}$ (Å^2, $\times 10^3$) и ФЗ(F) для статистически неупорядоченных атомов фтора в структуре I*

Атом	x	y	z	$U_{экв}/U_{изо}$	ФЗ(F)
S(1)	1509(1)	6279(1)	9995(1)	65(1)	
N(1)	3025(2)	5792(2)	9297(3)	55(1)	
N(2)	785(2)	7583(2)	5449(3)	55(1)	
C(1)	2143(2)	6238(2)	9039(2)	46(1)	
C(2)	1681(2)	6717(2)	7760(2)	42(1)	
C(3)	1314(2)	7628(2)	7681(3)	51(1)	
C(4)	884(2)	8049(2)	6506(3)	58(1)	
C(5)	1090(2)	6701(2)	5462(3)	50(1)	
C(6)	1574(2)	6265(2)	6638(2)	46(1)	
C(7)	897(3)	6258(3)	4192(3)	67(1)	
C(8)	1760(3)	6445(3)	3758(4)	77(1)	
Si(1)	0	9278(1)	2500	36(1)	
F(1)	462(6)	8296(5)	1989(7)	56(1)	0.284(5)
F(2)	1074(7)	9067(7)	3889(8)	54(2)	0.215(6)
F(3)	153(12)	9306(13)	4055(8)	47(2)	0.141(6)
F(4)	149(12)	9773(11)	3927(10)	71(3)	0.163(6)
F(5)	–504(9)	10324(5)	1871(10)	55(2)	0.176(5)
F(6)	1265(7)	9589(13)	2994(15)	53(3)	0.138(5)
F(7)	1237(7)	9021(11)	2782(14)	54(3)	0.142(5)
F(8)	635(12)	9947(10)	1853(17)	52(3)	0.135(5)
F(9)	598(13)	8245(8)	2891(19)	59(4)	0.116(5)
F(10)	–504(13)	10284(8)	2630(20)	59(3)	0.125(5)
F(11)	–177(11)	8906(9)	3777(11)	45(2)	0.142(5)
F(12)	–360(20)	9639(16)	3690(20)	70(5)	0.112(5)
F(13)	1125(11)	8680(14)	3170(20)	33(3)	0.069(6)
F(14)	720(15)	9328(12)	4091(9)	53(3)	0.115(6)
F(15)	1027(11)	10003(12)	3095(19)	52(4)	0.105(5)
F(16)	1063(12)	9885(14)	2520(30)	40(3)	0.092(5)
F(17)	947(15)	8597(13)	2420(20)	39(4)	0.073(5)
F(18)	1112(11)	9524(15)	3719(16)	49(4)	0.089(5)
F(19)	0	8109(7)	2500	46(6)	0.039(4)
F(20)	580(12)	8629(11)	1734(17)	34(3)	0.096(5)
F(21)	0	10447(7)	2500	42(4)	0.047(4)
F(22)	49(19)	10286(9)	1810(20)	36(4)	0.067(5)
F(23)	361(16)	8936(14)	4030(10)	26(3)	0.064(6)
F(24)	822(18)	8478(16)	3480(20)	47(5)	0.066(5)
F(25)	–170(20)	8202(8)	1880(20)	55(4)	0.083(6)
F(26)	1002(16)	9637(19)	2120(30)	38(5)	0.060(5)
F(27)	1279(9)	9117(17)	3480(20)	22(4)	0.053(7)
H(1)	330(3)	545(3)	1002(4)	76(11)	
H(2)	337(3)	579(2)	879(3)	65(10)	
H(5)	51(3)	787(3)	472(4)	84(12)	

* Приведены координаты атомов водорода, участвующих в ВС.

связей (**ВС**, табл. 3) типа N–H···F. Акцепторами ВС выступают практически все атомы фтора (за исключением F(10), F(13) и F(21)), донорами – атомы водорода аминогруппы и протонированного атома азота пиридина катиона.

В табл. 4 приведены характеристики ИК-спектров гексафторосиликатов *бис*(2-алкил-4-тиокарбамоил-4-пиридиния). В ИК-спектре **I** наблюдается высокочастотный сдвиг на 20 см$^{-1}$ двух из трех полос колебаний $\nu_{кольца}$ по сравнению с их положением в спектре L^1. Высокочастотный сдвиг претерпевает также полоса пульсационных колебаний кольца $\nu_{пульс}$, что указывает на протонирование тиоамидного лиганда по атому гетероцикла N [9] и согласуется с данными РСА. Появление более высокочастотной компоненты полосы $\nu(NH_2)$ в спектре **I** (~3300 см$^{-1}$) может являться следствием частичного разрыва ВС с участием NH_2-групп при протонировании. Полосы $\delta(NH_2)$ практически не меняют своего положения.

Незначительные изменения положения полос и перераспределение их интенсивностей в ИК-спектре **I** относительно соответствующих полос в спектре лиганда L^1 в области 1100–1050 см$^{-1}$, где проявляются сложные валентно-деформационные колебания связей C–N, C–S и деформационные маятниковые колебания NH_2-групп, связаны, по-видимому, с присутствием деформационных плоскостных колебаний группы $\geqslant N^+H$. Идентификация колебаний ν(CS) в области 800–600 см$^{-1}$ в спектре **I** проблематична в связи с наложением собственных колебаний лиганда ν(CS), δ(CCH), $\rho(NH_2)$ и колебаний ν(SiF) аниона SiF_6^{2-}.

В свободной от собственных колебаний лиганда области (490–435 см$^{-1}$) в спектре **I** четко фиксируются колебания $\delta(SiF_2)$ аниона в виде интенсивной полосы при 470 см$^{-1}$ и "плеча" около 440 см$^{-1}$.

Спектральные характеристики **I** и **II** весьма близки, что может указывать на аналогию в строении комплексов.

В табл. 5 представлены данные о растворимости соединений **I** и **II**, а также ряда других гексафторосиликатов пиридиния с функционализированными катионами, в воде и значения pH 0.001 М растворов солей. Ранее было отмечено [1, 2], что характер изменения растворимости гексафторосиликатов пиридиния нельзя объяснить в рамках представлений о гидрофильно-липофильном балансе структурных фрагментов соединений [13]. В то же время наблюдается взаимосвязь между растворимостью гексафторосиликатов и интенсивностью межионных ВС в структуре соли, для сравнительной оценки влияния которых предложено [2] использовать параметр h:

$$h = n/d(D\cdots A)_{ср},$$

Таблица 2. Основные длины связей (d) и валентные углы (ω) в катионе в L^1H^+

Связь	d, Å
S(1)–C(1)	1.654(3)
N(1)–C(1)	1.314(3)
N(2)–C(4)	1.331(4)
N(2)–C(5)	1.336(4)
C(1)–C(2)	1.497(3)
C(2)–C(6)	1.382(4)
C(2)–C(3)	1.397(3)
C(3)–C(4)	1.362(4)
C(5)–C(6)	1.380(4)
C(5)–C(7)	1.496(4)
C(7)–C(8)	1.498(5)
Si(1)–F(10)	1.641(8)
Si(1)–F(18)	1.650(9)
Si(1)–F(11)	1.652(7)
Si(1)–F(22)	1.663(9)
Si(1)–F(8)	1.666(8)
Si(1)–F(7)	1.668(8)
Si(1)–F(23)	1.673(9)
Si(1)–F(9)	1.674(9)
Si(1)–F(25)	1.676(9)
Si(1)–F(17)	1.676(9)
Si(1)–F(14)	1.676(8)
Si(1)–F(19)	1.680(10)
Si(1)–F(15)	1.681(9)
Si(1)–F(21)	1.682(9)
Si(1)–F(13)	1.682(9)
Si(1)–F(6)	1.686(8)
Si(1)–F(20)	1.687(8)
Si(1)–F(24)	1.687(10)
Si(1)–F(3)	1.688(8)
Si(1)–F(5)	1.692(7)
Si(1)–F(27)	1.699(9)
Si(1)–F(12)	1.702(9)
Si(1)–F(4)	1.702(8)
Si(1)–F(26)	1.702(10)
Si(1)–F(2)	1.710(6)
Si(1)–F(16)	1.714(9)
Si(1)–F(1)	1.744(5)
Угол	**ω, град**
C(1)N(1)H(1)	119(2)
C(1)N(1)H(2)	124(2)
H(1)N(1)H(2)	116(3)
C(4)N(2)C(5)	123.4(3)
C(4)N(2)H(5)	118(3)
C(5)N(2)H(5)	118(3)
N(1)C(1)C(2)	116.2(2)
N(1)C(1)S(1)	125.0(2)
C(2)C(1)S(1)	118.87(18)
C(6)C(2)C(3)	118.8(2)
C(6)C(2)C(1)	121.3(2)
C(3)C(2)C(1)	119.9(2)
C(4)C(3)C(2)	119.0(3)
N(2)C(4)C(3)	120.1(3)
N(2)C(5)C(6)	118.2(3)
N(2)C(5)C(7)	117.4(3)
C(6)C(5)C(7)	124.4(3)
C(5)C(6)C(2)	120.3(2)
C(5)C(7)C(8)	112.5(3)

Таблица 3. Геометрические параметры коротких межионных контактов в структуре I

Контакт D–H···A	Расстояние, Å			Угол DHA, град	Координаты атома A
	D–H	A···H	D···A		
N(1)–H(1)···F(18)	0.90(4)	1.88(4)	2.767(16)	167(3)	$-x+1/2, y-1/2, -z+3/2$
N(1)–H(1)···F(22)	0.90(4)	2.48(5)	3.19(2)	135(3)	$x+1/2, y-1/2, z+1$
N(1)–H(1)···F(14)	0.90(4)	2.09(4)	2.875(15)	145(3)	$-x+1/2, y-1/2, -z+3/2$
N(1)–H(1)···F(5)	0.90(4)	2.10(4)	2.893(10)	146(3)	$x+1/2, y-1/2, z+1$
N(1)–H(1)···F(15)	0.90(4)	2.06(5)	2.938(18)	164(3)	$-x+1/2, y-1/2, -z+3/2$
N(1)–H(1)···F(2)	0.90(4)	2.31(4)	3.144(10)	153(3)	$-x+1/2, y-1/2, -z+3/2$
N(1)–H(1)···F(6)	0.90(4)	2.42(50	3.309(16)	169(3)	$-x+1/2, y-1/2, -z+3/2$
N(1)–H(1)···F(4)	0.90(4)	2.23(4)	2.930(14)	134(3)	$-x+1/2, y-1/2, -z+3/2$
N(1)–H(1)···F(27)	0.90(4)	2.47(5)	3.33(2)	162(3)	$-x+1/2, y-1/2, -z+3/2$
N(1)–H(2)···F(26)	0.88(4)	1.72(4)	2.56(2)	160(3)	$-x+1/2, -y+3/2, -z+1$
N(1)–H(2)···F(20)	0.88(4)	1.98(4)	2.773(14)	148(3)	$-x+1/2, -y+3/2, -z+1$
N(1)–H(2)···F(16)	0.88(4)	2.18(4)	2.99(2)	153(3)	$-x+1/2, -y+3/2, -z+1$
N(1)–H(2)···F(11)	0.88(4)	2.09(4)	2.835(11)	142(3)	$x+1/2, -y+3/2, z+1/2$
N(1)–H(2)···F(8)	0.88(4)	2.10(4)	2.881(15)	147(3)	$-x+1/2, -y+3/2, -z+1$
N(1)–H(2)···F(7)	0.88(4)	2.09(4)	2.940(14)	162(3)	$-x+1/2, -y+3/2, -z+1$
N(1)–H(2)···F(12)	0.88(4)	1.93(4)	2.682(18)	143(3)	$x+1/2, -y+3/2, z+1/2$
N(1)–H(2)···F(17)	0.88(4)	2.16(4)	2.98(2)	155(3)	$-x+1/2, -y+3/2, -z+1$
N(1)–H(2)···F(6)	0.88(4)	2.34(4)	3.179(16)	158(3)	$-x+1/2, -y+3/2, -z+1$
N(2)–H(5)···F(25)	0.86(4)	1.75(5)	2.582(18)	164(4)	$-x, y, -z+1/2$
N(2)–H(5)···F(1)	0.86(4)	1.97(4)	2.802(8)	163(4)	$-x, y, -z+1/2$
N(2)–H(5)···F(20)	0.86(4)	2.06(4)	2.869(15)	157(4)	$-x, y, -z+1/2$
N(2)–H(5)···F(23)	0.86(4)	1.70(4)	2.441(14)	143(4)	x, y, z
N(2)–H(5)···F(24)	0.86(4)	1.85(5)	2.60(2)	144(4)	x, y, z
N(2)–H(5)···F(11)	0.86(4)	1.87(4)	2.640(10)	149(4)	x, y, z
N(2)–H(5)···F(3)	0.86(4)	2.19(4)	2.879(17)	137(3)	x, y, z
N(2)–H(5)···F(9)	0.86(4)	2.19(5)	2.96(2)	149(4)	x, y, z
N(2)–H(5)···F(14)	0.86(4)	2.28(4)	2.927(17)	132(3)	x, y, z
N(2)–H(5)···F(2)	0.86(4)	2.25(4)	2.902(10)	132(3)	x, y, z
N(2)–H(5)···F(19)	0.86(4)	2.35(4)	3.162(3)	158(4)	x, y, z

где n – число коротких межионных ВС (сильные и средние ВС, D···A ≤ 3.2 Å [14]), $d(\mathrm{D{\cdots}A})_{ср}$ – среднее расстояние донор–акцептор. Как следует из данных табл. 5, рост значений h (для I величина $d(\mathrm{D{\cdots}A})_{ср}$ рассчитывалась усреднением всех контактов разупорядоченных атомов фтора), отражающий относительную стабилизацию соответствующих комплексов, сопровождается закономерным уменьшением

Таблица 4. Волновые числа (см$^{-1}$) максимумов полос поглощения в ИК-спектрах гексафторосиликатов *бис*(2-алкил-4-тиокарбамоил-4-пиридиния)

L^1	$(L^1H)_2SiF_6$ I	$(L^2H)_2SiF_6$ II	Отнесение
	3300 ср.	3380 ср.	
		3305 ср.	$\nu(NH_2)$
3240 ср.		3220 ср.	
3170 ср.	3180 ср.ш.	3130 ср.	$\nu(N^+H)$
3075 пл.	3080 пл.	3080 пл.	
1645 пл.	1640 ср.	1640 ср.	$\delta(NH_2)$
1600 с.	1620 с.	1620 с.	$\nu_{кольца}$, $\delta(HNC)$
1565 с.	1585 ср.	1570 пл.	
1500 с.	1500 с.	1505 с.	
	1340 пл.	1330 пл.	
1320 ср.	1310 ср.	1310 ср.	$\delta(CCH)$, $\nu(CN)$, $r(NH_2)$
	1285 ср	1270 ср.	
1210 ср.	1230 ср.	1235 ср	
	1165 пл.		$\omega(NH_2)$, $\delta(CCH)$, $\delta(HCN)$
1145 с.	1140 сл.	1150 ср.	
1070 ср.	1075 ср.	1070 ср.	$\nu(CN) + \nu(CS) + r(NH_2)$, $\delta_{пл}(\geqslant^+NH)$
1040 пл.	1050 ср.	1045 пл.	
1005 ср.	1025 ср.	1025 ср.	$\nu_{пульс.}$
940 ср.	940 ср.	940 ср.	
860 ср.	840 ср.	840 пл.	$\delta(CCN)$, $\delta(CCH)$, $\delta_{непл}(\geqslant^+NH)$
	820 ср.	825 ср.	
805 пл.			
	745 с.	740 с.	
720 ср.	720 о.с.	720 о.с.	$\nu(CS)$, $\nu(SiF)$, $\rho(NH_2)$, $\delta(CCH)$
	690 пл.	690 пл.	
670 пл.	670 ср.	670 пл.	
615 пл.	610 пл.	615 пл.	
530 ср.	535 пл.	540 ср.	$\delta(SCN)$, $\delta(NCC)$
		490 пл.	
	470 ср.	475 ср.	
	440 пл.		$\delta(SiF_2)$
		425 пл.	

растворимости солей. При этом значения pH растворов I и II, указывающие на гидролитическую неустойчивость солей, близки к соответствующим величинам для других гексафторосиликатов пиридиния. При этом, как указывалось в [2], не наблюдается корреляции между величинами pH растворов солей и pK_a соответствующих пиридиновых лигандов.

Таким образом, продуктами взаимодействия КФК с 2-этил-4-тиокарбамоил-4-пиридином и 2-пропил-4-тиокарбамоил-4-пиридином являются

Таблица 5. Растворимость гексафторосиликатов пиридиния в воде и значения pH водных растворов солей

Соединение	Растворимость, мол. %, 25°C	h, Å^{-1}	pH 0.001 M растворов	Литература
$[2\text{-}CH_3C_5H_4NH]_2SiF_6$*	11.60**	0.71	3.27	[10]
$[2\text{-}HO(O)CC_5H_4NH]_2SiF_6$*	5.33**	0.76	–	[11]
$[3\text{-}HO(O)CC_5H_4NH]_2SiF_6$*	3.33**	1.09	–	[12]
$[4\text{-}HO(O)CC_5H_4NH]_2SiF_6$*	0.80**	1.08	–	[1]
$[2,5\text{-}(HOOC)_2C_5H_3NH]_2SiF_6$	0.07**	–	–	
$[2,6\text{-}(HOOC)_2C_5H_3NH]_2SiF_6$	0.02**	–	–	
$[2\text{-}H_2NC_5H_4NH]_2SiF_6$*	5.60**	1.38	3.30	[2]
$[3\text{-}H_2NC_5H_4NH]_2SiF_6$	1.86**	–	3.35	
$[4\text{-}H_2NC_5H_4NH]_2SiF_6H_2O$	3.88**	–	3.09	
$[2,6\text{-}(H_2N)_2C_5H_3NH]_2SiF_6$*	0.06**	2.35	3.33	[2]
$[2\text{-}C_2H_5\text{-}4\text{-}H_2N(S)CC_5H_3NH]_2SiF_6$	0.10	1.04	3.31	
$[2\text{-}C_3H_7\text{-}4\text{-}H_2N(S)CC_5H_3NH]_2SiF_6$	0.18		3.30	

* Структурно охарактеризованные соединения.

** Данные [1, 2].

гексафторосиликаты соответствующих замещенных пиридиниевых катионов. Данные РСА и ИК-спектральные характеристики солей указывают на протонирование пиридиновых лигандов по эндоциклическому атому N. В водных растворах гексафторосиликаты подвергаются гидролизу; растворимость солей коррелирует с характеристиками межионных ВС.

Авторы благодарны А.Б. Илюхину за помощь в расшифровке структуры I.

СПИСОК ЛИТЕРАТУРЫ

1. *Gelmboldt V.O., Koroeva L.V., Ganin Ed.V. et al.* // J. Fluor. Chem. 2008. V. 129. № 7. P. 632.
2. *Gelmboldt V.O., Ganin Ed.V., Fonar' M.S. et al.* // J. Fluor. Chem. 2009. V. 130. № 4. P. 428.
3. *Sheldrick G.M.* SADABS. Program for Scaling and Correction of Area Detector Data. University Göttingen, Germany. 1997.
4. *Sheldrick G.M.* SHELXS-97. Program for the Solution of Crystal Structures. Göttingen: Univ. Göttingen, 1997.
5. *Sheldrick G.M.* // SHELXL-97. Program for the Refinement of Crystal Structures. University Göttingen, Germany. 1997.
6. *Tandura S.N., Voronkov M.G., Alekseev N.V.* // Top. Curr. Chem. 1986. V. 131. P. 99.
7. *Colleter J.C., Gadret M.* // Acta Crystallogr. 1968. V. 24B. № 4. P. 513.
8. *Colleter J.C., Gadret M.* // Acta Crystallogr. 1968. V. 24B. № 4. P. 519.
9. Физические методы в химии гетероциклических соединений / Под ред. Катрицкого А.Р. М.-Л.: Химия, 1966. 658 с.
10. *Pevec A., Demšar A.* // J. Fluor. Chem. 2008. V. 129. № 8. P. 707.
11. *Gelmboldt V.O., Ganin E.V., Domasevitch K.V.* // Acta Crystallogr. 2007. V. C63. P. 530.
12. *Гельмбольдт В.О., Минячева Л.Х., Ганин Э.В., Сергиенко В.С.* // Журн. неорган. химии. 2008. Т. 53. № 6. С. 947.
13. *Кукушкин В.Ю., Кукушкин Ю.Н.* Теория и практика синтеза координационных соединений. Л.: Наука, 1990. 264 с.
14. *Steiner T.* // Angew. Chem. Int. Ed. 2002. V. 41. № 1. P. 48.

Додаток Ш.

Копія статті. “ Persistent CH... π Interactions in Mefenamic Acid Complexes with Cyclic and Acyclic Amines ”

CRYSTAL GROWTH & DESIGN
Article
XXXX, Vol. XXX
000–000

DOI: 10.1021/cg100518b

Persistent CH···π Interactions in Mefenamic Acid Complexes with Cyclic and Acyclic Amines

Marina S. Fonari,*,† Eduard V. Ganin,‡ Anna V. Vologzhanina,# Mikhail Yu. Antipin,# and Victor Ch. Kravtsov†

†Institute of Applied Physics, Academy of Sciences of Moldova, Academiei Street, 5 MD-2028 Chişinău, R. Moldova, ‡Odessa State Environmental University, Lvovskaya Street, 15, 65016, Odessa, Ukraine, and #A. N. Nesmeyanov Institute of Organoelement Compounds, Russian Academy of Sciences, 28 Vavilov St., B-334, 119991, Moscow, Russia

Received April 19, 2010; Revised Manuscript Received May 28, 2010

ABSTRACT: Interaction of mefenamic acid [2-(2,3-dimethylphenyl)aminobenzoic acid, maH] with piperazine (ppz), 1,4,7,10-tetraazacyclododecane (cyclen), *meso*-5,7,7,12,12,14-hexamethyl-1,4,8,11-tetraazacyclotetradecane (teta), and tris(hydroxymethyl)aminomethane (tris) resulted in crystalline proton-transfer complexes of the compositions $(ppzH_2)(ma)_2 \cdot 4H_2O$ **1**, $(cyclenH_2)(ma)_2 \cdot 2H_2O$ **2**, $(tetaH_2)(ma)_2 \cdot 2H_2O$ **3**, and $(trisH)(ma) \cdot H_2O$ **4**. Immediate cation−anion hydrogen bonds and those mediated by water molecules are the prime driving forces for the maH and amine assembly. Persistent CH···π interactions involving the aromatic rings were found to play an important role in the formation of final structures. All complexes reveal the pronounced segregation of hydrophilic and hydrophobic regions.

The active pharmaceutical ingredients (APIs) are most conveniently developed and delivered as solid dosage forms that contain a single crystalline form of an API due to the inherent stability of crystalline materials and the well-established impact of the crystallization processes on the purification and isolation of a chemical substance. However, there are often limitations in terms of solubility, stability, and bioavailability for the crystal form of a single organic molecule; thus the crystal form can be crucial to the performance of a dosage form.[1] Obviously, the variations in physicochemical properties can be achieved through structural variation, and pharmaceuticals may be manipulated, for example, by using different polymorphic forms, but the discovery of new polymorphs is often serendipitous and can be difficult to control.[2] Another possible way for modifying the physicochemical properties with the goal to improve pharmaceutical profile of drug is the creation of a multicomponent molecular complex (e.g., cocrystal or salt) without altering covalent bonding and therefore keeping the pharmacological behavior of the drug. Crystal engineering[3] has emerged into the pharmaceutical field with importance of its strategy in the design of multicomponent pharmaceutical solids.[4] The deliberate design of such organic solids, possessing controlled supramolecular structures, is generally based on conventional "strong" hydrogen bonds and robust, reproducible hydrogen bond motifs (synthons)[5] that occur with a high frequency in known crystal structures. Whereas stronger hydrogen bonds are ideal tools in this context, weaker interactions such as C−H···π, for example, are more problematic, although interactions involving aromatic systems are key processes in both chemical and biological recognition.[6] Moreover, in the structures rich with aromatic hydrocarbons the C−H···π interactions may dominate in molecular association, and packing thus playing an increasingly important role as a persistent structural motif in structure formation.[7] Therefore, it is believed that the C−H···π interactions are important in controlling the final structures of molecular assemblies, and it is a great challenge to make a full screen of various interactions changing from conventional strong hydrogen bonds to weak C−H···π interactions in the structure of relative molecular complexes.

Mefenamic acid [(2-(2,3-dimethylphenyl)aminobenzoic acid, maH] is a well-known representative of fenamates[8] showing a potent analgesic effect. Mefenamic acid is a nonsteroidal anti-inflammatory (NSAI), antipyretic, and analgesic agent that is used for the relief of postoperative and traumatic inflammation and analgesic treatment of rheumatoid arthritis, and antipyretic in acute respiratory tract infection.[9] Recently, it has been reported that maH is perspective as a therapeutic agent in Alzheimer's disease since it improves learning and memory impairment in an amyloid β peptide (Aβ1−42)-infused Alzheimer's disease rat model.[10] Low water solubility of maH limits its efficacy and therapeutic benefit as an API in the clinic; therefore, efforts have been done to enhance its solubility and dissolution rate.[11] The polymorphism of maH was studied for its effect on improvement physical properties. Similar to diclofenac, flufenamic, and tolfenamic acids that crystallize in three, two, and five polymorphic forms, respectively,[12] two crystalline polymorphic forms, stable Form I (CSD refcode XYANAC) and metastable Form II, were found for maH.[13] Since prodrugs are known to enhance numerous desirable qualities of pharmaceuticals and temporarily mask the acidic group to suppress gastrointestinal injury, the different esterified mefenamates were studied and approved as possible prodrugs.[14] Salts are usually considered as another alternative for drug delivery.[15] Sodium, manganese(II), cobalt(II), nickel(II), copper(II), and zinc(II) mefenamates were recently explored with the aim to solve the formulation and dissolution problems of maH.[16] On the other hand, the structural information for maH complexes with organic cocrystal partners is restricted by three salts with alkanolamines, *n*-propanol-, diethanol-, and triethanolamine (CSD refcodes NASBEP, NASBIT, NASBOZ, no fractional

*To whom correspondence should be addressed. E-mail: fonari.xray@phys.asm.md; kravtsov.xray@phys.asm.md; fax: +373 22 72 58 87; tel: +373 22 73 81 54.

©XXXX American Chemical Society

coordinates are available),[17] and an inclusion complex with cyclodextrin (CD).[18] As indicated by authors,[17] binary compounds of maH with alkanolamines represent the proton-transfer complexes sustained by the charge-assisted hydrogen bonds. Hydrophobic and hydrophilic regions exist in the crystal of each complex.

The diverse bases are successfully exploited nowadays as suitable cocrystallization partners for fatty, oxy-, and aromatic acids.[19,20] The advantages of polyazamacrocycles as *N*-bases are numerous.[21] In the polyprotonated form they are soluble in water. The high positive charge density and potential hydrogen-bonding sites promote complex formation with biologically relevant anionic substrates. The well-elaborated synthetic methodology provides the ring size readily varied in the synthetic scheme. Moreover, incorporated in the ring or attached as pendant arms organic moieties can vary their charge density and lipophilicity. For example, the pharmaceutically acceptable smallest in size cyclic diamine, piperazine, acts both in neutral and cationic forms giving rise to cocrystal with paracetamol,[22] and salts with salicylic, ascorbic, camphoric, pamoic acids, diclofenac, and phenylbutazone.[23]

Our previous research has been focused on the synthesis of multicomponent crystalline solids involving as APIs sulfa drugs,[24] or pharmaceutical acids, *p*-aminobenzoic acid,[25] salicylic acid,[26] and crown ethers (CEs) or azacycles as cocrystallization partners with an emphasis on the modes of interaction of the components in the solid state. *p*-Aminobenzoic acid yielded the binary molecular complexes of the 2:1 ratio with 18-membered CEs, while the proton-transfer complexes with mixed *N*,O-containing CEs and azacycles were obtained both for *p*-aminobenzoic and salicylic acids. In view of the above, our further attempts were aimed to design a system wherein an addition of a cyclic amine molecule could improve hydrogen bonding with maH, which in turn could impart physicochemical properties. For this purpose, the gradually increased in size aza cycles depicted in Scheme 1 along with one acyclic amine (tris) have been used. Piperazine and tris are pharmaceutically approved with their meaningful occurrence in the Cambridge Structural Database (CSD) as good crystal partners for APIs.[27] Within the past decade, tetraazacycles cyclen (1,4,7,10-tetraazacyclododecane) and cyclam (1,4,8,11-tetraazacyclotetradecane, the parent azacycle for teta) have found many applications in medicine. The advantages of cyclen and cyclam are their low toxicity, low molecular weight, and amphiphilic solubility.[21] All of these properties are beneficial for their investigation as suitable crystal partners. In general, ΔpK_a of an acid and a base is used as a rule of thumb to estimate the proton transfer.[28] The difference of 3.6−6 orders of magnitude between the acid dissociation constants of the base (pK_a 5.68 and 9.82 for ppz, 10.51 and 9.49 for cyclen, 12.60 and 10.40 for teta, and 8.06 for tris),[29] and the acid (pK_a 4.2 for maH[9a]) should lead to proton transfer and serves as an indication of the preferable formation of salts. So, with a high degree of probability we could expect the presence of ionic moieties in each structure under discussion.

Herein we report the synthesis and crystal structures of four novel complexes of maH with cyclic amines, piperazine (ppz), 1,4,7,10-tetraazacyclododecane (cyclen), *meso*-5,7,7,12,12,14-hexamethyl-1,4,8,11-tetraazacyclotetradecane (teta), and acyclic tris(hydroxymethyl)aminomethane (tris) of the compositions $(ppzH_2)(ma)_2 \cdot 4H_2O$ **1**, $(cyclenH_2)(ma)_2 \cdot 2H_2O$ **2**, $(tetaH_2)(ma)_2 \cdot 2H_2O$ **3**, and $(trisH)(ma) \cdot H_2O$ **4**.

Scheme 1. Target Mefenamic Acid and Amine Molecules with the Numbering Scheme

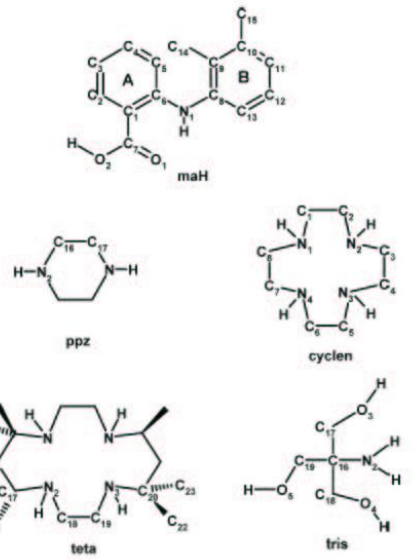

Experimental Section

General. All reagents (Scheme 1) were purchased from commercial sources and used as received. Solvents were obtained from commercial sources and distilled before use. Single crystals were obtained via slow evaporation of stoichiometric amounts of starting materials in an appropriate solvent. Compounds **1**−**4** were characterized by elemental analysis for C, H, and N in a Perkin-Elmer 240C device, X-ray powder diffraction (PXRD), and single crystal X-ray analysis.

$(ppzH_2)(ma)_2 \cdot 4H_2O$ 1. Piperazine hexahydrate (194 mg, 1 mmol) and maH (241 mg, 1 mmol) were dissolved upon boiling in methanol (25 mL). The solution was allowed to evaporate at room temperature when colorless transparent crystals appeared. mp 178−180 °C, found %: C 63.77; H 7.51; N 8.78 %, required for $C_{24}H_{48}N_4O_8$ %: C 63.73; H 7.55; N 8.74.

$(cyclenH_2)(ma)_2 \cdot 2H_2O$ 2. 1,4,7,10-Tetraazacyclododecane (86 mg, 0.5 mmol) and maH (241 mg, 1 mmol) were dissolved upon boiling in a mixture of methanol, ethylacetate, and water (20 mL/50 mL/1 mL). The solution was allowed to evaporate at room temperature when colorless transparent needles appeared. mp 148−150 °C, found %: C 66.11%; H 7.84; N 12.19, required for $C_{38}H_{54}N_6O_6$ %: C 66.06; H 7.88; N 12.16.

$(tetaH_2)(ma)_2 \cdot 2H_2O$ 3. *meso*-5,7,7,12,12,14-Hexamethyl-1,4,8,11-tetraazacyclotetra-decane (142 mg, 0.5 mmol) and maH (241 mg, 1 mmol) were dissolved upon boiling in a mixture of methanol and ethylacetate (10 mL/30 mL). The solution was allowed to evaporate at room temperature when colorless transparent crystals appeared. mp 215−218 °C, found %: C 68.85; H 8.77; N 10.49, required for $C_{46}H_{70}N_6O_5$ %: C68.80; H 8.79; N 10.46.

$(trisH)(ma) \cdot H_2O$ 4. 2-Amino-2-(hydroxymethyl)propane-1,3-diol (121 mg, 1 mmol) and maH (241 mg, 1 mmol) were dissolved in boiling water (15 mL). The solution was allowed to evaporate at room temperature when colorless transparent thin plates appeared. mp > 190 °C (melt. + dec.), found %: C 59.98; H 7.42; N 7.36, required for $C_{19}H_{28}N_2O_6$ %: C 59.93; H 7.45; N 7.39.

Single-Crystal X-ray Data Collection and Structure Determinations. The X-ray intensity data for **1**−**4** were recorded at 100 K on a Bruker-AXS SMART APEX/CCD diffractometer employing graphite monochromatized MoKα radiation (λ = 0.71073 Å) in ω scan mode. The structure solution and refinement proceeded similarly for all structures using SHELX-97 program package.[30] Direct

Table 1. Summary of the Crystal Data and Structure Refinement Parameters for 1−4

compound	1	2	3	4
formula	$C_{34}H_{48}N_4O_8$	$C_{38}H_{54}N_6O_6$	$C_{46}H_{70}N_6O_6$	$C_{19}H_{28}N_2O_6$
composition	$(C_4H_{12}N_2)(C_{15}H_{14}NO_2)_2\cdot 4H_2O$	$(C_8H_{22}N_4)(C_{15}H_{14}NO_2)_2\cdot 2H_2O$	$(C_{16}H_{38}N_4)(C_{15}H_{14}NO_2)_2\cdot 2H_2O$	$(C_4H_{12}NO_3)(C_{15}H_{14}NO_2)\cdot H_2O$
formula weight	640.76	690.87	803.08	380.43
crystal system	triclinic	monoclinic	triclinic	triclinic
space group	$P\bar{1}$	$C2/c$	$P\bar{1}$	$P\bar{1}$
a (Å)	6.9297(8)	32.809(4)	8.5654(14)	7.7773(16)
b (Å)	7.1741(8)	7.6594(10)	8.7181(14)	8.4070(17)
c (Å)	18.621(2)	29.684(4)	16.020(3)	15.127(3)
α (°)	85.995(2)	90.0	102.383(3)	90.642(4)
β (°)	83.245(2)	104.457(2)	91.415(3)	97.981(5)
γ (°)	65.812(2)	90.0	112.494(3)	97.970(4)
V (Å^3)	838.37(16)	7223.4(16)	1072.0(3)	969.6(3)
Z	1	8	1	2
D_c (Mg m^{-3})	1.269	1.271	1.244	1.303
μ (MoKα)/(mm^{-1})	0.091	0.087	0.083	0.097
F(000)	344	2976	436	408
reflections collected/unique	6659/3121 [R(int) = 0.0219]	26893/7094 [R(int) = 0.0563]	5612/3929 [R(int) = 0.0206]	7911/3797 [R(int) = 0.0284]
reflections with $I > 2\sigma(I)$	2565	5093	2886	2507
goodness-of-fit	1.008	1.008	0.999	0.963
R, wR [$I > 2\sigma(I)$]	0.0408, 0.1106	0.0545, 0.1236	0.0472, 0.1135	0.0361, 0.0705

methods yielded all non-hydrogen atoms. Hydrogen atoms bonded to nitrogen or oxygen atoms were localized in the difference Fourier map and refined freely with U_{iso}(H) = 1.5$_{eq}$(O), U_{iso}(H) = 1.2$_{eq}$(N). The remaining hydrogen atoms were placed in calculated positions and refined in "ride" mode. Structure graphics shown in the figures were created using the Mercury software package version 2.2.[31] Packing Index (PI) was calculated with the program PLATON.[32] Crystal data together with further details of the data collections and refinement are given in Table 1. CCDC reference numbers 759430−759433.

Results and Discussion

Commercially available maH, piperazine (ppz) hexahydrate, 1,4,7,10-tetraazacyclododecane (cyclen), *meso*-5,7,7,12,12,14-hexamethyl-1,4,8,11-tetraazacyclotetradecane (teta), and *tris*-(hydroxymethyl)methylamine (tris) were taken for cocrystallization. Crystalline products of the compositions (ppzH_2)(ma)$_2\cdot 4H_2O$ **1**, (cyclenH_2)(ma)$_2\cdot 2H_2O$ **2**, (tetaH_2)(ma)$_2\cdot 2H_2O$ **3**, and (trisH)(ma)$\cdot H_2O$ **4** were obtained in similar synthetic conditions in solution by direct mixing of maH with the basic component. The cycles gradually increase in size from 6 to 14 ring atoms, and contain two or four NH-amino groups capable of being protonated, contrary to one amino-group in tris. The purity of the synthesized compounds was confirmed by similarities between experimental and simulated X-ray powder diffraction patterns. The final complexes demonstrated the high stability within a long period of time. The melting point of all complexes falls between that of the partner and the drug substance, with no correlation with the melting points of initial bases (Table 2).[33] The variability in melting points for the series described herein may be attributed to the differences in structure, and primarily in the hydrogen bonding network. In **1**−**4** the acidic proton transfers from the carboxylic group of the maH molecule to the NH- or NH_2-group of the amine molecule give rise to the di- (**1**−**3**) or monocation (**4**). The crystallographic evidence for this proton transfer is the equalized C−O distances in the carboxylate group consistent with the carboxylate anion [bond distances C(7)−O(1) and C(7)−O(2) in Table 2, the most different values in the same COO^- group being 1.286(2) and 1.244(2) Å in **3**] and unbiased localization of the hydrogen atoms in close proximity to the nitrogen atoms in the *N*-basic cations, respectively. In all complexes the ma anion reveals an intramolecular N(1)−H···O(1) hydrogen bond of the $S_1^1(6)$ motif,[5] the N···O distance and N−H···O angle ranging within 2.624−2.675 Å and 132−143°, respectively (Table 3). The ma anion consists of the three planar fragments, the deprotonated carboxylic group, the phenyl ring **A** that carries it, and the xylyl ring **B** (Scheme 1). The conformation of the anion is defined by three torsion angles, O(1)−C(7)−C(1)−C(6), C(1)−C(6)−N(1)−C(8), and C(6)−N(1)−C(8)−C(9). These angles in **1**−**4** along with those in pure maH[13f] are given in Table 2. It can be clearly seen from Table 2 that the torsion angles C(1)−C(6)−N(1)−C(8) and C(6)−N(1)−C(8)−C(9) in **1**−**4** essentially vary. This fact indicates that the cocrystallization partner affects the observed conformation in the crystal structures.

Compound (ppzH_2)(ma)$_2\cdot 4H_2O$ **1** crystallizes in the triclinic space group $P\bar{1}$ (Figure 1). The piperazinium cation resides around an inversion center in chair conformation.

The seven-membered formula unit is stabilized by two charge-assisted $NH^+\cdots O(COO^-)$ hydrogen bonds using equatorial H-atoms, and two NH···O(H_2O) hydrogen bonds using axial H-atoms of azonia-groups, the cation···anion separation N(2)···O(1) of 2.713(2) Å (Table 3) being the shortest in the structure. There are no more direct cation−anion interactions, and the two-membered O(1w)···O(2w) (2.726 Å) water clusters additionally link the charged entities inside the formula unit giving rise to two $R_4^4(13)$ graph sets. The second H-atom of each water molecule, being involved in the OH(H_2O)···O(COO^-) hydrogen bonds combines the formula units in the layer propagated parallel to the *ab* crystallographic plane (Figure 2).

The layer comprises the hydrophilic core and the hydrophobic outer surfaces. The internal hydrophilic region is formulated by the combination of the above-mentioned $R_4^4(13)$ motifs within the formula units, and alternating $R_4^6(12)$ and $R_6^6(16)$ motifs involving water molecules and carboxylic group of ma. Summarizing, six symmetry independent H-bonds are responsible for the stabilization of the hydrophilic area where all donors (two water molecules and one cyclic cation) are involved in single H-bonds, while the carboxylic oxygens act as multiple acceptors, taking part in three [O(1)] and two [O(2)] hydrogen-bonds, respectively. The parallel ma anions related by the shortest *a* and *b* translations demonstrate the edge-to-face arrangements of the **A** and **B**

Table 2. Selected Parameters of 1-4

parameter	maH[13f]	1	2 a	2 b	3	4
ma:base:H_2O ratio		2:1:4	2:1:2		2:1:2	1:1:1
melting point/°C	230−232	178−180	148−150		215−218	>190 (dec)
melting point base/ °C[a]		106	108−113		146−148	171−172
water environment		DDA, DDA	DDA, DD		DDA	DDA
O(1)−C(7) (Å)	1.232	1.278(2)	1.265(2)	1.262(2)	1.286(2)	1.270(2)
O(2)−C(7) (Å)	1.318	1.258(2)	1.258(2)	1.273(2)	1.244(2)	1.273(2)
C(6)−N(1)−C(8)−C(9) (°)	120.0	117.8(2)	79.3(3)	73.0(3)	160.4(2)	85.2(2)
C(1)−C(6)−N(1)−C(8) (°)	179.3	−172.2(1)	165.0(2)	−175.6(2)	145.1(2)	171.2(2)
O(1)−C(7)−C(1)−C(6) (°)	1.71	−7.6(2)	−7.0(3)	−6.3(3)	13.4(3)	6.8(2)
A/B angle (°)	62.4	60.6	73.4	75.3	53.5	78.4
CH (sp^2) ···π (Å)	3.59	3.41	3.91			3.44
	3.66	3.90				3.41
CH(sp^3) ···π (Å)	3.63	3.55	3.54		3.63	3.64
			3.83		3.67	
			3.99		3.74	
NH···π (Å)			3.47			
thickness of the layer (Å)	14.0	18.5	18.5		16.7	13.6
thickness of the hydrophobic region (Å)	14.0	13.9	12.2		14.1	11.4
area per one **ma**/(Å^2)	45.4	45.4	56.8		69.0	64.8
packing index/(%)	68.2	69.1	69.8		70.9	69.4

[a] Melting point is given for anhydrous form.

Table 3. Hydrogen Bond Distances (Å) and Angles (°) for 1−4

D−H···A	d(D−H)	d(H···A)	d(D···A)	∠(DHA	symmetry transformation for acceptor
1					
N(1)−H(1N1)···O(1)	0.85(2)	2.00(2)	2.652(2)	133(2)	x, y, z
N(2)−H(1N2)···O(1)	0.98(2)	1.74(2)	2.713(2)	173(2)	x, y, z
N(2)−H(2N2)···O(2w)	0.91(1)	1.91(2)	2.808(2)	169(2)	$2 - x, 1 - y, -z$
O(1w)−H(1w1)···O(1)	0.87(2)	2.04(2)	2.851(2)	155(2)	$1 + x, y, z$
O(1w)−H(2w1)···O(2)	0.87(2)	1.96(2)	2.732(2)	147(2)	x, y, z
O(2w)−H(1w2)···O(1w)	0.90(2)	1.83(2)	2.726(2)	174(2)	x, y, z
O(2w)−H(2w2)···O(2)	0.92(2)	1.88(2)	2.802(2)	174(2)	$3 - x, -y, -z$
2					
N(1a)−H(1A)···O(1a)	0.88(2)	1.93(2)	2.641(2)	137(2)	x, y, z
N(1b)−H(1b)···O(1b)	0.88(2)	1.90(2)	2.625(2)	138(2)	x, y, z
N(1)−H(1N1)···O(2b)	0.96(2)	1.74(2)	2.697(2)	175(2)	x, y, z
N(1)−H(2N1)···N(4)	0.92(2)	2.37(2)	2.832(2)	111(2)	x, y, z
N(1)−H(2N1)···N(2)	0.92(2)	2.39(2)	2.874(2)	112(2)	x, y, z
N(1)−H(2N1)···O(1w)	0.92(2)	2.50(2)	3.021(2)	117(2)	x, y, z
N(3)−H(1N3)···O(1a)	1.01(2)	1.67(2)	2.664(2)	169(2)	x, y, z
N(3)−H(1N3)···O(2a)	1.01(2)	2.51(2)	3.192(2)	125(2)	x, y, z
N(3)−H(2N3)···N(2)	0.88(2)	2.35(2)	2.820(3)	114(2)	x, y, z
N(3)−H(2N3)···N(4)	0.88(2)	2.42(2)	2.885(2)	113(2)	x, y, z
N(4)−H(1N4)···O(2a)	0.92(2)	2.09(2)	2.925(2)	151(2)	$1/2 - x, 1/2 + y, 1/2 - z$
O(1w)−H(1w1)···O(2b)	0.87(3)	1.93(3)	2.806(2)	176(2)	$1/2 - x, 3/2 - y, 1 - z$
O(1w)−H(2w1)···O(1b)	0.88(3)	1.88(3)	2.752(2)	177(2)	x, y, z
O(2w)−H(1w2)···O(2a)	0.89(3)	1.95(2)	2.828(2)	170(3)	$1/2 - x, 1/2 + y, 1/2 - z$
O(2w)−H(2w2)···O(1w)	0.95(3)	1.94(3)	2.887(2)	175(3)	x, y, z
3					
N(1)−H(1N1)···O(1)	0.88(2)	1.91(2)	2.673(2)	144(2)	x, y, z
N(2)−H(1N2)···N(3)	0.90(2)	2.09(2)	2.829(2)	139(2)	$1-x, -y, -z$
N(2)−H(2N2)···O(1)	0.98(2)	1.81(2)	2.786(2)	171(2)	x, y, z
N(3)−H(1N3)···O(1w)	0.84(2)	2.34(2)	3.041(2)	141(2)	$1 - x, -y, -z$
O(1w)−H(1w1)···O(1)	0.87(3)	2.03(3)	2.873(2)	163(2)	x, y, z
O(1w)−H(2w1)···O(2)	0.87(3)	1.91(3)	2.777(2)	174(2)	$1-x, 1-y, -z$
4					
N(1)−H(1N1)···O(1)	0.84(2)	2.01(2)	2.676(2)	136(2)	x, y, z
N(2)−H(1N2)···O(3)	0.97(2)	1.88(2)	2.830(2)	167(2)	$1-x, -y, 1-z$
N(2)−H(2N2)···O(2)	0.95(2)	1.78(2)	2.723(2)	171(2)	x, y, z
N(2)−H(3N2)···O(5)	0.95(2)	1.83(2)	2.760(2)	169(2)	$-x, -y, 1-z$
O(1w)−H(1w)···O(2)	0.86(2)	1.93(2)	2.780(2)	174(2)	x, y, z
O(1w)−H(2w)···O(4)	0.89(2)	2.00(2)	2.859(2)	161(2)	$1 - x, 1 - y, 1 - z$
O(3)−H(3B)···O(1)	0.84	2.02	2.858(2)	176	$1 - x, 1 - y, 1 - z$
O(4)−H(4B)···O(1)	0.84	1.93	2.752(2)	167	x, y, z
O(5)−H(5B)···O(1w)	0.84	1.81	2.630(2)	166	$1-x, -y, 1 - z$

aromatic rings (Figure 2b, Table 2). The **A/B** dihedral angle of 60.6° between the interacting rings is equal to the **A/B** dihedral angle within the molecule. The layers meet by their hydrophobic surfaces and interactions across the layer boundary include the CH_3···π contacts[34] between the center-of-symmetry related xylyl rings (**B**) and directed outside the layer methyl groups, Figure 2c. The arrangement of ma anions both inside the layer and across the layer boundary closely

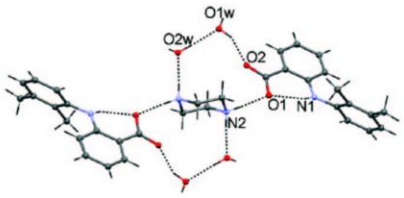

Figure 1. View of formula unit for **1** with the partial labeling scheme. Hydrogen bonds are shown by dashed lines.

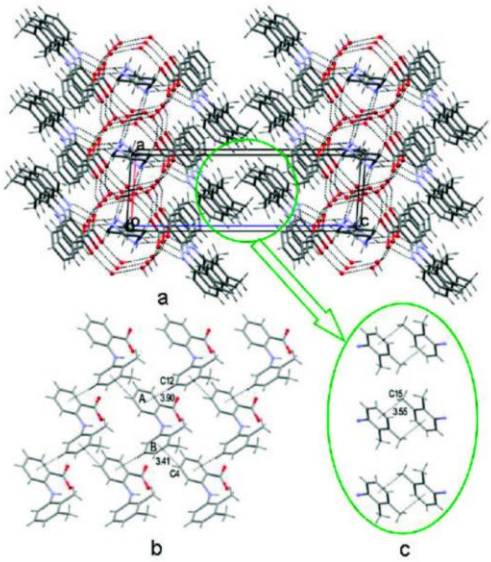

Figure 2. (a) Packing of two layers in **1**; (b) arrangement of ma anions in the slice parallel to the *ab* crystallographic plane. The edge-to-face CH(sp^2)$\cdots\pi$ interactions are shown by dotted lines; (c) the $CH_3\cdots\pi$ interactions of xylyl rings of ma anions in the interlayer region are shown by dashed lines.

resembles the crystal packing of the H-bonded centrosymmetric dimers of maH,[13f] which form similar layers with the hydrophilic carboxylic groups inside and two hydrophobic surfaces parallel to the crystallographic plane defined by the two shortest unit cell parameters. The only specific recognizable driving forces which hold the dimers within the layer are the edge-to-face **A/B** interactions between the related by translation maH molecules, C(4)−H$\cdots$Cg B(centroid B) = 3.59 Å, C(12) $\cdots$ Cg B = 3.66 Å; the **A/B** dihedral angle equals 62.4°, resulting in exactly the same packing motif as shown in Figure 2b for **1**. It is also noteworthy that maH in the pure phase and ma in **1** occupy the same area of 45.4 Å^2 in the slice of parallel entities shown in Figure 2b. The conformations of maH and ma in **1** are also identical as is evident from Table 2. At the same time, the thickness of the layer given by the distance between the parallel planes defined by the most distal C(15) atoms is essentially different, being 14.0 Å in the structure of maH and 18.5 Å in **1**. Thus, the insertion of *N*-base between the ma entities affords the lateral expansion of the layer but preserves the intra- and interlayer CH$\cdots\pi$

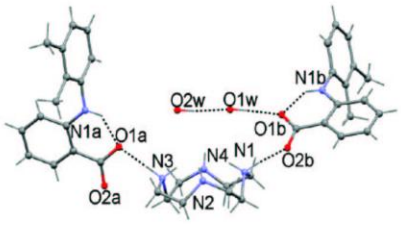

Figure 3. View of formula unit for **2** with the partial labeling scheme. Hydrogen bondings are shown by dashed lines.

interactions along with the relative arrangement of the anions in the structure.

Figure 3 depicts the five-membered complex (cyclenH_2)-(ma)$_2\cdot 2H_2O$ **2**, which crystallizes in the monoclinic space group *C*2/*c*. All the components, being the macrocyclic dication, two symmetry independent ma anions marked with the **a** and **b** trailers, and two water molecules, O(1w) and O(2w), occupy general positions. The anions **a** and **b** have similar conformations (Table 2). In the cyclic dication, each second nitrogen atom is additionally protonated, all four nitrogen atoms are perfectly coplanar (within 0.007 Å), and all *N*-bound hydrogen atoms display above this N_4 plane. The mode of protonation and the shape of the (cyclenH_2)$^{2+}$ moiety is identical to that found in its complex with *p*-aminobenzoic acid.[25b] The hydrogen atoms of the NH_2-groups are *endo*- and *exo*-oriented. The *endo*-oriented H-atoms participate in the bifurcated NH$\cdots$N intramolecular short contacts (Table 3). The *exo*-oriented H-atoms anchor the **a** and **b** anions via the charge-assisted $N^+\cdots O(COO^-)$ hydrogen bonds, N(1)$\cdots$O-(2b) 2.697(2) Å, and N(3)$\cdots$O(2a) 2.664(2) Å, being the shortest in **2** similar to **1** (Table 3). The formula unit is completed by the two-membered water cluster with the O(1w)$\cdots$O(2w) separation of 2.887(2) Å.

The neighboring complexes are associated in the tapes parallel to the *b* axis via the bridging carboxylic group of the anion **a** and the H-donor function of N(4) atom, the interaction being described by the $C_2^2(9)$ graph set. The water clusters additionally link the neighboring formula units into the tapes, mediating the **a** and **b** anions. The O(1w) water molecule uses one of its H-atoms for the cross-tape interactions giving rise to the layer spread parallel to the *bc* plane (Figure 4). These interactions generate the centrosymmetric heterotetramer, $R_4^4(12)$ that combines the two **b** anions and the two O(1w) water molecules.

Similar to **1**, the layer comprises the hydrophilic core and the hydrophobic outer surfaces and has the same thickness of 18.5 Å. However, the area occupied by one ma anion essentially increases and equals 56.8 Å^2, and the only one weak edge-to-face CH$\cdots\pi$ interaction with C(5a)$\cdots$Cg **B(b)** separation of 3.91 Å and the **A(a)**/**B(b)** dihedral angle of 76.8° preserves within the layer in **2**. It is a consequence of the insertion of the larger in size (cyclenH_2)$^{2+}$ cations which impose the increased separation between the pendant ma anions, while the more spongiose hydrophobic region of the layer facilitates the deeper interlayer interdigitation of the xylyl rings of the ma (Figure 4b, Table 2). Additionally, the structure reveals the NH$\cdots\pi$ interactions[35] of 3.47 Å, mediated by the cyclic NH-group and the unused π-acceptor function of ring **A** (anion **b**) Thus, the insertion of a larger cycle possessing an increased number of NH-binding sites does not enlarge the thickness of the layer but slides apart the neighboring ma anions.

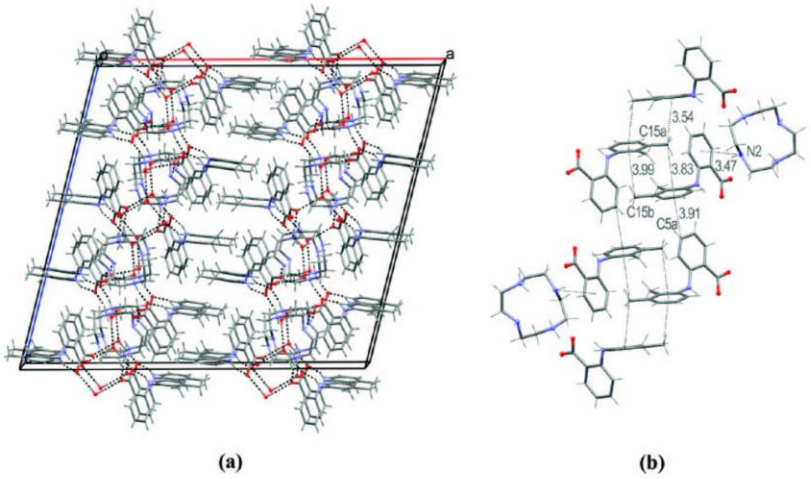

Figure 4. Crystal packing in **2**: (a) arrangement of two layers in the unit cell, (b) the CH···π and NH···π interactions involving aromatic rings are shown by dashed lines.

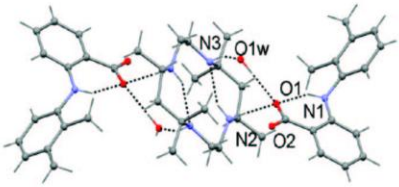

Figure 5. View of formula unit for **3** with the partial labeling scheme. Hydrogen bondings are shown by dashed lines.

Compound **3** of the composition $(tetaH_2)(ma)_2 \cdot 2H_2O$ crystallizes in the triclinic space group $P\bar{1}$. The centrosymmetric formula unit is shown in Figure 5.

The mode of protonation of teta molecule is identical to that found in its complexes with 3- and 4-hydroxybenzoic acids, 3,5-dihydroxybenzoic and phenylphosphonic acids.[36] The conformation of the cation is fixed by the two N(2)−H···N(3) hydrogen bonds. Complex **3** is stabilized by the combination of couples of $NH^+ \cdots O(COO^-)$, $NH \cdots O(H_2O)$, and $OH(H_2O) \cdots O(COO^-)$ hydrogen bonds (Table 3). The neighboring complexes translated along the *b* direction are bound in the columns of the edge-fused $R_2^3(10)$ and $R_4^4(12)$ rings due to the bridging function of water molecule. The $R_4^4(12)$ graph set describes the centrosymmetric heterotetramer identical to that one found in **2** which combines two ma anions and two water molecules at O···O distances of 2.776(2) and 2.871(2) Å, respectively (Figure 6). All possible hydrogen bonds are segregated inside the columns, which have the external hydrophobic surfaces.

The column size along the [001] direction defined as a separation between the parallel planes through the most distal C(15) atoms of the xylyl ring is 16.7 Å. The column size along the [100] direction defined by the planes through the C(3) atoms is 8.51 Å. The columns related by the translation along the *a* axis are connected by the CH···π interactions between the methyl group of the $(tetaH_2)^{2+}$ cation and ring **A** of the ma anion. To the opposite side of the **A** ring approaches the other

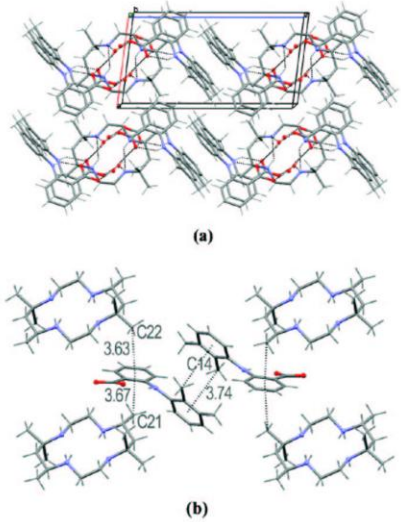

Figure 6. Crystal packing in **3** (a); the scheme of CH···π interactions shown by dashed lines (b).

methyl group of the $(tetaH_2)^{2+}$ showing the intracolumn CH···π interaction (Figure 6b). The methyl groups of the $(tetaH_2)^{2+}$ cation, intercalated into the slice of the parallel ma anions, substitute the edge-to-face interactions by the $CH_3 \cdots \pi$ ones, which unite the columns in the layer similar to that found in **1**−**2**. The intervention of the methyl groups slides ma anions apart and increases up to 69.0 $Å^2$ the area occupied by one ma. The neighboring layers are stacked along the *c* axis via CH-$(sp^3) \cdots \pi$ interactions of 3.74 Å acting exactly in the same mode as in the pure maH and in **1**−**2**.

The proton-transfer complex $(trisH)(ma) \cdot H_2O$ **4** is the only one where the acyclic amine (Scheme 1) is used as a base.

Complex represents a monohydrate of the 1:1:1 stoichiometry, which crystallizes in the triclinic space group $P\bar{1}$. The formula unit is shown in Figure 7.

It is a solitary complex in this series where both oxygen atoms of the ma anion interact with the same cation in a chelate mode via the $NH(NH_3^+)\cdots O(COO^-)$ and $OH\cdots O(COO^-)$ hydrogen bonds giving rise to the $R_2^2(9)$ asymmetric ring. Three hydroxymethyl groups of *N*-base adopt around the amino-methyl bond a propeller-like conformation, close to the C_3 symmetry. The tripod geometry of the cation decorated by one NH_3^+ and three OH-groups facilitates its self-assembling in the chains running along the *a* axis which via bridging water molecules are further combined in the well-defined H-bonded layer developed parallel to the *ab* plane.

The similar self-organization of the $(trisH)^+$ cations in the chains is found in its deoxycholate,[37] while in the layer − in {2-[(2,6-dichlorophenyl)amino]phenylacetate.[38] The ma anions in **4** attached to the cationic layer via hydrogen bonds form its hydrophobic surfaces. The slice of the parallel ma anions reveals the same **B**/**A** edge-to-face interaction previously found in **1**−**2** and characterized by the $CH(sp^2)\cdots\pi$ and $CH(sp^3)\cdots\pi$ interactions (Figure 8b). Besides, cycle **B** is involved in the $CH(sp^3)\cdots\pi$ interaction of 3.41 Å with the methylene group of the $(trisH)^+$ cation. Each ma occupies an area of 64.8 Å^2. The layer in **4** is the thinnest among the studied complexes with a thickness of 13.6 Å between the planes defined by the most distal C(4) atom of ring **A**. This is explained by the rearrangement of the xylyl rings inside the layer due to its involvement in the intralayer $CH_3\cdots\pi$ interactions (Figure 8b).

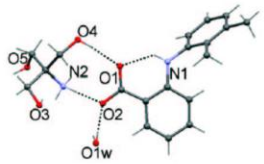

Figure 7. View of formula unit for **4** with the partial labeling scheme. Hydrogen bonds are shown by dashed lines.

The present study, our previous results,[25,26] and the literature data[20] unambiguously show that charge-assisted N−H···O hydrogen bonds are reliable and predictable interactions in the formation of organic complexes between aromatic carboxylic acids and cyclic amines in which nitrogen atom possesses sp^3-hybridization. These intermolecular interactions, being the shortest in the structure, determine the direct binding of *N*-base with aromatic carboxylate. A similar observation was made for the allied crystalline complexes with acyclic amines where the charge assisted N−H···O bonds were the driving forces for the aggregation of molecular components in the complex.[13] In all mefenamic acid−amine crystalline complexes known so far, the amine molecule inserts between the carboxylic groups of maH, disrupts the $R_2^2(8)$ carboxylic acid homomeric synthon, and replaces it by charge-assisted N−H···O hydrogen bonds. These strong H-bonds give the ability to control ma-amine assembly and represent an ideal tool for reproducing predesigned multicomponent crystals in this system.

The ability of organic crystals to form hydrated structures is very intriguing.[39,40] Structurally, hydrates of organic compounds have been categorized into two classes: isolated site hydrates and channel hydrates.[41] Because of their small size water molecules readily incorporate into crystal lattices and provide versatile hydrogen bonding patterns.[42] They can contribute to stabilization of crystal structures when there is an imbalance in the number of acceptors and donors[43] by forming a diverse arrangement of supramolecular heterosynthons. Our previous results for *p*-aminobenzoic acid complexes give such examples.[25] Referring to organic salts, the authors[27] based on the survey of CSD generalized the increasing hydrate formation with increasing charge on a single ion or with increasing number of carboxylate groups in a structure.[44] Recent studies represent the attempts to find correlations between the degree of hydration and thermal stability of the crystals.[45,46] Water molecules in **1**−**4** incorporate into the hydrophilic region of the crystals and feature different structural functions. The single water molecule point inclusion in the DDA (where D = H-donor, A = H-acceptor) environment is registered in **3** and **4**, while in **1**−**2** two crystallographically unique water molecules incorporate in the form

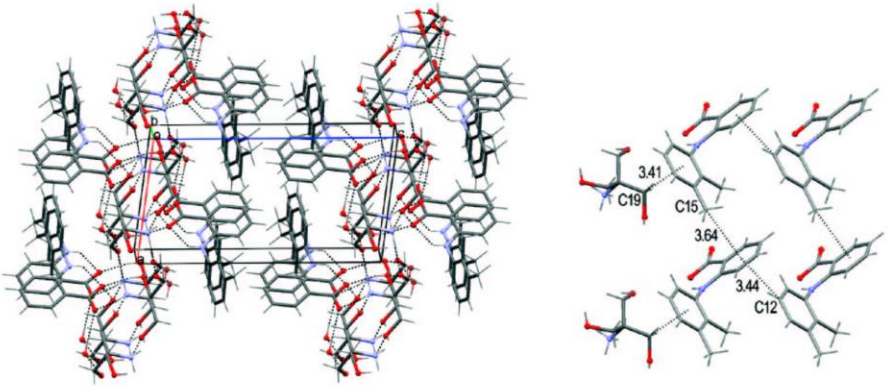

(a) (b)

Figure 8. (a) Crystal packing in **4** shows the arrangement of two layers; (b) $CH\cdots\pi$ interactions involving aromatic rings are shown by dashed lines.

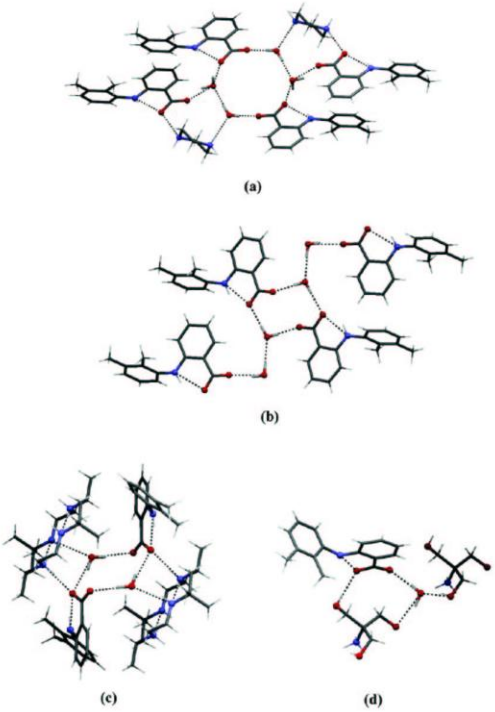

Figure 9. Water inclusion in **1** (a), **2** (b), **3** (c), and **4** (d).

of a two-membered cluster; in **1** both molecules exist in the same DDA environment, while in **2** exist in DDA and DD environments giving rise to the heteromeric clusters in the form of $R_6^4(16)$ (**1**), $R_4^4(12)$ (**2**, **3**), and $R_3^3(12)$ (**4**) H-bonded rings (Figure 9).

The contribution of CH···π intermolecular interactions to the overall system of interactions is the subject of intense debates nowadays.[47] The scientists agree that these interactions are very weak and being largely originated from the dispersion force they possess very weak directionality. For typical CHs in aliphatic and aromatic groups, the energy of one CH···π hydrogen bond is ca. 1.5−2.5 kcal mol^{-1}. Nevertheless, one of the most remarkable features of C−H···π interactions is that they work cooperatively, and this effect is most prominent in crystals.[48] For example, Kobayashi and Saigo[49] starting from the X-ray crystallographic structures for four less soluble organic salts sustained by the network of NH_3^+···O(COO$^-$) hydrogen bonds, using the periodic ab initio MO method presented computational evidence in favor of the cooperative effect of CH ··π interactions in the crystals. The common feature of four complexes discussed herein is their layered structure in which the hydrophilic area is isolated within the layer. Whereas strong hydrogen bonds determine the ma-*N*-base assembly, the rather weak C−H···π intermolecular interactions predominate in the hydrophobic interlayer region and reported structures demonstrate their persistence (Table 2). The intra- and interlayer aromatic C−H···π interactions in the complexes iterate or resemble those in the pure phase of maH, although some of them are replaced by C−H···π or even N−H···π interactions with the base. These interactions determine the thickness of interlayer hydrophobic region formally evaluated as the distance between the parallel to layer planes through the outer for this region C(7) atoms of carboxylic groups. This parameter varies in a relatively short-range of 11.4−14.1 Å (Table 2). The major discrepancy in interlayer interactions and in such integrated parameters as thickness of the hydrophobic region compared with the pure phase of mefenamic acid was found for **4** which also differs from three other complexes by an ma/amine stoichiometry of 1:1. Only in **4** the acyclic amine, rich in donor-acceptor groups, and water molecules associate to form the well-defined H-bonded layer, which dictates the orientation of the attached to it ma anions. In the complexes with cyclic amines the formation of H-bonded layers or even columns occurs with involvement of carboxylic groups of ma; thus, the role of ma and competitive ability of weak C−H···π interactions in the tuning of overall packing pattern increase.

The ma anion reveals the conformational mobility indicated by the difference in the values of torsion angles around N(1)−C(8) and N(1)−C(6) bonds which comes up to 87.5° and 42.7°, respectively. At the same time, the dihedral angle between the aromatic rings, which influences the geometry of the C−H···π interactions, deviates in a relatively short range of 24.9°. The most effective crystal packing with the largest packing coefficient of 70.9% was found in complex **3** with the teta base enriched by the methyl groups.

Conclusions

Four novel crystalline complexes of mefenamic acid with *N*-bases, cyclic piperazine, 1,4,7,10-tetraazacyclododecane (cyclen), *meso*-5,7,7,12,12,14-hexamethyl-1,4,8,11-tetraazacyclotetradecane (teta), and acyclic tris(hydroxymethyl)aminomethane (tris) have been synthesized and studied. All complexes are formed due to the proton transfer from the carboxylic group of mefenamic acid to the amino group of *N*-base. The components are packed in the layers where the hydrophilic region within the layer is surrounded by two nonpolar surfaces formed by mefenamate anions. Notwithstanding a diverse hydrogen-bonding system including the most reliable charge-assisted hydrogen bonds between the mefenamate anions and cationic amines, the structures demonstrate persistent CH···π interactions both *within* and *across* the layers that include the aromatic moieties of the mefenamate anions. These interactions are closely comparable to those in the crystal structure of mefenamic acid itself, where the packing of the hydrogen-bonded dimers is directed by the well-defined edge-to-face interactions between the phenyl rings. Insertion of piperazine or cyclen into the mefenamic acid layers results in a lateral expansion within the layers but a minimal change in the interlayer interactions. Cocrystallization with teta demonstrates the competitive involvement of its own methyl groups into the CH_3···π interactions within the layer but the preservation of the interlayer packing motif. Cocrystallization with tris buries the xylyl rings of mefenamate anions within the layer thus decreasing the layer thickness and partly rearranging the interlayer hydrophobic interactions.

Acknowledgment. This work is supported by the Russian Foundation for Basic Research and the Academy of Sciences of R. Moldova (Project No. 08-03-90103-Mol-a/08.820.05.037RF)

Supporting Information Available: X-ray crystallographic information in CIF format. This information is available free of charge via the Internet at http://pubs.acs.org.

References

(1) (a) Huang, L. F.; Tong, W. Q. *Adv. Drug Delivery Rev.* **2004**, *56*, 321 334. (b) Singhal, D.; Curatolo, W. *Adv. Drug Delivery Rev.* **2004**, *56*, 335 347.

(2) (a) Bernstein, J. *Polymorphism in Molecular Crystals*; Oxford University Press: United Kingdom, 2003. (b) Dunitz, J. D.; Bernstein, J. *Acc. Chem. Res.* **1995**, *28* (4), 193 200. (c) Vishweshwar, P.; McMahon, J. A.; Oliveira, M.; Peterson, M. L.; Zaworotko, M. *J. Am. Chem. Soc.* **2005**, *127*, 16802 16803. (d) Hilfiker, R.; Blatter, F; von Raumer, M. In *Polymorphism in the Pharmaceutical Industry*; Hilfiker, R., Ed.; Wiley-VCH Verlag: Weinheim, 2006; Chapter 1, p 1.

(3) (a) Lehn, J. M. *Supramolecular Chemistry*; VCH: Weinheim, 1995; (b) Desiraju, G. R. *Crystal Engineering: the Design of Organic Solids*; Elsevier: Amsterdam, 1989; (c) B. Moulton, B.; Zaworotko, M. J. *Chem. Rev.* **2001**, *101*, 1629 1658.

(4) (a) Almarsson, O.; Zaworotko, M. J. *Chem. Commun.* **2004**, 1889 1896. (b) Vishweshwar, P.; McMahon, J.; Bis, J.; Zaworotko, M. J. *J. Pharm. Sci.* **2006**, *95*, 499 516. (c) Trask, A. V.; Motherwell, W. D. S.; Jones, W. *Cryst. Growth Des.* **2005**, *5*, 1013 1021. (d) Reddy, L. S.; Babu, N. J.; Nangia, A. *Chem. Commun.* **2006**, 1369 1371. (e) Basavoju, S.; Boström, D.; Velaga, S. P. *Cryst. Growth Des.* **2006**, *6*, 2699 2708.

(5) (a) Etter, M. *Acc. Chem. Res.* **1990**, *23*, 120 126. (b) Etter, M. C.; Frankenbach, G. A. *Chem. Mater.* **1989**, *1*, 10 12. (c) Desiraju, G. R. *Angew. Chem., Int. Ed. Engl.* **1995**, *34*, 2311 2327. (d) Desiraju, G. R. *Curr. Opin. Solid State Mater. Sci.* **1997**, *2*, 451 454.

(6) (a) Desiraju, G. R.; Steiner, T. *The Weak Hydrogen Bond in Structural Chemistry and Biology*; Oxford University Press: Oxford, 1999; (b) Meyer, E. A.; Castellano, R. K.; Diederich, F. *Angew. Chem., Int. Ed.* **2003**, *42*, 1210 1250.

(7) (a) Biradha, K.; Zaworotko, M. J. *J. Am. Chem. Soc.* **1998**, *120*, 6431 6432. (b) Lewis, G. R.; Dance, I. *J. Chem. Soc., Dalton Trans.* **2000**, 299 306. (c) Lewis, G. R.; Dance, I. *J. Chem. Soc., Dalton Trans.* **2000**, 3176 3185. (d) Scudder, M.; Dance, I. *J. Chem. Soc., Dalton Trans.* **1998**, 329 344.

(8) Mei, X.; August, A. T.; Wolf, C. *J. Org. Chem.* **2006**, *71*, 142 149.

(9) (a) Winder, C. V.; Wax, J.; Scotti, L.; Scherre, R. A.; Jones, E. M.; Short, F. W. *J. Pharmacol. Exp. Ther.* **1962**, *38*, 405 413. (b) Reynolds, J. E. F. *Martindale: The Extra Pharmacopoeia*, 31rd ed.; The Pharmaceutical Press: London, 1998; p 58; (c) Gungor, S.; Yildiz, A.; Ozsoy, Y.; Cevher, E.; Araman, A. *Farmaco* **2003**, *58*, 397 401.

(10) (a) Joo, Y.; Kim, H.-S.; Woo, R.-S.; Park, C. H.; Shin, Ki-Y.; Lee, J.-P.; Chang, K.-A.; Kim, S.; Suh, Y.-H. *Mol. Pharmacol.* **2006**, *69*, 76 84. (b) Asanuma, M.; Nishibayashi-Asanuma, S.; Miyazaki, I.; Kohno, M.; Ogawa, N. *J. Neurochem.* **2001**, *76*, 1895 1904.

(11) (a) Park, K. H.; Evans, J. M. B.; Myerson, A. S. *Cryst. Growth Des.* **2003**, *3*, 991 995. (b) Otsuka, M.; Kato, F.; Matsuda, Y. *Solid State Ionics* **2004**, *172*, 451 453. (c) Singh, A.; Lee, I. S.; Myerson, A. S. *Cryst. Growth Des.* **2009**, *9*, 1182 1185.

(12) (a) Castellari, C.; Ottani, S. *Acta Crystallogr.* **1997**, *C53*, 794 797. (b) Surov, A. O.; Terekhova, I. V.; Bauer−Brandl, A.; Perlovich, G. L. *Cryst. Growth Des.* **2009**, *9*, 3265 3272.

(13) (a) Adam, A.; Schrimpl, L.; Schmidt, P. C. *Drug. Dev. Ind. Pharm.* **2000**, *26*, 477 487. (b) Panchagnula, R.; Sundaramurthy, R.; Pillai, O.; Agrawal, S. *J. Pharm. Sci.* **2004**, *93*, 1019 1029. (c) Aguair, A. J.; Zelmer, J. E. *J. Pharm. Sci.* **1969**, *58*, 983 987. (d) Umeda, T.; Ohnishi, N.; Yokoyama, T.; Kuroda, T.; Kita, Y.; Kuroda, K.; Tatsumi, E.; Matsuda, Y. *Chem. Pharm. Bull.* **1985**, *33*, 2073 2078. (e) Lee, E. H.; Byrn, S. R.; Carvajal, T. M. *Pharm. Res.* **2006**, *23*, 2375 2380. (f) McConnell, J. F.; Company, F. Z. *Cryst. Struct. Commun.* **1976**, *5*, 861 864. (g) Romero, S.; Escalera, B.; Bustamante, P. *Int. J. Pharm.* **1999**, *178*, 193 202.

(14) (a) Jilani, J. A.; Najib, N. M.; Ghariabeh, S. H. *Acta Pharm. Hung.* **1997**, *67*, 99 104. (b) Tantishaiyakul, V.; Wiwattanawongsa, K.; Pinsuwan, S.; Kasiwong, S.; Phadoongsombut, N.; Kaewnopparat, S.; Kaewnopparat, N.; Rojanasakul, Y. *Pharm. Res.* **2002**, *19*, 1013 1018.

(15) (a) Aakeröy, Ch. B.; Fasulo, M. E.; Desper, J. *Mol. Pharmaceutics* **2007**, *4*, 317 322. (b) Berge, S. M.; Bighley, L. D.; Monkhouse, D. C. *J. Pharm. Sci.* **1977**, *66*, 1 19. (c) Agharkar, S.; Lindenbaum, S.; Higuchi, T. *J. Pharm. Sci.* **1976**, *65*, 747 749.

(16) (a) Bani−Jaber, A.; Hamdan, I.; Al-Khalidi, B. *Chem. Pharm. Bull.* **2007**, *55*, 1136 1140. (b) Kovala−Demertzi, D.; Hadjipavlou-Litina, D.; Staninska, M.; Primikiri, A.; Kotoglou, C.; Demertzis, M. A. *J. Enzyme Inhibition Med. Chem.* **2009**, *24*, 742 752. (c) Andrews, G. P.; Zhai, H.; Tipping, S.; Jones, D. S. *J. Pharm. Sci.* **2009**, *98*, 4545 4556. (d) Gupta, U.; Agashe, H. B.; Asthana, A; Jain, N. K. *Biomacromolecules* **2006**, *7* (3), 649 658.

(17) Fang, L.; Numajiri, S.; Kobayashi, D.; Ueda, H.; Nakayama, K.; Miyamae, H.; Morimoto, Y. *J. Pharm. Sci.* **2004**, *93*, 144 154.

(18) (a) Pop, M. M.; Goubitz, K.; Borodi, G.; Bogdan, M.; De Ridder, D. J. A.; Peschar, R.; Schenk, H. *Acta Crystallogr.* **2002**, *B58*, 1036 1043. (b) Hladon, T.; Pawlaczyk, J.; Szafran, B. *J. Incl. Phenom* **1999**, *35*, 497 506.

(19) Allen, F. N. *Acta Crystallogr.* **2002**, *B58*, 380 388.

(20) Skovsgaard, S.; Bond, A. D. *CrystEngComm* **2009**, *11*, 444 453.

(21) (a) Mertes, M. P.; Mertes, K. B. *Acc. Chem. Res.* **1990**, *23*, 413 418. (b) Liang, F.; Wan, S.; Li, Zh.; Xiong, X.; Yang, Li.; Zhou, X.; Wu, C. *Curr. Med. Chem.* **2006**, *13* (6), 711 727. (c) Delgado, R.; Felix, V.; Lima, L. M. P.; Price, D. W. *Dalton Trans.* **2007**, 2734 2745. (d) Chen, T.; Wang, X.; He, Y.; Zhang, C.; Wu, Z.; Liao, K.; Wang, J.; Guo, Z. *Inorg. Chem.* **2009**, *48*, 5801 5809.

(22) Oswald, I. D. H.; Allan, D. R.; McGregor, P. A.; Motherwell, W. D. S.; Parsons, S.; Pulham, C. R. *Acta Crystallogr.* **2002**, *B58*, 1057 1066.

(23) (a) Wang, C. K.-W.; Pan, Y.-J.; Jin, Z.-M. *Z. Kristallogr.- New Cryst. Struct* **2002**, *217*, 435 443. (b) Nomura, H.; Nakamachi, H.; Wada, Y. *Chem. Pharm. Bull.* **1982**, *30*, 1024 1029. (c) Zakaria, C. M.; Ferguson, G.; Lough, A. J.; Glidewell, C. *Acta Crystallogr.* **2003**, *B59*, 118 131. (d) Du, M.; Zhang, Z.−H.; Guo, W.; Fu, X.−J. *Cryst. Growth Des.* **2009**, *9* (4), 1655 1657. (e) Castellari, C.; Sabatino, P. *Acta Crystallogr.* **1996**, *C52*, 1708 1712. (f) Castellari, C.; Ottani, S. *Acta Crystallogr.* **1998**, *C54*, 415 417. (g) Singh, T. P.; Vijayan, M. *J. Chem. Soc., Perkin Trans.* **1977**, *2*, 693 699.

(24) (a) Fonari, M. S.; Ganin, E. V.; Tang, S.-W.; Wang, W.-J.; Simonov, Yu. A. *J. Mol. Struct.* **2007**, *826*, 89 95. (b) Fonari, M. S.; Ganin, E. V.; Simonov, Yu. A.; Wang, W.-J. *Acta Crystallogr.* **2006**, *E62*, o911 o913. (c) Simonov, Yu. A.; Fonari, M. S.; Bocelli, G.; Calestani, G.; Lipkowski, J.; Suwinska, K.; Ganin, E. V. *Supramol. Chem.* **1995**, *4*, 251 258.

(25) (a) Basok, S. S.; Bocelli, G.; Fonari, M. S.; Ganin, E. V.; Simonov, Yu. A. *Acta Crystallogr.* **2006**, *C62*, o50 o52. (b) Moulton, B.; Luisi, B. S.; Fonari, M. S.; Basok, S. S.; Ganin, E. V.; Kravtsov, V. Ch. *New J. Chem.* **2007**, *31*, 561 568.

(26) Fonari, M. S.; Kravtsov, V. Ch.; Simonov, Yu. A.; Basok, S. S.; Ganin, E. V. Supramolecular Architecture in the Co-Crystals of Azacrown Ethers with Salicylic Acid. Moldavian-Polish-Ukrainian Symposium on Supramolecular Chemistry, Chisinau, Moldova, October 10−12, **2005**, Abstracts, p 65.

(27) Haynes, D. A.; Jones, W.; Motherwell, W. D. S. *J. Pharm. Sci.* **2005**, *94*, 2111 2120.

(28) (a) Ratajczak, H.; Sobczyk, L. *J. Chem. Phys.* **1969**, *50*, 556 557. (b) Li, Z. J.; Abramov, Yu.; Bordner, J.; Leonard, J.; Medek, A.; Trask, A. V. *J. Am. Chem. Soc.* **2006**, *128*, 8199 8210.

(29) (a) Hetzer, H. B.; Robinson, R. A.; Bates, R. G. *J. Phys. Chem.* **1968**, *72*, 2081 2086. (b) Kodama, M.; Kimura, E. *J. Chem. Soc., Dalton Trans.* **1980**, 327 333. (c) Pesavento, M.; Profumo, A.; Soldi, T.; Fabbrizzi, L. *Inorg. Chem.* **1985**, *24*, 3873 3875. (d) El-Harakany, A. A.; Abdel Halima, F. M.; Barakat, A. O. *J. Electroanal. Chem.* **1984**, *162* (1−2), 285 305.

(30) Sheldrick, G. M. *Acta Crystallogr.* **2008**, *A64*, 112 122.

(31) Macrae, C. F.; Edgington, P. R.; McCabe, P.; Pidcock, E.; Shields, G. P.; Taylor, R.; Towler, M.; van de Streek, J. *J. Appl. Crystallogr.* **2006**, *39*, 453 457.

(32) Spek, A. L. *J. Appl. Crystallogr.* **2003**, *36*, 7 13.

(33) The successful attempts are reported to fine-tune melting points and aqueous solubility by incorporation of an API within a series of crystalline solids characterized by considerable structural consistency: (a) Aakeroy, Ch. B.; Forbes, S.; Desper, J. *J. Am. Chem. Soc.* **2009**, *131*, 17048 17049. (b) Stanton, M. K.; Bak, A. *Cryst. Growth Des.* **2008**, *8*, 3856 3862.

(34) (a) Re, S.; Nagase, S. *Chem. Commun.* **2004**, 658 659. (b) Nishio, M. *CrystEngComm* **2004**, *6* (27), 130 158.

(35) Braga, D.; Grepioni, F.; Todesco, E. *Organometallics* **1998**, *17*, 2669 2672.

(36) Gregson, R. M.; Glidewell, C.; Ferguson, G.; Lough, A. L. *Acta Crystallogr.* **2000**, *B56*, 39 57.

(37) (a) Tusvik, P. H.; Mostad, A.; Dalhus, B.; Rosenqvist, E. *Acta Crystallogr.* **1999**, *C55*, 1113 1115. (b) Ng, S. W. Z. *Kristallogr.* **1995**, *210*, 287 289.

(38) Castellari, C.; Ottani, S. *Acta Crystallogr.* **1997**, *C53*, 482 486.

(39) Infantes, L.; Fabian, L.; Motherwell, W. D. S. *CrystEngComm* **2007**, *9*, 65 71.

(40) Rodriguez-Spong, B.; Price, Ch.P.; Jayasankar, A.; Matzger, A. J.; Rodriguez-Hornedo, N. *Adv. Drug. Delivery Rev.* **2004**, *56*, 241 274.

(41) Morris, K. R. In *Polymorphism in Pharmaceutical Solids*; Brittain, H. G., Ed.; Marcel Dekker Inc.: New York, 1999, 125−181.
(42) Gillon, A. L.; Feeder, N.; Davey, R. J.; Storey, R. *Cryst. Growth Des.* **2003**, *3*, 663 673.
(43) Desiraju, R. G. *J. Chem. Soc., Chem. Commun.* **1991**, 426 428.
(44) Infantes, L.; Chisholm, J.; Motherwell, S. *CrystEngComm* **2003**, *5*, 480 486.
(45) Kiang, Y.-H.; Xu, W.; Stephens, P. W.; Ball, R. G.; Yasuda, N. *Cryst. Growth Des.* **2009**, *9*, 1833 1843.
(46) Clarke, H. D.; Arora, K. K.; Bass, H.; Kavuru, P.; Ong, T. T.; Pujari, T.; Wojtas, L.; Zaworotko, M. J. *Cryst. Growth Des.* **2010**, *10*, 2152 2167.
(47) (a) Tsuzuki, S.; Honda, K.; Uchimaru, T.; Mikami, M.; Fujii, A. *J. Phys. Chem. A* **2006**, *110*, 10163 10168. (b) Tsuzuki, S.; Fujii, A. *Phys. Chem. Chem. Phys.* **2008**, *10*, 2584 2594.
(48) (a) Nishio, M.; Umezawa, Y.; Honda, K.; Tsuboyama, S.; Suezawa, H. *CrystEngComm* **2009**, *11*, 1757 1788. (b) Bissantz, C.; Kuhn, B.; Stahl, M. *J. Med. Chem.* doi: 10.1021/jm100112j.
(49) Kobayashi, Y.; Saigo, K. *J. Am. Chem. Soc.* **2005**, *127*, 15054 15060.

Додаток Щ.

Копія статті. “ Structural study of salicylic acid salts of a series of azacycles and azacrown ethers ”

Structural study of salicylic acid salts of a series of azacycles and azacrown ethers

Marina S. Fonari[a*], Eduard V. Ganin[b], Stepan S. Basok[c], Konstantin A. Lyssenko[d], Michael J. Zaworotko[e], Victor Ch. Kravtsov[a]

Dedicated to the memory of Yurii A. Simonov

[a] *Institute of Applied Physics, Academy of Sciences of Moldova, Academiei str., 5 MD-2028 Chişinău, R. Moldova. e-mail: fonari.xray@phys.asm.md; kravtsov.xray@phys.asm.md*
[b] *Odessa State Environmental University, Lvovskaya str., 15, 65016, Odessa, Ukraine*
[c] *A.V. Bogatsky Physico-Chemical Institute, National Academy of Sciences of Ukraine, Lustdorfskaya doroga 86, 650080, Odessa, Ukraine*
[d] *A. N. Nesmeyanov Institute of Organoelement Compounds, Russian Academy of Sciences, 28 Vavilov St., B-334, 119991, Moscow, Russia*
[e] *Department of Chemistry, University of South Florida, CHE205, 4202 East Fowler Avenue, Tampa, Florida 33620*

ABSTRACT: Interaction of salicylic acid (**saH**) with azacycles piperidine (**pipe**), and *meso*-5,7,7,12,12,14-hexamethyl-1,4,8,11-tetraazacyclotetradecane (**teta**), and aza-crown ethers, aza-12-crown-4 (**A12C4**), benzoaza-15-crown-5 (**BA15C5**), aza-18-crown-6 (**A18C6**), and diaza-18-crown-6 (**DA18C6**), afforded the proton-transfer complexes of the compositions **[pipeH][sa]**, **[tetaH$_2$][sa]$_2$**, **[BA15C5H][sa]**, **[A18C6H][sa]·2H$_2$O**, and **[DA18C6H$_2$][sa]$_2$·3H$_2$O**, whose structures were determined by single crystal X-ray diffraction. The same products were obtained in the same synthetic conditions starting from acetylsalicylic acid (aspirin) as a results of hydrolysis. Proton transfer is observed in all six structures, and the charge-assisted hydrogen-bond interactions provide the main driving force for direct binding of **sa** with protonated ammonium moieties. The crystal packing arrangement is also supported by weak hydrogen bonding, π-π and molecular dipole-dipole interactions.

The crystal engineering of multicomponent systems including active pharmaceutical ingredient (API) has attracted much attention in recent years because the physicochemical properties of the API can be changed, thereby altering the pharmaceutical profile of the APIs. Particularly relevant in this context is aqueous solubility, which can critically influence the ADMET (absorption, distribution, metabolism, excretion, and toxicity) properties of an API. Lipophilicity is another key parameter that influences ADMET properties as only APIs with the appropriate lipophilicity can cross the blood brain barrier for uptake by the brain. Modern strategies to affect these parameters typically focus on salt and cocrystal formation or medicinal chemistry approaches that rely on covalent transformations of the API.[1] Organic acids, especially carboxylic acids, represent ca. 30% of APIs and they are also widely used as salt or cocrystal formers.[2-3] We have recently reported five crystal structures formed by reacting of *p*-aminobenzoic acid, which is topically used as a sunscreen agent in various pharmaceutical preparations, with azacycles and aza-crown ethers.[4] We have also reported the crystal structures of four proton-transfer complexes of mefenamic acid, a poorly soluble anti-inflammatory agent, with aza-cycles of different dimensionality.[5] Our aim was to study the supramolecular synthons that occur between the cation and anion and to determine the contribution of weak interactions to the overall crystal packing. We report herein a new investigation along these lines by reporting how other aromatic pharmaceutical acids react with aza-cycles and crown ethers, thereby

For Review Only

offering a new opportunity to study how both strong and weak hydrogen bonding interactions as well as aromatic stacking interactions influence crystal packing of APIs. Salicylic acid (2-hydroxybenzoic acid, **saH**) represents an attractive target for this purpose. Salicylic acid, a key ingredient of skin-care products, has antiseptic, preservative, analgesic, and anti-inflammatory properties, covering a broad spectrum of applications,[6] and has also some similarities with aspirin both in its analgesic action and in its crystal packing arrangement[7] (the formation of a centrosymmetric $R_2^2(8)$ carboxylic acid dimer supramolecular homosynthon occurs in both aspirin polymorphs and the only reported crystal form of salicylic acid[8]). The planar dimers of **saH** are packed into a herringbone motif *via* interactions between *p*-H atoms and hydroxyl groups.[9] As with most APIs, **saH** is likely to be similar to other APIs in that it should be amenable to formation of cocrystals or salts,[10] form multiple stoichiometry variants of salts and cocrystals,[11] and dependening upon which method of preparation is employed, there also exist the possibilities of solvates, hydrates and polymorphic forms. Indeed, the reproducibility of the reaction products is unlikely to be consistent over "routine" solvent crystallization, mechanochemical approaches,[12] and melt crystallization *via* the Kofler mixed fusion method.[13] Along with the study of crystalline multicomponent compounds, the use of ionic liquids formed between pharmaceutically active ions and pharmaceutically acceptable counterions has recently been suggested by Rogers and co-workers. The salicylate anions has been used in this context.[14] **saH** has already been shown to exist as either a cocrystal former or an anions in multicomponent crystals within the cocrystal-salt continuum.[15] In the Commentary by Haynes and co-workers[16] based on the CSD statistics (ConQuest[17] version 1.6 on version 5.25 of the CSD[18]), salicylic acid is cited as a component of 19 salts, 7 neutral cocrystals, 1 ionic cocrystal, and 3 cocrystals of salts. This list has since been augmented by salicylic acid and DABCO, phenazine, diacetylpiperazine,[10] 3,5-dimethyl-1H-pyrazole,[11] caffeine,[12,19] and carbamazepine.[20] In this contribution we present details on the synthesis and structures of a new series of multiple component crystals that include salicylic acid and discuss in the context of a CSD analysis (version 5.31, release November 2009 including February and May 2010 updates). Table 1 presents a full list of compounds involving salicylic acid as a cocrystal former or counterion.

<Table 1 here>

Crown ethers represent a class of compound that are exceptionally versatile in that they can selectively bind a range of metal ions and a variety of organic neutral and ionic species.[57] Our long-term involvement in the crystal chemistry of crown ethers[58] explains our choice of crown ethers and aza-cycles as cocrystal formers or counterions. Structurally, when crown ethers are in their "crown" conformation they possess a hydrophobic ring surrounding a hydrophilic cavity, which enables them to form stable complexes with metal ions, and at the same time to be incorporated in the lipid fraction of the cell membrane. Aza-crowns have complexation properties that are intermediate between those of all-oxygen crown ethers, which complex strongly with alkali, alkaline earth, and primary ammonium cations, and those of all-nitrogen cyclams, which complex strongly with the transition metal and heavy metal cations. Contrary to azacycles (mainly cyclen and cyclam derivatives), which are widely studied and explored in medicinal chemistry,[59] the toxicity of crown ethers has limited their study to anticancer agents. In this context, recent studies demonstrate that crown compounds could either induce toxicities that are different from those of conventional antitumor drugs, or complement drugs in current use.[60] Our present study demonstrates the possibility to develop further multicomponent crystalline solids from such macrocycles and thereby modify their physicochemical properties. The cyclic *N*-bases, aza-cycles and aza-crown ethers studied herein represent a variety of sizes and number of *N*-basic centers, and are illustrated in Scheme 1.

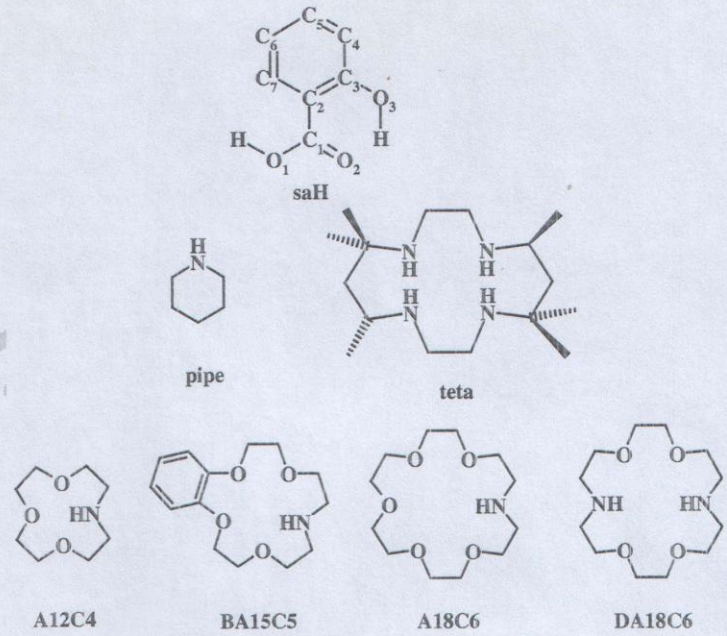

Scheme 1. Target salicylic acid and cyclic aza-molecules with the numbering scheme

In solution ΔpK_a is a useful measure of determining the outcome of an acid-base reaction since salt formation is expected to happen when ΔpKa is greater than 2 or 3.[15] In light of the relative strength of salicylic acid (pK_a = 2.97) and high pK_a values for the bases in Scheme 1 (they fall in the range 8.2-12.6)[61], we expect proton transfer to form proton-transfer complexes[62] or organic salts. Depending on the number and relative arrangement of nitrogen atoms within the molecule, the cyclic bases studied herein were expected to form with **saH** either of two different types of molecular assemblies sustained by hydrogen bonds. Formation of the 1:1 salts was expected for **pipe**, **A12C4**, **BA15C5**, and **A18C6** whereas **teta** and **DA18C6**, with four and two NH-groups, respectively, were expected to form 1:2 salts. In this study we also analyze the crystal packing in these new structures with an emphasis on the general features that could be more broadly relevant in the context of crystal design.

Experimental Section

All chemicals were of analytical grade and were used without further purification. Salts were obtained by mixing of equimolar amounts of the corresponding macrocycle and **saH** (or acetylsalicylic acid) dissolved in water-methanol solution. Suitable microanalyses for C, H, and N were obtained for all compounds using a Perkin Elmer 240 C device.

Salicylic acid with piperidine, [pipeH][sa]. Piperidine (85 mg, 1 mmol) and salicylic acid (138 mg, 1 mmol) were dissolved in methanol (25 ml) at 64 °C and then allowed to evaporate at room temperature. The yield of crystalline solid was close to quantitative. Transparent colorless crystals, soluble in methanol, ethanol, acetone, m.p. 108-110 °C. Found, % C, 64.51, H, 7.72, N, 6.29; required for $C_{12}H_{17}NO_3$%: C, 64.55%, H, 7.67%, N, 6.27%

Salicylic acid with *meso*-5,7,7,12,12,14-hexamethyl-1,4,8,11-tetraazacyclotetradecane, [tetaH$_2$][sa]$_2$. *Meso*-5,7,7,12,12,14-hexamethyl-1,4,8,11-tetraazacyclotetradecane (142 mg, 0.5 mmol) and salicylic acid (138 mg, 1 mmol) were

For Confidential ACS

dissolved in water: methanol (3ml : 10 ml) at 64 °C and allowed to slowly evaporate at room temperature. Transparent colorless crystals, soluble in methanol, ethanol, acetone, m.p. ≥ 280-282 °C (decomp). Found, % C, 64.31, H, 8.60, N, 9.94 required for $C_{30}H_{48}N_4O_6$ C, 64.26, H, 8.63, N, 9.99.

Salicylic acid with 1,4,7-trioxa-10-azacyclododecane, [A18C6H][sa]·2H$_2$O. 1,4,7-Trioxa-10-azacyclododecane (175 mg, 1 mmol) and salicylic acid (138 mg, 1 mmol) were dissolved in water: methanol (0.5 ml : 5 ml) at 64 °C and allowed to slowly evaporate at room temperature. The resulting solid was recrystallized from acetone : hexane (5ml : 5ml). Transparent colorless crystals, soluble in methanol, ethanol, acetone, m.p. 166-167°C (decomp). Found, % C, 57.54, H, 7.42, N, 4.43 required for $C_{15}H_{23}NO_6$: C, 57.50, H, 7.40, N, 4.47%.

Salicylic acid with 2,3,6,7,8,9,11,12-octahydro-5*H*-1,4,10,13,7-benzotetraoxazacyclopentadecine, [BA15C5H][sa]. 2,3,6,7,8,9,11,12-octahydro-5*H*-1,4,10,13,7-benzotetraoxaza-cyclopentadecine (134 mg 0.5 mmol) and salicylic acid (69 mg 0.5 mmol) were dissolved in water : methanol (1ml : 10 ml) at 64 °C and allowed to slowly evaporate at room temperature. Colorless, transparent crystals, soluble in methanol, ethanol, acetone, m.p. 140-141 °C. (decomp). Found, % C, 62.20, H, 6.75, N, 3.47 required for $C_{21}H_{27}NO_7$: C, 62.21, H, 6.71, N, 3.45.

Salicylic acid with 1,4,7,10,13-pentaoxa-16-azacyclooctadecane, [A18C6H][sa]·2H$_2$O. 1,4,7,10,13-pentaoxa-16-azacyclooctadecane (263 mg 1 mmol) and salicylic acid (138 mg 1 mmol) were dissolved in water : methanol (0.5 ml : 5 ml) at 64 °C, and allowed to slowly evaporate at room temperature. To obtain single crystals the resulting solid was recrystallized from acetone and hexane (5 ml : 5 ml). Transparent colorless crystals, soluble in methanol, ethanol, acetone, m.p. 83-85°C (decomp.). Found, % C, 52.13, H, 8.09, N, 3.26 required for $C_{19}H_{35}NO_{10}$: C, 52.16, H, 8.06, N, 3.20%.

Salicylic acid with 1,4,10,13-tetraoxa-7,16-diazacyclooctadecane, [DA18C6H$_2$][sa]$_2$·3H$_2$O. 1,4,10,13-tetraoxa-7,16-diazacyclooctadecane (132 mg 0.5 mmol) and (69 mg 0.5 mmol) salicylic acid were dissolved in water : methanol (1ml : 10 ml)at 64 °C, and allowed to slowly evaporate at room temperature. Transparent colorless crystals, soluble in methanol, ethanol, acetone, m.p. 156-157°C (decomp). Found, % C, 51.22, H, 8.33, N, 6.24 required for $C_{28}H_{44}N_4O_6S_4$ C, 50.87, H, 6.71, N, 8.48, S, 19.41.

Single-Crystal X-Ray Data Collection and Structure Determinations. X-Ray data for all complexes were collected on Bruker SMART-APEX CCD diffractometer using graphite-monochromated Mo-*K*α radiation at 100K. There was no intensity decay. Structure solutions were performed by direct methods (SHELXS-97) and refined by full-matrix least-squares methods on F^2 (SHELXL–97).[63] In all but **[DA18C6H$_2$][sa]$_2$·3H$_2$O** non–hydrogen atoms were refined anisotropically. In **[pipeH][sa]** all H-atoms were localized *via* the difference Fourier map and refined freely. In all the other structures H-atoms attached to carbons were included in idealized positions using a riding model with isotropic temperature factors 1.2 times that of the parent carbon atom, whereas those on N and O(water) atoms were found from difference Fourier maps and refined isotropically, except **[DA18C6H$_2$][sa]$_2$·3H$_2$O**, where such H atoms were not located. In **[A12C4H][sa]** the hydroxyl group in **sa** unit A is disordered with H atoms in the other *o*-position and was refined with occupancies of 0.55 and 0.45, respectively. The crystal structure of **[DA18C6H$_2$][sa]$_2$·3H$_2$O** was solved and refined in the centrosymmetric space group *P*-1. It is comprised of two similar but crystallographically independent complexes. In both complexes the crown ether molecule resides on the crystallographic inversion center, while both **sa** anions and water molecules occupy general positions and are disordered over two positions with equal occupancies. Analysis of the disordered positions and intermolecular contacts unambiguously showed that although each crown molecule resides on the inversion center, it has different-face environment, and each complex is non-centrosymmetric. The observed centrosymmetric structure is the result of superposition in the crystal of two generally non-centrosymmetric structures. Nevertheless, attempts to solve this structure in the non-centrosymmetric space group *P*1 did not change the disordering pattern for **sa** and water

molecules and did not show any deviation in geometrical parameters of macrocyclic molecule compared with that in centrosymmetric space group. The **sa** anions were refined isotropically using a rigid group approximation. The N-bound H-atoms were included in idealized positions in a riding model with isotropic temperature factors 1.2 times the parent nitrogen atom temperature factor. The disordered water molecule O1W was refined with the partial occupancy of 0.71. The poor crystal quality for compound **[DA18C6H$_2$][sa]$_2$·3H$_2$O** did not permit reliable placement of the H-atoms of the water molecules. Crystallographic data for structures reported in this paper have been deposited with the Cambridge Crystallographic Data Centre as supplementary publication CCDC Nos 779399 - 779404 Copies of these data can be obtained free of charge *via* http://www.ccdc.cam.ac.uk/conts/retrieving.html, or from the Director, CCDC, 12 Union Road, Cambridge CB2 IEZ, UK; fax: (+44) 1223-336-033; or e-mail: deposit@ccdc.cam.ac.uk. Structure graphics shown in the figures were created using the Mercury software package version 2.3.[64] Packing Index (PI) was calculated with the program PLATON.[65] Crystal data together with further details of the data collections and refinement are given in Table 2.

Results and Discussion

In two parallel series of synthesis we used as API acetylsalicylic acid (aspirin) or salicylic acid (**saH**), and as the bases aza cycles, piperidine and *meso*-5,7,7,12,12,14-hexamethyl-1,4,8,11-tetraazacyclotetradecane, aza-crown ethers, A12C4, BA15C5, A18C6, DA18C6, and crown ethers, 18C6, and *cis-syn-cis-* and *cis-anti-cis-* stereoisomers of dicyclohexyl-18C6. All reactions were carried out in similar synthetic conditions, by mixing of equimolar amounts of water-methanol solutions of **saH** or aspirin, and corresponding base. The new crystalline products were obtained only for *N*-bases, and their X-ray structural analysis indicated that in the reactions with aspirin due to its hydrolysis the final products represented the complexes of **saH** identical to those obtained starting from **saH** itself. The crystal structures of six new phases were determined by single-crystal X-ray diffraction. The structural features of all six solids are described below in succession. The carbon-oxygen bond distances in the carboxylic group in all structures were consistent with the deprotonated form (the C-O distances range within 1.240-1.278 Å, Table 3). In addition, the Fourier difference maps revealed that the acidic protons are positioned in the proximity to the *N*-atom of the cyclic molecule and the solids were classified as proton-transfer complexes or salts. Hydrogen bond parameters are listed in Table 4. The hydroxy group of **saH** is involved in an intramolecular O-H(hydroxy)···O(carboxy) hydrogen bond with the carboxylic group to form a $S_1(6)$ ring, consistent with other 2-hydroxybenzoic and 2-hydroxynaphthoic acids.[9,12]

[PipeH][sa] crystallizes in monoclinic $P2_1/c$ space group. The asymmetric unit consists of one piperidinium cation and one **sa** anion. Two cations and two anions form a centrosymmetric assembly giving rise to the $R_4^4(12)$ hetero synthon. The N(1)···O(1)(2-*x*, 1-*y*, 1-*z*) and N(1)···O(2) distances are equal to 2.721(1) and 2.771(1) Å, respectively (Fig. 1a, Table 4). The mean plane of piperidinium cation, which adopts chair conformation, and planar **sa** anion are inclined at a shallow angle of 39.4 °. The separated by the piperidinium cations two **sa** anions are at the O···O distance of 4.56 Å measured across an inversion center of heterotetramer. The heterotetramers are further combined into 2D layer parallel to the *bc* plane by C-H(**pipeH**)···O(3)(**sa**) hydrogen bond (C···O = 3.287, H···O = 2.39 Å, ∠CHO = 156°) which involves oxygen lone pare of 2-hydroxygroup. Thus, the layer is built of alternative four- and eight-membered H-bonded cycles. The **sa** anions related by the glide plane are arranged with *m/p* edge of one ring directed to the ring face of adjacent anion, and form a dihedral angle of 60.9°, the distance between centroids of aromatic rings being equal to 6.25 Å. The layer thickness corresponds to the shortest *a* axis (Fig. 1c). Adjacent layers are held together by van der Waals forces. The crystal density of 1.245 g cm^{-3} and packing coefficient (67.7%) of **[pipeH[[sa]** are significantly smaller than for salicylic acid itself (1.468 g cm^{-3}, 72.0%) and for the relative compounds discussed in[10].

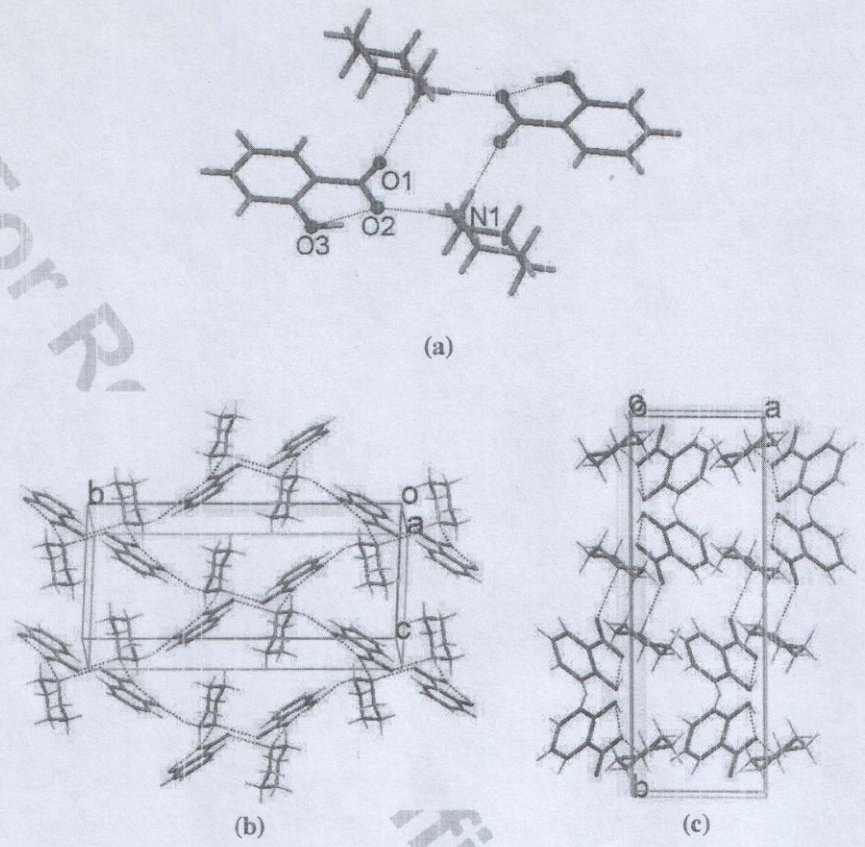

Fig. 1 Perspective views for **[pipeH][sa]**: (a) four-component complex defined by the $R_4^4(12)$ hydrogen-bond pattern; (b) H-bonded layer sustained by the combination of NH···O and CH···O interactions; (c) packing of the layers.

[TetaH$_2$][sa]$_2$. The anticipated hydrogen-bonded trimer **[sa][tetaH$_2$][sa]** resides around a crystallographic center of symmetry (Fig. 2a). The cation **[tetaH$_2$]**$^{2+}$ comprises four aminogroups, and generally captures two protons from acidic species to form a dication. The cycle conformation is folded by two intramolecular N(1)···N(2) = 2.775(2) Å hydrogen bonds (Table 4). The two **sa** anions act in a chelate mode across the macrocyclic cavity giving rise to two $R_3^3(8)$ rings, each including two intermolecular NH···O hydrogen bonds of 2.701(2) and 3.095(2) Å, and one above mentioned intramolecular hydrogen bond. The similar modes of the cycle protonation, and complex organization were registered in other complexes of teta with aromatic acids.[4,66] The **sa** moiety forms the dihedral angle of 70.5° with the mean plane of N_4-cyclic atoms. Although the O···O expansion between the inversion-related **sa** anions across the cycle increases up to 6.83 Å, the general packing motif bears close resemblance to **[pipeH][sa]**. The translated along *c* direction complexes are linked by the weak C-H· ·O hydrogen bonds involving 2-hydroxygroup (C···O = 3.474, H···O = 2.57 Å, ∠CHO = 153°) to form a ribbon (Fig. 2b). The edge-to-face arrangement of the **sa** anions across the ribbons is characterized by the dihedral angle of 84.08° and centroid-to-centroid distance of 5.28 Å, with the *m/p*-edge pointed towards the neighboring **sa** anion. Similar to **[pipeH][sa]** the layers pack along the shortest *a* axis, the thickness of the layer increases (Fig. 2c). The PI increases up to 69.4%.

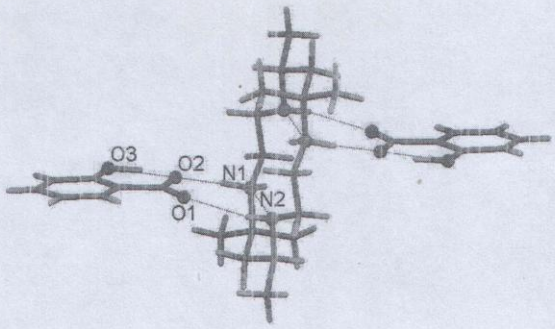

(a)

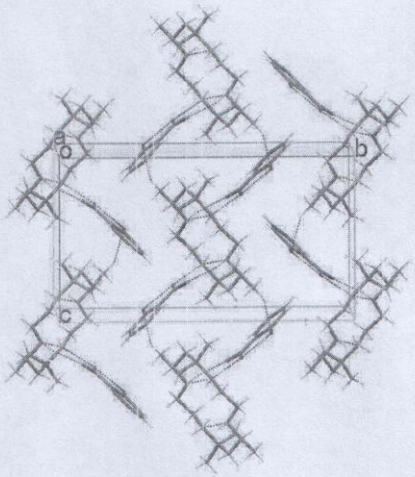

(b)

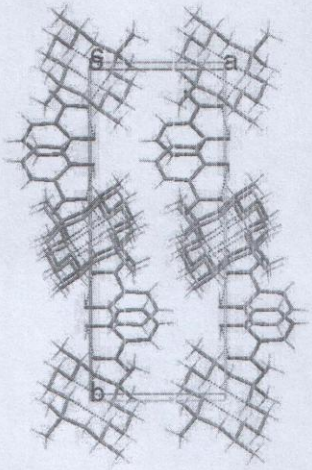

(c)

Fig. 2. Perspective views for **[tetaH$_2$][sa]$_2$**: (a) three-component complex defined by a $R_3^3(8)R_2^2(10)R_3^3(8)$ succession; (b) The layer sustained by the combination of NH···O, CH···O and π-π edge-to-face interactions; (c) packing of the layers.

[A12C4H][sa] crystallizes in monoclinic $P2_1/c$ space group. The asymmetric unit contains two **sa** anions (A and B), and two cyclic cations (A and B) (Fig. 3a,b). The conformation of both cycles is folded by the intramolecular N(1)···O(5) hydrogen bond (Table 4). The hydroxyl group in **sa** unit A is disordered with H atoms in the other *o*-position, while positions for all other atoms of the anion coincide.

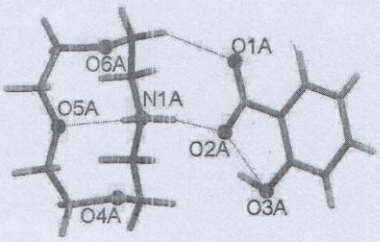

(a)

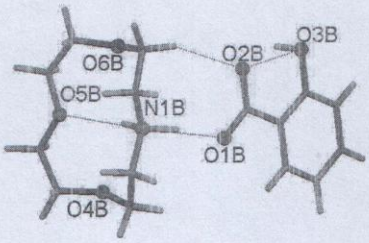

(b)

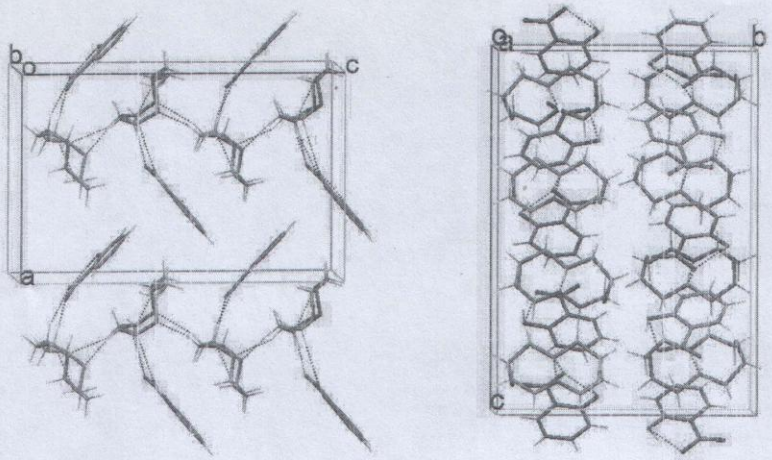

(c) (d)

Fig. 3. Perspective views for **[A12C4H][sa]**: (a-b) two-component units defined by $R_2^2(8)$ hydrogen-bond pattern. Only one position of hydroxyl group is shown for the disordered **sa**(A) anion; (c) the layer sustained by the combination of NH···O, CH···O, and π-π edge-to-face interactions; (d) packing of the layers.

The **sa**-cycle interactions occur in a chelate mode *via* strong NH···O hydrogen bonds, N(1A)···O(2A) = 2.655(3) and N(1B)···O(1B) = 2.635(3) Å, and weak CH···O hydrogen bonds, C(14A)···O(1A) = 3.356(4), C(14B)···O(2B) = 3.382(4) Å, giving rise to the $R_2^2(8)$ hydrogen-bonding non-planar pattern for both (A and B) formula units. The same mode of interaction was registered in the salt of *p*-aminobenzoic acid with **A12C4**.[4] The A and B complexes are associated into chains *via* weak CH(crown)···O(crown) interactions. The chains related by the translation *a* pack to maximize the edge-to-face interactions giving rise to the herringbone arrangement of the **sa** anions described by the **sa**(A)/**sa**(B) dihedral angle of 84.83°, and centroid-to-centroid distances of 5.19 Å and 5.29 Å for A/B and B/A pairs, respectively (Fig. 3c). The *p*-H atom of **sa**(B) pointed towards the hydroxyl group of the adjacent **sa**(A) anion, C(5B)···O(3A) = 3.741, H···O = 2.80 Å, while the *m/p* edge of **sa**(A) is above the translated B anion. The **sa** anions are completely buried within the layers parallel to the *ac* plane whose thickness is defined by the **A12C4H** cations (Fig. 3d). PI adopts the highest value of 71.5%.

[BA15C5H][sa] crystallizes in the triclinic *P*-1 space group. The asymmetric unit is comprised of one macrocyclic cation and one **sa** anion linked by single N(1)···O(1) = 2.626(2) Å hydrogen bond. The second oxygen atom of carboxylic group O(2) does not participate in any short intermolecular contacts (Fig. 4a). Although the second H-atom of azonia-group is pointed inside the macrocyclic cavity, all N(1)···O(crown) distances exceed the range of hydrogen-bonded contacts. The complexes stack along the shortest *a* direction (Fig. 4b, Table 2). The stacks related by the inversion center are packed in a way to maximize edge-to-face interactions between the **sa** anions and the aromatic rings of the macrocyclic cations providing the dihedral angle between the aromatic units of 89.1°, and the shortest centroid-to-centroid distance of 5.10 Å. The crystal structure reveals the dense crystal packing with PI being 70.7% (Fig. 4c).

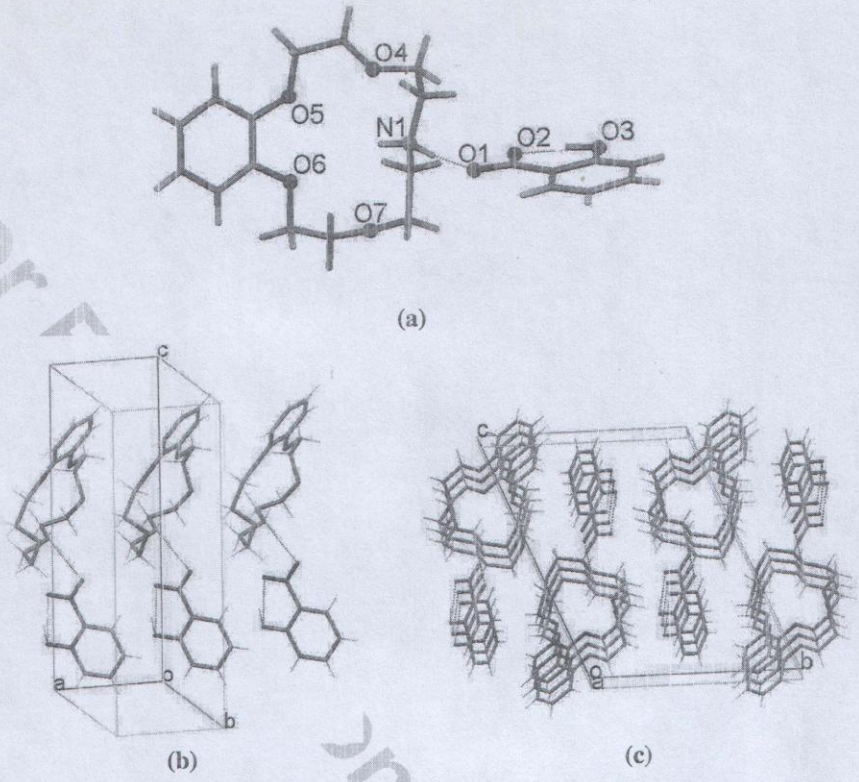

Fig. 4. Perspective views for **[AB15C5H][sa]**: (a) two-component complex; (b) stack along *a* direction; (c) crystal packing.

[A18C6H][sa]·2H$_2$O crystallizes in the orthorhombic *Pca*2$_1$ space group. The asymmetric unit is comprised of one macrocyclic cation, one **sa** anion and two water molecules (Fig. 5a). The charged units interact *via* a couple of hydrogen bonds, N(1)···O(1) = 2.775(2), and C(9)···O(2) = 3.413(3) Å acting in a chelate mode identical to that one registered in **[A12C4H][sa]** that in Etter's graph set notation can be described as $R_2^2(8)$ pattern. The **sa** anion is inclined at an angle of 43.9° to the NO_5-macrocyclic plane. Two water molecules fulfil different structural functions: water molecule associated with O1W centers the macrocyclic cavity, and acts as double H-bond donor and single H-bond acceptor forming three hydrogen bonds, and additionally links the O2W water molecule as H-acceptor (Table 4). The second water molecule O2W, acting as a double H-bond donor, bridges the complexes into chain along *c* axis (Fig. 5b). The related by the screw axis chains are packed in a double zipper-like mode with the partial mutual interdigitation of the macrocycles, and the herringbone edge-to-face arrangement of the **sa** anions being described by dihedral angle of 67.73° and centroid-to-centroid distance of 5.22 Å (Fig. 5c). The PI of 70.7% is the same as for **[BA15C5H][sa]**.

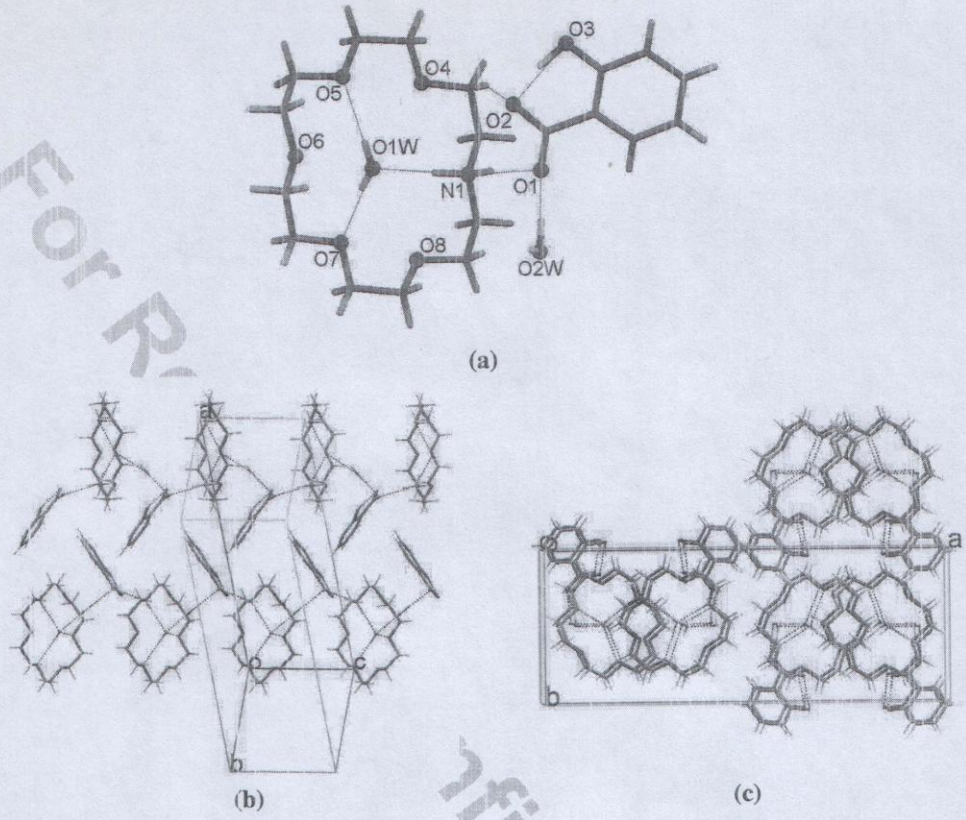

Fig. 5. Perspective views for **[A18C6H][sa]·2H$_2$O**: (a) formula unit; (b) edge-to-face interactions between adjacent chains; (c) crystal packing.

[DA18C6H$_2$][sa]$_2$·3H$_2$O crystallizes in the triclinic space group *P*-1. Crystal is built of two quite similar but crystallographically independent complexes [**sa** M][cycle A][**sa** N]·2H$_2$O and [**sa** P][cycle B][**sa** R]·2H$_2$O, so only one of them will be further discussed. The poor crystal quality does not permit to locate hydrogen atoms of water molecules and thus discuss the details of hydrogen bonding. Although the macrocyclic dication lies about an inversion center in the presented structure model, it has a different-face environment (see details in the experimental part, Fig. 6a, and Table 4). At one side of the crown ether the **sa** anion is linked with the macrocycle *via* NH···O(**sa**) hydrogen bond, while another oxygen atom of the carboxylate group interacts with the O1W water molecule being in a 'perching' position which mediates the macrocyclic cation and **sa** anion *via* short NH···Ow, Ocrown···Owater and Owater···O(sa) contacts. Another side of the macrocycle is also occupied by the water molecule O3W, that again mediates the **sa** anion and macrocycle, although being in a 'side position'. At this side the **sa** anion acts in a bidentate cyclic mode being coordinated to the same N(4) atom giving rise to the $R_1^2(4)$ hydrogen-bonding pattern. In both complexes the **sa** anions are arranged approximately perpendicular to the N_2O_4-plane of the macrocyclic cation, the corresponding dihedral angles being 80.3 and 86.45 ° for cycle A and 79.4 and 82.5° for cycle B, respectively. Water molecule O2W bridges the complexes in the chain along the *c* axis (Fig. 6b). Complexes in the chain are arranged in such a way that the dihedral angle between the N_2O_4 planes of A and B cycles equals to 58.0° that provides the arrangement of the adjacent **sa** anions being close to perpendicular (Fig. 6b). The adjacent chains meet by their **sa** anions that form again herringbone motif and are

arranged at an angle of about 87° with the centroid-to-centroid distances being in the range of 5.31-5.71 Å (Fig. 6c).

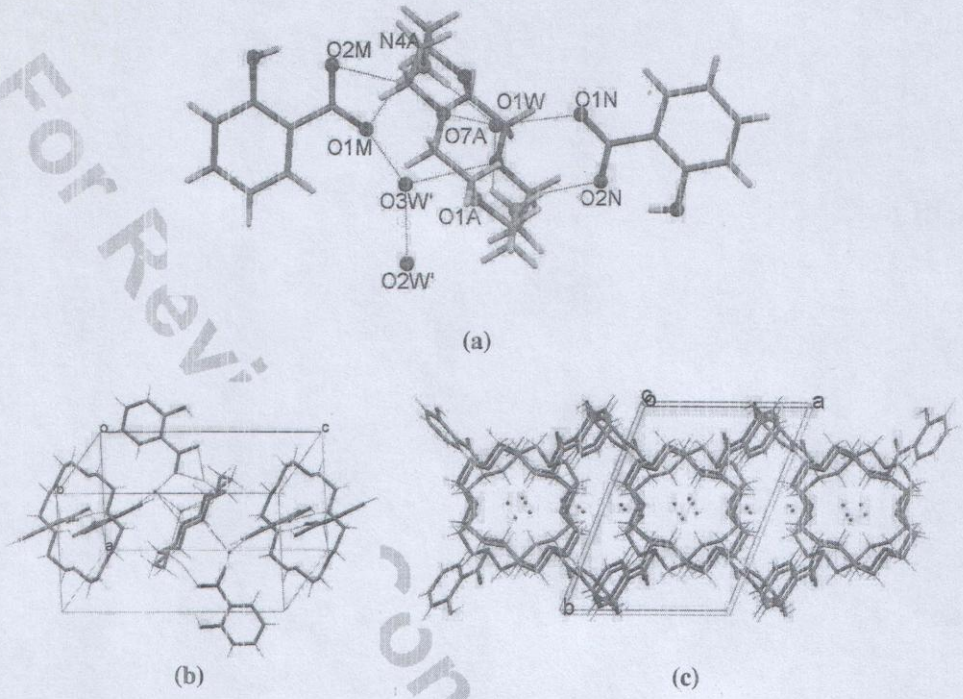

Fig. 6. Perspective views for **(DA18C6H$_2$)(sa)$_2$·3H$_2$O**: (a) view of the complex defined by macrocycle A; (b) hydrogen-bonding chain; (c) packing of the chains.

The examination of Table 1 and our results reveal that **saH** is readily co-crystallized with *N*-bases of aromatic and aliphatic nature. The cocrystals are predominantly formed *via* rearrangement of the $R_2^2(8)$ carboxylic acid homosynthon to the $R_2^2(8)$ carboxylic acid – amide (CSD refcodes DKPSAL10, SLCADC01, MOXWAY), $R_2^2(7)$ carboxylic acid – pyridine (SODDOF, ODOHEV, XOBCAT), or $R_2^2(8)$ carboxylic acid – amino–pyridine (GEYSAE) planar supramolecular heterosynthons sustained by two practically parallel hydrogen bonds. The proton transfer that follows the formation of salts is capable to occur either within the robust $R_2^2(8)$ hetero synthon in the case of topologic complementary of the components (EDATOS, FIXTAI, LEWROU, LOLDIA, DENXAW, CIQBIO, MIFWUT, SLCADB10, WEPTIV, XAGFAM), or disrupts it in favour of higher-dimensional aggregates (HURNEN, NIMDIW). In the case of salt bridges (BAKYES, BUSNIM, HABVIP, HABVOV, KAFSEQ, LUDDUJ, NICSAL, WANTOU, YAVRAO, YORJOF) hydrogen bond distances are shorter than those between neutral motifs and even one charge-assisted hydrogen bond as in NICSAL, and in **[BA15C5H][sa]** appears to be enough for stable structure. The water molecule that is typically inserted between the charged species often violates the predicted route of cocrystallization[67] and complicates the structural motifs (FIXTAI, HABVIP, HABVOV, KAFSEQ, WANTOU). The salts under discussion demonstrate the diverse modes of **sa** interactions with cyclic cations, being a bidentate-bridging mode in **[pipeH][sa]** built on two strong charge-assisted NH···O hydrogen bonds, chelate mode in **[tetaH$_2$][sa]$_2$** built again on a couple of strong NH···O hydrogen bonds, or on a combination of strong NH···O and weak CH···O hydrogen bonds in **[A12C4H][sa]**, and **[MA18C6H][sa]·2H$_2$O,** monodentate NH···O binding in **[BA15C5H][sa]**, and a combination of a bidentate cyclic $R_1^2(4)$ hydrogen bonding pattern and a bidentate chelate modes in

[DA18C6H$_2$][sa]$_2$·3H$_2$O. In spite of the variety of **sa**···cyclic azonia interactions all reported complexes invariably revealed at least one strong charge-assisted NH···O hydrogen bond. To estimate the reliability of such intermolecular interaction we have analyzed the CSD data (CSD v5.31, last update May 2010) involving in the search the aromatic carboxylic acids and cyclic amines relative to cyclic molecules reported herein in which nitrogen atom in sp^3-hybridization state may form H-bond. The searches were subjected to the following constraints: aromatic carboxylic group, either in neutral or deprotonated form, cyclic N$_{sp3}$-atom with at least two neighboring cyclic methylene groups, metal free structures, 3D coordinates present, repeated structures excluded. The survey of CSD revealed 165 hits that obey our requirements. These entries include structures with obviously wrong assigned type of atoms (C or N atoms) in piperazinediium moiety (KUFBIX, KUFBOD), disordered structures (EGODAF, NUKXOH) and structures where N-H atom was not located (JIHCIM, PIPCBZ, PIPHBZ, WIFBUI, ZEJNAD). In the last case the conclusions about the type of N···O bond was made on the basis of analysis of C-O distances in carboxylate group. Of 165 hits 132 (80%) exhibit NH$^+$···O(COO$^-$) hydrogen bond (Synthon I, Scheme 2), in 5 (3.0%) structures positively charged azonia-group forms H-bond with neutral carboxylic group (Synthon II), and 6 (3.6%) correspond to H-bonded interaction between neutral components (Synthon III). Thus, 143 (86.7%) hits revealed the intermolecular N···O H-bonded interaction. Of 132 structures with Synthon I type of interaction 61 represent hydrates, two hydrates were also observed in structures with synthons II (WIZXIN, WOVWEJ), and III (MIPVIQ, SIXBAD), respectively. Only in one structure (FIFFIK) insertion of water molecule destroys the robust NH$^+$···O(COO$^-$) Synthon I. The lack of the charge-assisted hydrogen bonds in the majority of remaining 22 structures (13.3%) is explained by the presence of competing more acidic groups. This observation and our previous investigations (*p*-aminobenzoic, mefenamic acids)[4,5] demonstrate the remarkable reliability of N···O interaction between cyclic amines/azonia and aromatic carboxylates, and promising potential for design of multiple component crystals on the base of such interactions.

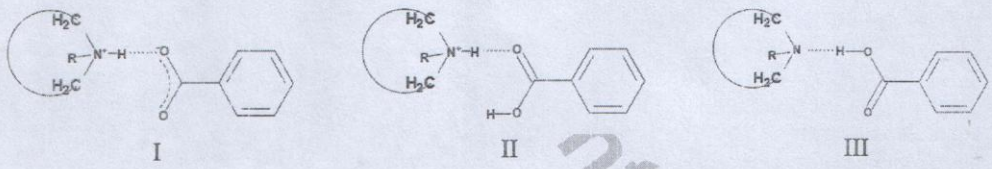

Scheme 2. Supramolecular heterosynthons observed between aromatic carboxylate ion or carboxylic acid, and cyclic azonia or amine molecule. R=H, C.

Along with the diverse types of **sa** – N-cycle interactions the salts demonstrate different mutual arrangement of the components, which changes from the 'side coordination' described by the shallow dihedral angle between the planes through the cyclic heteroatoms and planar skeleton of **sa** till the practically perpendicular arrangement. The corresponding dihedral angles are summarized in Table 3. In spite of the pronounced differences, the controlled by H-bonds packing motifs reveal some common features, namely the similar arrangement of the **sa** anions which preserve the herringbone edge-to-face packing pattern. Only in the case of **[BA15C5H][sa]**, where crown ether possesses the own aromatic moiety, the **sa/sa** interactions are substituted by the **sa/Ar** interactions, but the interactions between the aromatic units still preserve. Thus, our results are in line with the conclusion made by Childs with co-workers for carbamazepine containing structures[20] that interactions in the packing motif are cumulatively stronger than the hydrogen bonding motifs in the family of structures containing the same target molecule.

Conclusion

Six novel salts of salicylic acid (**saH**) with aza cycles piperidine, and *meso*-5,7,7,12,12,14-hexamethyl-1,4,8,11-tetraazacyclotetradecane, and aza-crown ethers aza-12C4, benzoaza-15C5, aza-18C6, and diaza-18C6 were synthesized in similar synthetic conditions and characterized by X-ray diffraction analysis. All salts are sustained by the combination of charge-assisted and conventional hydrogen bonds. The edge-to-face arrangement of the **sa** anions as the stable supramolecular motif preserves in all but one crystals.

Supporting Information Available: X-ray crystallographic information in CIF format This information is available free of charge via the Internet at http://pubs.acs.org.

References

(1) (a) Nehm, S. J.; Rodríguez-Spong, B.; Rodríguez-Hornedo, N. *Cryst. Growth Des.* **2006,** *6*, 592-600; (b) Trask, A. V. *Mol. Pharmaceutics* **2007,** *4(3)*, 301-309; (c) Stahl, P.H. Wermuth, C.G. Handbook of Pharmaceutical Salts : Properties, Selection, and Use; Wiley-VCH/VHCA: Weinheim/Zurich **2002**; (d) Aakeroy, C. B. *Acta Crystallogr.* **1997,** *B53*, 569-586; (e) Maheshwari, C.; Jayasankar, A.; Khan, N. A.; Amidon, G. E.; Rodríguez-Hornedo N. *CrystEngComm* **2009,** *11*, 493-500; (f) Shan, N.; Zaworotko, M. J. *Drug Discovery Today* **2008,** *13*, 440-446; (g) Lipinski, C. A.; Lombardo, F.; Dominy, B. W.; Feeney, P. J. *Adv. Drug Delivery Rev.* **1997**, *23*, 3-25; (h) Banks, W. A.; Kastin, A. J. *Brain Res. Bull.* **1985**, *15*, 287-292; (i) Begley, D. J. *J. Pharm. Pharmacol.* **1996**, *48*, 136-146; (g) Huang, L. F., Tong, W. Q. *Adv. Drug Delivery Rev.* **2004**, *56*, 321-334; (k) Lednicer, D.; *Strategies for Organic Drug Synthesis and Design;* Wiley: New York, **1998.**

(2) (a) Andrews, G. P.; Zhai, H.; Tipping, S.; Jones, D. S.; *J. Pharm. Sci.* **2009**, *98*, 4545-4556; (b) Fang, L.; Numajiri, S.; Kobayashi, D.; Ueda, H.; Nakayama, K.; Miyamae, H.; Morimoto, Y. *J. Pharm. Sci.* **2004**, *93*, 144-154; (c) Du, M.; Zhang, Z.-H.; Guo, W.; Fu, X.-J. *Cryst. Growth Des.* **2009**, *9*, 1655-1657; (d) Nichol, G. S.; Clegg, W. *Cryst. Growth Des.* **2009**, *9*, 1844-1850.

(3) (a) Remenar, J. F.; Morissette, S. L.; Peterson, M. L.; Moulton, B.; MacPhee, J. M.; Guzmán, H. R.; Almarsson, Ö. *J. Am. Chem. Soc.* **2003**, *125*, 8456-8457; (b) Childs, S. L.; Hardcastle, K. I. *Cryst. Growth Des.* **2007,** *7*, 1291-1304; (c) Childs, S. L.; Chyall, L. C.; Dunlap, J. T.; Smolenskaya, V. N.; Stahly, B. C.; Stahly, G. P. *J. Am. Chem. Soc.* **2004,** *126*, 13335-13342; (d) Schultheiss, N.; Lorimer, K.; Wolfe, S.; Desper, J. *CrystEngComm* **2010,** *12*, 742-749; (e) Orola, L.; Veidis, M. V. *CrystEngComm* **2009**, *11*, 415-417; (f) Bak, A.; Gore, A.; Yanez, E.; Stanton, M.; Tufekcic, S.; Syed, R.; Akrami, A.; Rose, M.; Surapaneni, S.; Bostick, T.; King, A.; Neervannan, S.; Ostovic, D.; Koparkar, A. *J. Pharm. Sci.* **2008,** *97*, 3942-3956; (g) Viertelhaus, M.; Hilfiker, R.; Blatter, F. *Cryst. Growth Des.* **2009,** *9*, 2220-2228; (h) Stanton, M. K.; Bak, A. *Cryst. Growth Des.* **2008,** *8*, 3856.

(4) Moulton, B.; Luisi, B. S.; Fonari, M. S.; Basok, S. S.; Ganin, E. V.; Kravtsov, V. Ch. *New J. Chem.* **2007** *31* 561-568.

(5) Fonari, M. S.; Ganin, E. V.; Vologzhanina, A. V.; Antipin, M. Yu.; Kravtsov, V. Ch. *Cryst. Growth Des.* 2010 DOI: 10.1021/cg100518b

(6) (a) Mackowiak, P.A. "Brief History of Antipyretic Therapy"; *Clinical Infectious Diseases*, **2000,** *31*(Suppl 5), S154-6; (b) Wu, K. K. *Anti-Inflammatory & Anti-Allergy Agents in Medicinal Chemistry,* **2007,** *6*, 278-292.

(7) (a) Wheatley, P. J. *J. Chem. Soc.* **1964,** 6036-6048; (b) Vishweshwar, P. McMahon, J.A. Oliveira, M. Peterson, M.L. Zaworotko, M. J. *J. Amer. Chem. Soc.* **2005,** *127*, 16802-

16803; (c) Caira, M. R. *J. Crystallogr. Spectrosc. Res.* **1992**, *22*, 193-200; (d) Caira, M.R. *J. Chem. Crystallogr.* **1994,** *24,* 695-701; (e) Bond, A. D.; Boese, R.; Desiraju, G. R. *Angew. Chem., Int. Ed.* **2007,** *46,* 618-622.

(8) Etter, M. C. *Acc. Chem. Res.* **1990,** *23,* 120-126.

(9) (a) Cochran, W. *Acta Crystallogr.* **1953,** *6,* 260-268; (b) Sundaralingam, M.; Jensen, L.H. *Acta Crystallogr.* **1965,** *18,* 1053-1058; (c) Bacon, G. E.; Jude, R. J. *Z. Kristallogr.,* **1973,** *138,* 19-40; (d) Bolte, M. *Private Communication* **2006**; (e) Munshi, P.; Row, T. N. G. *Acta Crystallogr.* **2006,** *B62,* 612-626.

(10) Skovsgaard, S.; Bond, A. D. *CrystEngComm* **2009**, *11*, 444-453.

(11) Lopez, C.; Claramunt, R. M.; Garcia, M. A.; Pinilla, E.; Torres, M. R.; Alkorta, I.; Elguero, J. *Cryst. Growth Des.* **2007,** *7,* 1176-1184.

(12) Bucar, D.-K.; Henry, R. F.; Lou, X.; Duerst, R. W.; MacGillivray, L.R.; Zhang, G. G. Z. *Cryst. Growth Des.* **2009,** *9,* 1932-1943.

(13) Berry, D. J.; Seaton, C. C.; Clegg, W.; Harrington, R. W.; Coles, S. J., Horton, P. N.; Hursthouse, M. B.; Storey, R.; Jones, W.; Friscic, T.; Blagden, N. *Cryst. Growth Des.* **2008,** *8,* 1697-1712.

(14) Bica, K.; Rogers, R. D. *ChemComm* **2010,** *46,* 1215-1217.

(15) (a) Aakeröy, C. B.; Fasulo, M. E.; Desper, J. *Mol. Pharmaceutics* **2007,** *4,* 317-322; (b) Childs, S. L.; Stahly, G. P.; Park, A. *Mol. Pharmaceutics*, **2007,** *4,* 323-338; (c) Hathwar,V. R.; Pal, R.; Guru Row, T. N. *Cryst. Growth Des.* Doi: 10.1021/cg100457r .

(16) Haynes, D. A.; Jones, W.; Motherwell, W. D. S. *J. Pharm. Sci.* **2005,** *94,* 2111-2120.

(17) Bruno, I. J.; Cole, J. C.; Edgington, P. R.; Kessler, M.; Macrae, C. F.; McCabe, P.; Pearson, J. ; Taylor, R. *Acta Crystallogr.* **2002,** *B58,* 389-397.

(18) Allen, F. N. *Acta Crystallogr.* **2002,** *B58,* 380-388.

(19) Lu, E.; Rodriguez-Hornedo, N.; Suryanarayanan, R. *CrystEngComm* **2008,** *10,* 665-668.

(20) Childs, S. L.; Wood, P. A.; Rodriguez-Hornedo, N.; Reddy, L. S.; Hardcastle, K. I. *Cryst. Growth Des.* **2009,** *9,* 1869-1888.

(21) Klepeis, J.-H. P.; Evans, W. J.; Zaitseva, N.; Schwegler, E.; Teat, S. J. *Acta Crystallogr.* **2009,** *E65,* o2062.

(22) Singh,T. P.; Vijayan, M. *Acta Crystallogr.* **1974,** *B30,* 557-562.

(23) Wang, K.-W.; Pan, Y.-J.; Jin, Z.-M.; *Z. Kristallogr.-New Cryst.Struct.* **2002,** *217,* 435-443.

(24) Shimizu, N.; Nishigaki, S.; Nakai, Y.; Osaki, K. *Acta Crystallogr.* **1983,** *C39,* 891-893.

(25) Shimizu, N.; Nishigaki, S.; Nakai, Y.; Osaki, K. *Acta Crystallogr.* **1984,** *C40,* 902.

(26) Thanigaimani, K.; Muthiah, P. T.; Lynch, D. E. *Acta Crystallogr.* **2007,** *E63,* o4555-o4556.

(27) Goswami, S.; Jana, S.; Hazra, A.; Fun, H.-K.; Anjum, S.; Atta-ur-Rahman, *CrystEngComm* **2006**, *8,* 712-718.

(28) Nishioka, F.; Nakanishi, I.; Fujiwara, T.; Tomita, K. *J. Incl. Phenom. Macrocycl. Chem.* **1984,** *2,* 701-714.

(29) Varughese, K. I.; Kartha, G. *Acta Crystallogr.* **1982,** *B38,* 301-302.

(30) Prabakaran, P.; Murugesan, S.; Muthiah, P. T.; Bocelli,G.; Righi, L. *Acta Crystallogr.* **2001,** *E57,* o933-o936.

(31) Bartoszak-Adamska, E.; Dega-Szafran, Z.; Przedwojska, M.; Jaskolski, M. *Pol. J. Chem.* **2003**, *77,* 1711-1722.

(32) Zhang, J.-N.; Shi, M.; Li, Q. *Chin. J. Struct. Chem.* **2005,** *24,* 151-158.

(33) Patel, U.; Haridas, M.; Singh, T. P. *Acta Crystallogr.* **1988,** *C44,* 1264-1267.

(34) Koh, L. L.; Xu, Y.; Gan, L.M., Chew, C.H.; Lee, K.C. *Acta Crystallogr.* **1993,** *C49* 1032-1035.

(35) Smith, G.; Wermuth, U. D.; White, J. M. *CrystEngComm* **2003,** *5,* 58-61.

For Review Confidential - ACS

(36) Byriel, K. A.; Gasperov, V.; Gloe, K.; Kennard, C. H. L.; Leong, A. J.; Lindoy, L. F.; Mahinay, M. S.; Pham, H. T.; Tasker, P. A.; Thorp, D.; Turner, P. *Dalton Trans.* **2003,** 3034-3040.
(37) Lynch, D. E.; Smith, G.; Freney, D.; Byriel, K. A.; Kennard, C. H. L. *Aust. J. Chem.* **1994,** *47,* 1097-1115.
(38) Byres, M.; Cox, P. J.; Kay, G.; Nixon, E. *CrystEngComm* **2009,** *11,* 135-142.
(39) Flippen-Anderson, J. L.; Deschamps, J. R.; Brossi, A.; Greig, N. H. *Acta Crystallogr.* **2002,** *E58,* o853-o855.
(40) Panneerselvam, P.; Stanley, N.; Muthiah, P. T. *Acta Crystallogr.* **2002,** *E58,* o180-o182.
(41) Kim, H. S.; Jeffrey, G. A. *Acta Crystallogr.* **1971,** *B27,* 1123-1131.
(42) Jebamony, J. R.; Muthiah, P. T. *Acta Crystallogr.* **1998,** *C54,* 539-540.
(43) Limmatvapirat, S.; Yamaguchi, K.; Yonemochi, E.; Oguchi, T.; Yamamoto, K. *Acta Crystallogr.* **1997,** *C53,* 803-805.
(44) Tamura, C.; Yoshikawa, M.; Sato, S.; Hata, T. *Chem. Lett.* **1973,** 1221-1224.
(45) Gellert, R. W.; Hsu, I.-N. *J. Crystallogr. Spectrosc. Res.* **1983,** *13,* 99-105
(46) Gellert, R. W.; Hsu, I-N. *Acta Crystallogr.* **1988,** *C44,* 311-313.
(47) Oleksyn, B. J.; Serda, P. *Acta Crystallogr.* **1993,** *B49,* 530-534.
(48) Muthiah, P. T.; Balasubramani, K.; Rychlewska, U.; Plutecka, A. *Acta Crystallogr.* **2006,** *C62,* o605-o607.
(49) Fleck, M.; Tillmanns, E.; Haussuhl, S. *Z. Kristallogr.-New Cryst. Struct.* **2000,** *215,* 105-106.
(50) McMahon, J. A.; Bis, J. A.; Vishweshwar, P.; Shattock, T. R.; McLaughlin, O. L.; Zaworotko, M. J. *Z. Kristallogr.* **2005**, *220,* 340-350.
(51) Pertlik, F.; Mikenda, W.; Steinwender, E. *J. Crystallogr. Spectrosc. Res.* **1993,** *23,* 389-395.
(52) Takata, N.; Shiraki, K.; Takano, R.; Hayashi, Y.; Terada, K. *Cryst. Growth Des.* **2008,** *8,* 3032-3037.
(53) Du, L.; Zeng, W.; Liu, X.; Jian, F.-F. *Acta Crystallogr.* **2009,** *E65,* o1791.
(54) Bartoszak-Adamska, E.; Dega-Szafran, Z.; Krociak, M.; Jaskolski, M.; Szafran, M. *J. Mol. Struct.* **2009,** *920,* 68-74.
(55) Chitradevi, A.; Athimoolam, S.; Sridhar, B.; Asath Bahadur S. *Acta Crystallogr.* **2009,** *E65,* o3041-o3042.
(56) Reddy, L. S.; Bethune, S. J.; Kampf, J. W.; Rodriguez-Hornedo, N. *Cryst. Growth Des.* **2009,** *9,* 378-385.
(57) Pedersen, C. J. *J. Am. Chem. Soc.* **1967,** *89,* 2495-2496.
(58) (a) Simonov, Yu. A.; Fonari, M. S.; Lipkowski, J.; Ganin, E. V.; Yavolovskii, A. A.; Kamalov, G. L. *J. Struct. Chem.* **2009,** 50(*Supp.*1), S136-S142; (b) Fonari, M. S.; Furmanova, N. G.; Simonov, Yu. A. *J. Struct. Chem.* **2009,** *50(Supp.1),* S124-S135.
(59) (a) Delgado, R.; Felix, V.; Lima, L. M. P.; Price, D. W. *Dalton Trans.* **2007,** 2734-2745; (b) Chen, T.; Wang, X.; He, Y.; Zhang, C.; Wu, Z.; Liao, K.; Wang, J.; Guo, Z. *Inorg. Chem.* **2009,** *48,* 5801-5809.
(60) (a) Gokel, G. W.; Leevy, W. M.; Weber, M. E. *Chem. Rev.* **2004,** *104,* 2723-2750; (b) Kralj, M.; Tusek-Bozić, L.; Frkanec, L. *ChemMedChem.* **2008,** *3,* 1478-1492; (c) Marjanović, M.; Kralj, M.; Supek, F.; Frkanec, L.; Piantanida, I.; Šmuc, T.; Tušek-Božić, L. *J. Med. Chem.* **2007,** *50,* 1007-1018.
(61) ACD Lab Version 4.56/26; Advanced Chemical Development Inc., Toronto, Canada **2000**.
(62) Li, Z. J.; Abramov, Y.; Bordner, J.; Leonard, J.; Medek, A.; Trask, A. V. *J. Am. Chem. Soc.* **2006,** *128,* 8199-8210.
(63) Sheldrick, G. M. *Acta Crystallogr.* **2008**, *A64*, 112-122.

(64) Macrae, C. F.; Edgington, P. R.; McCabe, P.; Pidcock, E.; Shields, G. P.; Taylor, R.; Towler, M.; van de Streek, J. *J. Appl. Crystallogr.* **2006,** *39,* 453-457.
(65) Spek, A. L. *J. Appl. Crystallogr.* **2003,** *36,* 7-13.
(66) (a) Gregson, R. M.; Glidewell, C.; Ferguson, G.; Lough, A. J. *Acta Crystallogr.* **2000,** *B56,* 39-57; (b) Lough, A. J.; Gregson, R. M.; Ferguson, G.; Glidewell, C. *Acta Crystallogr.* **2000,** *B56,* 85-93; (c) MacLean, E. J.; Teat, S. J.; Farrell, D. M. M.; Ferguson, G.; Glidewell, C. *Acta Crystallogr.* **2002,** *C58,* o470-o473.
(67) (a) Infantes, L.; Fabian, L.; Motherwell,W. D. S. *CrystEngComm* **2007,** *9,* 65-71; (b) Clarke, H. D.; Arora, K. K.; Bass, H.; Kavuru, P.; Ong, T. T.; Pujari, T.; Wojtas, L.; Zaworotko, M. J. *Cryst. Growth Des.* **2010**, *10*, 2152–2167

For Review - Confidential - ACS

Додаток Ю.

Копія статті. “ From chains to ladders in the co-crystals with 2,3-thiophene-15-crown-5, 2,3-naphtho-15-crown-5, and bis-(18-crown-6)-stilbene constructed by weak hydrogen bonding”

PAPER www.rsc.org/crystengcomm | CrystEngComm

From chains to ladders in co-crystals with 2,3-thiophene-15-crown-5, 2,3-naphtho-15-crown-5, and bis-(18-crown-6)-stilbene constructed by weak hydrogen bonding†

Eduard V. Ganin,[a] Stepan S. Basok,[b] Arkadii A. Yavolovskii,[b] Mark M. Botoshansky[c] and Marina S. Fonari*[d]

Received 30th April 2010, Accepted 6th August 2010
DOI: 10.1039/c005284c

For the first time a series of co-crystals of 2,3-thiophene-15-crown-5 **1**, 2,3-naphtho-15-crown-5 **2**, bis-(18-crown-6)-stilbene **3** with dithiooxamide **a**, 1,2,5-oxadiazole-3,4-diamine **b**, and 3-nitro-1H-1,2,4-triazole **c** of the compositions **1a**, **2a**, **2b**·H_2O, **2c**, and **3a**$_2$ were prepared and their structures were studied by X-ray crystallography. The components in the co-crystals demonstrate the different modes of mutual arrangement and contribution of diverse weak interactions to the final architecture. Infinite chains of the alternating component molecules linked by N–H···O hydrogen bonds characterise the structures of **1a** and **2a**, whereas in the case of **3a**$_2$ formation of the loosely packed ladder-type structure was observed. In **2b**·H_2O the planar naphtho- and oxadiazole moieties demonstrate their edge-to-face arrangement, while in **2c** the partially overlapping naphtho- and triazole moieties provide effective face-to-face π–π stacking interactions. The improved synthetic strategy for **1** and **2** is given.

Introduction

Crown ethers are widely utilised as efficient polydentate ligands for metal and ammonium ions as well as for neutral species.[1] Supramolecular systems combining crown ethers and light-absorbing groups attract considerable attention as they have a potential for use in optical sensors for metal ions[2] and in photoswitchable molecular devices.[3] The common approach in this area is the organic functionalisation of the classic crown ethers with chromophoric substituents (*e.g.*, anthracene,[4a,c] azobenzene,[4b,d] stilbene,[4e] or trityl[4f]). The photoswitchable crown compounds are created using functional groups that can undergo substantial structural changes under the action of light.[5]

So far typical 2,3-naphtho crown ethers, involving one or two large naphthylene groups, such as N15C5, N18C6 and DN18C6, have been widely used in the field of electrochemistry and some of their coordinating behaviors in solutions have been studied by CV and ESI-MS methods.[6] Alongside, classic crown ethers functionalised by the attachment of chromophoric or photoswitchable units to the crown ether skeleton or incorporation of a signal fragment into the crown framework,[7] bis-crown ethers with chromophoric or electron switchable bridges are the subject of great interest nowadays.[8] The crucial advantage of these crowns is their possibility to act in concern, thus forming sandwich complexes around the guest. This often leads to increased selectivity towards the complexing species. This is the case for photochromic crown ethers, which allow the photochemical control of cation binding, as well as for some optical sensors, designed for cation recognition. The intermolecular sandwich complexes based on bis-crown ethers range from discrete face-to-face arrangements to extended supramolecular architectures, which can generate nanosized aggregates and materials. The variety of possible combinations with cations bestows a particular interest in bis-crown dyes.

The crown ethers and co-crystal partners used in the present study are summarised in Scheme 1.

The present article is aimed at the co-crystals of 2,3-thiophene-15C5 **1**,[9] intensively exploited nowadays 2,3-naphtho-15C5 **2**, and perspective bis-18C6-stilbene **3** (Scheme 1). Owing to their bulky substituents, these crown ethers present non-covalent forces in the

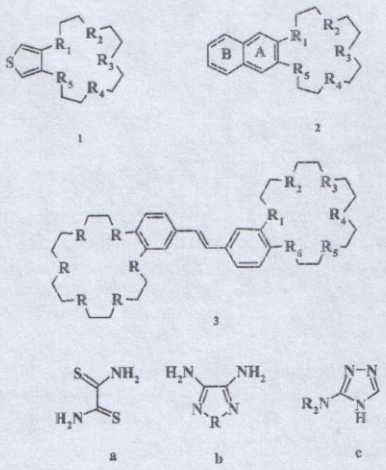

Scheme 1 Structural formulae with crystallographic numbering.

[a]*Odessa State Environmental University, Ministry of Education and Science of Ukraine, Lvovskaya str., 15, 65016 Odessa, Ukraine. E-mail: edganin@gmail.com*
[b]*A. V. Bogatsky Physico-Chemical Institute, National Academy of Sciences of Ukraine, Lustdorfskaya doroga 86, 650080 Odessa, Ukraine*
[c]*Schulich Faculty of Chemistry, Technion-Israel Institute of Technology, Technion City, 32000, Haifa, Israel. E-mail: botoshan@tx.technion.ac.il*
[d]*Institute of Applied Physics, Academy of Sciences of Moldova, Academy str., 5, MD2028 Chisinau, Moldova. E-mail: fonari.xray@phys.asm.md; Fax: (+373 22) 72 58 87; Tel: (+373 22) 73 81 54*

† CCDC reference numbers 771037–771042. For crystallographic data in CIF or other electronic format see DOI: 10.1039/c005284c

ART ■ C005284C

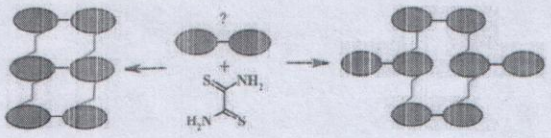

Scheme 2

crystal such as π–π stacking and cation–π interactions, occurring between themselves or with the guest molecules. Moreover, one can expect the contribution of sulfur from the thiophene moiety for intermolecular interactions. No structural data are available so far either for **1** or for its larger analogues both in pure or complexed form. For **3** such information is restricted by the macrocycle itself along with its two smaller homologues and photosensitive co-crystallisation compound of **3** with 1,2-bis[1-(3-ammoniopropyl)-4-pyridiniumyl]ethylene tetraperchlorate.[8] This complex has a very high thermodynamic stability that is provided by two-center host–guest bonding. Up until now, structurally studied 15- or 18-membered 2,3-naphtho crown ether complexes include preferably Na and K salts.[10,11] Dou and co-authors on a series of these complexes have demonstrated the contribution of π–π interactions between the naphtho-units to the supramolecular organisation of the complexes built on strong metal–O_{crown} interactions. Two types of the stacking models, between the inner and external aromatic rings were found and discussed. On the other hand, Kiviniemi and co-workers have studied the complexation of biologically important aromatic, nitrogen-containing cations with various crown ethers using ^{1}H NMR, mass spectrometric and crystallographic methods. Hydrogen bonding appears to be the most important interaction in complexation, but minor effects such as π-stacking or cation-π interactions have also been observed.[12]

In spite of the interest in **1–3**, no co-crystals with their base have been obtained so far. Along with others, we have previously shown that molecules **a–c** are good candidates for co-crystallisation with CEs.[13,14] They possess the different sets of H-donor groups for hydrogen bonding. On the other hand, they have the planar skeletons with the alternation of single and double bonds, so it is possible to expect different modes of stacking interactions and mutual arrangements with **1–3**, which in turn are possessed by extended aromatic systems. Dithiooxamide molecule **a** *via* its two *trans*-oriented amino-groups, preferably forms a 1 : 1 alternative chain with 15C5, B15C5, sterically hindered [1.5]dibenzo-18C6, and with lariat ethers, *N,N'*-bis(benzyl)-*N,N'*-diaza-18-crown-6 and *N,N'-bis*(4-methoxybenzyl)-*N,N'*-diaza-18-crown-6 as well as azacycles.[13,15] The conformationally flexible 18C6 and its dicyclohexyl-substituted analogues due to excess of their accessible O-atoms as H-bond acceptors provide the coordination of four dithiooxamide molecules to one CE makes it possible to expand the supramolecular architecture up to 2D layer with the second dithiooxamide molecule serving as a bridge between the (CE-dithiooxamide)$_n$ alternative chains. Based on the previously reported structures we could most probably expect the alternative chain motifs for **1–2**, while two scenarios, ladder-type chain motif or extended layer seem to be possible for **3** (Scheme 2).

Alongside the crystal structures for pure **1** and co-crystals based on crown ethers **1–3** of the compositions **1a**, **2a**, **2b**·H_2O,

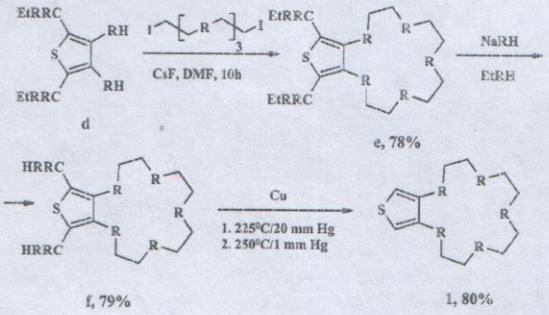

Scheme 3

2c and **3a**$_2$ (where **a** = dithiooxamide, **b** = 1,2,5-oxadiazole-3,4-diamine **b**, and **c** = 3-nitro-1*H*-1,2,4-triazole) we present herein the improved synthetic strategy for **1** and **2**.

Experimental

Synthesis

Commercially available **a–c** of the Aldrich Chemical Co trade were used in their initial state. **1** and all co-crystals were analysed for C, H, N and S in a Perkin Elmer 240C instrument. Crystals suitable for the X-ray diffraction experiments were isolated from the mass of crystals obtained. Suitable microanalyses were obtained for all compounds.

2,3-Thiophene-15-crown-5 **1** was obtained in three steps from 2,5-bis-(ethoxycarbonyl)-3,4-thiophendiol **d** using a modified procedure[16] (Scheme 3).

It should be noted that the use of 1,11-diiodine-3,6,9-trioxaundecane instead of tetraethyleneglycole ditosylate, and DMF as a solvent at the cyclisation stage, and a copper catalyst at the decarboxylation stage, allows us to simplify the synthetic procedure for **1** and increase its overall yield from 18.6% up to 49.3%.

Diethyl-2,3,5,6,8,9,11,12-octahydrothieno[3,4-b]-1,4,7,10,13-pentaoxacyclopentadecyn-14,16-dicarboxylate **e**. To a solution of 2,5-bis(ethoxycarbonyl)-3,4-thiophendiol **d**,[17] (13.0 g, 0.05 mol) in 900 ml of anhydrous DMF in an argon atmosphere at room temperature CsF (30.3 g, 0.199 mol) was added, and the mixture was stirred for 1 h followed by addition of 1,11-diiodine-3,6,9-trioxaundecane (21.3 g, 0.0515 mol) in 100 ml of anhydrous DMF. The temperature of the reaction mixture was gradually increased up to 80 °C, and the stirring at the same temperature continued for 10 h. DMF was distilled off under vacuum to a volume of 100 ml, the resulting solution was diluted twice with water and extracted by benzene (3 × 150 ml). The combined extracts were washed with water (100 ml), dried over $MgSO_4$ and evaporated to dryness. The resulting dry residue was purified on silica gel (Kiesilgel 60, 0.063–0.100 mm, "Merck"), eluent, hexane–ethyl acetate (3 : 1). The target product was additionally recrystallised from aqueous ethanol. Yield 16.3 g (78%). Mp 66–67 °C.[16]

2,3,5,6,8,9,11,12-Octahydro-thieno[3,4-b]-1,4,7,10,13-pentaoxacyclopentadecyn-14,16-dicarboxylic acid **f**. To a solution of diester **e** (25.1 g, 0.06 mol) in 300 ml of ethanol at room

This journal is © The Royal Society of Chemistry 2010

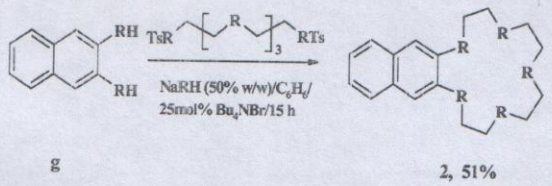

Scheme 4

temperature and stirring 300 ml of 5% aqueous NaOH was added. The reaction mixture was stirred for 2 h at 60 °C. After the reaction ethanol is distilled off in vacuum, water solution was washed by benzene (2 × 100 ml), acidified with $HCl_{conc.}$, cooled and the precipitate filtered off. Target product was purified by recrystallisation from minimal amount of hot water with 3–4 drops of HCl_{conc}. Yield 17.2 g (79%). Mp 244–245 °C.[16]

2,3-Thiophene-15-crown-5 (2,3,5,6,8,9,11,12-octahydro-thieno[3,4-b]-1,4,7,10,13-pentaoxacyclopentadecyne) **1**. Diacid **f** (13.8 g, 0.038 mol) and freshly prepared atomic copper (1.5 g) were placed in the refluxing unit for distillation and heated in an oil bath to 225 °C at 20 mm Hg. Thus there is a vigorous selection of CO_2, which ended after 1.5 h at 235 °C. Then the pressure was reduced to 1 mm Hg, bath temperature was increased to 250 °C and the resulting **1** was distilled off, followed by additional purification by crystallisation from heptane. Yield 8.3 g (80%). Mp 71–72 °C.[16]

2,3-Naphtho-15-crown-5 **2** was obtained by alkylation of 2,3-dihydroxynaphthalene by tetraethyleneglycole di-*p*-tosylate in conditions of phase catalysis (50% aqueous solution of NaOH, C_6H_6, 25 mol.% of tetrabutylammonium bromide),[18] allowing the 2.5 time output increase in comparison with the well-known Pedersen's method (Scheme 4).[19]

To a solution of 2,3-dihydroxynaphthalene **g** (8.0 g, 0.05 mol) and tetrabutylammonium bromide (4.0 g, 0,0125 mol) in 300 ml of benzene was added with stirring 100 ml of 50% solution of NaOH, the temperature was raised to 60 °C. The resulting mixture was stirred for 30 min at this temperature, then the solution of tetraethyleneglycol di-*p*-tosylate (25.85 g, 0.0515 mol) in 300 ml of benzene was added. The reaction mixture was boiled with stirring for 15 h. After cooling to room temperature, the organic layer was separated, washed successively with 5% solution of HCl (100 ml), water (3 × 200 ml), saturated solution of NaCl (100 ml) and dried over $MgSO_4$. The solvent was evaporated in vacuum; the resulting residue was extracted with boiling heptane (3 × 200 ml). The precipitate was filtered off and recrystallised from heptane. Yield 8.1 g (51%). Mp 118–119 °C (lit.[18] mp 117–119 °C).

3 was synthesised following a procedure previously described.[8c]

Preparation of co-crystals

Equimolar amounts of the corresponding crown ethers **1**–**3** and dithiooxamide **a** guest molecule were dissolved in boiling methanol–ethyl acetate mixture and allowed to crystallise slowly at room temperature. Similar synthetic procedure yielded the crystalline **2b·H₂O** from methanol–benzene–*n*-butanol mixture and **2c** from acetone–hexane mixture. The resulting co-crystals were separated by decanting. The crystallisation was repeated and the desired co-crystals were obtained in nearly quantitative yields. All the compositions were confirmed by elemental analysis. Melting points for co-crystals were determined and are presented in Table 1 along with the melting points for the starting compounds.

1 colorless crystals. Found, %: C, 52.59; H, 6.56; S, 11.64 for $C_{12}H_{18}O_5S$. Calcd, % C, 52.54; H, 6.61; S, 11.69.

1a (1/1) Yield 97%, transparent red crystals. Found, %: C, 42.66; H, 5.67; N,7.13; S, 24.35 for $C_{14}H_{22}N_2O_5S_3$. Calcd, %:C, 42.62; H, 5.62; N, 7.10; S, 24.38.

2a (1/1) Yield 94%, transparent red crystals. Found, %: C, 54.73; H, 5.96; N, 6.37; S, 14.68 for $C_{20}H_{26}N_2O_5S_2$. Calcd, %: C, 54.77; H, 5.98; N, 6.39; S, 14.62.

2b·H₂O (1/1/1) Yield 88%, transparent colorless crystals. Found, %:C, 55.01; H, 6.49; N, 12.89 for $C_{20}H_{28}N_4O_7$. Calcd, %:C, 55.04; H, 6.4; N, 12.84.

2c (1/1) transparent colorless crystals. Found, %:C, 55.54; H, 5.63; N, 12.92 for $C_{20}H_{24}N_4O_7$. Calcd, %: C, 55.55; H, 5.59; N, 12.96.

3a₂ (1/2) Yield 15%, transparent rosy crystals. Found, %: C, 51.37; H, 6.39; N, 6.35; S, 14.45 for $C_{38}H_{56}N_4O_{12}S_4$. Calcd, %: C, 51.33; H, 6.35; N, 6.30; S, 14.43.

Crystallography†

The crystallographic data collection for all six compounds was carried out on a Nonius Kappa CCD diffractometer at 293 K, using graphite-monochromatized Mo-Kα radiation ($\lambda = 0.71073$ Å).[20] The structure solution and refinement proceeded similarly using SHELX-97 program package[21] for all structures. Direct methods yielded all non-hydrogen atoms of the asymmetric unit. The non-hydrogen atoms were refined anisotropically by full-matrix least-squares calculations on F^2. Some disorder was found in **1a** and **3a₂**. In **1a** dithiooxamide molecule is disordered over two positions with occupancies of 0.75 and 0.25, correspondingly. The minor component was refined in isotropic

Table 1 Melting points for the studied co-crystals and starting materials

Co-crystal	Mp (°C)	Starting materials/Mp (°C)					
		1	2	3	a	b	c
1a	162–163	71–72			245		
2a	197–199		118–119		245		
2b·H₂O	84–85		118–119			160	
2c	111–113		118–119				212–214
3a₂	205–207			153	245		

approximation. Only for the major component were the hydrogen atoms of the amino-groups localised. $\mathbf{3a_2}$ was obtained in a miserable yield in the form of poor-quality crystals, and the X-ray experiment was carried out from the only selected very thin crystal. The whole structure is disordered over two positions with partial occupancies of 0.79 and 0.21, correspondingly. The minor component of the crown ether was refined using the SAME restraints to make equivalent bond distances and bond angles in two crown molecules equal. The crown and dithiooxamide molecules that correspond to the minor occupancies were refined in isotropic approximation. Only H-atoms of the amino groups in the major position of dithiooxamide molecule were localised and refined. In all structures C-bound hydrogen atoms were added theoretically, and were treated using a riding-model approximation, with $U_{iso}(H) = 1.2U_{eq}(C)$. The N- and O-bound H-atoms were determined from a difference Fourier map and were then allowed to refine isotropically with $U_{iso}(H) = 1.5U_{eq}(N/O)$. SADI restraints were applied to the N–H distances in amino-groups in $\mathbf{2b \cdot H_2O}$ and $\mathbf{3a_2}$. Details of the crystal data, data collection and processing are summarised in Table 2, hydrogen bonding geometry is given in Table 3. All packing diagrams were produced using Mercury.[22] Packing Index (PI) was calculated with the program PLATON.[23]

Results and discussion

Macrocycle **1** crystallises in orthorhombic space group *Pbca* with one molecule per asymmetric unit. The overall view of the molecule is shown in Fig. 1(a). The thiophene ring is almost exactly planar; the overall conformation of the molecule is chair-like with the dihedral angle between the thiophene ring and the mean plane of five oxygen atoms of 28.62(9)°. The molecule is deviating from ideal crown conformation as two of the O–C bonds adopt *gauche*-conformation being 83.3(3) for C(3)–O(2)–C(4)–C(5), and −82.4(4)° for C(8)–O(4)–C(7)–C(6), respectively. The molecules have voids that could, in principle, accommodate small guest molecules, although in the crystal structure access to these voids is blocked by neighboring molecules connected *via* CH···O weak interactions and packed in a herring-bone motif affording the dihedral angle between the planes through the thiophene rings in the neighboring molecules of 58.0° (Fig. 1(b)). Apropos, the same herring-bone packing motifs demonstrate the macrocycles **2**–**3** and their homologues in the solid state.[24]

Of **a**–**c** only molecule **a** forms co-crystals with all macrocycles **1**–**3**. Compound **1a** crystallises in the monoclinic $P2_1/n$ space group. The content of the asymmetric unit is shown in Fig. 2(a). The planar molecule **a** is inclined to the thiophene ring at an angle of 28.74(9)° and forms the dihedral angle of 72.95(5)° with the mean plane of crown oxygen atoms. The molecules in the co-crystal are held together *via* two NH···O crown hydrogen bonds provided by $H_2N(2)$-amino group. Through the second $H_2N(1)$-amino group that affords one single and one bifurcated NH···O crown hydrogen bonds the formula units are combined in the helical chains where the components alternate (Fig. 2(b)). Two NH_2-groups of molecule **a** use all their H-donor functions for hydrogen bonding with all crown oxygen atoms which are involved in these interactions, the corresponding N···O separations ranging within 2.993(12)–3.174(6) Å (Table 3). Although the separation of the macrocycles in the chain of *ca.* 7.93 Å (calculated as the distance between the centroids of pentagons of five crown oxygen atoms) provides space for partial interpenetration of the adjacent chains, the structure demonstrates the low packing efficacy (Fig. 2(c)) with the packing index (PI) of 66.6% practically equal to PI of 66.4% for pure **1**.

Co-crystallisation of 2,3-naphtho-15-crown-5 **2** with co-crystal partners **a**–**c** results in the compounds of the compositions **2a**, $\mathbf{2b \cdot H_2O}$, and **2c**, respectively which are sustained by the different sets of hydrogen bonds and auxiliary weak interactions. The co-crystals demonstrate the different modes of component arrangement. The extended naphthylene moiety imposes the rigidity to the attached O-atoms, which are perfectly coplanar with the aromatic unit, and prevents the 15C5 moiety from attaining the 'ideal crown' conformation. Similar to **1a**, **2a** represents a molecular complex of the 1 : 1 stoichiometry. The formula unit for **2a** is shown in Fig. 3(a). The compound crystallises in the monoclinic space group $P2_1/m$, with molecule **a** being displayed in a mirror plane which intersects the naphthalene moiety and the macrocyclic cavity through the O(3) atom; thus the planar units demonstrate the perfect T-shape arrangement. At the concave side of **2**, molecule **a** forms only one hydrogen bond, N(2)···O(3) = 3.287(3) Å, as the catechol oxygen atoms are removed from the possible interaction area. Similar to **1a** *via* the second $H_2N(1)$-amino group that participates in two NH···O hydrogen bonds, N(1)···O(1) = 3.051(2), and N(1)···O(3) = 2.943(3) Å the translated along direction *a* complexes are ordered in the linear chain with the separation of 7.97 Å between the neighboring crown molecules. The packing of the chains occurs in such mode to maximise the edge-to-face interactions between the planar skeletons of **a**, and naphthylene-units due to participation of S(1) atom in the bifurcated C(6)···S(1) contacts with H···S = 2.97, C(6)···S(1) = 3.894 Å, ∠CHS = 170° (Fig. 3(b)). Although visually no pronounced voids are evident in **2a** (Fig. 3(c)) contrary to **1a**, the PI indicates practically the same value of 66.7%, thus demonstrating the insignificantly improved packing efficacy in comparison with pure CE **2**, for which PI is 65.7% (calculated using YENMOT entry with geometrically generated H-atoms).

Co-crystal $\mathbf{2b \cdot H_2O}$ crystallises in monoclinic $P2_1/c$ space group, and represents a monohydrate of 1 : 1 : 1 stoichiometry. The formula unit for $\mathbf{2b \cdot H_2O}$ is shown in Fig. 4(a).

The *syn*-oriented amino-groups of molecule **b** are capable to co-ordinate either to two different molecules of CE (as in the co-crystals with 15C5, B15C5, dicyclohexano-18C6), thus generating the 1D chains built of alternative components, or to the same water molecule inserted between crown ether, (for example, [1.5]B18C6), and molecules **b**. In $\mathbf{2b \cdot H_2O}$ the water molecule is perching at 2.07 Å above the mean plane of five crown oxygen atoms. It acts as a double donor towards crown oxygen atoms at N···O distances of 2.842(3) and 3.134(3) Å, and as a double acceptor towards two amino groups of molecule **b**, thus generating the $R_2^1(7)$ graph set. It is noteworthy that each amino group uses only one of two hydrogen atoms in this hydrogen bonding pattern. The second H-atom of N(2)-amino group is pointed to the A cycle of the naphthalene moiety with the CgA···H = 2.69 and CgA···N(2) = 3.331 Å (where CgA is the center of gravity for ring A). The edge-to-face arrangement of molecule **b** and naphthalene unit is described by the dihedral angle of 77.1(1)°. Between the formula units related by the screw axis act

This journal is © The Royal Society of Chemistry 2010

ART ■ C005284C

Table 2 Crystallographic data for compounds **1**, **1a**, **2a**, **2b·H_2O**, **2c**, **$3a_2$**

Complex	**1**	**1a**	**2a**	**2b·H_2O**	**2c**	**$3a_2$**
Composition	$C_{12}H_{18}O_5S$	$C_{12}H_{18}O_5S\ C_2H_4N_2S_2$	$C_{18}H_{22}O_5\ C_2H_4N_2S_2$	$C_{18}H_{22}O_5\ C_2H_4N_4O\ H_2O$	$C_{18}H_{22}O_5\ C_2H_2N_4O_2$	$C_{34}H_{48}O_{12}\ (C_2H_4N_2S_2)_2$
CCDC numbers	771038	771040	771041	771042	771039	771037
Formula weight	274.32	394.52	438.55	436.46	432.43	889.11
Wavelength/Å	0.71073	0.71073	0.71073	0.71073	0.71073	0.71073
Space group	*Pbca*	$P2_1/n$	$P2_1/m$	$P2_1/c$	$P\bar{1}$	$P\bar{1}$
a/Å	16.674(3)	9.945(2)	7.965(2)	10.536(2)	7.219(1)	7.714(3)
b/Å	8.545(2)	15.102(3)	10.521(2)	15.585(4)	10.992(2)	9.760(2)
c/Å	19.279(4)	12.647(2)	13.080(3)	13.639(3)	13.356(3)	15.675(3)
α/°	90	90	90	90	89.43(2)	90.12(3)
β/°	90	91.68(2)	93.68(2)	91.17(2)	78.84(2)	96.87(30
γ/°	90	90	90	90	80.80(2)	107.23(3)
V/Å^3	2746.9(10)	1898.6(6)	1093.8(4)	2239.1(9)	1026.2(3)	1118.2(5)
Z	8	4	2	4	2	1
Dcalc/g cm^{-3}	1.327	1.380	1.332	1.295	1.400	1.320
μ/mm^{-1}	0.246	0.416	0.276	0.099	0.107	0.274
F(000)	1168	832	464	928	456	472
Reflections collected/unique	14103/2400	13416/3524	11441/2617	16152/3788	8141/3520	6161/3234
Reflections with $I > 2\sigma(I)$	1315	2206	1655	1560	1927	997
Refinement method	Full-matrix least-squares on F^2	Full-matrix least-squares on F^2	Full-matrix least-squares on F^2	Full-matrix least-squares on F^2	Full-matrix least-squares on F^2	Full-matrix least-squares on F^2
Data/restraints/parameters	2400/0/164	3524/0/261	2617/0/151	37882/299	3520/0/281	3234/54/401
Goodness-of-fit on F^2	1.038	0.980	1.005	0.846	0.930	0.772
R_1, wR_2 [$I > 2\sigma(I)$]	0.0511, 0.1407	0.0364, 0.0829	0.0423, 0.1143	0.0365, 0.0616	0.0478, 0.1088	0.0523, 0.0788
R_1, wR_2 (all data)	0.1118, 0.1580	0.0724, 0.0902	0.0707, 0.1213	0.1325, 0.0760	0.1119, 0.1294	0.2223, 0.1002
Extinction coefficient	0.0122(19)	0.0147(13)	0.050(7)	0.0109(6)	0.056(5)	—
Largest diff. peak/hole/e Å^{-3}	0.350/−0.308	0.186/−0.276	0.306/−0.300	0.137/−0.134	0.187/−0.175	0.099/−0.126
Packing index (%)	66.4	66.6	66.7	65.9	69.6	65.3

Table 3 Hydrogen bond distances (Å) and angles (°) for **1a**, **2a**, **2b·H$_2$O**, **2c**, **3a$_2$**

D–H···A	d(D–H)	d(H···A)	d(D···A)	∠(DHA)	Symmetry transformation for acceptor
1a					
N(1)–H(1N1)···O(1)	0.72(3)	2.47(3)	3.048(8)	138(4)	$x + 1/2, 1/2 - y, z + 1/2$
N(1)–H(1N1)···O(5)	0.72(3)	2.56(3)	3.140(12)	139(4)	$x + 1/2, 1/2 - y, z + 1/2$
N(1)–H(2N1)···O(3)	0.75(4)	2.28(3)	2.993(12)	159(4)	$x + 1/2, 1/2 - y, z + 1/2$
N(2)–H(1N2)···O(2)	0.82(3)	2.29(3)	3.097(5)	173(3)	x, y, z
N(2)–H(2N2)···O(4)	0.82(3)	2.46(3)	3.175(6)	147(4)	x, y, z
2a					
N(1)–H(1A)···O(3)	0.86(2)	2.27(3)	2.943(3)	135(2)	$x + 1, y, z$
N(1)–H(1B)···O(1)	0.79(3)	2.35(3)	3.051(2)	147(4)	$x + 1, 1/2 - y, z$
N(2)–H(2B)···O(3)	0.81(3)	2.48(3)	3.287(3)	176(3)	x, y, z
2b·H$_2$O					
O(1w)–H(1w)···O(2)	0.84(2)	2.07(2)	2.890(2)	168(2)	x, y, z
O(1w)–H(2w)···O(4)	0.86(2)	2.03(2)	2.886(2)	179(3)	x, y, z
N(1)–H(2N1)···O(1w)	0.85(1)	2.31(2)	3.131(3)	163(3)	x, y, z
N(2)–H(2N2)···O(1w)	0.94(2)	1.91(2)	2.839(3)	173(3)	x, y, z
2c					
N(4)–H(4)···O(4)	0.86	2.06	2.887(3)	161	x, y, z
N(4)–H(4)···O(3)	0.86	2.47	3.015(3)	122	x, y, z
C(8)–H(8A)···O(6)	0.97	2.54	3.245(4)	130	$1 - x, -y, 1 - z$
C(5)–H(5A)···O(7)	0.97	2.53	3.431(4)	154	$x, 1 + y, z$
3a$_2$					
N(1)–H(1N1)···O(6)	0.85(4)	2.49(5)	3.275(11)	153(6)	x, y, z
N(2)–H(2N1)···O(4)	0.85(4)	2.33(4)	3.166(12)	170(6)	x, y, z
N(2)–H(1N2)···O(3)	0.98(4)	2.35(5)	3.253(14)	152(6)	$x + 1, y, z$
N(2)–H(2N2)···O(1)	0.99(4)	2.38(5)	3.346(11)	166(6)	$x + 1, y, z$

the weak CH(CH$_2$)···N interactions of 3.398–3.478 Å (Fig. 4(b)) that combine them into helical chain. The insertion of water molecules in the structure increases a number of small voids and results in the lower PI of 65.9%.

The formula unit for **2c** that crystallises in triclinic $P\bar{1}$ space group is shown in Fig. 5(a). It is constructed by one bifurcated NH···O hydrogen bond, with N···O distances of 2.887(3) and 3.015(3) Å, respectively (Table 3). The CH···O crown distances for the neighboring NH CH-group pointed inside the heterocyclic cavity exceeding the reasonable value of CH···O hydrogen bonding (H···O = 2.6 Å).

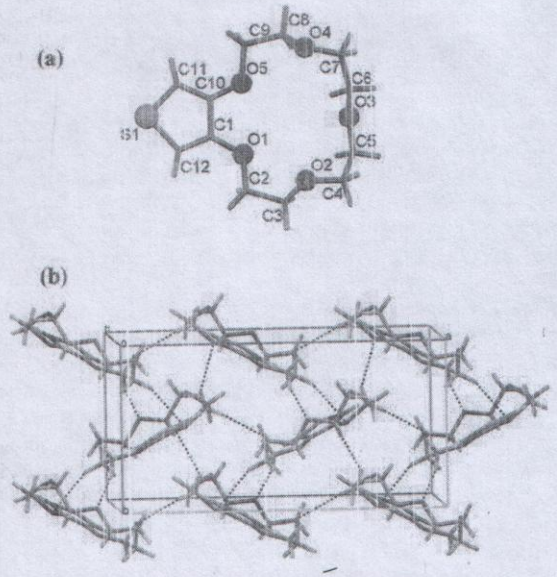

Fig. 1 Structure of **1**. View of molecule **1** with the numbering scheme (a); fragment of the layer sustained by CH···O hydrogen bonds (the marked CH···O contacts do not exceed 2.6 Å) (b).

The molecule of 3-nitro-1*H*-1,2,4-triazole **c** has a planar skeleton with all non-hydrogen atoms being coplanar within 0.034 Å. In the triazole cycle C–N distances range within 1.310(3)–1.332(3) Å, N–N distance being 1.342(3) Å. Of all herein discussed co-crystals only **2c** demonstrates the face-to-face heteromeric π–π interactions between the cyclic units, being inclined at an angle of 16.40(4)°. Further packing of the complexes is characterised by their pronounced segregation in stacks parallel to the *a* axis with the interplane separation between the naphthylene unit and the molecule **c** ranging within of 3.14–4.06 Å in the complex and 2.68–3.60 Å between the translated complexes (Fig. 5(b)). The inversion-related stacks are held in the crystal *via* weak CH···O interactions with participation of nitro-group of **c** as H-acceptor. The efficacy of the crystal packing of **2c** is the highest amongst described herein compounds as Kitaigorodskii's PI of 69.6% indicates.

Concluding this section we can unambiguously state that the imposed by bulky naphthalene moiety an essential increase of the rigidity of the crown ether framework in **2** reduces the number of O-crown atoms accessible for participation in the hydrogen bonding with neutral molecules **a–c** that results in an elaboration of part of potential H-donors from the overall interaction system. On the other hand, the formation of **1a** and **2a** with the predicted 1D topology confirms the previously demonstrated advantage of dithiooxamide molecule as a suitable bidentate linker even in the case of the asymmetric crown ethers with the reduced number of O-acceptors.

Complex **3a$_2$** further demonstrates the facilities of dithioxamide molecule **a** as a suitable bidentate linker giving rise to the

This journal is © The Royal Society of Chemistry 2010

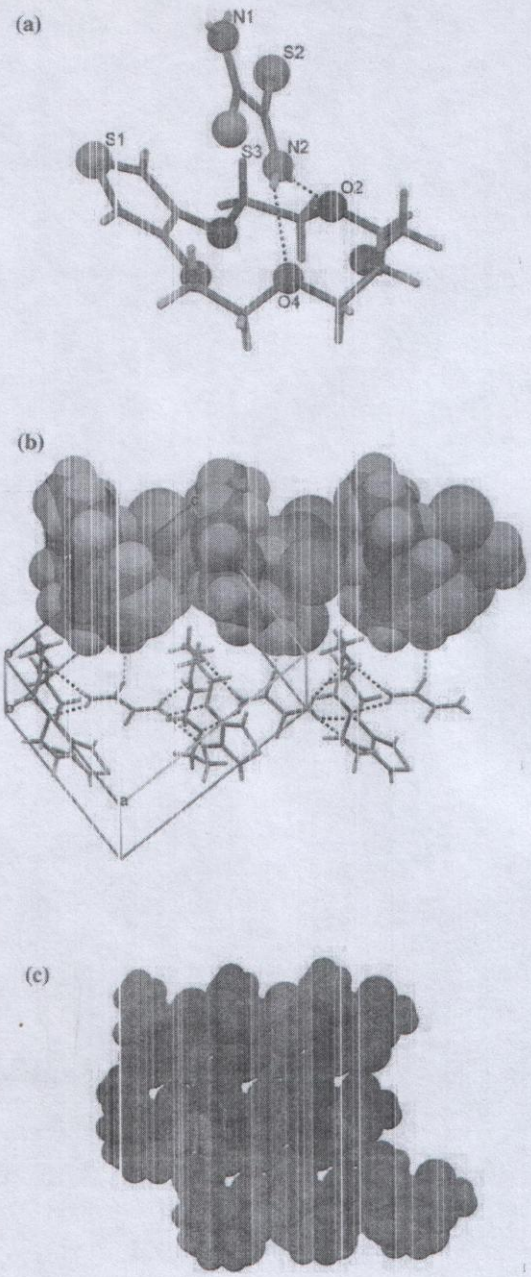

Fig. 2 View of **1a** with the partial numbering scheme, only major position for dithiooxamide molecule is shown (a); view of the helical chains with the intermolecular distances including the shortest CH···S contacts shown by pink color (H···S = 2.92, C(11)···S(2) = 3.844 Å, ∠CHS = 171°) (b); packing of the neighboring chains (c).

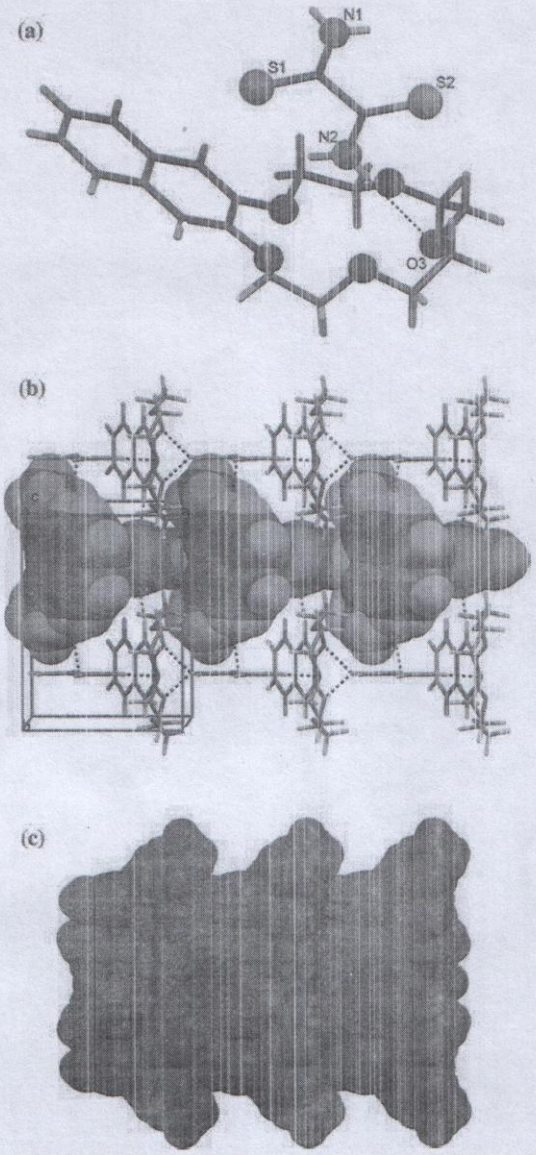

Fig. 3 View of **2a**. Formula unit with the partial numbering scheme (a); view of the linear chains with the shortest C···S intermolecular distances shown by pink color (b); packing of the neighboring chains (c).

first ladder-type co-crystal based on bis-(18C6)-stilbene. The formula unit for co-crystal $\mathbf{3a_2}$ is shown in Fig. 6(a). Molecule **3** lies about an inversion centre, its *E*-stilbene fragment being strictly planar. Dithiooxamide molecule occupies general position. In **3**, the oxygen atoms of the 18C6 subunit form a hexagon with the side varying within 2.60–2.92 Å. The least-squares mean plane through the oxygen atoms is inclined with respect to the benzene ring plane by 16.0° (39.7° in free macrocycle). The dithiooxamide molecule is inclined at an angle of 83.1° to the mean plane of six crown oxygen atoms. In the formula unit molecule **3** and two molecules **a** are held *via* a couple of NH···O hydrogen bonds, N(1)···O(6) = 3.275(11) and N(1)···O(4) =

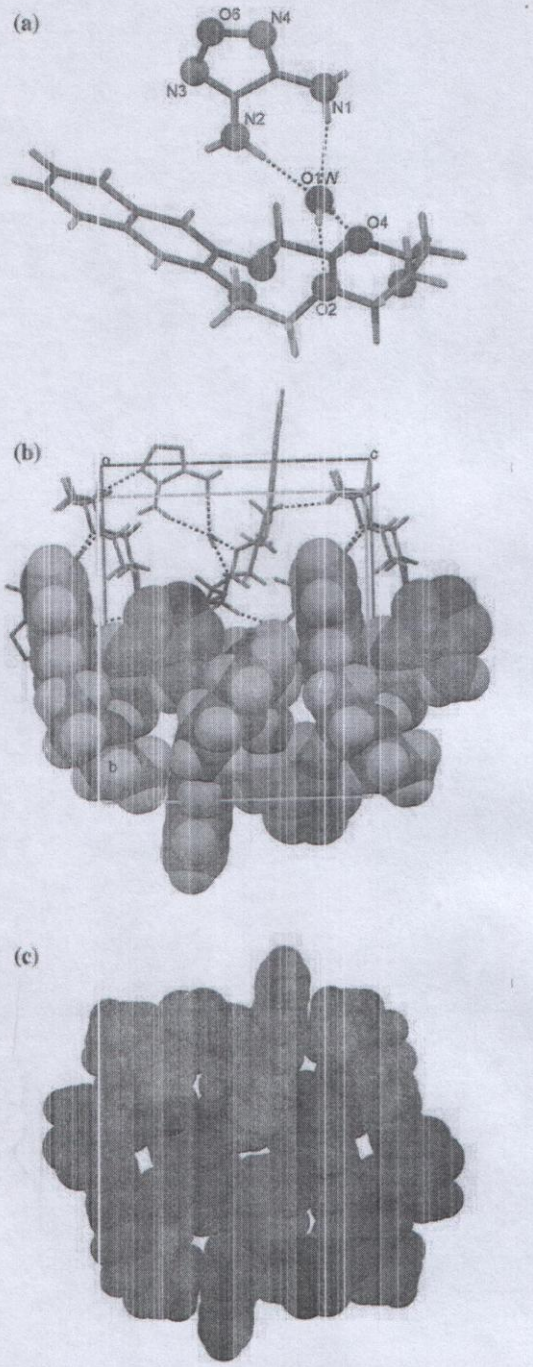

Fig. 4 View of **2b**·H_2O with the partial numbering scheme (a); space-filling presentation of crystal packing along the crystallographic *a* axis (b–c).

3.166(12) Å, the second $H_2N(2)$-amino group is responsible for the interaction with the translated crown molecule *via* two N(2)···O(3) = 3.253(14) and N(2)···O(1) = 3.346(11) Å hydrogen

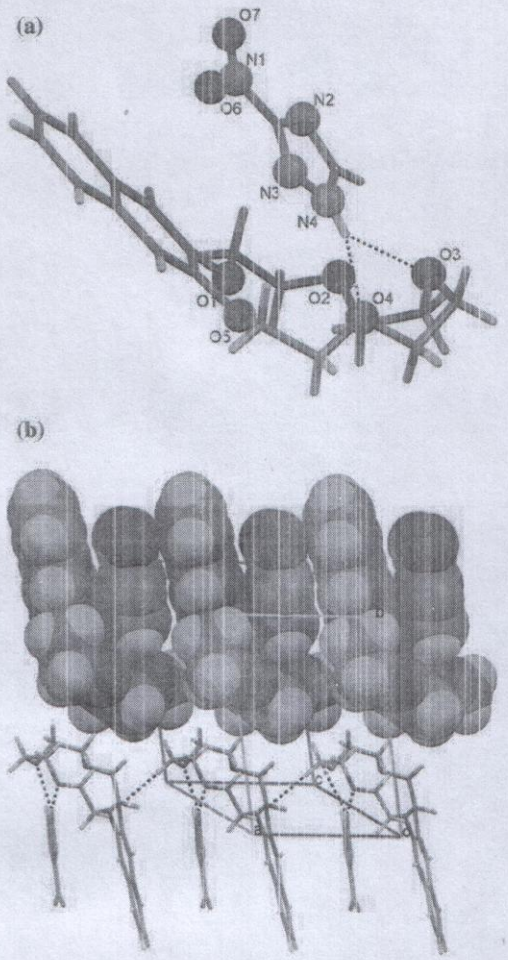

Fig. 5 View of **2c**. Formula unit with the partial numbering scheme (a); space-filling presentation of the crystal packing along the crystallographic *a* axis (b).

bonds. These rather weak NH···O hydrogen bonds multiply by the bis-nature of **3**, permit to build the rigid ladder-type framework with the parallel arrangement of the stilbene moieties and voids with the linear dimensions of 7.71 × 15.97 Å determined as the distances between the centroids of the crown ether rings separated by dithiooxamide molecule or stilbene fragment, respectively. The neighboring ladders stack in a partially interpenetrating mode with the part of oxyethylene chain buried within the voids *via* CH···S interactions, C(8)···S(1) = 3.939 Å. The PI for $\mathbf{3c_2}$ adopts the smallest value of 65.3% being essentially lower than 69.8% for pure **3** calculated using QASVUC cif file. Nevertheless the multiple hydrogen bonding providing by the *bis*-nature of crown ether affords the rather stable and predictable supramolecular architecture.

The reported data show that dithiooxamide can be used to control the supramolecular architecture. Besides the discussed crystal structures some physical properties change upon the formation of the co-crystals. First of all we should mention that

This journal is © The Royal Society of Chemistry 2010

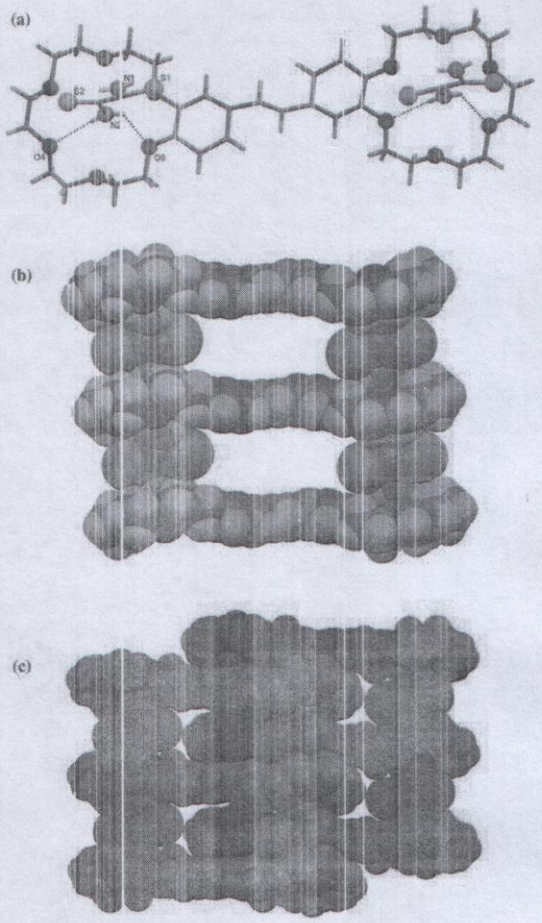

Fig. 6 View of $3c_2$ with the partial numbering scheme (a); ladder-type assembling (b); space-filling presentation of the ladders packing (c).

the red-colored dithiooxamide assigns its color to the co-crystals formed with the colorless CEs when the molecular mass of macrocyclic molecule does not essentially exceed the molecular mass of dithiooxamide.[13,14] Only in the case of bis-(18C6)-stilbene the co-crystal coloring becomes less intense being light rosy due to the increased mass portion of the colorless CE in the final co-crystal. Co-crystals **1a**, **2a**, and $\mathbf{3a_2}$ possess the melting points intermediate between the parent compounds, while monohydrate $\mathbf{2b \cdot H_2O}$, and weakly bound **2c** have melting points lower than the initial components (Table 1). Along with the decrease of melting point water insertion in $\mathbf{2b \cdot H_2O}$ also decreases the co-crystal PI by increasing the number of narrow void spaces in the crystal. The essentially improved PI registered for **2c** can be explained by the most effective packing of the extended planar moieties.

Conclusions

For the first time the co-crystals of 2,3-thiophene-15C5 **1**, 2,3-naphtho-15C5 **2**, and bis-(18C6)-stilbene **3**, with dithiooxamide alongside the co-crystals of naphtho-15C5 with 1,2,5-oxadiazole-3,4-diamine, and 3-nitro-1*H*-1,2,4-triazole were synthesised and their crystal structures were discussed. All the crown ethers used in this study possess the asymmetry imposed by the cyclic unit attached to the crown ether framework, which explains the generated asymmetric hydrogen-bonding patterns. Dithiooxamide as a suitable bidentate linker permits the control of the supramolecular architecture thus giving rise to the helical, linear, or ladder-type alternating component chains for **1**–**3**. The extended naphtho-moiety of **2** is responsible for the edge-to-face and face-to-face heteromeric stacking interactions with planar 1,2,5-oxadiazole-3,4-diamine and 3-nitro-1*H*-1,2,4-triazole molecules. Along with the crystal structure for **1** the improved synthetic strategy for **1** and **2** is reported.

Acknowledgements

The diffraction data were collected at the Schulich Faculty of Chemistry, Technion, Haifa, through the cooperation of Prof. Menahem Kaftory, whom we would like to acknowledge.

References

1 (*a*) *Cation Binding by Macrocycles*, ed. Y. Inoue and G. W. Gokel, Marcel Dekker, New York, 1990; (*b*) R. M. Izatt, K. Pawlak, J. S. Bradshaw and R. L. Bruening, *Chem. Rev.*, 1991, **91**, 1721; (*c*) J.-M. Lehn, *Supramolecular Chemistry. Concepts and Perspectives*, VCH, Weinheim, 1995; (*d*) G. W. Gokel, W. M. Leevy and M. E. Weber, *Chem. Rev.*, 2004, **104**, 2723.

2 (*a*) H.-G. Löhr and F. Vögtle, *Acc. Chem. Res.*, 1985, **18**, 65; (*b*) P. de Silva, H. Q. N. Gunaratne, T. Gunnlaugsson, A. J. M. Huxley, C. P. McCoy, J. T. Rademacher and T. E. Rice, *Chem. Rev.*, 1997, **97**, 1515; (*c*) M. V. Alfimov and S. P. Gromov, in *Applied fluorescence in chemistry, biology, and medicine*, ed. W. Rettig, B. Strehmel, S. Schrader and H. Seifert, Springer-Verlag, Berlin, 1999, pp. 161–178; (*d*) B. Valeur and I. Leray, *Coord. Chem. Rev.*, 2000, **205**, 3.

3 (*a*) V. Balzani, A. Credi and M. Venturi, *Molecular devices and machines – A Journey in the Nano World*, Wiley-VCH, Weinheim, 2003; (*b*) *Molecular Switches*, ed. B. L. Feringa, Wiley-VCH, Weinheim, 2001; (*c*) J. D. Badjic, V. Balzani, A. Credi, S. Silvi and J. F. Stoddart, *Science*, 2004, **303**, 1845; (*d*) D. S. Perekalin, M. V. Babak, V. V. Novikov, P. V. Petrovskii, K. A. Lyssenko, M. Corsini, P. Zanello and A. R. Kudinov, *Organometallics*, 2008, **27**, 3654.

4 (*a*) J.-P. Desvergne and H. Bouas-Laurent, *J. Chem. Soc., Chem. Commun.*, 1978, 403; (*b*) S. Shinkai, T. Minami, Y. Kusano and O. Manabe, *J. Am. Chem. Soc.*, 1983, **105**, 1851; (*c*) J. H. R. Tucker, H. Bouas-Laurent, P. Marsau, S. W. Rileya and J.-P. Desvergne, *Chem. Commun.*, 1997, 1165; (*d*) M. S. Fonari, E. Luboch, A. Collas, A. Bukrej, F. Blockhuys and J. F. Biernat, *J. Mol. Struct.*, 2008, **892**, 195; (*e*) M. V. Alfimov, S. P. Gromov, Y. V. Fedorov, O. A. Fedorova, A. I. Vedernikov, A. V. Churakov, L. G. Kuz'mina, J. A. K. Howard, S. Bossmann, A. Braun, M. Woerner, D. F. Jr. Sears and J. Saltiel, *J. Am. Chem. Soc.*, 1999, **121**, 4992; (*f*) K. Kimura, R. Mizutani, M. Yokoyama, R. Arakawa and Y. Sakurai, *J. Am. Chem. Soc.*, 2000, **122**, 5448.

5 (*a*) S. Shinkai, in *Comprehensive Supramolecular Chemistry*, ed. J.-M. Lehn, Pergamon Press, New York, 1996, 1; (*b*) S. P. Gromov and M. V. Alfimov, *Russ. Chem. Bull.*, 1997, **46**, 611; (*c*) V. Lokshin, A. Samat and A. V. Metelitsa, *Russ. Chem. Rev.*, 2002, **71**, 893; (*d*) D. G. Amirsakis, A. M. Elizarov, M. A. Garcia-Garibay, P. T. Glink, J. F. Stoddart, A. J. P. White and D. J. Williams, *Angew. Chem., Int. Ed.*, 2003, **42**, 1126; (*e*) M. V. Alfimov, O. A. Fedorova and S. P. Gromov, *J. Photochem. Photobiol., A*, 2003, **158**, 183.

6 (*a*) M. Yamauchi, A. Jyo and N. Ishibashi, *Anal. Chim. Acta*, 1982, **136**, 399; (*b*) M. Yamauchi, T. Imato, M. Katahira, Y. Inudo and N. Ishibashi, *Anal. Chim. Acta*, 1985, **169**, 59; (*c*) E. Luboch,

ART ■ C005284C

A. Cygan and J. F. Biernat, *Tetrahedron*, 1990, **46**, 2461; (*d*) Md. A. Rahman, H. Doe, N. Sakurada and R. Arakawa, *Electrochim. Acta*, 2001, **47**, 623.

7 (*a*) G. Koshkakaryan, L. M. Klivansky, D. Cao, M. Snauko, S. J. Teat, J. O. Struppe and Yi Liu, *J. Am. Chem. Soc.*, 2009, **131**, 2078; (*b*) E. Wagner-Wysiecka, M. Jamrogiewicz, M. S. Fonari and J. F. Biernat, *Tetrahedron*, 2007, **63**, 4414; (*c*) J. Szczygelska-Tao, M. S. Fonari and J. F. Biernat, *Supramol. Chem.*, 2008, **20**, 651; (*d*) N. G. Lukyanenko, T. I. Kirichenko, A. Yu. Lyapunov, C. Yu. Kulygina, Yu. A. Simonov, M. S. Fonari and M. M. Botoshansky, *Tetrahedron Lett.*, 2004, **45**, 2927; (*e*) N. G. Lukyanenko, T. I. Kirichenko, A. Yu. Lyapunov, A. V. Muzepa, Y. A. Simonov, M. S. Fonari and M. M. Botoshansky, *Chem.–Eur. J.*, 2005, **11**, 262; (*f*) N. G. Lukyanenko, A. Yu. Lyapunov, T. I. Kirichenko, M. M. Botoshansky, Y. A. Simonov and M. S. Fonari, *Tetrahedron Lett.*, 2005, **46**, 2109.

8 (*a*) W.-S. Xia, R. H. Schmehl and C.-J. Li, *J. Am. Chem. Soc.*, 1999, **121**, 5599; (*b*) S. P. Gromov, *Russ. Chem. Bull.*, 2008, **57**, 1325; (*c*) A. I. Vedernikov, S. S. Basok, S. P. Gromov, L. G. Kuzmina, V. G. Avakyan, N. A. Lobova, E. Yu. Kulygina, T. B. Titkov, Yu. A. Strelenko, E. I. Ivanov, G. A. K. Howard and M. V. Alfimov, *Russ. J. Org. Chem.*, 2005, **41**, 843(Engl. Transl.); (*d*) S. P. Gromov, A. I. Vedernikov, E. N. Ushakov, N. A. Lobova, A. A. Botsmanova, L. G. Kuz'mina, A. V. Churakov, Y. A. Strelenko, M. V. Alfimov, J. A. K. Howard, D. Johnels and U. G. Edlund, *New J. Chem.*, 2005, **29**, 881; (*e*) S. Fery-Forgues and F. Al-Ali, *J. Photochem. Photobiol., C*, 2004, **5**, 139.

9 (*a*) A. Berlin, G. Zotti, S. Zecchin and G. Schiavon, *Synth. Met.*, 2002, **131**, 149; (*b*) B. Jousselme, Ph. Blanchard, E. Levillain, J. Delaunay, M. Allain, P. Richomme, D. Rondeau, N. Gallego-Planas and J. Roncali, *J. Am. Chem. Soc.*, 2003, **125**, 1363; (*c*) D. T. McQuade, A. E. Pullen and T. M. Swager, *Chem. Rev.*, 2000, **100**, 2537.

10 (*a*) X.-K. Gao, J.-M. Dou, D.-C. Li, F.-Y. Dong and D.-Q. Wang, *J. Chem. Crystallogr.*, 2005, **35**, 107; (*b*) X. Gao, J. Dou, D. Li, F. Dong and D. Wang, *J. Coord. Chem.*, 2005, **58**, 1127; (*c*) J. F. Biernat, A. Cygan, E. Luboch, Yu. A. Simonov, T. I. Malinovski, V. K. Bel'skii and N. F. Bolotina, *J. Inclusion Phenom. Mol. Recognit. Chem.*, 1993, **15**, 369; (*d*) X.-K. Gao, J.-M. Dou, D.-C. Li, F.-Y. Dong and D.-Q. Wang, *J. Mol. Struct.*, 2005, **733**, 181; (*e*) X. Gao, J. Dou, D. Li, F. Dong and D.-Q. Wang, *J. Coord. Chem.*, 2005, **58**, 1597; (*f*) Yu. A. Simonov, A. A. Dvorkin, T. J. Malinovski, A. Cygan, E. Luboch and J. F. Biernat, *Pol. J. Chem.*, 1994, **68**, 1783.

11 (*a*) X.-K. Gao, J.-M. Dou, D.-C. Li, F.-Y. Dong and D.-Q. Wang, *J. Inclusion Phenom. Macrocyclic Chem.*, 2005, **53**, 111; (*b*) J. Dou, X.-K. Gao, F. Dong, D.-C. Li and D.-Q. Wang, *Dalton Trans.*, 2004, 2918; (*c*) C. B. Knobler, E. F. Maverick, K. N. Trueblood and R. M. Weiss, *Acta Crystallogr., Sect. C: Cryst. Struct. Commun.*, 1999, **55**, 2091.

12 (*a*) S. Kiviniemi, A. Sillanpää, M. Nissinen, K. Rissanen, M. T. Lämsä and J. Pursiainen, *Chem. Commun.*, 1999, 897; (*b*) M. Nissinen, S. Kiviniemi, K. Rissanen and J. Pursiainen, *CrystEngComm*, 2000, **2**, 102; (*c*) S. Kiviniemi, M. Nissinen, M. T. Lämsä, J. Jalonen, K. Rissanen and J. Pursiainen, *New J. Chem.*, 2000, **24**, 47.

13 (*a*) Y. A. Simonov, M. S. Fonari, M. J. Zaworotko, H. Abourahma, J. Lipkowski, E. V. Ganin and A. A. Yavolovskii, *Org. Biomol. Chem.*, 2003, **1**, 2922; (*b*) W. H. Watson, J. Galloy, D. A. Grossie, F. Vogtle and W. M. Muller, *J. Org. Chem.*, 1984, **49**, 347; (*c*) W. H. Watson and P. C. Jain, *J. Inclusion Phenom.*, 1986, **4**, 397; (*d*) M. S. Fonari, Yu. A. Simonov, L. Croitoru, S. S. Basok, E. V. Ganin and J. Lipkowski, *J. Mol. Struct.*, 2006, **794**, 110; (*e*) M. S. Fonari, E. V. Ganin, Yu. M. Chumakov, M. M. Botoshansky, K. Suwinska, S. S. Basok and Yu. A. Simonov, *New J. Chem.*, 2009, **33**, 1646.

14 (*a*) R. Luboradzki, J. Lipkowski, Y. A. Simonov, M. S. Fonari, E. V. Ganin and A. A. Yavolovskii, *J. Inclusion Phenom. Macrocyclic Chem.*, 2001, **40**, 59; (*b*) R. Luboradzki, J. Lipkowski, Y. A. Simonov, M. S. Fonari, E. V. Ganin and A. A. Yavolovskii, *J. Inclusion Phenom. Mol. Recognit. Chem.*, 1995, **23**, 181; (*c*) E. V. Ganin, M. S. Fonari, Yu. A. Simonov, G. Bocelli, S. S. Basok, V. V. Tkachuk, S. A. Kotlyar and G. L. Kamalov, *J. Inclusion Phenom. Macrocyclic Chem.*, 2005, **52**, 63.

15 B. Piotrkowska, A. Wasilewska, M. Gdaniec and T. Polonski, *CrystEngComm*, 2008, **10**, 1421.

16 T. Sone, K. Sato and Y. Ohba, *Bull. Chem. Soc. Jpn.*, 1989, **62**, 838.

17 E. W. Fager, *J. Am. Chem. Soc.*, 1945, **67**, 2217.

18 T. Bogaschenko, S. Basok, C. Kulygina, A. Lyapunov and N. Lukyanenko, *Synthesis*, 2002, 2266.

19 C. J. Pedersen, *J. Am. Chem. Soc.*, 1967, **89**, 7017.

20 Z. Otwinowski and W. Minor, in C. W. Carter & R. M. Sweet (ed.), *Methods in Enzymology, Macromolecular Crystallography, Part A*, Academic Press. London. 1996, 276, 307.

21 G. M. Sheldrick, *Acta Crystallogr., Sect. A: Found. Crystallogr.*, 2008, **64**, 112.

22 C. F. Macrae, P. R. Edgington, P. McCabe, E. Pidcock, G. P. Shields, R. Taylor, M. Towler and J. van de Streek, *J. Appl. Crystallogr.*, 2006, **39**, 453.

23 A. L. Spek, *J. Appl. Crystallogr.*, 2003, **36**, 7.

24 F. N. Allen, *Acta Crystallogr., Sect. B: Struct. Sci.*, 2002, **58**, 380.

This journal is © The Royal Society of Chemistry 2010

ART ■ C005284C

Додаток Я.

Копія статті. “ Транспортные взаимодействия краун-эфиров с фторокомплексными кислотами кремния”

УДК 547.89

М.Г. Васильева, Э.В. Ганин, *д.х.н.***, В.Ф. Шевченко,** *к.т.н.***, О.Н.Ласовская**
Одесский государственный экологический университет

ТРАНСПОРТНЫЕ ВЗАИМОДЕЙСТВИЯ КРАУН-ЭФИРОВ С ФТОРОКОМПЛЕКСНЫМИ КИСЛОТАМИ КРЕМНИЯ

Синтез диакватетрафторосиликата 18-краун-6 и стабилизация пентафторсиликата гидроксония с цис-син-цис-изомером дициклогексано-18-краун-6 при взаимодействии краун-эфиров с кремнефтороводородной кислотой, образующейся в результате транспортной реакции, могут быть учтены в качестве химической основы при моделировании самоорганизационных природных процессов.

Ключевые слова: *транспортные реакции, краун-эфиры, кремнефторо-водородная кислота, комплексы.*

Введение.

При химических транспортных реакциях твердое или жидкое вещество, реагируя с каким-либо газообразным веществом, образует газообразные продукты, которые после переноса в другую часть системы при изменении условий равновесия изменяются с выделением нового вещества. Так, Р. Бунзен, изучая вулканические газы, содержащие летучие кислоты, упомянул о возможности переноса железа в токе вулканических газовых извержений [1]. Видно, что гетерогенные реакции этого типа могут быть учтены при моделировании природных химических процессов.

Согласно данным [2] 45%-ная кремнефтороводородная кислота представляет собой лабильную равновесную смесь SiF_6^{2-} (30–40%), $[SiF_5 \bullet H_2O]^-$ (60–70%), $SiF_4 \bullet 2H_2O$ (5%). Источники [3-5] указывают на содержание в растворах кремнефтороводородной кислоты единственного комплекса SiF_6^{2-}. При полном испарении воды из 45%-ной кремнефтороводородной кислоты, по [6,7], образуется стабильный кристаллический фторокомплекс состава $(H_3O)_2SiF_6$.

Материалы и методы их исследования.

Исходные соединения использовали в виде коммерческих образцов, (фирмы Acros) без дополнительной очистки. ИК спектры регистрировали на приборе Spekord M-80 в вазелиновом масле, стекла KRS-5. ТСХ проводили на пластинах Silufol с элюированием смесью метанол—хлороформ, 1:5, проявление нингидрином. Комплексы (I) и (II) при ТСХ разлагаются на компоненты со значениями Rf 0 (красные пятна кремнийфторидов) ~ 0.53 и 0.70 (белые пятна краун-эфиров) соответственно.

Кристаллические супрамолекулярные комплексы (I, II).

Растворы 0.25 ммоля 1,4,7,10,13,16-гексаоксациклооктадекана или цис-син-цис-пергидродибензо[b,k][1,4,7,13,16]гексаоксациклооктадецина в 15 мл 45%-ной фтороводородной кислоты помещали в стеклянный эксикатор над серной

кислотой. После полного испарения растворителей с количественным выходом получали кристаллы комплексов (I, II).

Комплекс дигидрата 1,4,7,10,13,16-гексаоксациклооктадекана с *транс*-диакватетрафторосиликатом кремния, 2:1:2 (I), т. пл. 92-93 ^{o}C (т.пл 91-92 ^{o}C по [8]). ИК спектр, ν, см$^{-1}$: 3430 (HO), 1145-1095 (COC), 775, 702 (SiF). Найдено, %: C 32.85; H 7.47; F 17.60; Si 6.45. $C_{12}H_{32}F_4O_{10}Si$. Вычислено, %: C 32.72; H 7.32; F 17.25; Si 6.38.

Комплекс *цис-син-цис* пергидродибензо[*b,k*][1,4,7,10,13,16]гексаоксацикло-октадецина с пентафторосиликатом гидроксония, 1:1 (II), т. пл. 101-103 ^{o}C. ИК спектр, ν, см$^{-1}$: 3600 – 3500, 1650 (H_3O^+), 1165-1000 (COC), 875, 785 (SiF). Найдено, %: C 46.73; H 7.61; F 18.52; Si 5.55. $C_{20}H_{39}F_5O_7Si$. Вычислено, %: C 46.67; H 7.64; F 18.46; Si 5.46.

Результаты исследования и их анализ.

В рамках одной из приоритетных задач супрамолекулярной химии по выявлению селективных взаимодействий и стабилизации краун-эфирами («хозяевами») малоустойчивых соединений («гостей») в стабильные кристаллические соединения включения [9,10], в данной работе изучена возможность селективного синтеза кристаллических супрамолекулярных комплексов краун-эфиров с фторокомплексными кислотами кремния из растворов краун-эфиров во фтороводородной кислоте в условиях самопроизвольного образования в них кремнефтороводородной кислоты.

Установлено, что при испарении растворов 1,4,7,10,13,16-гексаоксациклооктадекана – (18К6) и *цис-син-цис* пергидродибензо[*b,k*][1,4,7,10,13,16] гексаоксациклооктадецина – (А-ДЦГ-6) во фтороводородной кислоте в стеклянном эксикаторе над серной кислотой, селективно образуются кристаллические супрамолекулярные комплексы:
нейтральный [(*trans*-SiF_4 • 2 H_2O) • 18К6 • 2 H_2O] – (I) и
ионный [H_3O^+ • (А-ДЦГ-6)] SiF_5^- – (II) соответственно.

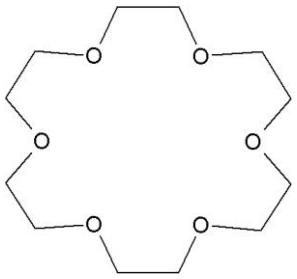

(18К6)

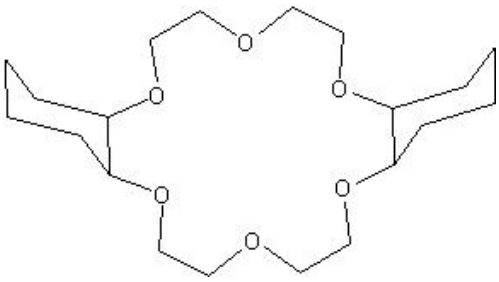

(А-ДЦГ-6)

18К6 – 1,4,7,10,13,16-гексаоксациклооктадекан,
А-ДЦГ-6 – *цис-син-цис* пергидродибензо[*b,k*][1,4,7,10,13,16]гексаоксациклооктадецин

Состав и строение комплексов (I и II) были охарактеризованы методом рентгеноструктурного анализа. Кристаллы комплекса (I) моноклинные, пространственная группа $P2_1/a$, a = 15.484(5), b = 9.651(3), c = 7.795(2) Å, γ =

121.45(3)°, Z = 2 для формулы $C_{12}H_{32}F_4O_{10}Si$. *На рис. 1 приведен фрагмент псевдополимерной цепи комплекса (I).*

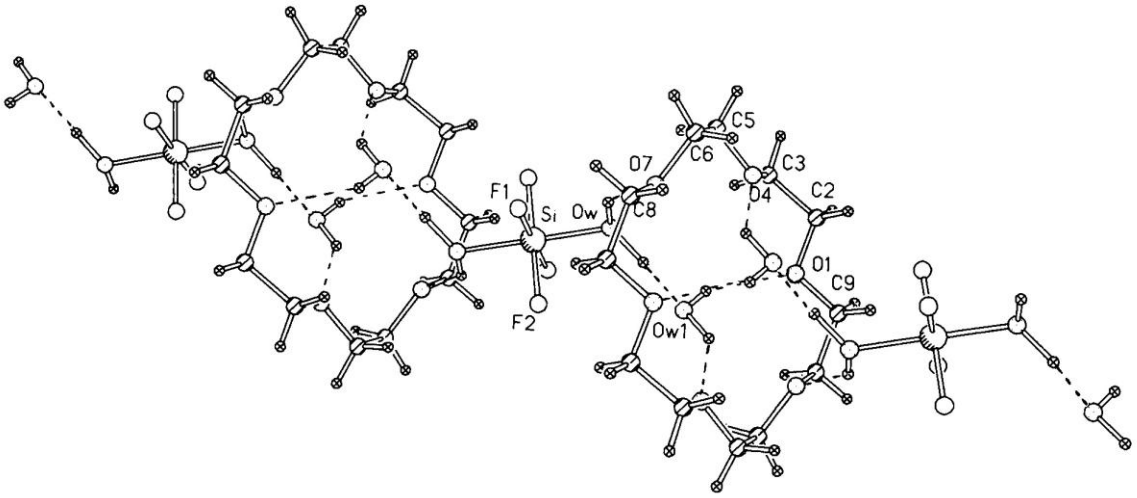

Рис. 1. Фрагмент псевдополимерной цепи комплекса (I) с водородными связями, отмеченными пунктирными линиями.

*В кристалле (I) псевдополимерная структура образована так, что вода и половинки [*trans-$SiF_4 \bullet 2\ H_2O$*] связаны меду собой и 18К6 системой O-H ... O водородных связей. Расстояния O (H) ... O находятся в пределах 2.60 (1) – 2.91 (1) Å. Транс-октаэдрические [*$SiF_4 \bullet 2\ H_2O$*] фрагменты образованы за счет гидратации тетраэдрического* SiF_4. *Длины связей Si-F и Si-O составляют 1.658 (7) и 1.853 (9) Å, соответственно. Между индивидуальными цепями имеются только ван-дер-ваальсовы взаимодействия.*

Строение комплекса (II) представлено на рис. 2. Кристаллы моноклинные: a = 12.476(1), b = 10.761(1), c = 19.840(5) Å, γ = 102.83(1)°, Z = 4, пространственная группа $P2_1/n$. *Структура комплекса образована из катионов [*H_3O^+ *• (А-ДЦГ-6)] и анионов* SiF_5, *связанных электростатическими взаимодействиями.*

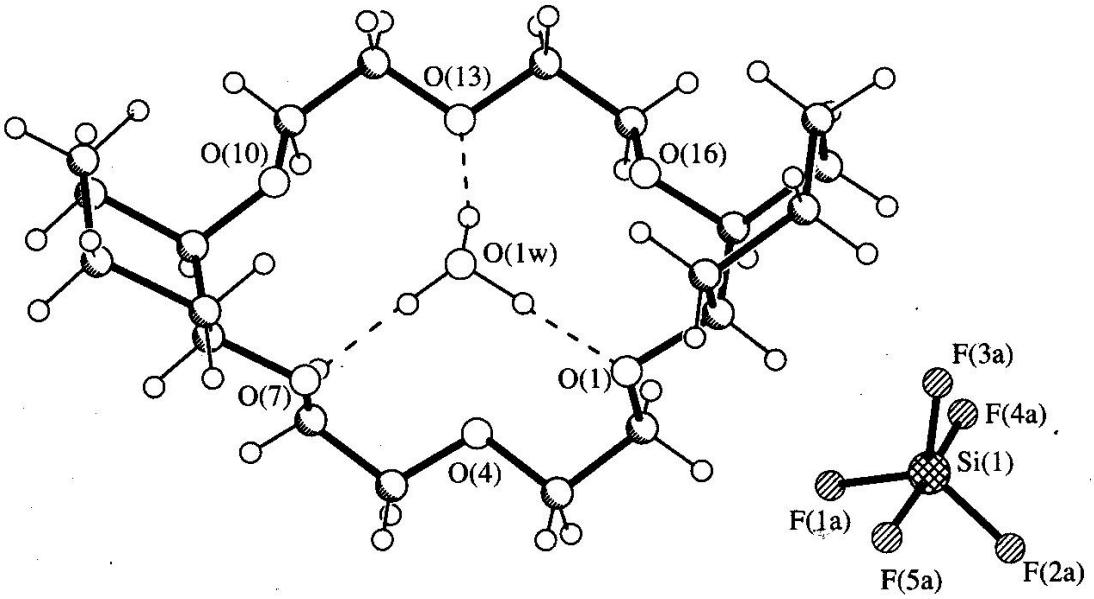

Рис. 2. Строение комплекса (II) в проекции на плоскость шести атомов кислорода макроцикла с указанием водородных связей.

В катионе реализуются три Н-связи типа OH ... O между ионом H_3O^+, внедренным в полость макроцикла, и каждым вторым атомом кислорода А-ДЦГ-6; соответствующие расстояния O ... O составляют 2.615(3) – 2.637(3) Å. Расстояния до трех других атомов кислорода цикла укорочены по сравнению с суммой ван-дер-ваальсовых радиусов для атома кислорода (1.52 Å) и принимают значения 2.833(4) – 2.882(3) Å. Изомер А-ДЦГ-6 характеризуется тем, что оба циклогексановых заместителя расположены по одну сторону от средней плоскости макроцикла. Атом кислорода иона гидроксония выходит из нее в ту же сторону, образуя так называемый "тесный комплекс". Макроцикл имеет наиболее выгодную гош-конформацию по связям С–С, кон-формация же связей С–О определяется десятью транс- *и двумя* гош-*фрагментами. Взаимное расположение шести эфирных атомов кислорода таково, что атомы кислорода O(1), O(7), O(10) и O(16) компланарны с точностью +0.074 Å, атомы кислорода O(4) и O(13) выходят из этой плоскости на –1.632 и –0.853 Å соответственно. Отклонение атома кислорода иона гидроксония от нее составляет 0.440 Å. Комплекс (II) относится к числу немногих структурно описанных соединений, в которых удалось фиксировать пентафторосиликатный анион как обособленную структурную единицу.*

Тригонально-бипирамидальный анион SiF_5^- (рис. 3) разупорядочен: атом кремния занимает одну, а атомы фтора – две равновероятные позиции.

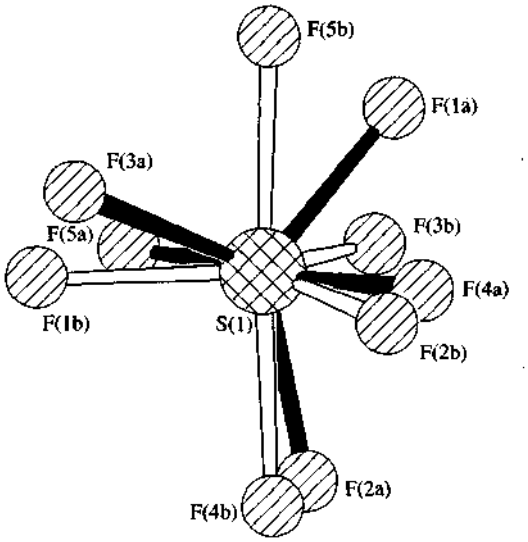

Рис. 3. Строение пентафторосиликатного аниона в комплексе (II).

Каждый пентафторосиликатный анион имеет кратчайшие межмолекулярные контакты с тремя катионами с расстояниями C... F находящимися в интервале 3.062(9) –3.364(10) Å. Основными факторами, способствующими стабилизации комплекса (II), на наш взгляд, являются: центрирование полости цикла "малым" ионом гидроксония по триподному типу с фиксированием конформации "хозяина" и комплексообразование с однозарядным анионом SiF_5^-, заполняющим полости к кристалле.

С учетом состава комплексов (I, II) видно, что смещение равновесия и селективность связывания «гостевых» компонент кремнефтороводородной кислоты определяется пространственным строением краун-эфиров 18К6 и А-ДЦГ-6.

Описанные превращения являются первым примером селективного синтеза кристаллических супрамолекулярных комплексов (I, II) в условиях самопроизвольного образования на границе раздела фаз (газообразная–HF/твердая–SiO_2) тетрафторида кремния (SiF_4), анти-направленным транспортом его в газовой фазе, образованием равновесной смеси «гостевых» компонент в жидкой фазе по схеме:

$$HF + SiO_2 \rightarrow SiF_4 + H_2O \rightarrow SiF_4 \bullet 2\,H_2O + H_3OSiF_5 + (H_3O)_2SiF_6 ,$$

и взаимодейсивием последних с краун-эфирами.

Образование комплексов (I, II) иллюстрирует, что жидкая и твердая фазы, могут существенно преобразовываться при нормальной температуре и давлении в атмосфере, теряющей воду. Результаты могут быть приняты во внимание в качестве химической основы при моделировании самоорганизационных природных процессов согласно [9,10]. Кристаллические супрамолекулярные соединения (I, II) стабильны и могут представлять интерес в качестве контейнеров [9] фторокомплексных кислот кремния.

Список литературы

1. *Шефер Г.* Химические транспортные реакции. Транспорт неорганических веществ через газовую фазу и его применение. – М: Мир, 1964. – 189 с.

2. *Буслаев Ю.А.,* Петросянц С.П. О составе фторокомплексов алюминия и кремнефтороводородной кислоты в водных растворах // Коорд. химия. – 1979. – Т.5, № 2. – С.163-170.

3. *Масалович В.М.,* Мошкарева Г.А., Агасян П.К. Изучение комплексообразования в растворах фтористоводородной и кремниевой кислот // Журн. неорганич. химии. – 1979. – Т. 24. № 2. – С. 353-356.

4. *Головнев Н.Н.,* Головнева И.И. Влияние pH на равновесия образования фторидных комплексов кремния в водном растворе // Журн. неорганич. химии. – 1984. – Т.29, № 5. – С.1173-1177.

5. *Головнев Н.Н.* Влияние pH на образование иона $SiF6^{2-}$ в водном растворе // Журн. неорганич. химии. – 1986. – Т.31, № 3. – С.643-646.

6. *Гельмбольдт В.О.,* Ганин Э.В., Сергиенко В.С., Миначева Л.Х. Необычный путь получения и кристаллическая структура гексафторосиликата гидроксония – простейшего "гидрата" кремнефтороводородной кислоты // Коорд. Хим. – 2004. Т. 30. № 9. – С. 720.

7. *Gel'mbol'dt V. O.,* Ganin E. V., Minacheva L. Kh., Sergienko V. S. Synthesis and Crystal Structure of Oxonium Hexafluorosilicate,a Stable Form of Fluosilicic Acid Dihydrate // Russ. J. Inorganic Chem. – 2005 – Vol. 50, No. 2. – P. 143-147.

8. *Simonov Y.A.*. Ganin E.V., Dvorkin A.A., et al. Stabilization of silicon tetrafluoride by crown ether complexation. Crystal and molecular structure of the host:guest complex 1:1:2 between trans-tetrafluorobis(aqua)silicon, 18-crown-6 and water // Supramol. Chem. – 1994. – Vol. 3. – P. 185-189.

9. *Comprehensive* supramolecular chemistry / eds.: J-M. Lehn, J. L. Atwood, J. E. D. Davies, D. D. MacNicol, F. Wogtle, Oxford – New York – Tokyo: Pergamon, 1996. – P. 418.

10. *Лен Ж-М.* Супрамолекулярная химия: Концепции и перспективы. – Новосибирск: Наука, 1998. – 334 с.